Université de Montréal

Molecular Basis of Native Inward Rectifier Currents: Role of Kir2 Subunits

par

Gernot Schram

Département de Médecine

Faculté de Médecine

Thèse présentée à la Faculté des études supérieures

en vue de l'obtention du grade de Philosophiae Doctor (Ph.D.)

en Sciences Biomedicales

Aout 2005

Université de Montréal

Faculté des études supérieures

Cette thèse intitulée :

Molecular basis of native inward rectifier currents: Role of Kir2 subunits

présentée par :

Gernot Schram

a été évaluée par un jury composé des personnes suivantes :

Dr. Bruce G. Allen, président-rapporteur

Dr. Stanley Nattel, directeur de recherche

Dr. Lucie Parent, membre du jury

Dr. Alvin Shrier, examinateur externe

Dr. Jacques Billette, représentant du doyen de la FES

Résumé

Les canaux potassiques à rectification entrante (Kir) sont d'importants régulateurs de l'excitabilité cellulaire. Dans le système nerveux central, ils contrôlent l'excitabilité, participent à la signalisation électrique et à la transmission d'information. Leur dysfonction est associée à l'épilepsie et aux paralysies périodiques. Au niveau cardiaque, le canal potassique à rectification entrante I_{K1} détermine le potentiel de repos membranaire et contribue à la phase 3 du potentiel d'action. Sa dysfonction est responsable d'arythmies chez les sujets atteints du syndrome d'Andersen. Au niveau vasculaire, I_{K1} détermine le potentiel de repos membranaire, régule l'influx de Ca^{2+} et la signalisation intracellulaire dépendante du Ca^{2+}.

Quatre membres de la sous-famille Kir 2 (Kir2.1-4) contribuent au courant I_{K1} endogène. Cependant, la contribution de chacune de ces sous-unités au courant I_{K1} natif est inconnue. Les propriétés biophysiques des sous unités homomériques Kir2 ne reproduisent pas les propriétés du courant I_{K1} cardiaque. De plus, l'expression relative de Kir2 au niveau ARNm et protéique ne permet pas d'expliquer plusieurs des ses caractéristiques.

Par l'utilisation de méthodes électrophysiologiques et biochimiques, nous avons étudié l'association des sous-unités Kir2.4 et Kir2.1 et montré qu'elles s'assemblaient pour former un hétéromère Kir2.1/Kir2.4 fonctionnel possédant des propriétés distinctes des sous-unités Kir2.1 ou Kir2.4 exprimées seules. Ce fut une des premières démonstrations de l'assemblage hétérométrique des sous-unités Kir2 et de sa contribution au phénotype du courant potassique à rectification entrante endogène. L'assemblage des sous-unités Kir2.1/Kir2.4 pourrait être physiologiquement important, particulièrement au niveau du cerveau où les deux sous-unités sont co-exprimées.

Nous avons par la suite comparé les propriétés de bloc par le Ba^{2+} des canaux homo- et hétéromères Kir2 exprimés dans des oocytes de *Xenopus* avec celles du courant I_{K1} endogène humain. Nous avons trouvé que le bloc par le Ba^{2+} des

hétéromères Kir2.x/Kir2.y n'était pas la simple résultante de la somme des réponses individuelles des sous-unités et que les propriétés du bloc par le Ba^{2+} de I_{K1} étaient plus proches de celles des sous-unités co-injectées que de celles des sous unités exprimées individuellement. Ces résultats suggèrent la possibilité qu'une portion de I_{K1} endogène puisse résulter de ces assemblages hétéromériques.

Des stratégies électrophysiologiques et biochimiques additionnelles ont été utilisées pour déterminer la composition des cellules endothéliales aortiques humaines (CEAHs) en sous-unités Kir2. Nous avons démontré que les CEAHs exprimaient les quatre types de sous-unités Kir2 mais que seules Kir2.2 et Kir2.1 étaient fonctionnellement importantes, Kir2.2 apparaissant être le déterminant principal de la conduction Kir dans ces cellules.

Nous concluons que les canaux hétéromères Kir2 pourraient représenter un mécanisme important dans la détermination de la diversité des canaux potassiques à rectification entrante fonctionnellement distincts et que l'importance relative des différentes sous-unités Kir 2 pourrait varier selon le tissu.

Mots-clés : Kir2.1, Kir2.2, Kir2.3, Kir2.4, canaux potassiques, I_{K1}, courants à rectification entrante, hétéromères, cerveau, cœur, endothélium aortique, distribution différentielle, canaux ioniques, expression fonctionnelle

Abstract

Inward rectifier potassium (Kir) channels are important regulators of cellular excitability. Central nervous system Kir channels participate in electrical excitability, electrical signalling and information processing. Their dysfunction is associated with epilepsy and paralysis. Cardiac inward rectifier current I_{K1} sets the resting membrane potential and contributes to phase 3 cardiac repolarization. Dysfunction of cardiac I_{K1} causes arrhythmias in Andersen's syndrome. Vascular inward rectifier currents determine the resting membrane potential, regulating Ca^{2+} influx and Ca^{2+} dependent intracellular signalling. Four members of the Kir2 subfamily (Kir2.1-4) contribute to the background inward rectifier I_{K1}. Their relative contribution to native Kir currents is unknown. Homomeric Kir2 subunit assembly fails to reproduce cardiac I_{K1} and the relative expression of Kir2 mRNA and protein cannot explain a variety of I_{K1} features. Using electrophysiological and biochemical methods, we studied co-assembly of Kir2.4 and Kir2.1, finding that Kir2.1 and Kir2.4 co-assemble to form functional Kir2.1/Kir2.4 heteromers with properties distinct from homomeric channels formed by either subunit alone. This was one of the first demonstrations that heteromeric Kir2 subunit assembly can occur and contribute to physiological inward rectifier phenotype. Kir2.1/2.4 assembly might be physiologically important in regions of the brain, where both subunits are co-expressed.

We then compared properties of Ba^{2+} block of homo- and heteromeric Kir2 channels in *Xenopus* oocytes to human cardiac I_{K1}. We found that Ba^{2+} block of heteromeric Kir2.x/Kir2.y subunits is not the simple sum of individual subunit responses and that Ba^{2+} blocking properties of I_{K1} are more similar to co-injected subunits than to each subunit expressed alone. These results suggest that a substantial proportion of native I_{K1} may result from Kir2 heteromultimer formation.

Complementary electrophysiological and biochemical strategies were used to determine Kir2-subunit composition of human aortic endothelial cells (HAECs). We found that HAECs express all four types of Kir2 subunits, but that only Kir2.2 and Kir2.1 are functionally relevant, with Kir2.2 appearing to be the primary determinant of Kir conductance.

We conclude that heteromeric Kir2 channels may represent an important mechanism to achieve diversity of functionally distinct inward rectifier channels and that the relative importance of different Kir2 subunits varies among tissues.

Keywords: Kir2.1, Kir2.2, Kir2.3, Kir2.4, potassium channels, I_{K1}, inward rectifier current, heteromultimer, brain, heart, aortic endothelium, differential distribution, ion channels, functional expression

Table of contents

List of Tables

List of Figures

List of acronyms and abbreviations

°C: Degrees Celsius

$[Ba^{2+}]_i$: Internal (cytosolic) Ba^{2+} concentration

$[Ba^{2+}]_o$: External (extracellular) Ba^{2+} concentration

$[K^+]$: K^+ concentration

$[K^+]_o$: Extracellular K^+ concentration

2TM: two transmembrane domains

4TM: four transmembrane domains

4-AP: 4-Aminopyridine

$5\text{-}HT_{1A}$: 5-hydroxytryptamine 1A

6TM: six transmembrane domains

A1 receptor: Adenosine receptor

A: Atrium

Å: Angström

AA: Amino acid

AAA: Sequence of three alanine residues; used to replace the GYG motif in the selectivity filter to create a dominant negative channel subunit

ABC: ATP-binding cassette (protein superfamily)

ACh: Acetylcholine

ADP: Adenosine diphosphate

AF: Atrial fibrillation

Ag^+: Silver ion

AGS: Activators of G-protein signalling

AP: Action potential

APD: Action potential duration

ARNm: Acide ribonucléotique méssager

ATP: Adenosine triphosphate

AV: Atrioventricular

AVN: Atrioventricular node

Ba^{2+}: Barium

BAEC: Bovine artery endothelial cell

BPAEC: Bovine pulmonary artery endothelial cell

BCE: Bovine corneal endothelial cell

BK channel: Ca^{2+} activated K^+ channel

Ca^{2+}: Calcium

CaM: Calmodulin

CCE: Capacitative Ca^{2+} entry

cDNA: Complementary Deoxyribonucleic acid

cRNA: Complementary Ribonucleic acid

CCPA: 2-chloro N6-cyclopentyl adenosine

Cd^{2+}: Cadmium

CEAHs: Céllules endothéliales aortiques humaines

CHO cells: Chinese hamster ovary cells

Cl^-: Chloride

cm: Centimetre

CNG channel: Cyclic nucleotide-gated channel

CNS: Central nervous system

Co^{2+}: Cobalt

COS cells: Monkey cell lines derived from the CV-1 cell line by transformation with a replication origin defective mutant of SV40 VIRUS, which codes for wild type large T antigen

CPPX: Dipeptidyl-peptidase-like protein

CRAC: Ca^{2+}-release activated Ca^{2+} channel

Cs^+: Caesium

CTX: Charybdotoxin

D2 receptor: Dopamine receptor

DAD: delayed after depolarization

DAG: 1,2-diacylglycerol

DMEM: Dulbecco's Modified Eagle Medium

DIDS: 4,4'-Diisothiocyanostilbene-2,2'-Disulfonic Acid

Dn: Dominant negative

Dn-Kir: Dominant negative Kir2 subunit

DNA: Deoxyribonucleic acid

DTX: Dendrotoxin

E. coli: Escherichia coli

EA1: Episodic ataxia type 1

EAD: Early after depolarization

Eag: ether-à-go-go

EC: Endothelial cell

ECG: Electrocardiogram

EDHF: Endothelium-derived hyperpolarizing factor

EGTA: ethylene glycol bis(2-aminoethyl ether)-N,N,N'N'-tetraacetic acid

EGM-2: Endothelium growth medium-2

E_M: Membrane potential

E_{Na}: Sodium equilibrium potential

Endo: Endocardium

Epi: Epicardium

ER: Endoplasmatic reticulum

ERG: ether-related gene

ERP: Effective refractory period

EPR: Electron paramagnetic resonance spectroscopy

E_K: Equilibrium potential for potassium

FBS: Fetal bovine serum

FEP: Free energy perturbation (computations)

Flag sequence: eight amino-acid sequence (Asp-Tyr-Lys-Asp-Asp-Asp-Asp-Lys)

$GABA_B$: γ-aminobutyric acid B

GAP: GTPase accelerating protein

GDP: Guanosine diphosphate

GFP: Green fluorescent protein

gK: Potassium conductance

gNA: Sodium conductance

GPCR: G-protein coupled receptor

GST: Gluthatione S-transferase

GTP: Guanosine triphosphate

H5-segment: putative pore forming segment

HAEC: Human aortic endothelial cell

HCEC: Human capillary endothelial cell

HEK: Human embryonic kidney cells

HCN: Hyperpolarization activated cyclic nucleotide-gated channel

HEPES: 4-(2-hydroxyethyl)-1-piperazineethanesulfonic acid

HERG: Human ether-related gene

HUGO: Human Genome Organization

HUVEC: Human umbilical vein endothelial cell

IC_{50}: Half-maximal inhibitory concentration

$I_{Ca,\,L}$: L-type calcium current

$I_{CA,\,T}$: T-type calcium current

I_f: Funny current, aka pacemaker current

I_{K1}: Inward rectifier current.

I_K: Delayed rectifier potassium current.

I_{KACh}: Acetylcholine-activated potassium current.

I_{KATP}: ATP-sensitive potassium current

I_{KNDP}: Vascular smooth muscle cell ATP-dependent K^+-current

I_{Kr}: Delayed rectifier potassium current, rapid component

I_{Ks}: Delayed rectifier potassium current, slow component

I_{Kur}: Ultrarapid delayed rectifier current

I_{Na}: Inward sodium current

IPC: Ischemic preconditioning

IPE cells: Iris pigment epithelial cells

IsK: Synonym for minK

IUPHAR: International Union of Pharmacology

I_{to}: Transient outward current

$I_{to,\,f}$: Transient outward current with fast inactivation kinetics

$I_{to,\,s}$: Transient outward current with slow inactivation kinetics

IP_3: Inositol-1,4,5-trisphosphate

K^+: Potassium

K_{Ach}: Acetylcholine-activated K^+ channel

K_{ATP}: ATP inhibited K^+ channel

KChIP2: Potassium Channel Interacting Protein 2

KCl: Potassium chloride

KCO: K^+ channel openers

KcsA: Potassium channel from *Streptomyces lividans*

Kd: Dissociation constant

kDa: Kilo Dalton

K_G-channel: G-protein activated K^+ channel

Kir: Inward rectifier potassium channel

KirBac: Eukaryotic Kir channel

K_{NDP}: Vascular smooth muscle cell ATP dependent K^+ channel

KO: Knockout

Kv: Voltage dependent potassium channel

KvAP: Voltage-gated potassium channel from Aeropyrum pernix

KvLQT1: Pore forming subunit of the I_{Ks} channel

LA: Left atrium

LB medium: Luria-Bertani medium

LC: Locus coeruleus

LC-CoA: Long chain CoA

LQT syndrome: Long QT syndrome

LV: Left ventricle

mA: Milli ampère

M-cell: Midmyocardial cell

M1-2 segments: Transmembrane segments one and two of 2TM K^+ channels

M2 receptor: Muscarinic receptor

MD: Molecular dynamics

MDP: Maximum diastolic potential

mM: Millimol

MinK: Minimal potassium channel

MiRP1: MinK Related Peptide 1

mRNA: Messenger Ribonucleic acid

ms: Milliseconds

mS: Millisiemens

MthK: Calcium-gated K^+ channel from *Methanobacterium thermoautotrophicum*

mV: Milli volts

MW: Molecular weight

Na^+: Sodium

nA: Nano Ampère

NBF: Nucleotide binding fold

NCX: Na^+/Ca^{2+} exchanger

NDP: Nucleoside diphosphate

NO: Nitric oxide

NOS: Nitric oxide synthase

NSC: Non-selective cation channel

P-region: Channel region containing putative pore forming segment, synonym to H5 segment

P2X4: Purinergic ligand-gated receptor channel complex

PAEC: Porcine aortic endothelial cell

PAF: Platelet activating factor

PC: Purkinje cells

PCR: Polymerase Chain Reaction

PECAM-1: EC-specific antiplatelet-endothelial cell adhesion molecule 1

PGI_2: Prostacyclin

PIP_2: Phosphatidylinositol-4,5-bisphosphate

PIP_3: Phosphatidyl-3,4,5-trisphosphate

PKA: Phosphokinase A

PLC: Phospholipase C

PMSF: Phenylmethylsulphonylfluoride

PSD-95: Postsynaptic density protein of 95 kDa

PTX: Pertussis toxin

QRT-PCR: Quantitative real-time PCR

QTc interval: Corrected QT interval in the ECG

r-*eag*: Rat ether-à-go-go

RA: Right atrium

RACC: Receptor activated cation channel

Rb^+: Rubidium ion

RCK: Regulator of K^+-conductance

RIPA buffer: Modified radioimmunoprecipitation buffer

RGS (protein): Regulators of G-protein signalling (protein)

RMP: Resting membrane potential

RNA: Ribonucleic acid

RPE cells: Retinal pigmental epithelial cells

RT: Reverse Transcription

RT-PCR: Reverse transcriptase-polymerase chain reaction

RV: Right ventricle

S1-6 segment: Transmembrane segments 1-6 of 6TM K^+ channels

SAN: Sinoatrial node

S.E.M.: Standard error of the mean

Slo: Large conductance K^+ channel

SNr: Substantia nigra pars reticulata

SOC: Store operated channel

Sr^{2+}: Strontium ion

SUR: Sulfonylurea receptor

T1 domain: Amino terminal assembly domain

T1/2: Time for 50% of steady-state time-dependent block

TASK: Twik-related acid-sensitive K^+ channel

TdP: Torsade de pointes

TEA: Tetra ethyl ammonium

TFPI: Tissue factor pathway inhibitor

TM: Transmembrane segment

TMD: Transmembrane domain

TP: Testpotential

tPA: Tissue plasminogen activator

TREK: Twik-related K^+ channel

TRPC: Transient receptor potential channel

TRPM: Transient receptor potential channel of the melastatin family

TVGYG: K^+ channel key sequence

TWIK: Tandem of p domains in a weak inward rectifier K^+ channel

V: Ventricle

$V_{1/2}$: Voltage at which half maximal activation or inactivation occurs

VF: Ventricular fibrillation

Vmax: Maximum phase 0 upstroke slope of the action potential

VRAC: Volume regulated anion channel

VT: Ventricular tachycardia

vWF: von Willebrand factor

WT: Wild type

Acknowledgements

I would like to thank Dr. Stanley Nattel for his exceptional support during my time in his laboratory. I greatly appreciate his scientific excellence as well as his qualities as a human being. Without his help the achievement of many goals would have taken much longer if not been impossible.

Amongst the staff at the Montreal Heart Institute, I am particulary indebted to Dr. Bruce Allen, Dr. Zhiguo Wang and Dr. Terence Hebert, who have substantially contributed to my success in the laboratory. Dr. Bruce Allen has provided indispensable help for my experiments involving western blots of Cav1.2 channels. He has been of great help as the president of my PhD jury and his meticulous work on the manuscript helped to eliminate many mistakes. Dr. Wang has introduced me to molecular biology and the two-electrode voltage-clamp technique. His recording setup has always been available for me. Dr. Hebert has always been supportive in solving any kind of scientific problems, theoretical or practical.

Dr Lucie Parent has helped me tremdendously with scientific discussions regarding experiments on the structural determinants of Ba^{2+} block of Kir2.4 channels. Her participation in the committee of my pre-doctoral examination started my interest in structure-function related research which has never ceased since. Her thourough reading of the first manuscript of this thesis resulted in countless changes that have greatly contributed to improving its quality.

When I started my research activities in Dr. Nattel's laboratory, Nathalie Ethier and Dr. Manjula Weerapura guided me through the many pitfalls of molecular biology, the handling of *Xenopus* oocytes and the two-electrode voltage clamp technique. I will never forget their essential help in times when I needed it the most. In this context I would also like to thank Dr. Hans Rindt and Kathy Schreiber, who provided both professional and personal support in the beginning.

A very special thank you goes to Maya Mamarbachi. Maya has never hesitated to help me. She was always approachable when I had questions. Whenever I

ran out of reagents, she would lend them to me. She was always there to lend me a hand when the deadline for an experiment approached too quickly.

During my time in Dr. Nattel's laboratory, I saw many people come and go. Only few of them became friends. I would like to thank Dr. Marc Pourrier for his exceptional help during all these years, both professionally and in personal life. Working with him has always been a pleasure owing to his exceptional reliability and great sense of humour. His help with the French version of the abstract of the final version of the manuscript was indispensable. Dr. Stephen Zicha has spent considerable effort in helping me with western blot experiments. He provided substantial help in a project that unfortunately never matured to publication. Dr. Joachim Ehrlich spent many late nights with me in the laboratory, recording HERG and minK/KvLQT1 currents. He became a dear friend who unfortunately had to return to Germany after the completion of his research fellowship. Daniel Herrera shares my passion for structure-function relationships of K^+ channels. It is due to his efforts that my final project can be continued and has finally supplied us with exciting results. Dr. Ricardo Caballero did not spend a long time with us in Montreal. I would like to thank him for his friendship and scientific collaboration.

During the last five years I had the opportunity to collaborate with many people who I would like to thank for letting me participate in their projects as well as their contribution to mine. In particular, I wish to express my gratitude to Dr. Irena Levitan at the University of Pennsylvania and Yun Fang, University of Pennsylvania, for giving me the opportunity to collaborate on the molecular basis of inward rectifier currents in a biological system I would have otherwise not had access to.

No experiment can succeed without proper preparation. Chantal St Cyr has impressed me with her exceptional reliability and accuracy. Xiao Fan Yang spent many evenings helping me with the injection of *Xenopus* oocytes. Evelyn Landry would never leave the laboratory if there was one final request from any of us and prepared anything on the last minute. Chantal Maltais and Nathalie L'Heureux have always been helpful.

No article would have been published and no poster presented without the excellent work of France Thériault, Diane Campeau, Daniela Giuliani, Nadine Vespoli, Luce Bégin and the audiovisual department at the Montreal Heart Institute.

For financial support, I sincerely want to thank the Ernst and Berta Grimmke Foundation, Düsseldorf, Germany who first believed in me and granted me funding for my research work in Montreal. I also wish to thank the Canadian Institutes of Health Research (CIHR) and Aventis Pharma for fellowship support. During my research, I have received substantial financial support from the University of Montreal, which awarded me a differential scholarship waiver while I was not a permanent resident of Canada, a "bourse d'excellence" and two "bourse de redaction". I feel honoured to have been awarded these scholarships. At the University of Montreal, I would like to thank Dr Daniel Lajeunesse for giving rapid attention to any arising problems during the course of my thesis submission.

Due to considerable experimental delays of a project that was intended to be included in this thesis, writing had been significantly delayed and finally coincided with the beginning of my residency training in Internal Medicine. I would like to thank Dr Richard Gauthier, Dr Geneviève Grégoire, Dr Guy Lalonde, Madame Monelle Beaulieu, Madame Maryse Campion, Dr Sandra Bernardin, and Dr Douglas Fish for their support and flexibility needed to finish my PhD training.

Last not least, I would like to thank Lena Rivard for all her support and patience during the writing of this thesis and her help with the manuscript and the French version of the abstract. She has always been there for me, in happy times and in times of frustration.

I am sincerely grateful to my parents, who accepted my decision to engage in several more years of financial hardship without any objection. I could have never realized this project without their substantial moral and financial support.

Finally, I would like to thank my grandmother for her faith and for her love. This thesis is dedicated to her memory.

Contributions of authors

1- Schram G, Melnyk P, Pourrier M, Wang Z, Nattel S, Kir2.4 and Kir2.1 K^+ channel subunits co-assemble: A potential new contributor to inward rectifier current heterogeneity, *J Physiol*, 544 (Pt2): 337 – 349, 2002

I designed the project and techniques to generate the chimeric Kir2.1-2.4 construct and Kir2.4-FLAG. I performed most of the molecular biology experiments (generation of Kir2.1-2.4 concatemer, FLAG-tagging of Kir2.4 and creation of dn-Kir2.4). Techniques used include PCR, DNA cloning, mutation and amplification. For heterologous expression in *Xenopus* oocytes, techniques used were preparation of cRNA, isolation and preparation of *Xenopus* oocytes, cRNA injection and recording of heterologously expressed currents using the two-electrode voltage clamp technique. All electrophysiological experiments were performed exclusively by me. The manuscript of the article was written entirely by myself and revised with the help of Dr. Nattel, who contributed largely to the discussion.

2- Schram G, Pourrier M, Wang Z, Nattel S., Barium block of Kir2 and human cardiac inward rectifier currents: evidence for subunit-heteromeric contribution to native currents, *Cardiovascular Research*, 59: 328-338, 2003

I designed the study and performed all experimental work including molecular biology and electrophysiological experiments. Techniques used for oocyte experiments include DNA handling (DNA amplification using *E.* coli, restriction enzyme digestions etc.), generation of cRNA, isolation and preparation of *Xenopus* oocytes and cRNA injection as well as two-electrode voltage clamp experiments. For patch clamp experiments, human tissue was obtained by right ventricular biopsy and single myocytes were prepared using standard enzyme digestion protocols. Currents were recorded using the patch clamp technique. I performed all statistical analysis, wrote the manuscript and prepared all figures.

3- Fang Y., **Schram G.**, Romanenko V., Shi C., Conti, L., Vandenberg CA., Peter F. Davies PF., Nattel S., Levitan I., Functional expression of Kir2.x in human aortic endothelial cells: the dominant role of Kir2.2, *Am J Physiol Cell Physiol.* 289: C1134-1144, 2005

I was approached by Dr Levitan who asked me to collaborate with her team on a project evaluating the molecular composition of native inward rectifier K^+-currents in human aortic endothelial cells (HAECs). I agreed and participated in the development of the experimental approach together with Dr. Levitan, Yun Fang (the first author) and Dr. Nattel. Based on our experience with dominant negative (dn-) Kir2 subunits (Schram *et al.*, 2002a) and the previous demonstration that these constructs provide a helpful tool to evaluate the role of Kir2 subunits in native Kir current (Zobel *et al.*, 2003) we decided to use a dominant negative approach to determine the functional role of various Kir2 subunits in native HAEC Kir current. I generated dn-Kir2.2, dn-Kir2.3 and dn-Kir2.4 constructs and subcloned dn-Kir2.1-4 from their respective cloning vectors into the bicistronic mammalian cell expression vector pIRES. Techniques used include PCR, DNA cloning, site directed mutagenesis and DNA amplification. To test the functionality of these dominant negative constructs, I co-expressed them with their respective Kir2.x-WT channels in *Xenopus* oocytes. Techniques applied include cRNA preparation, isolation of *Xenopus* oocytes, cRNA injection and the two-electrode voltage-clamp technique. I analyzed all the data obtained in the oocyte experiments and prepared the figure for our publication.

During the course of the project, I participated in the review of data obtained. At the writing stage, I co-wrote sections of the manuscript and participated in its corrections. During the revision process, I performed additional experiments (dn-Kir2.x/Kir2.x-WT co-expression), wrote additional sections of the manuscript, added one figure and revised the manuscript.

The dominant negative approach, which was designed by me, was recognized by the reviewers as one of two key experiments in our project to demonstrate the main objective of this article. Due to my extensive contribution to the project, both Dr. Levitan and Yun Fang, the first author, offered me the second author position.

Related studies not included in this thesis

Substantial effort had been invested in a publication reviewing the "Differential distribution of cardiac ion channel expression as a basis for regional specialization in electrical function" (Schram *et al.*, 2002b) which due to its nature can not be included in this thesis. This article has therefore been integrated in the introduction to the extent possible.

Due to its thematic restriction, the data presented in this thesis unfortunately under-represents the work done over the course of my PhD. For that reason I would like to mention that at the time of writing I have published four peer reviewed articles in which I am the first author (Schram *et al.*, 2002a; Schram *et al.*, 2002b; Schram *et al.*, 2003; Schram *et al.*, 2004) and one non-peer reviewed article, three articles in which I am the second author (Fang *et al.*, 2005; Shiroshita-Takeshita *et al.*, 2004; Pourrier *et al.*, 2003a) (one of which is presented in this thesis) and one article in which I am the last author (Nattel *et al.*, 2001). Important contributions to the work of co-workers in our laboratory resulted in five co-authorship publications (Wang *et al.*, 2001; Han *et al.*, 2002; Shinagawa *et al.*, 2003; Caballero *et al.*, 2003; Pourrier *et al.*, 2004). A last first authorship project examining structural determinants of voltage-dependence and sensitivity of Ba^{2+} block of Kir2.1 and Kir2.4 channels delayed the writing of this thesis and finally could not be completed in time due to recurring technical difficulties. This project is now close to publication. Preliminary data has been published in abstract form (Schram *et al.*, 2005; Herrera *et al.* 2005; Herrea *et al.* 2006) and presented at the Annual Meeting of the Biophysical Society in Long Beach, California, 2005, the Meeting of the Canadian Cardiological Association in Montreal, 2005 and the Annual Meeting of the Biophysical Society in Salt Lake City, Utah, 2006. Presentations at scientific reunions of the University of Montreal were awarded prizes.

For my grandmother

For my parents

For Lena

PART ONE:

INTRODUCTION AND REVIEW OF THE LITERATURE

CHAPTER I: INTRODUCTION TO CELLULAR ELECTROPHYSIOLOGY

Practically every process in the living being depends on electrical signalling. Charged particles, ions, cross the cell membrane through highly specialized transmembraneous passages, so called ion channels. At the end of the 18th century, Sidney Ringer demonstrated that a frog heart needs to be perfused with a solution containing potassium, sodium and calcium ions in a certain stoichiometry in order to keep on beating. A decade later, the "membrane breakdown" hypothesis of Julius Bernstein (Bernstein, 1902; Bernstein, 1912) suggested that the negative resting membrane potential of nerve and muscle cells is determined by a membrane selectively permeable to potassium (K^+) ions. During excitation, positively charged ions would move into the cell owing to their higher concentration in the extracellular solution than in the cytoplasm, causing a transient loss of the negative resting membrane potential. 1952, Hodgkin and Huxley showed that membrane currents in the giant squid axon were dependent upon membrane permeability changes to Na^+ and K^+ in a time and voltage dependent manner, implying a feedback mechanism between membrane voltage and transmembraneous ion movement (Hodgkin & Huxley, 1952). Thus, ion channels control the membrane potential and in return their state, open or closed, is controlled by the membrane potential.

During the twentieth century, many cellular roles were discovered for various anions and cations. It is now firmly established that electrical signalling of nerve and muscle cells depends on the transmembraneous movement of Na^+, K^+, Ca^{2+} and Cl^- ions through highly specialized ion channels. Complex interactions between inward and outward ionic currents result in transient membrane depolarization and subsequent repolarization. The ensemble of these changes in membrane potential is called action potential (AP) and represents the means by which excitable cells transfer information over large distances in short time intervals. A variety of non-excitable cells including blood cells, cells of the immune system, osteoblasts, fibroblasts and vascular endothelial cells, depend on the proper functioning of ion channels in cell signalling. In vascular endothelial cells (ECs), a complex interplay between many different types of ion channels regulates intracellular Ca^{2+} levels, which is crucial to many physiological functions of ECs (Nilius & Droogmans,

2001). However, current knowledge of the precise role of ion channels in various tissues is still very limited.

Potassium channels play a key role in regulation of cellular excitability. K^+ channels conduct K^+ ions across the cell membrane down their electrochemical gradient achieving flow rates of 10^8 ions per second while still maintaining perfect fidelity for K^+ (MacKinnon, 2003). Their function is essential for the regular automatic beating of the heart, proper functioning of the nervous system, memory and mood, secretion of hormones and enzymes and many other important physiological functions. K^+ channels set the resting membrane potential, keep fast action potentials short, terminate periods of intense activity, time the interspike intervals during repetitive firing, and generally lower the effectiveness of excitatory inputs to a cell when open (Hille, 2001). Potassium channels are targets of many antiarrhythmic drugs and are responsible for the pro-arrhythmic actions of various antiarrhythmic and non-cardiac drugs (Mitcheson *et al.*, 2000). In the heart, regional and transmural differences in K^+ channel expression and density contributes to regional specialization in electrical function (Schram *et al.*, 2002b). Malfunctions of ion channels have been implicated in the pathogenesis of a growing number of diseases termed "channelopathies" (Abraham *et al.*, 1999; Marban, 2002; Kullmann, 2002). Dysfunctions of K^+- channels underlie diseases of the brain such as epilepsy and episodic ataxia. In the heart, K^+- channel dysfunction is the cause of various forms of the genetic and acquired long QT syndrome (LQT1, LQT2, LQT5-7) (Splawski *et al.*, 2000; Plaster *et al.*, 2001) inducing potentially lethal cardiac arrhythmias. In Andersen's syndrome, dysfunction of inward rectifier K^+ channels is associated with cardiac arrhythmias, periodic paralysis and dysmorphic bone features (Plaster *et al.*, 2001). K^+ channel dysfunction in the ear, the kidney, muscles and the pancreas is associated with deafness, hypertension, myokymia and periodic paralysis and hyperinsulinaemic hypoinsulinemia, respectively (Shieh *et al.*, 2000; Bichet *et al.*, 2003).

A great variety of K^+ currents has been discovered in various tissues and species. Pharmacological and biophysical properties of these currents have been studied with the help of the patch-clamp technique. However, such properties could

only be explained on assumptions, since the molecular basis of these currents was unclear. Additionally, the presence of overlapping ionic currents made the characterization of specific K^+ currents difficult. Application of channel blocking compounds, specific ionic constituents of recording solutions and distinct recording protocols were used to minimize potential confounding factors. Nevertheless, it could not be excluded that such procedures also changed the properties of the current under investigation.

In 1987, the first voltage-gated K^+ channel subunit was cloned from the shaker locus of *Drosophila* melanogaster (Tempel *et al.*, 1987; Kamb *et al.*, 1987; Pongs *et al.*, 1988) and characterized in *Xenopus* oocytes (Timpe *et al.*, 1988). One year later, three more genes encoding subunits of voltage-gated K^+ channels were cloned and designated Shab, Shaw and Shal (Butler *et al.*, 1989). The following years saw an almost exponential discovery of new potassium channel clones and regulatory (beta-) subunits. In 1998, Roderick MacKinnon presented the crystal structure of a voltage gated K^+ channel from *Streptomyces lividans*, KcsA, allowing important insight into the structure-function relationship of K^+ channels at the atomic level (Doyle *et al.*, 1998). A series of publications following the crystallization of KcsA explained the structural basis of K^+ selectivity, ion conductance, channel inactivation and mechanisms of pharmacological channel blockade on the atomic level (Morais-Cabral *et al.*, 2001; Zhou *et al.*, 2001b; Zhou *et al.*, 2001a; Roux & MacKinnon, 1999). Whereas KcsA showed a K^+ channel in the closed state, the crystallization of MthK from *Methanobacterium thermoautotrophicum* captured a potassium channel in its open state and allowed important insight into basic mechanisms underlying channel opening and closure (Jiang *et al.*, 2002b; Jiang *et al.*, 2002c). The crystallization study of the cytoplasmic pore of Kir3.1 (Nishida & MacKinnon, 2002), the entire eukaryotic inward rectifier KirBac (Kuo *et al.*, 2003) and finally the cytoplasmic region of Kir2.1 (Pegan *et al.*, 2005) illustrated the structural basis of inward rectification. Most recently, the crystal structure of the voltage gated shaker channel Kv1.2 (Long *et al.*, 2005a) and its S4 voltage sensor (Long *et al.*, 2005b) clarified the local environment of the voltage-sensor, its relation to the ion-conducting pore and coupling of voltage-sensing and channel gating. Computational studies such as

molecular dynamics simulations provided insight to gating movements on a nanosecond timescale (Sansom *et al.*, 2002; Roux, 2005).

The first part of this thesis introduces the basics of electrogenesis in different biological systems, focusing on the central nervous system, the heart and vascular endothelial cells. A detailed section on the current knowledge of K^+ channel structure and the structural basis of their functioning is followed by a section on voltage-gated and inward rectifier K^+ channels. This part details the molecular basis, biophysical and pharmacological properties as well as the functional role of major K^+-currents in different organ systems.

The second part of this thesis consists of original publications. The common theme of the articles presented here is the contribution of distinct Kir2 subunits in homo- or heteromeric assembly to native inward rectifier K^+-current in different tissues.

The third part states the major novel scientific contributions presented in this thesis and discusses their scientific significance and potential limitations in the context of current literature as well as potential future directions.

I-1 The Action Potential in Neurons

Action potentials (APs) are pulse-like electrical messages that are rapidly propagated along a specific conduction system. Historically, APs and their underlying ionic mechanisms were first investigated in the squid giant axon (Figure 1). Axonal APs are very short, lasting only a few milliseconds, and propagate electrically in an all-or-none like fashion. APs encode time and frequency but not amplitude or duration of a signal. Axonal APs depend practically solely on K^+ and Na^+ conductances. At rest, the membrane potential of the axon is negative with typical values between -40 and -95 mV (Hille, 2001). When an electrical stimulus such as an AP reaches the membrane, it depolarizes. Na^+ channels open and Na^+ ions rush into the cell, further depolarizing the membrane until the membrane potential reaches values above 0 mV, an event termed "overshoot". Na^+ channels subsequently inactivate and delayed rectifier K^+ channels activate to conduct K^+ ions out of the cell causing the membrane potential to return to its previous negative value. The transient overshoot depolarizes the next stretch of cell membrane and so the AP travels along the axon to reach its effector site.

Larger axons differ from smaller axons in that they are covered by myelin, an electrically insulating layer of glial cells (Schwann cells). The myelin sheath is interrupted by the so-called "nodes of Ranvier", axonal sections where there is no myelin sheath and the density of Na^+ and K^+ channels is higher than in unmyelinated axons (Hille, 2001). In myelinated axons, ionic current can only flow at these interruptions. This causes the axonal AP to jumps from node to node, thereby boosting the signal and speeding up its rate of transmission.

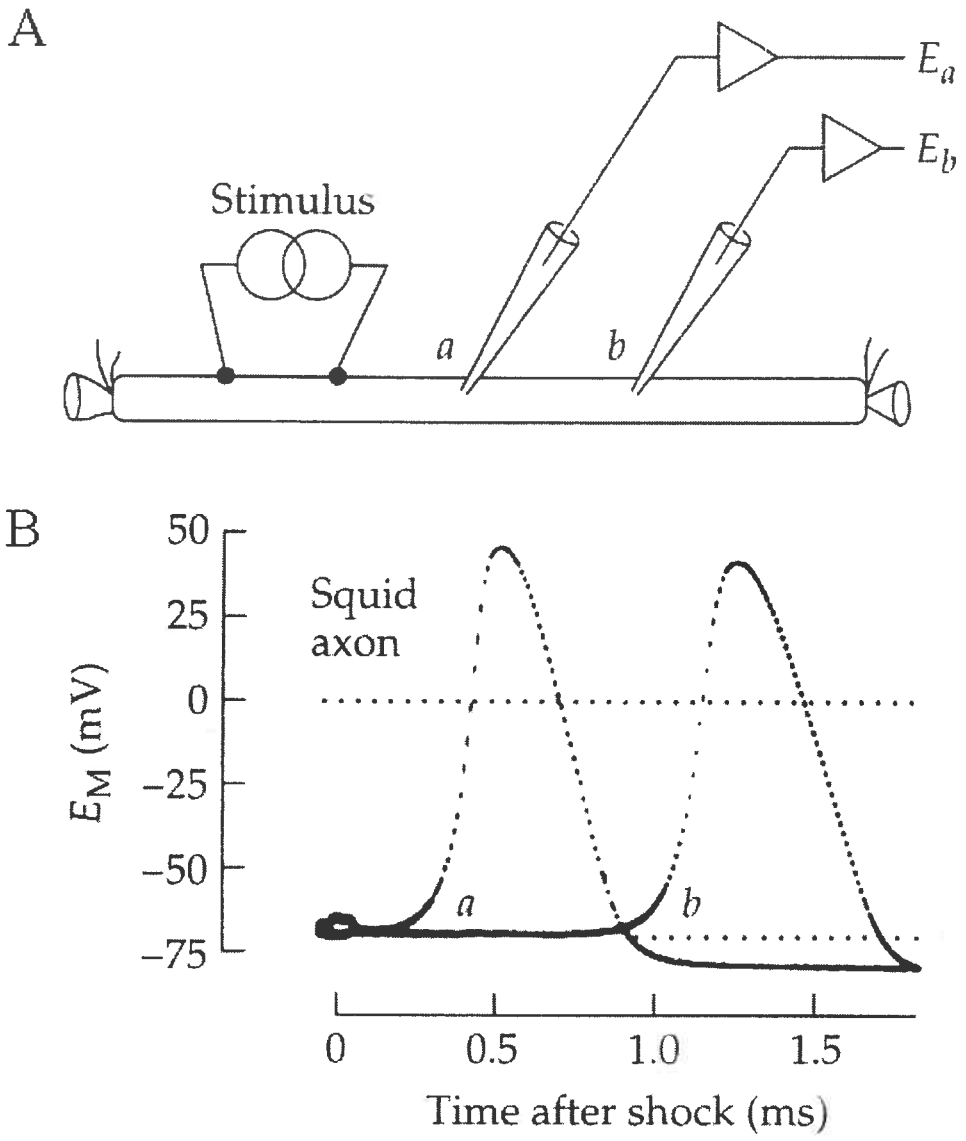

Figure 1: Schematic diagram of action potential recordings from the squid giant axon.

A. Schematic diagram of squid axon with stimulator and two recording microelectrodes *a* and *b*.

B. Action potential measured by electrodes *a* and *b*. Adapted from Del Castillo & Moore (1959) in Hille (2001).

Figure 2A illustrates current recorded from a squid axon after depolarization from a negative holding potential to a test potential of 0 mV. Upon depolarization, a large transient inward current is seen that reverses to a large maintained outward current. Figure 2B shows time course of Na^+ and K^+ conductances (g_{Na} and g_K) during a depolarizing voltage step from a holding potential of -65 mV to a test potential of -9 mV. Conductances were calculated using the Hodgkin & Huxley formula defining ionic conductances:

$$g_{Na} = \frac{I_{Na}}{E - E_{Na}}$$

$$g_K = \frac{I_K}{E - E_K}$$

As shown in Figure 2B, middle panel, the sodium conductance increases rapidly and decreases slowly after membrane depolarization, indicating that the transient inward current shown in Figure 2A is a Na^+ current that activates upon depolarization and subsequently inactivates. The slowly activating and non-inactivating outward current shown in Figure 2A corresponds to a K^+ current, as can be seen in Figure 2B, lower panel. Figure 2A shows an original current recording whereas Figure 2B displays calculated conductances under conditions different from those of the experiment shown in A. The purpose of panel B is not to show actual components of the current shown in panel A but simply to illustrate how the two different ionic components contribute to the native current. Therefore, the time course of currents shown in panels A and B is different.

A.

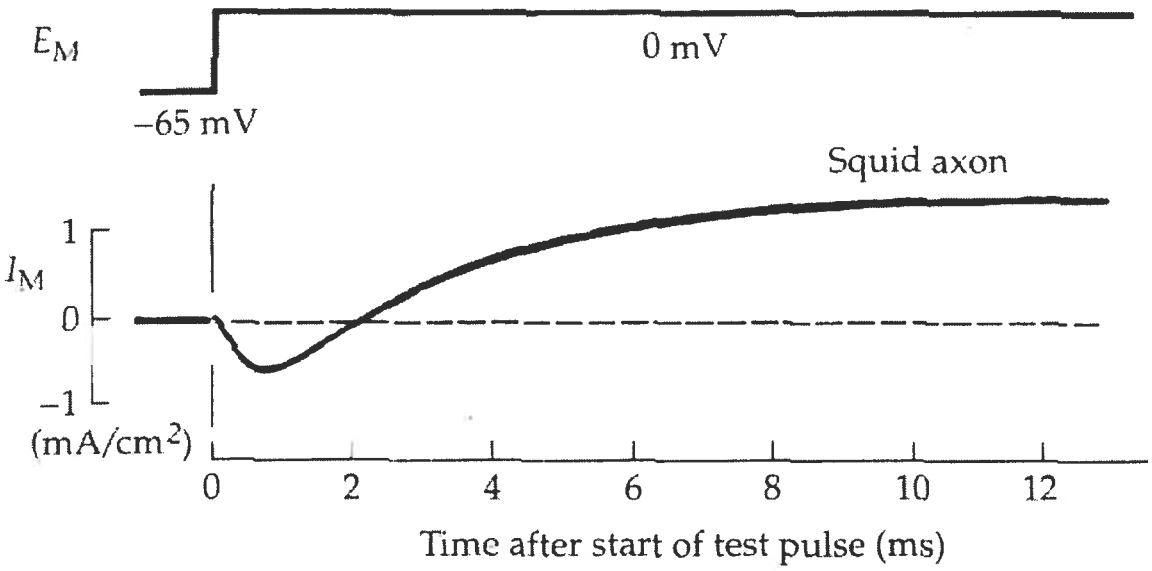
E_M
0 mV
−65 mV
Squid axon
I_M
1
0
−1
(mA/cm²)
0
2
4
6
8
10
12
Time after start of test pulse (ms)

B.

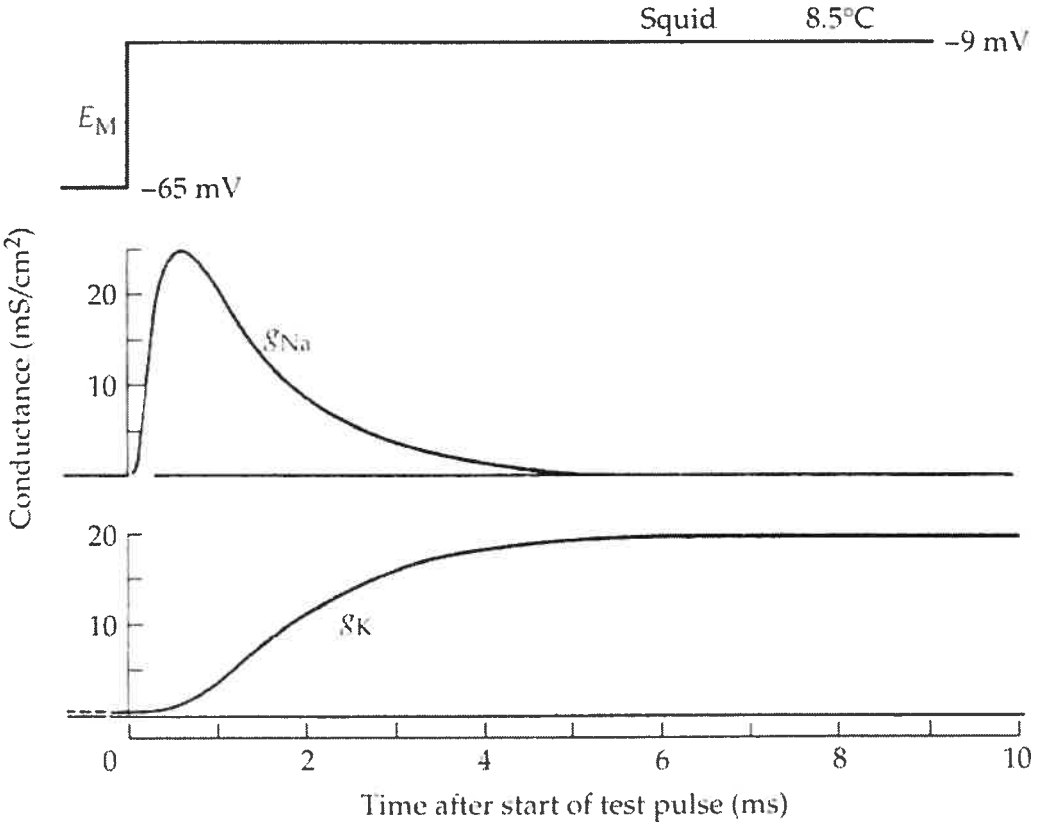
Squid
8.5°C
−9 mV
E_M
−65 mV
Conductance (mS/cm²)
20
10
g_{Na}
20
10
g_K
0
2
4
6
8
10
Time after start of test pulse (ms)

Figure 2: Action potential of the squid axon and underlying ionic conductances.

A. Depolarization of the squid axon from a holding potential from -65 mV to a test potential of 0 mV at 3.8°C elicits a large, biphasic current. Adapted from Hille (2001).

B. Calculated time course of Na^+ and K^+ conductances in the squid axon during membrane depolarization from -65 mV to -9 mV at a temperature of 8.5°C. Adapted from Hodgkin (1958) in Hille (2001).

I-2 The Cardiac Action Potential

The cardiac AP originates in the sinoatrial node (SAN). Propagation through the atria causes atrial contraction. The AP traverses the atrioventricular node (AVN) and then travels through the HIS-Purkinje system to reach the ventricles, where it triggers the contraction of ventricular muscle cells. In order to ensure appropriate timing of cardiac contraction, cardiac action potentials vary between different cardiac regions reflecting an adaptation to its specific function. Figure 3 illustrates cardiac APs recorded from different cardiac regions.

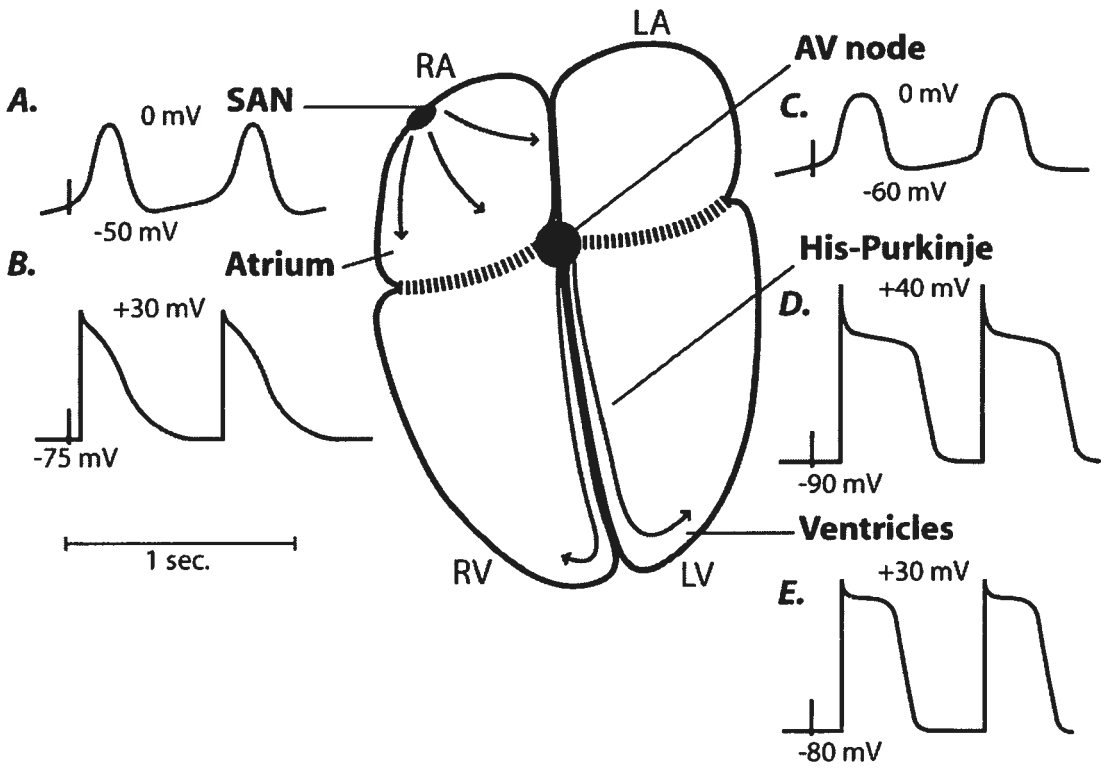

Figure 3: Schematic diagram of AP properties in different regions of the heart. Adapted from Schram *et al.* (2002b).

In contrast to axonal APs, the cardiac action potential is determined by a complex interplay between multiple depolarizing inward and repolarizing outward currents. A hallmark property is its long duration. Whereas the action potential of neurons lasts only a few milliseconds, the cardiac action potential can last up to several hundred milliseconds.

Figure 4 illustrates relative current contribution to representative atrial and ventricular action potentials. Per definition, upward deflections denote outward currents and downward deflections inward currents. Native ionic current will be discussed in detail in chapter two. Five phases of the cardiac action potential can be distinguished. Phase 0 is the initial upstroke during membrane depolarization, mainly due to inward Na^+ current. Following the rapid upstroke, the transient outward potassium current, I_{to}, shifts the membrane potential to a more negative potential (phase 1) at which depolarizing, inward L-type ($I_{Ca,L}$) and T-type ($I_{Ca,T}$) calcium currents activate, initiating phase two, which is also referred to as the plateau phase. At the same time, the repolarizing K^+ currents I_{Kur} (ultrarapid delayed rectifier potassium current) and I_{KACh} (acetylcholine activated potassium current) conduct potassium out of the cell. It has to be noted that ion channel RNA and protein expression differs between species and currents described here may not be expressed in all tissues. Outward delayed rectifier currents activate in late phase 2 and are active throughout the late phase 3 until the membrane has reached its negative resting potential. I_{K1} is the main K^+-conductance in diastolic phase 4. It becomes active in late phase 3 where its outward component contributes to phase 3 repolarization (see also Figure 20). During phase 4, I_{K1} is the main current governing the resting membrane potential. Spontaneous diastolic depolarization in pacemaker cells during phase 4 is mainly carried by the depolarizing inward pacemaker current I_f, conducted by Na^+ and K^+ ions, but in certain tissues also by the K^+ current I_{KACh} and the outward component of the inward rectifier current I_{K1}. As indicated in the upper two panels of Figure 4, atrial APs have faster initial repolarization, less positive plateau potentials, a shorter plateau phase and slower phase 3 repolarization.

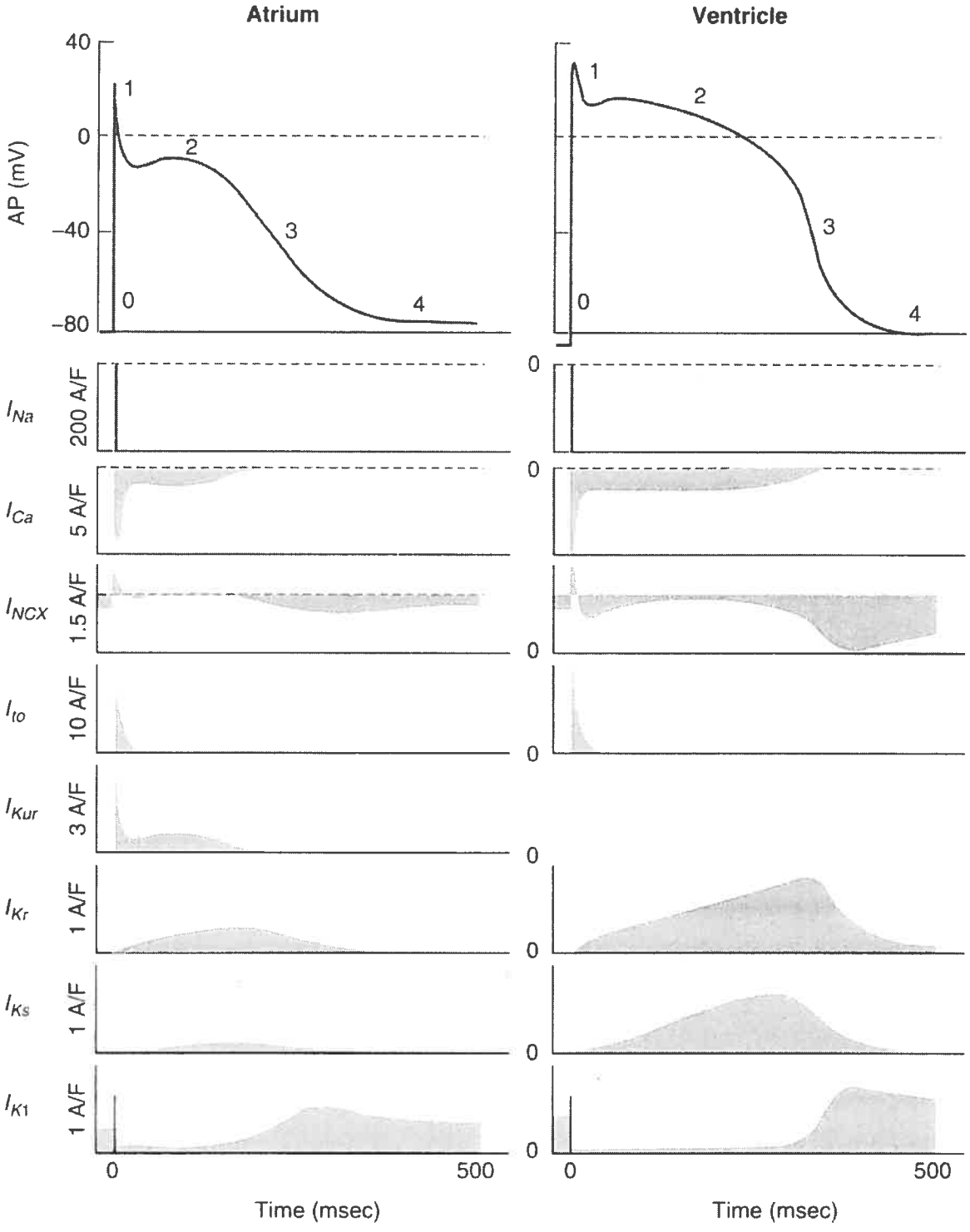
Atrium
Ventricle
AP (mV)
40
0
−40
−80
1
2
3
0
4
I_{Na}
200 A/F
I_{Ca}
5 A/F
I_{NCX}
1.5 A/F
I_{to}
10 A/F
I_{Kur}
3 A/F
I_{Kr}
1 A/F
I_{Ks}
1 A/F
I_{K1}
1 A/F
0
500
Time (msec)

Figure 4: Representative cardiac action potential waveforms.

Top panels show APs obtained from atrial (left) and ventricular (right) myocytes. The five phases of the AP are labelled. The rate of change of the AP is directly proportional to the sum of the underlying transmembraneous ion currents (lower panels). Inward currents depolarize the membrane, whereas outward currents contribute to repolarization. Compared with an atrial AP, the ventricular AP typically has a longer duration, higher plateau potential (phase 2), and a more negative resting membrane potential (phase 4). The presence of an ultra-rapid delayed rectifier potassium (K^+) current (I_{Kur}) in atrial myocytes contributes to the lower plateau phase in the atrial AP. Greater inward rectifier K^+ current (I_{K1}) in ventricular cells provides a faster phase 3 repolarization and a more negative resting membrane potential (phase 4). Adapted from Oudit *et al.* (2004).

The sinoatrial node is the primary pacemaker of the heart. Sinoatrial APs have a relatively positive maximum diastolic potential (MDP) of ~ 50 mV, a small phase 0 upstroke velocity (V_{max}, < 2 V/s) (Bleeker *et al.*, 1980) and prominent phase 4 depolarization to ensure SAN pacemaker predominance over distally located cardiac regions (Schram *et al.*, 2002b). Electrical coupling of the SAN to the atrium is complex and is designed to drive the large atrial muscle mass while protecting the SAN from hyperpolarizing atrial stimuli (Coppen *et al.*, 1999).

Isolated atrial myocytes have a MDP of around -70 mV (Yue *et al.*, 1997; Li *et al.*, 2001), slower phase 3 repolarization and almost no spontaneous depolarization (Schram *et al.*, 2002b). Spatial heterogeneity of atrial APs and APD within and between the atria (Hogan & Davis, 1968; Spach *et al.*, 1989; Feng *et al.*, 1998; Fareh *et al.*, 1998) plays an important role in atrial re-entrant arrhythmias, mostly due to shorter APD and ERP in the LA free wall than in the RA (Li *et al.*, 2001). Rapid AP conduction follows muscle fibre orientation (Spach, 1995) to the AV node.

APs from intact AVN have a MDP of approximately -64 mV, small amplitudes and slow phase 0 upstrokes (Hoffman *et al.*, 1959). AVN cells have low excitability and postrepolarization responsiveness (Merideth *et al.*, 1968) and display pacemaking activity (Munk *et al.*, 1996; Watanabe & Dreifus, 1968). Phase 4 depolarization results in takeoff potentials of at -60 mV, and V_{max} is <20 V/s (Billette, 1987). However, atrial electrotonic influences suppress spontaneous activity in AVN cells (Kirchhof *et al.*, 1988).

The His-Purkinje system directs the AP to the ventricles. Hence, Purkinje cells (PC) are specialized for rapid conduction. MDPs of PCs are very negative at around -90 mV and V_{max} is high (~400-800 V/s) (Davis & Temte, 1969; Kus & Sasyniuk, 1975; Carmeliet, 1977; Nattel & Quantz, 1988). APD is relatively long at slow rates (Carmeliet, 1977; Nattel & Quantz, 1988) and there is prominent spontaneous phase 4 depolarization (Callewaert *et al.*, 1984). PCs can generate drug-induced early afterdepolarizations (EADs) that trigger torsade de pointes arrhythmias (El Sherif *et al.*, 1996; Asano *et al.*, 1997).

Ventricular myocytes have a MDP of -85 mV and a relatively positive plateau of about +10 to 20 mV. Phase 3 repolarization is rapid. Similarly to atrial muscle cells, there is no significant phase 4 depolarization (Davis & Temte, 1969; Kus & Sasyniuk, 1975; Litovsky & Antzelevitch, 1989). Prominent regional and transmural heterogeneity of ventricular APs is well established. In rat ventricle, APD is shortest at the apex and longest in the septum (Gomez *et al.*, 1997). In canine ventricular myocardium, APs recorded from epicardium have a smaller overshoot, a more prominent phase 1 followed by a notch ("spike and dome") and a briefer APD than endocardial cells, resulting in the T-wave in the ECG. MDP and V_{max}, however, are similar in cells from both regions (Litovsky & Antzelevitch, 1988). A distinct cell population has been found in the midmyocardium and designated M-cells (Sicouri & Antzelevitch, 1991; Drouin *et al.*, 1995). M-cell APDs increase at slow heart rates and have a larger V_{max} (~300 V/s) than endo- or epicardial cells (Sicouri & Antzelevitch, 1991). RV M-cell APs have a smaller upstroke, a deeper notch and a shorter duration than LV M-cell APs (Volders *et al.*, 1999). Transmural APD heterogeneity has been implicated in the generation of torsade de pointes ventricular arrhythmias (Antzelevitch & Sicouri, 1994), especially under conditions that cause prolongation of APD such as APD prolonging drugs, hypokalemia or slow heart rates (Sicouri & Antzelevitch, 1993). Figure 5 compares action potentials of ventricular epicardium, midmyocardium and endocardium.

Region	MDP (mV)	V_{max} (V/s)	Phase 3 repolarization	Phase 4 depolarization
SAN	-50	< 2		rapid
Atrium	-70	150-300	slow	no
AVN	-64	< 20		yes
PC	-90	400-800		yes
Ventricle	-85	200-300	rapid	no

Table I: Actionpotential characteristics in different cardiac regions.

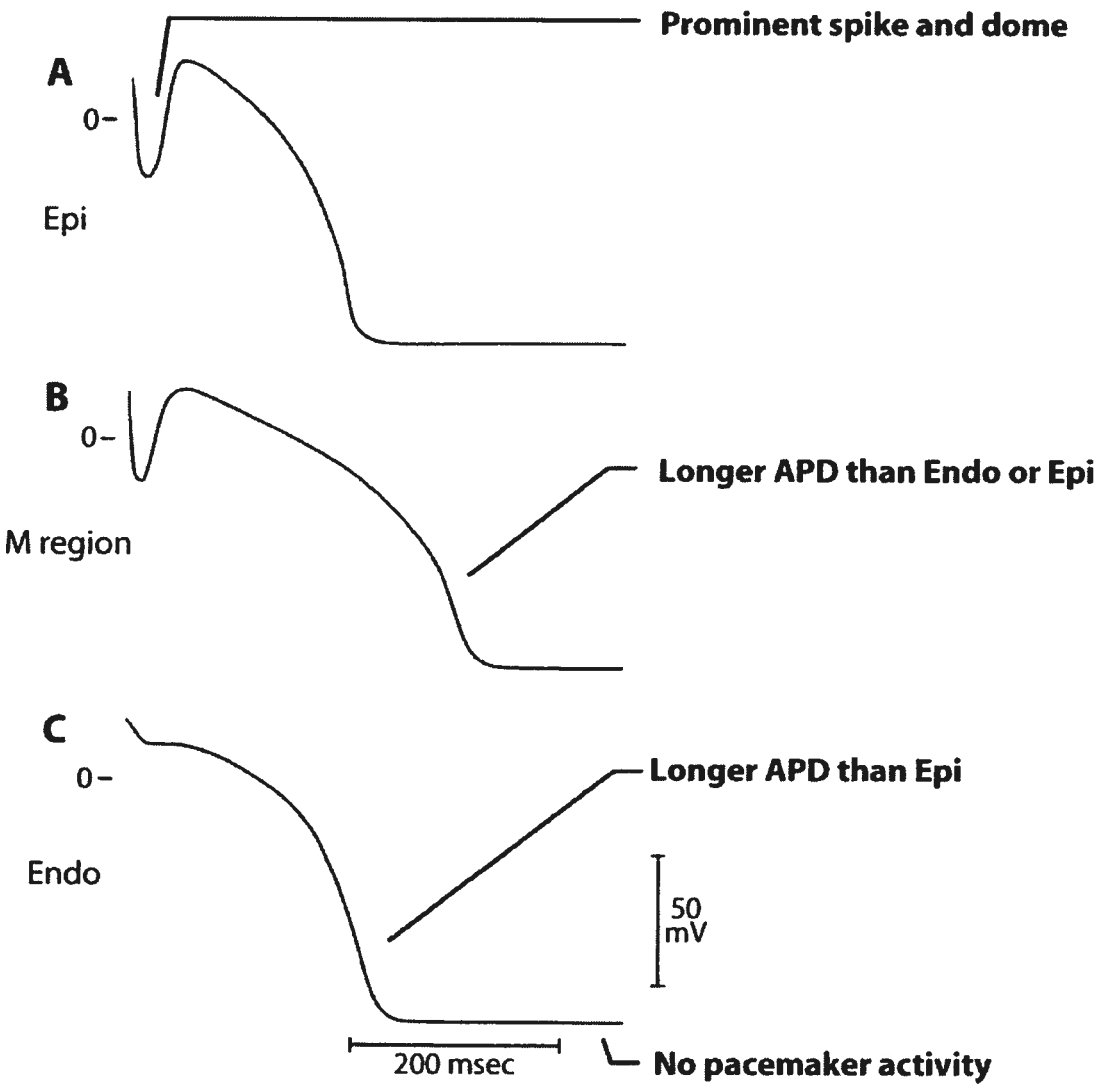

Figure 5: AP properties of canine ventricular epicardium, midmyocardium and endocardium.

A: Epicardium (Epi), **B:** midmyocardium (M region), **C:** Endocardium (Endo). Adapted from Schram *et al.* (2002c). APs are reproduced from Sicouri & Antzelevitch, 1991.

I-3 Electrogenesis in Vascular Endothelial Cells

The mechanisms of electrical signalling in non-excitable cells, such as vascular endothelial cells (ECs) are less understood. A multitude of different ion channels is found in endothelial cells, many of which have not been well characterised and whose molecular basis is yet unknown (Nilius *et al.*, 1997; Nilius & Droogmans, 2001).

Endothelial cells provide the pathway for oxygen delivery from blood to tissue. Control of permeability to metabolites, macromolecules and gas exchange are crucial for the proper functioning of cell metabolism (Born *et al.*, 1998). Modulation of vascular tone regulates blood pressure (Cannon, 1998). Endothelial cells are involved in control of blood coagulation, wound healing and angiogenesis (Shimokawa & Takeshita, 1995; Luscher, 1994; Born *et al.*, 1998). In cardiovascular disease, the endothelium plays a key role in vascular pathology and as a target for pharmacotherapy (Angus, 1996; Garcia-Palmieri, 1997; Born & Schwartz, 1997; Tan *et al.*, 2004; Deedwania, 2000). Endothelial cell functions depend on both constitutive EC properties and on active responses ("on demand") of ECs to chemical, mechanical or neuronal stimuli originating from the blood, tissue and coupling to neighboring ECs or adhering blood cells. Responses such as the release of vasoactive substances by the endothelium depend upon fluctuations in their membrane potential and in the intracellular Ca^{2+} concentration. Hyperpolarization of the membrane potential provides the main driving force for entry of extracellular Ca^{2+} (Nilius *et al.*, 1997; Nilius & Droogmans, 2001). The role of ion channels in the transduction of these signals is still controversial but it appears that they are involved in short-term EC responses in the range of seconds to minutes. Roles of ion channels have been determined for release of pro- and anticoagulants, growth factors, and regulators of vasotonus such as nitric oxide (NO), prostacyclin (PGI_2), platelet activating factor (PAF), endothelium-derived hyperpolarizing factor (EDHF), release of von Willebrand factor (vWF), tissue plasminogen activator (tPA), the anticoagulant tissue factor pathway inhibitor (TFPI) and protein S (Nilius & Droogmans, 2001). Ion channels are involved in regulation of vascular permeability and angiogenesis.

The resting membrane potential of ECs is negative when compared to blood cells and tissue compartments. However, RMPs vary considerably between tissues and conditions of cell isolation and culturing and values between 0 and -80 mV having been reported (Takeda *et al.*, 1987; Daut *et al.*, 1994; Nilius *et al.*, 1997; Yamamoto *et al.*, 1992; Zunkler *et al.*, 1995; Jow *et al.*, 1999; Hogg *et al.*, 1999). Non-selective cation channels, cyclic nucleotide-gated channels (CNG), hyperpolarization activated cyclic nucleotide-gated channels (HCN), K^+, Na^+, Cl^- and the Na^+ -K^+ -ATPase contribute to the negative RMP, with K^+ channels being the most important conductors in most tissues (Oike *et al.*, 1993; Seiss-Geuder *et al.*, 1992; Himmel *et al.*, 1993; Marchenko & Sage, 1994; Nilius *et al.*, 1997; Vargas *et al.*, 1994; Voets *et al.*, 1996; Nilius & Droogmans, 2001). Functional studies demonstrate that inhibition of K^+ channels by pharmacological blockade or depolarized membrane potentials results in inhibition of bradykinin-, acetylcholine- and flow-induced Ca^{2+}-influx and NO release as well as flow-induced vasodilation (Kwan *et al.*, 2003; Luckhoff & Busse, 1990; Wellman & Bevan, 1995). A bimodal distribution of RMPs has been found in several endothelial cell types. ECs mainly expressing inward rectifier K^+- (Kir-) channels have RMPs between -60 to -70 mV whereas cells with predominant chloride conductances have RMPs between -10 to -40 mV (Nilius & Droogmans, 2001).

The most important functional task of ion channels in ECs is regulation of intracellular Ca^{2+} (Nilius & Droogmans, 2001). Hormones or growth factors bind to their receptor which subsequently activates phospholipase C (PLC). PLC in turn converts phosphatidylinositol-4,5-bisphosphate (PIP_2) into inositol-1,4,5-trisphosphate (IP_3) and 1,2-diacylglycerol (DAG). These activate plasma membrane channels including transient receptor potential channels (TRPC) and extracellular Ca^{2+} enters into the cell (Freichel *et al.*, 2005). The degree of filling of intracellular Ca^{2+} stores modulates Ca^{2+} influx through a group of ion channel referred to as store-operated channels (SOC) and Capacitative Ca^{2+} entry (CCE).

The Ca^{2+} release activated Ca^{2+} channel CRAC (Mendelowitz *et al.*, 1992) is the major store-operated channel but other channels have been described (Luckhoff & Clapham, 1992; Vaca & Kunze, 1995). Store-operated channels are believed to

represent a major pathway for Ca^{2+} entry during agonist stimulation (Nilius & Droogmans, 2001). Charged stores prevent and discharged stores promote Ca^{2+} entry (Parekh & Penner, 1997).

Changes of intracellular Ca^{2+} concentration through uptake of extracellular Ca^{2+} into depleted intracellular Ca^{2+} stores are referred to as Capacitative Ca^{2+} Entry (CCE) (Nilius & Droogmans, 2001). CCE depends on various mechanisms including Ca^{2+} sequestration and buffering and is modulated by the plasma membrane Ca^{2+} pump (Klishin *et al.*, 1998), the Na^{+}/Ca^{2+} exchanger (Domotor *et al.*, 1999; Graier *et al.*, 1998; Paltauf-Doburzynska *et al.*, 1998) and changes in membrane potential (Nilius & Droogmans, 2001). Other potential Ca^{2+} entry channels are non-selective cation channels (NSC), including receptor-activated cation channels (RACCs), purinergic ligand-gated (P2X4-) receptor channel complexes, amiloride-sensitive NSCs, redox state-regulated NSCs regulated, and mechanosensitive channels (Nilius & Droogmans, 2001). When intracellular Ca^{2+} reaches a maximum level, non-selective cation channels activate. Possible candidates underlying this functions are the transient receptor potential channel (TRPC) related proteins TRPM4 and TRPM5, which allow Na^{+} entry into the cell, thereby causing membrane depolarization which in turn activates voltage-gated Ca^{2+} channels (Bkaily *et al.*, 1993; Bossu *et al.*, 1992a; Bossu *et al.*, 1992b; Bossu *et al.*, 1989; Vinet & Vargas, 1999) further increasing the intracellular Ca^{2+} concentration (Freichel *et al.*, 2005). Data supporting this signalling cascade has been obtained in T-lymphcytes (Badou *et al.*, 2005).

Two types of Ca^{2+} signalling, short oscillations and biphasic behaviour can be distinguished. Whereas oscillations are observed at low concentrations of agonists, biphasic behaviour is seen at higher agonist concentrations. Ca^{2+} release from intracellular Ca^{2+} stores results in a transient Ca^{2+} increase followed by an influx of extracellular Ca^{2+} resulting in a plateau-like phase. Dissociation of the agonist terminates the Ca^{2+} plateau (Figure 6). Increases in intracellular Ca^{2+} then modulate various EC responses such as NO release (Furchgott & Zawadzki, 1980; Graier *et al.*, 1992; Iouzalen *et al.*, 1996; Lantoine *et al.*, 1998), rapid synthesis and release of PGI_2 (Clark *et al.*, 1995; Frearson *et al.*, 1995; Patel *et al.*, 1996), production of PAF (Korth *et al.*, 1995), synthesis and release of EDHF (Edwards *et al.*, 1998; Nilius &

Droogmans, 2001), exocytosis of secretory granules containing vWF (Birch *et al.*, 1992), or tPA (Emeis *et al.*, 1997), decreased interaction between TFPI and phosphatidylserine resulting in TFPI release (Valentin & Schousboe, 1996), release of protein S from cell organelles (Stern *et al.*, 1986) and regulation of vascular permeability (Nilius & Droogmans, 2001; Kajimura & Curry, 1999; Moore *et al.*, 1998a; Moore *et al.*, 1998b).

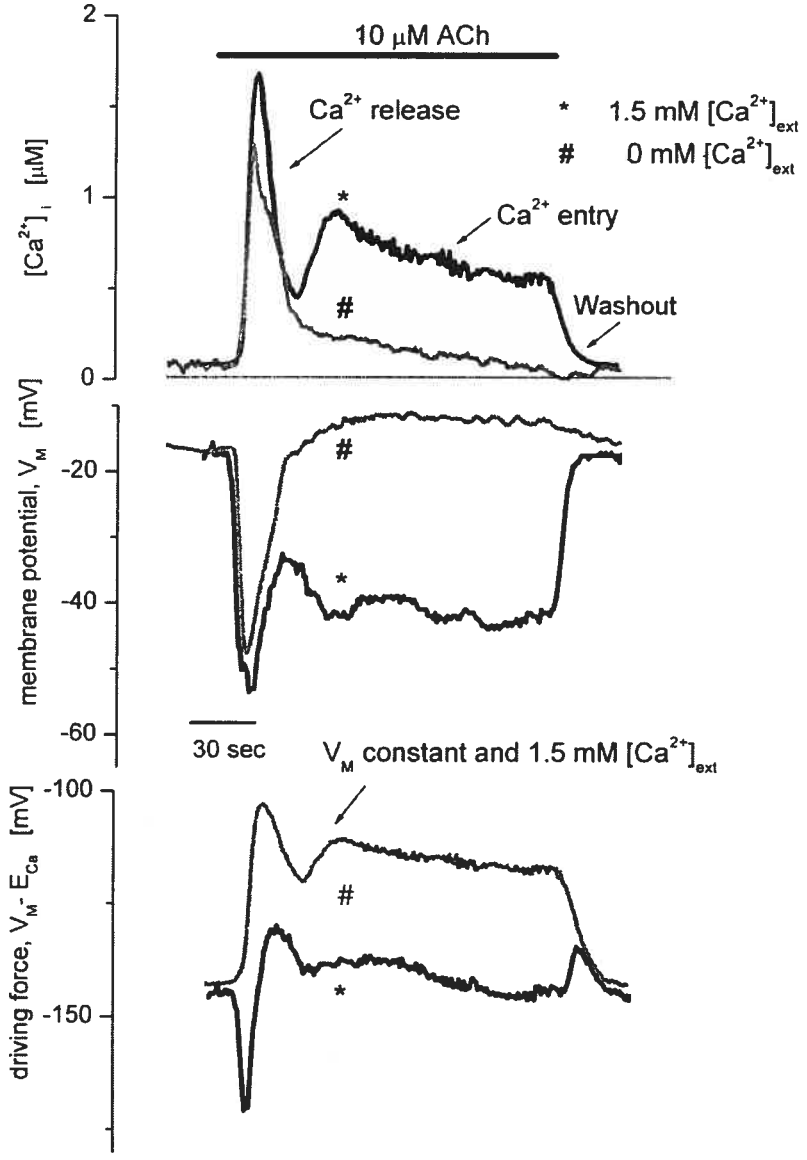

Figure 6: Two mechanisms of Ca^{2+} entry into endothelial cells.

Upper panel: EC stimulation with ACh causes a short transient Ca^{2+} influx through Ca^{2+} release from intracellular stores. Middle panel: Corresponding changes in membrane potential. In the presence of 1.5 mM external Ca^{2+}, influx of extracellular Ca^{2+} causes "plateau-like" membrane hyperpolarization stabilizing the driving force for Ca^{2+} entry (lower panel). In the absence of extracellular Ca^{2+} only the short Ca^{2+} transient can be observed. Results obtained in the presence (*) and absence (#) of 1.5 mM external Ca^{2+}. Adapted from Nilius & Droogmans (2001).

CHAPTER II: INTRODUCTION TO POTASSIUM CHANNELS

Potassium channels are ubiquitously expressed in eukaryotic and prokaryotic cells (Jan & Jan, 1997). K^+ channels contain a common, highly conserved segment known as the K^+ channel signature sequence (Heginbotham *et al.*, 1994) which forms a structural element now known as the selectivity filter (Doyle *et al.*, 1998). The main function of the selectivity filter is determination of ion selectivity and rate of ion conductance through the K^+ channel pore (Morais-Cabral *et al.*, 2001; Zhou *et al.*, 2001b). Even though all known K^+ channels are related members of a single protein family (MacKinnon, 2003), they are currently grouped into five classes: Voltage-gated potassium channels, inwardly rectifying potassium channels, potassium channels whose members might be a tandem fusion of 2 α-subunits of a more basic design, the large-conductance channel Slo, and a fifth distinct class of K^+- channels which has a 6TM segment linked in tandem with a 2TM segment. (Jan, 1999; Gutman *et al.*, 2003). Details are summarized in Table II.

A standardized nomenclature for voltage-gated K^+ channels, the Kv naming system, was suggested more than a decade ago. Based upon their phylogenetic relationship, channels sharing more than 65% sequence identity were assigned to one subfamily (Chandy, 1991; Chandy & Gutman, 1993). A similar naming system, the Kir naming system, was suggested for inward rectifier K^+ channels (Doupnik *et al.*, 1995). Both naming systems haves been widely adopted. A parallel nomenclature for naming genes, the KCN naming system, was developed by the Human Genome Organization (HUGO Nomenclature Committee) in 1997 (White *et al.*, 1997). The KCN naming system has significant shortcomings since it ignores the structural and phylogenetic relationship of ion channels. As a consequence, the International Union of Pharmacology (IUPHAR) has updated its Standardized K^+ Channel Nomenclature System based on phylogenetic relationships to include newly discovered ion channels and add the Eag/Erg/Elk and KvLQT families to the Kv system (Table II, Figures 7-9) (Gutman *et al.*, 2003).

Type	Gene	Nomenclature	Tissue distribution
Voltage-gated K^+ channels (*Shaker*)	*KCNA1*	Kv1.1	Neurons, heart, retina, pancreatic islet cells
	KCNA2	Kv1.2	Brain, heart, pancreatic islet cells
	KCNA3	Kv1.3	Lymphocytes, brain, lung, thymus, spleen
	KCNA4	Kv1.4	Brain, heart, pancreatic islet
	KCNA5	Kv1.5	Brain, heart, kidney, lung, skeletal muscle
	KCNA6	Kv1.6	Brain
	KCNA7	Kv1.7	Heart, pancreatic islet, skeletal muscle
Voltage- and cGMP gated K^+ channel	*KCNA10*	Kv1.10	Aorta, brain, kidney
β subunits for Kv channels	*KCNAB1*	Kvβ1	Brain (Kvβ1.1) Heart (Kvβ1.2)
	KCNAB2	Kvβ2	Brain, heart
	KCNAB3	Kvβ3	Brain
Shab	*KCNB1*	Kv2.1/2.2	Brain, heart, kidney, skeletal muscle, retina
Shaw	*KCNC1*	Kv3.1	Brain, muscle, lymphocyte
	KCNC2	Kv3.2	Brain
	KCNC3	Kv3.3	Brain, liver
	KCNC4	Kv3.4	Brain, skeletal muscle

Shal	*KCND1*	Kv4.1	Heart, brain, liver, kidney, lung, placenta, pancreas
	KCND2	Kv4.2	Heart, brain
	KCND3	Kv4.3	Heart, brain
Ether-a-go-go	*KCNH1*	EAG	Brain
Human *EAG*	*KCNH2*	hERG	Brain, heart
	KCNH3	BEC1	Brain
	KCNH4	BEC2	Brain
MinK	*KCNE1*	MinK	Kidney, uterus, heart, cochlea, retina
	KCNE2	MiRP1	Heart
	KCNE3	MiRP2	Kidney, colon, small intestine
KvLQT1	*KCNQ1*	KvLQT1	Heart, cochlea, kidney, lung, placenta, colon
	KCNQ2	KvLQT2	Brain, neuron
	KCNQ3	KvLQT3	Brain, neuron
	KCNQ4	KvLQT4	Outer hair cells, inner ear, central auditory pathway
	KCNQ5	KvLQT5	Brain, skeletal muscle
Inward rectifier	*KCNJ1*	Kir1.1-1.3	Kidney, pancreatic islets
	KCNJ2	Kir2.1	Heart, brain, smooth muscle, lung, placenta, kidney, aorta
	KCNJ3	Kir3.1	Heart, brain
	KCNJ4	Kir2.3	Heart, brain, skeletal muscle, aorta
	KCNJ5	Kir3.4	Heart, pancreas
	KCNJ6	Kir3.2	Cerebellum, pancreatic islet

	KCNJ8	Kir6.1/uK_{ATP}-1	Various
	KCNJ9	Kir3.3	Brain
	KCNJ11	Kir6.2	Various
	KCNJ12	Kir2.2	Atrium, ventricle
	KCNJ13	Kir7.1	GI, kidney, brain
	KCNJ14	Kir2.4	Brain, retina, peripheral nerves
Sulfonylurea receptor	*SUR1*	Sulfonylurea receptor 1	Pancreas, neurons, skeletal muscle
	SUR2	Sulfonylurea receptor 2 (2A, 2B)	2A : Heart, skeletal muscle 2B : Brain, liver, skeletal and smooth muscle
Two-pore K^+ channels	*KCNK1*	TWIK1	Brain, kidney, heart
	KCNK2	TREK	Brain, lung
	KCNK3	TASK	Heart, brain, pancreas, placenta
	KCNK5	TASK2	Kidney
	KCNK6	TWIK2, TOSS	Eyes, lung, stomach, embryo
	KCNK7	TRAAK	Brain, spinal cord, retina
		CTBAK-1	Heart, brain, kidney
		TALK-1, TALK-2	Exocrine pancreas

Table II: Potassium channel genes, ancillary subunits and tissue distribution.

Modified from Shieh *et al.* (2000).

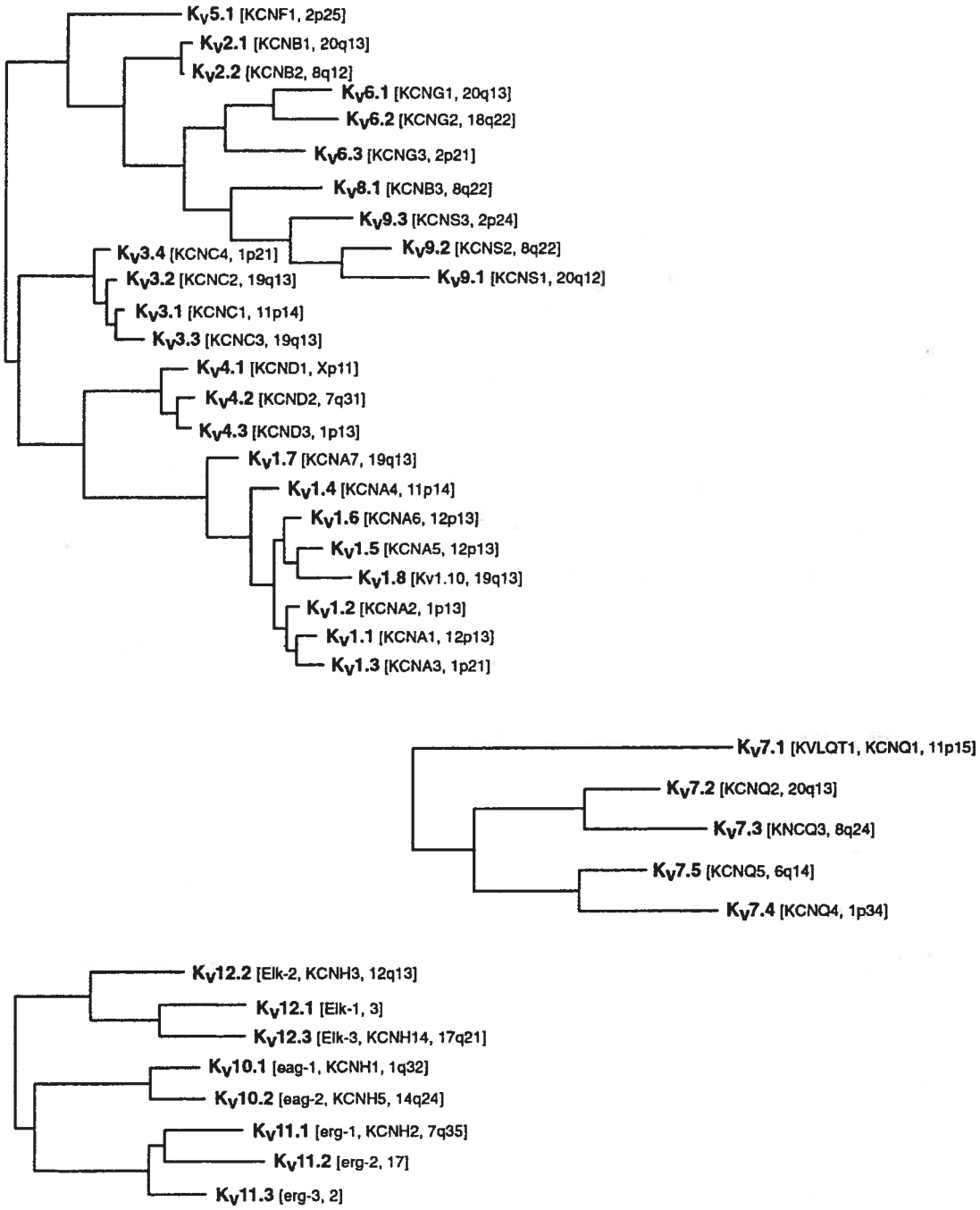

Figure 7: Phylogenetic tree of Kv (6TM) channels.

Adapted from Gutman *et al.* (2003).

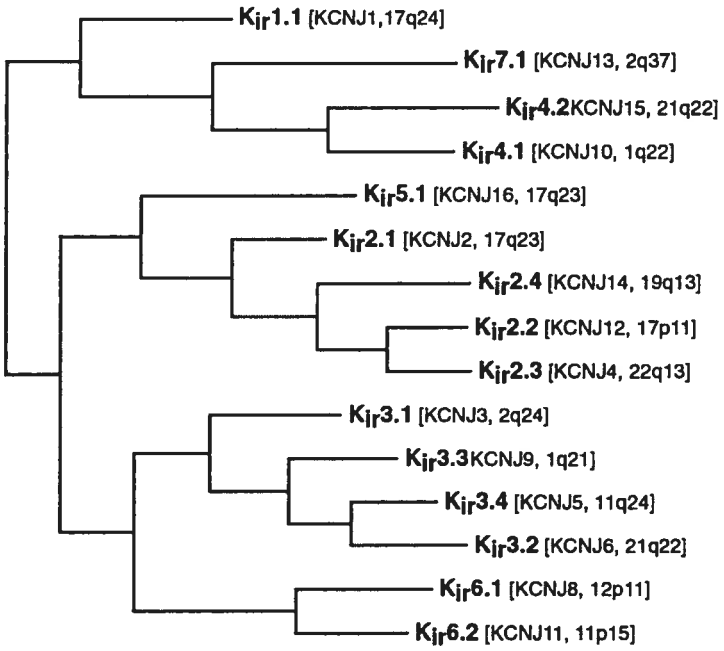

Figure 8: Phylogenetic tree of Kir (2TM) channels.

Adapted from Gutman *et al.* (2003).

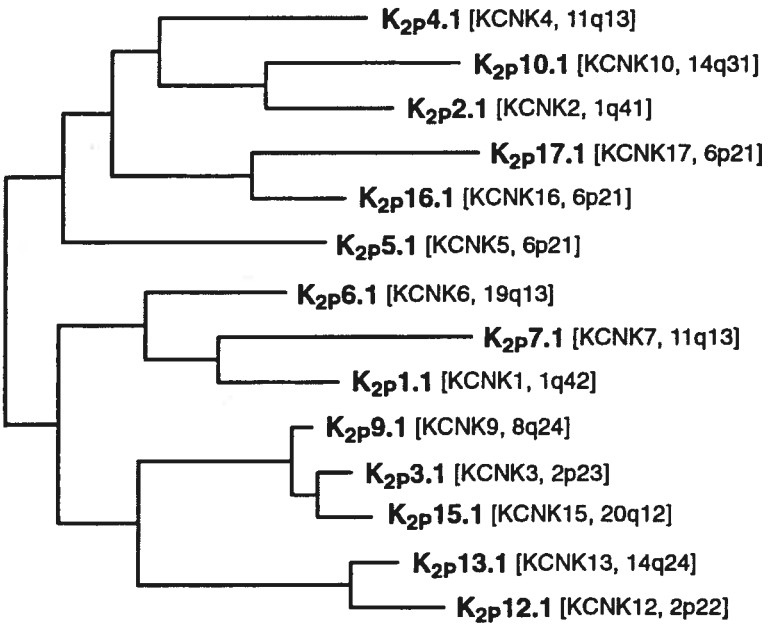

Figure 9: Phylogenetic tree of K2P (4TM) channels.

Adapted from Gutman *et al.* (2003).

CHAPTER III: STRUCTURE-FUNCTION RELATIONSHIP OF POTASSIUM CHANNELS

III-1 Introduction

Crystal structures of seven potassium channels have been obtained in the last seven years from prokaryotic and eukaryotic cells (Doyle *et al.*, 1998; Chang *et al.*, 1998; Jiang *et al.*, 2002b; Bass *et al.*, 2002; Jiang *et al.*, 2003a; Kuo *et al.*, 2003; Long *et al.*, 2005a). In addition, partial structures such as the cytoplasmic T1 domain (Gulbis *et al.*, 2000), the intracellular vestibule of the inward rectifier channel Kir2.1 and Kir3.1 (Pegan *et al.*, 2005; Nishida & MacKinnon, 2002) and regulatory beta subunits (Gulbis *et al.*, 1999) have been crystallized. Information obtained from these studies has given important insight into the molecular basis of ion channel conduction, ion selectivity and ion channel gating. Molecular dynamics simulations have provided further insight into how these structures achieve their respective tasks on the atomic level on a timescale of nanoseconds (Sansom *et al.*, 2002; Domene & Sansom, 2003; Holyoake *et al.*, 2004; Domene *et al.*, 2004; Faraldo-Gomez *et al.*, 2004; Sands *et al.*, 2005). Section III-2 describes general principles of ion channel structure and outlines structural differences between ion channels belonging to different families. Section III-3 outlines structural determinants of rapid ion conductances in the context of high selectivity and mechanisms of channel gating.

III-2 K^+ Channel Structure is Modular

Potassium channels consist of two transmembrane segments and a pore region (Doyle *et al.*, 1998; Jiang *et al.*, 2002b; Kuo *et al.*, 2003; Long *et al.*, 2005a). The highly conserved K^+ channel signature sequence TVGYG is located within the selectivity filter in the pore region near the extracellular surface of the membrane, between the pore helix and the outer helix (Heginbotham *et al.*, 1994; Doyle *et al.*, 1998). While it has been believed for a long time that voltage-gated K^+ channels consist of six transmembrane subunits, newer data suggests that the ion conducting pore and the voltage-sensor are essentially two independent structural domains (Lu *et al.*, 2001b; Jiang *et al.*, 2003a; Long *et al.*, 2005a; Long *et al.*, 2005b). This is in analogy with the concept that diverse structural domains are attached to the conserved K^+ channel pore in a modular fashion according to the gating mechanism of the ion channel (MacKinnon, 2003). The main difference between K^+-ion channels thus lies within the auxiliary domain (Doyle, 2004). Other examples of auxiliary domains are RCK domains (regulators of K^+ conductance) attached to the MthK channel (Jiang *et al.*, 2002b), the T1 domain of Kv-channels (Long *et al.*, 2005a) and the cytoplasmic pore of Kir channels (Nishida & MacKinnon, 2002; Kuo *et al.*, 2003; Pegan *et al.*, 2005). The next section will discuss the structure of the ion conduction pore in detail. For descriptive reasons, original terminology will be used. Thus the term "pore" will refer to the ion conduction pore consisting of the turret (see below), the pore α-helix and the selectivity filter (Doyle *et al.*, 1998).

III-2.1 The Ion-Conduction Pore

The crystallization of the bacterial KcsA channel in 1998 by the laboratory of Roderick MacKinnon (Doyle *et al.*, 1998) was a major scientific breakthrough. The KcsA crystal shows a channel in its closed state. Four subunits assemble with four-fold symmetry about a central pore. Each subunit contains two transmembrane α-helices designated inner (closer to the ion pathway, corresponding to S6) and outer helix (bordering the membrane, S5) and a tilted pore helix. The selectivity filter containing the K^+ channel key sequence TVGYG (Heginbotham *et al.*, 1994) is

located between the outer helix and the pore helix. A short loop into the extracellular space between S5 and the selectivity filter has been termed "turret". The C-terminal negative end-charges of the tilted pore helix point towards the ion conducting pathway. Two layers of aromatic amino acids, twelve in total, are positioned like a cuff around the selectivity filter. Valine and Tyrosine side chains from the Val-Gly-Tyr-Gly sequence of the selectivity filter interact with Trp residues of the pore helix. Hydrogen bonding between Tyr hydroxyls and Trp nitrogens (Tyr68, Trp67 and Tyr68) and extensive van der Waals contacts within the sheet anchor the pore in the lipid bilayer like a "layer of molecular springs", holding the channel open (Doyle *et al.*, 1998). It was proposed that this structure contributes importantly to how channels achieve selectivity for K^+ over Na^+ (Doyle *et al.*, 1998). However, data obtained from molecular dynamics (MD) simulations indicates that loss of selectivity still occurs when these residues are "frozen", indicating that flexibility of the filter does not affect ion selectivity (Noskov *et al.*, 2004). The selectivity filter of voltage-gated channels is essentially identical to KcsA with some small differences in a few hydrophobic amino acid side chains within the hydrophobic core surrounding the filter (Jiang *et al.*, 2003a). To attract cations, both the intra- and extracellular entryways of the pore are negatively charged by acidic amino acids.

The selectivity filter opens into a ~ 10 Å wide water filled cavity. Four inner helices (one from each subunit) are packed against each other to line the pore on the intracellular side of the selectivity filter with a right handed bundle, a structure referred to as the "inner bundle helix". This structure forms an expandable constriction (the "bundle crossing") important for channel gating. Whereas the selectivity filter is lined exclusively by polar amino acid side chain atoms belonging to the signature sequence amino acids, the wall lining of the internal pore and the cavity is predominantly hydrophobic (Doyle *et al.*, 1998). This is easily understandable if one considers the specific functions of these structures. While the outer pore and the selectivity filter attract, select and conduct K^+-ions at a rate of approximately one ion per ten nanoseconds, the central cavity has to overcome the dielectric barrier (barrier to ion flow across the membrane), which is maximal at the center of the membrane (Parsegian, 1969). The cavity overcomes the dielectric barrier

by pointing the carboxyl ends of the four pore α-helices directly at the center of the cavity, thus imposing a negative electrostatic potential via the helix dipole effect (Doyle *et al.*, 1998; MacKinnon, 2003). Interestingly, in the closed state of KirBac, the four pore helixes are misaligned. It has been suggested that the loss of the combined dipole effect results in destabilization of the ion in the center of the cavity thus impeding ion conduction. Weak, broken electron density in this area in the KirBac crystal supports this notion (Kuo *et al.*, 2003).

In KcsA, the inner helix is tilted by about 25 degrees with respect to the membrane and slightly kinked, narrowing the ion pathway below the cavity to a 3.5 Å wide tunnel creating a structure resembling an "inverted tepee". In MthK, the inner helices are bent at a hinge point and opened wide, forming a tunnel of approximately 20 Å in diameter allowing an open connection between the cytoplasm and the water filled cavity. This conformation is believed to represent the open channel configuration. By generating a continuum between the central cavity and the cytoplasm, the channel reduces the dielectric barrier of the membrane to equal the size of the selectivity filter (Jiang *et al.*, 2002b). In prokaryotic K^+ channels, a glycine residue located just below the selectivity filter (Gly83) is believed to act as a "gating hinge" (Jiang *et al.*, 2002b; Jiang *et al.*, 2002c; Jiang *et al.*, 2003a). Mutation of this residue in Kir3 channels reduces channel conductance (Jin *et al.*, 2002). Sequence alignments show that this residue is not conserved in all Kir families, and instead a different glycine residue corresponding to Gly143 in KirBac, which is more conserved, might act as the gating hinge (Kuo *et al.*, 2003). If both glycines are present, the channel might bend at either point (Doyle, 2004). In eukaryotic channels, a highly conserved triplet Pro-X-Pro sequence (Pro-Val-Pro in Kv1.2, (Long *et al.*, 2005a)) serves the same purpose. Applying lateral force on the C-terminal extension of the inner helices would place a torque on the gating hinge, thereby opening the channel (Jiang *et al.*, 2002c). Structure-based sequence alignment suggests that the conformational changes underlying gating are conserved. Consistent with this notion, functional studies in *Shaker* channels show that cysteines introduced at positions "above" the bundle crossing can only react with sulfhydryl reagents added to the intracellular side of the membrane when the channel opens (del Camino *et al.*, 2000;

Liu *et al.*, 1997; del Camino *et al.*, 2000). Gate closure occurs while maintaining the size of the cavity (Jiang *et al.*, 2002b). This mechanism is consistent with the "trapping" of cations in the channel pore (Armstrong, 1971; Holmgren *et al.*, 1996; del Camino *et al.*, 2000). However, more recent data indicates that in fully closed channels, the volume of the cavity might be decreased (Kuo *et al.*, 2003). Data obtained from KvAP and Kv1.2 show that the adjacent inner and outer helices maintain an antiparallel relationship to one another, suggesting that they move as one unit (Jiang *et al.*, 2003a; Long *et al.*, 2005a). An "activation gate" has been demonstrated in KirBac. In the closed state, the side chain of Phe146 blocks the ion conduction pathway (Kuo *et al.*, 2003). Molecular dynamics simulations suggest that a hydrophobic-lined pore acts as an effective gate, preventing water and ion movement (Chang *et al.*, 1998). Based on sequence alignment, amino acids with large hydrophobic aromatic or aliphatic side chains are favoured in this position in Kir (Kuo *et al.*, 2003) and other channels (Unwin, 1993; Unwin, 1995; Chang *et al.*, 1998).

An additional helical structure, designated "slide helix", is present in the transmembrane structure of KirBac. This amphipathic helix runs in parallel with the membrane / cytoplasmic interface (Kuo *et al.*, 2003) and has also been demonstrated in KcsA (Cortes *et al.*, 2001). In KirBac, the negatively charged end of the slide helix interacts with a conserved Arg148 side chain tethering the inner helix to the slide helix. Movement of the slide helix would hence move the inner helix, suggesting a role of the slide helix in channel gating. It was proposed that the slide helix couples the initial gating signal to the activation gate Phe146 of KirBac (Kuo *et al.*, 2003) in a similar fashion as the S4-S5 linker couples movements of the voltage-sensor to the inner helix of voltage-gated K^+ channels (Lu *et al.*, 2002; Jiang *et al.*, 2003a; Long *et al.*, 2005a).

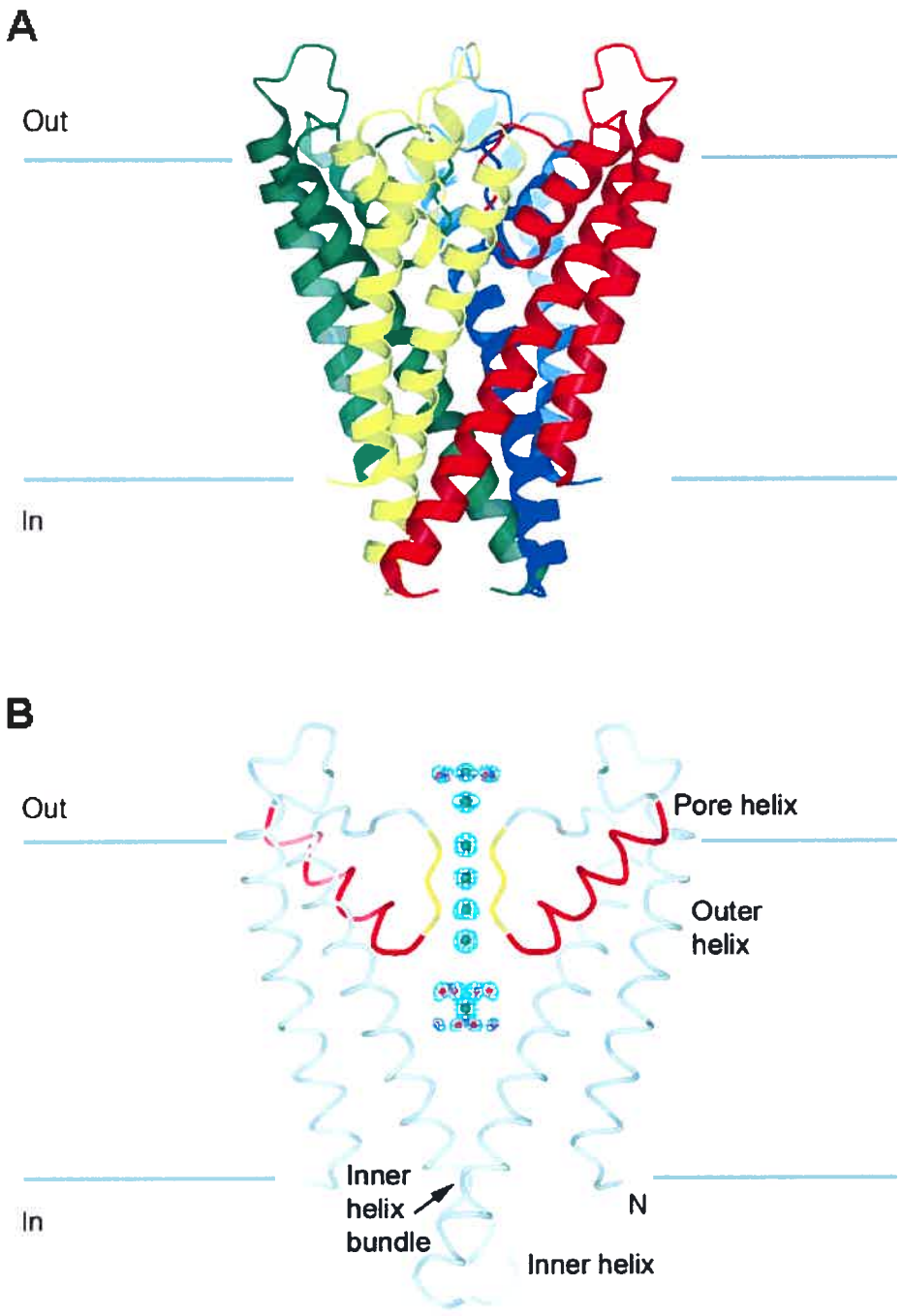

Figure 10: Ribbon presentation of the KcsA K^+- channel.

A. Four subunits are shown in different colors. The extracellular end is on top.

B. The KcsA K^+ channel with front and back subunits removed. The pore helices are shown in red and selectivity filter in yellow; the electron density along the ion pathway is shown in a blue mesh. Adapted from MacKinnon (2004).

III-2.2 Modular Cytoplasmic K^+ Channel Domains

The major difference between K^+ channels lies within the auxiliary cytoplasmic domain (Doyle, 2004). Ligand-binding domains in ligand-gated channels (Finn *et al.*, 1996; Jiang *et al.*, 2001), long cytoplasmic pores in inwardly rectifying channels (Nishida & MacKinnon, 2002; Kuo *et al.*, 2003) and voltage-sensors in voltage-gated channels (Jiang *et al.*, 2003a; Long *et al.*, 2005a) are attached to the conserved K^+ channel pore on the cytoplasmic side of the membrane in a modular fashion. The function of these domains is to translate the energy of the channel activation signal into mechanical work on the activation gate causing the channel to open or close.

III-2.2.1 RCK-Domains of Ligand-Gated K^+-Channels

Regulators of K^+ conductance (RCK-) domains are a commonly occurring structural element of ligand-gated channels (Jiang *et al.*, 2001). RCK domains are prominent among pro- and eukaryotic channels and occur as single or tandem soluble cytoplasmic proteins or as single or tandem units attached to the C- and / or N-terminus of a K^+ channel (Jiang *et al.*, 2002b).

In MthK, eight identical RCK domains form a gating ring on the cytoplasmic side. One RCK domain is attached to one channel α-subunit through a polypeptide chain whereas a second RCK domain comes from the cytoplasm. The two surfaces where two RCK subunits connect are unique so that one channel-attached RCK unit has to interact with a cytoplasmic unit in order to form a ring. One of these two interfaces is fixed whereas the other one is flexible. In this way, the gating ring is assembled of four rigid units consisting of two RCK units attached to each other through the fixed interface in a tilted left-handed bundle. Two neighboring flexible interfaces form a cleft in which the ligand (Ca^{2+}) can bind. Near the Ca^{2+} binding site at the base of the cleft is a flexible hinge, allowing the rigid assembly to move. Binding of Ca^{2+} reshapes the cleft causing the rigid units to tilt thereby expanding the diameter of the gating ring. This in turns pulls on the inner helix causing the channel to open (Jiang *et al.*, 2002b).

III-2.2.2 The Voltage Sensor: Coupling Electrical Work to Channel Gating

Voltage-gated K^+ channels activate and deactivate as a function of the membrane potential. Charged amino acids, "gating charges", are electromechanically coupled to the gating mechanism of the ion channels causing channel opening or closure when moving through the membrane electrical field. Gating charges can be measured (Armstrong & Bezanilla, 1974) and correspond to approximately 12-14 electron charges crossing the membrane voltage difference in tetrameric K^+ channels (Schoppa *et al.*, 1992; Seoh *et al.*, 1996; Aggarwal & MacKinnon, 1996). Sensing of the membrane potential and transmembraneous movement of gating charges is accomplished by a structure known as the "voltage sensor", which consists of four transmembraneous segments S1 to S4. The S4 segment contains several charged amino acids. Of these, the first four arginines account for most of the gating charge (Seoh *et al.*, 1996; Aggarwal & MacKinnon, 1996).

III-2.2.2.1 Voltage-Sensor Structure: KvAP and Kv1.2

Crystal structures of voltage gated channels are available for KvAP (Jiang *et al.*, 2003a), a prokaryotic channel and of Kv1.2 (Long *et al.*, 2005a; Long *et al.*, 2005b), an eukaryotic channel. These show the S1 and S2 segments loosely packed against the outer helix of the channel pore. In KvAP, the conventional S3 segment is divided into two individual helices S3a and S3b connected by a S3-loop (Jiang *et al.*, 2003a), a distinction not made in Kv1.2 (Long *et al.*, 2005b). S3b and the N-terminal end of the mainly hydrophobic S4 segment are tightly packed together in an anti-parallel relationship forming a mainly hydrophobic "helix-turn-helix" structure termed the "voltage-sensor paddle". The paddles are located at the outer perimeter of the channel. Conserved arginine residues (Bezanilla, 2000), important for gating (Seoh *et al.*, 1996; Aggarwal & MacKinnon, 1996), are located on the highly conserved N-terminal part of the S4 segment. The voltage-paddles are flexibly attached to S2 and S5, and are movable with respect to the pore because of their flexible attachment via the S3 loops. Acidic amino acids in the S2 helix could help to stabilize positive charges on the paddles as they move across the membrane (Jiang *et al.*, 2003b). Several salt-bridges connect S3a to the C-terminal half of S2. Exchange

of salt-bridge pairs has been shown to be important for paddle movements between closed and open states of the channel (Tiwari-Woodruff *et al.*, 2000; Papazian *et al.*, 2002). Loss of Arg377 in *Shaker* channels (which corresponds to Arg133 in KvAP) results in loss of channel functions (Bezanilla, 2000).

The C-terminal S4-segment is poorly conserved and connects to the S5 segment forming an amphipathic α-helix called the S4-S5 linker. This structure runs parallel to the membrane on its cytoplasmic side with hydrophobic residues facing the membrane and hydrophilic amino acids pointing towards the inside of the cell. It crosses over the top of the inner helix of the same subunit and makes many amino acid interactions with it. Multiple glycine residues allow the S4-S5 linker to bend at various points making it a highly flexible helix. The inner helix in return bends at the Pro-Val-Pro region and curves parallel to the membrane plane creating a "receptor" for the S4-S5 linker. The interaction between S4-S5 and the inner pore helix is important to allow linkage of paddle movement to movement of the S5 helices while maintaining free movement of the voltage-sensor in the membrane with respect to the ion channel pore according to the gating state. The importance of this interaction is emphasized by functional studies. Mutations in the S4-S5 linker or the Pro-X-Pro sequence have profound effects on channel gating (Liu *et al.*, 1997; Schoppa & Sigworth, 1998; Hackos *et al.*, 2002; Yifrach & MacKinnon, 2002; Sukhareva *et al.*, 2003). To confer voltage-dependence to KcsA, both the "S4-S5 linker receptor" on S6 and the S4-S5 linker have to be transferred together with the voltage-sensor onto the ion conduction pore of KcsA (Lu *et al.*, 2001b; Lu *et al.*, 2002).

In KvAP, the voltage-sensor was captured in a non-native configuration emphasizing its capability to undergo domain-like movements with respect to the pore. Its great flexibility suggests that it is essentially an independent domain in the membrane (MacKinnon, 2004). This notion is supported by data from Kv1.2. Crystals of Kv1.2 show the voltage-sensors located at the corner of the pore "floating as separate domains from the pore" (Long *et al.*, 2005b). Aside the S4-S5 linker, the voltage-sensor makes contact with the ion-conduction pore in only two places: The S1 helix touches S5 in one place near the outer membrane surface and the S4 helix

comes in contact with the outer edge of S5. Most of the surface of the hydrophobic sides of the pore and the voltage-sensor face the lipid of the membrane.

In summary, voltage-sensors are independent, flexible domains within the membrane loosely attached to the ion-conduction pore by the S4-S5 linker. In this respect they represent, similar to ligand-binding domains in ligand-gated channel, a modular gating domain. Segments S3 and the N-terminal part of the S4 segment form a helix-turn-helix structure called the "voltage-sensor paddle" which carries the gating charges in form of four arginines. Interaction between the S4-S5 linker and the C-terminal S6 segment is essential for channel gating.

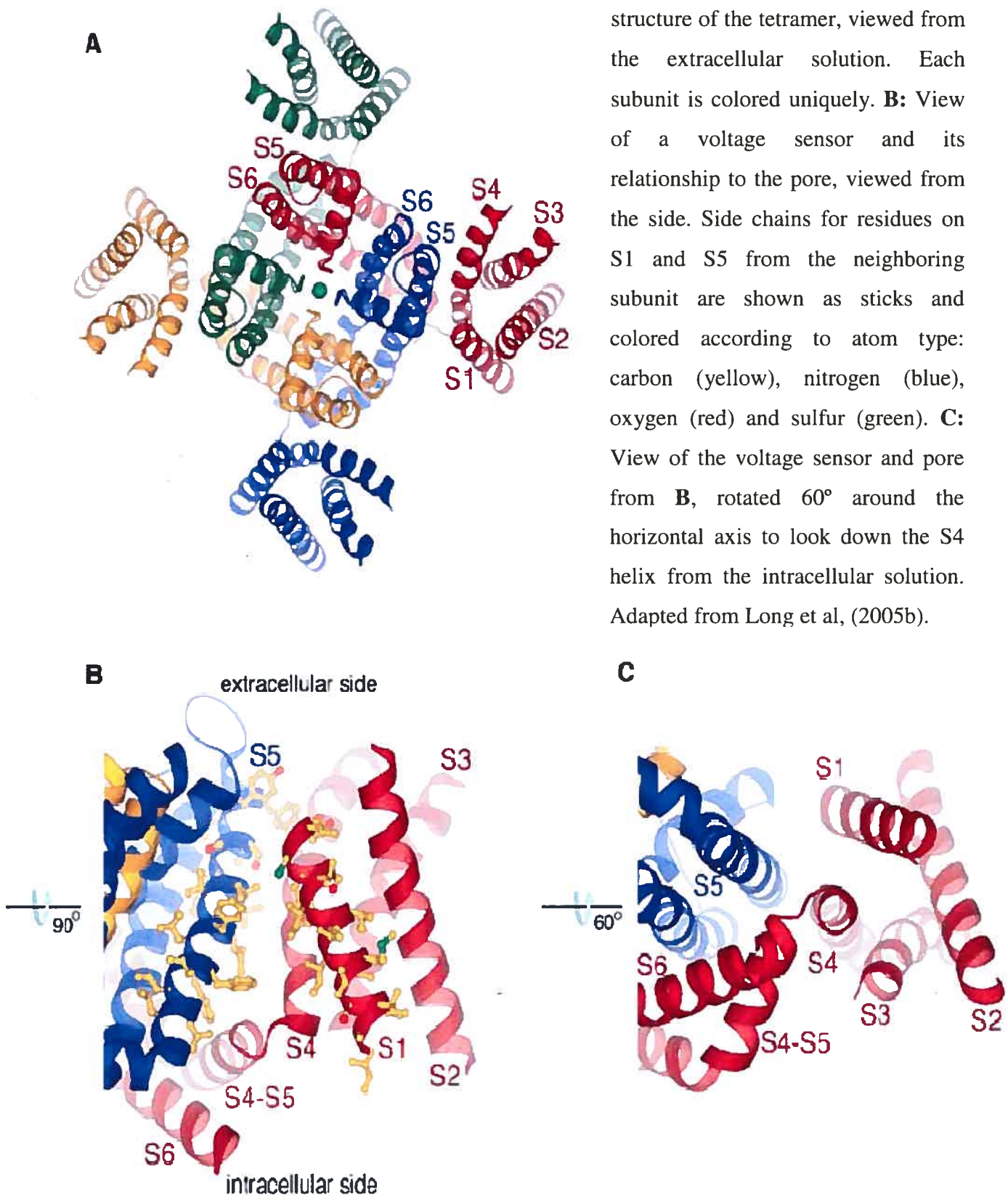

Figure 11: Pore and voltage sensors of the Kv1.2 channel. **A:** Overall structure of the tetramer, viewed from the extracellular solution. Each subunit is colored uniquely. **B:** View of a voltage sensor and its relationship to the pore, viewed from the side. Side chains for residues on S1 and S5 from the neighboring subunit are shown as sticks and colored according to atom type: carbon (yellow), nitrogen (blue), oxygen (red) and sulfur (green). **C:** View of the voltage sensor and pore from **B**, rotated 60° around the horizontal axis to look down the S4 helix from the intracellular solution. Adapted from Long et al, (2005b).

III-2.2.2.2 How do Gating Charges cross the Membrane?

Electrophysiological data suggests that the S4 segment moves through the lipid membrane thereby carrying gating charges through the electrical field (Swartz & MacKinnon, 1997; Baker *et al.*, 1998; Larsson *et al.*, 1996a; Yusaf *et al.*, 1996). These charges are located on the first four arginine residues on the S4 segment, Arg117, Arg120, Arg123, Arg126 and Arg294, Arg297, Arg200 and Arg303 in KvAP and Kv1.2, respectively. Experiments with biotin-tethered voltage-sensor paddles showed that biotin is accessible to avidin from the intracellular side when the channel is closed and from the extracellular side when the channel is in the open state indicating that biotin is being dragged all the way across the membrane during channel gating (Jiang *et al.*, 2003b).

Several models of transmembrane charge movement have been published. The common ground of these models is that the S4 helix is mostly (Elinder *et al.*, 2001) or completely (Bezanilla, 2002; Horn, 2002; Gandhi & Isacoff, 2002) separated from the membrane to protect the arginine charges from the low dielectric environment of the lipid membrane (Long *et al.*, 2005b). The *canonical model* (or *sliding-helix model*) suggests that movement of the S4 segment occurs in a protein-lined "caniculus" formed by the inner and outer pore helices on one side and by the voltage-sensor's S1, S2 and S3 segments on the other side (Horn, 2002; Gandhi & Isacoff, 2002; Bezanilla, 2002; Li-Smerin *et al.*, 2000). In this way, the charged amino acids of the moving S4 segment are completely protected from the lipid environment. The *transporter model* also proposes protection of the S4 segment between S1 – S3 and the channel pore domain. However, this model suggests that instead of the S4 segment moving in the membrane, charges are moved over S4 by alternately opening and closing surrounding "crevices" to the internal and external solutions (Cha *et al.*, 1999; Starace & Bezanilla, 2004). The *paddle-mode*" of KvAP indicates that movement of the voltage-paddles within the membrane occurs while contacting the lipid membrane on one side and the channel protein on the other side (Jiang *et al.*, 2003b). The *twisted S4 model* is based on spin labelling experiments of KvAP in a lipid bilayer. Here, the S4 helices are at the protein-lipid interface and not buried in a

"caniculus" A flexible linker in the middle of S4 enables one half to rotate versus the other allowing the positive charges to point inward towards the remainder of the protein. Differential rearrangement of the S4 segment would occur in response to voltage changes (Cuello *et al.*, 2004).

Consistent with EPR data from KvAP in lipid membranes (Cuello *et al.*, 2004), the Kv1.2 crystal shows that Arg294 and Arg297 are located on the lipid facing surface of the voltage-sensor while Arg300 and Arg303 face helices S1 and S2 making salt bridges with acidic amino acids (Long *et al.*, 2005b), thus supporting the *paddle model*. The S3 segment and the S4 segment move together as the voltage-sensor paddle with S3 providing rigidity to S4. S3 is facing the extracellular side of the membrane with its top never penetrating deeper than the membrane's outer leaflet (Jiang *et al.*, 2003b). This position is energetically more stable than in the hydrophobic core because of the presence of both hydrophobic and hydrophilic amino acids. S4 is facing the intracellular side of the membrane. During inward movement, the paddle must counterbalance the energetic preference of S3 to stay at the extracellular interface. It has been suggested that in this way the S3 segment might serve as a "recoil device" causing the voltage-sensor to "spring open" during depolarization (Long *et al.*, 2005b).

In summary, various models have been developed to explain gating charge movement across the membrane. Recent crystal data is in support of the *paddle model*. Two arginines on the voltage-sensor paddle are exposed to the lipid membrane whereas the other two face the protein surface of helices S1 and S2 indicating that all charge shielding from the membrane and compensation by counter charges comes from the voltage-sensor itself. When going from the closed to the open state, the voltage sensor paddles travel through the entire membrane, moving gating charges through the electric field. The S3 segment stabilizes S4 and serves as a recoil device causing the channel to "spring open".

III-2.2.2.3 Mechanical Coupling of Voltage-Sensor Movements to the Pore

How does the voltage-sensor achieve the task of electromechanical coupling? MacKinnon and colleagues proposed a model suggesting that in the closed channel

formation the paddles are held close to the cytosolic membrane interface through the electric field imposed by the negative resting potential. In this state, the inner and outer helices are bent like in KcsA thereby closing the pore. When the membrane depolarizes, the paddles move approximately 20 Å (assuming a membrane thickness of 35 Å) through the membrane. Transfer of the four arginine residues (each carrying approximately one electron charge unit) across the membrane is in agreement with the gating charge movement of 12-14 electrons in *Shaker* channels (Schoppa *et al.*, 1992; Seoh *et al.*, 1996; Aggarwal & MacKinnon, 1996). An upward displacement of the paddles would pull on the S4-S5 linker helices thereby decompressing the inner helices and opening the pore. Closure of the channel involves bringing the positive arginine charges inward, resulting in downward movement of the voltage-sensor paddles pushing down the S4-S5 helices thus compressing the inner helices which closes the pore (Jiang *et al.*, 2003b; Long *et al.*, 2005b).

III-2.2.3 The T1 Domain of Voltage-Gated K^+ Channels

III-2.2.3.1 Crystal Structure

Eukaryotic Kv channels differ from prokaryotic channels by the presence of a cytoplasmic T1 domain. The crystal structure of Kv1.2 shows the T1-Kvβ-subunit complex to be a 40 Å long rigid structure with four fold symmetry about the pore axis. A α-helical T1-S1 linker spreads out radially from the pore creating 15 – 20 Å wide side portals separating cytoplasmic from transmembraneous domains. The side portals provide room for the inner helix to move during gating and provide low resistance perfusion pathways between the cytoplasm and the pore. Multiple negatively charged amino acids attract cations (Long *et al.*, 2005a), a mechanism similar to the cytoplasmic pore of inward-rectifier channels (Nishida & MacKinnon, 2002; Kuo *et al.*, 2003).

III-2.2.3.2 Functional Role

T1 domains contribute to regulation of channel trafficking and determine specificity of Kv channel subunit co-assembly. T1 domains may be receptor sites for regulation of Kv-channel activity by Kvβ-subunits (Li *et al.*, 1992; Shen &

Pfaffinger, 1995; Schulteis *et al.*, 1998; Tu *et al.*, 1996; Kobertz & Miller, 1999; Li *et al.*, 1992; Papazian, 1999; Gulbis *et al.*, 2000; Zhou *et al.*, 2001a; Tu *et al.*, 1996; Kobertz & Miller, 1999; Papazian, 1999; Long *et al.*, 2005a). A key role of the T1 domain in N-type inactivation was suggested in 1990 (Hoshi *et al.*, 1990; Zagotta *et al.*, 1990). Electric charges on the large side portals between the T1 domain and the pore might steer inactivation peptides of N-terminal channel domains or Kvβ-subunits (Long *et al.*, 2005a).

III-2.2.4 The Cytoplasmic Pore of Inward Rectifier Channels

III-2.2.4.1 Structure

The concept of a cytoplasmic pore protruding from the membrane into the cytoplasm of Kir channels was first proposed by Lu et al. (1999) and later confirmed by the crystal structures of Kir3.1 (Nishida & MacKinnon, 2002; Pegan *et al.*, 2005), KirBac (Kuo *et al.*, 2003) and Kir2.1 (Pegan *et al.*, 2005). Structures of Kir2.1, Kir3.1 and KirBac show marked similarity (Figure 12). Nearly 40 amino acids preceding the first transmembrane domain and the approximately 200 first amino acids of the C-terminal of inward-rectifier K^+ channels are conserved (Nishida & MacKinnon, 2002). N- and C-termini form a globular cytoplasmic pore of β-sheets with a protruding α-helix. The cytoplasmic pore is between 7 and 10 Å wide and approximately 30 Å long, thereby extending the ion pathway to about 60-88 Å (Nishida & MacKinnon, 2002; Kuo *et al.*, 2003). The N-terminus runs in a groove between two adjacent C-termini interacting with the C-terminus of the same subunit through a short parallel β-sheet. A more recent study reported this interaction to occur between C- and N-termini of adjacent Kir2.1 subunits (Pegan *et al.*, 2005), which is in line with interactions between the C- and N-termini in Kir2 channel assembly (Preisig-Muller *et al.*, 2002). In Kir2.1, the distal end of the C-terminus was disordered and could not be visualized suggesting that it is highly mobile and requires the N-terminus, binding to PSD-95 or other cytoplasmic factors to obtain structural stability (Pegan *et al.*, 2005; Cohen *et al.*, 1996). Flexible linkers connect the cytoplasmic domain to the transmembraneous pore. Positively charged arginine and lysine residues in the linker make it unlikely that K^+ ions can enter the channel

through gaps between the linkers (Kuo *et al.*, 2003). Contrary to the four-fold symmetry of the transmembraneous pore, two cytoplasmic domains form an asymmetric unit with two-fold symmetry about the pore axis, a configuration referred to as dimer-of-dimers (Kuo *et al.*, 2003). The attempt to obtain a crystal of heteromeric Kir3.2/Kir3.4 N- and C- termini also resulted in the formation of dimers, however, these constructs were unstable over time and the experiments were not pursued (Pegan *et al.*, 2005). Two highly conserved pore-facing β-sheet loop regions (CD-loop and HI-loop, Figure 11) form the narrowest part of the cytoplasmic pore, acting like a girdle. In the HI-loop a section designated "G-loop" differs between Kir2.1 and Kir3.1. In Kir2.1, Gly300, Met301, Ala306 and Met307 form two hydrophobic rings, allowing openings of 2.8-5.7 Å. Thus, four opposing G-loops form openings which are too small for a hydrated K^+-ion to pass (Pegan *et al.*, 2005). Conserved and backbone-flexible glycines anchor these loops in the cytoplasmic pore. Conformational differences between Kir2.1, Kir3.1 (Pegan *et al.*, 2005) and the first reported Kir3.1 structure (Nishida & MacKinnon, 2002) suggest that these loops are intrinsically flexible and can undergo large conformational changes during conduction (Pegan *et al.*, 2005). This structure is crucial for channel modulation by intracellular regulators and voltage-dependence of inward rectification (Bichet *et al.*, 2003).

III-2.2.4.2 Potential Functional Role

In contrast to the hydrophobic inner lining revealed by the crystal structures of KcsA and MthK, the cytoplasmic pore of Kir channels is lined by polar, negatively charged amino acid (mostly Glu and Asp) interspersed with hydrophobic residues, creating an overall negative electrostatic potential. Such an environment is consistent with a role of the cytoplasmic pore in the mechanism of "long pore plugging" by cytoplasmic polyamines underlying inward rectification (Lopatin *et al.*, 1995). The importance of the N- and C-termini for inward-rectification was already described by Taglialatela and colleagues in 1994 (Taglialatela *et al.*, 1994). Residues important for inward rectification of Kir2.1 are Asp172 in the inner helix (Lu & MacKinnon, 1994; Stanfield *et al.*, 1994), and Glu224 and Glu229 in the cytoplasmic domain (Kubo &

Murata, 2001; Taglialatela *et al.*, 1995; Yang *et al.*, 1995). In KirBac, equivalent residues are Ile138, Glu187 and Glu258. The side chains of Glu187 and Glu258 are oriented towards the center of the ion conduction pathway forming two electrostatic rings of negative charge ~ 35 Å apart. This is too far apart for a single spermine molecule (~ 20 Å long) to overlap. Shape, charge and hydrophobicity determine polyamine binding affinity and diffuse anionic charge appears to be a configuration that favours binding of linear positively charged polyamines over compact Mg^{2+} ions (Kuo *et al.*, 2003). The degree of binding affinity for blocking cations is directly related to the degree of inward rectification (Bichet *et al.*, 2003). The presence of blocking particle binding residues in both the transmembraneous pore and the cytoplasmic membrane led to the suggestion of a two-site blocking model. In this model, the cytoplasmic pore might serve as an intermediate binding site, attracting and increasing the concentration of polyamines, whereas the plugging site is in the transmembrane segment of the pore (Kubo & Murata, 2001; Lopatin *et al.*, 1995; Lee *et al.*, 1999; Xie *et al.*, 2002). The precise mechanism coupling rectification to channel gating is presently unknown. It has been proposed that the C-terminus might interact with the outer helix through the slide helix, causing movement of the inner helices through interactions with the outer helices (Kuo *et al.*, 2003).

Four charged amino-acids, Arg228, Asp255, Asp259 and Arg260, in the Kir2.1 cytoplasmic pore differentially modulate rectification properties. Charge neutralization at Asp259 decreases rectification to a greater extent than at Asp255 whereas mutation of Arg228 and Arg260 produces only very little changes in rectification when respective mutant Kir2.1 channels were expressed in *Xenopus* oocytes (Pegan *et al.*, 2005).

Inward-rectification is caused by voltage-dependent block of the pore by intracellular Mg^{2+} and polyamines (Matsuda *et al.*, 1987; Vandenberg 1987; Lopatin *et al.*, 1994; Ficker *et al.*, 1994; Lopatin *et al.*, 1995). Movement of Mg^{2+} and polyamines towards the extracellular space pushes a queue of K^+ ions in front of the blocker out into the extracellular solution. The movement of charges through the transmembrane electric field is thought to underlie the voltage dependence of inward rectification (Nishida & MacKinnon, 2002; Bichet *et al.*, 2003). In addition, the

interaction of the polyamine amine group with Asp172 in the pore cavity and with the selectivity filter might contribute to voltage-dependence of polyamine block (Pearson & Nichols, 1998).

A wide variety of cytoplasmic factors regulating the activity of Kir channels have been discovered. Phosphatidylinositol-4,4-bisphosphate (PIP_2) is essential for Kir channels to open (Huang *et al.*, 1998; Lopes *et al.*, 2002; Shyng *et al.*, 2000b). On the whole cell level, PIP_2 enhances Kir currents and its depletion causes current rundown (Huang *et al.*, 1998; Sui *et al.*, 1998; Baukrowitz *et al.*, 1998; Shyng *et al.*, 2000b). PIP_2-binding domains have been identified in the C- and N-terminus (Shyng *et al.*, 2000b; Soom *et al.*, 2001; Lopes *et al.*, 2002). When mapped on KirBac, these residues lie within a pocket built by the N- and C-termini just below the cytoplasmic side of the pore (Kuo *et al.*, 2003). Betagamma-subunits of G-proteins ($G\beta\gamma$), pH, ATP, Na^+, Mg^{2+}, arachidonic acid, and phosphorylation and oxidation / reduction are important cytoplasmic regulators (Bichet *et al.*, 2003). Kir3 channels are activated by $G\beta\gamma$ (Logothetis *et al.*, 1987). The crystal structure of Kir3.1 shows four α-helical prongs protruding into the cytoplasm with a C-terminal hydrophobic end (Nishida & MacKinnon, 2002). These residues are well conserved within the Kir3 family (Mirshahi *et al.*, 2002) and are believed to represent the binding site for $G\beta\gamma$ (Nishida & MacKinnon, 2002). Intracellular acidosis inhibits Kir1.1 and Kir2.1 channels (Jiang *et al.*, 2002a; Mao *et al.*, 2003) via protonation of C-terminal histidines (Chanchevalap *et al.*, 2000; Qu *et al.*, 2000). Enhanced interaction between N- and C-termini at low pH (Qu *et al.*, 2000) might affect gating through interactions between the C-terminus and the outer helix (Kuo *et al.*, 2003). A similar mechanism might underlie Kir6.2 channel inhibition through ATP binding in an ATP binding pocket (Trapp *et al.*, 2003) located in the β-sheet connecting N- and C-terminus (Nishida & MacKinnon, 2002; Kuo *et al.*, 2003). Proximity of C-terminal binding sites for Na^+, Mg^{2+}, PIP_2 and arachidonic acid binding sites as well as protonation sites suggests additive, synergistic and/or competitive mechanisms in the regulation of Kir channels (Bichet *et al.*, 2003). The G-loop of Kir2.1 and Kir3.1 appears to be a functionally coupled to PIP_2 and / or $G\beta\gamma$ binding (Pegan *et al.*, 2005).

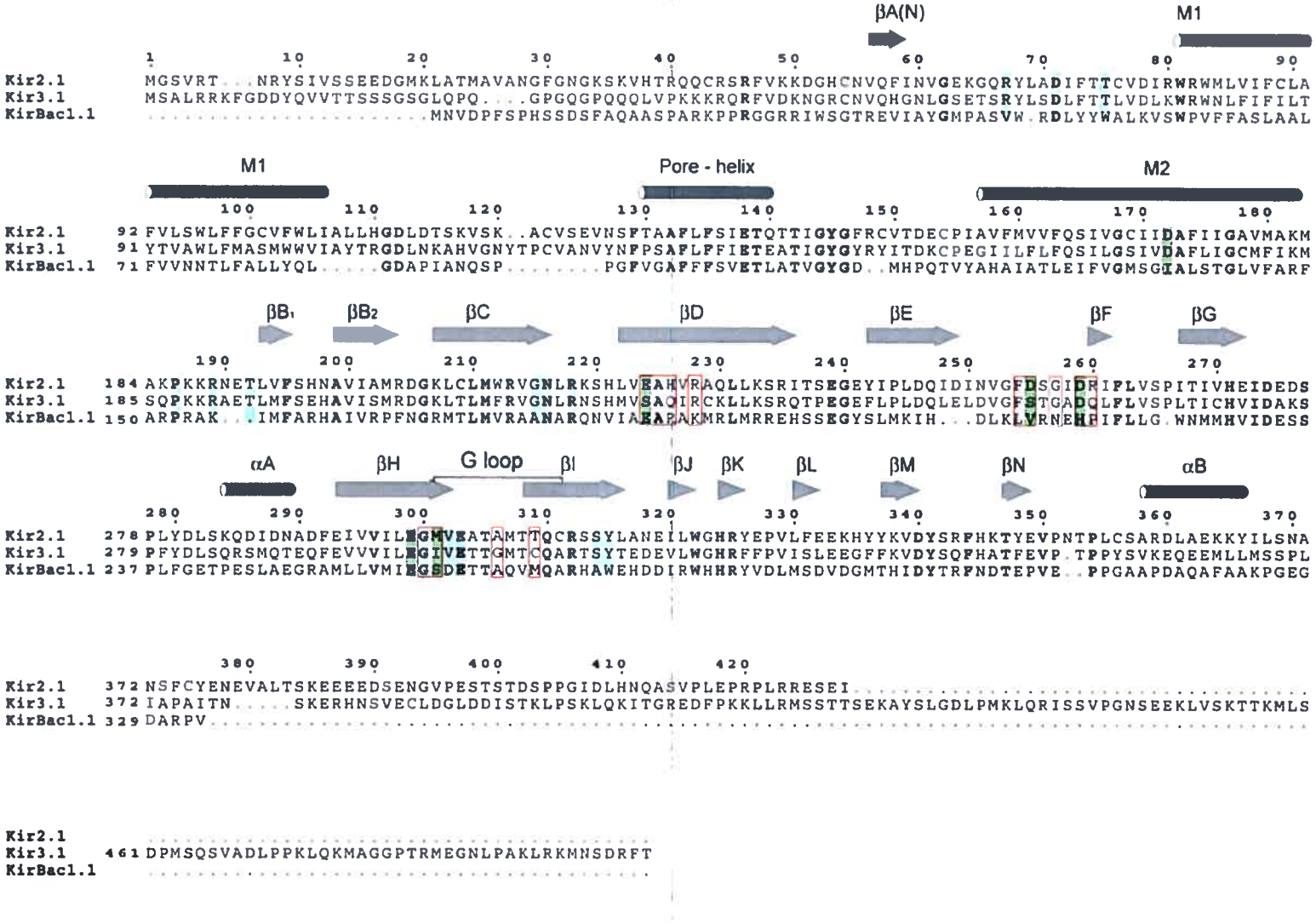
βA(N)
M1
M1
Pore - helix
M2
βB1
βB2
βC
βD
βE
βF
βG
αA
βH
G loop
βI
βJ
βK
βL
βM
βN
αB
Kir2.1
Kir3.1
KirBac1.1

Figure 12: Sequence alignment of Kir3.1, Kir2.1, and KirBac1.1 with secondary structure elements noted.

Pore-facing residues within the cytoplasmic domains based on the structure of Kir2.1 are boxed in red. The selectivity filter residues GYG are highlighted in pink. Mutations known to be related to Andersen syndrome (blue) and six positions implicated for inward rectification (green) are highlighted. Reproduced from Pegan *et al*, 2005.

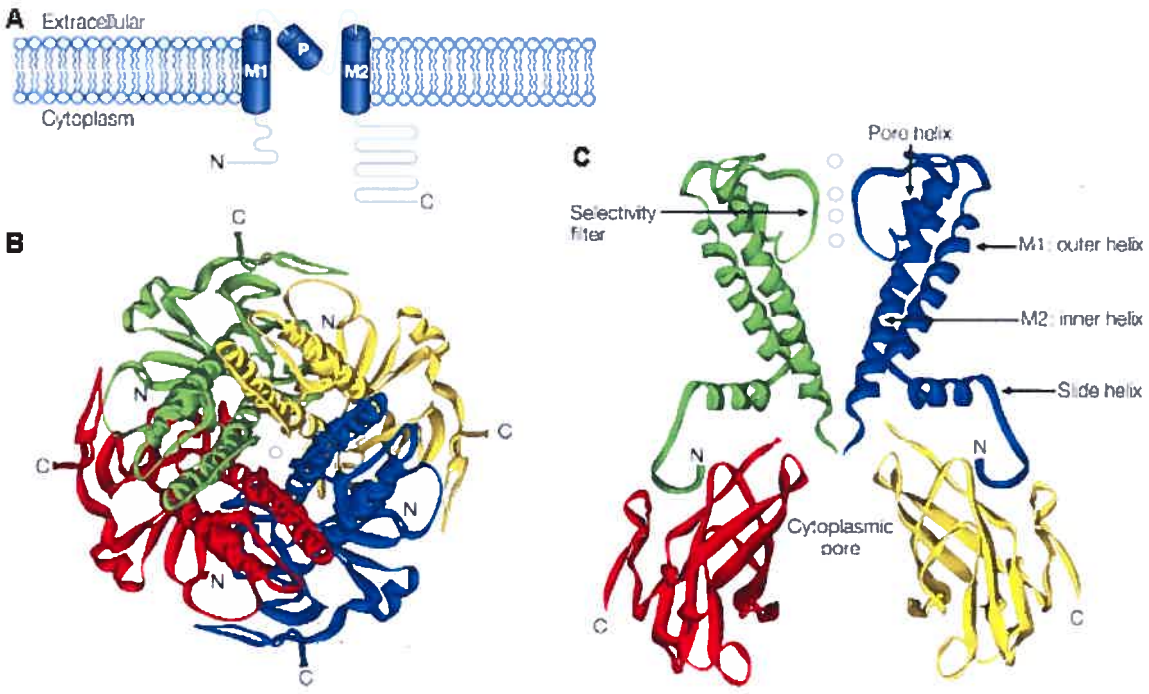

Figure 13: Overall architecture of inwardly rectifying K^+ (Kir) channels.

A. Schematic drawing of a Kir channel subunit. Each subunit comprises two transmembrane helices (M1 and M2), a pore-forming region containing the pore-helix (P), and a cytoplasmic domain formed by the amino (N) and carboxy (C) termini.

B. View of the tetrameric structure of the KirBac1.1 channel from the extracellular side. Monomers are individually coloured red, green, yellow and blue. A K^+ ion (white) indicates the conduction pathway. **C.** Side view of the KirBac1.1 structure showing the transmembrane domain of two subunits (green and blue) and the C-terminal domains of their neighboring subunits (red and yellow). White spheres represent K^+ ions in the selectivity filter. Reproduced from Bichet *et al.* 2003.

III-3 Structural Basis of Ion Channel Function

A K^+ channel transports K^+ -ions across the membrane. To achieve this, it has to fulfill three essential tasks: 1.) Distinguish between different available ions and allow only K^+ ions to cross the membrane (selective ion conduction), 2.) Conduct K^+-ions rapidly (high conduction rate) and 3.) Switch between conducting and non-conducting states in response to cellular stimuli (gating) (MacKinnon, 2003).

Since the publication of the KcsA crystal structure, a multitude of studies have investigated the atomic mechanisms of high K^+ selectivity in the context of high conduction rates and gating mechanisms. Methods applied include experimental approaches, structural data, molecular dynamics simulations, electron spin resonance and mass spectroscopy. For recent reviews see (Sansom *et al.*, 2002; Roux, 2005). The following section will introduce structural determinants of K^+ permeation through K^+ channels and then discuss how these relate to selectivity and high conduction rate.

III-3.1. Basis of Ion Permeation

Two structures of the K^+ channel are imperative for its function: 1.) the selectivity filter (Doyle *et al.*, 1998) and 2.) the water filled cavity at the center of the membrane (Roux & MacKinnon, 1999).

In an aqueous solution, monovalent potassium ions are stabilized by eight polarized water molecules that point their negative oxygen atoms in the direction of the K^+-ion. Four water molecules are located in a plane "above" and four "below" the K^+-ion (Zhou *et al.*, 2001b) (Figures 10 and 14). In this state, the ion is said to be "hydrated". Molecular dynamics simulations and the crystal structure of KcsA have identified seven K^+ binding sites in the channel pore (Berneche & Roux, 2001) (Figure 14). K^+ is needed to maintain stability of the channel pore and prevent the channel from assuming a non-functional "defunct" state (Loboda *et al.*, 2001; Zhou & MacKinnon, 2003; Domene & Sansom, 2003; Domene *et al.*, 2004). Thus, it is considered a structural element of the selectivity filter.

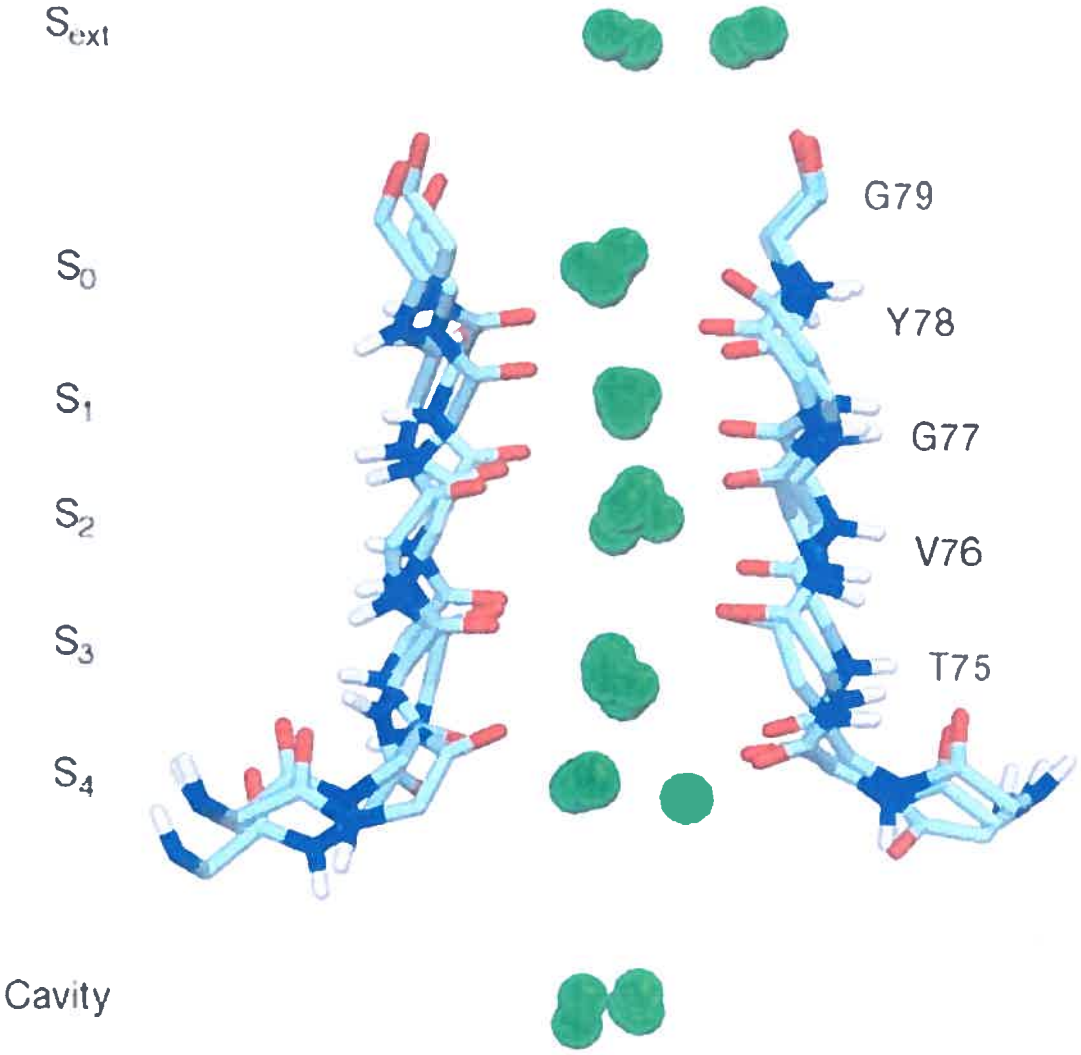

Figure 14: Permeant ion binding sites in the KcsA K^+ channel.

The outer site (S1), the upper inner site (S3), the lower inner site (S4) and the diffuse cavity site detected in the initial X-ray structure are shown (Doyle *et al.*, 1998). Furthermore, K^+ can occupy the site where crystallographic water was previously detected (S2), as well as two additional sites termed S0 and Sext. The ions in S1, S2 and S3 are in contact with the main chain carbonyl oxygen atoms (S1, Gly77 and Tyr78; S2, Val76 and Gly77; S3, Thr75 and Val76) and only 1–2 water molecules, whereas the ion in S4 is hydrated by 2–3 water molecules and makes intermittent contacts with the carbonyl oxygens and the side chain of Thr75. The ion in S0 is in contact with Tyr78 and is hydrated by 3–4 water molecules. The ion in Sext is almost fully hydrated. Reproduced from Berneche & Roux (2001).

The outermost position Sext is located on the extracellular side of the channel. At this position, the K^+ ion is fully hydrated by eight water molecules (Berneche & Roux, 2001). S0 is located at the external mouth of the channel. Negative charges from the carbonyl oxygen atoms from the four Tyr78 (or Gly79 (Doyle *et al.*, 1998; Zhou *et al.*, 2001b)) residues replace half of the ion's hydration shell, mimicking four water molecules thereby stabilizing the ion by acting as surrogate water (Berneche & Roux, 2001). Sext and S0 site were initially not seen in the crystal structure of KcsA, however, more recent high resolution x-ray data of KcsA has revealed these two sites as well (Berneche & Roux, 2001). Negative charges from four carbonyl oxygen atoms from the Gly79 residues are directed straight into the extracellular solution, providing an electronegative environment, which attracts extracellular cations. A second layer of negative charges near the entryway is provided by carboxy-carboxylate pairs formed by Glu71 and Asp80 (Doyle *et al.*, 1998; Zhou *et al.*, 2001b).

Inside the selectivity filter, the K^+-ion is almost completely dehydrated (Berneche & Roux, 2001). Four layers of carbonyl oxygen atoms from the Gly-Tyr-Gly-Val residues and one layer of threonine hydroxyl oxygen groups create four K^+-ion binding sites near the center of a distorted cube (a "square antiprism"). These sites have been designated S1 (Gly77 and Tyr78), S2 (Val76 and Gly77), S3 (Thr75 and Val76) and S4 (Thr75) with S1 being closest to the external mouth of the ion channel. Glycine residues in the TVGYG sequence are imperative for structural flexibility of the selectivity filter (Berneche & Roux, 2005). It was suggested that sites S1 – S4 stabilize the dehydrated K^+-ion by the negative charges of their surrounding eight carbonyl groups (Zhou *et al.*, 2001b). However, more recent data from MD simulations indicates that the number of K^+-coordinating charges in the filter varies, resulting in distinct selectivities of the various ion-binding sites (Noskov *et al.*, 2004; Berneche & Roux, 2005). Only position S2 appears to supply eight coordination charges (Berneche & Roux, 2005) consistent with the highest selectivity for K^+ at this site (Aqvist & Luzhkov, 2000; Noskov *et al.*, 2004) and its role in C-type activation (Berneche & Roux, 2005).

A seventh K^+ binding site is found in the water-filled central cavity where the K^+-ion remains stabilized by eight water molecule suspended at the center of the cavity on the pore axis. Additional water molecules are present in the cavity but they are disordered. The order of water in the K^+-hydration shell is probably due to weak, indirect hydrogen-bonding interactions from the hydroxyl group of Thr107 as well as the carbonyl oxygen atoms from the pore and inner helices with the hydrated K^+-ion (Roux & MacKinnon, 1999; Zhou *et al.*, 2001b). Ordering of water molecules does not impede the movement of K^+-ions through the pore because rearrangement of water molecules occurs faster than ion movement through the pore. The cavity achieves a K^+-concentration of about 2M (Zhou *et al.*, 2001b).

III-3.2. Mechanism of High Conduction Rate

The selectivity filter is where the driving force arising from the transmembrane potential is predominant (Berneche & Roux, 2003; Jiang *et al.*, 2002c). Rapid conduction in the context of selectivity for K^+ is the hallmark feature of K^+ channels. Under physiological conditions, K^+ channels achieve conduction rates of up to 10^8 K^+-ions per second, approaching the limit of free diffusion (MacKinnon, 2004). Dehydration, transfer and rehydration of a K^+-ion occur in about ten nanoseconds (Morais-Cabral *et al.*, 2001). How can such a high conduction rate be achieved while still maintaining perfect fidelity for potassium ions?

Two basic mechanisms account for the channel's high conduction rates: 1.) Reduction of the membranes dielectric field by the water filled cavity and 2.) Conduction of K^+ ions through the selectivity filter at near diffusion limits.

As proposed by Hodgkin and Keynes 50 years ago (Hodgin & Keynes, 1955), K^+-ions move through the ion channel pore in a single file (Doyle *et al.*, 1998; Morais-Cabral *et al.*, 2001; Zhou *et al.*, 2001b; Berneche & Roux, 2001; Shrivastava & Sansom, 2000). The conduction rate of an ion channel is a function of how many ions can pass through the channel per unit of time. A major obstacle to rapid ion conduction across the membrane is electrostatic repulsion by the membrane dielectric barrier. The water filled cavity concentrates K^+ ions in the axis of the pore. Its hydrophobic wall-lining (Ile100, Phe103) from the inner helix prevents the

interaction of water with the surface of the cavity which is therefore available to stabilize the K^+ ion. The order of water molecules is most likely imposed by weak indirect hydrogen bonding mediated by the hydroxyl group of Thr107 and the carbonyl oxygen atoms from the pore and inner helices. Roux and McKinnon showed by modeling that 80% of ionic stabilization comes from the pore helices and 20% from the carbonyl group of Thr107 (Roux & MacKinnon, 1999). Exchange of ordered water molecules occurs faster than conduction. Therefore, the hydration shell does not impede ion migration through the pore. In the open channel state, the water filled cavity is in equilibrium with the intracellular solution, thus diminishing the dielectric barrier to the distance of the selectivity filter. This is in accordance with functional data showing that when TEA binds to the top of the cavity at more than 50% of the physical distance across the membrane, it crosses only about 20% of the transmembraneous voltage difference, indicating that the selectivity filter imposes 80% of the transmembrane voltage field (Yellen *et al.*, 1991).

K^+ channels have "multi-ion pores", which means that multiple permeant ions are in the channel pore at a given time (Doyle *et al.*, 1998; Berneche & Roux, 2001). Depending on the K^+-concentration, the filter adopts two different conformational states, a conducting and a non-conducting one (Morais-Cabral *et al.*, 2001; Berneche & Roux, 2001). Structural data and data obtained from MD simulations has shown that in the conducting state, two or three K^+-ions must be in the selectivity filter (Morais-Cabral *et al.*, 2001; Zhou & MacKinnon, 2003; Berneche & Roux, 2001; Berneche & Roux, 2005; Allen & Chung, 2001). Computations indicate that three-K^+-ion configurations are [cavity, S3, S1] and [S4, S2, S0]. Electrostatic repulsions oppose the simultaneous occupancy of the cavity and sites S4 or sites S1 and S0 (Roux, 2005). If the filter is exposed to a low K^+-concentration as is the case in the "closed state" where the filter "sees" the low (5 mM) extracellular K^+-concentration, only one K^+-ion at either site S1 or S4 is present in the filter (Morais-Cabral *et al.*, 2001). In this state, a conformational change occurs, switching the channel into a non-conducting state. In the context of a high K^+ concentration (higher than 50 mM), which is the case in the context of an open activation gate where the filter "sees" the high (145 mM) cytoplasmic K^+ concentration, an additional K^+ ion enters the

selectivity filter resulting in a configuration where two binding sites are occupied causing the filter to "snap into the main configuration" (Zhou *et al.*, 2001b). Under physiological conditions, K^+-ion occupancy in the selectivity filter alternates between energetically balanced S0-S2-S4 and S1-S3 configurations (Shrivastava & Sansom, 2000; Berneche & Roux, 2001; Domene & Sansom, 2003) which by itself does not control ion throughput. The largest free energy barrier between these positions is around 2-3 kcal/mol, approaching the limit of free diffusion (Berneche & Roux, 2001). An incoming ion from the cavity induces a concerted movement to the S4-S2-S0 configuration followed by dissociation of the outermost ion into site Sext and subsequent dissociation from the channel (Roux, 2005). Electrostatic repulsion between permeant ions is essential for rapid conduction. When two ions are in the central cavity and one at site S3, a deep energy well impedes the outer ion to exit the channel. When an ion approaches site S4, the ion at site S3 moves to S2 decreasing the energy barrier between sites S1 and S0 to 1 kcal/mol. This causes site S1 to become unstable and the exit becomes barrierless, causing the outer ion to leave the channel (Berneche & Roux, 2001). MD simulations have shown that the approach of an ion on the intracellular site is energetically neutral whereas dissociation from the channel is accelerated by electrostatic ion-ion repulsions (Berneche & Roux, 2001; Berneche & Roux, 2003). The proposed model for ion conduction (Berneche & Roux, 2005) is therefore:

$$[S3, S1] \leftrightarrow [Cavity, S3, S1] \leftrightarrow [S4, S2, S0] \leftrightarrow [S4, S2] \leftrightarrow [S3, S1]$$

In summary, the cavity overcomes the dielectric barrier by concentrating K^+-ions at its center, ready to enter the selectivity filter thus limiting the dielectric barrier to the length of the filter. Two permeant ions are constantly present in the filter. An incoming ion causes a concerted movement of K^+-water-K^+-water within the filter causing the outermost ion to exit due to electrostatic repulsion. The key mechanism underlying high conduction is the concerted transition between the two ion state S3-S1 and the three ion state S4-S2-S0.

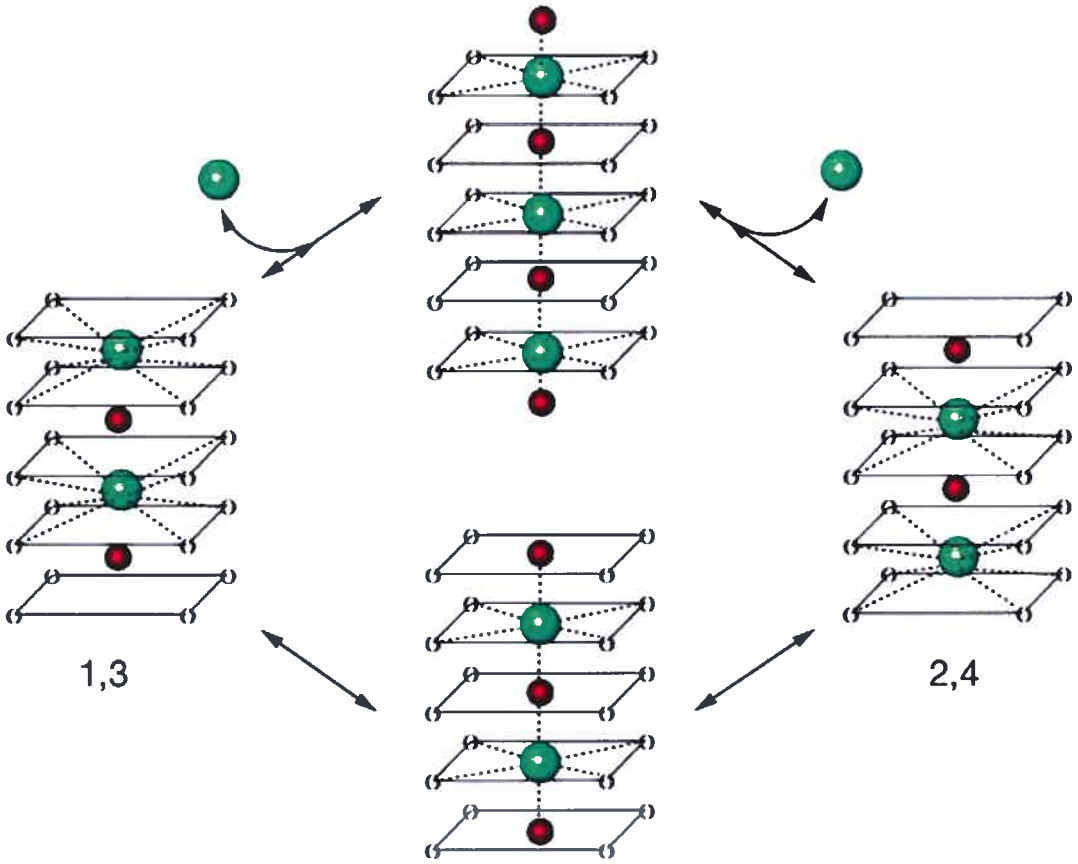

Figure 15: Ion occupancy in the selectivity filter.

The selectivity filter is depicted as five sets of four in-plane oxygen atoms (the top is outside the cell), with K^+ ions and water molecules shown as green and red spheres, respectively. K^+ ions undergo coordination by eight oxygen atoms when in the 1,3 and 2,4 configurations. Movement along either the concentration-independent path (bottom) or the concentration-dependent path (top) would involve octahedral coordination by six oxygen atoms, two provided by the intervening water molecules. Adapted from Morais-Cabral *et al.* (2001).

III-3.3 Current Concepts of Ion Selectivity

Ion selectivity is critical to survival of the cell. Selectivity for K^+ is about 1000 times higher than for Na^+ thus practically excluding conduction of Na^+ ions (MacKinnon, 2003). How does the K^+ channel achieve such high selectivity for K^+ over Na^+?

Ion selectivity is controlled by the relative free energy of K^+ and Na^+ in the pore and the extra- or intracellular solution (Roux, 2005). Potassium ions have an atomic radius of 1.33 Å while that of sodium is only 0.95 Å. In 1972, Bezanilla and Armstrong proposed the "snug-fit" hypothesis, suggesting that Na^+-ions cannot pass through the narrowest part of the channel pore because they are too small to fit the "coordination cage" provided by the channel as replacement for the water molecules in aqueous solution. This hypothesis has subsequently been strengthened by experimental data obtained from KcsA (Doyle *et al.*, 1998; Zhou *et al.*, 2001b) suggesting that the structure of the selectivity filter is perfectly tuned to accommodate K^+-ions, balancing energetic costs and gains (Doyle *et al.*, 1998; Hille *et al.*, 1999). In order to maintain the precise fit between K^+-ions and the coordinating carbonyl groups of pore-lining residues, the filter must be rigid. Filter flexibility would allow approach of its carbonyl oxygen atoms enabling it to assume an energetically favourable configuration to compensate for the cost of dehydration of Na^+-ions (Doyle *et al.*, 1998) resulting in loss of selectivity for K^+. Rigidity of the selection filter is accomplished by "molecular springs" anchoring the filter in the membrane. Bonding of Glu71 with Asp80 as well as a buried water molecule to the amide nitrogen of Gly79 is believed to hold the filter in a stable position (Zhou *et al.*, 2001b). Additionally, side chains of Val76 and Tyr78 in the selectivity filter are directed into the surrounding protein stabilizing the configuration of the selectivity filter (MacKinnon, 2004).

The flexible nature of proteins (Zaccai, 2000; Allen *et al.*, 2004) has challenged the "snug-fit" hypothesis (Noskov *et al.*, 2004; Roux, 2005). Structural data (Morais-Cabral *et al.*, 2001) and MD simulation studies (Allen *et al.*, 2000; Berneche & Roux, 2001; Shrivastava & Sansom, 2000; Shrivastava *et al.*, 2002;

Domene & Sansom, 2003; Domene *et al.*, 2004; Noskov *et al.*, 2004; Berneche & Roux, 2005) have shown that the filter can undergo significant conformational changes ("filter distortion") due to flexibility of the selectivity filter backbone at the glycine residues (Berneche & Roux, 2005). Molecular dynamics simulations show that filter distortion is sufficient to accommodate Na^+ at little energetic cost, resulting in a loss of K^+-selectivity (Guidoni *et al.*, 1999; Biggin *et al.*, 2001; Domene & Sansom, 2003). However, alchemical free energy perturbation (FEP) computations (Aqvist & Luzhkov, 2000; Berneche & Roux, 2001; Luzhkov & Aqvist, 2001) and ion-flux measurements (Neyton & Miller, 1988; Nimigean & Miller, 2002) indicate that occupancy by Na^+ in the selectivity filter is indeed energetically unfavourable. How can this apparent paradox be resolved?

Current data suggests that ion channel selectivity is achieved through electrostatic interactions between ion-coordinating carbonyl groups of the selectivity filter themselves as with the permeant ion (Noskov *et al.*, 2004). MD simulations show that removal of carbonyl-carbonyl interactions in a flexible KcsA channel results in loss of ion-selectivity for K^+ over Na^+. Without these carbonyl-carbonyl interactions, channel rigidity required to maintain K^+-selectivity would render the channel practically non-functional. Interestingly, carbonyl-carbonyl repulsions have only a very moderate effect on pore structure, which is mainly controlled by strong interactions between permeant ions and the carbonyl groups of the filter. Even when geometric restraints are optimized to accommodate a Na^+-ion, carbonyl-carbonyl repulsions result in thermal fluctuations "rescuing" selectivity for K^+ (Noskov *et al.*, 2004).

While MacKinnon and colleagues suggested that K^+ ions have an equal affinity to K^+ binding sites with an average occupancy of 0.53 for each site (Morais-Cabral *et al.*, 2001; Zhou & MacKinnon, 2003), data from MD simulations indicates that selectivity of sites S1 to S4 is distinct (Aqvist & Luzhkov, 2000; Berneche & Roux, 2001; Noskov *et al.*, 2004; Berneche & Roux, 2005) with highest selectivity at site S2 and lowest selectivity at site S4 (Berneche & Roux, 2001; Noskov *et al.*, 2004; Domene *et al.*, 2004). The cavity does not display any selectivity, however, the

hydration type around cations appears to be different with only K^+ having a complete hydration shell (Zhou *et al.*, 2001b;Zhou & MacKinnon, 2004).

In summary, permeant ion binding sites in the selectivity filter have distinct selectivities for K^+ over Na^+. Selectivity in the filter arises locally as a function of carbonyl-carbonyl repulsion of ligands coordinating the permeant ion rather than due to geometrical restraints. Electrostatic repulsion between carbonyl groups influences ion-binding energetics but has only little effect on pore radius indicating that selectivity is a robust feature of a dynamical fluctuating pore.

III-3.4 K^+ Channel Gating

In order to control ion flux across the membrane, ion channels need to be able to switch between a conducting and a non-conducting state, a process called "gating". Three gating states are known: "Activation" refers to the channel assuming an ion-conducting, open configuration. During "deactivation", the channel pore is closed and the channel does not conduct. "Inactivation" denotes a non-conducting state in which the pore is open. Two different kinds of inactivation have been described, C- and N-type inactivation. C-type inactivation is slow and due to conformational changes of the outer pore region (Yellen *et al.*, 1994). N-type inactivation occurs rapidly, within the order of milliseconds. Insertion of the cytoplasmic amphipathic N-terminal chain of the channel protein itself or from attached Kvβ-subunits occludes the cytoplasmic channel pore. It is important to note that inactivation is a process distinct from deactivation.

Current knowledge of gating processes is derived from structural data and MD simulations. This chapter will briefly discuss structural changes involving the transmembrane helices and the selectivity filter thought to underlie channel opening / closure and C-type inactivation, respectively.

III-3.4.1 Structural Changes during Activation and Deactivation

The primary activation / deactivation gating event responsible for channel opening or closure occurs by modification of the diameter of the ion conducting pore near the cytoplasmic membrane (Jiang *et al.*, 2002b; Jiang *et al.*, 2002c; Kuo *et al.*,

2003; Doyle, 2004; Domene *et al.*, 2005). Structural information about ion channel gating first came from KcsA. Here, the inner helices are nearly straight, forming a bundle ("inner helix bundle") near the intracellular solution thereby giving the channel the appearance of an "inverted tepee". At the inner helix bundle, which is formed by hydrophobic amino acids from the inner helices, the pore is as narrow as 3.5 Å, making it impossible for the K^+-ion to pass (Doyle *et al.*, 1998). In MthK, the inner helices are bent at a hinge point (Gly89) and splayed wide open (12 Å at its narrowest point, Ala88), so that the cavity becomes continuous with the cytoplasm (Jiang *et al.*, 2002b). This conformation indicates that the inner helix bundle must be able to undergo conformational changes, i.e. open and close. This hypothesis is supported by experimental data showing that thiol-reactive compounds and metal ions applied to the cytoplasm can not access the pore in *Shaker* channels when the channel is closed (del Camino *et al.*, 2000; del Camino & Yellen, 2001). The structure of the hydrophobic "activation gate" has been further elaborated in KirBac (Kuo *et al.*, 2003). Here, four phenylalanine residues (Phe146) form a tight constriction completely occluding the ion conduction pathway when the inner helix bundle is closed. Bending of the inner helices occurs at glycine residues in prokaryotic channels (Doyle, 2004) whereas in *Shaker* channels a Pro-X-Pro sequences corresponding to Gly143 in KirBac serves as the gating hinge (del Camino *et al.*, 2000; Long *et al.*, 2005a). Glycine residues are more or less conserved and it is believed that bending of the inner helices can occur at various positions or even several different positions depending on the state of gating (Doyle, 2004). MD simulations have confirmed gating by movement of the inner helices (Sansom *et al.*, 2002; Grottesi *et al.*, 2005; Domene *et al.*, 2005).

III-3.4.2 Filter distortion might underlie C-type Inactivation

In 2001, Zhou et al. described that low potassium concentrations cause the selectivity filter to adopt a non-conducting conformation involving residues Val76 and Gly77 (Zhou *et al.*, 2001b). As outlined in section III.3.3, the backbone structure of the selectivity filter is flexible. Reorientation of the Val76-Gly77 peptide link has been seen to undergo spontaneous reorientation in MD simulations of KcsA (Berneche & Roux, 2000; Domene & Sansom, 2003), Kir6.2 (Capener *et al.*, 2003) and KirBac (Domene *et al.*, 2004), a behaviour that has been termed "filter distortion". In KirBac, the corresponding Val111 can flip and thereby widen the filter towards its extracellular end. This distortion functionally closes the channel by directing the NH groups of Gly112 towards the lumen producing an electrostatic barrier to permeant cations (Domene *et al.*, 2004). Similar observations have been made in Kir6.2. It was suggested that these distortions underlie "fast" gating in Kir channels (Lu *et al.*, 2001a; Proks *et al.*, 2001; Bichet *et al.*, 2003) and C-type inactivation in Kv-channels (Liu *et al.*, 1996; Starkus *et al.*, 1997; Kiss *et al.*, 1999; Berneche & Roux, 2005).

What are the structural changes underlying gating in the selectivity filter? In KcsA, transition from the stable conducting to the stable non-conducting state takes place in two steps. First, the backbone carbonyl oxygen of Val76 flips away from the conduction pathway causing the amide plane Val76–Gly77 to undergo a 180 degree reorientation, leading to the "intermediate state of marginal stability" (Berneche & Roux, 2005) similar to Val76–Gly77 interactions initially described by Zhou et al. (2001). However, Zhou et al saw only a 45 degree reorientation (Zhou *et al.*, 2001b). This intermediate state is readily reversible since the amide plane can rapidly return to its original orientation (Berneche & Roux, 2000). As a second step, the amide group of Thr75 forms a strong hydrogen bond with the carbonyl group of Glu71 while the carbonyl oxygen and side chain of Thr75 coordinate the K^+-ion in site S3. This "locks" the selectivity filter in a state breaking the fourfold symmetry. The K^+-ion in site S3 remains well coordinated by seven or eight oxygen ligands, yet loss of favourable interaction with the Val76 carbonyl creates a large energetic barrier

preventing translocation of K^+ from [Cavity, S3, S1] to [S4, S2, S0] (Figure 16) necessary for rapid ion conduction resulting in significant reduction of K^+-currents as shown by MD simulations (Berneche & Roux, 2005). Interestingly, the state of broken symmetry decreases K^+ selectivity over Na^+ (Berneche & Roux, 2005) which is in accordance with experimental data showing that during C-type inactivation the channel becomes transiently permeable for Na^+ (Starkus *et al.*, 1997; Starkus *et al.*, 2000). The lifetime of the non-conducting state is about 0.14 ms.

What are the structural determinants of Val76–Gly77 reorientation? Reorientation of Val76 is prohibited by K^+ occupation of site S2 due to its stabilization by eight carbonyl oxygens and can not occur in more than one subunit at a time due to large free energy barriers or resulting excessive deformation of the selectivity filter. The presence of glycine residues in the GYG sequence is imperative for the transition to occur. Inter-subunit hydrogen bonds involving Tyr78 and Trp68 have been implicated in the "molecular spring" mechanism stabilizing the filter (Doyle *et al.*, 1998). Even though these interactions are not essential for channel selectivity (see section III-3.3) (Noskov *et al.*, 2004), they are involved in channel gating. When Tyr78 makes strong hydrogen bonds with Trp68 of an adjacent subunit, the probability of Val76 and Gly77 reorientation is reduced (Berneche & Roux, 2005). Asp80 to Arg89 inter-subunit salt bridges have similar effects (Figure 16).

In summary, the selectivity filter of K^+ channels can undergo a transition involving Val76–Gly77 and Thr75–Val76 in KcsA resulting in "trapping" of K^+ in site S3. This turns the filter into a non-conductive state. Occupation of site S2 by K^+ prohibits reorientation. Val76 reorientation bears many similarities with and might underlie C-type inactivation in Kv-channels as well as "fast gating" in Kir channels.

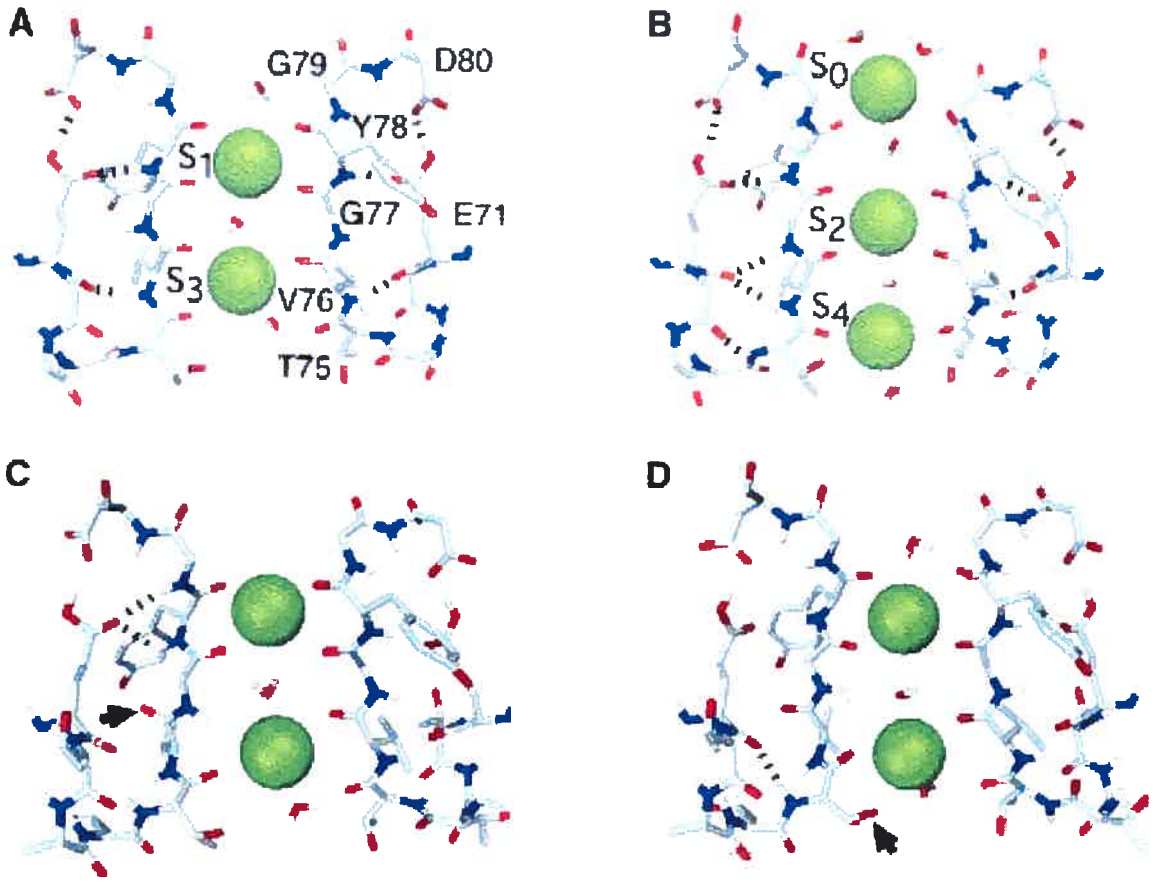

Figure 16: Gating in the selectivity filter of the KcsA K^+ Channel.

For clarity, only two of the four subunits are shown and some side chains are omitted. The dashed lines highlight the hydrogen bonds stabilizing the selectivity filter. Five specific cation binding sites, hereafter referred to as S0 to S4, are disposed along the narrow pore of the KcsA K^+ channel. The Figures in **A** and **B** correspond to the two main intermediate states that enable fast ion conduction with K^+ in sites S1 and S3 (**A**) and in sites S2 and S4 (**B**). The latter configuration is enforced by the presence of a third K^+-ion in the binding site S0 located at the extracellular end of the selectivity filter. The Figures in **C** and **D** illustrate the conformational transition of the selectivity filter as observed in Bernèche & Roux (2000). The complete transition takes place in two steps, respectively involving the Val76-Gly77 (**C**) and Thr75-Val76 (**D**) amide planes in one of the four monomers. **C**: In a first step, the carbonyl group of Val76 points away from the pore (indicated by an arrow). **D**: In a second step, the carbonyl

and side chain hydroxyl group (indicated by an arrow) of Thr75 closely coordinate the ion in S3, while the amide group forms a strong hydrogen bond with the carbonyl group of Glu71 (dashed line). Reproduced from Bernèche & Roux (2005).

CHAPTER IV: VOLTAGE-GATED POTASSIUM CHANNELS

IV-1 The Delayed Rectifier Current I_K

The delayed rectifier current I_K is mainly responsible for late phase 2 and phase 3 repolarization of the cardiac action potential (Apkon & Nerbonne, 1991; Tseng, 2001; Kurokawa *et al.*, 2001). It was first described in 1969 by Noble and Tsien (Noble & Tsien, 1969). In 1993, Wang, Fermini and Nattel demonstrated I_K in myocytes isolated from human atrium (Wang *et al.*, 1993b). Studies conducted in myocytes isolated from the ventricles of guinea pigs showed that I_K consists of two components I_{Kr} and I_{Ks} with distinct biophysical and pharmacological properties. One year later, Sanguinetti and Jurkiewizc identified both I_{Kr} and I_{Ks} in guinea pig atrium (Sanguinetti & Jurkiewicz, 1991) and in 1994, Wang et al. described I_{Kr} and I_{Ks} in human atrium (Wang *et al.*, 1994b). An ultra-rapidly activating delayed-rectifier current was identified by Wang and colleagues in human atrium and designated I_{Kur} (Wang *et al.*, 1993c). Since I_{Kur} is not found in human ventricle it is an interesting target for pharmacotherapy of atrial arrhythmias such as atrial fibrillation.

IV-1.1 Biophysical Properties

I_{Kr} activates rapidly at membrane potential of -40 to -30 mV and plateaus at voltages between +20 to +30 mV (Tseng, 2001). Its half activation voltage $V_{1/2}$ is -14 mV (Wang *et al.*, 1994b). Outward I_{Kr} current peaks at around 0-10 mV and displays inward rectification at potentials positive to +10 mV due to rapid inactivation that occurs at a faster rate than current activation (Tseng, 2001). When the membrane potential falls below 0 mV, I_{Kr} recovers from inactivation and further repolarizes the cell membrane during phase 3 of the cardiac AP. Kinetics of I_{Kr} activation and deactivation differ between species (Tseng & Hoffman, 1989) and cardiac regions (Gintant, 2000), possibly due to different channel subunit compositions or regionally distinct intrinsic α-subunit gating properties (London *et al.*, 1997; Lees-Miller *et al.*, 1997; Abbott *et al.*, 1999).

I_{Ks} activates slowly at potentials positive to 0 mV, has a linear current-voltage relationship and displays rapid current deactivation properties (Gintant, 1996; Wang

et al., 1994b). In human atrial myocytes, its half activation voltage $V_{1/2}$ averages +19.9 mV (Wang *et al.*, 1994b).

I_{Kur} activates near -30 mV and has a half-activation voltage of -4.3 mV. Activation is very rapid, about two orders of magnitude faster than the rapid component of the delayed rectifier K^+ current and displays temperature-dependent activation kinetics. The fully activated current-voltage relation shows outward rectification. Inactivation is limited. Selective inhibition of I_{Kur} prolongs APD in human atrial myocytes by 66 ± 11% (Wang *et al.*, 1993c).

IV-1.2. Pharmacology

I_{Kr} is selectively inhibited by methanesulfonanilides such as E4031 and Dofetilide (Spector *et al.*, 1996; Carmeliet, 1992). A wide variety of other therapeutic substances including antiarrhythmic drugs of various categories (Numaguchi *et al.*, 2000; Zhang *et al.*, 1999; Walker *et al.*, 2000; Busch *et al.*, 1998), prokinetic drugs (Mohammad *et al.*, 1997), antihistaminic agents (Suessbrich *et al.*, 1996; Zhou *et al.*, 1999), or antibiotics (Abbott *et al.*, 1999), and psychoactive drugs such as fluoxetine (Thomas *et al.*, 2002) and haloperidol (Suessbrich *et al.*, 1997) block I_{Kr} in a non-specific fashion, causing acquired long QT-syndrome possibly leading to potentially fatal cardiac arrhythmias.

I_{Ks} is E-4031 resistant and selectively blocked by Chromanol 293B (Busch *et al.*, 1996) and L-735821 (Propenamide) (Cordeiro *et al.*, 1998) in a frequency independent manner (Varro *et al.*, 2000).

I_{Kur} is highly sensitive to 4-AP and Quinidine and is resistant to TEA, DTX, Ba^{2+} and atropine (Wang *et al.*, 1995). In rabbit atrium, a depolarisation induced I_{Kur} is carried by Cl^- ions and is inhibited by the Cl^--transport blocker DIDS (Duan *et al.*, 1992). In human myocytes, I_{Kur} is a K^+ selective current that is insensitive to DIDS. Selective inhibition of I_{Kur} by 50 μM 4-AP causes a prolongation of atrial APD without affecting AP morphology (Wang *et al.*, 1993c).

IV-1.3 Functional relevance of I_K

IV-1.3.1 Role of Cardiac I_K

Regional variation of I_K in the heart is well recognized. In the SAN, deactivation of I_K contributes to diastolic depolarization (Zhang *et al.*, 2000; DiFrancesco, 1993; Irisawa *et al.*, 1993). In rabbits, a smaller I_{Kr} component is found in central SAN cells compared with peripheral cells possibly contributing to a more positive membrane potential and longer APD (Lei *et al.*, 2001). Atrial I_K consists of both I_{Kr} and I_{Ks} (Sanguinetti & Jurkiewicz, 1991; Yue *et al.*, 1996b; Wang *et al.*, 1994b). I_{Kr} density in the LA free-wall is higher than in the RA accounting for shorter LA APDs and ERPs (Li *et al.*, 2001). I_{Kur} has been described in atrial myocytes of various species (Boyle & Nerbonne, 1991; Bou-Abboud *et al.*, 2000; Wang *et al.*, 1993c; Yue *et al.*, 1996a) and is absent in the ventricles of humans and dogs (Li *et al.*, 1996;Yue *et al.*, 2000).

In the AVN, I_{Kr} predominates over I_{Ks} (Sato *et al.*, 2000). In AV nodal cells, I_{Kr} activation contributes to repolarization and deactivation of I_K, which is faster in the AVN than in the ventricle (Howarth *et al.*, 1996), contributes to diastolic depolarization (Hancox & Mitcheson, 1997).

In Purkinje cells, I_{Kr} is similar to atrial and ventricular I_{Kr} (Han *et al.*, 2000). In ventricular myocytes, a larger epicardial I_{Kr} (Bryant *et al.*, 1998; Main *et al.*, 1998), contributes to shorter APD in epicardial myocytes (Litovsky & Antzelevitch, 1988). Midmyocardial (M-) cells have larger I_{Kr} (Bryant *et al.*, 1998) than endocardial cells and smaller I_{Ks} than epi- and endocardial cells contributing to longer M-cell APD (Liu & Antzelevitch, 1995; Gintant, 1995). I_{Ks} is larger in RV M-cells, possibly explaining their shorter APD compared to LV M-cells (Volders *et al.*, 1999). Even though I_{Kr} appears to be larger in apical myocytes, smaller apical I_{Ks} might contribute to longer APD in apical myocytes (Cheng *et al.*, 1999).

Blockade of I_{Kr} lengthens cardiac APD (Singh & Vaughan Williams, 1970; Strauss *et al.*, 1970; Jurkiewicz & Sanguinetti, 1993) exerting an antiarrhythmic effect by increasing refractory wavelength. I_{Kr} block occurs in a reverse use-dependent fashion (Hondeghem & Snyders, 1990), limiting its therapeutic usefulness.

At faster heart rates, when I_{Kr} block is desired to prolong APD and break the tachycardia, block of I_{Kr} is small. Conversely, at slow heart rates block is high and APD is greatly prolonged, predisposing to early afterdepolarizations (EADs), potentially triggering torsade de pointe ventricular arrhythmias in the His-Purkinje system (El Sherif *et al.*, 1996; Asano *et al.*, 1997).

Selective block of I_{Ks} occurs in a frequency independent manner (Varro *et al.*, 2000). Contradictory findings on the effect of selective I_{Ks} blockade on APD have been published. Whereas application of Chromanol 293B and L-735821 increased APD in human and guinea pig ventricular myocytes (Bosch *et al.*, 1998) and rabbit PC (Cordeiro *et al.*, 1998), other authors found that Chromanol 293B only slightly lengthened APD in guinea pig right papillary muscle (Schreieck *et al.*, 1997) or dog PC and ventricular muscle (Varro *et al.*, 2000). Differences observed have been explained by differences in I_{Ks} expression and current availability due to its activation at relatively positive membrane potentials and fast deactivation kinetics (Varro *et al.*, 2000). Recordings of I_{Ks} during test pulses mimicking action potentials resulted in outward currents with less than one tenth of the magnitude of I_{Kr} throughout all phases of the AP-like test pulse. However, when APD was lengthened by application of E-4031 and the sodium channel agonist veratrine, selective block of I_{Ks} markedly increased APD (Varro *et al.*, 2000). These results suggest that under physiological conditions I_{Ks} plays a little role in AP repolarization due to its slow activation kinetics. When APD becomes longer, I_{Ks} has more time to activate and its amplitude and thus contribution to repolarization increases. In accordance with the lack of APD prolongation under physiological conditions, Chromanol 293B did not increase QTc in anaesthetized dogs (Varro *et al.*, 2000).

In summary, regional differences in ventricular I_K current density may play an important role in the pathogenesis of ventricular fibrillation (Choi *et al.*, 2001). I_{Kr} is the main repolarizing current of the cardiac action potential. I_{Ks} appears to play little role in cardiac repolarization under normal conditions but limits excessive APD lengthening when repolarization is abnormally lengthened thus providing an important safety mechanism (Varro *et al.*, 2000). The effect of I_{Ks} block in the presence of sympathetic stimulation on APD is controversial (Vanoli *et al.*, 1995;

Schreieck *et al.*, 1997; Varro *et al.*, 2000). In humans and dogs, I_{Kur} contributes solely to atrial repolarization, making it an interesting target for antiarrhythmic therapy of supraventricular arrhythmias without the risk of ventricular pro-arrhymia

IV-1.3.2 Role of I_K-like Currents in Endothelial Cells

Endothelial cells are non-excitable and changes in membrane potential in these cells are slow and small, suggesting little role in voltage-dependent currents in ECs. Hogg et al. (1999) found a voltage-dependent current in rat pulmonary artery ECs. This current activated at -37 mV and exhibited time-dependent activation and little inactivation. It was highly sensitive to 4-AP but insensitive to TEA. Immunohistochemical staining revealed extensive expression of Kv1.5 protein in rat pulmonary artery endothelium (Hogg *et al.*, 1999). Thus, I_{Kur} might play a role in control of the resting potential in these cells.

A 10 mM TEA sensitive non-inactivating delayed rectifier current was found in 60% of freshly isolated human capillary endothelial cells (HCEC). However, no detailed analysis of biophysical or pharmacological properties was performed. The molecular basis of this current was not investigated (Jow *et al.*, 1999).

In summary, delayed rectifier currents have been demonstrated in endothelial cells. However, their physiological significance is not clear. It was suggested that depolarization activated K^+-currents may play a role in membrane potential oscillations of endothelial cells (Dittrich & Daut, 1999)

Genes, nomenclature and tissue distribution of voltage-gated K^+ (Kv) channel α- and β-subunits are summarized in Table II.

IV-1.4 Molecular Basis of I_K

IV-1.4.1 MinK and KvLQT1 underlie I_{Ks}

A structurally unusual K^+ channel was cloned from rat kidney and designated IsK or minK (for minimal K^+ channel) (Takumi *et al.*, 1988; Murai *et al.*, 1989). Surprisingly, minK was found to consist of only one transmembrane segment. The functional role of minK was controversial for a long time. Many authors believed that

despite its unusual structure, minK was acting as a channel by itself. This view changed in 1996 when the laboratories of Mark Keating and George Romey showed in a back to back publication in Nature that minK co-assembles with the voltage-gated channel subunit KvLQT1 (KCNQ1) to form the slow component of the cardiac inward-rectifier current I_{Ks}. Expression of KvLQT1 cDNA in CHO cells produces a small, rapidly activating outwardly rectifying current. Co-expression with minK increases current size and slows down activation kinetics tenfold (Sanguinetti *et al.*, 1996; Barhanin *et al.*, 1996). Inherited mutations of minK are associated with long-QT syndrome and the Jervell-Lange Nielsen syndrome, possibly through decreased I_{Ks} caused by mutant minK subunits (Sesti & Goldstein, 1998). It is now firmly established that minK does not form functional channels but acts as a β-subunit to modulate properties of the delayed outward rectifier current I_{Ks}.

IV-1.4.2 HERG and MiRP: The Molecular Basis of I_{Kr}?

In 1991, Warmke and colleagues cloned a new subgroup of voltage gated K^+ channels from the Drosophila "ether-à-go-go" (*eag*) locus (Warmke *et al.*, 1991). Expression of *eag* in *Xenopus* oocytes resulted in cAMP modulated K^+ and Ca^{2+} permeable channels (Bruggemann *et al.*, 1993). Subsequently, homologues of *eag* were cloned from rat brain (*r-eag,* Ludwig *et al.* (1994)) and mouse chromosome 17 (Hoglund *et al.*, 1992). A human *eag* related gene was discovered by screening a human hippocampus cDNA library (Warmke & Ganetzky, 1994) and was designated HERG (for "human ether-related gene). HERG is predominantly expressed in human heart and mutations in this gene underlie the long QT syndrome type 2 (LQT2) (Curran *et al.*, 1995).

McDonald and colleagues demonstrated that minK can upregulate current density of I_{Kr} through assembly with HERG without changing kinetics (McDonald *et al.*, 1997). A subunit similar to minK was discovered in 1999 by Abbott and colleagues and designated minK related peptide 1 (MiRP1) (Abbott *et al.*, 1999). Mutations in MiRP1 are linked to dysfunction of I_{Kr} causing a congenital long-QT syndrome (LQT6). Co-expression of MiRP1 with HERG resulted in currents with properties more similar to I_{Kr} than when HERG alone was expressed (Abbott *et al.*,

1999). This led to the assumption that HERG co-assembles with MiRP1 to form I_{Kr}. However, effects of MiRP on HERG differ when different expression systems are used (Abbott *et al.*, 1999; Mazhari *et al.*, 2001) challenging the notion of a MiRP/HERG complex as molecular basis of I_{Kr} (Weerapura *et al.*, 2002) and leaving the role of MiRP1 in the heart unclear (Pourrier *et al.*, 2003a) until today (Anantharam & Abbott, 2005).

IV-1.4.3 Molecular Basis of Physiological Function in the Heart

KvLQT1, minK and ERG transcripts are present in atrium (Brahmajothi *et al.*, 1997a; Pond *et al.*, 2000) consistent with the presence of both I_{Kr} and I_{Ks} (Sanguinetti & Jurkiewicz, 1991; Yue *et al.*, 1996b; Wang *et al.*, 1994b). ERG protein levels in dogs are larger in the LA (Li *et al.*, 2001). Kv1.2/Kv1.5 currents have been recorded from rat atrium (Bou-Abboud & Nerbonne, 1999) and antisense directed against Kv1.5 inhibits I_{Kur} in human atrium (Feng *et al.*, 1997). In dogs, Kv3.1 encodes I_{Kur} and is present in atrium but undetectable in ventricle, just like the corresponding current (Yue *et al.*, 2000). Both ERG and KvLQT1 RNA and protein are expressed.

In ventricular myocytes, ERG protein expression is stronger in the epicardium than in the endocardium (Brahmajothi *et al.*, 1997b) possible explaining a larger epicardial I_{Kr} (Bryant *et al.*, 1998; Main *et al.*, 1998). ERG mRNA in canine ventricle is 1.5-fold more abundant than Kv4.3 consistent with its predominant role in ventricular repolarization (Wymore *et al.*, 1997). MinK mRNA levels in humans are similar in epi-, mid- and endocardial tissues. A dominant negative KvLQT is more strongly expressed in midmyocardial cells potentially accounting for lower M-cell I_{Ks} (Pereon *et al.*, 2000).

IV-1.4.4 Role of I_K-like Currents in the Central Nervous System

Mutations in Drosophila *eag* cause repetitive firing and enhanced transmitter release in motor neurons (Ganetzky & Wu, 1983; Wu *et al.*, 1983). Even though HERG is predominantly expressed in the heart, it was initially cloned from a human hippocampal cell line (Warmke & Ganetzky, 1994), suggesting potential functional importance in the control of neuronal excitability. In drosophila, ERG-type channels

sharing 71% homology with HERG are expressed throughout the CNS of embryonic Drosophila (Titus *et al.*, 1997). Lesions in the ERG-coding sequence are associated with temperature-sensitive paralysis due to spontaneous increase in neuronal activity of flight motoneurons (Wang *et al.*, 1997). However, no such role has been described so far in mammals (Ganetzky *et al.*, 1999) and the functional role of HERG in the CNS of mammals is unclear.

Mutations in KvLQT1 are associated with Jervell and Lange-Nielsen syndrome, an autosomal recessive syndrome with bilateral deafness and QT interval prolongation, and Romano Ward syndrome (Jentsch, 2000). KvLQT1 is not expressed in the CNS and consequently does not have a functional role in the CNS (Jentsch, 2000).

IV-2 The Transient Outward Current I_{to}

A transient outward current was first described in neurons and designated A-type current (Hagiwara *et al.*, 1961). In the heart, it was first described in 1964 in sheep Purkinje cells and thought to be a chloride current (Deck & Trautwein, 1964). Subsequent studies showed that I_{to} consisted of two components, a Ca^{2+} independent 4-AP sensitive K^+ current I_{to1} and a Ca^{2+} sensitive, 4-AP insensitive Cl^- current. I_{to2} is a short, Ca^{2+}-insensitive Cl^- current that activates slower but inactivates faster than I_{to1}. It is inhibited by caffeine, Co^{2+} or a previous transient outward current. Caffeine, isoproterenol or increased Ca^{2+} concentrations increase I_{to2} suggesting its physiological activation by increased Ca^{2+} release from the sarcoplasmatic reticulum. In rabbit ventricular myocytes, both I_{to1} and I_{to2} activate at potentials between -30 and -20 mV (Fermini *et al.*, 1992). At the same test potential, I_{to1} is larger and activates faster than I_{to2}. For the purpose of simplification, the term I_{to} will be used to refer to I_{to1} from now on and there will be no further mentioning of I_{to2}.

I_{to} was demonstrated in various species, including humans (Escande *et al.*, 1987; Coraboeuf & Carmeliet, 1982; Salkoff, 1983; Tseng & Hoffman, 1989; Hiraoka & Kawano, 1989) and is present in various cardiac regions including the atria (Clark *et al.*, 1988), the AV-node (Nakayama & Irisawa, 1985), the crista terminalis (Giles & van Ginneken, 1985), Purkinje cells (Kenyon & Gibbons, 1979) and the ventricles (Giles & Imaizumi, 1988; Josephson *et al.*, 1984).

IV-2.1 Pharmacology and Biophysical Properties

I_{to} is a K^+ selective current and is sensitive to 4-AP, flecainide, quinidine and Ba^{2+} (Fermini *et al.*, 1992; Yeola & Snyders, 1997; Himmel *et al.*, 1999) as well as to various toxins such as heteropodatoxins (Xu *et al.*, 1999a; Sanguinetti *et al.*, 1997; Brahmajothi *et al.*, 1999), hanatoxin (Himmel *et al.*, 1999; Swartz & MacKinnon, 1997) phrixotoxins (Diochot *et al.*, 1999) and Tarantula toxins (Escoubas *et al.*, 2002). Native cardiac I_{to} has been stratified into $I_{to,f}$ and $I_{to,s}$ (fast and slow) according to their rate of inactivation (Nerbonne, 2000). Activation of both types is very rapid (τ_a ~ 2-10 ms) but rates of inactivation and recovery from inactivation are differing

($\tau_{iIto,f}$ ~ 25-80 ms and $\tau_{iIto,s}$ ~ 80-200 ms; $\tau_{recIto,f}$ ~ 25-80 ms and $\tau_{recIto,s}$ ~ 1-2 s) (Oudit *et al.*, 2001; Nabauer *et al.*, 1996). I_{to} in human (Han *et al.*, 2001b) and canine (Han *et al.*, 2000) PCs display unique properties including sensitivity to 10 mM TEA and sensitivity to 4-AP which is about one order of magnitude greater than in ventricular myocytes and slower reactivation.

IV-2.2 Functional Role of A-type Currents

IV-2.2.1 Role of Cardiac I_{to}

I_{to} is primarily responsible for early repolarization of atrial and ventricular APs (Oudit *et al.*, 2004). Therefore, it affects L-type Ca^{2+} current magnitude thus indirectly modulating excitation-contraction coupling, myocardial contractility and repolarization. Because of interactions with delayed-rectifier K^+- and L-type Ca^{2+}-current (Courtemanche *et al.*, 1998; Greenstein *et al.*, 2000), I_{to} can have differential consequences on APD (Oudit *et al.*, 2001). For example, inhibition of I_{to} in dogs results in a shortening of the cardiac AP (Litovsky & Antzelevitch, 1988) whereas selective inhibition of I_{to} in rodents results in APD prolongation and can cause EADs (Shimoni *et al.*, 1992; Barry *et al.*, 1998; Xu *et al.*, 1999b; Guo *et al.*, 2000). Complete loss of ventricular I_{to} is associated with susceptibility to ventricular tachycardia (Kuo *et al.*, 2001). Heterogeneity of I_{to} density is believed to contribute to regional AP variability (Oudit *et al.*, 2001) resulting in more synchronous repolarization (Antzelevitch *et al.*, 1991) and contributing to regional modulation of contractility (Volk *et al.*, 1999).

I_{to} current density varies among different regions of the heart as well as among species. The general pattern observed is that $I_{to,s}$ density is generally high in regions with longer APD such as the septum, left ventricular endocardium and apex of the heart, while $I_{to,f}$ is favoured in epicardial regions, the right ventricle and the base of the heart (Oudit *et al.*, 2001). Rabbits preferentially express $I_{to,s}$ in both atrium and ventricle (Giles & Imaizumi, 1988; Fedida & Giles, 1991; Wang *et al.*, 1999) while most other species express predominantly $I_{to,f}$ (Barry & Nerbonne, 1996; Nerbonne, 2000).

I_{to} is absent in the SAN (Guo *et al.*, 1997). In the atrium, regional expression differences might possibly contribute to the short plateau phase, relatively slow phase 3 repolarization and AP heterogeneity (Schram *et al.*, 2002b). Little is known about the functional role of I_{to} in AVN but targeted deletion of the gene encoding $I_{to,f}$ in mice causes AV block (Guo *et al.*, 2000). Purkinje cell I_{to} in humans (Han *et al.*, 2001b) and dogs (Han *et al.*, 2000) shows striking differences compared to ventricular I_{to} including sensitivity to TEA, a ~ 9-fold greater sensitivity to 4-AP and slower reactivation compatible with Kv3.4 potentially encoding PC I_{to} (Han *et al.*, 2001a).

In the ventricles, peak I_{to} density is higher in the RV than in the LV (Di Diego *et al.*, 1996) and larger in epicardium than endocardium (Liu *et al.*, 1993; Furukawa *et al.*, 1990; Fedida & Giles, 1991; Wettwer *et al.*, 1994). Larger epicardial I_{to} underlies the prominent spike and dome configuration of the epicardial AP (Figure 5) (Sicouri & Antzelevitch, 1991). In humans, epicardial I_{to} shows faster recovery from inactivation than endocardial I_{to} (Nabauer *et al.*, 1996). Although it is believed that I_{to} does not contribute to specific M-cell properties (Antzelevitch *et al.*, 1991), it can not be excluded that in addition to a larger RV I_{Ks}, I_{to} might contribute to shorter RV M-cell APDs (Volders *et al.*, 1999).

In summary, I_{to} is of crucial importance for early repolarization of atrial and ventricular APs. I_{to} expression shows great regional variability and properties differ between species. Loss of ventricular I_{to} might cause potentially life threatening tachycardia.

IV-2.2.2 Role of A-Type Currents in Endothelial Cells

A depolarization activated outward current with characteristics of a transient outward (A-type) current in endothelial cells was first described by Takeda et al. in cultured BAECs (Takeda *et al.*, 1987). This current was seen in about 30% of the cells, activated near -10 mV, was inactivated by depolarizing prepulses and blocked by 5 mM 4-AP. In human capillary endothelial cells (HCECs) cultured in conditioned media, a 3 mM 4-AP sensitive transient outward current was observed in 24.7% of the cells. This current was fully inactivated at a membrane potential of -20 mV. Mean

steady state half activation ($V_{1/2}$) occurred at +12.0±1.8 mV and $V_{1/2}$ of inactivation was -40.0±1.6 mV (Jow *et al.*, 1999). In rabbit corneal epithelium, 94% of the cells contained a 4-AP and quinidine sensitive, rapidly activating A-type current with $V_{1/2}$ of activation +3.5 mV and $V_{1/2}$ of inactivation of -42 mV (Watsky *et al.*, 1992). A-type currents were also observed in bovine pulmonary artery endothelial cells (Silver & DeCoursey, 1990).

In summary, A-type currents have been detected in endothelial tissue cells. Their presence suggests a role in regulation of EC cell function by repolarization of depolarized membrane potentials. However, endothelial cells undergo profound changes in metabolism and electrical properties during culture (Tracey & Peach, 1992; Nilius & Droogmans, 2001) and studies examining a functional role of these currents in freshly isolated ECs are lacking. Thus, the physiological relevance of voltage-gated channels in ECs remains yet to be determined. As previously stated, depolarization activated K^+-currents may play a role in membrane potential oscillations of endothelial cells (Dittrich & Daut, 1999).

IV-2.3 Molecular Basis of A-type currents

IV-2.3.1 Transmembrane Alpha-subunits

Up to date, nine families of Kv channels are known (Table II, Figure 7). Whereas channels belonging to Kv1–Kv4 subfamilies conduct ionic current, Kv5–Kv9 subfamily members are have regulatory function and do not conduct current by themselves. The IUPHAR proposed in its most recent update on K^+ channel nomenclature to include *eag* and KCNH related K^+ channels in the Kv nomenclature and categorized KCNH, *eag*, erg and Elk related K^+ channels in the Kv7, Kv10, Kv11 and Kv12 subfamilies, respectively (Gutman *et al.*, 2003).

Four α-subunits co-assemble to form a functional ion channel (MacKinnon, 1991). A channel protein consisting of four identical subunits is called a homotetramer. If subunits are different the channel is termed a heterotetramer. Formation of heterotetrameric channels is an important way to adjust ion channel function to physiological requirements. Alpha-subunit co-assembly among voltage

gated channels is limited to the channel subfamily (i.e. Kv1 channels will only co-assemble with Kv1 channels, Kv2 only with Kv2 and so on), a property conferred by the N-terminus (Isacoff *et al.*, 1990). Kv α-subunits Kv5 - Kv9 are the exception to the rule. As mentioned above, these channels remain silent when heterologously expressed but co-assemble with and modulate the properties of Kv2 and Kv3 subunits (Hugnot *et al.*, 1996; Stocker *et al.*, 1999). Co-assembly of Kv1-Kv4 channels is coordinated by the N-terminal T1 domain (Papazian, 1999; Kreusch *et al.*, 1998; Gulbis *et al.*, 2000). The "turret" (the external helix between segment S5 and the P-helix) serves as a binding site for toxins and several K^+ channel blockers such as charybdotoxin (Goldstein & Miller, 1993; MacKinnon & Miller, 1988) and TEA (Pascual *et al.*, 1995). In addition to external block at the turret, cytosolic application of TEA blocks the channel in the central cavity (Lopez *et al.*, 1994; Shieh & Kirsch, 1994). Interestingly, tarantula toxin binds to the S4 segment and inhibits channel function by inhibition of S4 movement within the membrane without affecting the pore (Ruta & MacKinnon, 2004).

IV-2.3.2 Auxiliary Subunits

Auxiliary beta-subunits modulate biophysical and pharmacologic properties of associated α-subunits and regulate α-subunit trafficking and tissue distribution of ion channels. Interaction between α- and β-subunits can be dynamic and/or can be modulated by other cytoskeletal proteins (Pourrier *et al.*, 2003a) such as Kvβ subunits (Kuryshev *et al.*, 2001).

IV-2.3.2.1 Kvβ-Subunits

Kvβ subunits are cytoplasmatic subunits that associate with the T1 domain of Kv1 and Kv2 channels (Gulbis *et al.*, 2000). Kvβ1 and 2 were cloned from rat brain in 1994 and confer channel inactivation to Kv1 channels (Rettig *et al.*, 1994; Majumder *et al.*, 1995). Three different β-subunits, Kvβ1-3, arise through alternative splicing of the Kvβ1 gene (England *et al.*, 1995). These subunits regulate inactivation as well as channel maturation and cell surface localization (Shi *et al.*, 1996). A fourth subunit, Kvβ4, increases functional expression of Kv2 subunits and is not expressed in the heart (Fink *et al.*, 1996b).

IV-2.3.2.2 K^+ channel Interacting Protein (KChIP)

KChIPs are cytoplasmatic proteins with a C-terminal domain containing 4 EF-hand like Ca^{2+} binding domains (An *et al.*, 2000). They are encoded by at least four genes, KChIP1-4, and consist of a conserved core region and a variable N-terminal peptide (An *et al.*, 2000). All four KChIP genes are widely expressed in the brain, whereas only KChIP2 mRNA is abundant in the heart (An *et al.*, 2000; Rosati *et al.*, 2001). At least three isoforms of KChIP2 encoding 220, 252 and 270 amino acid proteins sharing 70% homology are expressed in the heart (An *et al.*, 2000; Bahring *et al.*, 2001; Rosati *et al.*, 2001; Ohya *et al.*, 2001; Decher *et al.*, 2001; Deschenes *et al.*, 2002). KChIP effects are specific for Kir4 subunits. The first 40 N-terminal amino acids of Kv-channels interact with KChIPs (An *et al.*, 2000; Bahring *et al.*, 2001). The crystal structure of the core domain of KChIP1 in complex with the N-terminus of Kv4.2 shows a clam-shaped dimeric assembly. The major interface between theses two proteins is formed by the N-terminal end of the α-helix of Kv4.2 and the C-terminal α-helix of KChIP. A pair of these helices is deeply buried in a hydrophobic groove between two shells in an anti-parallel fashion, and is crucial for stability of the dimer. Hydrophobic interactions are essential for KChIP mediated modulation of Kv-channels (Zhou *et al.*, 2004).

In heterologous systems, KChIP increases Kv4.2 current density, shifts inactivation $V_{1/2}$ to more positive potentials, slows inactivation and accelerates recovery from inactivation (An *et al.*, 2000). Similar effects on Kv4.3 subunits have been described (Bahring *et al.*, 2001; Decher *et al.*, 2001; Deschenes *et al.*, 2002). Association of with Kv4.2 and Kv4.3 subunits might contribute to regulation of the transient outward current I_{to} (Deschenes *et al.*, 2002; Rosati *et al.*, 2001).

IV-2.3.2.3 K^+ channel Associated Peptide (KChAP)

The cytoplasmatic K^+ channel accessory subunit, KChAP, was cloned in 1998 (Wible *et al.*, 1998). It belongs to the family of transcription factor binding proteins and increases Kv1.3/2.1/2.2/4.3 subunit current density without any effect on current kinetics and gating. Although KChAP interacts with the N-termini of Kv1 channels it only affects Kv1.3 current expression. Other than Kvβ subunits that form stable

Kvα/β heteromultimers, KChAP interacts only transiently with Kv α-subunits (Wible *et al.*, 1998; Kuryshev *et al.*, 2000). Effects of KChAPs may be indirectly regulated by an interaction with Kvβ subunits (Kuryshev *et al.*, 2001).

IV-2.3.2.4 MinK Related Peptide (MiRP)

Association between MiRP2 and Kv3.4 in skeletal muscle affects unitary conductance, voltage-dependent activation, recovery from inactivation and steady-state open probability. A missense mutation in MiRP2 is associated with periodic paralysis (Abbott *et al.*, 2001). Association of MiRP1 with Kv4.3 increases Kv4.3 current density and affects gating kinetics. The physiological significance of this finding is uncertain (Deschenes & Tomaselli, 2002). MiRP1 might have a role in native I_{to}, particularly in Purkinje fibres where mRNA expression is high (Pourrier *et al.*, 2003b).

IV-2.3.2.5 MinK

MinK modulates Kv4.3 currents in HEK93 cells. Co-expression of minK and Kv4.3 increases Kv4.3 current and slows its activation, inactivation and recovery from inactivation without affecting voltage-dependence of inactivation (Deschenes & Tomaselli, 2002). The physiological significance of these results is unclear.

IV-2.3.3 Molecular Basis of Cardiac I_{to} Heterogeneity

Principal subunits encoding I_{to} include Kv1.4, Kv4.2 and Kv4.3 (Nerbonne, 2000). Kv1.4 is the predominant subunit in rabbit atrium (Wang *et al.*, 1999) consistent with high $I_{to,s}$ density (Giles & Imaizumi, 1988; Fedida & Giles, 1991; Wang *et al.*, 1999). Kv1.4 protein is almost undetectable in rat atrium and ventricle (Barry *et al.*, 1995) and Kv4.3 protein is selectively expressed in human atrium (Wang *et al.*, 1999) accounting for high $I_{to,f}$ current density (Barry & Nerbonne, 1996; Nerbonne, 2000).

Little is known about the functional role of I_{to} in AVN but targeted deletion of the Kv1.4 and Kv4.3 in mice causes AV block (Guo *et al.*, 2000).

Ventricular I_{to} is predominantly encoded by Kv4.2 and Kv4.3 (Barry *et al.*, 1995; Wickenden *et al.*, 1999; Fiset *et al.*, 1997; Yeola & Snyders, 1997). In rats, the gradient in I_{to} density in the LV wall correlates with Kv4.2 mRNA expression (Dixon & McKinnon, 1994) whereas the transmural I_{to} gradient in ferrets is due to stronger endocardial expression of Kv1.4 versus epicardial predominance of Kv4.2 and Kv4.3 mRNA expression (Dixon *et al.*, 1996; Kaab *et al.*, 1998). In dogs and humans, ventricular I_{to} is entirely encoded by Kv4.3 (Dixon *et al.*, 1996; Kaab *et al.*, 1998; Zhu *et al.*, 1999b). Higher protein expression of the regulatory subunit KChIP in epicardial cells is thought to underlie the transmural I_{to} gradient (Rosati *et al.*, 2001). Kv1.4 is thought to encode $I_{to,s}$ in rodents whereas $I_{to,f}$ is encoded by Kv4.2 and Kv4.3 (Guo *et al.*, 1999). Kv4.1 mRNA expression is very low suggesting limited relevance to native I_{to} (Dixon & McKinnon, 1994). The functional importance of KChIP for I_{to} has been demonstrated by elimination of I_{to} in a KChIP knockout model in mice (Kuo *et al.*, 2001). KChAP may be a chaperone for Kv-channels that form I_{to} (Wible *et al.*, 1998) and modulate regulation by Kvβ-subunits (Kuryshev *et al.*, 2001).

In summary, Kv1.4 subunits are believed to underlie $I_{to,s}$ in rodents, whereas Kv4.2 and Kv4.3 conduct $I_{to,f}$. Heterogeneity of I_{to} expression might be caused by differential Kv subunit and/or KChIP expression and is believed to contribute to regional modulation of contractility.

IV-2.3.4 Molecular Basis of A-Type Currents in the CNS

Electrical signalling in the CNS is largely determined by the action of voltage-gated ion channels (Trimmer & Rhodes, 2004). Kv subunits are widely expressed in the CNS.

The three most abundant Kv1 subunits in the CNS, Kv1.1, Kv1.2 and Kv1.4 are predominantly expressed on axons and nerve terminals and often form heteromeric channel complexes. Heteromeric Kv1.1/Kv1.4 complexes are expressed in the globus pallidus and pars reticulata of the substantia nigra (Rhodes *et al.*, 1997; Sheng *et al.*, 1992) whereas Kv1.1/Kv1.2 complexes localize in the cerebellar basket cell terminals (McNamara *et al.*, 1993; McNamara *et al.*, 1996; Wang *et al.*, 1994a) and the juxtaparanodal membrane adjacent to nodes of Ranvier (Wang *et al.*, 1993a).

Kv1.1, Kv1.2 and Kv1.4 expression in the hippocampus displays complex heterogeneity of subunit association (Trimmer & Rhodes, 2004). Kv1.1, Kv1.2 and Kv1.4 proteins are also highly abundant along axons and in the preterminal axonal membrane (Cooper *et al.*, 1998; Wang *et al.*, 1993a; Wang *et al.*, 1994a) suggesting a key role in regulation of nerve terminal depolarization and neurotransmitter release (Trimmer & Rhodes, 2004). In hippocampal mossy fibre terminals, complexes of Kv1.1/Kv1.4 and Kvβ1 are thought to underlie a DTX- and TEA Kv-channel conductance regulating frequency-dependent spike broadening, which controls the extent and duration of neurotransmitter release as a function of AP frequency (Geiger & Jonas, 2000; Bischofberger *et al.*, 2002). In cerebellar large basket cells, DTX-sensitive Kv1 channels underlie the low-threshold Kv current, which modulates GABA release from basket cell terminals (Southan & Robertson, 1998; Southan & Robertson, 2000). Kv1.3, Kv1.5 and Kv1.6 protein expression in the mammalian brain is lower. Kv1.3 is predominantly expressed in the cerebellar cortex where it might form heteromeric channel complexes with Kv1.1 (Rhodes *et al.*, 1997). Expression of Kv1.5 protein may be restricted to glial cells (Khanna *et al.*, 2001; Chittajallu *et al.*, 2002) and overall expression in the CNS is low (Felix *et al.*, 1999). Kv1.6 is expressed throughout the brain on principal cell dendrites and found predominantly in interneurons (Rhodes *et al.*, 1997). Kv1.7 is not expressed in the brain. Missense mutations of Kv1.1 causing episodic ataxia type 1 (EA1) were first described by Browne *et al.* (1994). EA1 is an autosomal dominant disorder in which cerebellar incoordination is triggered by exertion, stress or startle. Phenotypes vary and can include epilepsy, infantile contractions and isolated myotonia. Meanwhile a great variety of Kv1.1 mutations underlying EA1 has been described. Failure of motor axon repolarization might cause neuromyotonia. Since Kv1.1 is present in both Purkinje cells and axons of cerebellar basket cells (which inhibit Purkinje cells) it is not clear whether ataxia is due to increased or decreased output from the cerebellar cortex (Kullmann, 2002). Kv1.1 knockout mice suffer from seizures and shaking attacks at low temperatures caused by repetitive firing of preterminal motor neurons (Zhou *et al.*, 1998).

Kv2 channels are abundant in mammalian brain and localize to somatodendritic domains of neurons in large clusters (Trimmer, 1991; Hwang *et al.*, 1993b; Du *et al.*, 1998; Maletic-Savatic *et al.*, 1995; Scannevin *et al.*, 1996). The physiological significance of this clustering is unknown (Trimmer & Rhodes, 2004). Pyramidal cells in the cortex and hippocampal cells express particularly high levels of Kv2.1 (Du *et al.*, 1998). Kv2.2 expression is found on dendrites of most cells expressing Kv2.1 (Hwang *et al.*, 1993a; Lim *et al.*, 2000). Due to differences in subcellular localization, formation of heteromultimeric channels is unlikely (Trimmer & Rhodes, 2004) though structurally possible (Blaine & Ribera, 1998). Kv2.2 is highly expressed in olfactory bulb and cortical pyramidal neurons (Trimmer & Rhodes, 2004). Somatodendritic Kv channels control subthreshold excitatory responses, as well as amplitude and duration of back-propagating action potentials (Hoffman *et al.*, 1997; Hoffman *et al.*, 1959). Dendritic Kv channels regulate contributions of dendritic Cav and Nav channels to somatodendritic excitation (Trimmer & Rhodes, 2004). Activation or inhibition of somatic Kv channels might play a crucial role in determining whether or not the summed level of excitation reaching the soma is sufficient to elicit an action potential (Murakoshi & Trimmer, 1999).

Kv3.1 and Kv3.2 transcript expression in the cerebral cortex and hippocampus is low (Perney *et al.*, 1992; Weiser *et al.*, 1995) and displays a distinct expression pattern (Weiser *et al.*, 1995) suggesting that different subtypes of Kv3 channels may differentially regulate neuronal firing patterns. Subcellular localization of Kv3 subunits is partially determined by alternative splicing (Ponce *et al.*, 1997; Ozaita *et al.*, 2002). Kv3.3 subunit mRNA is expressed in Purkinje cells of the cerebellar cortex and deep cerebellar nuclei (Goldman-Wohl *et al.*, 1994). Heteromeric Kv3.1/Kv3.3 channels may regulate excitability of brainstem auditory neurons and Purkinje cell somata and dendrites (Martina *et al.*, 2003). In the neocortex and the hippocampus (Weiser *et al.*, 1995; Rettig *et al.*, 1992), Kv3.4 is localized to axons and nerve terminal similarly to Kv1 subunits. Even though expression of Kv3.4 overlaps with Kv1.1 and Kv1.4 in cerebellar basket cell terminals, the subcellular location of these subunits is distinct (Laube *et al.*, 1996). A high-voltage activated

conductance with biophysical properties similar to Kv3 subunits has been recorded in these terminals (Southan & Robertson, 2000). In certain fast-spiking cells, Kv3.4/Kv3.1 and/or Kv3.4/Kv3.2 heteromeric channels might underlie a fast-delayed rectifier current (Baranauskas *et al.*, 2003). In Purkinje cell dendrites, Kv3.3/Kv3.4 might be involved in shaping responses to relatively strong depolarizing events (Martina *et al.*, 2003).

Kv4 subunits are primarily expressed in the dendrites of central neurons. High levels of Kv4.2 and Kv4.3 mRNA are expressed in the hippocampus and CA3 pyramidal neurons. Absence of Kv4.3 mRNA suggests a unique role for Kv4.2 homomeric channels in CA2 and CA1 pyramidal cells. Kv4.3 homomeric channels might play a functional role in many interneurons where Kv4.2 mRNA is absent (Trimmer & Rhodes, 2004; Rhodes *et al.*, 2004). In the neocortex, Kv4.2 protein is expressed in pyramidal cell layer V whereas Kv4.3 is expressed in layer II as well as in interneurons throughout layers II-VI (Trimmer & Rhodes, 2004). Somatodendritic A-type currents in mammalian central neurons are largely mediated by Kv4 channel subunits, that might co-assemble with KChIPs (An *et al.*, 2000) or dipeptidyl-peptidase-like proteins (DPPX) (Nadal *et al.*, 2003) as an accessory subunit. A-type currents control subthreshold excitation and amplitude of back-propagating action potentials thereby regulating synaptic integration and plasticity (Hoffman *et al.*, 1997; Johnston *et al.*, 2000). In neocortical and hippocampal cells, A-type current density increases with distance from the soma conferring increasing inhibition of postsynaptic excitation as a function of distance from the cell soma (Hoffman *et al.*, 1997), or in other words less inhibition of the soma suggesting that distal dendrites respond more strongly to excitatory stimuli. This current decrease towards the soma is at least in part accompanied by a decrease in Kv4 immunostaining in proximal apical dendrites of CA1 pyramidal cells (Sheng *et al.*, 1992). This A-type current gradient is not observed along apical dendrites in neocortical layer V pyramidal cells (Storm, 2000; Hoffman *et al.*, 1997; Bekkers, 2000; Korngreen & Sakmann, 2000) consistent with uniform Kv4.2 and KChIP immunoreactivity along the dendritic shaft (Trimmer & Rhodes, 2004). The presence of these channels along the dendrites of neocortical pyramidal cells suggests modulation of excitatory input along the entire

dendrite. The functional significance of differences in dendrite regulation between different brain regions is unclear.

In summary, expression of Kv-channels in the CNS is diverse. Kv channel subunit co-localize in many regions of the brain, suggesting that formation of heterotetrameric channels might contribute to fine tuning of cellular excitability in different regions of the brain. Dysfunction of Kv channels in the CNS is associated with epilepsy and myotonia.

Current	$V_{Act.}$ (mV)	$V_{1/2}$ (mV)	Localization	Blocker	Subunit	Primary Function in the Heart
I_{Kr}	-40 - -30	-14	SAN, LA>RA, AVN, PC, V: Epi + M > Endo Brain	E4031, Dofetilide, d-Sotalol, MK-499, Ibutilide, Azimilide	*HERG*, MiRP1	Phase-3 repolarization
I_{Ks}	> 0	+19.9	SAN, atrium, V: Epi + Endo > M	Chromanol 293B, L-735821, Azimilide	KvLQT1, minK	Phase-3 repolarization
I_{Kur}	-30	-4.3	Atrium, ECs	4-AP, Quinidine	Kv1.5, Kv3.1	Phase 1-2 repolarization
A-type	-30 - -20	-25 – -9.5	Atrium, ?AVN, RV>LV; Epi>Endo, ?M; Brain; ECs	4-AP, Ba^{2+}, Flecainide, Quinidine, Sotalol, various toxins	Kv1.x-4.x, (I_{to}: Kv1.4, Kv4.2, Kv4.3); KChIP, ?MiRP1, ?minK	Phase-1 repolarization

Table III: Summary of voltage-gated channels and resulting currents. $V_{Act.}$: Activation voltage; $V_{1/2}$: Half maximal activation voltage, V: Ventricle; Epi: Epicardial; Endo: Endocardial; M: Midmyocardial; EC: Endothelial cells

CHAPTER V: INWARD RECTIFIER POTASSIUM K^+- (KIR-) CHANNELS

V-1 Introduction

In 1949, Bernard Katz described a current in skeletal muscle showing "anomalous rectification" (Katz, 1949). The term "rectification" denotes a voltage-dependant change in conductance. Delayed (outward) rectifier channels conduct greater outward K^+ flow at a given voltage (membrane or test potential) than inward K^+ current at the opposite voltage. The term used by Katz denotes an opposite behaviour: An increase in K^+-conduction with hyperpolarization and a decrease with depolarization - inward rectification. Six years later, Weidmann found an inwardly rectifying conductance with similar properties in sheep Purkinje fibres (Weidmann, 1955) and subsequently, inward rectifier currents were demonstrated in Purkinje fibres (Hall *et al.*, 1963), in frog atrial (Rougier *et al.*, 1968) and in canine ventricular muscle (Mascher & Peper, 1969; Beeler, Jr. & Reuter, 1970). In the CNS, inward rectifying currents have been demonstrated in neuronal (Hestrin, 1987; Nakajima *et al.*, 1988; Yamaguchi *et al.*, 1990; Brown *et al.*, 1990; Wimpey & Chavkin, 1991; Newman, 1993; Karschin & Karschin, 1999; Pruss *et al.*, 2005) and non-neuronal cells (Brismar & Collins, 1989; Tse *et al.*, 1992; Karschin *et al.*, 1994a). Kir channels open on hyperpolarization as a function of the extracellular $[K^+]$. Because of the coupling between $[K^+]_o$ and Kir gating mechanisms, inward rectification is said to depend on the voltage shift from the equilibrium potential for potassium, $E\text{-}E_K$, and not on the membrane potential E alone (Hille 2001). Higher $[K^+]_o$ shifts the resting membrane potential to more positive values thus increasing $E\text{-}E_K$, resulting in larger Kir currents at a given hyperpolarized membrane potential. Thus, inward Kir currents increase as the concentration of external potassium increases (Figure 17). Cells expressing a sufficient quantity of Kir channels are expected to have a resting potential near to E_K (Nichols & Lopatin, 1997; Isomoto *et al.*, 1997; Lopatin & Nichols, 2001).

Inward rectifier currents regulate cellular excitability and K^+ transport across the membrane in a multitude of cells and system including the heart, the CNS, the kidneys, endocrine organs and blood (Lopatin & Nichols, 2001; Nichols & Lopatin, 1997; Isomoto *et al.*, 1997; Lopatin & Nichols, 2001; Fang *et al.*, 2005). Dysfunction

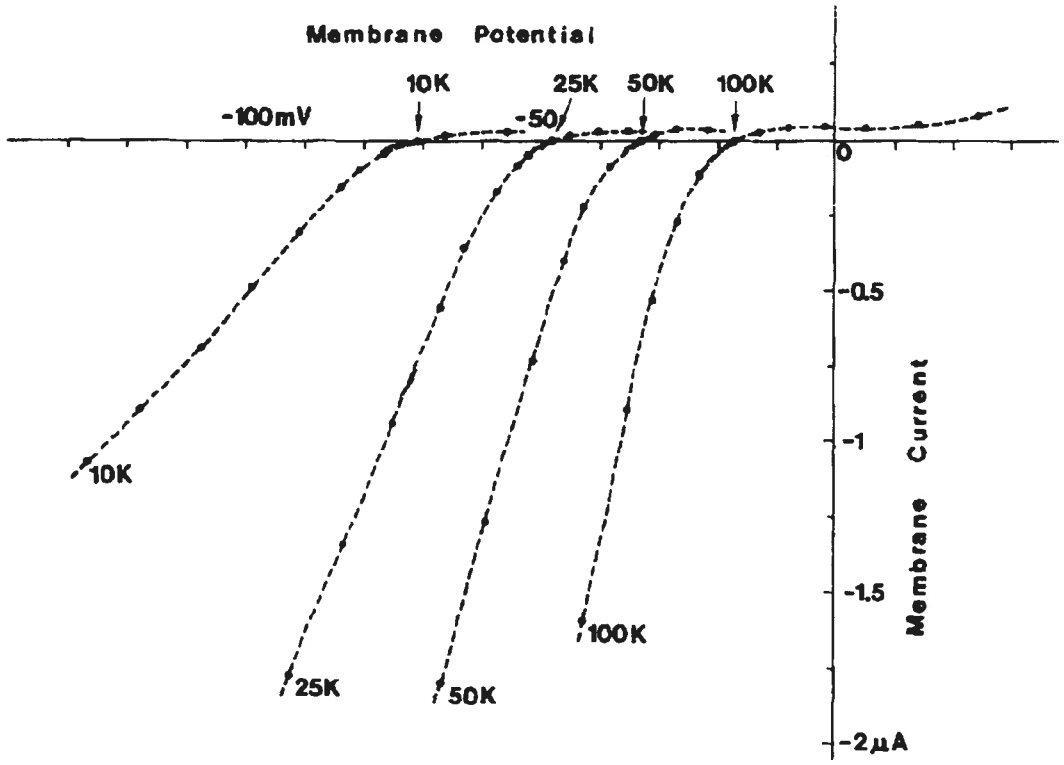

Figure 17: Inward rectification of steady state current in a Starfish egg.

Current-voltage relations of a *Mediaster* egg at four different external K^+ concentrations (10, 25, 50 and 100 mM) in Na^+-free media. The membrane is held at the zero-current potential and holding membrane potentials at resting potentials are -71 mM in 10 mM K^+, -48 mV in 25 mM K^+, -33 mV in 50 mM K^+, and -17 mM in 100 mM K^+. Currents were elicited with the two-electrode voltage clamp technique by 10 mV depolarizing or hyperpolarizing voltage-steps. Steady state current is shown by broken lines. T=21° C. Adapted from Hagiwara S. *et al.*, J. Gen. Physiol. 1976; 67:621-638.

of inward rectifier channels is associated with a multitude of pathologies including cardiac arrhythmias, paralysis, dysmorphic bone growth (Plaster *et al.*, 2001) convulsions (Signorini *et al.*, 1997), and kidney disease (Derst *et al.*, 1997).

V-2 The Cardiac Inward Recifier Current I_{KI}

V-2.1 Biophysical Properties

Measurements of I_{K1} single channel conductances have revealed a great variety of unitary inward rectifier conductances in different cardiac tissues and species (Table IV). Atrial I_{K1} is about 3-10 times larger in ventricle than in atrium (Figure 18) (Wang *et al.*, 1998; Varro *et al.*, 1993). These observations have been interpreted as differences in the molecular basis of I_{K1} between different cardiac regions and species.

I_{K1} shows strong inward rectification that shifts with the K^+ reversal potential (Noble, 1965; Vandenberg, 1994). Voltage-dependent block of the pore by intracellular cations as a mechanism of inward rectification was first suggested by Armstrong (1969). Matsuda *et al.* (1987) and Vandenberg (1987) demonstrated that pore blocking by Mg^{2+} resulted in inward rectification, however, the magnitude of voltage dependence of rectification induced by Mg^{2+} in ventricular myocyte and PCs of various species was weaker than that of native currents and strong inward rectification could often still be demonstrated after removal of Mg^{2+} (Martin *et al.*, 1995; Oliva *et al.*, 1990). In 1994 and 1995, a series of publications from different laboratories demonstrated that the polyamines spermine, spermidine and putrescine, a family of cationic cytoplasmic proteins, determine inward rectification by plugging the pore from the intracellular site in a voltage dependent manner (Lopatin *et al.*, 1994; Ficker *et al.*, 1994; Fakler *et al.*, 1994; Fakler *et al.*, 1995; Lopatin *et al.*, 1995). Block by putrescine, spermidine and spermine shows increasing steepness (Lopatin *et al.*, 1995; Guo & Lu, 2000) and total cellular polyamine levels are sufficient to produce the degree of rectification seen at physiologically important membrane potentials (Tabor & Tabor, 1984; Lopatin & Nichols, 2001).

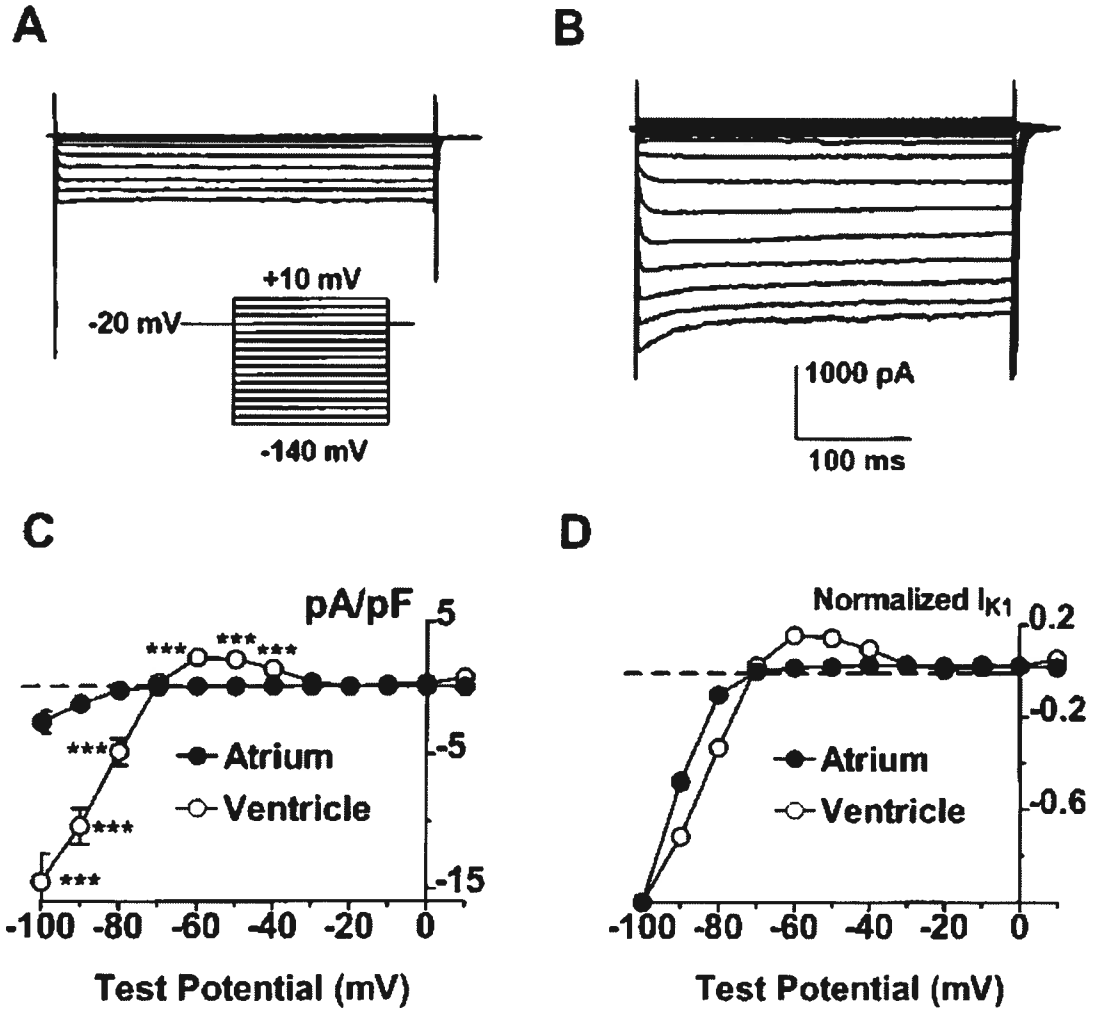

Figure 18: Inward rectifier K^+ current (I_{K1}) in human atrial and ventricular myocytes. **A** and **B**, Original recordings from representative experiments. Currents were elicited by 300-ms voltage steps to between -140 and +10 mV from a holding potential of -20 mV. **C**, Current density-voltage relation of I_{K1} obtained from types of current recordings shown in A before and after adding 1 mmol/L Ba^{2+} (Ba^{2+}-sensitive current). Data are mean±SEM (n=5 cells for atrium and 6 for ventricle). ***P<0.001 for atrium vs ventricle. **D**, Current-voltage relations normalized to current at -100 mV. Reproduced from Wang *et al.* (1998).

Tissue	Conductances (pS)	Reference
Human atrium	9, 21, 35, 41	Wible *et al.*, 1995
Rat Ventricle	20 - 40	Josephson & Brown, 1986
Guinea pig myocytes	10.5, 22, 32.5	Liu *et al.*, 2001
Guinea pig ventricle	27	Sakmann & Trube, 1984a
Nakamura	8, 14, 21, 35, 43, 80	Nakamura *et al.*, 1998

Table IV: Inward recitifier single channel conductances in different tissues and species.

V-2.2 Pharmacology

Inward rectifyer K^+ channels have a high affinity for various monovalent and divalent cations. Kir channel block by monovalent (Na^+, Cs^+, Rb^+, Ag^+) or divalent cations (Ba^{2+}, Mg^{2+}, Ca^{2+}, Sr^{2+}) has been studied in native tissues, as well as in cloned channels expressed in various heterologous systems (Standen & Stanfield, 1978, 1980; Ohmori, 1978; Biermans et al. 1987; Harvey & Ten Eick, 1989; Shioya et al. 1993; Reuveny et al. 1996; Sabirov et al. 1997a; Shieh et al. 1998; Doring et al. 1998; Dart et al. 1998).

V-2.2.1 Relevance and Models of Barium block

Voltage- and concentration dependent block by Ba^{2+} block is a hallmark property of I_{K1}. The crystal radius of Ba^{2+} is similar to that of K^+ (1.35 Å and 1.33 Å, respectively). Barium's size therefore allows it to fit into the selectivity filter but its higher charge causes it to bind to tightly causing Ba^{2+} to block the channel rather than to permeate it (Jiang & MacKinnon, 2000). These properties have been used to investigate the amino acid lining of the K^+ channel pore (Eaton & Brodwick, 1980;

Armstrong & Taylor, 1980; Vergara & Latorre, 1983; Neyton & Miller 1988, Taglialatela *et al.*, 1993; Navaratnam *et al.*, 1995; Shieh *et al.*, 1998).

Ba^{2+} blocks K^+-channels from the extracellular and the cytoplasmic side (Taglialatela et al., 1993; Harris et al., 1998; Shieh et al., 1998). It has been proposed that interactions of divalent cations with the K^+-channel pore occur at two distinct binding sites. A shallow site at the external end of the channels mediates block by Mg^{2+} and Ca^{2+} whereas block by Ba^{2+} and Sr^{2+} ions is mediated by a deeper site (Standen & Stanfield, 1978; Shioya *et al.*, 1993; Reuveny *et al.*, 1996; Sabirov *et al.*, 1997b; Shieh *et al.*, 1998). An amphipathic Arginine, Arg148, located between these two sites might act as a barrier preventing Mg^{2+} and Ca^{2+} ions to reach the deeper site (Sabirov *et al.*, 1997b). Ba^{2+} block of the Ca^{2+} activated K^+ channel (BK) is sensitive to the presence of K^+ in the pore. Low external K^+ concentrations prevent Ba^{2+} from exiting into the extracellular space while high K^+ concentrations cause Ba^{2+} to exit the channel into the cytoplasm. Based upon these observations, Neyton & Miller (1988 a,b) proposed the presence of multiple K^+ binding sites in the channel pore. Occupation of an external "lock-in" site by K^+ ions would inhibit the exit of Ba^{2+} into the extracellular solution while K^+ ion occupation of both sites (the site closer to Ba^{2+} was termed the "enhancement site") destabilizes Ba^{2+} binding and so facilitates its exit into the cytoplasm. A third site, the "internal lock-in site", was proposed to be located at the cytosolic side of the Ba^{2+} binding site (Neyton & Miller, 1988 a,b). Similar observations were made by Harris et al. (1998) and Vergara et al. (1999) in Shaker channels. Using x-ray diffraction data from frozen KcsA K^+ channel, Jiang and MacKinnon (2000) found structural confirmation of this hypothesis. An Rb^+ ion was seen very near the extracellular solution in the selectivity filter, compatible with the "external lock-in" site. However, the enhancement site, located closer to the Ba^{2+} ion in the selectivity filter, could not be precisely determined. The ion at the "internal lock-in" site was proposed to be the cavity ion (Figure 19). This model is consistent with the concept of a "multi-ion pore" (Doyle *et al.*, 1998; Berneche & Roux, 2001) where two or three K^+-ions must be in the selectivity filter (Morais-Cabral *et al.*, 2001; Zhou & MacKinnon, 2003; Berneche & Roux, 2001; Berneche & Roux, 2005; Allen & Chung, 2001). When a fourth ion enters the channel, occupying the "external

enhancement site", it pushes the queue along and thus Ba^{2+} out into the intracellular solution (Jiang & MacKinnon, 2000).

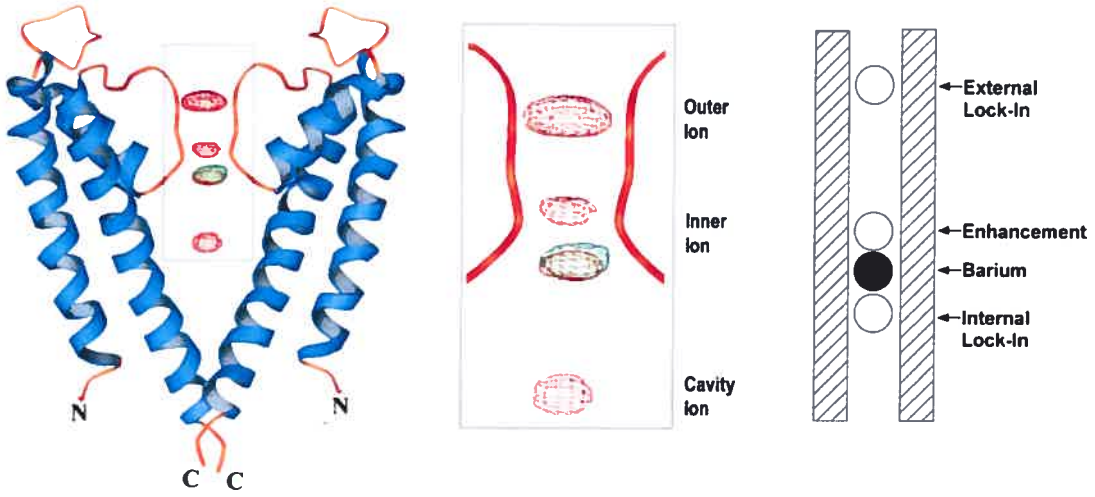

Figure 19: Visualization of barium in the KcsA K^+ channel by x-ray crystallography and in a Ca^{2+}-activated K^+ channel by analysis of single channel function.

Left: A ribbon diagram showing two subunits of the KcsA K^+ channel (blue and orange) with difference electron density showing the positions of Rb^+ (red mesh) and Ba^{2+} (green mesh) in the pore.

Middle: Magnified view of the boxed region on the left. The Rb^+ difference maps were calculated at 3.8-Å resolution and contoured at 9.0 s. Three ion positions are labeled outer, inner, and cavity ion. The inner ion shows two peaks reflecting alternative positions. The Ba^{2+} difference map was calculated at 5.0-Å resolution and contoured at 10.0 s; $Ba2^+$ is located at the innermost position of the inner ion.

Right: Diagram adapted from Neyton and Miller (1988) depicting the relative locations of Ba^{2+} and K^+ or Rb^+ sites (external lock-in, enhancement, and internal lock-in) as determined by examination of single-channel records. The ions are positioned according to their electrical distance across the membrane potential difference. Reproduced from Jiang & McKinnon (2000).

V-2.3 Functional Role of cardiac I_{K1}

In the heart, I_{K1} plays a key role in the maintenance of the resting membrane potential and contributes importantly to phase 3 of the cardiac action potential (Sakmann & Trube, 1984b; Hume & Uehara, 1985; Ibarra *et al.*, 1991; Shimoni *et al.*, 1992; Carmeliet, 1993). High conductances at negative potentials keep the RMP stable whereas small conductances at more positive membrane potentials avoid short-circuiting the AP and contribute to phase 3 repolarization (Figure 20) (Nichols & Lopatin, 1999). I_{K1} is practically absent in the SAN (Guo *et al.*, 1997), explaining the relatively depolarized MDP and allowing spontaneous phase 4 depolarization. In the atrium, I_{K1} is 6 to 10 times smaller than in ventricular myocytes (Giles & Imaizumi, 1988; Wang *et al.*, 1998) resulting in a more depolarized MDP and a less steep phase 3 depolarization in atrial compared to ventricular myocytes. I_{K1} density in the AVN is low (Hancox & Mitcheson, 1997), consistent with its positive MDP. PC I_{K1} is smaller (Verkerk *et al.*, 1999; Cordeiro *et al.*, 1998) or similar (Han *et al.*, 2001b) to ventricular I_{K1}. In the ventricles, the outward component of epicardial I_{K1} is smaller in cats (Furukawa *et al.*, 1992) but not in guinea pig (Main *et al.*, 1998) or dog epicardium (Liu & Antzelevitch, 1995). There are no differences in M-cell I_{K1} (Liu *et al.*, 1993). Regional differences in I_{K1} may be a significant determinant of VF (Samie *et al.*, 2001; Warren *et al.*, 2003).

V-2.3 Clinical Significance of I_{K1} Dysfunction

I_{K1} is reduced in heart failure (Beuckelmann *et al.*, 1993). Dysfunction of I_{K1} causes depolarization of the resting membrane potential resulting in complex effects on cardiac excitability. Mild depolarization decreases the amount of depolarization needed to reach threshold, thus increasing excitability and facilitating arrhythmias from abnormal automaticity and triggered activity. Strong membrane depolarization decreases excitability and conduction velocity by inactivating Na^+ channels promoting re-entry (Schram *et al.*, 2002b). Block of I_{K1} results in increased automaticity (Imoto *et al.*, 1987; Miake *et al.*, 2002; Miake *et al.*, 2003). I_{K1} dysfunction depolarizes the resting membrane potential, prolongs APD and decelerates phase 3 repolarization (Miake *et al.*, 2003) possibly promoting EADs that

could trigger torsade de pointes arrhythmias (El Sherif *et al.*, 1996; Asano *et al.*, 1997). Reduction of I_{K1} contributes to larger amplitude DADs potentially triggering an arrhythmogenic AP (Pogwizd *et al.*, 2001). Dysfunction of I_{K1} in Andersen's syndrome (LQT7) causes prolongation of the QT interval resulting in potentially lethal arrhythmias (Plaster *et al.*, 2001).

In chronic atrial fibrillation, upregulation of I_{K1} and Kir2.1 mRNA expression in human atrial myocytes causes shortening of APD in AF patients (Dobrev *et al.*, 2001). However, in dogs subjected to rapid atrial pacing, Kir2.1 mRNA and I_{K1} were not changed (Yue *et al.*, 1999), possibly reflecting distinct pathophysiological mechanisms in this model.

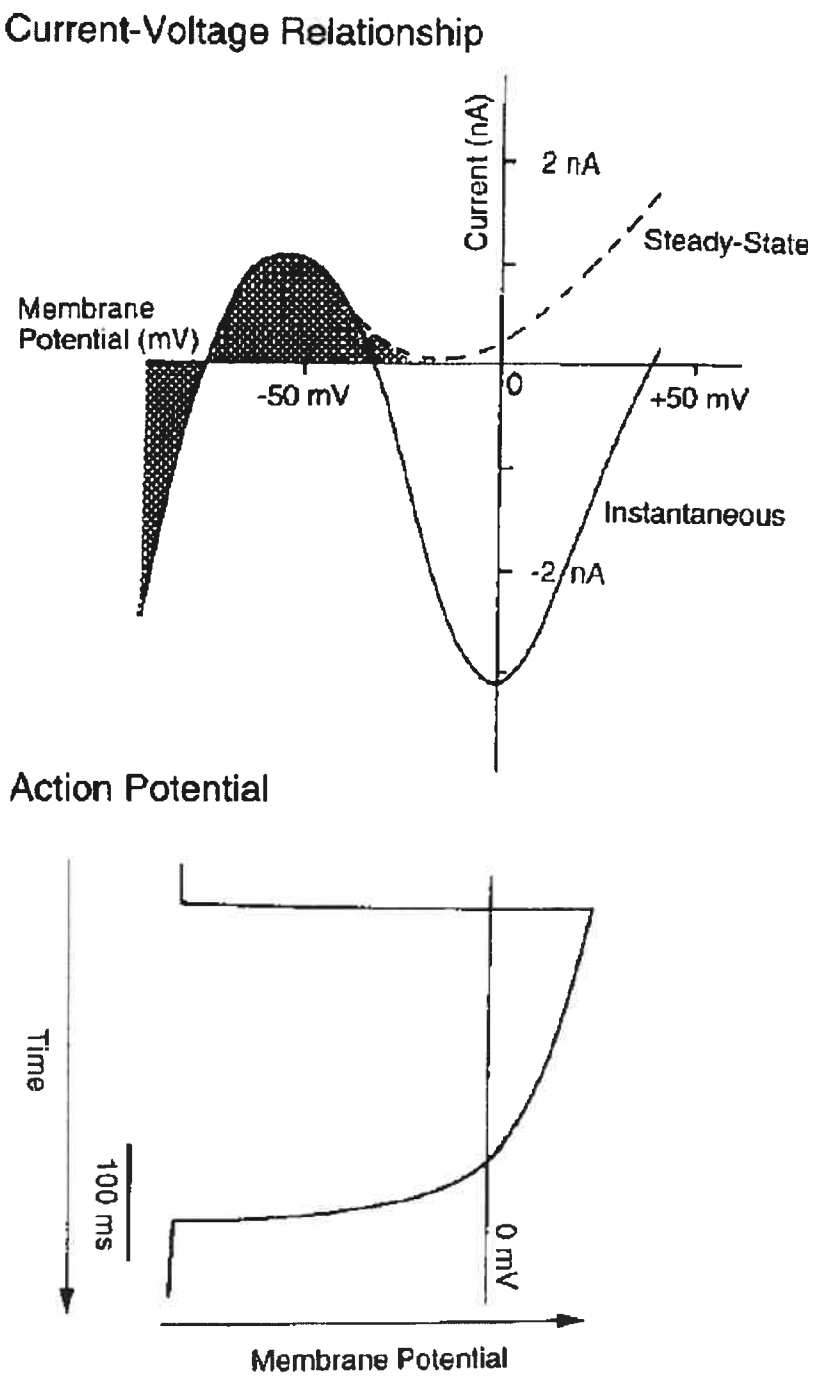

Figure 20: I_{K1} urrent-voltage relationship and action potential in the ventricular cell.

The current-voltage relationship in the voltage clamp experiment for the instantaneous current is indicated by the solid line and that for the steady-state current at 1s by the broken line. The action potential is drawn sideways to correlate it to the above current-voltage relationship. Shaded area shows I_{K1} currents. Reproduced from Isomoto *et al.* (1997).

V-2.4 Molecular Basis of I_{K1}

V-2.4.1 Regional Heterogeneity of Cardiac Kir2 Subunit Expression

Four distinct Kir2 subfamily members have been cloned from various species and tissues (Kubo *et al.*, 1993a. Ishii *et al.*, 1994; Wible *et al.*, 1995; Raab-Graham *et al.*, 1994; Koyama *et al.*, 1994; Makhina *et al.*, 1994; Morishige *et al.*, 1994; Perier *et al.*, 1994; Tang & Yang, 1994; Tang *et al.*, 1995; Topert *et al.*, 1998; Hughes *et al.*, 2000; Liu *et al.*, 2001) (Figure 25). In the heart, only Kir2.1-3 subunits are believed to underlie the inward rectifier current I_{K1} (Liu *et al.*, 2001).

Kir2.1 is the most abundant Kir2-subunit mRNA in atrium and ventricle and is equally expressed in each while Kir2.1 protein expression is about 80% higher in ventricle (Figure 21, Tables V and VI). Kir2.3 transcripts are more abundant in atrium than in ventricle, consistent with a 2.3-fold greater atrial Kir2.3 expression. Kir2.2 mRNA is equally expressed in atrium and ventricle, yet about an order of magnitude less abundant than Kir2.1 (Wang *et al.*, 1998; Melnyk *et al.*, 2002). Consequently, differences in Kir2 mRNA expression cannot account for atrio-ventricular I_{K1} differences in I_{K1}. Post-translational processes might account for lower atrial Kir2.1 protein expression resulting in lower atrial I_{K1} thereby providing a potential partial explanation for differences observed. In ferret SAN, Kir2.1 transcript expression is very limited (Brahmajothi *et al.*, 1996) in accordance with the absence of I_{K1} in the SAN (Guo *et al.*, 1997). No data on Kir2 subunit expression in the AVN or PCs is available.

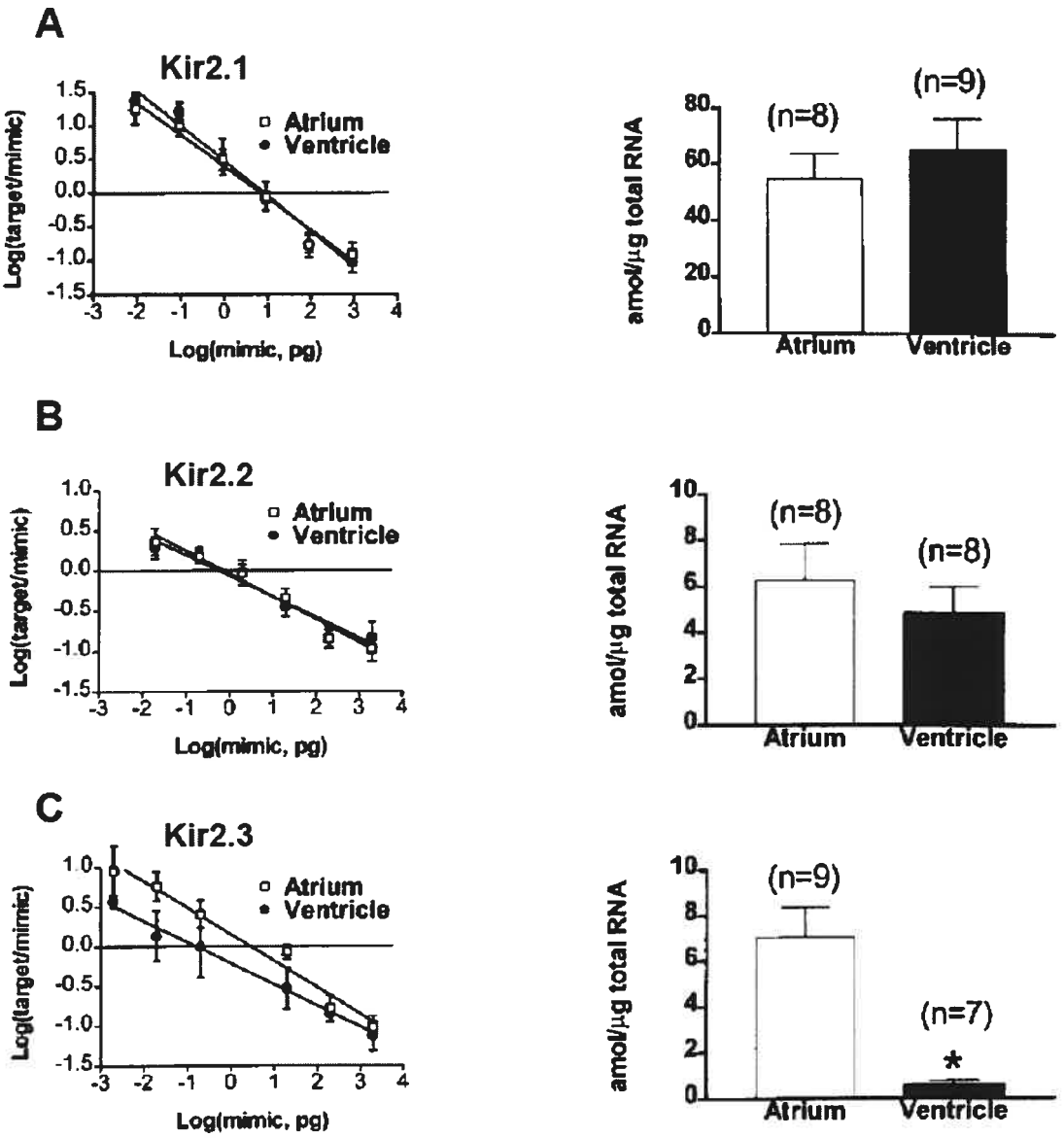

Figure 21: Quantification of Kir2 mRNA in human atrium and ventricle.

Left, Log-amplified target Kir2/internal standard ratio versus known amount of RNA mimics. *x*-intercepts of linear regression to mean data in which log (target/mimic) equals zero indicate initial amount of target mRNA. **Right**, Amount of Kir2 transcript (amol/µg total RNA) calculated by dividing initial amount of target mRNA by molecular weight of respective PCR products (number of nucleotides x average molecular weight of single nucleotide, 310). Reproduced from Wang *et al.* (1997).

Subunit	Atrium	Ventricle
Kir2.1	1	1
Kir2.2	0.1	0.1
Kir2.3	0.1	0.01

Table V: Relative concentration of Kir2 mRNA in human atrium and ventricle. Concentrations are normalized to Kir2.1 in atrium (Wang *et al.*, 1998).

Subunit	Atrium	Ventricle
Kir2.1	1	1.8
Kir2.3	1	0.41

Table VI: Relative concentration of Kir2.1 and Kir2.3 protein in canine atrium and ventricle. Values are normalized to atrial protein concentrations (Melnyk *et al.*, 2002).

V-2.4.2 Functional Role of Kir2 Subunits in the Heart

Zaritsky *et al.* (2000) showed that myocytes from Kir2.1 KO mice displayed longer APD and more frequent spontaneous AP than myocytes from WT mice. The study, however, was limited by the early demise of homozygous Kir2.1 KO mice. In neonatal mice, sinus rhythm was maintained but heart rates were consistently slower. Using adenoviral transfer of a dominant negative Kir2.1 construct, Miake *et al.* (2002) demonstrated two different phenotypes in myocytes from transduced guinea pigs: 1.) Myocytes with a stable resting membrane potential from which prolonged action potentials could be elicited and 2.) Myocytes displaying spontaneous activity. Myocytes with spontaneous activity had depolarized MDPs of ~ -61 mV and displayed repetitive regular activity. Action potentials showed gradual phase 4 depolarization and slow upstroke velocity. ECGs obtained from these animals in vivo were characterized by a steady ventricular rhythm at faster rates than the physiological pacemaker. A second study by the same group investigated effects of I_{K1} upregulation by overexpression of Kir2.1 as well as a quantitative approach of I_{K1} knockout with a dominant negative Kir2.1 subunit in guinea pig ventricular myocytes. Myocytes from animals with Kir2.1 upregulation had more than 100% higher I_{K1} density and slightly more negative MDPs (-79.1 ± 0.8 mV vs. -74.7 ± 4.5 mV). This was functionally manifested by shortened APD (~50%), mostly due to an accelerated phase 3 repolarization as seen by a 7.5% shortening of the QTc interval in the ECG. Animals with 50-80% I_{K1} suppression showed prolongation of APD (~ 9%), decelerated phase 3 repolarization and depolarized MDPs (-68.0 ± 2.3 mV vs. -74.7 ± 4.5 mV). ECGs showed a 14% prolongation of the QTc interval. As expected, reduction of I_{K1} by more than 80% resulted in a pacemaker phenotype (Miake *et al.*, 2003). Effects on APD and phase 3 repolarization are illustrated in Figure 22.

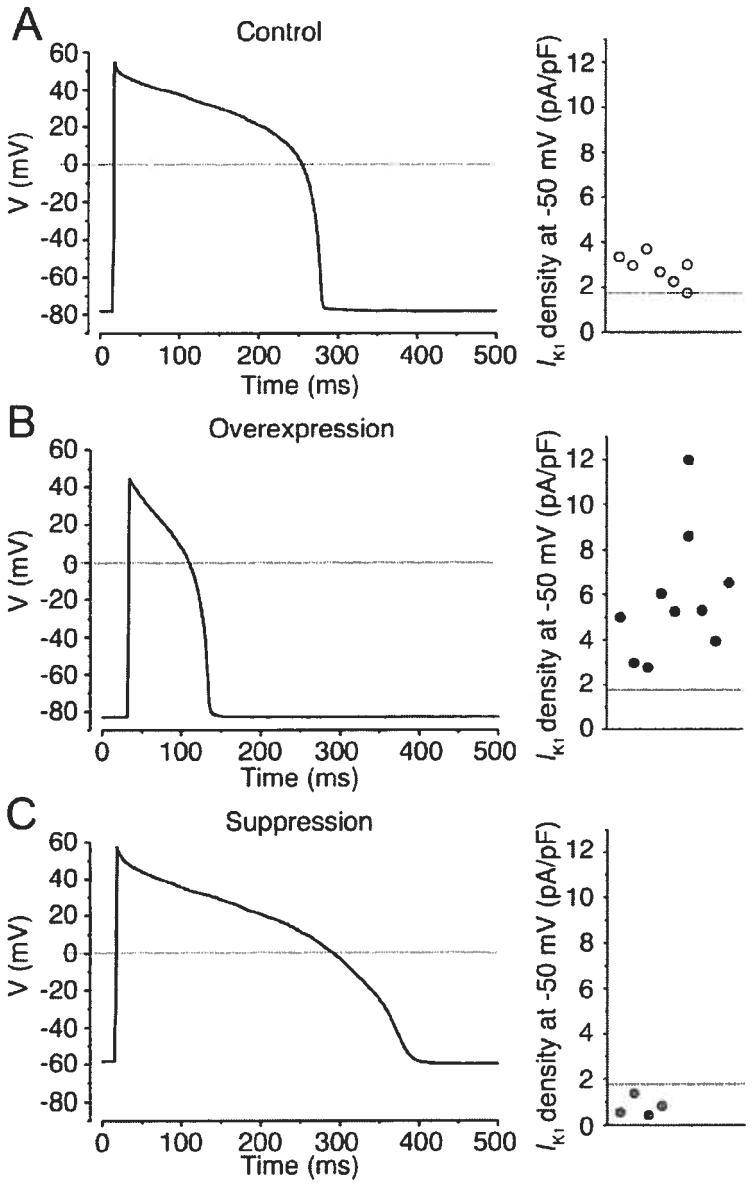

Figure 22: AP phenotype is determined by I_{K1} density.

A: Stable APs evoked by depolarizing external stimuli in control myocytes.

B: APs recorded in overexpressed myocytes with a robust I_{K1} are abbreviated.

C: In dn-Kir2.1-transduced myocytes with moderately depressed I_{K1}, APs with a long-QT phenotype were evoked. The actual I_{K1} density measurements from the individual myocytes comprising each group are plotted to the right of each AP waveform. Adapted from Miake *et al.* (2003).

V-2.4.3 Potential Role of Kir2 Subunits in the Brain

In situ hybridization has shown Kir2.1-Kir2.3 protein expression in most brain regions (Bredt *et al.*, 1995; Falk *et al.*, 1995; Horio *et al.*, 1996; Karschin *et al.*, 1996; Koyama *et al.*, 1994; Topert *et al.*, 1998). Kir2 mRNA as detected by RT-PCR overlaps with Kir2 protein expression in most areas (Isomoto *et al.*, 1997; Karschin & Karschin, 1999). Kir2 subunits are localized in the somata and dendrites of many neurons and appear to be absent from glial cells. Instead, glial cells express Kir4.1 and/or Kir5.1 homo-/heteromeric channels in a region-specific manner, suggesting regionally distinct physiological roles of homomeric Kir4.1 and heteromeric Kir4.1/Kir5.1 channels in K^+-buffering of brain astrocytes (Hibino *et al.*, 2004; Kalsi *et al.*, 2004; Neusch *et al.*, 2001). A recent study by Prüss et al. (2005) has shown that Kir2 subunits are widely expressed in different tissues and cell types. A principal novelty of this study is the demonstration that Kir2.4 protein expression is widely distributed in the brain and not as previously thought restricted to motoneurons in the brainstem (Topert *et al.*, 1998). Substantial differences in subcellular localization of Kir2 subunits are differentially regulated by interacting proteins. For example, Kir2.1-Kir2.4 express PDZ binding motifs, whereas Kir2.4 does not (Hughes *et al.*, 2000; Topert *et al.*, 1998; Topert *et al.*, 2000).

Table VII summarizes Kir2.1-4 protein expression in the brain. High Kir2.2 and Kir2.3 expression in layer 5 pyramidal cells might be of physiological importance since layer V comprises the main output system of the cerebral cortex. Both Kir2.2 and Kir2.3 are associated with apical dendritic processes of large pyramidal neurons, suggesting the formation of heteromeric Kir2.2/Kir2.3 complexes.

The nucleus accumbens and the caudate putamen express protein of all Kir2 subunits. Kir2.1 and Kir2.3 expression in the brain is highest in these regions (Karschin & Karschin, 1999; Karschin *et al.*, 1996; Pruss *et al.*, 2003). Kir2.1 and Kir2.2 are co-expressed and co-localize in all parts, whereas Kir2.3 localizes to the shell part of the nucleus accumbens suggesting a physiological role of Kir2.1/Kir2.2 heteromultimers in the nucleus accumbens. In the mesencephalon, high Kir2.2/Kir2.3 co-expression in the neuropil of the pars reticulata of the substantia nigra suggests

formation of heteromeric complexes. The cerebellum and spinal cord show remarkable expression differences in Kir2 subunit protein expression. Kir2.2 expression in the cerebellar cortex is strong but restricted to the granulate cell layer, consistent with in situ data (Bredt *et al.*, 1995; Karschin & Karschin, 1999). Kir2.3 is intensely expressed by large neurons in the deep cerebellar nuclei, Purkinje cells and Purkinje cell dendritic arborations radiating into the superficial molecular layer, in line with previous publications (Falk *et al.*, 1995). In the spinal cord, all four Kir2 subunits are found in the grey matter, the dorsal and ventral horns, where they are associated with neuronal somata and motoneurons. Kir2.2 expression in these structures is particularly high, consistent with previously published data (Karschin *et al.*, 1996; Stonehouse *et al.*, 1999).

Co-localization of different Kir2 channel subunits strongly suggests formation of heterotetrameric Kir2 channels (Preisig-Muller *et al.*, 2002; Schram *et al.*, 2002a). As shown in this thesis, Kir2 heterotetramers have distinct biophysical and pharmacological properties. Hence, differential heteromerization between Kir2 subunits might contribute to fine tuning of regulation of cellular excitability in tissues where different Kir2 subunits co-localize (Karschin *et al.*, 1996; Liu *et al.*, 2001). Dysfunction of Kir2 subunits in Andersen's syndrome causes periodic paralysis (Plaster *et al.*, 2001). However, the phenotype can greatly vary and in general, neurologic symptoms are not prominent in patients with Andersen's syndrome. Similarly, Kir2.1/Kir2.2 knockout mice do not display neurological symptoms (Zaritsky *et al.*, 2000; Zaritsky *et al.*, 2001). It has therefore been suggested, that the strong heterogeneity of neuronal Kir2 subunit expression might provide a safety mechanism, in which one Kir2 subunit might substitute the loss of another Kir2 subunit in the brain (Pruss *et al.*, 2003). Strong expression of Kir2.3 and Kir2.4 protein in basal ganglia might make these channels a potential target of pharmacological intervention in diseases of the basal ganglia, such as Parkinson's disease (Pruss *et al.*, 2003).

Brain region	**Kir2.1**	**Kir2.2**	**Kir2.3**	**Kir2.4**
Telencephalon				
Olfactory bulb				
Glomerular layer	++++	+	0	+
External plexiform layer	+	0	++++	0
Mitral cell layer	+	+	+	+
Granule cell layer	++	0	+	+
Olfactory tubercle	++	+	+++	0
Island of Calleja	+	0	0	0
Piriform cortex	++	+	++	+
Neocortex				
Layer I	0	+	+	0
Layer II	+++	++	+++	++
Layer III	+++	++	+++	+
Layer IV	++	+	++	++
Layer V	++	+++	++	++
Layer VI	++	+	+	+
Hippocampus				
Dentate gyrus				
Molecular layer	+	+++	+	0
Granule cell layer	+++	++	++	++
Polymorphic layer	0	+	+	0
CA1–CA2				
Oriens layer	0	+	++	+
Pyramidal cell layer	+	++	++	+
Radiate layer	0	+	++	0
Lacunosum moleculare layer	+	++	+	0
CA3				
Oriens layer	0	+	+	+
Pyramidal cell layer	+	+	+	+
Radiate layer	0	+	+	+

Telencephalon				
Basal forebrain				
Substantia innominata	0	+	0	+
Basal nucleus of Meynert	+	++	++	+
Basal ganglia				
Caudate putamen (Striatum)	++	+++	+++	+
Nucleus accumbens	++	++	++	+
Globus pallidus	+	++	++	+
Claustrum	0	+	0	+
Endopiriform nucleus	+	+	+	+
Lateral olfactory tract nucleus	+++	0	+	+
Amygdala				
Cortical nuclei	+	0	0	0
Medial nucleus	+	0	0	0
Basomedial nucleus	+	0	0	0
Diencephalon				
Thalamus				
Anterodorsal nucleus	+++	0	0	0
Anteroventral nucleus	++	0	0	0
Anteromedial nucleus	+	0	0	0
Laterodorsal nucleus	+	+	0	0
Mediodorsal nucleus	+	0	0	0
Centrolateral nucleus	0	++	0	+
Paraventricular nucleus	+	++	0	+
Reuniens nucleus	+	+	0	0
Reticular nucleus	++	++	++	+
Posterior nucleus	++	+	0	0
Medial geniculate nucleus	+	+	0	0
Paratenial nucleus	+	++	0	+
Stria terminalis	+	+++	+++	0

Diencephalon				
Hypothalamus				
Anterior area	+	++	0	+
Ventrolateral nucleus	0	+	0	+
Lateral area	+	+	0	0
Preoptic nucleus	+	++	0	+
Periventricular nucleus	+	+	0	0
Paraventricular nucleus	+	+	0	+
Supraoptic nucleus	+	++	0	++
Epithalamus				
Medial habenula	++	++++	+	0
Lateral habenula	+	+	0	0
Mesencephalon				
Red nucleus	0	+	+	+
Substantia nigra				
Pars compacta	+	++	+	+
Pars reticulata	0	+++	++	0
Ventral tegmental area	+	0	0	0
Interpeduncular nucleus	++	+++	++	+
Superior colliculus	++++	++	+	0
Central gray	+	++	0	+
Edinger–Westphal nucleus	+	+	0	+
Oculomotor nucleus (III)	+	++	0	+++
Metencephalon				
Cerebellum				
Deep nuclei	+	0	+++	+
Molecular layer	+	0	+	0
Granule cell layer	0	+++	0	+

Metencephalon				
Cerebellum				
Purkinje cells	0	0	++	0
Myelencephalon				
Spinal medulla				
Substantia gelatinosa	+	++++	+	0
Motoneurons	++	+++	+	+

Table VII: Distribution of individual Kir2 subunits in different brain regions. Reproduced from Pruss *et al.*, 2005.

V-2.4.3 Role of Kir2 Currents in Endothelial Cells

The negative resting potential in endothelial cells is of crucial importance for entry of extracellular Ca^{2+} (Nilius & Droogmans, 2001). Kir2 channels are thought to be the major conductance setting the resting membrane potential in these cells (Voets *et al.*, 1996; Jow *et al.*, 1999; Forsyth *et al.*, 1997; Nilius & Droogmans, 2001; Eschke *et al.*, 2002; Adams & Hill, 2004). Kir2.1 channels are differentially expressed in ECs and found predominantly in macrovascular endothelial cells such as bovine pulmonary artery ECs (BPAECs), bovine aortic ECs (BAECs), coronary endothelial cells and to some extent human umbilical vein ECs (HUVECs) whereas expression of Kir2.1 channels in microvascular ECs appears to be tissue specific. For example, Himmel et al. did not detect inward rectifier K^+ current in endothelial cells from human omentum (Himmel *et al.*, 2001) whereas Eschke and colleagues demonstrated inwardly rectifying currents and Kir2.1 mRNA in bovine retinal and choroidal microvascular ECs (Eschke *et al.*, 2002).

Even though Kir2.1 channels appear to be more abundant in cultured cells than in primary ECs, functional data points to an important physiological role of these channels in vivo. Exposure of endothelial cells to Ba^{2+} results in membrane depolarization in cultured bovine pulmonary artery endothelial cells (Voets *et al.*, 1996), native bovine corneal endothelial (BCE) cells (Yang *et al.*, 2003a) and vascular endothelial cells (Lieu *et al.*, 2004). Hemodynamic (shear) stress produces vasodilatation through Kir2.1 mediated (Hoger *et al.*, 2002) hyperpolarization of the RMP (Olesen *et al.*, 1988;Lieu *et al.*, 2004). The functional importance of Kir2.1 channels in vasodilatation was further confirmed in a Kir2.1 mouse knockout model. Whereas an increase of the extracellular K^+ concentration caused Ba^{2+}-sensitive dilatation of pressurized cerebral arteries from Kir2.1-WT and Kir2.2 mice, arteries obtained from mice lacking the Kir2.1 gene did not dilate (Zaritsky *et al.*, 2000). Romanenko et al. (2002) have recently demonstrated that hypercholesterolemia results in suppression of endothelial Kir2 current in BAECs suggesting that such currents might be implicated in the pathogenesis of hypercholesterolemia-induced abnormalities of the vasculature (Romanenko *et al.*, 2002). Other functions of Kir2

channels in ECs include K^+-sensing as well as regulation of peptide mediated vasoconstriction through angiotensin II, vasopressin, vasoactive intestinal peptide, and histamine mediated inhibition of Kir2 channels (Nilius & Droogmans, 2001).

In summary, structural and functional data demonstrate an important physiological role of Kir2.1 channels in regulation and pathophysiological conditions of endothelial cells in a variety of different tissues including the inner lining of coronary arteries. Kir2.1 channels contribute importantly to the negative resting membrane potential required for Ca^{2+} influx and regulation of Ca^{2+} dependant intracellular signalling in endothelial cells.

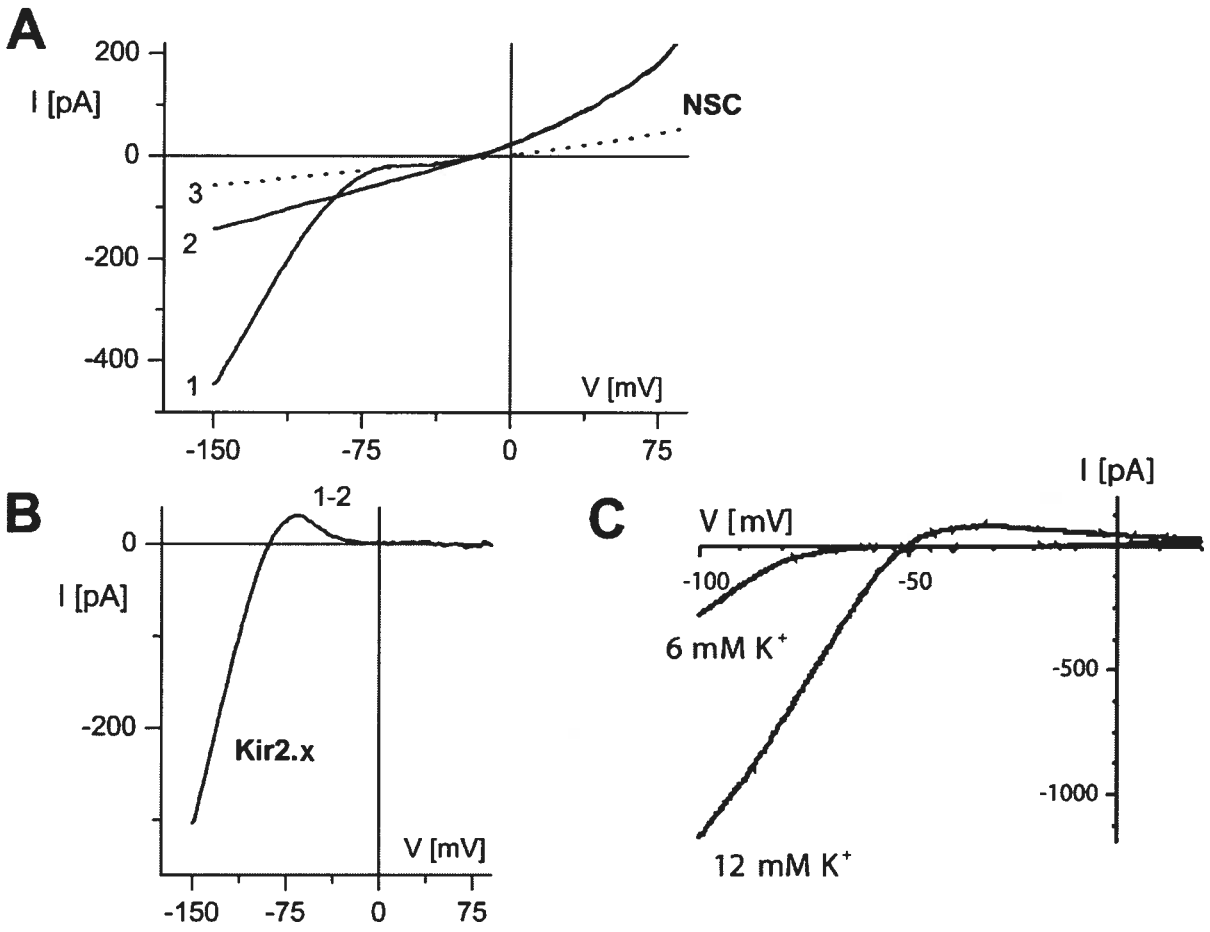

Figure 23: Current-voltage relationships in non-stimulated bovine endothelial cells.

A: IV-curves of currents recorded from BPAECs with linear voltage-ramps (-150 mV to +100 mV) under control conditions (1), in the presence of 1mM Ba^{2+} to block Kir2.x (2), and remaining non-selective cation current (NSC) after shrinking the cell with 100 mM mannitol to inhibit volume regulated anion channels (VRAC) and application of 1 mM Ba^{2+} to inhibit Kir2 current (3). **B:** Difference current 1-2 is a strongly inwardly rectifying current supposedly of the Kir2.x family. **C:** Net current recorded from a BAEC in the presence of 12 mM and 6 mM extracellular K^+. As expected from Kir2.x currents, increasing the extracellular K^+ concentration increases current conductance. Adapted from Nilius & Droogmans (2001).

V-2.4.4 Barium block of Kir2 channels

High-potency block by Barium ions is a hallmark property of I_{K1} and thus of cloned Kir2 channels. Ba^{2+} ions block Kir2.1 channels from both the intra- and extracellular side. Intracellular Ba^{2+} inhibits Kir2.1 at positive but not at negative membrane potentials (Shieh *et al.*, 1998; Figure 24). Block of steady-state Kir2.1-3 current by extracellular Ba^{2+} ions is concentration-, time-, and voltage-dependent (Kubo *et al.* 1993; Makhina *et al.*, 1994; Morishige *et al.*, 1994; Perier *et al.*, 1994; Ashen *et al.*, 1995; Shieh *et al.*, 1998; Schram *et al.*, 1999b; Liu *et al.*, 2001; Preisig-Müller *et al.*, 2002). The work presented in this thesis studied block by external Ba^{2+} ions only. Therefore, the term "Ba^{2+} block" will refer to block by extracellular Ba^{2+} for the remainder of this thesis and block by internal Ba^{2+} ions will not be discussed any further. The articles presented in "Part 2: Original contributions" of this thesis used Ba^{2+} block as a tool to infer on native inward rectifier current composition based upon its Ba^{2+} blocking properties. Ba^{2+} block was not used to speculate on pore structure / function of potential heteromeric inward rectifier channels or to investigate mechanisms of Ba^{2+} block in these channels. However a subsequent study that could not be completed within the time allotted for this research project focused on the molecular mechanisms responsible for the different properties of Ba^{2+} block of Kir2.4. Preliminary results of this study, which is currently being pursued by one of my former coworkers, are being presented and discussed in the section on molecular determinants of Ba^{2+} block of Kir2.1.

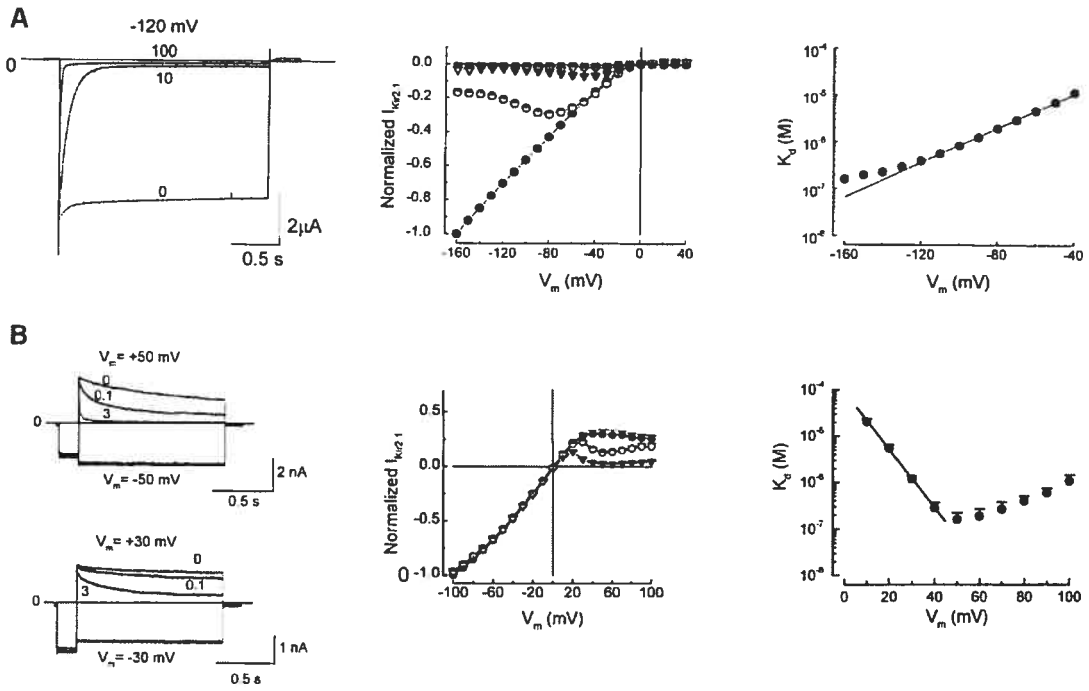

Figure 24: Ba^{2+} block of Kir2.1.

A: Blockade of Kir2.1 by extracellular Ba^{2+}. Left: Representative currents elicited by voltage steps to −120 mV from a holding potential of 0 mV in the presence of the indicated $[Ba^{2+}]_o$ (μM). Middle: Normalized average (4-12 cells) current-voltage (*I-V*) relationships for the steady-state inward $I_{Kir2.1}$ in the presence of 0 (•), 1 (○), 10 (▼), 100 (▽), and 1000 μM Ba^{2+} (■). Right: K_d values obtained from the concentration-dependent inhibition of the steady-state $I_{Kir2.1}$ as function of the membrane potentials. The solid line is the best fit of the data obtained at V_m ranging from −120 mV to −40 mV, using the Boltzmann equation.

B: Blockade of Kir2.1 channels by intracellular Ba^{2+}. Left: $I_{Kir2.1}$ at +50 (upper panel) and −50 mV and +30 and −30 mV (lower panel) in the presence of 0, 0.1, and 3 μM $[Ba^{2+}]_i$. Middle: Normalized *I-V* relationships in the presence of 0 (control, •, $n = 5$), 0.1 (○, $n = 5$), and 3 μM $[Ba^{2+}]_i$ (▼, $n = 5$). Right: Voltage-dependence of K_d. K_d at V_m between +10 and +40 mV were fitted (*continuous line*) with the Boltzmann equation. Adapted from Shieh *et al.*, (1998).

V-2.4.4.1 Molecular determinants of Kir2 Ba^{2+} block

Kir2 channels display different sensitivity to barium with Kir2.2 being about an order of magnitude more sensitive and Kir2.4 an order of magnitude less sensitive than Kir2.1 or Kir2.3 (Schram et al, 1999a; Schram et al. 2000a; Topert *et al.*, 1998; Liu *et al.*, 2001). Barium block of steady-state Kir2.1–3 is voltage dependent with higher sensitivity at more negative potentials. Steady state block of Kir2.4 does not show clear voltage dependence (Schram et al. 2002a). The molecular determinants of Kir2 Ba^{2+} block are largely unknown. Research has focused on polar amino acids inside the channel pore and around the outer mouth of the channel. In Kir2.1, Glu125, Arg148 and Thr141 have been identified to be important structural determinants of Ba^{2+} block (Navaratnam *et al.*, 1995; Sabirov *et al.*, 1997; Doring *et al.*, 1998; Alagem *et al.*, 2001; Murata *et al.*, 2002; Table VIII, Figure 25). Glu125 and Thr141 appear to be determinants of Kir2.1 Ba^{2+} sensitivity while Arg148, located between these two sites, might act as a barrier preventing cations to reach the deeper site (Sabirov *et al.*, 1997b). Thr141 and Arg148 are conserved amongst all four Kir2 family members and thus unlikely to acoount for differences observed between Kir2.1 and Kir2.4. The corresponding amino acid to Kir2.1-Glu125 in Kir2.2 is glutamine (Kir2.2-Gln126). Murata et al. (2002) showed that a Kir2.1-E125Q mutant was less sensitive to Ba^{2+} than Kir2.1-WT. VDB was not affected by the E125Q mutation. Ba^{2+} block of the reverse mutation, Kir2.2-Q126E was not studied. However, a Kir2.2.-Q126E mutant showed decreased sensitivity to block by Mg^{2+}. Like Kir2.2, Kir2.4 has a glutamine in the corresponding position (Kir2.4-Gln129). Nonetheless, despite Gln126, Ba^{2+} sensitivity of Kir2.2 is about one order of magnitude higher than that of Kir2.1. It is therefore difficult to infer on the functional importance of Kir2.4-Gln129. Kir2.1 has an aspartic acid in the turret (Asp114), whereas the corresponding amino acid in Kir2.4 is alanine. To determine the importance of Asp114, we created a Kir2.1 mutant where Asp114 was replaced by alanine. Kir2.1-D114A did not display altered Ba^{2+} sensitivity or voltage dependence of block (Schram, G., unpublished data) suggesting that Asp114 does not play a key role in Kir2.1 Ba^{2+} block. Kir2.4 has a phenylalanine, a large hydrophobic amino acid, at position 120 in the turret (Phe120). The corresponding amino acid in Kir2.1 is

Lys117. We hypothesized that Phe120 might act as a hydrophobic barrier to Ba^{2+} entry into the channel pore, acting in a similar fashion as Arg148 in Kir2.1 (Sabirov *et al.* 1997). To investigate this hypothesis, we created a Kir2.1-K117P mutant. Ba^{2+} block of this construct was similar to Kir2.1-WT (Schram, G., unpublished data) suggesting that Phe120 is not responsible for the lower Ba^{2+} or absence of VDB of Kir2.4.

To better understand underlying molecular determinants, we studied Ba^{2+} block of chimeric and point mutant constructs of Kir2.1 and Kir2.4 subunits in *Xenopus* oocytes and compared properties to Kir2.1-WT and Kir2.4-WT. Chimeras were created by replacing the Kir2.1 N-terminal (Kir2.1-2.4-NT), the first transmembrane domain (Kir2.1-2.4-M1), the turret (Kir2.1-2.4-ECL1), the pore region (Kir2.1-2.4-H5), the pore-helix-M2 linker (Kir2.1-Kir2.4-ECL2) and the C-terminal (Kir2.1-2.4-CT) of Kir2.1 by the respective region of Kir2.4.

Ba^{2+} sensitivity of Kir2.1-WT and Kir2.1-Kir2.4 constructs was not significantly different. Voltage-dependence of Ba^{2+} block (VDB) was assessed by fitting the IC_{50} as a function of the test potential by a Boltzmann equation. VDB of most of the chimeras was not altered significantly from Kir2.1-WT values. However, replacement of Kir2.1-H5 and Kir2.1-ECL2 by respective regions of Kir2.4 (Kir2.1-2.4-H5 and Kir2.1-2.4 ECL2) resulted in the loss of VDB, similar to Kir2.4-WT. Comparison of amino acid sequences between Kir2.1 and Kir2.4 identified four potential candidates in the pore region and three in the pore-helix-M2 linker, respectively. Point mutant constructs of Kir2.1-2.4-H5 and Kir2.1-2.4–ECL2 were created by replacing differing amino acids in the H5 or ECL2 region of Kir2.4 by the corresponding residues of Kir2.1. Insertion of Thr in place of Ser142 in Kir2.1-2.4-H5 (Kir2.1-2.4-S142T) and Cys in place of Ser149 in Kir2.1-2.4-ECL2 (Kir2.1-2.4-S149C) restored VDB to values similar to Kir2.1-WT. To confirm these results, we mutated the two residues that seemed to be responsible for carrying the characteristic VDB directly in the full length Kir2.1-WT. Ba^{2+} sensitivity was not significantly different for either the Kir2.1-C149S or Kir2.1-T142S mutants compared to Kir2.1 WT. As expected both mutants showed no voltage-dependence of Ba^{2+} block.

Our results indicate that voltage dependence of Ba^{2+} block and sensitivity to Ba^{2+} are determined by different regions of the Kir2.1 channel subunit.

Residue	Mutation	Location	Effect on Ba^{2+} block	Reference
D114	D114A	ECL1	No effect	Schram *et al.*, 2003 unpublished results
K117	K117P	ECL1	No effect	Schram *et al.*, 2003 unpublished results
E125	E125Q	ECL1	↓ sensitivity ↔ VDB ↓ rate of recovery	Murata *et al.*, 2002
	E125N	ECL1	↓ sensitivity ↓ VDB ↓ rate of recovery	Alagem *et al.*, 2001
	E125Q	ECL1	↓ sensitivity ↔ VDB ↓ rate of recovery	Alagem *et al.*, 2001
	E125D	ECL1	? sensitivity ↔ VDB ↑ rate of recovery	Alagem *et al.*, 2001
D125*	D125E	ECL1	↑↑ sensitivity	Navaratnam *et al.*, 1995
T141	T141A	H5	↓ sensitivity ↓ VDB	Alagem *et al.*, 2001
T142	T142S	H5	↔ sensitivity ↓↓↓ VDB	Herrera *et al.*, 2006
R148	R148H	H5	↔ sensitivity ↑ onset of block	Sabirov *et al.*, 1997
C149	C149S	ECL2	↔ sensitivity ↓↓↓ VDB	Herrera *et al.*, 2006

Table VIII: Effect of amino acid point mutations on Kir2.1 Ba^{2+} block.

↓: decrease; ↔: no change; ↑: increase. ECL1: Extracellular loop between the M1 and H5 segments. H5: pore region. ECL2: Extracellular loop between H5 and M2 segments. VDB: Voltage dependence of block. *: The chick ear clone has D125 instead of E125. All experiments were performed in *X.* oocytes.

```
Kir2.1      1 -MGSVRTNRYSIVSSEEDGMKLATMAVA------NGFGNGKSKVHTRQQCRSRFVKKDGH
Kir2.2      1 MTAASRANPYSIVSSEEDGLHLVTMSGA------NGFGNG--KVHTRRRCRNRFVKKNGQ
Kir2.3      1 MHGHSR--------------------------------NGQAHVPRRKR-RNRFVKKNGQ
Kir2.4      1 -MGLARALRRLSGALEPGNSRAGDEEEAGAGLCRNGWAPGPVAGNRR---RGRFVKKDGH

                                                        M1
Kir2.1     54 CNVQFINVGEKGQRYLADIFTTCVDIRWRWMLVIFCLAFVLSWLFFGCVFWLIALLHGDL
Kir2.2     53 CNIEFANMDEKSQRYLADMFTTCVDIRWRYMLLIFSLAFLASWLLFGIIFWVIAVAHGDL
Kir2.3     28 CNVYFANLSNKSQRYMADIFTTCVDTRWRYMLMIFSAAFLVSWLFFGLLFWCIAFFHGDL
Kir2.4     57 CNVRFVNLGGQGARYLSDLFTTCVDVRWRWMCLLFSCSFLASWLLFGLTFWLIASLHGDL

                                                    H5
Kir2.1    114 DTS--K------------------VSKACVSEVNSFTAAFLFSIETQTTIGYGFRCVTDE
Kir2.2    113 EPAEGR------------------GRTPCVMQVHGFMAAFLFSIETQTTIGYGLRCVTEE
Kir2.3     88 EAS--PGVPAAGGPAAGGGGAAPVAPKPCIMHVNGFLGAFLFSVETQTTIGYGFRCVTEE
Kir2.4    117 AAP--P------------------PPAPCFSQVASFLAAFLFALETQTSIGYGVRSVTEE
                                       *          *↑     *↑

                  M2
Kir2.1    154 CPIAVFMVVFQSIVGCIIDAFIIGAVMAKMAKPKKRNETLVFSHNAVIAMRDGKLCLMWR
Kir2.2    155 CPVAVFMVVAQSIVGCIIDSFMIGAIMAKMARPKKRAQTLLFSHNAVVALRDGKLCLMWR
Kir2.3    146 CPLAVIAVVVQSIVGCVIDSFMIGTIMAKMARPKKRAQTLLFSHHAVISVRDGKLCLMWR
Kir2.4    157 CPAAVAAVVLQCIAGCVLDAFVVGAVMAKMAKPKKRNETLVFSENAVVALRDRRLCLMWR

Kir2.1    214 VGNLRKSHLVEAHVRAQLLKSRITSEGEYIPLDQIDINVGFDSGIDRIFLVSPITIVHEI
Kir2.2    215 VGNLRKSHIVEAHVRAQLIKPRVTEEGEYIPLDQIDIDVGFDKGLDRIFLVSPITILHEI
Kir2.3    206 VGNLRKSHIVEAHVRAQLIKPYMTQEGEYLPLDQRDLNVGYDIGLDRIFLVSPIIIVHEI
Kir2.4    217 VGNLRRSHLVEAHVRAQLLQPRVTPEGEYIPLDHQDVDVGFDGGTDRIFLVSPITIVHEI

Kir2.1    274 DEDSPLYDLSKQDIDNADFEIVVILEGMVEATAMTTQCRSSYLANEILWGHRYEPVLFEE
Kir2.2    275 DEASPLFGIS-QDLETDDFEIVVILEGMVEATAMTTQARSSYLANEILWGHRFEPVLFEE
Kir2.3    266 DEDSPLYGMGKEELESEDFEIVVILEGMVEATAMTTQARSSYLASEILWGHRFEPVVFEE
Kir2.4    277 DSASPLYELGRAELARADFELVVILEGMVEATAMTTQCRSSYLPGELLWGHRFEPVLFQR

Kir2.1    334 KHYYKVDYSRFHKTYEVPNTPLCSARDLAEKKYILSNA-----N---------SFCYENE
Kir2.2    334 KNQYKIDYSHFHKTYEVPSTPRCSAKDLVENKFLLPSA-----N---------SFCYENE
Kir2.3    326 KSHYKVDYSRFHKTYEVAGTPCCSARELQESKITVLPAPPPPPS---------AFCYENE
Kir2.4    337 GSQYEVDYRHFHRTYEVPGTPVCSAKELDERAEQASHS-----PKSSFPGSLAAFCYENE

Kir2.1    380 VALTSKEEEEDSEN---------GVPESTSTD--SPPG---I----------DLHN-QAS
Kir2.2    380 LAFLSRDEEDEAD----------GDQDGRSRDGLSPQARHDF----------DRLQ-AGG
Kir2.3    377 LALMSQEEEEMEEEAAAAAAVAAGLGLEAGSK--EEAG---IIRMLEFGSHLDLERMQAS
Kir2.4    392 LAL-SCCQEEDEEE---------DTKEGTSAE--TP------------------D-RAA

Kir2.1    415 VPLEPRPLRRESEI-
Kir2.2    419 GVLEQRPYRRESEI-
Kir2.3    432 LPLDNISYRRESAI-
Kir2.4    420 SPQALTPTLALTLPP
```

Figure 25: Comparison of Kir2.1-4 amino acid sequences.

Kir2.2, Kir2.3 and Kir2.4 share 69%, 57% and 57% identity on the amino acid level, respectively. Residues are shaded in blue if they share > 60 identity. Transmembrane segments M1 and M2 and the pore region H5 are indicated by black bars. The turret is located between M1 and H5, the pore helix-M2 linker between H5 and M2. Amino acids relevant for Ba of Kir2.1 (corresponding to Kir2.1: E125, T141 and R148) are indicated by asterixes, newly discovered amino acids responsible for VDB (T142 and C149) by arrows.

How can these observations be interpreted? Residues Thr142 in H5 and Cys149 in ECL2 are essential for voltage dependent Ba^{2+} block but not for Ba^{2+} sensitivity (Schram *et al.*, 2005; Herrera *et al.*, 2006). The C-terminal end of the pore helices (T142 in Kir2.1) is crucial for stabilization of K^+ ions in the central cavity, providing 80% of the energy necessary to coordinate the hydrated K^+ ion in the center of the cavity (Roux & MacKinnon, 1999). Ba^{2+} has almost the identical crystal radius (1.35 Å) as K^+ (1.33) suggesting that a similar amount of energy might be necessary to stabilize a Ba^{2+} ion in the cavity. Thr142 of Kir2.1 is conserved amongst Kir2.1-3, which all display similar VDB. The corresponding amino acid in Kir2.4 is a serine. It is thus reasonable to speculate that substitution of threonine by serine results in lack of stabilization of Ba^{2+} in the central cavity, causing loss of voltage-dependence of block. The second residue identified, Kir2.1-Cys149, is located at the extracellular end of the selectivity filter in the H5-M2 linker. Kir2.4 has a serine (Kir2.4-Ser152) at this position. Both cysteine and serine are neutral amino acids so charge can not account for their role in voltage-dependence of Ba^{2+} block. Cysteine interaction with other residues might result in conformational changes or stabilization of the pore thus affecting ion permeation. Modelling studies will help to answer these questions.

The molecular mechanisms determining Ba^{2+} sensitivity of Kir2.4 remain unclear. Glu125 in the turret (ECL1) of Kir2.1 appears to be important for Ba^{2+} sensitivity of this subunit. The corresponding amino acid in Kir2.4 is Gln129. Even though it can not be excluded that Gln129 contributes to the lower Ba^{2+} sensitivity of Kir2.4, Ba^{2+} sensitivity of a Kir2.1-2.4-ECL1 chimera was not different from Kir2.1-WT. In addition, glutamine is also found in the corresponding position in Kir2.2 (Gln126), which displays the highest Ba^{2+} sensitivity of all four Kir2 subunits, suggesting that Glu129 might not be an essential determinant of Kir2.4 Ba^{2+} sensitivity. This speculation is in contrast to results published by Murata et al. (2002) suggesting that Glu125 is crucial for Ba^{2+} sensitivity of Kir2.1. No experimental data on Ba^{2+} sensitivity of Kir2.2-Q126E is available even though such a mutant exists (Murata *et al.*, 2002). Potential explanations include that Ba^{2+} sensitivity is determined by complex interactions between residues located in different regions of the channel or affected by channel regulation. Ba^{2+} block of Kir2.3 is modulated by

pH (Vandenberg, C., University of Santa Barbara, California, personal communications). Likewise, Kir2.4 is a pH sensitive channel (Hughes *et al.*, 2000). Thus, pH dependent channel regulation might affect Ba^{2+} binding or permeation properties of Kir2.4.

IC_{50} (μM)				TP	$[K^+]_o$	Clone		Expression	Reference
Kir2.1	*Kir2.2*	*Kir2.3*	*Kir2.4*	*(mV)*	*(mM)*	*Species*	*Tissue*	*System*	
8.0	6.0	-	390.0	-80	96	Rat	Brain	*X.* oocytes	Topert *et al.*, 1998
3.2	0.5	10.3	235.0	-100	60	Guinea pig	Myocardium	*X.* oocytes	Liu *et al.*, 2001

Table IX: Ba^{2+} sensitivity of Kir2.1-4 cloned from various tissues and species as indicated. Test potentials as well as the external K^+ concentration at which IC_{50}'s were obtained are indicated. TP: Test potential. $[K^+]_o$: External K^+ concentration.

V-3 The G-protein activated cardiac inward rectifier I_{KACh}

V-3.1 The G-protein Signalling Pathway

K_G-currents are inwardly rectifying currents that primarily control slow postsynaptic inhibitory signalling and hormone secretion. These currents are found in (but not limited to) the heart, the central and peripheral nervous system and in endocrine tissues (Sadja *et al.*, 2003). Several Gα-protein classess are known: G_s, G_i, G_t, G_q, G_o, G_{12} and G_{13}. G_i, G_o and G_t are pertussis toxin (PTX) sensitive (Gilman AG, 1987). G_K is supposed to be a member of the G_i class in some systems (Kozasa *et al.*, 1996). G_i-proteins are heterotrimeric GTP-binding regulatory proteins that are present in all eukaryotic cells. They control metabolic, humoral, neural, and developmental functions (Simon *et al.*, 1991), and play a critical role in signal propagation from the cell surface to the cell interior (Neer & Clapham, 1988; Gilman, 1995; Neer, 1995; Lanier, 2004). Important effector proteins include the muscarinic cardiac K^+ channel I_{KACh}, adenylyl cyclase and phospholipase C (Navarro *et al.*, 1999). G-proteins consist of three subunits, Gα, Gβ, and Gγ that form together the heterotrimeric protein Gαβγ. The interaction between the M2 receptor and the α-subunit can be blocked by PTX (Kurose *et al.*, 1986) resulting in interruption of signal transduction. G-proteins are associated with the cytoplasmic side of the cell membrane by hydrophobic anchors.

K_G-currents are regulated by G-protein coupled receptors (GPCR). In the resting state, GDP is bound to Gα. Upon GPCR stimulation, G-protein bound GDP is exchanged for a cytoplasmatic GTP resulting in dissociation of Gαβγ into Gα-GTP and the free βγ heterodimer (Clapham & Neer, 1997). Both Gα-GTP and the βγ subunit can interact with effector proteins such as ion channels or enzymes (Yamada *et al.*, 1998). Hydrolysis of Gα-GTP into Gα-GDP, which subsequently re-associates with Gβγ terminates the activation signal. Regulators of G-protein signalling (RGS) proteins (Hepler, 1999; Ross & Wilkie, 2000) control activation of GTPase (GAP) activity, accelerating activation, desensitization, deactivation and agonist

concentration- and time-dependent relaxation of Kir3 currents (Doupnik *et al.*, 1997; Saitoh *et al.*, 1997; Fujita *et al.*, 2000; Stanfield *et al.*, 2002) (Figure 26).

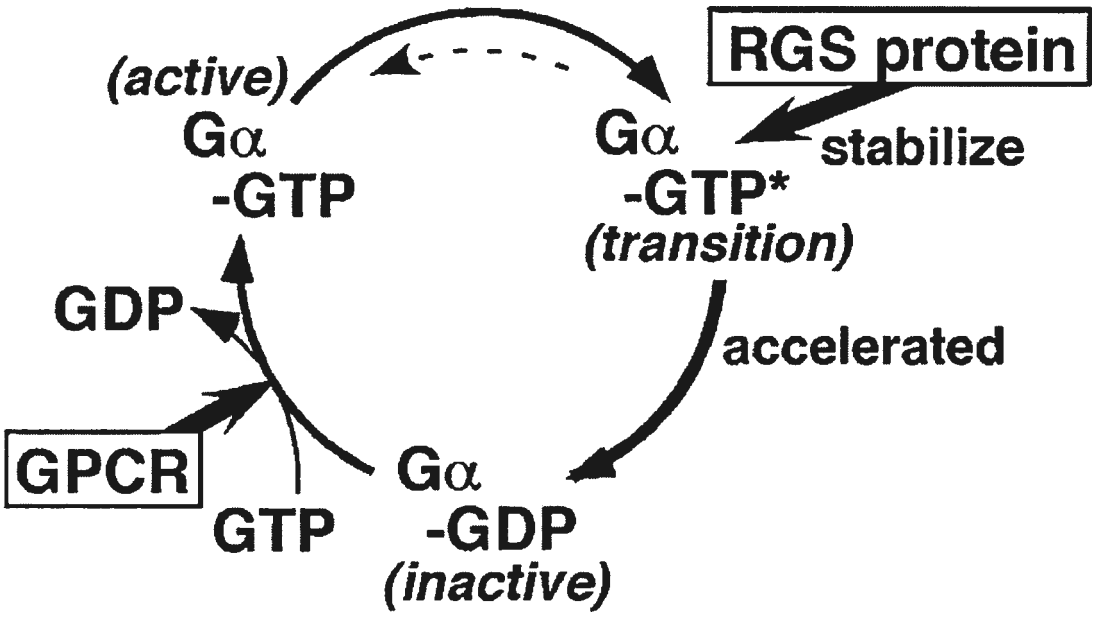

Figure 26: Schematic representation of the action of RGS protein.

RGS proteins stabilize the transition state (Gα-GTP*) of GTP hydrolysis on the Gα subunit, which results in the acceleration of intrinsic GTPase-activity on the subunit (GTPase-accelerating protein; GAP). GPCR, G protein-coupled receptor. Reproduced from Kurachi & Ishii (2004).

Another group of accessory proteins regulating the signal transfer from receptor to G-protein or the activation state of G-proteins independently of a classical G-protein coupled receptor are so-called Activators of G-protein Signalling (AGS) proteins (Lanier, 2004). The usage of a membrane-delimited system as opposed to (slower changes in) intracellular messengers has been implicated in the rapid cellular response of I_{KACh} to vagal stimulation (Hartzell *et al.*, 1991). Recent studies suggest the formation of heteromeric complexes consisting of Kir3 channels, G-protein, GPCR and RGS protein (Jeong & Ikeda, 2001; Zhang *et al.*, 2002; Benians *et al.*, 2003).

The system of G-protein regulated activation of K_G-channels represents an important regulator of cardiac and neuronal cellular excitability. A wide variety of membrane receptors including M2-muscarinic, A1-adenosine, α_2-adrenergic, D2-dopamine, various opioid receptors, 5-HT_{1A}-serotonin, somatostatin, $GABA_B$ to only name a few use this pathway to inhibit cell excitation in various organs (Yamada *et al.*, 1998). More than sixteen genes encoding Gα subunits, four genes encoding β-subunits and multiple genes encoding γ-subunits are known (Simon *et al.*, 1991).

V-3.2 Direct Activation of I_{KACh} by βγ-subunits

Almost one century ago, Otto Loewi discovered that the release of "Vagusstoff" (Acetylcholine) upon stimulation of vagal nerves caused slowing of the heart rate (Loewi, 1921; Loewi & Navaratil, 1926). Membrane hyperpolarization induced by ACh in the frog heart was subsequently demonstrated by two groups (Burgen & Terroux, 1953; Del Castillo & Katz, 1955). A series of publications from Trautwein and colleagues led to the proposition that ACh induces activation of muscarinic K^+ channels termed I_{KACh} resulting in deceleration of pacemaker activity in sino-atrial node cells (Hutter & Trautwein, 1955; Trautwein & Dudel, 1958; Noma & Trautwein, 1978; Osterrieder *et al.*, 1981). Single channel recordings of I_{KACh} displayed unique channel kinetics (Sakmann *et al.*, 1983). A scientific breakthrough was the discovery that acetylcholine binds to M2-muscarinic and A1-adenosine receptors activating I_{KACh} via a PTX-sensitive G_i-protein (Pfaffinger *et al.*, 1985; Breitwieser & Szabo, 1985; Kurachi *et al.*, 1986a; Kurachi *et al.*, 1986b). After a long

controversy which part of the G-protein is responsible for activation of K_G-channels, it was shown that I_{KACh} is directly activated (Kurachi *et al.*, 1986a; Kurachi *et al.*, 1986b) through βγ-subunits (Logothetis *et al.*, 1987) and not the Gα-GTP subunit (Codina *et al.*, 1987; Yatani *et al.*, 1987; Yatani *et al.*, 1988). Confirmation was obtained from molecular studies (Krapivinsky *et al.*, 1995b; Inanobe *et al.*, 1995). Direct binding of Gβγ to the I_{KACh} channel increases channel open probability (Logothetis *et al.*, 1987; Kurachi *et al.*, 1989; Clapham, 1994; Wickman *et al.*, 1994).

V-3.3 Biophysical Properties

Inward rectifier channels activated by G-proteins or other second messenger systems display intermediate rectification properties (Kubo *et al.*, 1993b; Bond *et al.*, 1994; Yamada *et al.*, 1998). I_{KACh} shows a sigmoidal activation time course (Breitwieser & Szabo, 1988). Upon hyperpolarization, current increases instantaneously to a certain level and then continuous to increase slowly to a steady state level. Membrane depolarization causes the reverse biphasic reaction, slow and then fast decreases in current amplitude. Whereas the fast component of g_K is due to voltage-dependent unblocking of polyamines and Mg^{2+} (Horie *et al.*, 1987; Matsuda *et al.*, 1987; Fakler *et al.*, 1995; Yamada & Kurachi, 1995), a different mechanism designated "relaxation" accounts for the slow phase (Kurachi & Ishii, 2004). Relaxation is caused by slow recovery from inhibition at depolarized voltages mediated by the RGS domain of the RGS protein with the PTX-sensitive Gα subunit (Inanobe *et al.*, 2001). At diastolic potentials, GAP activity of RGS proteins is inhibited by phosphatidyl-3,4,5-trisphosphate (PIP_3). Depolarization induces Ca^{2+} influx, which subsequently binds to Calmodulin (CaM) to form a Ca^{2+}-CaM complex. The Ca^{2+}-CaM complex binds to RGS protein, relieves the PIP_3-mediated inhibition, restores GAP activity of RGS proteins, and accelerates the hydrolysis of GTP on Gα. GDP- Gα re-associates with free Gβγ and thus decreases active K_G channel number. Therefore, at depolarized potentials the G-protein cycle is negatively regulated and the number of active K_G channels is decreased (Ishii & Kurachi, 2003). Deactivation of I_{KACh} after agonist washout occurs within seconds (Gilman, 1987). The single channel conductance of I_{KACh} and neuronal K_G channels is 32-35 pS and the mean

open time ~ 1-2 ms (Logothetis *et al.*, 1987; Miyake *et al.*, 1989; Grigg *et al.*, 1996; Wickman *et al.*, 1998; Bettahi *et al.*, 2002).

V-3.4 Pharmacological Properties

I_{KACh} can be activated by acetylcholine and other agonists including adenosine (Hartzell, 1979). Ba^{2+} and Cs^{+} ions block I_{KACh} (and other K_G-currents) in a concentration- and voltage-dependent but time-independent manner (Carmeliet & Mubagwa, 1986; Gahwiler & Brown, 1985; Inoue *et al.*, 1988). Sodickson et al. reported voltage-independent Ba^{2+} block of a $GABA_B$ activated K^{+} current in hippocampal neurons (Sodickson & Bean, 1996). Sensitivity to Ba^{2+} and CS^{+} ions is about one order of magnitude lower than for that of strong inward rectifiers. Interestingly, Ehrlich et al. described a time-dependent hyperpolarization-induced G-protein activated current in canine myocytes from pulmonary vein myocardial sleeve and the left atrium with Ba^{2+} sensitivity about twice as high as the strong inward rectifier current I_{K1} in human ventricle (Ehrlich *et al.*, 2004).

K_G-currents are sensitive to quinidine and quinine (Kurachi *et al.*, 1987; Katayama *et al.*, 1997), verapamil (Ito *et al.*, 1989), flecainide (Inomata *et al.*, 1991) and cibenzoline (Wu *et al.*, 1994). No effect has been reported for TEA, 4-AP, apamine, charybdotoxin, disopyramide and procainamide (Lacey *et al.*, 1987; Lacey *et al.*, 1988; Inoue *et al.*, 1988; Nakajima *et al.*, 1989; Katayama *et al.*, 1997). Tertiapin, a 22-amino acid peptide isolated from the venom of the honey bee (Gauldie *et al.*, 1976) blocks I_{KACh} and I_{KATP} channels but not I_{K1} with nanomolar affinities (Jin & Lu, 1998). A more stable, synthetic form of Tertiapin, Tertiapin-Q, has recently been synthesized (Jin & Lu, 1999) and used to study acetylcholine-dependent current in the heart (Drici *et al.*, 2000).

V-3.5 Role of Cardiac I_{KACh}

In the heart, I_{KACh} is responsible for acetylcholine (ACh) mediated deceleration of the heart rate and heart rate variability (Krapivinsky *et al.*, 1995a; Wickman *et al.*, 1998). I_{KACh} is found in the conduction system, the SA node, the atria, the AV node, Purkinje cells (Kurachi *et al.*, 1992) and the ventricular

myocardium (Koumi *et al.*, 1997; Ito *et al.*, 1995; Boyett *et al.*, 1988; Hartzell & Simmons, 1987; Kovoor *et al.*, 2001). In SA nodal cells, acetylcholine induces slowing of the heart rate (DiFrancesco, 1993). However, the precise ionic determinants causing this effect are not completely understood. While earlier studies indicated that parasympathetic regulation of the heart rate was due to ACh-mediated activation of I_{KACh} (Giles & Noble, 1976; Noma & Trautwein, 1978; Garnier *et al.*, 1978; Sakmann *et al.*, 1983), later studies provided evidence that the pacemaker current I_f (DiFrancesco & Tromba, 1988; DiFrancesco *et al.*, 1989; Bywater *et al.*, 1990; Hirst *et al.*, 1992), the L-type Ca^{2+} channel $I_{Ca,L}$ and the sustained inward current I_{st} might be implicated in autonomic regulation of the heart rate (Noma *et al.*, 1983; Hagiwara *et al.*, 1988; Guo *et al.*, 1995).

Expression of I_{KACh} in atrial cells is approximately six times higher than in the ventricles (Kurachi *et al.*, 1992; Wickman *et al.*, 1994). Atrial I_{KACh} has been proposed to play an important role in the control of the resting membrane potential and repolarization in rabbit atrial myocytes (Kaibara *et al.*, 1991) and might contribute to modulation of RMP and APD in human atrium (Dobrev *et al.*, 2001). Activation of I_{KACh} produces shortening of atrial and ventricular APD as well as a negative inotropic effect in rat cardiomyocytes (McMorn *et al.*, 1993).

In guinea pig heart, the selective I_{KACh} blocker Tertiapin prevents acetylcholine induced third degree AV block in a dose dependent fashion suggesting a role of I_{KACh} in genesis of AV block. Similar effects are observed in isolated rabbit hearts (Drici *et al.*, 2000; Kitamura *et al.*, 2000). In ventricular myocytes, Tertiapin produces non-significant shortening of the QTc interval suggesting an effect on ventricular repolarization (Drici *et al.*, 2000). I_{KACh} activation through adenosine might underlie the profound bradycardia and AV block after adenosine administration (DiMarco *et al.*, 1983; Clemo & Belardinelli, 1986; Kurachi *et al.*, 1986b).

V-3.6 Role of I_{KACh} in Disease

Patch clamp studies have shown greater I_{KACh} density in LA than in RA (Sarmast *et al.*, 2003). A greater dose-dependent increase in LA than RA rotor frequency due to greater I_{KACh} was suggested to underlie cholinergic AF (Sarmast *et*

al., 2003) and might contribute to shorter APD and ERP in the LA free wall (Li *et al.*, 2001). In chronic AF, I_{KACh} is down regulated and muscarinic receptor mediated shortening of APD is attenuated. It was suggested that down regulation of I_{KACh} presents a mechanism to counteract upregulation of I_{K1} in AF thereby preventing ERP shortening, decreasing ERP heterogeneity and so vulnerability to atrial tachyarrhythmia (Dobrev *et al.*, 2001).

V-3.7 Molecular Basis of K_G-Currents

K_G-currents are conducted by members of the Kir3 subfamily. Kir3 channels are activated by βγ-subunits of heterotrimeric G-proteins (Logothetis *et al.*, 1987) in a membrane-delimited fashion. Four members, Kir3.1-4, are currently known (Shieh *et al.*, 2000; Gutman *et al.*, 2003). Three different isoforms of Kir3.2 channels are obtained by alternative splicing (Isomoto *et al.*, 1996a).

V-3.7.1 Role of Kir3 Subunits in the Heart

I_{KACh} is encoded by heterotetramers of Kir3.1 and Kir3.4 (Krapivinsky *et al.*, 1995a; Wickman *et al.*, 1998). Kir3.1 protein has been detected in rat, ferret, and guinea pig SAN where it co-localises with the M2-receptor. Kir3.4 protein was found in rat SAN (Dobrzynski *et al.*, 2001). Kir3.1/Kir3.4 mRNA (DePaoli *et al.*, 1994; Karschin *et al.*, 1994b) and protein expression (Dobrzynski *et al.*, 2001) is higher in the atria than in the ventricles, consistent with higher I_{KACh} current density in atrium (Kurachi *et al.*, 1992; Wickman *et al.*, 1994). Homomeric Kir3.4 channels might also contribute to atrial I_{KACh} (Corey & Clapham, 1998; Bender *et al.*, 2001) unlike Kir3.1 which can not form homomeric channels due to lack of membrane expression (Krapivinsky *et al.*, 1995a; Hedin *et al.*, 1996). No data exists for the AVN or His-Purkinje system.

Kir3.1 or Kir3.4 KO mice exhibit modest resting tachycardia, suggesting loss of inhibitory influences on heart rate, and depolarization of the MDP (Kovoor *et al.*, 2001; Bettahi *et al.*, 2002). Heart rate variability (beat-to-beat variations of the heart rate due to parasympathetic and sympathetic tonus (Akselrod *et al.*, 1981)) is greatly attenuated in Kir3.1 and Kir3.4 KO mice at rest and after vagal stimulation with

methoxamine and vagus-independent cholinergic stimulation with the A1-receptor selective agonist 2-chloro, N6-cyclopentyl adenosine (CCPA). Methoxamine and CCPA also greatly attenuate the bradycardic response in Kir3.1 and Kir3.4 KO mice. No effects on AVN conduction are noted in either KO mice (Wickman *et al.*, 1998; Bettahi *et al.*, 2002). Taken together, these results suggest an important role of I_{KACh} in regulation of the heart rate, even at baseline, when parasympathetic tone is not elevated.

V-3.7.2 Role of Kir3 Subunits in the CNS

In the central nervous system (CNS), Kir3 channels contribute to regulation of firing rates, membrane potential and neurotransmitter responses (Isomoto *et al.*, 1997) by decreasing membrane excitability (Isomoto *et al.*, 1997). Alternative splicing of the Kir3.2 gene might contribute to Kir3 encoded inward rectifier current diversity in the brain (Isomoto *et al.*, 1996a) where functional heterotetramers of Kir3.1 and Kir3.2 exist (Lesage *et al.*, 1995). Activation of Kir3 channels in the CNS hyperpolarizes the MDP thereby slowing membrane depolarization (Isomoto *et al.*, 1997).

G-protein activated inward rectifier currents in the brain play a key role in neurotransmitter-regulated changes of cellular excitability (North, 1989; Grigg *et al.*, 1996) and are involved in the postsynaptic inhibitory action of many neurotransmitters such as γ-aminobutyric acid through $GABA_B$ receptors, adenosine through A1 receptors and serotonin through $5\text{-}HT_{1A}$ receptors (Luscher *et al.*, 1997).

Kir3.1 mRNA is abundantly expressed throughout the brain in rats (DePaoli *et al.*, 1994; Karschin *et al.*, 1994b; Ponce *et al.*, 1996) and mice (Kobayashi *et al.*, 1995). Kir3.1 protein is found mainly on somata and dendrites in a matching distribution (Ponce *et al.*, 1996; Bausch *et al.*, 1995; Liao *et al.*, 1996; Ponce *et al.*, 1996; Miyashita & Kubo, 1997). Abundant Kir3.1 mRNA is expressed in the olfactory system, hippocampus, dentate gyrus, amygdale, neocortex, lateral septal nuclei, thalamus, red nucleus, cerebellar granule cells, deep cerebellar nuclei and the brainstem. No Kir3.1 mRNA is detected in hypothalamus and basal ganglia (Karschin & Karschin, 1999). Kir3.2 protein expression is prominent in neuronal somata and

dendrites in a distribution pattern similar to that of Kir3.1 (Liao *et al.*, 1996; Adelbrecht *et al.*, 1997). Differences between Kir3.1 and Kir3.2 tissue distribution are found in dopaminergic neurons of the substantia nigra pars compacta and the ventral tegmental area where Kir3.1 is absent and only Kir3.2 is expressed, in the caudate-putamen complex, where Kir3.1 is moderately expressed and Kir3.2 is absent and in cerebellar deep nuclei, where Kir3.1 expression is prominent. Kir3.3 is the most widely distributed Kir3 subunit in the brain and shows moderate to strong mRNA expression in almost all brain regions (Dissmann *et al.*, 1996; Karschin *et al.*, 1996). Expression is particularly strong in the olfactory system, the all layers of neocortex, hippocampus, and in cerebellar Purkinje cells, where Kir3.1 and Kir3.2 are not detected. Kir3.4 expression in the brain is restricted (Karschin & Karschin, 1997). Moderate Kir3.4 protein xpression is found in the medial habenula, the superior colliculus and cerebellar Purkinje cells (Murer *et al.*, 1997).

Functional importance of Kir3 channel subunits has been investigated using Kir3 knockout mice. Whereas Kir3.1 and Kir3.4 knockout mice do not display neurological abnormalities (Wickman *et al.*, 1998; Bettahi *et al.*, 2002), mice lacking the Kir3.2 gene develop spontaneous seizures and are more susceptible to pharmacologically induced seizures. In weaver mice (Lane, 1964) a G156S mutation in the Kir3.2 channel (Patil *et al.*, 1995) is associated with cerebellar atrophy due to loss of granule cell neurons resulting in gait abnormalities (weaver for "weaving gait"), fine rapid tremor and hyperactivity. The G156S mutation in weaver mice is within the GYG of the selectivity filter, resulting in a SYG sequence. This mutation causes loss of K^+ selectivity and makes the channel permeable for Na^+. Na^+ influx into the cell activates the channel further (Silverman *et al.*, 1996a), leading to increased Na^+/Ca^{2+} exchanger activity causing intracellular Ca^{2+} overload and cell death. Mice in which the Kir3.2 gene has been deleted (Kir3.2 knockout mice) are morphologically indistinguishable from wild-type mice confirming that the weaver phenotype is due to abnormal Kir3.2 function (Signorini *et al.*, 1997). Data based on biochemical and functional properties indicates that functional K_G channels composed of Kir3.2 and Kir3.3 subunits exist in brain (Jelacic *et al.*, 2000). Knockout of Kir3.2 and / or Kir3.3 depolarizes RMP in locus coeruleus (LC) neurons of mice

by 15 to 20 mV compare to WT mice. In these animals, [Met]^{5}enkephalin-induced hyperpolarization and whole-cell current were reduced by 40% in LC neurons from Kir3.2 knockout mice and by 80% in neurons from Kir3.2/3.3 double knockout mice indicating that both Kir3.2 and Kir3.3 subunits contribute to native K_G current in locus coeruleus neurons (Torrecilla *et al.*, 2002).

In summary, Kir3 subunits are abundant throughout the brain where they modulate hormone- and neurotransmitter-regulated changes of neuronal excitability. Biochemical, biophysical and functional data indicates that native neuronal K_G-channels are composed of heterotetramers consisting of Kir3.1, Kir3.2 and Kir3.3 channels. Kir3.4 channels are unlikely to play a major role in neuronal K_G channels. Dysfunction of K_G-channels in the brain is associated with increased neuronal excitability and a decrease in seizure threshold. The functional importance of Kir3 channels in endothelial cells is unknown.

V-4 The ATP-sensitive Inward Rectifier Current I_{KATP}

An ATP-sensitive K^+ channel was discovered 1983 by Noma in guinea pig ventricular myocytes (Noma, 1983). Subsequently, K_{ATP} channels have been found in a variety of tissues including brain, pancreas, pituitary gland, smooth and skeletal muscle, intestine and kidney (Gross & Peart, 2003). Distinct sarcolemmal, mitochondrial and nuclear K_{ATP} channels have been described. The molecular composition of K_{ATP} channels varies between tissues (Zhuo *et al.*, 2005). K_{ATP} channels are regulated by intracellular ADP and ATP concentrations and thus provide a feedback mechanism between cell metabolism and membrane electrical activity (Gross & Peart, 2003; Zhuo *et al.*, 2005). Cell metabolism regulates K_{ATP} gene expression and products of cell metabolism control channel activity. K_{ATP} channels in return control membrane potentials, regulation of vascular smooth muscle tone, insulin secretion in the pancreas, release of synaptic neurotransmitter release and cell activities such as energy metabolism, cellular homeostasis, apoptosis and gene expression (Ashcroft & Rorsman, 1989; Ho *et al.*, 1993; Nichols & Lederer, 1991; Zhuo *et al.*, 2005). In the heart, K_{ATP} channels protect the myocardium against ischemic injuries. Sarcolemmal K_{ATP} (sarc K_{ATP}) may contribute to energy sparing while mitochondrial K_{ATP} (mito K_{ATP}) channels are involved in ischemic preconditioning (IPC) (Zhuo *et al.*, 2005). When intracellular ATP is low such as under ischemic conditions, I_{KATP} channels open and conduct inward K^+-current. The resulting shortening of cardiac APD decreases the risk of cardiac arrhythmias (Nichols & Lederer, 1991). I_{KATP} shows only weak inward rectification allowing conduction of substantial current at potentials positive to the K^+ equilibrium potential (Noma, 1983; Nichols & Lederer, 1991). The field of K_{ATP} channels is vast and impossible to cover in its entirety in the context of this thesis. The following section will thus only briefly discuss biophysical properties, pharmacology, molecular structure and the functional role of K_{ATP} channels in key organs.

V-4.1 Biophysical and Pharmacological properties

K_{ATP} channels have weak inwardly rectifying properties, are closed when intracellular ATP is high and open when ATP is low, i.e. the ATP/ADP ratio increases. ATP inhibits K_{ATP} channels with an IC_{50} of ~ 10 – 50 μM in excised patches and MgADP reverses the effect (Ashcroft, 1988; Nichols *et al.*, 1996; Gribble *et al.*, 1997; Haider *et al.*, 2005). Intracellular nucleoside diphosphates (NDP) activate I_{KATP} (Noma, 1983). Pancreatic, cardiac and skeletal muscle K_{ATP} channels have single-channel conductances of ~ 70-90 pS under symmetrical K^+-conditions (Ashcroft, 1988; Terzic *et al.*, 1995) and are blocked by Mg^{2+} and Na^+ at membrane potentials positive to E_K (Horie *et al.*, 1987). K_{ATP} channels are selectively inhibited by sulfonylurea derivatives including glibenclamide and tolbutamide. K_{ATP} channels are activated by a class of drugs known as K^+ channel openers (KCO) which include pinacidil and diazoxide, however, sensitivities differ between channels from different tissues (Weik & Neumcke, 1989; Hamada *et al.*, 1990; Allard *et al.*, 1995; Ashcroft & Ashcroft, 1990; Zhang & Bolton, 1995; Quayle *et al.*, 1997). Application of PIP_2 and long chain acyl CoAs (LC-CoA) increases open probability and decreases ATP sensitivity (Baukrowitz *et al.*, 1998; Shyng & Nichols, 1998; Fan & Makielski, 1997; Larsson *et al.*, 1996b; Gribble *et al.*, 1998a) through interaction with residues in the C-terminus (Shyng *et al.*, 2000b) providing another potential mechanism for channel activation in physiological ATP concentrations (Xie *et al.*, 1999; Shyng *et al.*, 2000a).

V-4.2 Functional Role of K_{ATP} channels

V-4.2.1 Regulation of Pancreatic Insulin Secretion

A physiological role of K_{ATP} channels has first been characterized in pancreatic β-cells. Increase in intracellular ATP due to increased glucose metabolism closes K_{ATP} channels. This leads to depolarization of the RMP leading to Ca^{2+} influx into the cell through the opening of voltage-gated Ca^{2+} channels. Rise in the intracellular Ca^{2+}-concentration in β-cells triggers exocytosis of insulin-containing granules (Seino & Miki, 2003). Insulin secretion from β-cells can be stimulated by pharmacological treatment with sulfonylureas which inhibit I_{KATP} through direct closing of K_{ATP} channels (Trube *et al.*, 1986; Dunne *et al.*, 1987; Sturgess *et al.*,

1985; Seino & Miki, 2003). When glucose level fall low, the ADP to ATP ratio increases, K_{ATP} channels open and hyperpolarize the cell thereby shutting off the release of insulin.

Hypothalamic K_{ATP} channels might play a critical role in the modulation of glucose homeostasis through regulation of the counter-regulatory hormones such as glucagon and catecholamines (Taborsky, Jr. *et al.*, 1998). Mice lacking the gene encoding the pore-forming subunit of K_{ATP} channels display a markedly impaired recovery from insulin-induced hypoglycaemia (Miki *et al.*, 2001), consistent with this notion.

V-4.2.2 Role of Cardiac I_{KATP}

In the heart, K_{ATP} channels are involved in cellular reactions to metabolic stress during ischemia and hypoxia (Fujita & Kurachi, 2000). Cardiac I_{KATP} is regulated via cell metabolites (fast regulation) or regulation of K_{ATP} gene expression (slow regulation) (Zhuo *et al.*, 2005). Decreased arrhythmogenicity through K_{ATP} channel increased K^+-efflux during ischemia is not due to membrane hyperpolarization but to inhibition of cellular excitability (Nichols & Lederer, 1991; Nakaya *et al.*, 1991; Findlay, 1994; Isomoto *et al.*, 1997). Mice lacking I_{KATP} have a deficit in repolarization reserve. Adrenergic challenges in these animals provoke EADs, triggered activity and torsades de pointes ventricular tachycardia (Liu *et al.*, 2004) emphasizing the important functional role of K_{ATP} in modulation of membrane excitability during sympathetic stress. Cardiac sarc K_{ATP} channels may also provide protection against ischemia by energy sparing while both sarc K_{ATP} and mito K_{ATP} channels are important for IPC, minimizing cardiac damage during hypoxia (Grover *et al.*, 1992; Yao *et al.*, 1993; Zhuo *et al.*, 2005). Sarc K_{ATP} contributes to acceleration of phase 3 repolarization and slowing of depolarization. This causes shortening of APD and prevents the reversal of the Na^+/Ca^{2+} exchanger thereby inhibiting Ca^{2+} entry into the cell (Suzuki *et al.*, 2001). A decrease in intracellular Ca^{2+} results in reduction of mechanical contraction and energy sparing. In ischemic preconditioning, brief intermittent periods of ischemia protect the myocardium against a more sustained episode of ischemia resulting in a marked reduction of

infarct size (Murry *et al.*, 1986). Both sarc K_{ATP} and mito K_{ATP} contribute to IPC through different, complementary mechanisms (Zhuo *et al.*, 2005) which might include activation of protein kinase C (PKC), increase in nitric oxide (NO) via induction of endothelial NO synthase and activation of the Na^+/K^+ ATPase (Gross *et al.*, 2003; Gross & Peart, 2003).

V-4.2.3 Role of K_{ATP} in the CNS

K_{ATP} channels in the brain exert a protective function against neuronal damage and neurodegeneration during metabolic stress (Heurteaux *et al.*, 1995; Blondeau *et al.*, 2000). Within two minutes of ischemia, ATP levels in the brain fall to about 5 – 15% of their normal value (Katsura *et al.*, 1992; Lipton, 1999). K_{ATP} channels have been shown to be involved in hypoxia induced hyperpolarization in the hippocampus (Fujiwara *et al.*, 1987). K_{ATP} channels in the brain have been detected in many regions including the substantia nigra pars reticularis (Roper & Ashcroft, 1995), the neocortex (Ohno-Shosaku & Yamamoto, 1992), the hippocampus (Zawar *et al.*, 1999) and the hypothalamus (Ashford *et al.*, 1990) and show particularly high expression in the substantia nigra pars reticulata (SNr) (Mourre *et al.*, 1989; Hicks *et al.*, 1994). The SNr is an essential structure in suppressing generalized seizures, and K_{ATP} channels might play a critical role in modulating SNr excitability. Studies with mice lacking the pore forming subunit of K_{ATP} have demonstrated an important functional role of K_{ATP} in seizure control during hypoxia. Rapid minimization of oxygen consumption through control of seizures minimizes irreversible cell damage caused by a high metabolic demand during seizure (Yamada & Inagaki, 2005).

V-4.2.4 Role of Vascular I_{KATP}

In coronary arteries, K_{ATP} channels mediate vasodilation during ischemia (Daut *et al.*, 1990; Beech *et al.*, 1993; Dart & Standen, 1995). Mice lacking I_{KATP} suffer from coronary artery vasospasm ("Prinzmetal angina"), arterial hypertension and sudden death (Miki *et al.*, 2002; Chutkow *et al.*, 2002). Activation of K_{ATP} channels in the vascular system by KCOs leads to smooth muscle relaxation, decreases vascular resistance and lowers blood pressure (Edwards & Weston, 1993; Nelson & Quayle, 1995; Quayle *et al.*, 1995; Quayle *et al.*, 1997). The role of I_{KATP}

and K_{ATP} channel opener in myocardial ischemia-reperfusion is controversial (Zhuo *et al.*, 2005).

Data on K_{ATP} channels in endothelial cells is sparse. K_{ATP} currents in endothelial cells were first described in endothelial cells from rat brain and aorta (Janigro *et al.*, 1993; Janigro *et al.*, 1996), rabbit arteries (Katnik & Adams, 1995) and aorta (Katnik & Adams, 1997). Liu et al. (1997) showed that endothelium-dependent relaxation in response to hypoxia can overwhelm hypoxia induced vasoconstriction in small porcine coronary arteries. Pharmacological studies indicate that this relaxation is likely to be mediated by a mechanism independent of nitric oxide or prostacyclin which involves activation of smooth muscle K_{ATP}-channels (Liu & Flavahan, 1997). Endothelial K_{ATP} channels have also been implicated in adenosine induced potentiation of vasodilation of porcine subepicardial coronary arterioles (Kuo & Chancellor, 1995). Chatterjee et al (2003) have shown that shear stress in pulmonary microvascular endothelial cells induces expression of K_{ATP} currents which contribute to membrane hyperpolarization. Membrane depolarization due to an acute decrease in sheer stress can be prevented by cromakalim, indicating a role of K_{ATP} channels in endothelial cell membrane depolarization response due to ischemia induced flow changes (Chatterjee *et al.*, 2003). Endothelial dysfunction, an important contributor to reperfusion injury during ischemia (Hearse, 1998), is reduced by IPC (Yellon & Downey, 2003). In animal models, K_{ATP} openers such as diazoxide mimic IPC while K_{ATP} blockers such as glibenclamide inhibit it (Garlid *et al.*, 1997; Liu *et al.*, 1998; Pain *et al.*, 2000; Gross & Auchampach, 1992; Sanada *et al.*, 2001). K_{ATP} channel-mediated induction of endothelial IPC in vivo has recently been demonstrated in humans (Broadhead *et al.*, 2004). Left ventricular hypertrophy in pigs is associated with a loss of endothelial K_{ATP} channel-dependent, NO-mediated dilatation of endocardial resistance coronary arteries (Gendron *et al.*, 2004).

V-4.3 Molecular Basis of K_{ATP} channels

V-4.3.1 Molecular Basis of K_{ATP} channel assembly

K_{ATP} channels are heterooctameric complexes consisting of four pore-forming Kir6 subunits and four regulatory sulfonylurea receptor (SUR) subunits which co-

assemble to Kir6/SUR tandems in a 4:4 stoichiometry (Inagaki *et al.*, 1997; Clement *et al.*, 1997; Isomoto *et al.*, 1997; Shyng & Nichols, 1997; Reimann & Ashcroft, 1999).

The first member of the Kir6 family, Kir6.1, was cloned in 1995 from a rat pancreatic islet cDNA library. Kir6.1 is ubiquitously expressed including in the brain, heart, pancreatic islets, pituitary, and skeletal muscle (Inagaki *et al.*, 1995b). A second isoform, Kir6.2 sharing 71% identity at the primary sequence level with Kir6.1, was cloned from a human genomic library by homology screening using Kir6.1 as probe. Kir6.2 mRNA expression is strong in the pancreas, but is also found at lower levels in the brain, heart and skeletal muscle (Inagaki *et al.*, 1995a). Instead of Gly-Tyr-Gly, Kir6 channels have Gly-Phe-Gly in their signature sequence.

Sulfonylurea receptors are part of the ATP-binding cassette (ABC) protein superfamily (Higgins, 1992). SUR1 was cloned from rat insulinoma and hamster-insulin secreting tumor cells (Aguilar-Bryan *et al.*, 1995). The sulfonylurea receptor has been proposed to have three transmembrane domains, TMD0, TMD1 and TMD2 consisting of five, five and six transmembrane spanning regions. N- and C-termini are on the cytoplasmic side. Two nucleotide binding folds (NBF-1 and NBF-2) each containing a Walker type A and Walker type B motif (Walker *et al.*, 1982) are located in the loop between TMD1 and TMD2 and in the C-terminus, respectively (Conti *et al.*, 2001). Mutations in SUR1 are associated with familiar hyperinsulinaemic hypoglycaemia (Thomas *et al.*, 1995). Co-expression of Kir6.2 and SUR1 (Aguilar-Bryan *et al.*, 1995) reconstitute the pancreatic ATP sensitive K_{ATP} channel responsible for the regulation of insulin secretion (Inagaki *et al.*, 1995a). SUR1 mRNA expression is high in the pancreas, however, it is also found in heart and brain (Inagaki *et al.*, 1995b). SUR1 shows high affinity binding for glibenclamide suggesting that it confers sulfonylurea binding (Aguilar-Bryan *et al.*, 1995). Other SUR1 splice variants have been identified (Sakura *et al.*, 1999; Hambrock *et al.*, 2002).

SUR2 was cloned from a rat brain library and shares 68% homology with SUR1. In the same year, a splice variant of SUR2 with 97% homology to SUR2 was

cloned and designated SUR2B. SUR2 was subsequently renamed to SUR2A (Isomoto *et al.*, 1996b). Whereas SUR2B mRNA is ubiquitously expressed, SUR2A mRNA expression appears to be restricted to brain, heart and skeletal muscle (Isomoto *et al.*, 1996b). Co-expression of Kir6.2 with SUR2A results in channels resembling cardiac I_{KATP} (Inagaki *et al.*, 1996; Okuyama *et al.*, 1998) whereas co-expression of Kir6.2 with SUR2B results in a channel with pharmacological properties and nucleotide regulation distinct from Kir6.2/SUR2A (Yamada *et al.*, 1997). It is believed that SUR2B co-assembles with Kir6.1 to form the vascular K_{ATP} channel (Isomoto *et al.*, 1996a; Yamada *et al.*, 1997). Meanwhile, additional SUR2 variants derived from alternative splicing have been discovered (Chutkow *et al.*, 1996; Chutkow *et al.*, 1999). SUR2A affinity for sulfonylureas is much lower than that of SUR1 (Inagaki *et al.*, 1996).

Co-assembly of Kir6 and SUR occurs in the ER. Both Kir6 and SUR possess RKR, an endoplasmic reticulum retention signal, that prevents export from the ER (Zerangue *et al.*, 1999). In Kir6 it is present in the C-terminus, whereas in SUR it is located in a loop between TM11 and NDF-1. Co-assembly of Kir6 with SUR masks the signal allowing the complex to traffic to the membrane (Tucker *et al.*, 1997). Additional trafficking signals on the C-terminus of SUR are required to exit the ER/cis-Golgi compartments and traffic to the membrane (Sharma *et al.*, 1999). K_{ATP} trafficking to the membrane appears to be complex (Babenko *et al.*, 1998; Sakura *et al.*, 1999).

V-4.3.2 Molecular Basis of K_{ATP} channel Regulation

Ligand docking has modelled the ATP-binding site at the interface between the C- and N- terminal domains of the same subunit and part of the N-terminus of a neighbouring subunit (Trapp *et al.*, 2003). Native channels have four ATP binding sites (one per Kir6 subunit), yet binding of one ATP molecule is sufficient to induce channel closure (Markworth *et al.*, 2000). The tail phosphate of the ATP molecule makes contact with Lys185 and Arg201 in the C-terminus of one subunit and Arg50 in the N-terminus of another Kir6.2 subunit (Seino & Miki, 2003; Antcliff *et al.*, 2005). The ATP-binding site lies within a pocket lined by side chains of residues 179-

182 on one side and residues 38-40 and Arg 301 on the other (Antcliff *et al.*, 2005). MgADP activates K_{ATP} channels (Gribble *et al.*, 1997; Shyng *et al.*, 1997). Nucleotide binding studies have revealed the interaction of MgADP with NBF-2 of SUR1 (Ueda *et al.*, 1997). In addition, MgADP and MgATP stabilize ATP-binding at NBF-1 on SUR1 through conformational changes at NBF-2 (Ueda *et al.*, 1997; Ueda *et al.*, 1999a; Matsuo *et al.*, 1999a; Matsuo *et al.*, 1999b). When ATP/ADP is decreased, NBF-1 binds ATP and NBF-2 binds MgADP. This state reduces the affinity of Kir6.2 to ATP resulting in channel opening. Increase in the ATP/ADP ratio induces dissociation of MgADP from NBF-2 resulting in release of ATP from NBF-1 and channel closure (Ueda *et al.*, 1999b). Gating in K_{ATP} channels is suggested to occur in the Kir6 filter ("fast gating"), the inner helices and the cytoplasmic ring ("slow gating"). The slide helix might be involved in coupling ATP binding to channel closure. However, the precise mechanism is yet to be determined (Haider *et al.*, 2005)

V-4.3.3 Molecular Basis of K_{ATP} channel Pharmacology

Two major classes of therapeutic drugs regulate the activity of K_{ATP} channels (Ashcroft & Gribble, 2000a; Gribble & Reimann, 2003). Sulfonylureas bind to SUR subunits. TM15 and TM16 on TMD2 are critical for binding of sulfonylureas (Babenko *et al.*, 1999b; Babenko *et al.*, 1999a; Ashfield *et al.*, 1999). Glibenclamide contains both sulfonylurea and benzamido moieties, enabling it to bind to SUR1 at two regions (Ashcroft & Gribble, 2000b). Tolbutamide contains only a sulfonylurea moiety and can only bind to the tolbutamide binding site of SUR1 (Gribble *et al.*, 1998b). SUR1 and SUR2 both possess a benzamido binding site but SUR2 lacks the sulfonylurea binding site (Seino & Miki, 2003).

K^+ channel openers (KCOs) activate K_{ATP} channels leading to membrane hyperpolarization and decreased cellular excitability (Ashcroft & Gribble, 2000a). KCOs bind to SUR subunits which display varying sensitivities to KCOs. SUR1 confers sensitivity to diazoxide but not pinacidil while SUR2A confers sensitivity to pinacidil and cromakalim but not diazoxide. Kir6.2/SUR2B channels are activated by all three, pinacidil, diazoxide and cromakalim (Seino & Miki, 2003). Interaction of

KCOs with SURs stimulates ATP hydrolysis at NBF-2, which stabilizes channels in the MgADP bound state and promotes channel opening (Zingman *et al.*, 2001). SUR2 specific KCOs bind to the loop between TM13 and TM14 as well as between TM16 and TM17 on TMD2 (Seino & Miki, 2003). Lys1249 and Thr1253 of SUR2A are critical for KCO binding (Moreau *et al.*, 2000). The binding site for diazoxide is somewhat elusive yet thought to be located on TMD1 on TM8 to TM11 (Moreau *et al.*, 2005). Lack of cooperativity between KCOs indicate that binding sites are highly specific (Moreau *et al.*, 2005).

V-4.3.4 Molecular Identity of K_{ATP}

Heterologous expression of Kir6 channels with SUR subunits in different combinations reconstitutes K_{ATP} channels with distinct electrophysiological and pharmacological properties reflecting I_{KATP} in various tissues. It is currently believed that Kir6.2/SUR1 complexes underlie I_{KATP} in the pancreatic beta-cells (Inagaki *et al.*, 1995a) and Kir6.2/SUR2A reconstitute cardiac sarcoplasmatic K_{ATP} channels (Inagaki *et al.*, 1996). Two different types of smooth muscle cell I_{KATP} are known. Whereas Kir6.2/SUR2B is thought to underlie non-vascular smooth muscle cell I_{KATP} (Yamada *et al.*, 1997), Kir6.1/SUR2B form channels with properties similar to vascular smooth muscle cell I_{KATP}, also referred to I_{KNDP}. I_{KNDP} is rather insensitive to ATP, activated by nucleoside diphosphates, inhibited by glibenclamide and has a single channel conductance that is about half the single channel conductance of K_{ATP} channels (Yamada *et al.*, 1997). Mitochondrial K_{ATP} was discovered in 1991 (Inoue *et al.*, 1991). Its molecular composition has not yet been clarified (Zhuo *et al.*, 2005). I_{KACh} in excised patches of nuclear membranes has kinetics and pharmacological properties similar to K_{ATP} in the plasma membrane (Quesada *et al.*, 2002). Its molecular basis is unknown (Zhuo *et al.*, 2005).

In the brain, a Kir6.2/SUR1 complex reconstitutes I_{KATP} in ventromedial hypothalamus (Miki *et al.*, 2001) and neurons of the SNr (Thomzig *et al.*, 2001). Kir6.1 but not Kir6.2 is expressed in astrocytes and only in very few neurons in the brain. Immunoreactivity to Kir6.1 is primarily located at distal perisynaptic and peridendritic astrocyte plasma membrane processes (Thomzig *et al.*, 2001).

Overexpression of SUR1 in the forebrain of mice leads to about 9-12 fold increased K_{ATP} channel expression in the cortex, hippocampus, and striatum (Hernandez-Sanchez *et al.*, 2001). Interestingly, overexpression of SUR1 in the forebrain protects both WT and transgenic mice from seizures and neuronal damage without interfering with locomotor or cognitive function. These results strongly indicate a critical role of SUR1-containing K_{ATP} channels neuroprotection during acute or chronic metabolic stress such as ischemia (Heurteaux *et al.*, 1993).

V-5 Role of other Inward Rectifier Channels

Kir1 channels encode weakly inwardly rectifying channels. They are predominantly expressed in the kidney (Ho *et al.*, 1993; Isomoto *et al.*, 1997) and in the brain (Kenna *et al.*, 1994). The Kir1 gene contains at least five exons and alternate splicing of the 5' coding and the 3' non-coding region generates multiple variants (Ho *et al.*, 1993; Boim *et al.*, 1995). A putative phosphate-binding loop in the C-terminal of Kir1.1 (Ho *et al.*, 1993) allows channel inhibition by cytoplasmic ATP (McNicholas *et al.*, 1994). Direct phosphorylation by PKA is involved in channel regulation and PKA-dependent phosphorylation and regulation by protein kinase A is essential for channel activity (Xu *et al.*, 1996).

Kir4 channels are widely expressed and are thought to supply the major K^+ conductance in oligodendrocytes. Their functioning is crucial for myelination of axons (Neusch *et al.*, 2001). Formation of heteromeric Kir2.1/Kir4.1 (Fakler *et al.*, 1996), heterotetrameric Kir4.1/Kir5.1 (Pessia *et al.*, 1996; Tanemoto *et al.*, 2000; Yang *et al.*, 2000; Lourdel *et al.*, 2002) and Kir4.2/Kir5.1 (Tanemoto *et al.*, 2000) channels has been described and may play a role in the kidney and the CNS.

Kir5.1 subunit diversity is achieved by alternative splicing of exon 3. Kir5.1 protein expression is high in kidney and brain (Tanemoto *et al.*, 2000). Only little is known about its functional relevance. Kir5.1 was reported to form non-functional channels when expressed alone in heterologous expression systems (Bond *et al.*, 1994; Pessia *et al.*, 1996) but has been shown to be an important regulator of Kir channels such as Kir4.0 (see above) or possibly Kir2.1 (Derst *et al.*, 2001b). Recent data suggests that the scaffolding protein PSD-95 is necessary for functional homomeric Kir5.1 channel expression. When Kir5.1 is co-expressed with PSD-95 in HEK293 cells, Kir5.1 channels cluster in the cell membrane and conduct a K^+ selective current that is strongly rectifying and blocked by Barium. Phosphorylation of the Kir5.1 C-terminal leads to detachment from PSD-95 resulting in prompt Kir5.1 current suppression, possibly due to internalization (Tanemoto *et al.*, 2002). Given the high Kir5.1 abundance as well as the presence of Kir5.1/PSD-95 complexes in the

brain homomeric Kir5.1 channels might play an important role in neuronal excitability.

Kir7.1 was cloned from rat and human cDNA (Doring *et al.*, 1998). Kir7.1 shares less than 37% homology with other Kir subunits and shows various unique residues at conserved sites, particularly near the pore region. High Kir7.1 mRNA levels are detected in rat brain, lung, kidney, and testis (Doring *et al.*, 1998) as well as in the thyroid gland, small intestine, stomach, and spinal cord (Nakamura *et al.*, 1999a). Kir7.1 protein as shown by immunohistochemistry is expressed in follicular and epithelial cells of rat thyroid, intestine and choroid plexus, suggesting a contributory role to regulation of membrane potentials in these specialized cells (Nakamura *et al.*, 1999a).

Heterologous expression of Kir7.1 cRNA in *Xenopus* oocytes generates macroscopic Kir currents that show shallow dependence on external K^+. Mutation of methionine 125 to the conserved arginine 125 confers the pronounced dependence of K^+ permeability on external potassium which is characteristic for other Kir channels. Additionally, Kir7.1-M125R mutants display Ba^{2+} sensitivity which is apprixmately 25 fold higher than that of Kir7.1-WT. These results suggest an important role of this site in the regulation of K^+ permeability in Kir channels by extracellular cations (Doring *et al.*, 1998).

Kir7.1 importantly contributes to maintenance of the resting membrane potential in epithelial cells in various organs and species. In the kidney, Kir7.1 transcript expression is high in the proximal tubule but weak in glomeruli and thick ascending limb in guinea pigs. Immunocytochemical studies in guinea pig identified Kir7.1 protein in the basolateral membrane of epithelial cells of the proximal tubule. In isolated human tubule fragments, Kir7.1 mRNA is expressed in proximal tubule and thick ascending limb, suggesting that Kir7.1 may contribute to basolateral K^+ recycling in the proximal tubule and in the thick ascending limb (Derst *et al.*, 2001a). Kir7.1 plays a major role in K^+-excretion during kidney development in rats (Suzuki *et al.*, 2003).

In rat brain, Kir7.1 mRNA is absent from neurons and glia but strongly expressed in the secretory epithelial cells of the choroid plexus (Doring *et al.*, 1998; Nakamura *et al.*, 1999a). In retinal pigmented epithelial (RPE) cells, Kir7.1 channels are localized specifically at the proximal roots of the apical processes of RPE cells and co-localize with Na^+/K^+-ATPase and Kir4.1 suggesting that Kir7.1, possibly in heteromeric Kir7.1/Kir4.1 complexes, may contribute to K^+ recycling to maintain Na^+/K^+-ATPase activity and thus is essential for K^+ handling in RPE cells (Kusaka *et al.*, 2001; Kusaka *et al.*, 1999). A similar role has been suggested in rat and human thyroid follicular cells (Nakamura *et al.*, 1999a). Whole-cell recordings from freshly isolated bovine RPE cells showed a predominant mild inwardly rectifying K^+ conductance with properties compatible with Kir7.1. Cell-attached recordings revealed inwardly rectifying currents with the same unitary conductances as Kir7.1 in nine of 12 patches of RPE apical membrane but only in one of one of 13 basolateral membrane patches. Consistent with other data (Yang *et al.*, 2003a), these results suggest, that Kir7.1 channel subunits comprise the K^+ conductance of the RPE apical membrane in bovine retinal pigmented cells (Shimura *et al.*, 2001). Kir7.1 mRNA is also expressed in native porcine iris pigment epithelial cells (IPE) consistent with mild inwardly rectifying whole cell K^+ currents that display little dependence on extracellular K^+. However, current density of Kir conductance in IPE cells is much smaller than that in RPE cells (21.7 S/F vs. 205.6 S/F) suggesting that Kir channels other than Kir7.1 might underlie Kir conductance in these cells (Yang *et al.*, 2003b).

CHAPTER VI: POTENTIAL ROLE OF HETEROMULTIMER FORMATION IN K^+ CHANNELS

VI-1 Structural Determinants of Kv-channel Assembly

Four pore-forming α-subunits co-assemble to form a functional ion channel (MacKinnon, 1991). If four identical subunits co-assemble the resulting channel protein is said to be a homotetramer, if subunits are different the channel is called a heterotetramer. Alpha-subunit co-assembly among voltage gated channels usually only occurs within a subfamily, but not between members of different Kv subfamilies (Li *et al.*, 1992; Shen *et al.*, 1993). Kv channel co-assembly is determined by the T1 domain located at the channel N-terminus. While it was initially believed that the T1 domain is essential for subunit co-assembly or channel trafficking (Li *et al.*, 1992; Shen & Pfaffinger, 1995; Schulteis *et al.*, 1998), conflicting studies reported that channel assembly was still possible in the absence of the T1 domain (Tu *et al.*, 1996; Kobertz & Miller, 1999). It is now generally accepted, that the role of the amino terminal assembly domain is to coordinate channel assembly amongst compatible subunits (Papazian, 1999). The expression and localization of Kv4 channels can be regulated by various auxiliary channel-interacting proteins including Kv α-subunits (Nakahira *et al.*, 1996; Yang *et al.*, 2001), Kvβ subunits (Shi *et al.*, 1996), the minK related peptide 1 (MiRP1) (Zhang *et al.*, 2001), K^+ channel interacting protein (KChIP) (An *et al.*, 2000) and the chaperon-like KChAP protein (Kuryshev *et al.*, 2000).

The exception to the rule in Kv-channel assembly are so-called modulatory Kv α-subunits, also referred to as γ-subunits. These subunits designated Kv5, Kv6, Kv8 and Kv9, (Kramer *et al.*, 1998; Zhu *et al.*, 1999a; Sano *et al.*, 2002) remain silent when heterologously expressed but co-assemble and modulate the properties of co-assembled Kv α-subunits. Kv5 and Kv6 subunits only co-assemble with Kv2 channels whereas Kv8 and Kv9 subunits co-assemble with Kv2 and Kv3 channels (Hugnot *et al.*, 1996; Stocker *et al.*, 1999).

VI-2 Physiological Role of Kv-channel Heterotetramers

In the heart, both Kv4.2 and Kv4.3 are expressed in the ventricles (Barry *et al.*, 1995; Wickenden *et al.*, 1999; Fiset *et al.*, 1997; Yeola & Snyders, 1997). Even though antisense experiment did not support formation of Kv4.2/Kv4.3 heteromeric channels in L-cells (Fiset *et al.*, 1997), biochemical and electrophysiological data suggests that Kv4.2/Kv4.3 heteromultimeric channels coassemble with KChIP to form I_{to} in mouse ventricular myocytes (Guo *et al.*, 2002).

Kv channel subunits co-localize in the brain (see section IV-2.4). Heteromeric Kv1.1/Kv1.4 complexes are expressed in the globus pallidus, the SNr (Rhodes *et al.*, 1997; Sheng *et al.*, 1992) and in hippocampal mossy fibre terminals (Geiger & Jonas, 2000; Bischofberger *et al.*, 2002)}. Kv1.1/Kv1.2 colocalize in cerebellar basket cell terminals (McNamara *et al.*, 1993; McNamara *et al.*, 1996; Wang *et al.*, 1994a). Formation of Kv2 heteromeric complexes is structurally possible (Blaine & Ribera, 1998) yet unlikely due to different subcellular localization (Trimmer & Rhodes, 2004). Heteromeric Kv3.1/Kv3.3 may regulate excitability of brainstem auditory neurons and Purkinje cell somata and dendrites (Martina *et al.*, 2003). In certain fast-spiking cells in the neocortex and hippocampus, heteromeric Kv3.4/Kv3.1 and/or Kv3.4/Kv3.2 channels might underlie a fast-delayed rectifier current (Baranauskas *et al.*, 2003). Kv4.2 and Kv4.3 channels show differential localization suggesting formation of homomeric Kv4 channel complexes in the brain (Trimmer & Rhodes, 2004).

VI-3 Structural Determinants of Kir Channel Assembly

First evidence for Kir2 subunit heteromeric assembly came from Fakler et al (1996) who presented data suggesting the formation of Kir2.1/Kir4.1 heterotetramers. Fink et al (1996a) constructed dominant negative- (dn-) chimeras of Kir3 with the C-terminal, central and N-terminal part of Kir2.3, respectively. Kir2.1 and Kir2.3 channel current was inhibited when coexpressed with dn-Kir2.3 or dn-Kir1.1 chimeras carrying the N-terminus of Kir2.3. The authors concluded that the N-terminal of Kir2 channels is essential for channel assembly and that Kir2.1 and Kir2.3

can coassemble. A milestone publication came from Andrew Tinker, who used Kir2 deletion mutants to demonstrate that the Kir2 C-terminus and distal M2 segment are essential for Kir channel assembly (Tinker *et al.*, 1996). Using a yeast two-hybrid system, Preisig-Müller et al. (2002) showed that the N- and C-terminal intracellular domains of different Kir2.x subunits interact, thus resolving the controversy between the data of Fink and Tinker.

VI-4 Potential Physiological Significance of Heteromeric Kir Channel Complexes

Heteromerization of Kir3 channels has been shown to be functionally important. In the heart, Kir3.1 and Kir3.4 underlie I_{KACh} (Krapivinsky *et al.*, 1995a; Wickman *et al.*, 1998). Silverman et al suggested that heteromeric Kir3.1/Kir3.4 channels are only conducting when both subunits assemble in a 1:1 stoichiometry (Silverman *et al.*, 1996b). A more recent study by the same group however showed that Kir3.1/Kir3.4 channels are also functional when assembled in a Kir3.1(1)-Kir3.4(3) conformation (Silverman *et al.*, 1998). Several subunit arrangements around the pore appear to be possible (Silverman *et al.*, 1996b).

In the brain, Kir3 subunit expression vastly overlaps suggesting that native K_G currents in the brain are heterotetramers of two or more Kir3 subunits. Due to the restricted expression of Kir3.4, neuronal Kir3 channels are thought to be formed primarily by various combinations of Kir3.1, Kir3.2, and Kir3.3 subunits (Chen *et al.*, 1997; Dascal, 1997; Karschin *et al.*, 1996; Wickman *et al.*, 2000). As shown by immunohistochemical studies, Kir3.1 and Kir3.2 co-localize in the same subcellular compartments (Bausch *et al.*, 1995; Ponce *et al.*, 1996; Drake *et al.*, 1997; Miyashita & Kubo, 1997; Kofuji *et al.*, 1996; Slesinger *et al.*, 1996; Lauritzen *et al.*, 1997). Kir3.1 and Kir3.2 proteins are solely detected postsynaptically on dendrites, but not on mossy fibre axons (Liao *et al.*, 1996; Ponce *et al.*, 1996; Miyashita & Kubo, 1997; Murer *et al.*, 1997). Evidence for Kir3.1/Kir3.2 heterotetramers as molecular basis of native neuronal K_G-currents comes from co-immunoprecipitation studies showing that Kir3.1 and Kir3.2 co-precipitate from mouse cerebrum, cerebellum and

hippocampus (Liao *et al.*, 1996). Evidence for functional Kir3.2/Kir3.3 heteromeric currents in the brain was obtained from biochemical and electrophysiological experiments as well as from Kir3.3 knockout mice (Jelacic *et al.*, 2000; Torrecilla *et al.*, 2002).

Various studies suggest that assembly of Kir channels might be more promiscuous than Kv channel assembly. Tucker et al. (1996) showed that Kir4.1 subunits can associate with Kir3 family members. However, resulting channels are not functional due to trafficking defects. Glowatzki et al (1995) showed that co-assembly of Kir4.1 subunits with Kir1.1 subunits results in channels with distinct functional properties. Co-assembly of Kir2.1 with Kir4.1 has been shown by Fakler et al. (1996) and might play a physiological role in the kidney, where both subunits are expressed. Co-expression of Kir4.2 with Kir5.1 in *Xenopus* oocytes results in increases of Kir4.2 current amplitude. Kir4.2/Kir5.1 channels have distinct kinetics and higher Ba^{2+} sensitivity at negative potentials (Pearson *et al.*, 1999), similar to Kir4.1/Kir5.1 channels (Pessia *et al.*, 1996). Formation of heteromeric channel complexes might therefore be important for physiological current modulation of Kir4 currents.

Co-assembly of Kir5.1 with Kir2.1 suppresses Kir2.1 currents in a dominant negative fashion. Such modulation of Kir2.1 channel activity might be physiologically relevant in the brain, where Kir5.1 mRNA overlaps with Kir2.1 mRNA in the superior/inferior colliculus and the pontine region (Derst *et al.*, 2001b). However, Kir5.1 homomeric channels are functional when co-expressed with PSD-95 (Tanemoto *et al.*, 2002) and it can not be excluded that Kir2.1/Kir5.1 channels conduct currents when assembled with PSD-95. Kir1.1 and Kir5.1 co-localize in the proximal tubule in the kidney (Derst *et al.*, 2001b), where heteromeric channels Kir4.x/Kir5.1 have also been demonstrated. Kir4.1 and Kir5.1 co-immunoprecipitate from kidney and an inwardly-rectifying current with properties similar to co-assembled Kir4.1/Kir5.1 and Kir4.2/Kir5.1 currents but different from Kir4.1 or Kir4.2 homomeric currents is observed in the basolateral membrane of the distal convoluted tubule of the kidney (Tanemoto *et al.*, 2000; Lourdel *et al.*, 2002). Heteromeric assembly with Kir5.1 increases Kir4.1 pH sensitivity and single channel

conductance. Kir4.1/Kir5.1 heteromers might play a role in the pH-dependent regulation of K^+ fluxes and acid-base homeostasis in the kidney and the pancreas (Pessia *et al.*, 1996; Tanemoto *et al.*, 2000; Pessia *et al.*, 2001) and may function as CO_2 chemoreceptor in neurons (Yang *et al.*, 2000). Interestingly Kir5.1 seems to regulate Kir4 currents only when connected in a 4-5-4-5 but not when connected in a 4-4-5-5 manner indicating an importance of subunit positioning in heterotetrameric assembly (Pessia *et al.*, 1996).

Differential expression of Kir2 subunits has been shown in the brain, the heart and endothelial cells. The physiological importance of Kir2 channels in these tissues is subject of this thesis and will be discussed in the context of respective publications in part III of this thesis.

CHAPTER VII: BASIS FOR HYPOTHESIS TESTED IN THIS THESIS

Ion channels control cellular function in excitable and non-excitable cells. Channel properties need to be adjusted to distinct physiological requirements in different organ systems and tissues. On the protein level, functional diversity can be achieved by assembly of different ion channel subunits to heterotetrameric K^+ channel complexes. Since four channel subunits are needed to form one functional ion channel, heteromeric assembly could theoretically result in 256 structurally different channel proteins. Different lines of research have provided evidence in favour of differential heteromeric K^+-channel assembly. For example, the molecular subunit composition of cardiac K_G currents differs from K_G currents in the brain. Subcellular co-localization of different Kv1 subunits in various brain regions suggests formation of discrete native heteromeric channels. Crystal structures of ion channel subunits demonstrate that the subunit interface is perfectly suited to allow heteromeric ion channel assembly. Distinct biophysical and pharmacological properties of native ionic currents might reflect potential differential ion channel subunit composition of native channels.

For a long time, Kir2 subunits were thought to form only homotetrameric channels (Tinker *et al.*, 1996) even though participation of Kir2 channels in heteromeric channel complexes seemed to be possible (Fakler *et al.*, 1996; Fink *et al.*, 1996a; Tinker *et al.*, 1996). However, a number of important aspects of the molecular biology of Kir2- related native channels were unclear. For example, the differential expression of various Kir2 subunits did not appear to explain important functional findings such as atrial-ventricular differences in I_{K1} density (Melnyk *et al.*, 2002), I_{K1} downregulation in heart failure (Wang *et al.*, 1998) and the functional properties of I_{K1}. More distinct single-channel conductances were reported for cardiac inward rectifier currents than there are family members (Sakmann & Trube, 1984b; Josephson & Brown, 1986; Shioya *et al.*, 1993; Wible *et al.*, 1995; Nakamura *et al.*, 1998) and inward rectifier conductances were found to change during myocardial development (Josephson & Sperelakis, 1990; Chen *et al.*, 1991; Wahler, 1992). Formation of Kir2 heteromeric channels could explain some of the properties of endogenous I_{K1} channels. Heteromultimer formation could produce channels with properties different from what might be expected from the simple sum of properties

of homomeric channels, thus contributing importantly to biological diversity in I_{K1}. Inward rectifier currents have been associated with cardiac arrhythmias, epilepsy, paralysis and impaired K^+ mediated vasodilatation. Knowledge about their molecular basis is essential for development of novel pharmaceutical or gene therapies of diseases related to their dysfunction. Differences in the molecular basis of native currents might allow a targeted approach to such pathologies thereby limiting potentially important side effects of therapy such as cardiac arrhythmias.

This thesis was designed to address three principal questions:

1. Can Kir2 channels assemble to functional heteromeric complexes? If so, do properties of heteromultimeric Kir2 channel-based currents differ from those of homomultimers of the subunits that form them?

2. Is there evidence for a role of Kir2 heteromultimers in native cardiac cells?

3. Does the native Kir2 subunit composition of non-cardiac cells in the cardiovascular system differ from that of cardiac cells?

PART TWO:
ORIGINAL CONTRIBUTIONS

CHAPTER VIII: KIR2.4 AND KIR2.1 K^+ CHANNEL SUB UNITS CO-ASSEMBLE: A POTENTIAL NEW CONTRIBUTOR TO INWARD RECTIFIER CURRENT HETEROGENEITY.

Reprinted from The Journal of Physiology (London), 59, Schram G, Melnyk P, Pourrier M, Wang Z, Nattel S, Kir2.4 and Kir2.1 K-channel subunits co-assemble: A potential new contributor to inward rectifier current heterogeneity, 544 (Pt2): 337 – 349, 2002 with permission from Blackwell Publishing, Oxford, United Kingdom.

Kir2.4 and Kir2.1 K^+ channel subunits co-assemble: A potential new contributor to inward rectifier current heterogeneity

Gernot Schram, Peter Melnyk, Marc Pourrier, Zhiguo Wang, Stanley Nattel

Running title: Inward rectifier current and Kir2.4

Word Count: 8,157

From the Department of Medicine and Research Center, Montreal Heart Institute (G.S., P.M., M.P., Z.W., S.N.), Department of Medicine, University of Montreal, (G.S., Z.W., S.N.), Departments of Pharmacology (S.N.) and Pathology (P.M.), McGill University, and Pharmacology (M.P.) University of Montreal, Quebec.

Correspondence to Stanley Nattel, Montreal Heart Institute Research Center, 5000 Belanger Street East, Montreal, Quebec, H1T 1C8, Canada. Tel.: (514)-376-3330; Fax: (514)-376-1355; E-mail [redacted]

VIII-1 Abstract

Heteromeric channel assembly is a potential source of physiological variability. The potential significance of Kir2-subunit heterotetramerization has been controversial, but recent findings suggest that heteromultimerization of Kir2.1-3 may be significant. This study was designed to investigate whether the recently-described Kir2.4 subunit can form heterotetramers with the important subunit Kir2.1, and if so, to investigate whether resulting heterotetrameric channels are functional. Co-expression of either dominant-negative Kir2.1 or Kir2.4 subunits in *Xenopus* oocytes with either of wild-type Kir2.1 or 2.4 strongly decreased resulting current amplitude. To examine physical association between Kir2.1 and Kir2.4, Cos-7 cells were co-transfected with a His6-tagged Kir2.1 subunit (Kir2.1-His6) and a Flag-tagged Kir2.4 subunit (Kir2.4-Flag). After pulldown with a His6-binding resin, Kir2.4-Flag could be detected in the eluted cell lysate by Western blotting, indicating co-assembly of Kir2.1-His6 and Kir2.4-Flag. Expression of a tandem construct containing covalently linked Kir2.1 and 2.4 subunits led to robust current expression. Kir2.1-Kir2.4 tandem subunit expression, as well as co-injection of Kir2.1 and Kir2.4 cRNA in *Xenopus* oocytes, produced currents with barium sensitivity greater than that of Kir2.1 or Kir2.4 subunit expression alone. These results show that Kir2.4 subunits can co-assemble with Kir2.1 subunits, and that co-assembled channels are functional, with properties different from those of Kir2.4 or Kir2.1 alone. Since Kir2.1 and Kir2.4 mRNA has been shown to co-localize in the CNS, Kir2.1 and Kir2.4 heteromultimers might play a role in the heterogeneity of native inward rectifier currents.

VIII-2 Introduction

Inward rectifier potassium channels play a key role in setting the membrane potential and regulating excitability in various tissues including the central nervous system and the heart (Nichols & Lopatin, 1997). Despite their obvious importance, little is known about the molecular basis of native inward rectifier currents. Subunits of the Kir2 family are thought to underlie the inward rectifier current (I_{K1}) in the heart and play an important role in the central nervous system. Kir2.1 was first cloned from a macrophage cell line in 1993 (Kubo et al., 1993). Over the past few years, the properties of currents carried by heterologous expression of Kir2.1, 2.2 and 2.3 subunits cloned from various tissues including the heart (Raab-Graham et al., 1994; Ishii et al., 1994; Ashen et al., 1995; Wood et al., 1995; Wible et al., 1995) and the brain (Koyama et al., 1994; Perier et al., 1994; Tang & Yang, 1994; Morishige et al., 1994; Makhina et al., 1994; Tang et al., 1995) have been studied in detail. Recently, a fourth subunit of the Kir2 group, with somewhat different properties from the other Kir2 subunits, was cloned from rat brain (Topert et al., 1998) and human retina (Hughes et al., 2000) and designated Kir2.4. A human genomic clone corresponding to Kir2.4 was assigned to chromosome 19q13 and designated KCNJ14 (Topert et al., 2000).

Biochemical and electrophysiological experiments on cardiac myocytes support the theory of a diversity of inward rectifier K^+ channels contributing to cardiac I_{K1} (Wang et al., 1998; Wible et al., 1995; Josephson & Brown, 1986). During myocardial development, different I_{K1} channels with distinct unitary conductances and properties are present (Chen et al., 1991; Wahler, 1992; Josephson & Sperelakis, 1990). Kir2.1 transcripts are about 10 times more abundant than those of Kir2.2 or 2.3 in human atrium and ventricle, with similar concentrations in each, despite a much larger I_{K1} current density in ventricle (Wang et al., 1998). In the central nervous system, co-localization of various Kir2 subunits has been noted (Fink et al., 1996; Horio et al., 1996; Karschin et al., 1996). The ability of different subunits to form heteromultimers could partly explain the great diversity observed among native inward rectifiers channels in various cells and tissues.

Heteromultimerization among inward rectifier subunits of the Kir3 family has been shown to occur and to be functionally important in the heart and the central nervous system (Krapivinsky et al., 1995; Lesage et al., 1994; Lesage et al., 1995). The results of studies on Kir2 heteromultimerization are conflicting. Fink et al. (1996) studied co-assembly between Kir2.1 and Kir2.3 with the use of a dominant negative chimera consisting of the N-terminus, the central part or the C-terminus of Kir2.3 and Kir3.2. The results of co-injection of chimeric constructs with either Kir2.1 or Kir2.3 into *Xenopus* oocytes suggested that co-assembly occurs if the N-terminus is preserved (Fink et al., 1996), similar to findings with voltage gated K^+ channel (Kv) subunits (Lee et al., 1994a; Green & Millar, 1995). On the other hand, Tinker et al. (1996) found that the C-terminus and a part of the M2 segment are essential determinants of co-assembly among Kir2 channels, and their results were not consistent with important heteromultimerization between Kir2.1 and Kir2.3 (Tinker et al., 1996). On the other hand, strong evidence has recently been provided that suggests that co-assembly among Kir2.1-3 subunits might contribute to inward rectifier diversity in the guinea-pig heart (Preisig-Müller et al., 2002).

Co-localization between the important subunit Kir2.1 and the recently cloned Kir2.4 occurs in various tissues (Kubo et al., 1993; Takahashi et al., 1994; Derst et al., 2001; Topert et al., 1998). The goals of our study were 1) to determine whether Kir2.4 can co-associate with Kir2.1, 2) to assess whether channels formed by co-assembled Kir2.1 and 2.4 subunits are functional, and 3) to compare Ba^{2+}-blocking properties of currents carried by channels composed of co-assembled Kir2.1-2.4 subunits with those of homomeric Kir2.1 and 2.4 channels.

VIII-3 Methods

VIII-3.1 Construction of Dominant Negative (dn) Kir2.4 and Kir2.1 Constructs

A PCR-based approach was used to engineer Kir2.4 subunits with the GYG motif important for ion selectivity and permeability (Heginbotham et al., 1994; Slesinger et al., 1996) replaced by 3 alanine residues (AAA). A 5' and a 3' fragment were generated and combined by overlap extension. Primers used to synthesize the 5' fragment were ACAGAATTCAGCATGGGCTTGGCCAGGGCCCTGCGCC (sense) and GACGCTGCGCACAGCAGCGGCTATGGACGTCTG (antisense). Primers used to generate the 3' fragment were CAGACGTCCATAGCCGCTGCTGTGCGCAGCGTC (sense) and ACACTCGAGTCATGGAGGCAGGGTCAGTGCCAG (antisense). Both fragments were combined by overlap extension PCR using the 5' sense and the 3' antisense primer. The resulting construct was subcloned into the *Xenopus* oocyte expression vector psGEM. The sequence and the presence of the mutation were verified by sequencing. Dn-Kir2.1 was a generous gift from Dr. Andrew Tinker, London.

VIII-3.2 Co-Precipitation of Kir2.1 and Kir2.4

To evaluate potential physical association between Kir2.4 and Kir2.1 a His-pulldown approach was used. A six-histidine tag was engineered to the N-terminus of Kir2.1 as previously described (Tinker et al., 1996), allowing high-affinity specific purification by a His6-binding resin. Kir2.1-His6 was generously provided by Dr. A. Tinker, London. Kir2.4 was tagged with an eight amino-acid sequence (Asp-Tyr-Lys-Asp-Asp-Asp-Asp-Lys) known as "Flag sequence" that can be recognized by a commercially available monoclonal antibody. Cos-7 cells were then co-transfected with Kir2.1-His6 and Kir2.4-Flag. Kir2.1-His6-containing complexes were purified under non-denaturing conditions from the detergent-solubilized cell homogenate, washed and eluted from the His6-binding resin. Proteins were then subjected to Western blotting. If protein–protein interactions occur between Kir2.1 and Kir2.4 the two proteins should copurify (Hoffmann & Roeder, 1991), allowing Kir2.4-Flag detection by the Flag epitope.

VIII-3.3 Construction of Kir2.4-FLAG

Kir2.4 in pcDNA3 (Invitrogen) was a friendly gift from Dr. Andreas Karschin, Göttingen, Germany. Using the PCR technique, an Eco RI restriction enzyme site and a sequence coding for the Flag protein (GACTATAAAGACGACGACGACAAA) were introduced by the sense primer to the 5' end of Kir2.4. The antisense primer introduced an Eco47 III restriction enzyme site which is present only once in Kir2.4 and not present in pcDNA3 (Invitrogen). The Kir2.4-pcDNA3 construct as well as the Kir2.4-FLAG PCR construct were digested with Eco RI and Eco47 III (Boehringer-Mannheim) and fragments were cleaned on a 1% agarose gel. Kir2.4-FLAG was then ligated into pcDNA3 with T4 DNA polymerase (Promega). After transformation of competent JM109 E. coli cells (Promega), culture in ampicillin containing LB medium and plasmid isolation, the presence of the construct was verified by restriction enzyme digestion with Eco RI and Eco47 III (Boehringer Mannheim). Cos-7 cells were transfected with Kir2.4-FLAG and after subsequent cell lysis the presence of Kir2.4 was shown by Western blot. The sense primer for construction of Kir2.4-FLAG was TTAGAATTC*ACGATG†GACTATAAAGACGACGACGACAAA‡ATGGGCTT GGCCAGG, with the ends of the ECO RI, Kozac and FLAG sequences designated by *, † and ‡ respectively, followed by the Kir2.4 sequence. The antisense primer consisted of ACAGGCGCT*GCGGTCTCGCAGAGCCAC, with the Eco47 III sequence identified by the asterisk, followed by the Kir2.4-specific sequence.

VIII-3.4 Cos-7 Cell Maintenance and Transfection

Cos-7 cells were cultured in Dulbecco's Modified Eagle Medium (DMEM) supplemented with heat-inactivated 10% fetal bovine serum (FBS) and 100 Units/ml Na-penicillin-G plus 100 µg/ml streptomycin-sulfate. Cells (2×10^5) were plated into 35 mm culture dishes with DMEM for 24 h (37°C, 5% CO_2) to reach ~70% confluence. Sample cDNA (2.5 µg of Kir2.4-FLAG, Kir2.1-His or both) was mixed with 5.5 µl lipofectamine, brought to a final volume of 200 µl with DMEM and added to an 800 µl FBS- and antibiotic-free DMEM cell suspension. After 6 hours of

incubation at (37°C, 5% CO_2), 1 ml of 20% FBS was added to achieve a 10% FBS final concentration.

VIII-3.5 His-Pulldown

After Cos-7 cell transfection (48-72 h), cells were incubated in RIPA buffer (Igepal 1% v/v, sodium deoxycholate 0.5%, SDS 0.1% and β-mercaptoethanol 10 mM) with protease inhibitors (benzamidine, trypsin inhibitor, leupeptin, PMSF and aprotinin) for 20 min on ice to solubilize membrane proteins. The lysates were then passed through a HiTrap Chelating Column (Amersham) that binds His-tagged proteins. The washing and elution buffers contained 20 and 40 mM imidazole, respectively, to eliminate non-specific binding. After elution, the collected fractions were concentrated by centrifugation in Ultrafree-MC filter units (Millipore).

VIII-3.6 Western Blotting

The solubilized membrane proteins were fractionated on 8% SDS-polyacrylamide gels. The proteins were electrophoretically transferred to Immobilon-P polyvinylidene fluoride membranes (Millipore) in 25 mM Tris-base, 192 mM glycine and 5% methanol at 0.07 A for 16 h. The membranes were blocked using 5% non-fat dry milk (Bio-Rad) in TBS (Tris-HCl 50 mM, NaCl 500 mM; pH 7.5) containing 0.05% Tween-20 (TTBS) for 2 h at room temperature. Membranes were then incubated for 1 h in primary antibody solutions in 1% non-fat dry milk in TTBS. The primary antibody against the histidine tag (Anti-His; Amersham Pharmacia Biotech) was used at a dilution of 1:3000 and the Anti-FLAG M2 antibody (Sigma) was used at a dilution of 1:1000. After incubation, the membranes were washed in TTBS and reblocked in 1% non-fat dry milk in TTBS for 10 min. They were then incubated with horseradish peroxidase-conjugated anti-mouse IgG (1:3000) in 5% non-fat dry milk in TTBS for 30 min and washed in TTBS 3 more times. Antibody detection was performed with Western blot chemiluminescence reagent plus (NEN Life Science Products).

VIII-3.7 Construction of Kir2.1-Kir2.4 Tandem

A BamHI and a SacII restriction enzyme site were introduced at the N-terminus and after ten aminoacids of the 5'-untranslated region of Kir2.4 by PCR. An XhoI restriction enzyme site was introduced at the C-terminus. A stop codon in the 5'-untranslated region was mutated to glycine by site directed mutagenesis. The PCR product and pcDNA3.1+ (Invitrogen) were then digested with BamHI and XhoI and the PCR product was subcloned into pcDNA3.1+. After transformation of competent JM109 cells (Promega) with the construct and amplification, the presence of the insert was verified by digestion with BamHI and XhoI. A BamHI restriction enzyme site was engineered to the N-terminus of Kir2.1 by PCR. A BamHI and a SacII restriction enzyme site were introduced to the N-terminus. The stop codon of Kir2.1 was mutated by site directed mutagenesis to GGA (glycine). The PCR product and the previously obtained Kir2.4-pcDNA3.1+ construct were digested with BamHI. The Kir2.1 sequence was then introduced upstream of the Kir2.4 sequence into pcDNA3.1+. The correct orientation of Kir2.1 was verified by restriction enzyme digestion and subsequent electrophoresis on a 1% agarose gel. The presence of Kir2.1 and Kir2.4 were verified by complete sequence confirmation. A 10-aminoacid sequence of the 5' UTR of Kir2.4 (GQIGKGSPHL) was preserved as a linker between Kir2.1 and Kir2.4, based on previous studies showing a 10-aminoacid linker to be sufficient for functional integration of linked subunits in the membrane (Lee *et al.*, 1994b). A second stop codon in this linker region was mutated to glycine.

The primers for tandem construction were:

GGATCCAGCATGGGCAGTGTGMGAAC (Kir2.1, sense);
GGATCCCCGCGG*TCC*TATCTCCGAYTCTCGCCG (Kir2.1, antisense);
GGATCCCCGCGGGGACAAATC*GGG*AAGGGGTCTCC (Kir2.4, sense);
CTCGAGTCATGGAGGCAGGGTCAGTGC (Kir2.4, antisense).

For heterologous expression in *Xenopus* oocytes the Kir2.1-2.4 tandem was subcloned into the polyadenylation transcription vector pSGEM. The BamHI site between Kir2.1 and Kir2.4 was removed by restriction enzyme digestion with SacII. After purification on a 1% agarose gel with the QIAquick Gel Extraction Kit, Qiagen Inc., Mississauga, Ontario, Canada, the construct was religated with T4 DNA polymerase (Promega). After transformation of competent JM109 cells (Promega) with the construct and amplification, the tandem was harvested by digestion with BamHI and XhoI, isolated on a 1% agarose gel and further subcloned into pSGEM.

III-8 Kir2.1 / Kir2.4 co-injection

We then investigated the properties of channels formed by spontaneous Kir2.1 and Kir2.4 co-assembly. To ensure comparable expression of Kir2.1 and 2.4, a sequence based on the tandem construct was used, but leaving a stop codon in place of glycine at the distal end of Kir2.1.

The primers were:

GGATCCAGCATGGGCAGTGTGMGAAC (Kir2.1, sense);
CCGCGGTCCTATCTCCGAYTCTCGCCG (Kir2.1 antisense);
GGATCCCCGCGGGGACAAATCTAGAAGGGGTCTCC (Kir2.4 sense);
CTCGAGTCATGGAGGCAGGGTCAGTGC (Kir2.4 antisense).

VIII-3.8 Electrophysiology

Female *Xenopus* laevis were anaesthetized in 0.13 % w/v tricaine (Sigma Chemicals, St Louis, MO, USA) for 30 min at 4°C. Segments of the ovarian lobe were removed through a small abdominal incision. The follicular layer was removed by digestion with 2 U/ml collagenase type V (Sigma) in OR2 solution (mM: NaCl, 82.5; KCl, 2; $MgCl_2$, 1; HEPES, 5; pH 7.6; 50 mg/l gentamycine solution). The procedures followed for surgery and maintenance of frogs were approved by the Animal Research Ethics Committee of the Montreal Heart Institute. Oocytes were stored at 17°C in SOS solution (mM: NaCl, 100; KCl, 2; $CaCl_2$, 1.8; $MgCl_2$, 1; HEPES, 5; pH 7.6; 50 mg/l gentamycine solution). For heterologous expression, 6-12 ng of cRNA were injected into stage IV-V *Xenopus* oocytes, followed by two-electrode voltage clamp 1 to 3 days later. When co-injected with dominant negative constructs, equal amounts of dominant negative and wild-type cRNA were injected. Currents were elicited at room temperature by 750-ms voltage steps from a holding potential of -60 mV with a GeneClamp-500 amplifier and pClamp 6.0 software (Axon). The external solution contained (mM): 5 KCl, 100 NaCl, 2 $MgC1_2$, 10 HEPES, 0.3 $CaC1_2$; pH adjusted to 7.4 with NaOH. Niflumic acid (10 μM) was added to block Ca^{2+}-dependent Cl^- current. Ba^{2+}-containing solutions were superfused until steady-state block occurred (generally ~10 minutes) before repeating full voltage-clamp protocols. Glass microelectrodes (3-M KCl^- filled) had 1.3-1.8 MΩ resistances.

VIII-3.9 Data analysis

Data analysis was conducted using Axon Clampfit 6.0, Graphpad Prism 3, SPSS 10 and Microsoft Excel 2000. Data are presented as the mean ± S.E.M. Statistical comparisons were made with Student's *t* test. Analysis of variance (ANOVA) was used for multiple comparison. A 2-tailed probability <0.05 was taken to indicate statistical significance.

VIII-4 Results

VIII-4.1 Co-expression of Kir2.1 or 2.4 Channels with Dominant Negative Subunits

Figure 27 compares representative currents ($I_{Kir2.x}$) recorded from *Xenopus* oocytes injected with Kir2.1 or Kir2.4 cRNA (left panels) with those of oocytes co-injected with dn-Kir2.1/Kir2.1 or dn-Kir2.1/Kir2.4 cRNA (middle panels). Corresponding mean current-voltage relations are shown in the right panels. Injection of either subunit alone produced robust inward-rectifier currents (left panels). The middle panels show the results of co-injection of dn-Kir2.1 with Kir2.1 or 2.4, into the same sets of oocytes studied on the same days as the corresponding homomeric wild-type constructs. Mean data are shown at the right. As expected, co-expression of Kir2.1 with dn-Kir2.1 strongly suppressed Kir2.1 currents ($P < 0.001$, Panel A). Co-injection of Kir2.4 with dn-Kir2.1 (panel B) substantially reduced $I_{Kir2.4}$ ($P < 0.001$) in a fashion quite similar to the co-expression of Kir2.1 with dn-Kir2.1 shown in panel A.

Figure 28 shows results of complementary experiments, in which dn-Kir2.4 was co-injected with either Kir2.1 or Kir2.4 subunits. Once again, results obtained following co-injection (middle panels) are compared with results obtained upon injection of the corresponding homomeric wild-type constructs (left panels), with injection and study occurring on the same days and into the same batches of oocytes. Mean data are at the right. Co-expression of dn-Kir2.4 with Kir2.1 and Kir2.4 strongly suppressed Kir2.x currents (Kir2.1/dn-Kir2.1 $P < 0.001$, Panel A, Kir2.4/dn-Kir2.4 $P < 0.001$, Panel B). The results in Figures 27 and 28 suggest co-assembly of Kir2.1 and Kir2.4 subunits.

VIII-4.2 Kir2.1-His_6 / Kir2.4-Flag Co-Precipitation

Figure 29 shows Western blots of lysates obtained from Cos-7 cells transfected with Kir2.1-His_6 alone, Kir2.4-Flag alone or both. A cell lysate of Kir2.4-Flag-transfected cells probed with Anti-Flag antibody (lane 1) reveals a single band of molecular weight 55 kDa. Lanes 2-7 are data obtained with His-pulldown. Lanes

2 and 3 were obtained from cells transfected with Kir2.1-His_6 and probed with antibodies directed against Kir2.1 (Anti-Kir2.1, Alomone Labs, Jerusalem, Israel, lane 3) or the His_6-epitope (lane 4). Both antibodies detect a specific band with a molecular weight of 67 kDa, corresponding to Kir2.1. Tinker *et al.* (1996) have published a molecular weight of 50 kDa for Kir2.1 expressed in HEK cells. The noted difference in molecular weight might be due to differences in the post-translational modification of Kir2.1 in HEK versus Cos-7 cells. Incubation and probing with the Flag-antibody of the cell lysate of co-transfected cells after His-pulldown (lane 4) detected a band with a molecular weight of 55 kDa corresponding to Kir2.4, indicating protein-protein interactions between His-tagged Kir2.1 (purified by His-pulldown) and Flag-tagged Kir2.4. In addition to detecting Flag-tagged Kir2.4 in the Kir2.1-His_6/Kir2.4-Flag co-transfected cell His pulldown experiment (lane 4), Flag antibody also detected a band with the molecular weight of Kir2.1 (67 kDa). We suspected that this was due to cross-reactivity of the Flag antibody with the Kir2.1-His_6 product. Lane 5 shows an experiment to test this notion. The band shown was obtained from cells transfected with Kir2.1-His_6 alone subjected to His-pulldown. The Flag antibody detects a single band with a molecular weight of ~67 kDa, corresponding to Kir2.1 suggesting that the band with a molecular weight of 67 kDa in lane 4 is indeed Kir2.1 detected by the anti-Flag antibody.

Lane 6 was obtained with His-pulldown of lysate from cells transfected with Kir2.4-Flag alone, followed by probing with Flag antibody. The lack of a signal indicates that association with His-tagged Kir2.1 is essential for Flag-tagged Kir2.4 to be detected in the sample obtained by His pulldown. Furthermore, the results shown in lane 6 exclude nonspecific binding of the Flag sequence or Kir2.4 to the His-binding resin. Lane 7 shows a Western blot of crude (non-transfected) Cos-7 cell lysate incubated with anti-Kir2.1. The band with the molecular weight of ~67 kDa shown in lane 1 was not detected, indicating that it does not represent nonspecific binding of anti-Kir2.1. Western blotting was also performed with anti-Kir2.1 preincubated with the antigenic peptide supplied by the manufacturer. After pre-incubation with antigen, anti-Kir2.1 no longer identified the band at 67 kDa (data not shown). Similar results were obtained in 4 such experiments.

VIII-4.3 Properties of Co-Expressed Kir2.1 and Kir2.4 and of a Covalently linked Kir2.1/2.4 Tandem Construct

The experiments shown in Figures 27-29 strongly suggest co-assembly of Kir2.1 and 2.4, but provide no information about the ability of heteromeric channels to carry current. We therefore addressed the issue of whether co-assembled channels can conduct current by studying the results of expression of a covalently linked Kir2.1-Kir2.4 tandem construct. Figure 30 shows currents carried by Kir2.1 alone (Figure 30A), Kir2.4 alone (Figure 30B), Kir2.1-Kir2.4 tandem constructs (Figure 30C) and Kir2.1/2.4 co-expression resulting from co-injection (Figure 30D) under control conditions (left panels) and then in the presence of 10, 100 μM and 1 mM Ba^{2+}. Recordings for each construct were obtained under all 4 conditions in each oocyte studies. From the data shown in Figure 30C it is clear that channels consisting of co-assembled, covalently-linked Kir2.1 and Kir2.4 carry substantial currents. Currents carried by Kir2.1-Kir2.4 tandem constructs (Figure 30C), as well as by co-injected Kir2.1/2.4 (Figure 30D) are more sensitive to Ba^{2+} than currents carried by Kir2.1 (Figure 30A) or Kir2.4 (Figure 30B) alone. Currents carried by Kir2.1-Kir2.4 tandem constructs appear smaller than those carried by Kir2.1 or Kir2.4 alone, or resulting from co-injection of Kir2.1 and Kir2.4. Corresponding mean current-voltage relationship at the onset of the pulse (left panels) and under steady state conditions (right panels) are shown in Figure 31. These data confirm the fact that currents carried by the tandem construct are smaller than those carried by homomeric Kir2.1 or 2.4 injection, or by co-injected (but not covalently linked) Kir2.1 and 2.4. They also suggest that co-injected and tandem constructs are more sensitive to Ba^{2+} than homomeric channels. For example, 10 μM Ba^{2+} produces near-maximal inhibition of tandem and co-injected constructs in the right panels of Figures 31C and 31D, whereas it clearly does not for homomeric Kir2.1 and 2.4 in the corresponding panels of Figures 31A and 31B.

We have previously shown that the concentration and voltage-dependence of Ba^{2+} blockade is a signature property of various Kir2.x clones and native I_{K1} channels (Schram *et al.*, 1999). We therefore determined the voltage-dependent Ba^{2+}-blocking properties of Kir2.1 and Kir2.4 and compared them with Ba^{2+}-block of the tandem

construct and co-expressed Kir2.1/2.4. Figure 32 (left panels) shows currents recorded upon stepping to –120 mV in oocytes expressing Kir2.1 (panel A), Kir2.4 (panel B), the tandem construct (panel C), or co-expressed Kir2.1 and Kir2.4 (panel D). Results are shown under control conditions (open circles) and after exposure to 10 (diamonds), 100 (squares), 1000 (filled circles) and 10,000 (stars) μM $[Ba^{2+}]$. Note that 10 μM Ba^{2+} produced about 30% inhibition of end-pulse Kir2.1 current in the example shown in panel A, whereas the same Ba^{2+} concentration (10 μM) produced much weaker inhibition of the Kir2.4 current shown in panel B. Current resulting from the tandem construct (C) and co-expressed Kir2.1/2.4 (D) was inhibited strongly by 10 μM Ba^{2+}. Corresponding mean Ba^{2+} concentration-response relations at –120 mV based on all cells studied are shown for each construct in the middle panels. The curves in the middle panels are best-fit relations of the form $B = 1 / (1 + IC_{50}/C)$, where B is Ba^{2+}-block at a concentration C. The Ba^{2+} IC_{50} at –120 mV for Kir2.1 (15.9 μM, Fig. 32A, middle panel) is about one forth the value for Kir2.4 (72.3 μM, Fig. 32B, middle). On the other hand, the values for the Kir2.1/2.4 tandem (Fig. 32C) and co-expressed Kir2.1 and 2.4 (Fig. 32D) are of the same order, in the range of 4-5 μM, a value one third that of Kir2.1 and less than one tenth that of Kir2.4. Significant differences were found between groups (Analysis of variance, $P < 0.0001$) and the different test potentials (Analysis of variance, $P < 0.0001$). There was also a significant group x voltage interaction (Analysis of variance, $P = 0.0003$), indicating significant voltage-dependence of intergroup differences. The right panels of Fig. 32 show mean IC_{50}s for each construct as a function of test potential in comparison to Kir2.1, represented by the circles and a dashed line. Significant differences between Kir2.4, Kir2.1-2.4 tandem and Kir2.1/2.4 co-expression, on one hand, and Kir2.1, on the other, are denoted in asterisks. Kir2.4 is clearly less sensitive to Ba^{2+} than Kir2.1 over the entire voltage range. The tandem and co-expressed channels are significantly more sensitive to Ba^{2+} than either Kir2.1 or 2.4 alone. Ba^{2+} block of Kir2.4 (Fig. 32B) is not clearly voltage dependent and shows limited time dependence, in contrast to block of Kir2.1, which is clearly time and voltage dependent, suggesting that the principle Ba^{2+}-blocking site in Kir2.4 may be much more shallow than that in Kir2.1. The tandem (Fig. 32C) and co-expressed constructs

(Fig. 32D) show a direct voltage-dependent Ba^{2+} sensitivity, like that of Kir2.1 and different from that of Kir2.4. This observation may provide supplementary evidence for Kir2.1/2.4 heteromultimer formation.

VIII-5 Discussion

In the present study, we showed that Kir2.4 associates with Kir2.1 subunits, that heteromeric Kir2.1-2.4 channels conduct robust inward rectifying currents and that they have Ba^{2+}-blocking properties different from those of homomeric channels resulting from expression of either individual subunit alone.

VIII-5.1 Heteromultimer Formation in Inward Rectifier Channels

The formation of heterotetrameric K^+ channels has been well-described for the Shaker-related voltage gated K^+ (Kv) channels. Heteromultimerization usually occurs only within a subfamily, but not between members of different Kv subfamilies (Li *et al.*, 1992; Shen *et al.*, 1993). It is believed that the main regions responsible for co-assembly of Kv family subunits are located in the N-terminus and the S1 segment (Li *et al.*, 1992; Shen *et al.*, 1993). Deletion of the N-terminus has the potential to remove the specificity of subfamily co-assembly (Lee *et al.*, 1994b).

Co-assembly in the inward rectifier group is less well understood. Heteromultimerization of inward rectifier K^+ channels has been shown to occur and to be functionally important in the Kir3 group. The molecular basis of the G-protein gated inward rectifier potassium current acetylcholine-dependent current (I_{KACh}) is a heterotetramer of the inward rectifier channels Kir3.1 and Kir3.4 (Krapivinsky *et al.*, 1995). Functional heteromultimers consisting of Kir3.1 and Kir3.2 exist in the central nervous system (Lesage *et al.*, 1994; Lesage *et al.*, 1995). Tucker *et al.* (1996) showed that Kir4.1 subunits form heteromeric channels when co-expressed with members of the Kir3 subfamily, but that the resulting channels are not functional (Tucker *et al.*, 1996). The inhibition of Kir4.1 current is likely due to degradation of the co-assembled channels rather than to the formation of stable nonconducting heteromeric channels (Tucker *et al.*, 1996). Glowatzki et al showed that Kir1.1 and 4.1 subunits can co-assemble, and that co-assembled channels have distinct functional properties (Glowatzki *et al.*, 1995). Oocytes co-injected with cRNA for Kir4.2 and Kir5.1 displayed currents with properties distinct from those expressing Kir4.2 alone. Co-injected oocytes displayed larger currents than Kir4.2, with novel kinetic

properties and an increased sensitivity to Ba^{2+} block at negative potentials, suggesting that Kir4.2 forms functional heteromultimeric channels with Kir5.1, as has been shown for Kir4.1 (Pearson *et al.*, 1999).

Fakler *et al.* (1996) reported the formation of functionally distinct heterotetramers between Kir2.1 and Kir4.1 (Fakler *et al.* 1996). When co-expressed in *Xenopus* oocytes, Kir5.1 and Kir2.1 are efficiently targeted to the cell surface but form electrically silent channels in a stoichiometry dependent manner. In vivo there is overlapping Kir5.1 and Kir2.1 mRNA expression in the brain and the kidney. Kir5.1 thus appears to function as a negative regulator of Kir2.1 channel activity in native cells (Derst *et al.*, 2001). Pessia *et al.* (1996) showed that co-expression of Kir4.1 subunits with Kir5.1 subunits results in functionally distinct channels (Pessia *et al.*, 1996). In contrast to Kir4.1 subunits, which form homomeric channels with a single-channel conductance of 12 pS, and Kir5.1, which does not form conducting channels upon heterologous expression, Kir4.1/5.1 co-expression produces channels with single-channel conductance of 43 pS. The properties of Kir4.1/5.1 heteromeric channels depend on the order of subunits, and Kir5.1 co-injection did not modify the properties of currents carried by Kir1.1, 2.2, 2.3, 3.1, 3.2 or 3.4 (Pessia *et al.*, 1996). Heteromeric Kir4.1-5.1 channels may function as a proton sensor in kidney (Tanemoto *et al.*, 2000) and play a role in CO_2 chemoreception in central nervous system neurons (Yang *et al.*, 2000). Co-injection of Kv1.1 and Kir2.1 subunits produces currents compatible with the sum of homomeric channels formed by each alone, and injection of a Kir2.1-Kv1.1 tandem construct fails to produce measurable currents despite detection by Western blot of protein with a molecular weight corresponding to the predicted size of the tandem (Tytgat *et al.*, 1996). These results suggest that Kir2.1 and Kv1.1 subunits do not co-assemble to produce functional channels.

Conflicting data have been reported for heteromultimerization within the Kir2 family. Tinker *et al.* (1996) addressed the regions responsible for homo- and heteromultimer formation among Kir2.1, Kir2.2 and Kir2.3 subunits (Tinker *et al.*, 1996). Their results indicate that the formation of homomultimers is by far the preferred reaction when Kir2.1 and Kir2.2 or Kir2.3 are co-expressed. The principal

regions responsible for the co-assembly of homomeric channels and for the lack of co-assembly between Kir2.1 and Kir2.2, 2.3 and 6.1 appear to be the M2 segment and the proximal C-terminus (Tinker *et al.*, 1996). Fink *et al.* (1996) studied the structural determinants that define the specificity of co-assembly of Kir2 channels and preclude the formation of heteromers between Kir2.3 and Kir3.2 subunits (Fink *et al.*, 1996). They found that chimeric constructs containing the N-terminal of Kir2.3 and the M1-M2-proximal C-terminal moiety of Kir3.2 have a dominant negative effect upon co-injection with Kir2.3, irrespective of whether the C-terminal of the chimeric protein corresponds to Kir2.3 or Kir3.2. Fink *et al.* (1996) also noted suppression of Kir2.1 currents when Kir2.1 was co-injected along with chimeras containing the Kir2.3 N-terminal and the Kir3.2 M1-M2-proximal C-terminal, irrespective of whether the distal C-terminal was derived from Kir2.3 or 3.2. These findings, along with the co-localization of Kir2.1 and 2.3 in similar brain regions, led the authors to conclude that the N-terminus of Kir2.3 determines co-assembly and that Kir2.1 and 2.3 likely form heterotetramers in vivo (Fink *et al.*, 1996). Very recently Preisig-Müller *et al.* (2002) showed that Kir2.1, Kir2.2 and Kir2.3 can form heterotetramers with distinct properties and suggested that diversity of inward rectifier channel co-assembly might underlie different phenotypes of Andersen's syndrome. Using a yeast two-hybrid system they found that co-assembly occurs between the C- and N-termini of Kir2 subunits (Preisig-Müller *et al.*, 2002).

Our findings were similar to those of Preisig-Müller *et al.* (2002), in that we found that Kir2.1 can co-assemble with Kir2.4 to form functional heterotetramers and that channels consisting of different subunits may have specific properties different from those of homomeric channel composed of either subunit alone. Furthermore, we found that co-assembly of Kir2.1 and Kir2.4, whether via co-injection or expression of concatemers, led to currents with Ba^{2+} IC_{50}'s lower than those of Kir2.1 and Kir2.4 alone. Preisig-Müller *et al.* (2002) found that co-assembled Kir2.1-3 channels had Ba^{2+} sensitivities of the same order as those of the more sensitive homomeric constituent subunit.

VIII-5.2 Novelty and Potential Significance

Heteromultimerization is a potentially important contributor to the functional diversity of K^+ channels (Coetzee *et al.*, 1999). The native I_{KACh} current, an ion conducting pathway of central importance to parasympathetic nervous system effector pathways, is composed of heteromultimeric Kir3.1 and Kir3.4 subunits (Krapivinsky *et al.*, 1995). There is evidence that the important transmembrane gradient in the slow delayed rectifier current I_{Ks}, a key determinant of the cardiac ventricular transmural gradient in action potential duration, (Liu & Antzelevitch, 1995) is caused by differential transmural distribution of a splice variant of KvLQT1 with dominant negative function (Pereon *et al.*, 2000). Heteromultimer formation may contribute to the properties of cardiac transient outward currents in tissues that express both Kv1.4 and Kv1.5 proteins (Po *et al.*, 1993). Differential heteromultimerization among Kir2.1-3 might underlie the different phenotypes of Andersen's syndrome (Preisig-Müller *et al.*, 2002).

In the present study, we demonstrate with both biochemical and electrophysiological methods that Kir2.4 subunits co-assemble with Kir2.1 subunits. Kir2.1 and 2.4 were co-purified by His_6 pulldown when only Kir2.1 was covalently bound to His_6, dominant negative Kir2.1 suppressed Kir2.4 currents upon co-expression and a tandem Kir2.1/2.4 construct carried Ba^{2+} sensitive currents with voltage-dependent Ba^{2+} sensitivity similar to that of co-expressed Kir2.1 and 2.4. The results of our Kir2.1/2.4 co-expression and Kir2.1/2.4 chimeric channel studies suggest that heteromeric Kir2.1/2.4 channels have properties that are different from those of homomeric channels formed by either subunit alone. In particular, the Ba^{2+} sensitivity of heteromeric channels is clearly greater than that of homomeric Kir2.1 channels and much greater (by an order of magnitude) than that of Kir2.4 channels, similar to the findings of Pearson *et al.* (1999), who showed that co-expression of Kir4.2 and Kir5.1 results in currents with higher Ba^{2+} sensitivity than when Kir4.2 is expressed alone (Pearson *et al.*, 1999). Currents resulting from Kir2.1 and Kir2.4 co-expression were of the same magnitude as Kir2.1 or Kir2.4 currents whereas currents carried by Kir2.1/2.4 chimeras were reduced by approximately 50%, possibly due to structural constraints limiting functional insertion.

Overlapping expression of Kir2.1-3 mRNA in the rat brain has been reported (Horio *et al.,* 1996; Fink *et al.*, 1996; Morishige *et al.*, 1993; Karschin *et al.*, 1996). Northern blot analysis and RT-PCR have shown that Kir2.1 and Kir2.4 mRNA is expressed in the brain, heart, kidney and skeletal muscle (Kubo *et al.*, 1993; Takahashi *et al.*, 1994; Derst *et al.*, 2001; Topert *et al.*, 1998). In situ hybridization studies of rat brain tissue have shown both Kir2.1 and Kir2.4 to be expressed in the pons, the facial nucleus and strongly in the midbrain (Topert *et al.*, 1998; Karschin *et al.*, 1996). The fact that Kir2.1 and Kir2.4 channels are expressed in the same regions, as well as their ability to co-assemble, raise the possibility that Kir2.1/2.4 heterotetramers may contribute to inward rectifier function in the CNS. A recent study by Liu et al. (2001) found Kir2.4 to be present in guinea pig heart, but immunocytochemical studies showed Kir2.4 to be present only in neuronal elements. More experiments are warranted to determine whether Kir2.4 is present in myocardial tissues of other species.

VIII-5.3 Potential Limitations

Changes in subunit arrangement can affect channel properties, as has been shown for Kir4.1 and Kir5.1 (Pessia *et al.*, 1996). The formation of heteromeric channels with different Kir2.1/Kir2.4 subunit arrangements and stoichiometry might therefore lead to the expression of channels with functionally different properties. Further studies are required to assess the effects of different subunit arrangements and stoichiometries on the properties of currents carried by systems co-expressing Kir2.1 and 2.4 subunits. There are discrepant observations regarding the structural determinants of Kir2.x subunit co-assembly (Tinker *et al.*, 1996; Fink *et al.*, 1996; Preisig-Müller *et al.*, 2002). Further work is necessary to establish the structural basis for the ability of Kir2.4 subunits to co-assemble with Kir2.1, as well as to establish whether Kir2.4 can also co-assemble with other inward rectifier channels. The structural basis for the differing Ba^{2+} sensitivities of Kir2 subfamily channels, as well as the mechanisms that lead to enhanced Ba^{2+} sensitivity of Kir2.1-2.4 heteromultimers, is a subject of considerable potential interest that our study raises but cannot answer. Single-channel experiments to evaluate the detailed biophysical

properties of the channels formed by the tandem construct in comparison with homomeric Kir2.1 and 2.4 would be quite interesting, but are beyond the scope of the present work. Finally, more detailed studies of the quantity and localization of Kir2.x protein expression would be of interest in order to assess the potential physiological importance of Kir2.4-Kir2.1 heteromultimerization.

VIII-6 References

ASHEN, M. D., O'ROURKE, B., KLUGE, K. A., JOHNS, D. C., & TOMASELLI, G. F. (1995). Inward rectifier K^+ channel from human heart and brain: cloning and stable expression in a human cell line. *American Journal of Physiology* **268**, H506-H511.

CHEN, F., WETZEL, G. T., FRIEDMAN, W. F., & KLITZNER, T. S. (1991). Single-channel recording of inwardly rectifying potassium currents in developing myocardium. *Journal of Molecular and Cellular Cardiology* **23**, 259-267.

COETZEE, W. A., AMARILLO, Y., CHIU, J., CHOW, A., LAU, D., MCCORMACK, T., MORENO, H., NADAL, M. S., OZAITA, A., POUNTNEY, D., SAGANICH, M., VEGA-SAENZ, D. M., & RUDY, B. (1999). Molecular diversity of K^+ channels. *Annuals of the New York Academy of Sciences* **868**, 233-285.

DERST, C., KARSCHIN, C., WISCHMEYER, E., HIRSCH, J. R., PREISIG-MULLER, R., RAJAN, S., ENGEL, H., GRZESCHIK, K., DAUT, J., & KARSCHIN, A. (2001). Genetic and functional linkage of Kir5.1 and Kir2.1 channel subunits. *FEBS Letters* **491**, 305-311.

FAKLER, B., BOND, C. T., ADELMAN, J. P., & RUPPERSBERG, J. P. (1996). Heterooligomeric assembly of inward-rectifier K^+ channels from subunits of different subfamilies: Kir2.1 (IRK1) and Kir4.1 (BIR10). *Pflugers Archiv* **433,** 77-83.

FINK, M., DUPRAT, F., HEURTEAUX, C., LESAGE, F., ROMEY, G., BARHANIN, J., & LAZDUNSKI, M. (1996). Dominant negative chimeras provide evidence for homo and heteromultimeric assembly of inward rectifier K^+ channel proteins via their N-terminal end. *FEBS Letters* **378**, 64-68.

GLOWATZKI, E., FAKLER, G., BRANDLE, U., REXHAUSEN, U., ZENNER, H. P., RUPPERSBERG, J. P., & FAKLER, B. (1995). Subunit-dependent assembly of inward-rectifier K^+ channels. *Proceedings of the Royal Society of London. Series B. Biological Sciences* **261**, 251-611.

GREEN, W. N. & MILLAR, N. S. (1995). Ion-channel assembly. *Trends in Neurosciences* **18**, 280-287.

HEGINBOTHAM, L., LU, Z., ABRAMSON, T., & MACKINNON, R. (1994). Mutations in the K^+ channel signature sequence. *Biophysical Journal* **66**, 1061-1077.

HOFFMANN, A. & ROEDER, R. G. (1991). Purification of His-tagged proteins in non-denaturing conditions suggests a convenient method for protein interaction studies. *Nucleic Acids Research* **19**, 6337-6338.

HORIO, Y., MORISHIGE, K., TAKAHASHI, N., & KURACHI, Y. (1996). Differential distribution of classical inwardly rectifying potassium channel mRNAs in the brain: comparison of IRK2 with IRK1 and IRK3. *FEBS Letters* **379,** 239-243.

HUGHES, B. A., KUMAR, G., YUAN, Y., SWAMINATHAN, A., YAN, D., SHARMA, A., PLUMLEY, L., YANG-FENG, T. L., & SWAROOP, A. (2000). Cloning and functional expression of human retinal Kir2.4, a pH- sensitive inwardly rectifying K^+ channel. *American Journal of Physiology - Cell Physiology* **279**, C771-C784.

ISHII, K., YAMAGISHI, T., & TAIRA, N. (1994). Cloning and functional expression of a cardiac inward rectifier K^+ channel. *FEBS Letters* **338**, 107-111.

JOSEPHSON, I. R. & BROWN, A. M. (1986). Inwardly rectifying single-channel and whole cell K^+ currents in rat ventricular myocytes. *The Journal of Membrane Biology* **94**, 19-35.

JOSEPHSON, I. R. & SPERELAKIS, N. (1990). Developmental increases in the inwardly-rectifying K^+ current of embryonic chick ventricular myocytes. *Biochimica et Biophysica Acta* **1052**, 123-127.

KARSCHIN, C., DISSMANN, E., STUHMER, W., & KARSCHIN, A. (1996). IRK(1-3) and GIRK(1-4) inwardly rectifying K^+ channel mRNAs are differentially expressed in the adult rat brain. *The Journal of Neuroscience* **16**, 3559-3570.

KOYAMA, H., MORISHIGE, K. I., TAKAHASHI, N., ZANELLI, J. S., FASS, D. N., & KURACHI, Y. (1994). Molecular cloning, functional expression and localization of a novel inward rectifier potassium channel in the rat brain. *FEBS Letters* **341**, 303-307.

KRAPIVINSKY, G., GORDON, E. A., WICKMAN, K., VELIMIROVIC, B., KRAPIVINSKY, L., & CLAPHAM, D. E. (1995). The G-protein-gated atrial K^+ channel I_{KACh} is a heteromultimer of two inwardly rectifying K^+ channel proteins. *Nature* **374**, 135-411.

KUBO, Y., BALDWIN, T. J., JAN, Y. N., & JAN, L. Y. (1993). Primary structure and functional expression of a mouse inward rectifier potassium channel. *Nature* **362**, 127-133.

LEE, T. E., PHILIPSON, L. H., KUZNETSOV, A., & NELSON, D. J. (1994a). Structural determinant for assembly of mammalian K^+ channels. *Biophysical Journal* **66**, 667-673.

LEE, T. E., PHILIPSON, L. H., KUZNETSOV, A., & NELSON, D. J. (1994b). Structural determinant for assembly of mammalian K^+ channels. *Biophysical Journal* **66**, 667-673.

LESAGE, F., DUPRAT, F., FINK, M., GUILLEMARE, E., COPPOLA, T., LAZDUNSKI, M., & HUGNOT, J. P. (1994). Cloning provides evidence for a family of inward rectifier and G- protein coupled K^+ channels in the brain. *FEBS Letters* **353**, 37-42.

LESAGE, F., GUILLEMARE, E., FINK, M., DUPRAT, F., HEURTEAUX, C., FOSSET, M., ROMEY, G., BARHANIN, J., & LAZDUNSKI, M. (1995). Molecular properties of neuronal G-protein-activated inwardly rectifying K^+ channels. *The Journal of Biological Chemistry* **270**, 28660-28667.

LI, M., JAN, Y. N., & JAN, L. Y. (1992). Specification of subunit assembly by the hydrophilic amino-terminal domain of the Shaker potassium channel. *Science* **257**, 1225-1300.

LIU, D. W. & ANTZELEVITCH, C. (1995). Characteristics of the delayed rectifier current (I_{Kr} and I_{Ks}) in canine ventricular epicardial, midmyocardial, and endocardial myocytes. A weaker I_{Ks} contributes to the longer action potential of the M cell. *Circulation Research* **76**, 351-365.

LIU, G. X., DERST, C., SCHLICHTHORL, G., HEINEN, S., SEEBOHM, G., BRÜGGEMANN, A., KUMMER, W., VEH, R. W., DAUT, J., & PREISIG-MULLER, R. (2001). Comparison of cloned Kir2 channels with native inward rectifier K^+ channels from guinea-pig cardiomyocytes. *The Journal of Physiology* **532**, 115-126.

MAKHINA, E. N., KELLY, A. J., LOPATIN, A. N., MERCER, R. W., & NICHOLS, C. G. (1994). Cloning and expression of a novel human brain inward rectifier potassium channel. *The Journal of Biological Chemistry* **269**, 20468-20744.

MORISHIGE, K., TAKAHASHI, N., FINDLAY, I., KOYAMA, H., ZANELLI, J. S., PETERSON, C., JENKINS, N. A., COPELAND, N. G., MORI, N., & KURACHI, Y. (1993). Molecular cloning, functional expression and localization of an inward rectifier potassium channel in the mouse brain. *FEBS Letters* **336**, 375-380.

MORISHIGE, K., TAKAHASHI, N., JAHANGIR, A., YAMADA, M., KOYAMA,M., ZANELLI, J.S., & KURACHI, Y. (1994). Molecular cloning and functional expression of a novel brain-specific inward rectifier potassium channel. *FEBS Letters* **346**, 251-256.

NICHOLS, C. G. & LOPATIN, A. N. (1997). Inward rectifier potassium channels. *Annual Review of Physiology* **59,** 171-191.

PEARSON, W. L., DOURADO, M., SCHREIBER, M., SALKOFF, L., & NICHOLS, C. G. (1999). Expression of a functional Kir4 family inward rectifier K^+ channel from a gene cloned from mouse liver. *The Journal of Physiology* **514**, 639-653.

PEREON, Y., DEMOLOMBE, S., BARO, I., DROUIN, E., CHARPENTIER, F., & ESCANDE, D. (2000). Differential expression of KvLQT1 isoforms across the human ventricular wall. *The American Journal of Physiology – Heart and Circulatory Physiology* **278**, H1908-H1915.

PERIER, F., RADEKE, C. M., & VANDENBERG, C. A. (1994). Primary structure and characterization of a small-conductance inwardly rectifying potassium channel from human hippocampus. *Proceedings of the National Academy of Sciences of the United States of America* **91**, 6240-6244.

PESSIA, M., TUCKER, S. J., LEE, K., BOND, C. T., & ADELMAN, J. P. (1996). Subunit positional effects revealed by novel heteromeric inwardly rectifying K^+ channels. *The EMBO Journal* **15**, 2980-2987.

PO, S., ROBERDS, S., SNYDERS, D. J., TAMKUN, M. M., & BENNETT, P. B. (1993). Heteromultimeric assembly of human potassium channels. Molecular basis of a transient outward current? *Circulation Research* **72**, 1326-1336.

PREISIG-MÜLLER, R., SCHLICHTHÖRL, G., GOERGE, T., HEINEN, S., BRUGGEMANN, A., RAJAN, S., DERST, C., VEH, R. W., & DAUT, J. (2002). Heteromerization of Kir2.x potassium channels contributes to the phenotype of Andersen's syndrome. *Proceedings of the National Academy of Sciences of the United States of America* **99**, 7774-7779.

RAAB-GRAHAM, K. F., RADEKE, C. M., & VANDENBERG, C. A. (1994). Molecular cloning and expression of a human heart inward rectifier potassium channel. *Neuroreport* **5**, 2501-2555.

SCHRAM, G., WANG, Z., & NATTEL, S. Molecular composition of human cardiac I_{K1} evaluated by barium blocking profile. *Circulation* **100**, I633. 1999.

SHEN, N. V., CHEN, X., BOYER, M. M., & PFAFFINGER, P. J. (1993). Deletion analysis of K^+ channel assembly. *Neuron* **11**, 67-76.

SLESINGER, P. A., PATIL, N., LIAO, Y. J., JAN, Y. N., JAN, L. Y., & COX, D. R. (1996). Functional effects of the mouse weaver mutation on G protein-gated inwardly rectifying K^+ channels. *Neuron* **16**, 321-311.

TAKAHASHI, N., MORISHIGE, K., JAHANGIR, A., YAMADA, M., FINDLAY, I., KOYAMA, H., & KURACHI, Y. (1994). Molecular cloning and functional expression of cDNA encoding a second class of inward rectifier potassium channels in the mouse brain. *The Journal of Biological Chemistry* **269**, 23274-23299.

TANEMOTO, M., KITTAKA, N., INANOBE, A., KURACHI, Y. (2000). In vivo formation of a proton-sensitive K^+ channel by heteromeric subunit assembly of Kir5.1 with Kir4.1. *The Journal of Physiology* **525**, 587-592.

TANG, W., QIN, C. L., & YANG, X. C. (1995). Cloning, localization, and functional expression of a human brain inward rectifier potassium channel (hIRK1). *Receptors & Channels* **3**, 175-833.

TANG, W. & YANG, X. C. (1994). Cloning a novel human brain inward rectifier potassium channel and its functional expression in *Xenopus* oocytes. *FEBS Letters* **348**, 239-433.

TINKER, A., JAN, Y. N., & JAN, L. Y. (1996). Regions responsible for the assembly of inwardly rectifying potassium channels. *Cell* **87**, 857-868.

TOPERT, C., DORING, F., DERST, C., DAUT, J., GRZESCHIK, K. H., & KARSCHIN, A. (2000). Cloning, structure and assignment to chromosome 19q13 of the human Kir2.4 inwardly rectifying potassium channel gene (KCNJ14). *Mammalian Genome* **11**, 247-249.

TOPERT, C., DORING, F., WISCHMEYER, E., KARSCHIN, C., BROCKHAUS, J., BALLANYI, K., DERST, C., & KARSCHIN, A. (1998). Kir2.4: a novel K^+ inward rectifier channel associated with motoneurons of cranial nerve nuclei. *Journal of Neuroscience* **18**, 4096-1055.

TUCKER, S. J., BOND, C. T., HERSON, P., PESSIA, M., & ADELMAN, J. P. (1996). Inhibitory interactions between two inward rectifier K^+ channel subunits mediated by the transmembrane domains. *The Journal of Biological Chemistry* **271**, 5866-5870.

TYTGAT, J., BUYSE, G., EGGERMONT, J., DROOGMANS, G., NILIUS, B., & DAENENS, P. (1996). Do voltage-gated Kv1.1 and inward rectifier Kir2.1 potassium channels form heteromultimers? *FEBS Letters* **390**, 280-244.

WAHLER, G. M. (1992). Developmental increases in the inwardly rectifying potassium current of rat ventricular myocytes. *The American Journal of Physiology* **262**, C1266-C1272.

WANG, Z., YUE, L., WHITE, M., PELLETIER, G., & NATTEL, S. (1998). Differential distribution of inward rectifier potassium channel transcripts in human atrium versus ventricle. *Circulation* **98**, 2422-2428.

WIBLE, B. A., DE BIASI, M., MAJUMDER, K., TAGLIALATELA, M., & BROWN, A. M. (1995). Cloning and functional expression of an inwardly rectifying K^+ channel from human atrium . *Circulation Research* **76**, 343-500.

WOOD, L. S., TSAI, T. D., LEE, K. S., & VOGELI, G. (1995). Cloning and functional expression of a human gene, hIRK1, encoding the heart inward rectifier K^+ channel. *Gene* **163**, 313-317.

YANG, Z., XU, H., CUI, N. QU, Z., CHANCHEVALAP, S., SHEN, W., JIANG, C. (2000). Biophysical and molecular mechanisms underlying the modulation of heteromeric Kir4.1-Kir5.1 channels by CO_2 and pH. *The Journal of General Physiology* **116**, 33-45.

VIII-7 Acknowledgments

The authors wish to thank Drs. Terence E. Hebert and Bruce G. Allen, Montreal Heart Institute for helpful discussions on construction of Kir2.4-Flag and His-pulldown, and Chantal St-Cyr, Evelyn Landry and Xiao Fan Yang for their excellent and reliable technical assistance. They thank Dr. Lily Y. Jan, San Francisco for Kir2.1, Dr. Barbara A. Wible, Cleveland for Kir2.2, Dr. Carol A. Vandenberg, Santa Barbara for Kir2.3, Dr. Andreas Karschin, Göttingen, Germany for the gift of Kir2.4 and Dr. Andrew Tinker, London, England for the generous gift of dn-Kir2.1 and Kir2.1-His_6. Dr. Schram wishes to thank the Ernst and Berta Grimmke Foundation, Düsseldorf, Germany, the Canadian Institutes of Health Research (CIHR) and Aventis Pharma for fellowship support, as well as CIHR and the Quebec Heart and Stroke Foundation for operating support.

VIII-8 Figures and Figure Legends

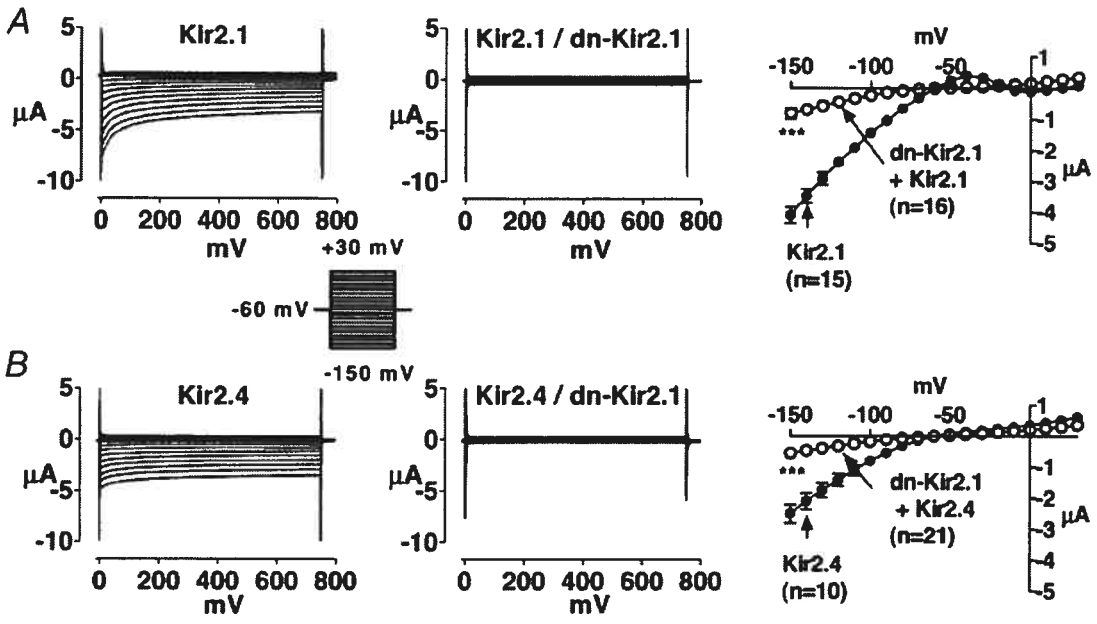

Figure 27: Effects of dn-Kir2.1 on Kir2.1 and Kir2.4 currents in *Xenopus* oocytes.

Currents recorded from *Xenopus* oocytes injected with Kir2.1 or 2.4 cRNA alone (left panels) or together with dn-Kir2.1 (middle panels). Results are shown for Kir2.1 (**A**) and Kir2.4 (**B**). Mean ± S.E.M. current-voltage relations for 15 (Kir2.1), 16 (Kir2.1/dn-Kir2.1), 10 (Kir2.4), and 21 (Kir2.4/dn-Kir2.1) oocytes are illustrated on the right. Closed symbols represent currents recorded from oocytes injected with Kir2.x cRNA alone, whereas corresponding open symbols represent currents recorded from oocytes co-injected with equal amounts of Kir2.x cRNA and dn-Kir2.1 cRNA. *** $P < 0.001$ for significance of difference between current density in co-injected oocytes vs. Kir2.x.

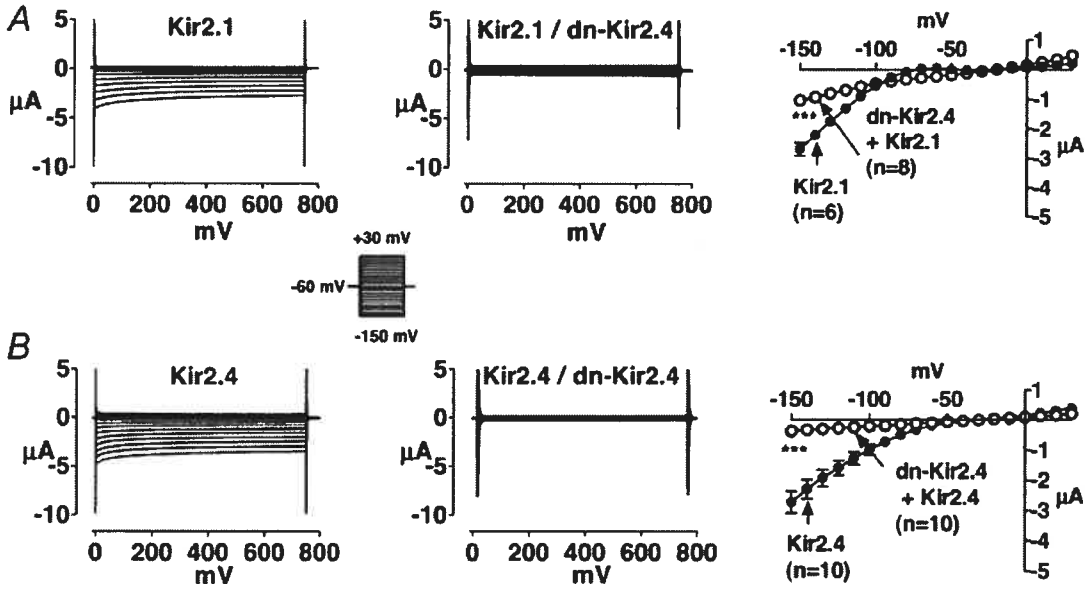

Figure 28: Effects of dn-Kir2.4 on Kir2.1 and Kir2.4 currents in *Xenopus* oocytes.

Currents recorded from *Xenopus* oocytes injected with Kir2.1or 2.4 cRNA alone (left panels) or together with dn-Kir2.4 (middle panels). Results are shown for Kir2.1 (**A**) and Kir2.4 (**B**). Mean ± S.E.M. current-voltage relations for 6 (Kir2.1), 8 (Kir2.1/dn-Kir2.4), 10 (Kir2.4), and 10 (Kir2.4/dn-Kir2.4) oocytes are illustrated on the right. Closed symbols represent currents recorded from oocytes injected with Kir2.x cRNA alone, whereas corresponding open symbols represent currents recorded from oocytes co-injected with equal amounts of Kir2.x cRNA and dn-Kir2.4 cRNA. *** $P < 0.001$ for significance of difference between current density in co-injected oocytes vs. Kir2.x.

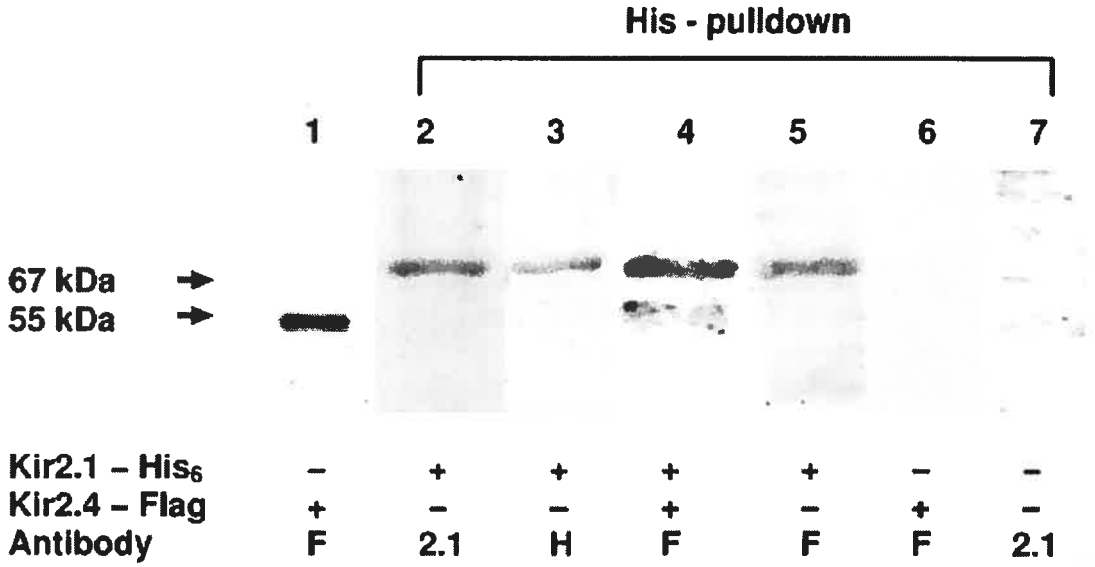

Figure 29: Western blots of cell lysates from Cos-7 cells transfected with either Kir2.1-His6, Kir2.4-Flag or both.

The constructs transfected and antibody probes used are indicated at the bottom. + indicates construct transfected, - indicates construct not present. Primary antibodies are designated by F for anti-Flag, 2.1 for anti-Kir2.1 and H for anti-His. Arrows on the left indicate molecular weights of specific bands detected by specific primary antibodies. Molecular weights are given in kilodaltons (kDa). Lane 1 is a Western blot of Cos-7 cell lysate transfected with Kir2.4-Flag and purified on a Flag-Affinity gel (Sigma). Cell lysates in lanes 2 to 7 were subjected to His_6-pulldown prior to incubation with the primary antibody. Lane 2 and 3 were obtained with a lysate of cells transfected with Kir2.1-His_6 only and lane 4 was obtained with a lysate of cells co-transfected with Kir2.4-Flag and Kir2.1-His_6. Lane 5 was obtained from cells transfected with Kir2.1-His_6 and incubated with anti-Flag after His-pulldown. Lane 6 is a western blot of lysate of Cos-7 cells transfected with Kir2.4-Flag only incubated with anti-Flag. Lane 7 is a Western blot with crude (non-transfected) Cos-7 cell lysate incubated with anti-Kir2.1.

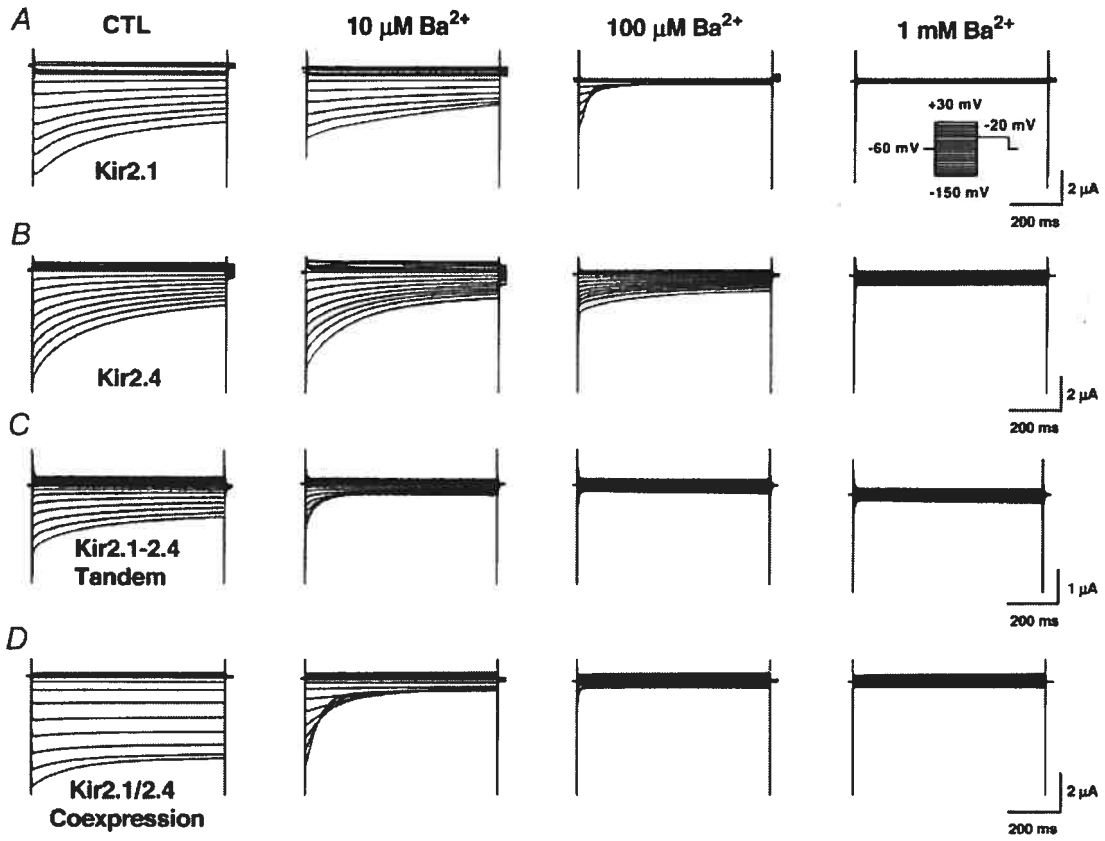

Figure 30: Ba^{2+} block of Kir2.1, Kir2.4, Kir2.1-Kir2.4 tandem and co-injected Kir2.1 and Kir2.4, original recordings.

Original current recordings obtained from oocytes injected with Kir2.1 (**A**), Kir2.4 (**B**), the Kir2.1-Kir2.4 tandem (**C**) and co-injected Kir2.1 and 2.4 (**D**) under control conditions (left panels) and in the presence of 10 μM (left middle panels), 100 μM (right middle panels) and 1 mM (right panels) Ba^{2+}.

Currents were elicited by voltage steps from a holding potential of -60 mv to step potentials between -150 mV and +30 mV in 10 mV increments as shown by the voltage protocol in the insert.

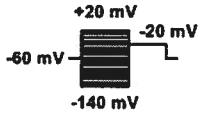

A Kir2.1

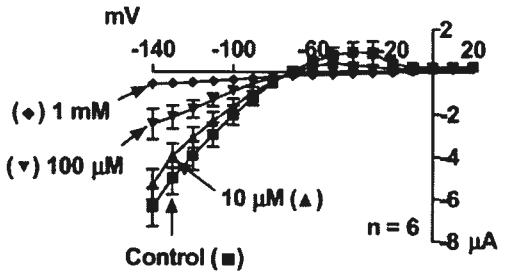

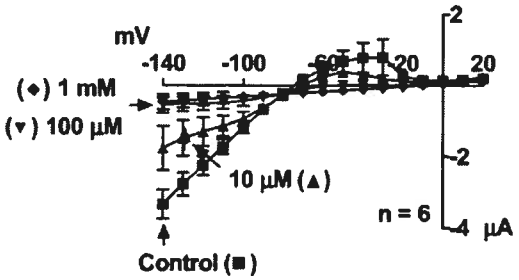

B Kir2.4

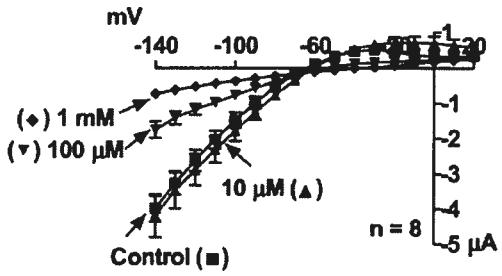

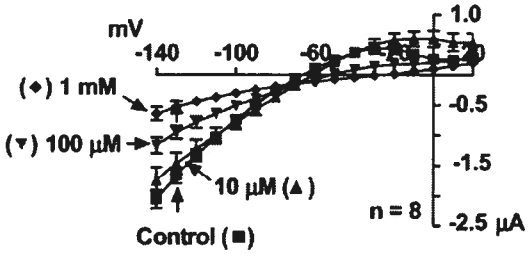

C Kir2.1-2.4 Tandem

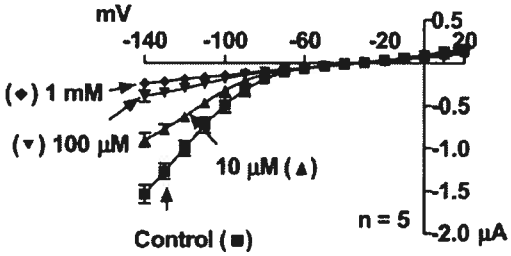

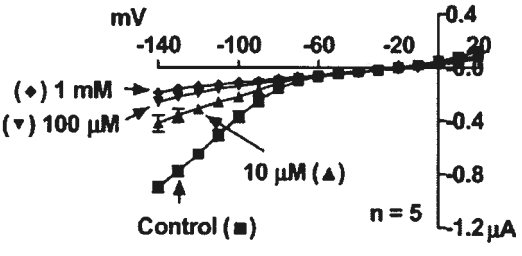

D Kir2.1/2.4 co-expression

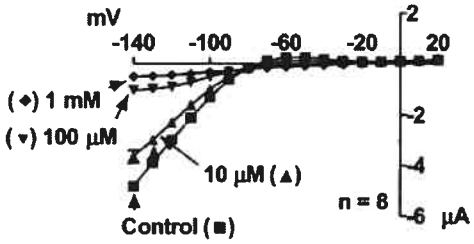

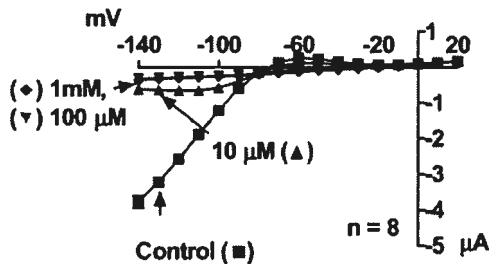

Figure 31: Ba^{2+} block of Kir2.1, Kir2.4, Kir2.1-Kir2.4 tandem and co-injected Kir2.1 and Kir2.4, mean ± S.E.M. current-voltage relations.

Mean ± S.E.M. current-voltage relations just after the onset of the voltage step (left panels) and under steady-state conditions (right panels).

N= 6, 8, 5 and 8 oocytes for Kir2.1 (**A**), Kir2.4 (**B**), tandem (**C**) and co-injected constructs (**D**).

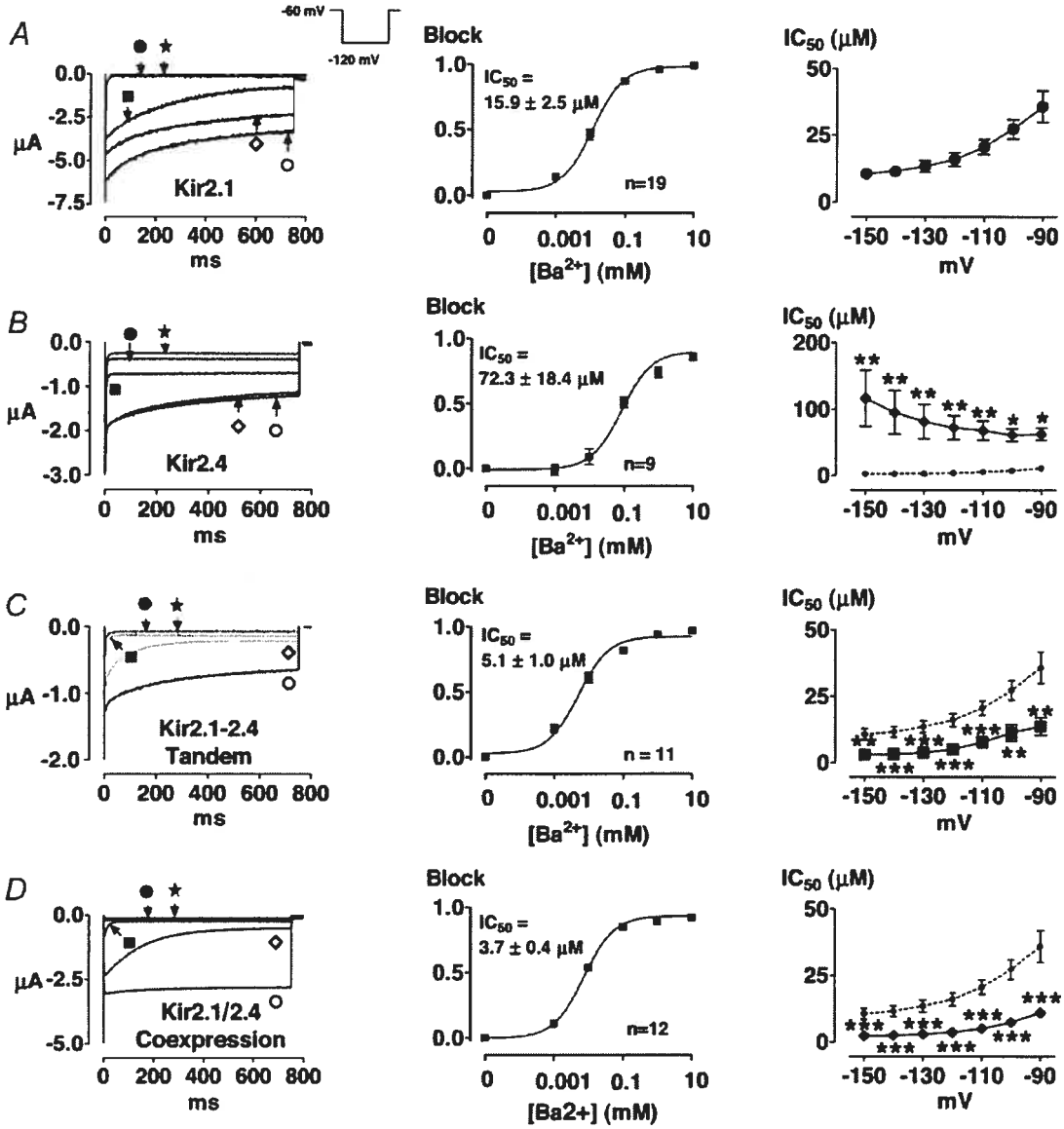
A
-60 mV
-120 mV
0.0
-2.5
-5.0
-7.5
μA
Kir2.1
0 200 400 600 800
ms
Block
1.0
0.5
0.0
IC50 =
15.9 ± 2.5 μM
n=19
0 0.001 0.1 10
[Ba2+] (mM)
IC50 (μM)
50
25
0
-150 -130 -110 -90
mV
B
0.0
-1.0
-2.0
-3.0
μA
Kir2.4
0 200 400 600 800
ms
Block
1.0
0.5
0.0
IC50 =
72.3 ± 18.4 μM
n=9
0 0.001 0.1 10
[Ba2+] (mM)
IC50 (μM)
200
100
0
-150 -130 -110 -90
mV
C
0.0
-1.0
-2.0
μA
Kir2.1-2.4
Tandem
0 200 400 600 800
ms
Block
1.0
0.5
0.0
IC50 =
5.1 ± 1.0 μM
n = 11
0 0.001 0.1 10
[Ba2+] (mM)
IC50 (μM)
50
25
0
-150 -130 -110 -90
mV
D
0.0
-2.5
-5.0
μA
Kir2.1/2.4
Coexpression
0 200 400 600 800
ms
Block
1.0
0.5
0.0
IC50 =
3.7 ± 0.4 μM
n=12
0 0.001 0.1 10
[Ba2+] (mM)
IC50 (μM)
50
25
0
-150 -130 -110 -90
mV

Figure 32: Comparison of Ba^{2+} block of Kir2.1, Kir2.4, Kir2.1-Kir2.4 tandem and co-expressed Kir2.1 and Kir2.4. Dose-response curves and IC_{50}/TP.

Ba^{2+} block of currents resulting from the expression of Kir2.1 (**A**), Kir2.4 (**B**), Kir2.1-2.4 tandem (**C**), co-expressed Kir2.1 and 2.4 (**D**). Left panels show original recordings from one oocyte under control conditions (open circles) and in the presence of Ba^{2+} at the following mM concentrations: 0.01 (open diamonds), 0.1 (closed squares), 1 (closed circles) and 10 (stars). The middle panels show corresponding mean ± S.E.M. concentration-response curves based on end-pulse block at each concentration upon hyperpolarisation to –120 mV (N= 19, 9, 11 and 12 oocytes for Kir2.1, Kir2.4, tandem and co-injected constructs respectively). The right panels show mean IC_{50}s obtained from the type of analysis illustrated in the middle panels, at each test potential studied (N= 19, 9, 11 and 12 oocytes for Kir2.1, Kir2.4, tandem and co-injected constructs respectively). To facilitate direct comparison of data obtained in oocytes following injection of Kir2.4 and engineered constructs with data for Kir2.1, data for Kir2.1 are reproduced in the right panels, as indicated by the dashed lines. $^{*}P < 0.05$, $^{**}P < 0.01$, $^{***}P < 0.001$ vs. Kir2.1 at the same voltage.

CHAPTER IX: BARIUM BLOCK OF KIR2 AND HUMAN CARDIAC INWARD RECTIFIER CURRENTS: EVIDENCE FOR SUBUNIT-HETEROMERIC CONTRIBUTION TO NATIVE CURRENTS

Reprinted from Cardiovascular Research, 59, Schram G, Pourrier M, Wang Z, Nattel S., Barium block of Kir2 and human cardiac inward rectifier currents: evidence for subunit-heteromeric contribution to native currents, 328-338, 2003, with permission from the European Society of Cardiology.

Barium block of Kir2 and human cardiac inward rectifier currents: evidence for subunit-heteromeric contribution to native currents

Gernot Schram[a,b], Marc Pourrier[a,d], Zhiguo Wang[a,b], Michel White[a,b], Stanley Nattel[a,b,c,*]

[a]Departments of Medicine and Research Center, Montreal Heart Institute, 5000 Belanger Street East, Montreal, Quebec, H1T 1C8, Canada

[b]Department of Medicine, University of Montreal, Montreal, Quebec, Canada

[c]Department of Pharmacology, McGill University, Montreal, Quebec, Canada

[d]Department of Pharmacology, University of Montreal, Montreal, Quebec, Canada.

Running title: Kir2 heteromers and I_{K1}

Word count: 5,208

---

*Corresponding author. Tel.: (514)-376-3330; fax: (514)-376-1355.

E-Mail address: [redacted]

IX-1 Abstract

Background: Kir2 subunits are believed to underlie the cardiac inwardly rectifying current I_{K1}. The subunit composition of native I_{K1} currents is uncertain, and it has been suggested that heteromultimer formation may play a role. **Methods:** We studied Ba^{2+} block of homo- and heteromeric Kir2 channels in *Xenopus* oocytes and compared the properties observed to those of human cardiac I_{K1} in cells isolated from myocardial biopsies of normal human hearts. **Results:** Homomeric expression of Kir2.1 and Kir2.3 produced currents with similar Ba^{2+} sensitivities (e.g. IC_{50} at -120 mV: 16.2±3.4, n=11 and 18.5±2.1, n=10 respectively), but these were less sensitive to Ba^{2+} than native I_{K1} (4.7±0.5 μM, n=10, P=0.001, P<0.001, respectively) and had different Ba^{2+} blocking kinetics from cardiac I_{K1}. Kir2.2 sensitivity was similar to cardiac I_{K1} (e.g. 2.8±0.4 μM, Kir2.2, n=9, versus 4.7±0.5 μM for I_{K1}), but the blocking kinetics of Kir2.2 were faster than those of I_{K1}. Currents resulting from co-expression of Kir2 subunits had similar Ba^{2+} sensitivities and blocking kinetics among groups and were similar to I_{K1} in both Ba^{2+} sensitivity (e.g. IC_{50} at -120 mV: 4.5±1.0, 2.5±0.5, and 2.3±0.4 μM for co-injected Kir2.1/2.2, n=6, Kir2.1/2.3, n=5, and Kir2.2/2.3, n=4 respectively) and blocking kinetics. **Conclusion:** Co-injection of Kir2 subunits results in currents with Ba^{2+} blocking properties different from homomeric Kir2 expression but similar to cardiac I_{K1}. These observations suggest that a substantial proportion of native I_{K1} may result from heteromultimer formation among diverse Kir2 family subunits.

Keywords: Ion transport; K^+ channel; Arrhythmia (mechanisms); Ion channels; Sudden death

IX-2 Introduction

The inward rectifier current (I_{K1}) was first described in 1949 in skeletal muscle [1]. In the heart, I_{K1} sets the resting potential close to the K^+ equilibrium potential [2] and contributes significantly to cardiac repolarization [3-5]. Dysfunction of I_{K1} causes cardiac arrhythmias in Andersen's syndrome (LQT7) [6].

A variety of genes encoding inwardly rectifying K^+ (Kir) channel subunits have been cloned and grouped into 7 families (Kir1-7). Subunits of the Kir2 family are believed to underlie I_{K1} in the heart [2]. Three pore-forming α-subunits of the Kir2 family, Kir2.1-3, are expressed in cardiomyocytes [7]. In the human heart, Kir2.1 transcripts are 10-fold more abundant than those of Kir2.2 or Kir2.3 [8]. The relative expression of Kir2 transcripts fails to explain a variety of cardiac I_{K1} properties [8]. Heteromultimer formation among Kir2 subunits results in currents distinct from those produced by homomeric Kir2 subunit expression [9,10], potentially contributing to phenotypic diversity in Andersen's syndrome [9]. However, no study in the literature has compared directly currents carried by homomeric and heteromeric Kir2 channels to native I_{K1}.

High-potency block by extracellular Ba^{2+} is a striking pharmacological property of I_{K1} [10]. Kir2-based channels have different sensitivities to Ba^{2+} [7,9-11]. The goal of the present study was to compare Ba^{2+}-blocking properties of currents carried by single Kir2 subunits with currents carried by coexpressed subunits and with human cardiac I_{K1}.

IX-3 Methods

IX-3.1 Functional Expression of Cloned Inward Rectifier Subunits in *Xenopus* Oocytes

Kir2.1 and Kir2.2 were subcloned into a modified expression vector (pCRII, Invitrogen) containing a poly (A+) tail (A+-pCRII). Kir2.1-A+-pCRII was a kind gift of Lily Leh Jan, San Francisco, California. Kir2.2-A+-pCRII was a kind gift of Barbara Wible, Cleveland, Ohio. After linearization with *Bam*HI, cRNA for injection into *Xenopus* oocytes was prepared with T7 RNA polymerase. Kir2.3 was a kind gift of Carol Vandenberg, Santa Barbara, California. Kir2.3 cDNA was subcloned into a Bluescript SK- (Stratagene) vector. After linearization with HindIII, cRNA was prepared with T3 RNA polymerase, and 6 to 12 ng cRNA of either a single clone or a mixture of equal amounts of different cRNAs (two at a time) to a total amount of 6 to 12 ng were injected into stage IV-V *Xenopus* oocytes, followed by two-electrode voltage clamp 24-72 h later. Currents were elicited at 22°C by 750-ms voltage steps from a holding potential of -60 mV to test potentials between -150 mV and +30 mV in 10 mV increments with a GeneClamp-500 amplifier and pClamp 6.0 software (Axon). The external solution consisted of (mM) 5 KCl, 100 NaCl, 2 $MgCl_2$, 10 HEPES, 0.3 $CaCl_2$. Niflumic acid (10 μM) was added to block the Ca^{2+}-dependent Cl^- current. The external pH was adjusted to 7.4 with NaOH and the pipette was filled with 3-M KCl. Ba^{2+}-containing solutions were superfused until steady-state block occurred (generally after ~10 min) at each concentration before repeating full voltage-clamp protocols. Glass microelectrodes (3-M KCl-filled) had 1.3-1.8 MΩ resistances. All cRNA transcriptions were performed with the mMESSAGE mMACHINE kit, Ambion Inc., Austin, Texas.

IX-3.2 Cell Isolation

Human right ventricular myocytes were obtained via endomyocardial biopsies from patients undergoing routine follow-up after heart transplantation. Ca^{2+}-tolerant myocytes were isolated and stored for use within 12 h according to previously-described procedures [8]. Written informed consent was obtained as approved by the Ethics Committee of the Montreal Heart Institute. Cells were dispersed by trituration with a Pasteur pipette and stored in a high K^+-storage medium (in mM: KCl 20, K-glutamate 70, KH_2PO_4 10, glucose 25, β-hydroxybutyuric acid 10, taurine 20, EGTA 10, albumin 0.1%, and mannitol 40) at 4°C. All chemicals were purchased from Sigma Chemical Co., St Louis, MO, USA, unless otherwise specified.

IX-3.3 Whole-Cell Patch-Clamp Recordings

Experiments were conducted at 22°C and ionic currents were recorded under whole-cell voltage-clamp mode using an Axopatch 200B amplifier (Axon Instruments Inc. USA). Borosilicate glass electrodes (1-mm O.D.) had tip resistances of 2-4 MΩ when filled with pipette solution (mM): 0.1 GTP, 110 K-aspartate, 20 KCl, 1 $MgCl_2$, 5 Mg-ATP, 10 HEPES, 5 EGTA, 5 Na_2-phosphocreatine. The pH was adjusted to 7.4 with NaOH. Command pulses were generated by a D-A converter controlled by pClamp 6.05 software (Axon Instruments). Tip potentials were zeroed before formation of the membrane-pipette seal in Tyrode solution. The capacitance and series resistance (Rs) were electrically compensated to minimize the duration of the capacitive surge on the current recording and the voltage drop across the clamped cell membrane. 200 μM Cd^{2+}, 500 μM 4-aminopyridine (4-AP) and 1 μM atropine were added to the extracellular solution to inhibit current contamination by L-type Ca^{2+}-current, transient outward K^+-current and acetylcholine-dependent K^+-current respectively. Adenosine triphosphate (ATP)-dependent K^+-current was minimized by including ATP (Mg-salt, 5 mM) in the pipette and glyburide (10 μM) in the bath solution.

IX-3.4 Statistical Analysis

Data analysis was conducted with Axon Clampfit 6, SPSS 11, Graphpad Prism 3 and Microsoft Excel 2000. Group data are expressed as the mean±S.E.M. Statistical comparisons were made with one-way ANOVA followed by Tukey's post-test (SPSS 11). A 2-tailed probability <0.05 was taken to indicate statistical significance. Concentration-response data were analyzed using curve-fitting functions of Prism 3 software (GraphPad Software, Inc. CA, USA).

IX-4 Results

Fig. 33 shows original recordings in oocytes injected with Kir2.1 (A), Kir2.2 (B) or Kir2.3 (C) cRNA and from a human cardiomyocyte (D). Left panels show currents recorded in the absence of Ba^{2+} (Control). Left middle panels, right middle panels and right panels show currents in the presence of 10 μM, 100 μM and 1 mM Ba^{2+}, respectively. Ba^{2+}-block was concentration- and voltage-dependent for all currents. Fig. 34 shows respective Kir2 mean end-pulse current-voltage relationships under control conditions and in the presence of 1, 10 and 100 μM Ba^{2+}. Kir2.1 and Kir2.3 showed similar Ba^{2+}-sensitivity, with high-level block requiring 100-μM Ba^{2+}. Both Kir2.2 and cardiac I_{K1} were reduced by >60% with 10-μM Ba^{2+} and completely blocked by 100-μM Ba^{2+}, indicating qualitatively-similar sensitivity that was greater than that of Kir2.1 or Kir2.3.

Fig. 35 shows original current recordings obtained from *Xenopus* oocytes co-injected with both Kir2.1 and Kir2.2 (A), Kir2.1 and Kir2.3 (B) or Kir2.2 and Kir2.3 (C) cRNA, under control conditions (left panels) and in the presence of 10, 100 μM and 1 mM Ba^{2+}. Panel D shows the results from the same human cardiomyocyte as in Figure 33, for comparison purposes. The response of co-injected oocytes was qualitatively like that of the human cardiomyocyte. Corresponding mean current-voltage relationships are shown in Fig. 36. The current-voltage relationships of co-injected oocytes qualitatively resemble those of cardiac I_{K1} in both the absence of Ba^{2+} and in the presence of various Ba^{2+} concentrations. The Ba^{2+}-sensitivity of homomeric channels and channels resulting from co-injected Kir2 subunits showed significant group differences over the entire voltage range tested (-150 to -90 mV, $P<0.001$).

IX-4.1 Concentration and Time Dependence of Ba^{2+} Block of Homomeric Kir2 Subunits and Cardiac I_{K1}

To pursue the issue of Ba^{2+}-block of the various constructs studied, we analyzed the block quantitatively. Fig. 37, left panels, shows original currents recorded from one oocyte before and after each of 3 Ba^{2+} concentrations for cells

expressing Kir2.1 (A), Kir2.2 (B) or Kir2.3 (B), along with corresponding data from a human cardiomyocyte (D). For clarity, currents obtained at only one voltage (upon hyperpolarization to -120 mV) are shown. Whereas Kir2.1 and Kir2.3 showed similar Ba^{2+} sensitivity (approximately 30% current reduction at end of pulse by 10 μM Ba^{2+}, Fig. 37A and C), Kir2.2 was approximately one order of magnitude more sensitive to Ba^{2+} than Kir2.1 or Kir2.3. For example, 10 μM Ba^{2+} almost completely inhibited Kir2.2 end-pulse current (Fig. 37B, left), similar to the effect of 100 μM Ba^{2+} on Kir2.1 (Fig. 37A, left) or Kir2.3 (Fig. 37C, left). Cardiac I_{K1} was more sensitive to Ba^{2+} than Kir2.1 or Kir2.3 (e.g. approximately 70% end-pulse current inhibition by 10 μM Ba^{2+}, Fig. 37D, left), displaying Ba^{2+}-sensitivity more similar to that of Kir2.2.

The time-dependence of block is illustrated in the middle column of Fig. 37. Fractional block was calculated as control current (I_{Ctl}) minus current in the presence of Ba^{2+} (I_{Ba}) divided by control current ($[I_{Ctl} - I_{Ba}] / I_{Ctl}$), and expressed as a function of time during the pulse. For Kir2.1 and 2.3, block at 10 μM was virtually time-independent. At the same concentration, block of Kir2.2 showed a very rapid onset. The time-dependent block of cardiac I_{K1} was substantial at 10 μM and showed a slow onset. The onset of Ba^{2+} block was quantified as the time for 50% of steady-state time-dependent block ($t_{½}$), since the kinetics did not consistently follow simple mono- or biexponential models. Block onset was analyzed at approximately equi-effective concentrations (10 μM for Kir2.2 and I_{K1}, 100 μM for Kir2.1 and 2.3). The $t_{½}$ values of homomeric constructs were smaller than the value for I_{K1} (Table X).

The right panels show mean concentration-response curves of the form $B = 1/(1 + IC_{50}/C)$, where B is Ba^{2+}-block at any concentration C and IC_{50} is the 50%-blocking concentration. The Ba^{2+} IC_{50}s were comparable for Kir2.1 and 2.3 (16.2±3.6 and 18.5±2.1 μM respectively), about an order of magnitude greater than for Kir2.2 (2.3±0.4 μM). Cardiac I_{K1} had an IC_{50} (4.7±0.4 μM) of the same order as that of Kir2.2 and much smaller than for Kir2.1 or 2.3 (Table X).

IX-4.2 Concentration and Time Dependence of Ba^{2+}-Block of Co-Injected Kir2 Subunits and Cardiac I_{K1}

Fig. 38, left panels show original current recordings obtained from *Xenopus* oocytes co-injected with either Kir2.1/Kir2.2 (A), Kir2.1/Kir2.3 (B) or Kir2.2/Kir2.3 (C), in comparison with human cardiac I_{K1} (D), upon hyperpolarization to -120 mV. Currents resulting from co-injected Kir2 subunits showed qualitatively similar Ba^{2+}-sensitivity to cardiac I_{K1}. The middle column shows time-dependent block onset. Like I_{K1}, block of Kir2.1/Kir2.2 and Kir2.1/2.3 showed significant, slow time-dependent onset at 10 μM Ba^{2+}. The $t_{½}$ values for Kir2.1/2.2 and Kir2.1/2.3 coinjected were similar to those of I_{K1} (Table X). The $t_{½}$ was somewhat faster for Kir2.2/2.3 subunits. The corresponding concentration-response relations are shown in the right column. In contrast to the homomeric subunit-based currents, the currents resulting from co-injection showed similar and low IC_{50}s (Table X). This was the case even for Kir2.1/Kir2.3 currents, despite the fact that both Kir2.1 and Kir2.3 had much higher IC_{50}s when expressed alone. The IC_{50}s for all co-injected subunit combinations were comparable to the values for I_{K1}.

IX-4.3 Comparison of Ba^{2+} Blocking Properties of Homomeric and Co-Injected Kir2 Subunits with Cardiac I_{K1}

Fig. 39 shows a comparison of block at -120 mV for each pair of co-injected Kir2 subunits with that of I_{K1} (middle panels) and for each of the corresponding homomeric currents with I_{K1} (left panels). The right panels show Ba^{2+} IC_{50} values as a function of voltage for each of the corresponding currents. The asterisks in the right panels show the statistical significance of differences for blocking potency at each voltage versus that of I_{K1}. For Kir2.1 and 2.2 (A), block is less potent for Kir2.1 and more potent for Kir2.2 at -120 mV compared to cardiac I_{K1} (left panel). Block of Kir2.1/2.2 co-injected currents at -120 mV is quite similar to that of I_{K1} (middle). Comparing results at all voltages (right panels), results for Kir2.1 were significantly different from those of I_{K1}. Results for Kir2.2, 2.1/2.3 and I_{K1} were not statistically distinguishable. For Kir2.1 and 2.3 (panel B), either homomer resulted in currents less sensitive to Ba^{2+} than I_{K1} (left panel), but co-injected oocytes showed a

sensitivity comparable to that of I_{K1} (middle panel). Examining the entire voltage range, homomeric Kir2.1 and 2.3 were each significantly less sensitive than currents resulting from Kir2.1/2.3 co-injection, which were indistinguishable from I_{K1} (right). The corresponding data for Kir2.2 and 2.3 (C) indicates that once again co-injected oocytes have currents with Ba^{2+}-sensitivity similar to that of I_{K1}.

IX-5 Discussion

We have compared the Ba^{2+}-blocking response of currents carried by homomeric channels composed of Kir2.1, Kir2.2 and Kir2.3 with the response of currents resulting from co-expressed subunits and with human cardiac I_{K1}. The principle novel findings are that the response of co-expressed subunit-currents is not the simple algebraic sum of individual subunit responses, and that the response of native human I_{K1} is more similar to that of co-injected subunits than of each subunit expressed alone.

IX-5.1 Importance and Molecular Basis of I_{K1}

I_{K1} is crucial in cardiac electrophysiology [2,11], setting the resting potential and contributing to terminal repolarization [5]. Resting potential depolarization has complex effects on cardiac excitability (Dominguez and Fozzard, ca. 1975). Mild depolarization increases excitability by decreasing the depolarization needed to reach threshold, but stronger depolarization decreases excitability and conduction velocity by inactivating Na^+-channels. Increased excitability facilitates arrhythmias arising from abnormal automaticity and triggered activity, whereas impaired conduction promotes reentry. Impaired phase-3 repolarization caused by I_{K1} dysfunction could lead to excess action potential prolongation and early afterdepolarizations. Thus, I_{K1} abnormality can promote a wide range of arrhythmia mechanisms, any of which might be implicated in ventricular tachyarrhythmias associated with Kir2.1 dysfunction in Andersen's Syndrome [6].

Our understanding of the molecular basis of I_{K1} is limited. At the mRNA level, the most abundant Kir2 subunit is Kir2.1, with ventricular concentrations that are >10-fold greater than those of Kir2.2 or Kir2.3 [8]. Although Kir2.1-4 have been detected in the heart [12-17], only Kir2.1-3 appear to be expressed in cardiomyocytes, whereas Kir2.4 is found in cardiac neuronal tissue [7]. There is 78% greater abundance of Kir2.1 protein in ventricle versus atrium and 228% greater abundance of Kir2.3 in atrium versus ventricle, but the relative quantities of Kir2.1 versus Kir2.3 protein are unknown [18]. Unitary I_{K1} conductances change with

development, suggesting developmentally-based molecular alterations [19,20]. Four different I_{K1} single-channel conductances are displayed in human atrial cells, compatible with molecular heterogeneity [15]. Kir2.1 anti-sense oligonucleotides suppressed, but did not eliminate, I_{K1} in rat ventricular myocytes, but residual current was detected, suggesting other contributors [21]. In mice genetically engineered to lack Kir2.1 completely, I_{K1} is absent in the presence of physiological (4-mM) extracellular [K^+] [22]. Knockout of Kir2.2 reduces I_{K1} by ~50% [22]. These results suggest that Kir2.1 is a component of virtually all murine I_{K1} channels, whereas Kir2.2 subunits are present in about half. This possibility would be most easily explained by the formation of Kir2.1-Kir2.2 heteromers [22].

IX-5.2 Potential Role of Kir2 Heteromultimers

Initial studies suggested possible co-assembly between Kir2.1 and Kir2.3 subunits, mediated by N-terminal interactions [23]. Subsequent work suggested little or no heteromultimer formation between Kir2.1 and 2.2 or 2.3, with determinants for co-assembly localized to the M2 segment and proximal C-terminus [24]. Preisig-Müller et al. recently provided extensive evidence for Kir2.1, Kir2.2 and Kir2.3 heteromultimer formation [9]. They showed that concatemers of different Kir2 subunits form functional channels, that dominant negative Kir2.1, Kir2.2 or Kir2.3 constructs suppress currents carried by wild-type subunits of each subtype upon co-injection, that Kir2.1 and Kir2.3 subunits can be co-immunoprecipitated, that cytosolic carboxyterminal domains play a key role in protein-protein interaction, and that Andersen syndrome Kir2.1 mutations have dominant-negative effects upon co-expression with Kir2.1, Kir2.2 or Kir2.3.

We have shown that Kir2.1 and 2.4 subunits co-assemble, and that Ba^{2+}-blocking properties of co-assembled channels differ from homomeric Kir2.1 or 2.4 [10]. In fact, the Ba^{2+}-sensitivity of Kir2.1-2.4 channels was greater than those of either Kir2.1 or 2.4 alone, suggesting that heteromeric channels are not merely an intermediate hybrid form, but may have distinct properties of their own [10]. In our study of Kir2.1-Kir2.4 interaction, as in Preisig-Müller's studies of Kir2.1, Kir2.2 and Kir2.3 interaction, currents carried by co-injected subunits behaved like channels

formed by concatemers (which of necessity consist of co-assembled subunits, since the subunits are covalently linked). In the present study, currents carried by Kir2.2 co-injected with either Kir2.1 or 2.3 subunits had a Ba^{2+} IC_{50} indistinguishable from Kir2.2-subunit homomeric channels, rather than between the IC_{50} of Kir2.2 and the larger IC_{50} of Kir2.1 or Kir2.3. Moreover, the IC_{50} of co-injected Kir2.1/Kir2.3 is lower than for either homomeric subunit and of the same order as the IC_{50} for Kir2.2. This observation resembles our previous findings for Kir2.1/Kir2.4 and supports the notion of distinct properties for heteromeric Kir2 channels.

The present study is the first direct comparison between properties of currents carried by combinations of Kir2 subunits with those of native I_{K1}. The response to Ba^{2+} of currents carried by all combinations of co-injected subunits was more similar to that of human I_{K1} in terms of sensitivity, and Kir2.1/2.2 and Kir2.1/2.3 current Ba^{2+} blocking kinetics were more like those of I_{K1}, than homomeric channels. This finding supports the notion that a significant portion of I_{K1} may be carried by Kir2 heteromers, as initially suggested by Zaritsky et al. [22] and recently reinforced by the elegant studies of Preisig-Müller and co-workers [9].

Our results help to resolve an issue arising from a recent study that compared homomeric guinea pig Kir2 subunits to guinea-pig cardiac I_{K1} [7]. Based upon Ba^{2+}-blocking properties, the authors concluded that Kir2.2 was likely the predominant subunit underlying I_{K1}. However, in both human [8] and mouse [22] heart, Kir2.1 transcripts are much more abundant than those encoding Kir2.2. We found that Ba^{2+}-blocking sensitivity of heteromeric Kir2 channels is similar to those of Kir2.2. Thus, the guinea-pig findings [7] are compatible with a prominent role for heteromeric Kir2 channels in native I_{K1}, and do not necessarily imply predominance of Kir2.2 per se. This notion would fit well with results of Kir2.1 knock-down [21] and knockout [22] studies, while being agreeing with the guinea-pig Ba^{2+}-sensitivity data [7].

IX-5.3 Potential Limitations

We did not study single-channel Kir2 or I_{K1} properties. Single-channel studies of native I_{K1} have provided a wide variety of results. Wible et al. described four distinct conductances (41, 35, 21 and 9 pS) in human atrium [15], whereas Liu et al.

found only three conductances (10.5, 22 and 32.5 pS) in guinea-pig cardiomyocytes [7]. Nakamura et al. described six diverse conductances (8, 14, 21, 35, 43 and 80 pS) in rat ventricle [21]. Conductances of native I_{K1} channels may differ from those of heterologously-expressed Kir2 subunits of the same species [7]. Furthermore, homomeric mouse Kir2.1 channels show a broad range of conductances ranging from 2 to 33 pS [25]. Thus, single-channel analyses have not to date provided clear insights into the molecular composition of I_{K1} channels.

We used *Xenopus* oocytes as a heterologous expression system. Although this system has been widely used to study biophysical properties of Kir2 subunits in the past, we cannot exclude the possibility that intracellular protein processing pathways in oocytes may be different from mammalian cells and cardiomyocytes. This might represent a potential confounding factor in the interpretation of how the various Kir2 subunits co-assemble. Co-assembly of Kir2.1 and Kir2.3 has been shown in to occur in HEK293 cells, from which both subunits could be co-immunoprecipitated [9].

IX-6 Conclusions

This is the first study to compare properties of heteromeric Kir2 currents with those of native cardiac I_{K1}. Our results support the notion that a substantial proportion of native I_{K1} may result from heteromultimer formation among Kir2 subunits.

IX-7 Acknowledgements

The authors thank Chantal St-Cyr, Evelyn Landry, and Xiao Fan Yang for excellent technical assistance, and Diane Campeau, Daniela Giuliani and France Thériault for secretarial help with the manuscript. They thank Lily Jan for providing Kir2.1, Barbara Wible for Kir2.2, and Carol Vandenberg for Kir2.3. Dr. Schram was supported by the Ernst and Berta Grimmke Foundation, the Canadian Institutes of Health Research (CIHR) and Aventis Pharma. Marc Pourrier was supported by a Heart and Stroke Foundation of Canada studentship. Zhiguo Wang and Michel White are research scholars of the Fonds de la recherche en santé du Québec. Operating support was received from CIHR, the Quebec Heart and Stroke Foundation, and the Mathematics of Information Technology and Complex Systems (MITACS) Network.

IX-8 References

1. **Katz B.** Les constantes électrique de la membrane du muscle. *Arch Sci Physiol 1949;3:285-299.*
2. **Nichols CG, Lopatin AN.** Inward rectifier potassium channels. *Annu Rev Physiol 1997;59:171-191.*
3. **Sakmann B, Trube G.** Conductance properties of single inwardly rectifying potassium channels in ventricular cells from guinea-pig heart. *J Physiol (Lond) 1984;347:641-657.*
4. **Ibarra J, Morley GE, Delmar M.** Dynamics of the inward rectifier K^+ current during the action potential of guinea pig ventricular myocytes. *Biophys J 1991;60:1534-1539.*
5. **Shimoni Y, Clark RB, Giles WR.** Role of an inwardly rectifying potassium current in rabbit ventricular action potential. *J Physiol (Lond) 1992;448:709-727.*
6. **Plaster NM, Tawil R, Tristani-Firouzi M et al.** Mutations in Kir2.1 cause the developmental and episodic electrical phenotypes of Andersen's syndrome. *Cell 2001;105:511-519.*
7. **Liu GX, Derst C, Schlichthorl G et al.** Comparison of cloned Kir2 channels with native inward rectifier K^+ channels from guinea-pig cardiomyocytes. *J Physiol (Lond) 2001;532:115-126.*
8. **Wang Z, Yue L, White M, Pelletier G, Nattel S.** Differential distribution of inward rectifier potassium channel transcripts in human atrium versus ventricle. *Circulation 1998;98:2422-2428.*
9. **Preisig-Muller R, Schlichthorl G, George T et al.** Heteromerization of Kir2.x potassium channels contributes to the phenotype of Andersen's syndrome. *Proc Natl Acad Sci USA 2002;99:7774-7779.*
10. **Schram G, Melnyk P, Pourrier M, Wang Z, Nattel S.** Kir2.4 and Kir2.1 K^+ channel subunits co-assemble: A potential new contributor to inward rectifier current heterogeneity. *J Physiol (Lond) 2002;544:337-349.*

11. **Lopatin AN, Nichols CG.** Inward rectifiers in the heart: an update on I_{K1}. *J Mol Cell Cardiol 2001;33:625-638.*

12. **Ishii K, Yamagishi T, Taira N.** Cloning and functional expression of a cardiac inward rectifier K^+ channel. *FEBS Lett 1994;338:107-111.*

13. **Raab-Graham KF, Radeke CM, Vandenberg CA.** Molecular cloning and expression of a human heart inward rectifier potassium channel. *Neuroreport 1994;5:2501-2555.*

14. **Ashen MD, O'Rourke B, Kluge KA, Johns DC, Tomaselli GF.** Inward rectifier K^+ channel from human heart and brain: cloning and stable expression in a human cell line. *Am J Physiol (Heart Circ Physiol) 1995;268:H506-H511.*

15 **Wible BA, De Biasi M, Majumder K, Taglialatela M, Brown AM.** Cloning and functional expression of an inwardly rectifying K^+ channel from human atrium. *Circ Res 1995; 76:343-500.*

16. **Wood LS, Tsai TD, Lee KS, Vogeli G.** Cloning and functional expression of a human gene, hIRK1, encoding the heart inward rectifier K^+ channel. *Gene 1995;163:313-317.*

17. **Topert C, Doring F, Wischmeyer E et al.** Kir2.4: a novel K^+ inward rectifier channel associated with motoneurons of cranial nerve nuclei. *J Neurosci 1998;18:4096-4105.*

18. **Melnyk P, Zhang L, Shrier A, Nattel S.** Differential distribution of Kir2.1 and Kir2.3 subunits in canine atrium and ventricle. *Am J Physiol (Heart Circ Physiol) 2002;283:H1123-H1133.*

19. **Josephson IR, Sperelakis N.** Developmental increases in the inwardly-rectifying K^+ current of embryonic chick ventricular myocytes. *Biochim Biophys Acta 1990;1052:123-127.*

20. **Wahler GM.** Developmental increases in the inwardly rectifying potassium current of rat ventricular myocytes. *Am J Physiol 1992;262:C1266-C1272.*

21. **Nakamura TY, Artman M, Rudy B, Coetzee WA.** Inhibition of rat ventricular I_{K1} with antisense oligonucleotides targeted to Kir2.1 mRNA. *Am J Physiol 1998;274:H892-H900.*

22. **Zaritsky JJ, Redell JB, Tempel BL, Schwarz TL.** The consequences of disrupting cardiac inwardly rectifying K^+ current (I_{K1}) as revealed by the targeted deletion of the murine Kir2.1 and Kir2.2 genes. *J Physiol (Lond) 2001;533:697-710.*

23. **Fink M, Duprat F, Heurteaux C et al.** Dominant negative chimeras provide evidence for homo and heteromultimeric assembly of inward rectifier K^+ channel proteins via their N-terminal end. *FEBS Lett 1996;378:64-68.*

24. **Tinker A, Jan YN, Jan LY.** Regions responsible for the assembly of inwardly rectifying potassium channels. *Cell 1996;87:857-868.*

25. **Picones A, Keung E, Timpe LC.** Unitary conductance variation in Kir2.1 and in cardiac inward rectifier potassium channels. *Biophys J 2001;81:2035-2049.*

IX-9 Tables

	IC_{50} μM (n)	$T_{1/2}$ ms (n)
Homomeric constructs		
Kir2.1	16.2±3.6 (11) **	67±10 (7)*
Kir2.2	2.3±0.4 (9)	75±10 (7)*
Kir2.3	18.5±2.1 (10) ***	118±20 (7)
Co-expressed constructs		
Kir2.1 + Kir2.2	4.5±2.2 (6)	355±60 (5)
Kir2.1 + Kir2.3	2.5±0.5 (5)	205±30 (5)
Kir2.2 + Kir2.3	2.3±0.4 (4)	87±10 (4)
Cardiac I_{K1}	4.5±0.4 (10)	205±50 (7)

* $P<0.05$; ** $P<0.01$; *** $P<0.001$ versus corresponding value for cardiac I_{K1}

Table X: Potency and time-course of Ba^{2+} block of various constructs.

IX-10 Figures and Figure Legends

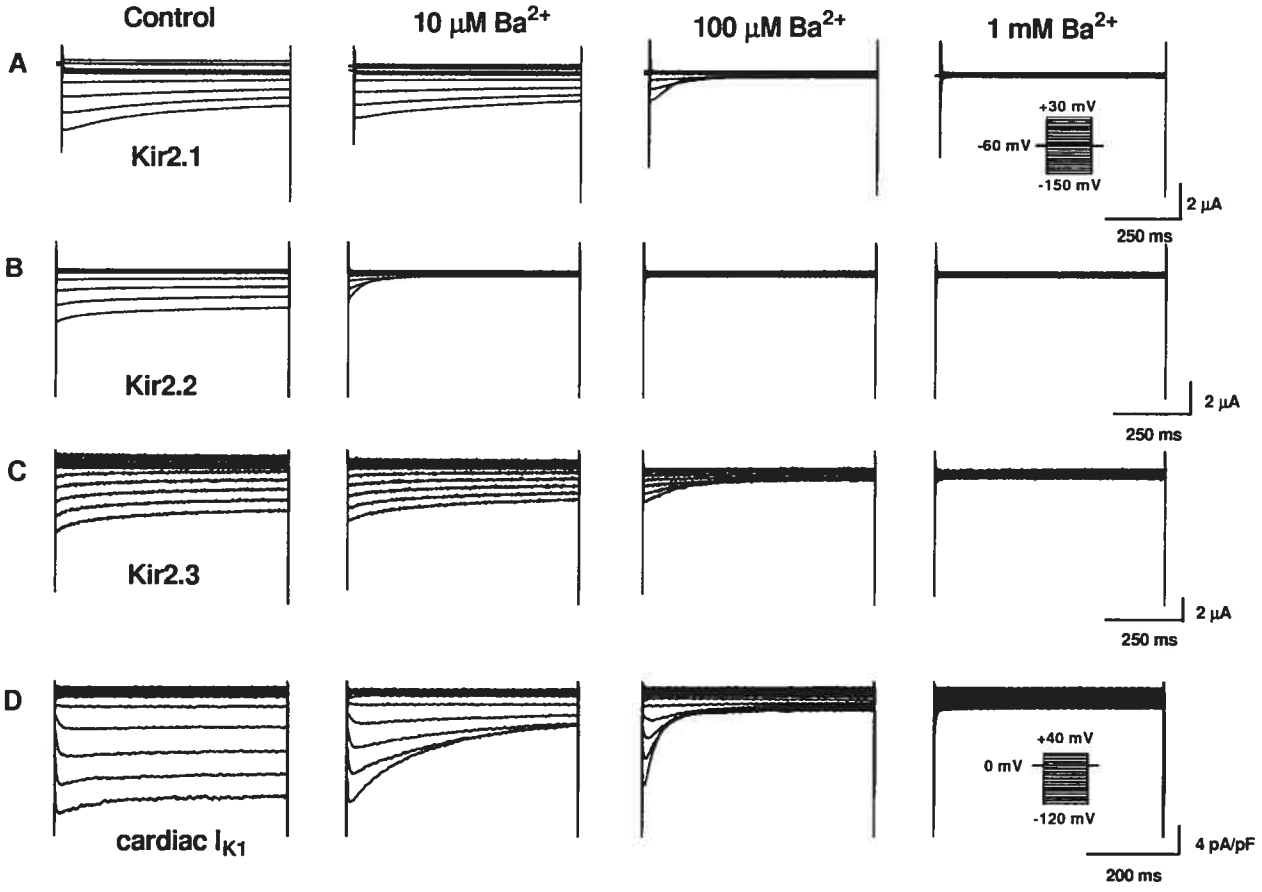

Figure 33: Ba^{2+} block of Kir2.1, Kir.2.2, Kir2.3 and cardiac I_{K1}, original current recordings.

Original current recordings obtained from oocytes injected with Kir2.1 (**A**), Kir2.2 (**B**) or Kir2.3 (**C**) and from human right ventricular myocytes (**D**) under control conditions (left panels) and in the presence of 10 μM (left middle panels), 100 μM (right middle panels) and 1 mM (right panels) Ba^{2+}. Kir2 currents were elicited by voltage steps from a holding potential of -60 mv to step potentials between -150 mV and +30 mV in 10 mV increments as shown by the voltage protocol in the inset. I_{K1} was elicited by voltage steps from a holding potential of 0 mV to step potentials between -120 mV and +40 mV in 10 mV increments as shown by the voltage protocol in the inset.

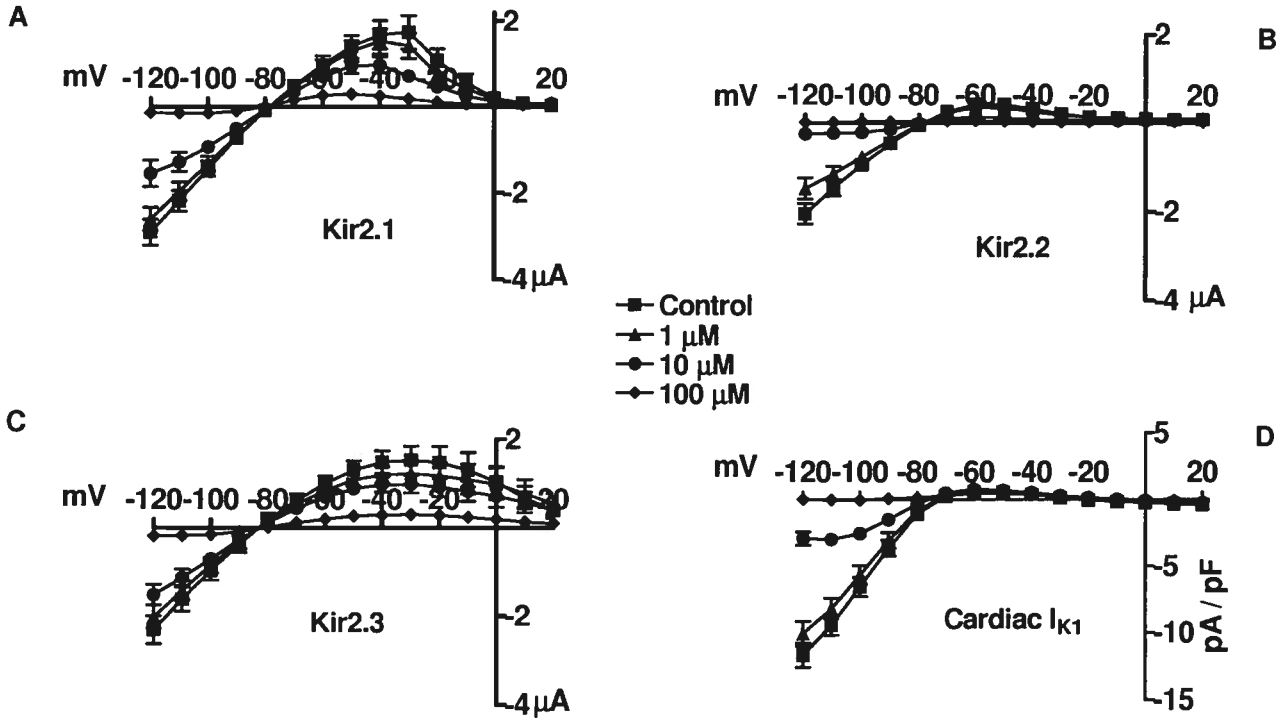

Figure 34: Ba^{2+} block of Kir2.1, Kir.2.2, Kir2.3 and cardiac I_{K1}, Mean±S.E.M. current-voltage relations.

Mean±S.E.M. current-voltage relations under steady-state conditions without drug (Control, squares) and in the presence of 1, 10 and 100 µM Ba^{2+} (triangles, circles and diamonds, respectively). n=14, 9, 11 and 10 cells for Kir2.1 (**A**), Kir2.2 (**B**), Kir2.3 (**C**) and cardiac I_{K1} (**D**).

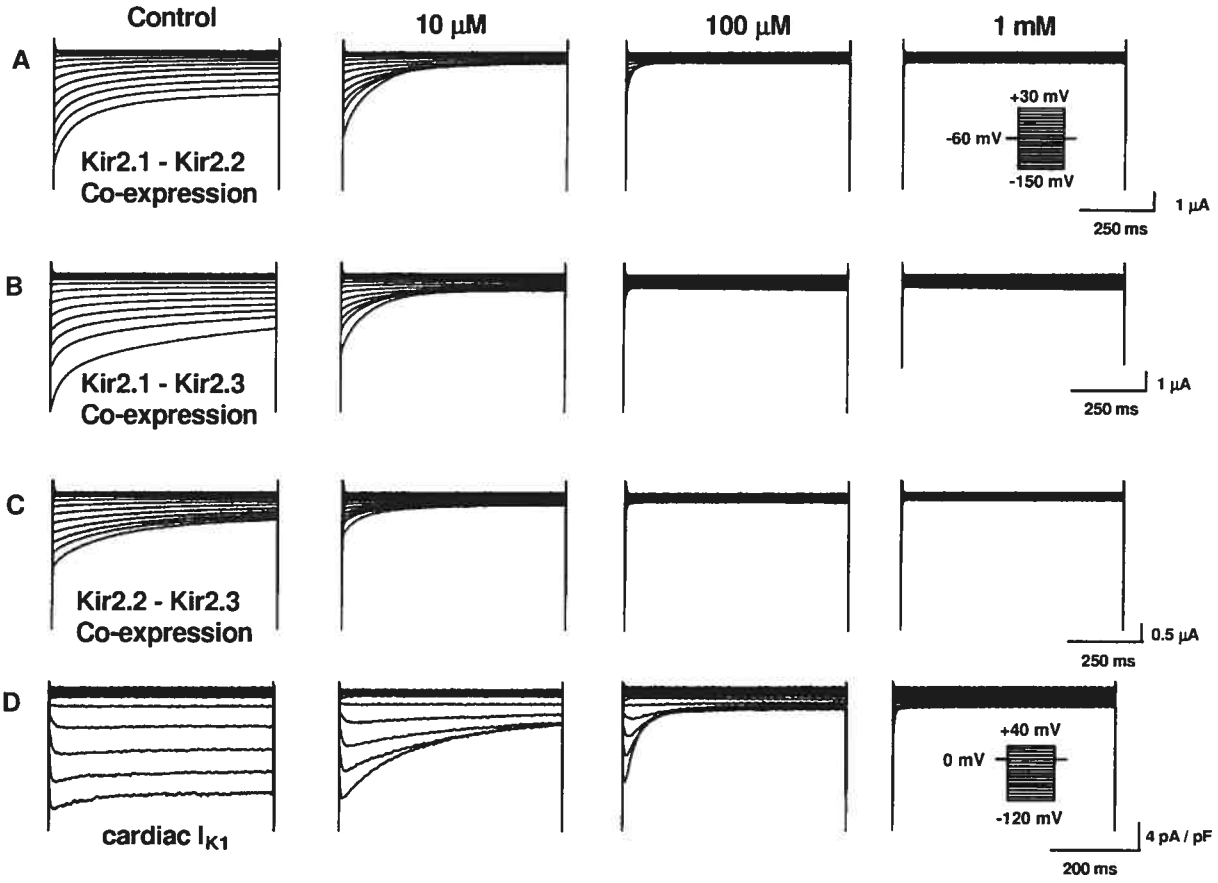

Figure 35: Ba^{2+} block of Kir2.x/Kir2.y heteromers and cardiac I_{K1}, original current recordings.

Original current recordings obtained from oocytes co-injected with Kir2.1/Kir2.2 (**A**), Kir2.1/Kir2.3 (**B**) or Kir2.2/2.3 (**C**) and from a human right ventricular myocyte (**D**) under control conditions (left panels) and in the presence of 10 µM (left middle panels), 100 µM (right middle panels) and 1 mM (right panels) Ba^{2+}. Kir2 currents were elicited by voltage steps from a holding potential of -60 mV to step potentials between -150 mV and +30 mV in 10 mV increments, as shown by the voltage protocol in the inset. I_{K1} was elicited by voltage steps from a holding potential of 0 mV to test potentials between -120 mV and +40 mV in 10 mV increments, as shown by the voltage protocol in the inset.

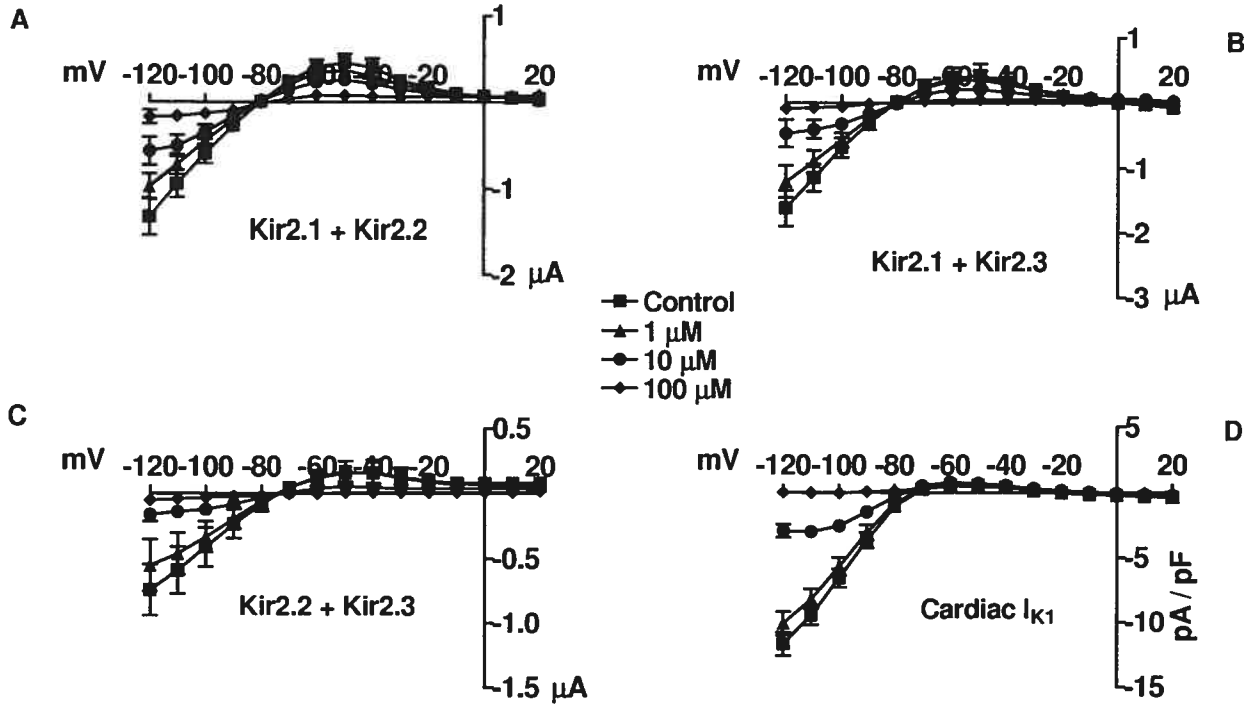

Figure 36: Ba^{2+} block of Kir2.x/Kir2.y heteromers and cardiac I_{K1}, mean±S.E.M current-voltage relations.

Mean±S.E.M current-voltage relations under steady-state conditions without drug (control, squares) and in the presence of 1, 10 and 100 µM Ba^{2+} (triangles, circles and diamonds, respectively). n=7, 6, 4 and 10 cells for Kir2.1 / Kir2.2 (**A**), Kir2.1 / Kir2.3 (**B**), Kir2.2 / Kir2.3 (**C**) and cardiac I_{K1} (**D**).

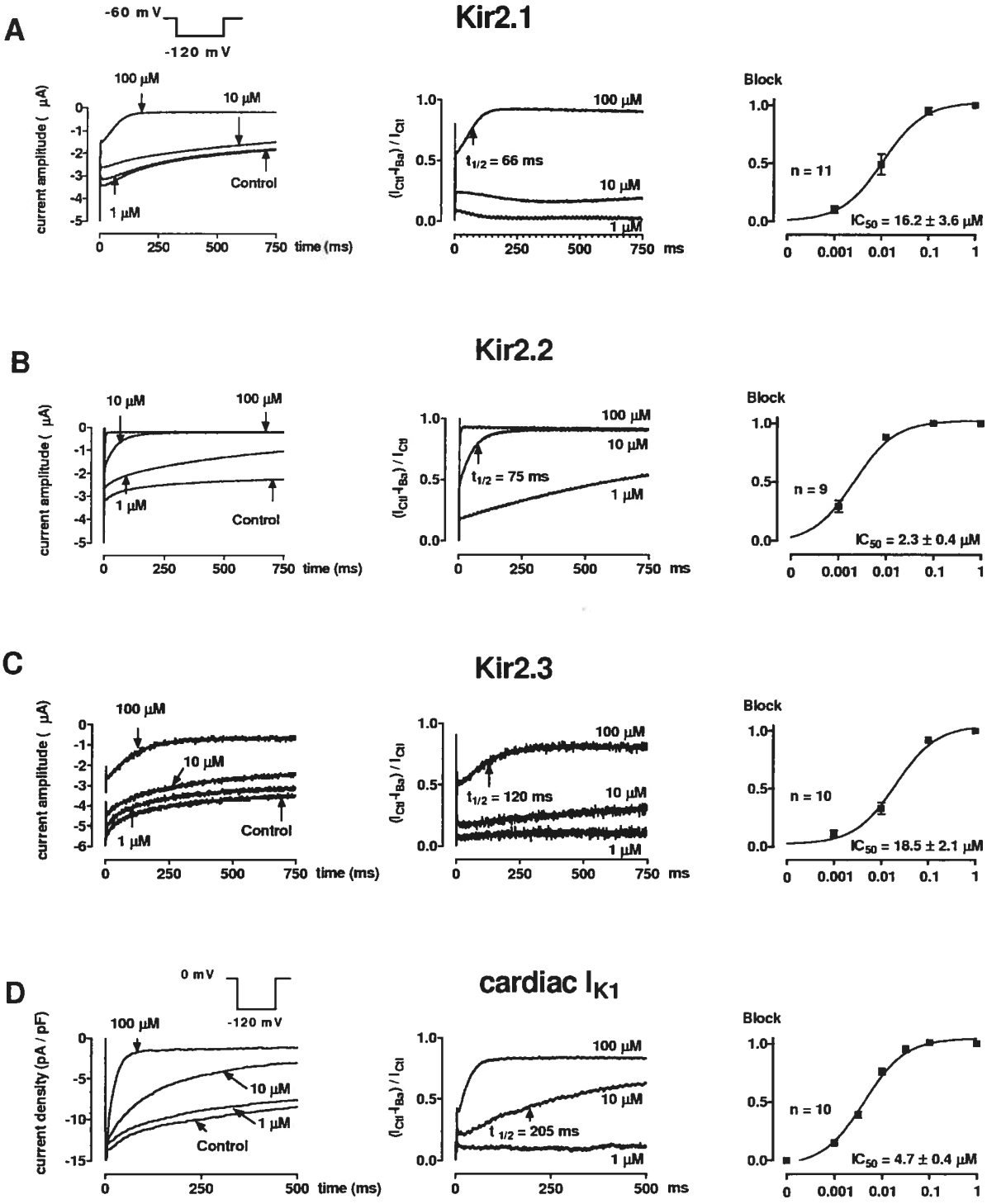
A
-60 mV
-120 mV
Kir2.1
100 µM
10 µM
1 µM
Control
current amplitude (µA)
time (ms)
$t_{1/2}$ = 66 ms
$(I_{Ctl}-I_{Ba})/I_{Ctl}$
ms
Block
n = 11
IC_{50} = 16.2 ± 3.6 µM
B
Kir2.2
$t_{1/2}$ = 75 ms
n = 9
IC_{50} = 2.3 ± 0.4 µM
C
Kir2.3
$t_{1/2}$ = 120 ms
n = 10
IC_{50} = 18.5 ± 2.1 µM
D
0 mV
-120 mV
current density (pA / pF)
cardiac I_{K1}
$t_{1/2}$ = 205 ms
n = 10
IC_{50} = 4.7 ± 0.4 µM

Figure 37: Kinetics of Ba^{2+} block of Kir2.1, Kir.2.2, Kir2.3 and cardiac I_{K1}.

Ba^{2+}-block of currents resulting from the expression of Kir2.1 (A), Kir2.2 (B), Kir2.3 (C) and human ventricular I_{K1} (D). Left panels show original recordings obtained from one oocyte under control conditions and in the presence of 1, 10 and 100 μM Ba^{2+}. Currents were elicited by steps from a holding potential of -60 mV to -120 mV in oocytes and by steps from 0 mV to -120 mV in myocytes, as shown in the protocols in the insets. Kinetics of Ba^{2+} block in the same oocyte or myocyte, respectively, are shown as fractional block in the middle panels. Fractional block was calculated as control current (I_{Ctl}) minus current in the presence of Ba^{2+} (I_{Ba}) divided by control current ($[I_{Ctl} - I_{Ba}]/ I_{Ctl}$). The positions of the $t_{½}$s for each example are shown by arrows. The right panels show corresponding mean±S.E.M concentration-response curves based on end-pulse block at each concentration upon hyperpolarization to -120 mV (n=11, 9, 10 and 10 cells for Kir2.1, Kir2.2, Kir2.3 and cardiac I_{K1} respectively).

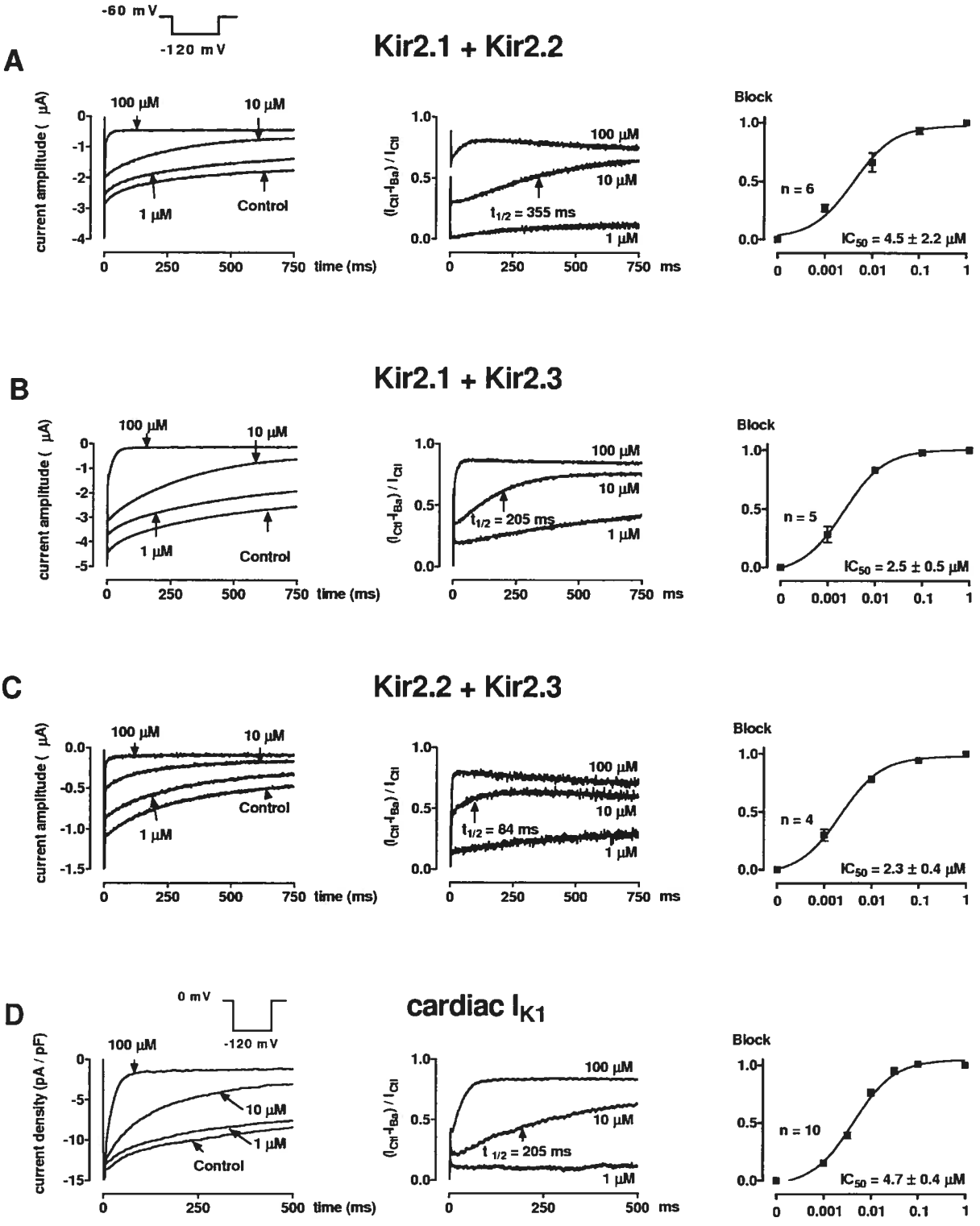
A
-60 mV
-120 mV
Kir2.1 + Kir2.2
current amplitude (µA)
100 µM
10 µM
1 µM
Control
time (ms)
(I_Ctl-I_Ba) / I_Ctl
t1/2 = 355 ms
ms
Block
n = 6
IC50 = 4.5 ± 2.2 µM
B
Kir2.1 + Kir2.3
t1/2 = 205 ms
n = 5
IC50 = 2.5 ± 0.5 µM
C
Kir2.2 + Kir2.3
t1/2 = 84 ms
n = 4
IC50 = 2.3 ± 0.4 µM
D
0 mV
-120 mV
current density (pA / pF)
cardiac IK1
t 1/2 = 205 ms
n = 10
IC50 = 4.7 ± 0.4 µM

Figure 38: Kinetics of Ba^{2+} block of Kir2.x/Kir2.y heteromers and cardiac I_{K1}.

Ba^{2+} block of currents resulting from the co-expression of Kir2.1 / Kir2.2 (**A**), Kir2.1 / Kir2.3 (**B**), Kir2.2 / Kir2.3 (**C**) and human ventricular I_{K1} (**D**). Left panels show original recordings obtained from one oocyte under control conditions and in the presence of 1, 10 and 100 μM Ba^{2+}. Currents were elicited by steps from a holding potential of -60 mV to -120 mV in oocytes and by steps from 0 mV to -120 mV in myocytes, as shown in the protocol in the inset. Kinetics of Ba^{2+}-block in the same oocyte or myocyte, respectively, are shown as fractional block in the right panels. Fractional block was calculated as control current (I_{Cl}) minus current in the presence of Ba^{2+} (I_{Ba}) divided by control current ($[I_{Cl} - I_{Ba}]/ I_{Cl}$). The positions of the $t_{½}$s are indicated by arrows in the middle panels. The right panels show corresponding mean±S.E.M. concentration-response curves based on end-pulse block at each concentration upon hyperpolarization to -120 mV (n=7, 6, 4 and 10 cells for Kir2.1, Kir2.2, Kir2.3 and cardiac I_{K1} respectively).

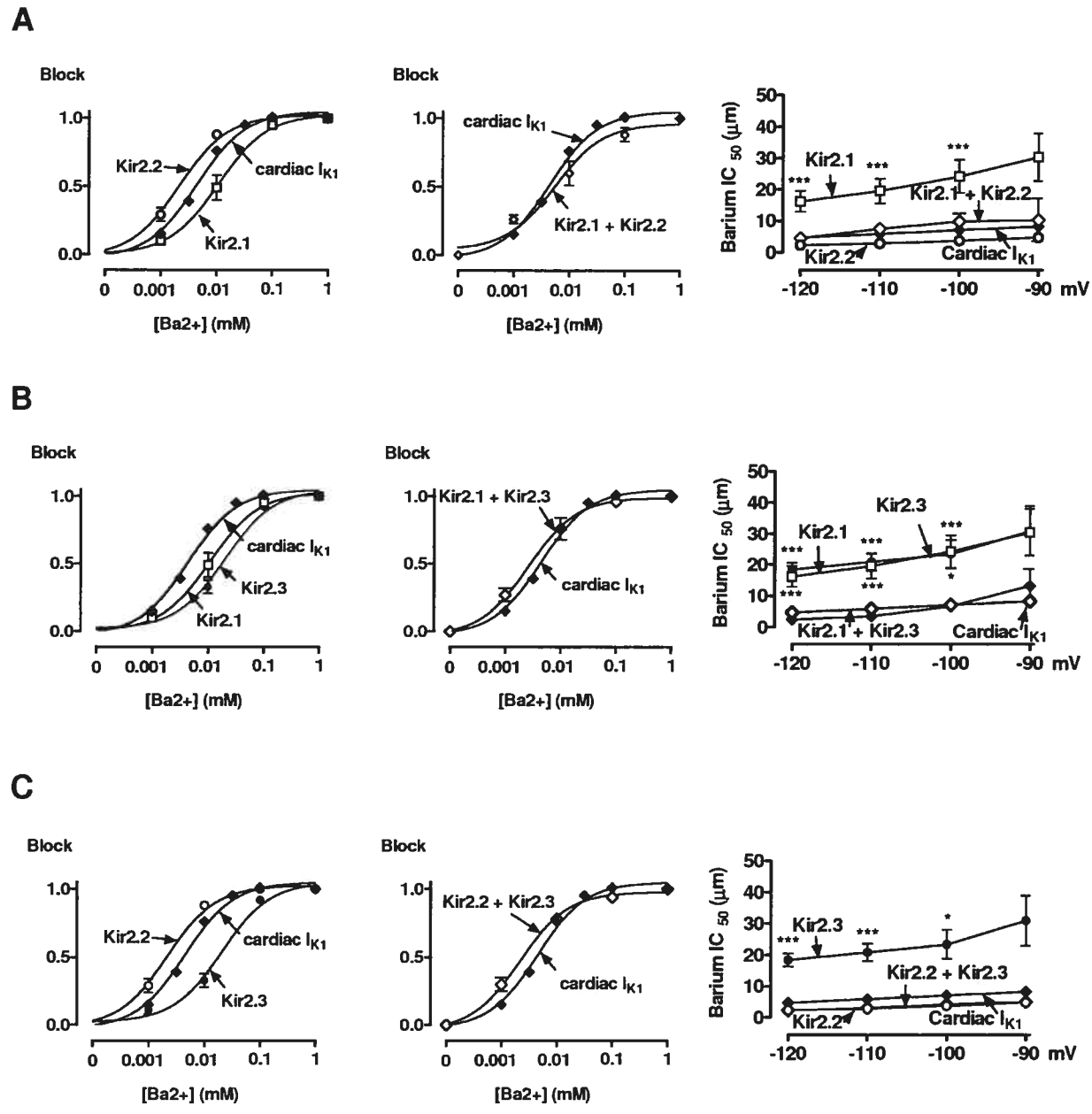
A
Block
1.0
0.5
0.0
Kir2.2
cardiac I_{K1}
Kir2.1
0 0.001 0.01 0.1 1
[Ba2+] (mM)
Block
cardiac I_{K1}
Kir2.1 + Kir2.2
[Ba2+] (mM)
Barium IC_{50} (μm)
50
40
30
20
10
0
Kir2.1
Kir2.1 + Kir2.2
Kir2.2
Cardiac I_{K1}
-120 -110 -100 -90 mV
B
Block
Kir2.3
[Ba2+] (mM)
Block
Kir2.1 + Kir2.3
[Ba2+] (mM)
Kir2.1 + Kir2.3
C
Block
Kir2.3
[Ba2+] (mM)
Block
Kir2.2 + Kir2.3
[Ba2+] (mM)

Figure 39: Comparison of mean±S.E.M. concentration-response curves based on end-pulse block at each concentration at a test potential of -120 mV.

Left panels compare Ba^{2+} block of currents carried by homomeric Kir2 channels with cardiac I_{K1}. Heteromeric channels composed of subunits shown in left panels are compared to cardiac I_{K1} in the middle panels. Right panels: comparison of homomeric and heteromeric Kir2 and cardiac I_{K1} mean Ba^{2+} IC_{50}s at test potentials between -120 mV and -90 mV. $*P<0.05$, $**P<0.01$, $***P<0.001$ versus cardiac I_{K1} at the same voltage.

A, left panels: Kir2.1, Kir2.2 and cardiac I_{K1} (open squares, open circles and filled diamonds, respectively; n=11, 9 and 10 cells for Kir2.1, Kir2.2 and cardiac I_{K1}). Middle panels: Kir2.1 / Kir2.2 (open diamonds, n=7) and cardiac I_{K1} (filled diamonds; n=10).

B, left panels: Kir2.1 (open squares, n=11), Kir2.3 (filled circles, n=10) and cardiac I_{K1} (filled diamonds, n=10). Middle panels: Kir2.1 / Kir2.3 (open diamonds, n=6) and cardiac I_{K1} (filled diamonds, n=10).

C, left panels: Kir2.2 (open circles, n=9), Kir2.3 (filled circles, n=10) and cardiac I_{K1} (filled diamonds, n=10). Middle panels: Kir2.2 / Kir2.3 (open diamonds, n=4) and cardiac I_{K1} (filled diamonds, n=10).

CHAPTER X: FUNCTIONAL EXPRESSION OF KIR2.X IN HUMAN AORTIC ENDOTHELIAL CELLS: THE DOMINANT ROLE OF KIR2.2.

Reprinted from The American Journal of Physiology Cell Physiology, 289, Fang Y., Schram G., Romanenko V., Shi C., Vandenberg CA., Davies PF., Nattel S., Levitan I., Functional expression of Kir2.x in human aortic endothelial cells: the dominant role of Kir2.2, C1134-C1144, 2005.

Functional expression of Kir2.x in human aortic endothelial cells: the dominant role of Kir2.2

Yun Fang[1], Gernot Schram[2], Victor Romanenko[1], Congzhu Shi[1], Lisa Conti[3], Carol A. Vandenberg[3], Peter F. Davies[1], Stanley Nattel[2] and Irena Levitan[1]

[1]Institute for Medicine and Engineering and Department of Pathology and Laboratory Medicine,
University of Pennsylvania, Philadelphia, PA 19104
[2]Department of Medicine, Montreal Heart Institute, and University of Montreal, Montreal, PQ, Canada
[3]Department of Molecular, Cellular and Developmental Biology, and Neuroscience Research Institute, University of California, Santa Barbara, CA 93106.

Short title: Molecular identity of Kir in HAECs

Corresponding author:
Irena Levitan
University of Pennsylvania, IME
1160 Vagelos Research Labs
3340 Smith Walk, Philadelphia, PA 19104
tel: 215-573-8161, fax: 215-573-6815
e-mail: [redacted]

X-1 Abstract

Inwardly-rectifying K^+ (Kir) channels are a significant determinant of endothelial-cell membrane potential, which plays an important role in endothelium-dependent vasodilatation. Several complementary strategies were applied to determine the Kir2-subunit composition of human aortic endothelial cells (HAECs). Expression levels of Kir2.1, 2.2 and 2.4 mRNAs were similar, whereas Kir2.3 mRNA-expression was significantly weaker. Western blot analysis showed clear Kir2.1 and Kir2.2 protein expression but Kir2.3 protein was undetectable. Functional analysis of endothelial inwardly-rectifying K^+ current demonstrated that: (i) inwardly-rectifying K^+ current sensitivity to Ba^{2+} and pH were consistent with currents determined by Kir2.1 and Kir2.2 but not Kir2.3 and Kir2.4, and (ii) unitary-conductance distributions showed two prominent peaks corresponding to known unitary conductances of Kir2.1 and Kir2.2 channels with a ratio of approximately 4:6. When HAECs were transfected with dominant negative- (dn-) Kir2.x mutants, endogenous current was reduced ~50% by dn-Kir2.1 and ~85% by dn-Kir2.2, whereas no significant effect was observed with dn-Kir2.3 or dn-Kir2.4. These studies suggest that Kir2.2 and Kir2.1 are primary determinants of endogenous K^+ conductance in HAECs under resting conditions and that Kir2.2 is the dominant conductance in these cells.

Key words: K^+ channels, aortic endothelium, Kir2.2, inward rectifier potassium channel

X-2 Introduction

Vascular endothelial cells constitute the inner lining of blood vessels and are actively involved in the regulation of vascular tone. K^+ channels set the negative resting membrane potential of endothelial cells, providing the driving force for Ca^{2+} influx and regulating Ca^{2+} dependent intracellular signalling [29]. Clamping the membrane potential at a depolarized value or blocking K^+ channels inhibits bradykinin-, acetylcholine- and flow-induced Ca^{2+} influx and NO release [17, 23] as well as flow-induced vasodilatation [47], consistent with the proposed role of K^+ channels in flow-mediated vasorelaxation [4, 12, 31]. Inward rectifier K^+ channels composed of Kir subunits are one of the most prominent types of K^+ channels in endothelial cells, and are believed to be important in maintaining endothelial-cell resting membrane potential [1, 29]. Indeed, several studies have shown that exposing endothelial cells to Ba^{2+}, a known blocker of Kir channels, results in significant membrane depolarization [21, 44, 50]. Conversely, activation of endothelial Kir channels by shear stress produces membrane hyperpolarization, underscoring their potential physiological importance [20, 21, 31]. Physiological significance of Kir channels in the vasculature was further supported by a recent study showing that disruption of the Kir2.1 gene impaired K^+-mediated vasodilatation in genetically engineered mice [51]. Furthermore, we have recently demonstrated that endothelial Kir currents are strongly suppressed by hypercholesterolemia [37] suggesting that these channels may also play a significant role in hypercholesterolemia-induced vasodilatation abnormalities.

Currently, four key Kir2 subunits have been identified (Kir2.1-Kir2.4) in a variety of tissues. Three of these (Kir2.1-Kir2.3) are expressed in cardiac cells [24, 25, 52], vascular smooth muscle cells [14, 51] and neurons [27], whereas expression of Kir2.4 has only been reported in neuronal cells [35, 43]. To date, only Kir2.1 mRNA has been identified in vascular endothelial cells [7, 9, 13, 50]. Here we show that all four Kir2.x channels are expressed in HAECs at the transcript level, but provide evidence suggesting that only Kir2.1 and Kir2.2 contribute significantly to

native endothelial Kir current. Furthermore, our results suggest that Kir2.2 is the dominant K^+ conductance in HAECs under resting conditions.

X-3 Materials and methods

X-3.1 Cell Culture

Human aortic endothelial cells (HAECs) were purchased at passage 2 from BioWhittaker Cambrex (Rutherford, NJ) and maintained between passages 3 and 5 in 2% fetal bovine serum endothelium growth medium-2 (EGM-2, Cambrex). Porcine aortic endothelial cells were freshly harvested from adult pig aortas (Juvenile Yorkshire females), as previously described [32]. Briefly, endothelial cells were gently scraped from a 2-cm^2 region located at the inner wall of descending thoracic aorta and transferred directly to endothelial culture media EGM-2. Cell purity was confirmed by immunostaining with EC-specific antiplatelet-endothelial cell adhesion molecule 1 (PECAM-1, CD31) and anti-von Willebrand Factor (vWF) antibodies. No positive α-SMA (smooth muscle cell specific anti-α-actin antibodies) staining was observed, indicating the absence of contaminating smooth muscle cells.

X-3.2 Electrophysiology

Ionic currents were measured with the whole cell and cell-attached configurations of the standard patch clamp technique. Pipettes were pulled (SG10 glass; Richland Glass, Richland, NJ) to give a final resistance of 3-5 MΩ and generated high resistance seals without fire polishing. A saturated salt agar bridge was used as a reference electrode. Currents were recorded with an EPC9 amplifier (HEKA Electronik, Lambrecht, Germany) and accompanying acquisition and analysis software (Pulse & PulseFit, HEKA Electronik, Lambrecht, Germany) running on a PowerCenter 150 (Mac OS) computer. Pipette and whole-cell capacitance was automatically compensated. Whole-cell capacitance and series resistance were compensated and monitored throughout each recording. Whole-cell current was recorded during 500-ms linear voltage ramps or a series of voltage steps from –160 or –110 mV to +60 mV at an interpulse interval of 5 s. The standard external solution contained (in mM) 150 NaCl, 6 KCl, 10 HEPES, 1.5 $CaCl_2$, 1 $MgCl_2$ and 1 EGTA, pH 7.3. In some experiments, 156, 96, or 60 mM extracellular KCl was used with equimolar substitution of KCl for NaCl to maintain osmolarity.

The pipette contained (in mM) 145 KCl, 10 HEPES, 1 $MgCl_2$, 1 EGTA, and 4 ATP, pH 7.3. For cell-attached configuration, single-channel recordings were obtained in 1.6-s sweeps with a 0.1-ms sampling interval and filtered at 500 Hz. Bath and pipette solutions for single-channel recordings contained (in mM): 156 KCl, 10 HEPES, 1.5 $CaCl_2$, 1 $MgCl_2$, and 1 EGTA, pH 7.3. All experiments were performed at room temperature (22-25°C).

X-3.3 RNA Isolation and RT-PCR

Total RNA was extracted using the Absolutely RNA™ Miniprep Kit (Stratagene, La Jolla, CA). Highly-purified total RNA was treated with DNAse I to remove traces of genomic DNA. The integrity and quantity of RNA were evaluated with an Agilent 2100 Bioanalyzer and the RNA 600 Nano Chips assay kit (Agilent Technologies, Waldbronn, Germany). cDNA was generated using Superscript II reverse transcription reagents (Invitrogen, Carlsbad, CA) with oligo (dT) primers. PCR primers (Table XI) were designed based on known human Kir2.1 (Genbank Accession # U12507), Kir2.2 (Accession # AB074970), Kir2.3 (Accession # U07364 & # U24056) and Kir2.4 (Accession # AF081466) sequences with Oligo Primer Analysis Software (Molecular Biology Insights, Inc., Cascade, CO). Primer specificity was confirmed by BLAST search. PCR was performed for 35 cycles consisting of: denaturation (98°C), annealing (60°C), and extension (72°C).

X-3.4 Quantitative Real-Time PCR (QRT-PCR)

Quantitative real-time PCR (QRT-PCR) was performed using the FastStart DNA Master SYBR Green I Kit and the LightCycler® System (Roche Applied Science, Indianapolis, IN). Mg^{2+} concentration, annealing temperature and primer concentration were optimized for each gene according to the manufacturer's instructions. To distinguish specific amplicons from non-specific amplifications, a melting (dissociation) curve for amplicons was generated. Melting curve analysis of Kir2.x amplicons resulted in a single peak indicating the formation of a single amplicon for each targeted gene and the lack of primer-dimer formation. Standard curves were generated with serial dilutions of known cDNA copy number for each gene in order to determine the copy number in the experimental sample. The standard

curves were log-linear for at least four orders of magnitude (10^2-10^6 copies). To measure relative abundance of Kir2.x mRNA in HAECs, cDNAs were synthesized from 1.5 μg total RNA in a 20 μl reaction. 0.1 μl of the cDNA reaction was used in 20 μl QRT-PCR reactions under optimized conditions. RNA extraction and cDNA synthesis, followed by QRT-PCR, were performed for all targeted Kir2.x genes in each of 4 biological samples. Each QRT-PCR measurement was performed in triplicate.

X-3.5 Immunoblotting

For preparation of total membrane (TM) samples, cells were scraped into Buffer A (in mM): 150 NaCl, 20 HEPES, 5 EDTA, pH 7.4, Protease Inhibitor Cocktail (PIC), 1 μg/ml pepstatin; homogenized in a Dounce tissue grinder and centrifuged for 10 min at 1,000 g. The pellet was resuspended in Buffer A, homogenized, and re-centrifuged for 10 min at 1,000 g. The combined supernatant was centrifuged for 1 h at 200,000 g (SW40Ti rotor, Beckman). The pellet was resuspended in Laemmli buffer and sonicated. Sample protein was measured using BCA Protein Assay Kit (BioRad). Proteins were resolved with 12% SDS PAGE at reducing conditions followed by transfer to PVDF membranes (Amersham). Channel-specific rabbit anti-peptide antibodies to Kir2.1 (rat amino acids 390-411), Kir2.2 (rat amino acids 390-410) and Kir2.3 (human amino acids 2-19) were prepared and purified by affinity chomatography or Protein A chromatography as previously described for Kir2.2 [36]. The membranes were probed with anti-Kir2.1 (1:1000), anti-Kir2.2 (1:250), and anti-Kir2.3 (1:1000), with dilutions optimized by probing CHO cells over-expressing Kir2.x subunits. Kir2.x-specific bands were detected using secondary antibodies conjugated with Horseradish Peroxidase (Jackson Laboratories). Finally, immunoreactivity was visualized with ECL Plus reagent (Amersham). The specificity of the antibodies was tested by transfecting COS-1 cells with Kir2.x constructs and harvesting the cells 2 days after transfection as previously described [19]. Samples were run on 10% SDS-PAGE, transferred to nitrocellulose, and probed with affinity- or Protein A purified-antibodies (1:250) to Kir2.1, Kir2.2,

or Kir2.3, followed by probing with secondary antibodies conjugated to horseradish peroxidase, and visualized with Supersignal West Dura (Pierce).

X-3.6 Construction and functional Assessment of Dominant Negative (dn) Kir2.x Constructs

Dominant negative (dn)Kir2.x subunits were engineered by replacing the GYG motif of the selectivity filter by 3 alanine residues (AAA). A 5' and a 3' fragment were generated by PCR (Elongase® Amplification System, Invitrogen) and combined by overlap extension. The resulting constructs were cloned into pCRII®-TOPO® (Invitrogen) and verified by sequencing. (Dn)Kir2.x constructs were subcloned into the bicistronic mammalian cell expression vector pIRES2-EGFP (CLONTECH laboratories, Inc.). Kir2.2/pCRII and Kir2.4/pSGEM were kind gifts from Barbara Wible, (Case Western Reserve University, Cleveland, Ohio) and Andreas Karschin (University of Göttingen, Germany) respectively. Kir2.3/BluescriptSK was previously described [33]. Kir2.x and dn-Kir2.x cRNA was generated using the mMESSAGE mMACHINE kit (Ambion Inc., Austin, Texas). Functionality of dn-Kir2.x constructs was verified by co-expression of Kir2.x-WT with the respective dn-Kir2.x-WT in *Xenopus* oocytes as previously described in detail [40].

X-3.7 Transfection

CHO cells and HAECs were transfected with wild-type or dn-Kir2.x constructs using Lipofectamine (Gibco-BRL) according to the manufacturer's instructions. Electrophysiological recording and Western blotting were performed 24h after transfection.

X-3.8 Data Analysis

Statistical analyses of the data were performed using a standard two-sample Student's t test assuming unequal variances of the two data sets. Statistical significance was determined using a two-tail distribution assumption and was set at 5% ($p<0.05$). The time-constants of voltage-dependent inactivation were measured by fitting a single exponential function $V(t)=Ae^{-t/\tau}$ where A is current amplitude and τ is

the time constant. The fits were obtained with the Levenberg-Marquardt algorithm using PulseFit software (HEKA Electronik, Lambrecht, Germany). Single-channel events were analyzed with TAC software (Braxton, Seattle, WA). The frequency distribution of single channel conductance was fitted by a weighted sum of two Gaussians (bimodal distribution) assuming unequal means and equal variance using Origin 6.0 software (Microcal Software, Inc. MA).

X-4 Results

X-4.1 Membrane Conductance in HAECs is dominated by strong Inwardly-Rectifying K^+ Current

Under resting conditions, 85% of HAECs showed a pronounced inwardly-rectifying K^+ current with significant inward currents at voltages below the reversal potential and small outward currents at voltages above the reversal potential (Fig. 40A). The reversal potential averaged -79 ± 2 mV, close to the theoretical reversal potential of a K^+-specific current under these recording conditions (-80 mV). No Ca^{2+} was added to the pipette solution to suppress Ca^{2+}-activated K^+ channels. The strong rectification of the endogenous current in HAECs suggests that it is carried by members of the Kir2 inward-rectifier family [28]. Indeed, the current-voltage (IV) relationship of the endogenous HAEC current appears to be identical to the IV relationship of currents carried by Kir2.x subunits expressed in Chinese hamster ovary cells (CHO), a cell line that has no endogenous inwardly-rectifying K^+ current. Typical current recordings of Kir2.1, Kir2.2, Kir2.3, and Kir2.4 are shown in the inset to Fig. 40A. Each subunit was expressed separately in CHO cells. Endogenous HAEC current shows two typical features of the Kir2 channels: sensitivity to the level of extracellular K^+ (Fig. 40B) and voltage-dependent inactivation at hyperpolarizing voltages (Fig. 40C) [28, 29].

To verify that similar inwardly-rectifying K^+ currents are observed in freshly-isolated native cells, the currents were also recorded from freshly isolated porcine aortic endothelial cells (PAECs) within 1-4 hours after their isolation. Pronounced inwardly-rectifying K^+ currents were recorded in ~76% of PAECs examined, similar to HAECs. Both IV relationships and current densities of K^+ currents in freshly-isolated PAECs were virtually identical to those in HAECs (Fig. 41). Maintaining the cells in culture for 5 passages had no significant effect on Kir current densities or rectification properties (Fig. 41B), supporting the physiological relevance of the HAEC system.

X-4.2 HAEC Kir2.x mRNA Expression.

To determine which Kir2.x transcripts are expressed in HAECs, RT-PCR was performed. For all experiments, the RNA profile revealed two strong 28S and 18S ribosomal peaks, present at an approximate 2:1 ratio, with little tailing and a flat baseline, as expected for high integrity RNA (Fig. 42A). Table XI lists the primer pairs used for RT-PCR of each of the four known Kir2 subunits. Fig. 42Ba shows clear bands of the predicted size for all four Kir2.x PCR products (all primers were designed within the single exon that contains the reading frame of each subunit). No bands were observed when PCR was performed directly on RNA samples (RT-negative controls), indicating that the PCR products were free of contaminating genomic DNA. Note that the band for Kir2.3 is much weaker than the bands for the other three subunits, suggesting weaker Kir2.3 mRNA expression. To exclude further the possibility of genomic contamination, expression of Kir2.1 and Kir2.4 was tested with intron-spanning primers for Kir2.1 and Kir2.4 (Fig. 42Bb). Kir2.2 has no intron, and therefore only non-spanning primers can be designed for this channel. The specific expression of all four Kir2.x subunits in HAECs was confirmed by sequencing of the PCR products. All four PCR products were 99-100% identical to the reported sequences of human Kir2.x.

X-4.3 Relative Abundance of HAEC Kir 2.x mRNA by quantitative Real Time PCR.

Quantitative RT-PCR was utilized to determine the relative expression levels of Kir2.x transcripts in HAECs. The melting curves of all PCR products showed single prominent peaks, indicating the specificity of the primers (Fig. 43A) and a lack of primer-primer dimerization [48]. Fig. 43B shows the PCR amplification standard curves generated with known amounts of Kir2.x cDNAs. In this panel, threshold PCR cycle number was plotted as a function of the Kir2.x cDNA amount, where the threshold cycle is defined as the onset of the log increase in PCR amplification. The relationship between the threshold cycle number and log [concentration] of the Kir2.x cDNA was linear. The standard curves were used to calculate the relative abundance of Kir2.x subunits in HAECs (Fig. 43C). Consistent with the RT-PCR results

presented above, the expression of Kir2.3 was significantly lower than that of the other subunits. The mRNA level of Kir2.2 was higher than that of Kir2.1 in each of the four independent cell-derived samples. These observations suggest that not only Kir2.1 but also other Kir2.x subunits, Kir2.2 in particular, are candidates to contribute substantially to the endogenous inwardly-rectifying K^+ current in HAECs.

X-4.4 Kir2.x Protein Expression in HAECs.

The presence of Kir2.x protein in HAECs was assessed using western blot analysis. Kir2.1, Kir2.2 and Kir2.3 proteins were probed with polyclonal antibodies raised against rat (for 2.1 and 2.2) or human (2.3) Kir2.x subunits [36] (no antibody against Kir2.4 subunit was available). Kir2.x antibodies provided clear bands upon probing COS-1 cells transfected with mouse Kir2.1, rat Kir2.2 or human Kir2.3 subunits (Fig. 44A). Signal was detected only in the lane corresponding to the specific Kir2.x subunit to which the antibody was designed, and no signal was present in lanes containing other Kir2.x subunits or with non-transfected COS-1 cells, demonstrating the specificity of these antibodies for individual Kir2.x subunits. Similar bands were also observed upon probing CHO cells transfected with mouse Kir2.1 or Kir2.2 subunits or human Kir2.3 subunits (Fig. 44B) but no signal with non-transfected CHO cells pointing to antibody specificity. CHO cells transfected with Kir2.x subunits presented prominent bands at approximately 50 kDa (MW for Kir2.1, Kir2.2, and Kir2.3 subunits predicted from their primary structures are 48, 49 and 49.5 kDa respectively). Probing of HAECs showed corresponding bands for Kir2.1 and Kir2.2 subunits but not for Kir2.3 subunit (Fig. 44B). The molecular weights of Kir2.1 and Kir2.2 in HAECs were similar to mouse Kir2.1 and Kir2.2 expressed in CHO cells. The specificity of the Kir2.2 band was further confirmed by blocking the antibody with the antigen [36]. In addition, a larger band (~65-70 kDa) was observed in some experiments for Kir2.2 subunits. The latter observation is consistent with an earlier study showing that Kir2.2 isolated from rat brain presented a band at approximately 64 kDa (36). A lack of a Kir2.3 band in HAECs suggests that the channel is either not expressed at the protein level or that its expression is

below the detection limit of the antibodies. Indeed, this is consistent with the low level of Kir2.3 mRNA expression.

X-4.5 Sensitivity of endothelial Inwardly-Rectifying K^+ Current to Ba^{2+} Block and to pH.

Differences in sensitivity of Kir2.x currents to extracellular Ba^{2+} and pH provided a valuable assay to further distinguish among Kir2.x subunit contributions to endogenous HAEC currents. All Kir2.x currents are blocked by extracellular Ba^{2+}, but while the sensitivities of Kir2.1, Kir2.2 and Kir2.3 are known to overlap [22, 34, 41], currents carried by Kir2.4 subunits have significantly lower Ba^{2+} sensitivity than other Kir2.x subunits: the IC_{50}s of Kir2.1-Kir 2.3 range between 3-16 μM for Kir2.1, 0.5-2.3 μM for Kir2.2, and 10-18.5 μM for Kir 2.3, whereas the IC50 of Kir2.4 is more than 200 μM at voltages -100 to -120 mV [22, 40, 41]. It is also important to note that Ba^{2+} sensitivity of Kir2.x channels may depend on the extracellular K^+ concentration [22, 40, 41]. In this study, Ba^{2+} sensitivity was determined at 60 mM extracellular K^+, under which conditions the IC_{50} values for Ba^{2+} block were 3.2, 0.5, 10.3 and 235 μM for Kir2.1, Kir2.2, Kir2.3 and Kir2.4 respectively [22]. Our data show that the IC_{50} for Ba^{2+} block of the endogenous inwardly-rectifying K^+ current in HAECs at –100 mV was 3.2 μM, whereas above 100 μM Ba^{2+} there was virtually no current (Fig. 45A&B). Since homotetrameric Kir2.4 channels are known to be only slightly inhibited by 100 μM Ba^{2+} [15], these observations suggest that homotetrameric Kir2.4 does not contribute significantly to native inwardly-rectifying K^+ current in HAECs.

Consistent with an earlier study of inwardly-rectifying K^+ current in bovine endothelial cells [13], endogenous inwardly-rectifying K^+ current in HAECs is not sensitive to extracellular pH (Fig. 45C). Since both Kir2.3 and Kir2.4 currents show strong sigmoidal dependence on pH with the currents being inhibited at low extracellular pH and enhanced at high pH [3, 11], a lack of pH sensitivity of the endogenous currents in HAECs suggests that neither Kir2.4 nor Kir2.3 contribute significantly to the whole-cell inwardly-rectifying K^+ current in HAECs as homotetramers. Therefore, on the basis of low transcript and undetectable protein

expression (for Kir2.3), a lack of pH sensitivity, and the range of Ba^{2+} sensitivity of the current, we conclude that the contribution of Kir2.3 and Kir2.4 homotetrameric channels to the endogenous current in HAECs is negligible. These observations, of course, do not exclude the possibility that Kir2.3 and/or Kir2.4 subunits may form functional heterotetramers with Kir2.1 and/or Kir2.2.

X-4.6 Distribution of Kir Unitary Conductance.

To further assess which Kir2.x channels constitute the endogenous inwardly rectifying potassium conductance in HAECs, unitary conductance was evaluated using single-channel analysis. The typical values of Kir2.x unitary conductances are 20-30 pS for Kir2.1, 35-40 pS for Kir2.2, 10-15 pS for Kir2.3, and 14-15 pS for Kir2.4 respectively [16, 22, 26, 33, 42, 43]. In HAECs, 90% of the channels had unitary conductances between ~20 and 45 pS (Fig. 46), as would be expected if only Kir2.1 and Kir2.2 channels contribute significantly to the whole cell endogenous inwardly-rectifying K^+ currents in these cells. Furthermore, there appear to be two distinct peaks in the distribution of the unitary conductances, one with a mean at 25 pS and another at 35 pS (Fig. 46B), supporting the notion that both Kir2.1 and Kir2.2 contribute to the endogenous inwardly-rectifying K^+ current in HAECs. It is also noteworthy that the peak at 35 pS is more prominent, suggesting that Kir2.2 is the major Kir2.x channel in HAECs. The ratio between the integrals for the major and the minor histogram peaks is 1.58, suggesting that Kir2.1 channels constitute approximately 40% and Kir2.2 constitute 60% of the channel population. A double-peak histogram of unitary conductances, however, does not exclude the possibility that multiple channel populations contribute to the endogenous Kir current in HAECs. This possibility is addressed further using dominant-negative Kir2.x constructs.

X-4.7 Inhibition of endogenous Inwardly-Rectifying K^+ Current by dn-Kir2.x.

Specific inhibition of currents in HAECs by dominant negative Kir2.x subunits was utilized to further discriminate between channel subunits that underlie the endogenous currents. dn-Kir2.x constructs were generated by replacing the GYG region of the pore by AAA, a substitution known to prevent ion throughput [34, 40].

The efficiency of the constructs was tested by coinjecting dn-Kir2.x RNA with the respective Kir2.x wild type into *Xenopus* oocytes. All four Kir2.x were efficiently inhibited by the appropriate dn-Kir2.x (Fig. 47). To evaluate the relative contributions of Kir2.x channels to the endogenous inwardly-rectifying K^+ in HAECs, cells were transfected with dn-Kir2.x constructs, one at a time, subcloned into a bi-cistronic vector containing an EGFP fluorescent marker. This system allowed much higher fidelity for the identification of successfully transfected cells than standard co-transfection procedures and by subcloning the constructs into the bi-cistronic vector, complications inherent in tagging GFP to the molecule of interest were minimized. To avoid possible non-specific effects of over-expression, only cells with moderate fluorescence were used for current recordings. Transfection of HAECs with the EGFP marker alone had no effect on inwardly-rectifying K^+ current. However, transfecting the cells with dn-Kir2.1 and dn-Kir2.2 significantly inhibited native Kir current. It is also noteworthy that the effect of dn-Kir2.2 was significantly stronger than that of dn-Kir2.1 (Fig. 48A,B). In contrast to dn-Kir2.1 and dn-Kir2.2, no significant effects were elicited by dn-Kir2.3 and dn-Kir2.4 (Fig. 48A,B). These observations are consistent with assignment of the major Kir conductances to Kir2.1 and Kir2.2 based on the double peak histogram of Kir unitary conductances as well as with the dominance of Kir2.2. The lack of dominant negative effects of dn-Kir2.3 and dn-Kir2.4 suggests that Kir2.3 and Kir2.4 subunits do not contribute significantly to functional Kir channels in HAECs.

Since dn-Kir2.1 only partially inhibited the macroscopic currents in HAECs, it was possible to extend the analysis to the single-channel level, and investigate whether one or both peaks of unitary conductances were specifically affected by dn-Kir2.1. When dn-Kir2.1 constructs were expressed in HAECs, we observed a shift in the distribution of unitary conductance of endothelial Kir channels, so that under these conditions the histogram presented a single peak at 35 pS corresponding to the unitary conductance of Kir2.2, whereas the minor peak at 25 pS, whose unitary conductance corresponded to Kir2.1 channels, was absent (Fig. 48C). These observations support the hypothesis that HAECs express two distinct populations of Kir2.x channels.

X-5 Discussion:

In this study we performed a detailed analysis of the molecular identity of inwardly-rectifying K^+ channels in HAECs. The general biophysical characteristics of whole-cell inwardly-rectifying K^+ current in HAECs are similar to those reported earlier in other types of endothelial cells [9, 13]. Here, however, we show that HAECs express not only Kir2.1 mRNA as previously described [7] [9, 13, 50], but also Kir2.2, 2.3 and 2.4 mRNA. Furthermore, analyses of biochemical and pharmacological properties of whole cell HAEC Kir current as well as of biophysical properties of single-channel events suggest that Kir2.2 contributes prominently and that Kir2.1 provides a significant but smaller contribution to endogenous HAEC current. Kir2.3 and Kir2.4 on the other hand do not appear of physiological importance in HAECs. Consistent with these observations, a dominant negative Kir2.2 construct strongly suppressed endogenous inwardly-rectifying K^+ currents in HAECs, whereas a dominant negative Kir2.1 construct had a smaller effect. Dn-constructs of Kir2.3 and Kir2.4 had no significant effect on HAEC Kir current. Together, these observations suggest that Kir2.2 channels provide the primary K^+ conductance in HAECs under resting conditions.

X-5.1 Consideration of the System

Low-passage HAECs as used in this study appear to be the best available cell model to investigate inwardly-rectifying K^+ currents in human aortic endothelium. Although it was reported earlier that aortic endothelial cells freshly isolated from mouse or from rabbit aortas lack inwardly-rectifying K^+ channels [39], we show here that inwardly-rectifying K^+ currents are clearly active in freshly isolated PAECs. Furthermore, inwardly-rectifying K^+ currents in low-passage PAECs were similar to those in freshly-isolated cells. Thus, the fraction of cells that express inwardly-rectifying K^+ currents (~80%) and the average current density of the current are similar in low-passage HAECs, low-passage PAECs and freshly isolated PAECs, supporting the relevance of the low-passage HAEC system. The difference between the endothelial cells isolated from mouse, rabbit or pig aorta could be due to inter-species differences in Kir expression or due to different isolation protocols. Inter-

species differences in cardiac Kir-subunit expression are well recognized [24, 5]. It is not surprising that inwardly-rectifying K^+ currents in HAECs and in PAECs are more similar than inwardly-rectifying K^+ currents in mouse or rabbit endothelium because it is generally accepted that pig vasculature is more similar to human than that of mice or rabbits. Kir expression appears to vary in different types of endothelial cells. Nilius & Schwarz showed that only a fraction of endothelial cells freshly isolated from human umbilical vein express inwardly-rectifying K^+ currents [30] and Himmel et al. showed that microvascular endothelial cells from human omentum lack inwardly-rectifying K^+ current [10]. In contrast, freshly isolated coronary endothelial cells show pronounced inwardly-rectifying K^+ current with a unitary conductance similar to that observed in aortic endothelium [45]. It is also possible that the expression profiles of Kir channels are modified under different physiological or pathological conditions. Thus, it is important to take into account both the differences among species and between endothelial cells isolated from different vascular beds when comparing the properties of endothelial inwardly-rectifying K^+ channels.

X-5.2 Molecular Diversity of Kir2-based Native Currents

In HAECs, the molecular diversity of Kir2 subunits at the transcript level is higher than the diversity of functional inwardly-rectifying K^+ channels. While for Kir2.3 this discrepancy could be explained by undetectable level of protein expression due to very low transcription, the transcript level of Kir2.4 is similar to that of Kir2.1 suggesting that Kir2.4 functional expression is regulated at a posttranscriptional level. A discrepancy between the heterogeneity of K^+ channels at transcript and at functional levels has been reported earlier for Kir2.x channels in human myoblasts [8] and for voltage-gated K^+ channels in rat cardiomyocytes [2, 49] and it has been proposed that translational/posttranslational steps may contribute a rate-limiting step to channel expression [38]. Protein expression of Kir2.x subunits in HAECs is consistent with the functional expression of the channels.

The peak Kir unitary conductances in HAECs (25 and 35 pS) are similar to previously-reported values in human umbilical vein endothelial cells (29 pS) and in bovine aortic and pulmonary artery endothelial cells (30-42 pS) [13, 29, 30, 37]. We

observed a dual-peak distribution of Kir unitary conductances in HAECs. A similar distribution with an additional peak at a lower value (34 pS, 24 pS and 11 pS) was reported in guinea pig cardiac myocytes [22]. These peak values are consistent with the unitary conductances of Kir2.2, Kir2.1 and Kir2.3 expressed in *Xenopus* oocytes (34-36 pS, 21 pS, and 8-15 pS respectively) [16, 33, 42].The exact values of Kir2.x unitary conductances can vary among cell types but an ~ 10 pS difference between Kir2.1 and Kir2.2 is maintained. For example, Kir 2.1 and Kir 2.2 have conductances of 21 pS and 28 pS respectively when expressed in human myoblasts [8] and 31 pS and 42 pS respectively when expressed in HEK293 cells (human embryonic kidney cells [22]). These variations have been attributed to possible binding of an intracellular ligand [22]. We propose that the observed bimodal distribution of unitary conductances suggests that both Kir2.1 and Kir2.2 contribute to the endogenous inwardly-rectifying K^+ current in HAECs. Taking into account the difference in unitary conductances between both channels, Kir2.2 appears to be the dominant conductance, contributing ~70% of the whole cell K^+ current. These ideas are supported by the observation that dn-Kir2.1 suppressed only the lower-conductance portion of the single-channel current histogram.

Dissecting the contributions of different Kir2.x subunits to the endogenous inwardly-rectifying K^+ current with dn-Kir 2.x constructs further supports the hypothesis that both Kir2.1 and Kir2.2 are the main constituents of endothelial inwardly-rectifying K^+ with Kir2.2 having the dominant role. Earlier studies showed that co-expression of wild type and dn-Kir2.x subunits resulted in formation of Kir2.x heterotetramers [34, 40]. Furthermore, Zobel et al. [52] demonstrated that both dn-Kir2.1 and dn-Kir2.2 inhibited endogenous inwardly-rectifying K^+ current in myocytes by more that 50%, suggesting formation of heterotetramers between dn-Kir2.x and endogenous Kir2.x subunits. Consistent with these findings, our data show that the sum of current inhibition by dn-Kir2.x in HAECs (dn-Kir2.2 ~85% and dn-Kir2.1 ~50%) produces a value greater than 1, implying possible heteromultimerization of native Kir2.x subunits. It is important to note, however, that heteromultimerization between over-expressed dn-Kirs and native Kirs does not necessarily mean that native Kirs form heterotetramers. As was pointed out by Zobel

et al. [52], if a significant proportion of endogenous Kir channels were Kir2.1-Kir2.2 heterotetramers, then dn-Kir2.1 and dn-Kir2.2 would be expected to equally inhibit endogenous Kir. That was indeed the case for rabbit cardiomyocytes, but in HAECs dn-Kir2.1 had a weaker effect than dn-Kir2.2.

X-5.3 Potential Significance of our Findings

Multiple Kir2.x subunits are expressed in individual cells of several types, including cardiomyocytes [22, 46] and smooth muscle cells [14]. It is noteworthy that since Kir2.x subunits have differential sensitivities to several modulatory systems, such as those related to protein kinase C [15], G-protein coupled receptors [6], and chaperone molecules [18, 19], the expression pattern of multiple Kir2.x subunits may underlie differences in tissue electrophysiological properties. Indeed, differential expression of multiple Kir2.x in atrial vs. ventricular myocytes was suggested to account for different resting potentials and excitability properties between the two heart tissues [15] and it was suggested that changes in Kir2.x expression profile may be important for plasticity of electrophysiological responses in arterial smooth muscles [14]. In summary, this study is the first to demonstrate the expression of multiple Kir2.x subunits in endothelial cells and to identify the relative roles of specific subunits of endogenous endothelial inwardly-rectifying K^+ current.

X-6 Acknowledgements

We thank Dr. Emile R. Mohler III for kindly providing pig aortas and Rebecca Riley for superb technical assistance. We also thank Dr. Yoshihisa Kurachi, Andrew Tinker, Dr. Barbara Wible and Dr. Andreas Karschin and Dr. Caroline Dart for the gifts of Kir2.1, Kir2.2, and Kir2.4 constructs. This work was supported by the American Heart Association Predoctoral fellowship 0415409U (to Y.F.), the American Heart Association Scientist Development grant 0130254N (to I.L.), and the NIH grant HL073965-01A1 (to I.L.), NIH grant HL64388 (to P.F.D), California Tobacco-related Disease Research Program 11RT-0114 (to C.A.V.), NS43377 (to C.A.V.), and a Canadian Institutes of Health Research Award (MOP 44365, to S.N.).

X-7 References

1. **Adams DJ and Hill MA.** Potassium channels and membrane potential in the modulation of intracellular calcium in vascular endothelial cells. *J Cardiovasc Pharmacol Electrophysiol* 15: 598-610, 2004.
2. **Barry DM, Trimmer JS, Merlie JP, and Nerbonne JM.** Differential expression of voltage-gated K^+ channel subunits in adult rat heart. Relation to functional K^+ channels? *Circ Res* 77: 361-369, 1995.
3. **Coulter KL, Perier F, Radeke CM, and Vandenberg CA.** Identification and molecular localization of a pH-sensing domain for the inward rectifier potassium channel HIR. *Neuron* 15: 1157-1168, 1995.
4. **Davies PF.** Flow-mediated endothelial mechanotransduction. *Physiol Rev* 75: 519-560, 1995.
5. **Dhamoon AS, Pandit SV, Sarmast F, Parisian KR, Guha P, Li Y, Bagwe S, Taffet SM, and Anumonwo JM.** Unique Kir2.x properties determine regional and species differences in the cardiac inward rectifier K^+ current. *Circ Res* 94: 1332-1339, 2004.
6. **Du X, Zhang H, Lopes C, Mirshahi T, Rohacs T, and Logothetis DE.** Characteristic interactions with PIP_2 determine regulation of Kir channels by diverse modulators. *J Biol Chem* 279:37271-37281, 2004.
7. **Eschke D, Richter M, Brylla E, Lewerenz A, Spanel-Borowski K, and Nieber K.** Identification of inwardly rectifying potassium channels in bovine retinal and choroidal endothelial cells. *Ophthalmic Res* 34: 343-348, 2002.
8. **Fischer-Lougheed J, Liu JH, Espinos E, Mordasini D, Bader CR, Belin D, and Bernheim L.** Human myoblast fusion requires expression of functional inward rectifier Kir2.1 channels. *J Cell Bio* 153: 677-686, 2001.
9. **Forsyth SE, Hoger A, and Hoger JH.** Molecular cloning and expression of a bovine endothelial inward rectifier potassium channel. *FEBS Lett* 409: 277-282, 1997.

10. **Himmel HM, Rauen U, and Ravens U.** Microvascular endothelial cells from human omentum lack an inward rectifier K^+ current. *Physiol Res* 50: 547-555, 2001.

11. **Hughes BA, Kumar G, Yuan Y, Swaminathan A, Yan D, Sharma A, Plumley L, Yang-Feng TL, and Swaroop A.** Cloning and functional expression of human retinal Kir2.4, a pH-sensitive inwardly rectifying K^+ channel. *Am J Physiol Cell Physiol* 279: C771-784, 2000.

12. **Hutcheson IR and Griffith TM.** Heterologous populations of K^+ channels mediate EDRF release to flow but not to agonists in rabbit aorta. *Am J Physiol Heart Circ Physiol* 266: H590-596, 1994.

13. **Kamouchi M, Van Den, Bremt K, Eggermont J, Droogmans G, and Nilius B.** Modulation of inwardly rectifying potassium channels in cultured bovine pulmonary artery endothelial cells. *J Physiol* 504: 545-556, 1997.

14. **Karkanis T, Li S, Pickering JG, and Sims SM.** Plasticity of KIR channels in human smooth muscle cells from internal thoracic artery. *Am J Physiol Heart Circ Physiol* 284(6): H2325-2334, 2003.

15. **Karle CA, Zitron E, Zhang W, Wendt-Nordahl G, Kathofer S, Thomas D, Gut B, Scholz E, Vahl CF, Katus HA, and Kiehn J.** Human cardiac inwardly-rectifying K^+ channel Kir(2.1b) is inhibited by direct protein kinase C-dependent regulation in human isolated cardiomyocytes and in an expression system. *Circulation* 106: 1493-1499, 2002.

16. **Kubo Y, Baldwin TJ, Jan YN, and Jan LY.** Primary structure and functional expression of a mouse inward rectifier potassium channel. *Nature* 362: 127-132, 1993.

17. **Kwan HY, Leung PC, Huang Y, and Yao X.** Depletion of intracellular Ca^{2+} stores sensitizes the flow-induced Ca^{2+} influx in rat endothelial cells. *Circ Res* 92: 286-292, 2003.

18. **Leonoudakis D, Conti LR, Anderson S, Radeke CM, McGuire LMM, Adams ME, Froehner SC, Froehner SC, Yates JR 3rd, and Vandenberg CA.** Protein trafficking and anchoring complexes revealed by proteomic analysis of inward rectifier potassium channel (Kir2.x)-associated proteins. *J Biol Chem* 279:22331-22346, 2004.

19. **Leonoudakis D, Conti LR, Radeke CM, McGuire LM, and Vandenberg CA.** A multiprotein trafficking complex composed of SAP97, CASK, Veli, and Mint1 is associated with inward rectifier Kir2 potassium channels. *J Biol Chem* 279: 19051-19063, 2004.

20. **Levitan I, Helmke BP, and Davies PF.** A chamber to permit invasive manipulation of adherent cells in laminar flow with minimal disturbance of the flow field. *Ann Biomed Eng* 28: 1184-1193, 2000.

21. **Lieu DK, Pappone PA, and Barakat AI.** Differential membrane potential and ion current responses to different types of shear stress in vascular endothelial cells. *Am J Physiol Cell Physiol* 286: 1367-1375, 2004.

22. **Liu GX, Derst C, Schlichthorl G, Heinen S, Seebohm G, Bruggemann A, Kummer W, Veh RW, Daut J, and Preisig-Muller R.** Comparison of cloned Kir2 channels with native inward rectifier K^+ channels from guinea-pig cardiomyocytes. *J Physiol* 532: 115-126, 2001.

23. **Luckhoff A and Busse R.** Calcium influx into endothelial cells and formation of endothelium-derived relaxing factor is controlled by the membrane potential. *Pflugers Arch* 416: 305-311, 1990.

24. **Melnyk P, Zhang L, Shrier A, and Nattel S.** Differential distribution of Kir2.1 and Kir2.3 subunits in canine atrium and ventricle. *Am J Physiol Heart Circ Physiol* 283: H1123-1133, 2002.

25. **Miake J, Marban E, and Nuss HB**. Functional role of inward rectifier current in heart probed by Kir2.1 overexpression and dominant-negative suppression. *J Clin Invest* 111 1529-36, 2003.

26. **Morishige K, Takahashi N, Jahangir A, Yamada M, Koyama H, Zanelli JS, and Kurachi Y.** Molecular cloning and functional expression of a novel brain-specific inward rectifier potassium channel. *FEBS Lett* 346: 251-256, 1994.

27. **Neusch C, Weishaupt JH, and Bahr M.** Kir channels in the CNS: emerging new *roles* and implications for neurological diseases. *Cell Tissue Res* 311: 131-138, 2003.

28. **Nichols CG and Lopatin AN.** Inward rectifier potassium channels. *Annu Rev Physiol* 59: 171-191, 1997.

29. **Nilius B and Droogmans G.** Ion channels and their functional role in vascular endothelium. *Physiol Rev* 81: 1415-1459, 2001.

30. **Nilius B, Schwarz G, and Droogmans G**. Modulation by histamine of an inwardly rectifying potassium channel in human endothelial cells. *J Physiol* 472: 359-371, 1993.

31. **Olesen SP and Clapham DE, and Davies PF.** Hemodynamic shear stress activates a K^+ current in vascular endothelial cells. *Nature* 331: 168-170, 1988.

32. **Passerini AG, Polacek DC, Shi C, Francesco NM, Manduchi E, Grant GR, Pritchard WF, Powell S, Chang GY, Stoeckert CJ Jr, and Davies PF.** Coexisting proinflammatory and antioxidative endothelial transcription profiles in a disturbed flow region of the adult porcine aorta.. *Proc Natl Acad Sci USA* 101: 2482-2487, 2004.

33. **Perier F, Radeke CM, and Vandenberg CA.** Primary structure and characterization of a small-conductance inwardly rectifying potassium channel from human hippocampus *Proc Natl Acad Sci USA* 91: 6240-6244, 1994.

34. **Preisig-Muller, R., G. Schlichthorl, T. Goerge, S. Heinen, A. Bruggemann, S. Rajan, C. Derst, R.W. Veh, and J. Daut**, Heteromerization of Kir2.x potassium channels contributes to the phenotype of Andersen's syndrome. *Proc Natl Acad Sci USA* 99: 7774-7779, 2002.

35. **Pruss H, Wenzel M, Eulitz D, Thomzig A, Karschin A, and Veh RW.** Kir2 potassium channels in rat striatum are strategically localized to control basal ganglia function. *Brain Res Mol Brain Res* 110: 203-219, 2003.

36. **Raab-Graham KF, and Vandenberg CA.** Tetrameric subunit structure of the native brain inwardly rectifying potassium channel Kir 2.2. *J Biol Chem* 273: 19699-19707, 1998.

37. **Romanenko, V.G., G.H. Rothblat, and I. Levitan**, Modulation of endothelial inward rectifier K^+ current by optical isomers of cholesterol. *Biophys J* 83:3211-3222, 2002.

38. **Rosati, B. and McKinnon D.** Regulation of Ion Channel Expression. *Circ Res* 94: 874-883, 2004.

39. **Rusko J, Tanzi F, van Breemen C, and Adams DJ.** Calcium-activated potassium channels in native endothelial cells from rabbit aorta: conductance, Ca^{2+} sensitivity and block. *J Physiol* 455: 601-621, 1992.

40. **Schram G, Melnyk P, Pourrier M, Wang Z, and Nattel S.** Kir2.4 and Kir2.1 K^+ channel subunits co-assemble: a potential new contributor to inward rectifier current heterogeneity. *J Physiol* 544: 337-349, 2002.

41. **Schram G, Pourrier M, Wang Z, White M, and Nattel S.** Barium block of Kir2 and human cardiac inward rectifier currents: evidence for subunit-heteromeric contribution to native currents. *Cardiovasc Res* 59: 328-338, 2003.

42. **Takahashi N, Morishige K, Jahangir A, Yamada M, Findlay I, Koyama H, and Kurachi Y.** Molecular cloning and functional expression of cDNA encoding a second class of inward rectifier potassium channels in the mouse brain. *J Biol Chem* 269: 23274-23279, 1994.

43. **Topert C, Doring F, Wischmeyer E, Karschin C, Brockhaus J, Ballanyi K, Derst C, and Karschin A.** Kir2.4: a novel K^+ inward rectifier channel associated with motoneurons of cranial nerve nuclei. *J Neurosci* 18: 4096-4105, 1998.

44. **Voets T, Droogmans G, and Nilius B.** Membrane currents and the resting potential in cultured bovine pulmonary artery endothelial cells. *J Physiol* 497: 95-107, 1996.

45. **von Beckerath N, Dittrich M, Klieber HG, and Daut J.** Inwardly rectifying K^+ channels in freshly dissociated coronary endothelial cells from guinea-pig heart. *J Physiol* 491: 357-365, 1996.

46. **Wang Z, Yue L, White M, Pelletier G, and Nattel S.** Differential distribution of inward rectifier potassium channel transcripts in human atrium versus ventricle. *Circulation* 98: 2422-2428, 1998.

47. **Wellman GC, Bevan JA.** Barium inhibits the endothelium-dependent component of flow but not acetylcholine-induced relaxation in isolated rabbit cerebral arteries. *J Pharmacol Exp Ther* 274: 47-53, 1995.

48. **Wilhelm, J. and Pingoud A.** Real-time polymerase chain reaction. *Chembiochem* 4: 1120-1128, 2003.

49. **Wymore RS, Gintant GA, Wymore RT, Dixon JE, McKinnon D, and Cohen IS.** Tissue and Species Distribution of mRNA for the I_{Kr}-like K^+ Channel, erg. *Circ Res* 80: 261-268, 1997.

50. **Yang D, MacCallum DK, Ernst SA, and Hughes BA.** Expression of the inwardly rectifying K^+ channel Kir2.1 in native bovine corneal endothelial cells. *Invest Ophthalmol Vis Sci* 44: 3511-9, 2003.

51. **Zaritsky JJ, Eckman DM, Wellman GC, Nelson MT, and Schwarz TL.** Targeted disruption of Kir2.1 and Kir2.2 genes reveals the essential role of the inwardly rectifying K^+ current in K^+-mediated vasodilation. *Circ Res* 87 160-166, 2000.

52. **Zobel C, Cho HC, Nguyen TT, Pekhletski R, Diaz RJ, Wilson GJ, and Backx PH.** Molecular dissection of the inward rectifier potassium current (I_{K1}) in rabbit cardiomyocytes: evidence for heteromeric co-assembly of Kir2.1 and Kir2.2. *J Physiol* 550: 365-72, 2003.

X-8 Tables

Kir gene	Primer			Size
Kir2.1	Kir2.1	Forward Reverse	5'GATGTGTCACGGATGAATGC3' 5'ACTCGCCACATCAAACACAG3'	199 bp
	Kir2.1S	Forward Reverse	5'AAACCACTGGATCTTACATGCC 3' 5'TCGGGTGTGGACTTTACTCT3'	410 bp
Kir2.2	Kir2.2	Forward Reverse	5'CCTCATGTGGCGTGTGGGTAAC 3' 5'GTCCAGGCCCTTGTCGAA3'	151 bp
Kir2.3	Kir2.3	Forward Reverse	5'GAAGAACGGCCAATGCAAC3' 5'TGTCACGCACCGGAACCCATAG3'	361 bp
Kir2.4	Kir2.4	Forward Reverse	5'CGCTGACCCTGCCTCCAT3 5'CTATACCATTGGCTTCTCACCC3'	362 bp
	Kir2.4S	Forward Reverse	5'CCCAAGAAGCGCAACGAGA3' 5'TCGGCACGTCCTAGCTCATACA3'	302 bp

Table XI: Molecular sequence and expected length of RT-PCR products for the different human Kir2.1, Kir2.2, Kir2.3, and Kir2.4 primers.

X-9 Figures and Figure legends

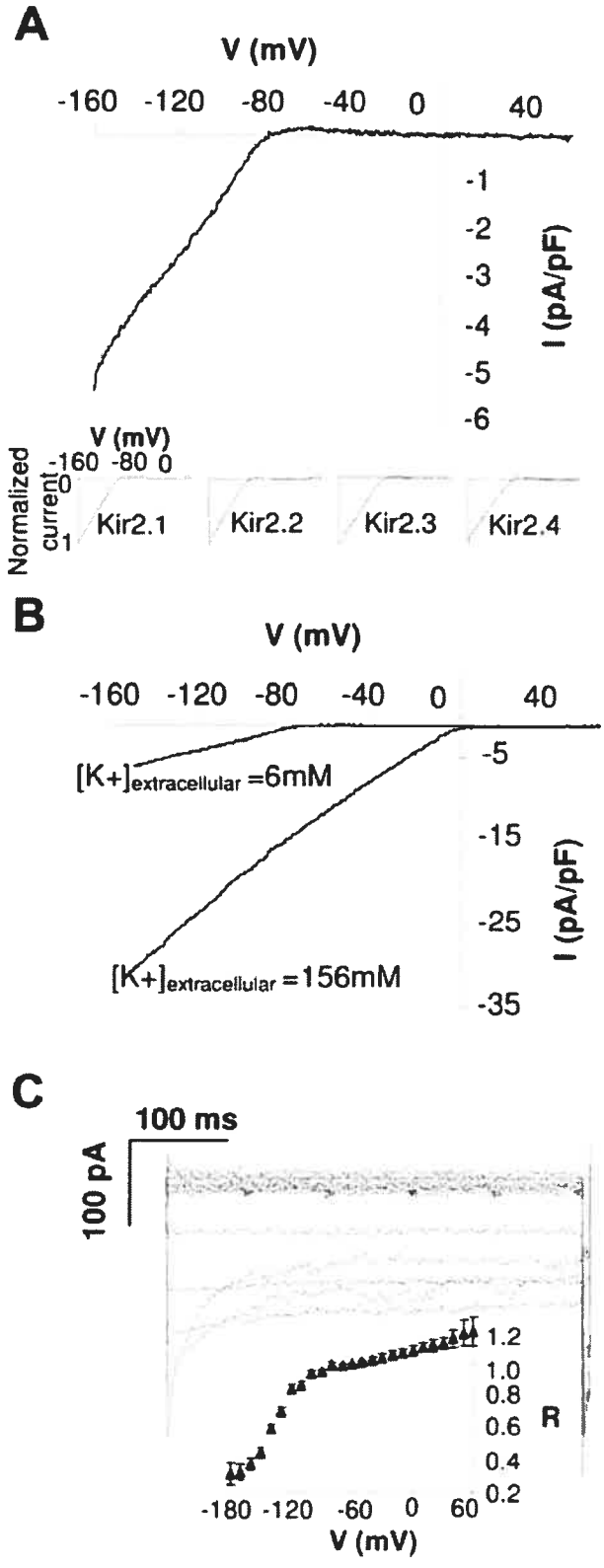

Figure 40: Basic properties of the inward rectifier K^+ current (I_K) in human aortic endothelial cells (HAECs).

***A*:** Typical currents recorded from HAECs at low (6 mM) extracellular K^+ concentration ($[K^+]$); *inset*, current recordings from Chinese hamster ovary (CHO) cells transfected with the four subunits of inward rectifier K^+ channels (Kir): Kir2.1–Kir2.4.

***B*:** Comparison of currents recorded at low (6 mM) and high (156 mM) extracellular $[K^+]$ solutions in the same cell. Note a shift in the reversal potential from –79 to –2 mV.

***C*:** Voltage-sensitive inactivation of the I_K as measured using a two-pulse voltage protocol. Inactivation ratio (R; *inset*) was determined as the ratio of the current amplitude in response to a test voltage pulse administered after prepulses to different voltages and a control test pulse given from the holding potential of –60 mV.

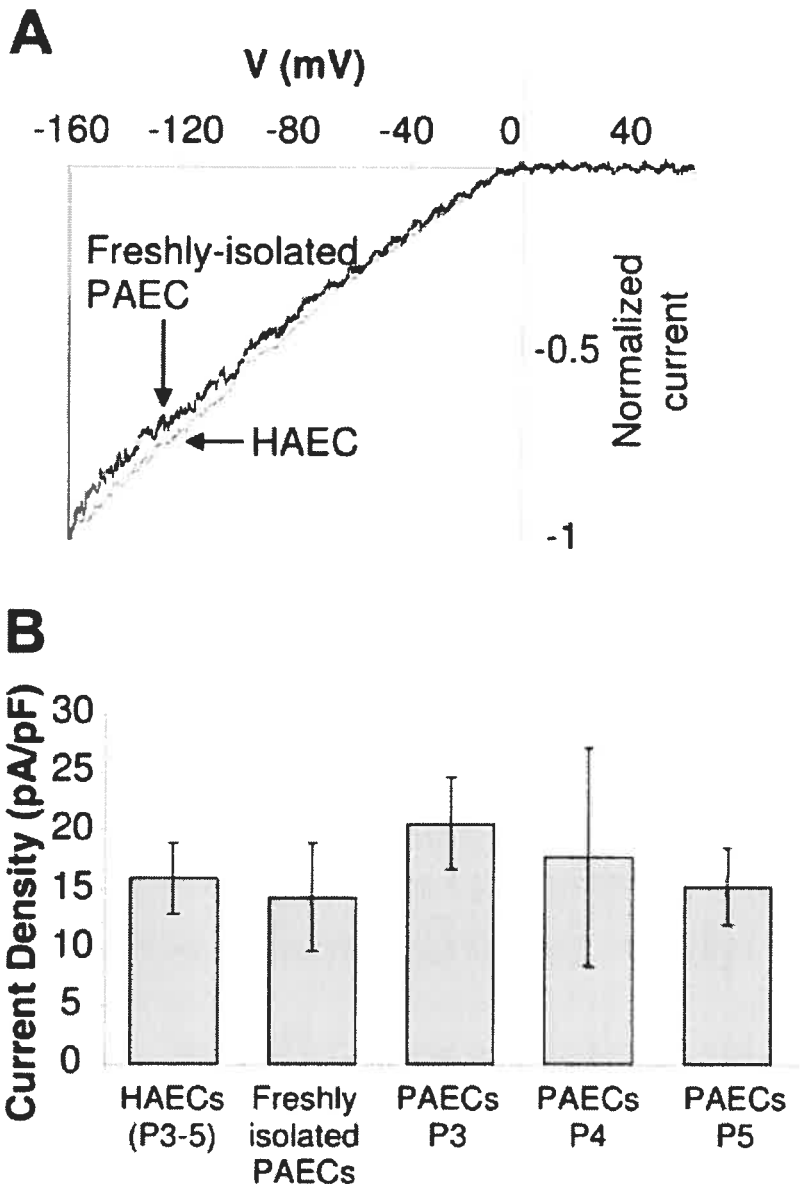

Figure 41: Comparison of I_K in HAECs and in freshly isolated or low-passage cultured porcine aortic endothelial cells (PAECs).

***A*:** Superimposed currents recorded from freshly isolated PAECs and from HAECs at 156 mM extracellular [K^+] solutions.

***B*:** Average current densities recorded in HAECs (*passages 3–5*; n = 17), freshly isolated PAECs (n = 23), and low-passage cultured PAECs (*passage 3*, n = 5; *passage 4*, n = 3; *passage 5*, n = 6). Each data set is expressed as the mean ± S.E.M.

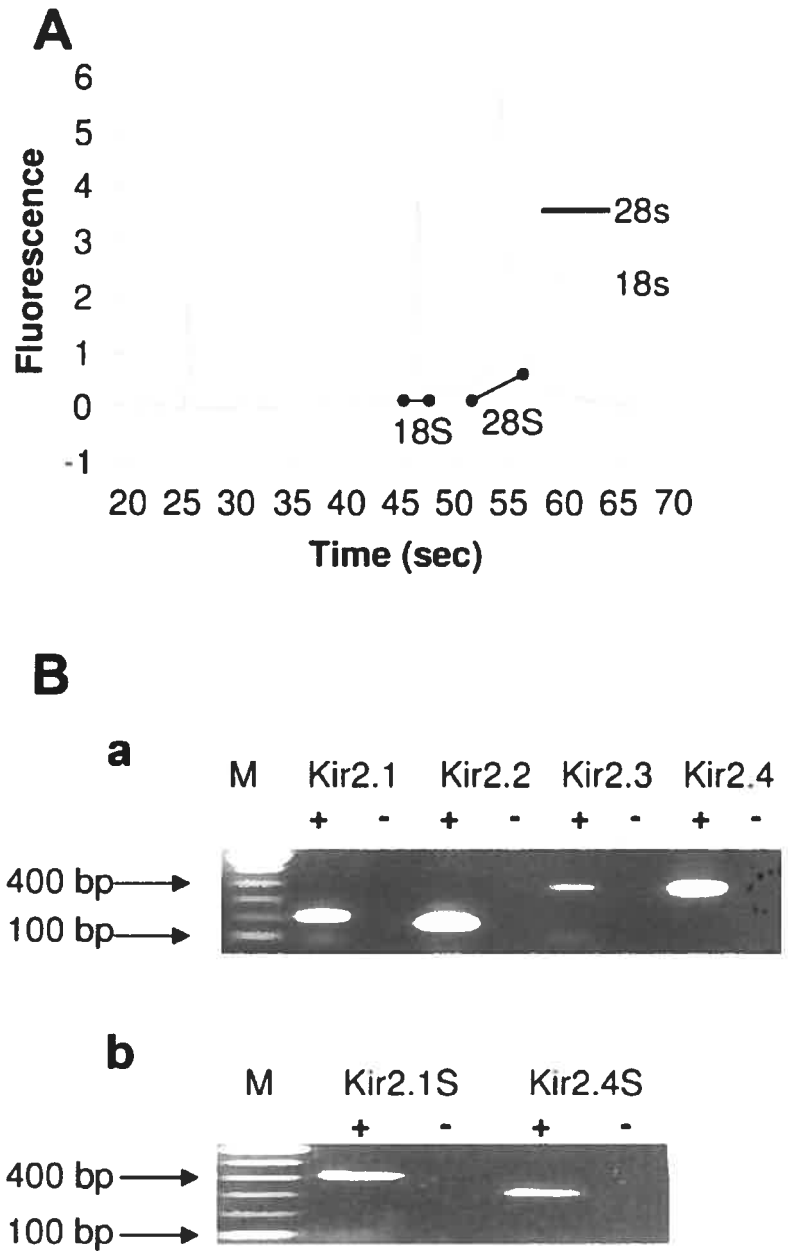

Figure 42: RT-PCR analysis of mRNA encoding different types of Kir2 channel subunits in HAECs.

***A*:** Typical profile for total RNA of HAECs. ***B*:** PCR products for Kir2.x channels amplified with exon-based primers (*a*) or intron-spanning primers (*b*). Lanes marked with minus signs correspond to negative controls in which amplification was performed without adding RT during cDNA synthesis.

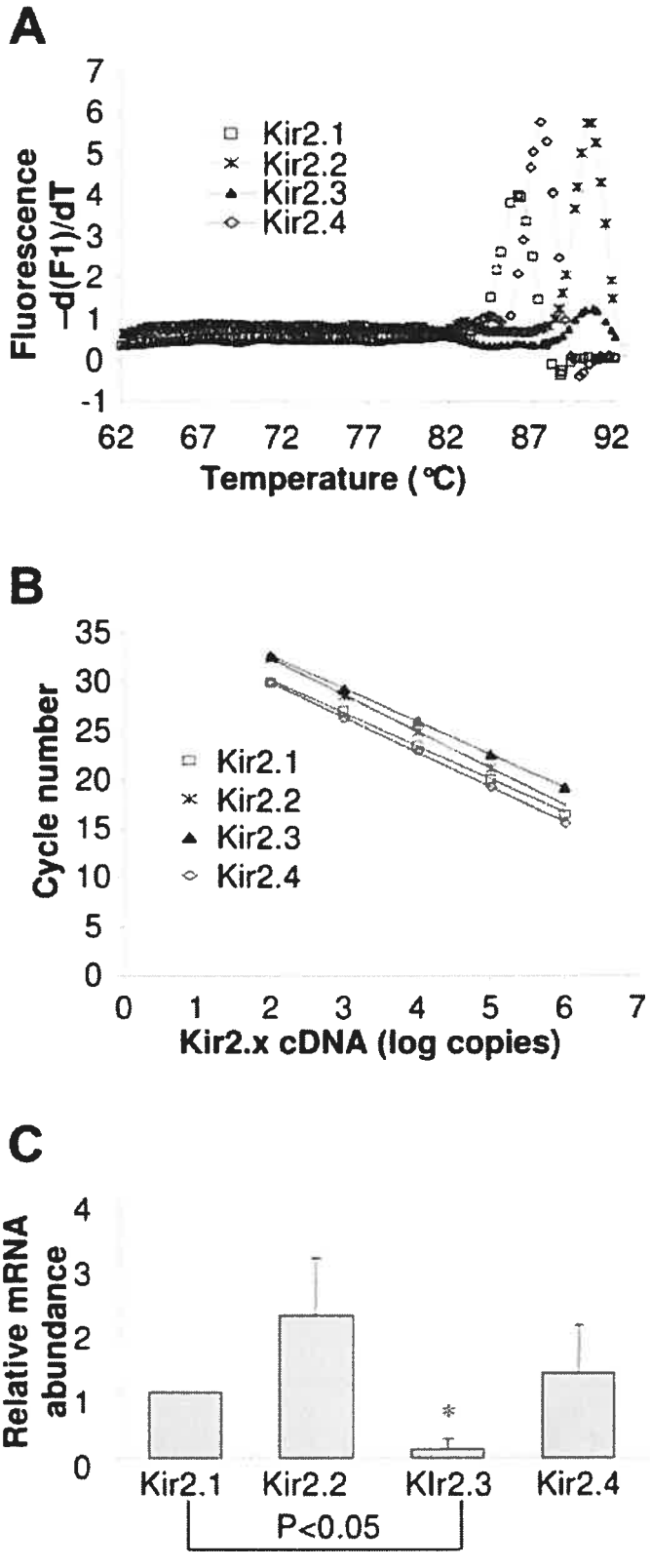
A
Fluorescence
−d(F1)/dT
7
6
5
4
3
2
1
0
-1
62
67
72
77
82
87
92
Temperature (°C)
Kir2.1
Kir2.2
Kir2.3
Kir2.4
B
Cycle number
35
30
25
20
15
10
5
0
0
1
2
3
4
5
6
7
Kir2.x cDNA (log copies)
Kir2.1
Kir2.2
Kir2.3
Kir2.4
C
Relative mRNA abundance
4
3
2
1
0
Kir2.1
Kir2.2
KIr2.3
Kir2.4
*
P<0.05

Figure 43: Quantification of Kir2.x mRNA level in HAECs using quantitative real-time PCR (QRT-PCR).

***A*:** Melting curves of Kir2.x amplicons representing plots of fluorescence ($-dF1/dt$) vs. temperature (°C).

***B*:** Standard curves for the real-time PCR amplification of human Kir2.x cDNA representing threshold cycle number vs. the copies of purified human Kir2.x cDNA.

***C*:** mRNA expression levels for Kir2.x channels estimated from cDNA copy numbers normalized to Kir2.1 in the same biological sample. Four independent experiments (RNA isolation and cDNA synthesis, followed by QRT-PCR) were performed, and the values shown are means ± S.E.M. $^*P < 0.05$.

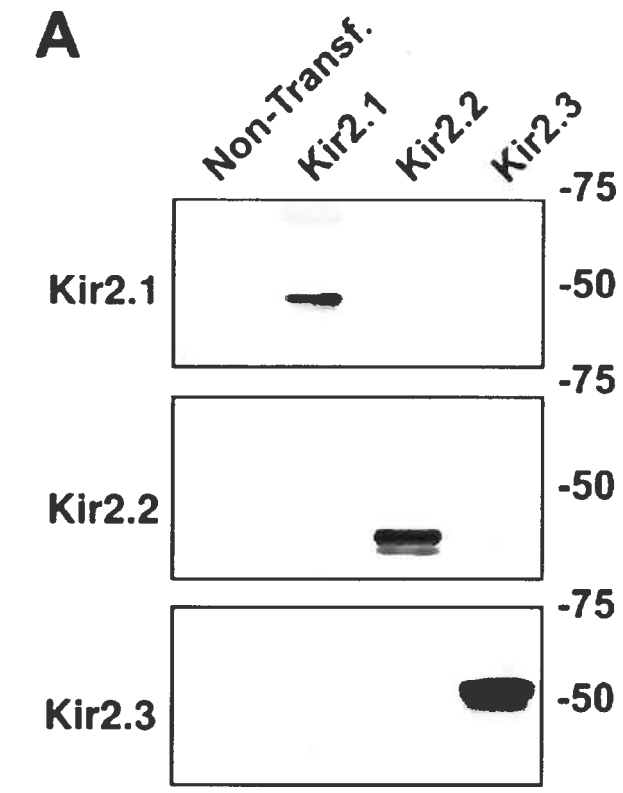
A
Non-Transf.
Kir2.1
Kir2.2
Kir2.3
-75
-50
-75
-50
-75
-50
Kir2.1
Kir2.2
Kir2.3

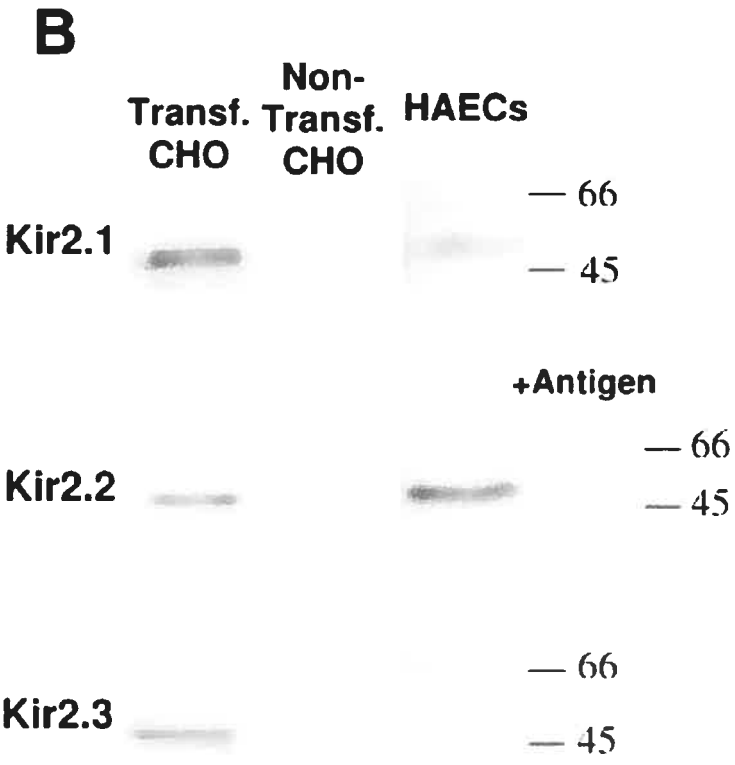
B
Transf. CHO
Non-Transf. CHO
HAECs
— 66
— 45
+Antigen
— 66
— 45
— 66
— 45
Kir2.1
Kir2.2
Kir2.3

Figure 44: Protein expression of Kir2.x in HAECs.

Typical examples of Kir2.x immunoblots of total membrane fractions of COS-1 or CHO cells transfected with cDNA encoding mouse or rat Kir2.1 and Kir2.2 and human Kir2.3, as well as HAECs.

***A*:** characterization of antibody specificity. The same amount of cell lysate (5–10 μg/lane) was loaded for COS-1 cells transfected with mouse Kir2.1, rat Kir2.2, human Kir2.3, and nontransfected cells. Blots were probed with antibodies to Kir2.1 (*top*), Kir2.2 (*middle*), and Kir2.3 (*bottom*).

***B*:** same amount of protein (30 μg/lane) was loaded for transfected and nontransfected CHO cells. For HAECs, the gels were loaded with the maximal sample volume (80 μg total proteins) for all three Kir subunits. The Kir2.2 band was completely abolished by preabsorbing the antibody with the specific antigen. All of the experiments were repeated in at least three independent biological samples.

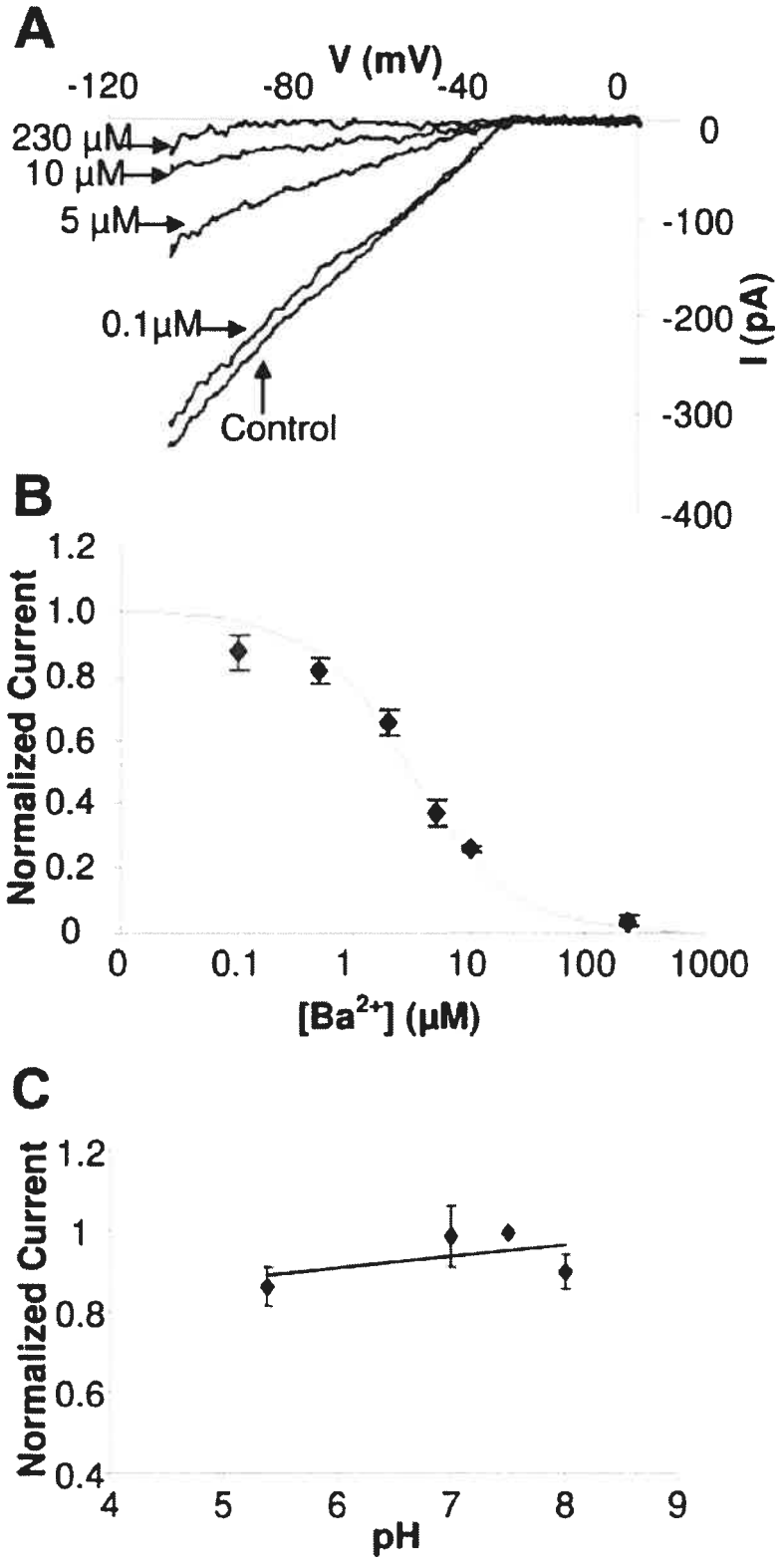
A
V (mV)
-120
-80
-40
0
230 µM
10 µM
5 µM
0.1µM
Control
0
-100
-200
-300
-400
I (pA)
B
Normalized Current
1.2
1.0
0.8
0.6
0.4
0.2
0
0
0.1
1
10
100
1000
[Ba2+] (µM)
C
Normalized Current
1.2
1
0.8
0.6
0.4
4
5
6
7
8
9
pH

Figure 45: Ba^{2+} block and pH sensitivity of the I_K in HAECs.

***A*:** I_K recorded in a single HAEC at 0.1, 5, 10, and 230 μM extracellular Ba^{2+} (extracellular $[K^+]$ was 60 mM).

***B*:** Concentration dependence of Ba^{2+} block. Fractional block was determined at –100 mV and calculated as $(I_{control} - I_{Ba}{}^{2+})/I_{control}$, where $I_{control}$ is the current recorded before application of Ba^{2+} and $I_{Ba}{}^{2+}$ is the current recorded at a specific Ba^{2+} concentration. Each point is the mean ± S.E.M. (n = 5). The data were fitted with the function $I_{Ba}{}^{2+}/I_{control} = 1/(1 + [Ba^{2+}]/K_d)$ where K_d is the dissociation constant.

***C*:** I_K amplitudes plotted as a function of extracellular pH normalized to the current measured with pH 7.5 solution in the same cell. The amplitudes were measured at –100 mV. The protocol for current recording and K^+ concentration ($[K^+]$) in bath and pipette solutions were identical to those in Fig. 5. Data are means ± S.E.M. (n = 5).

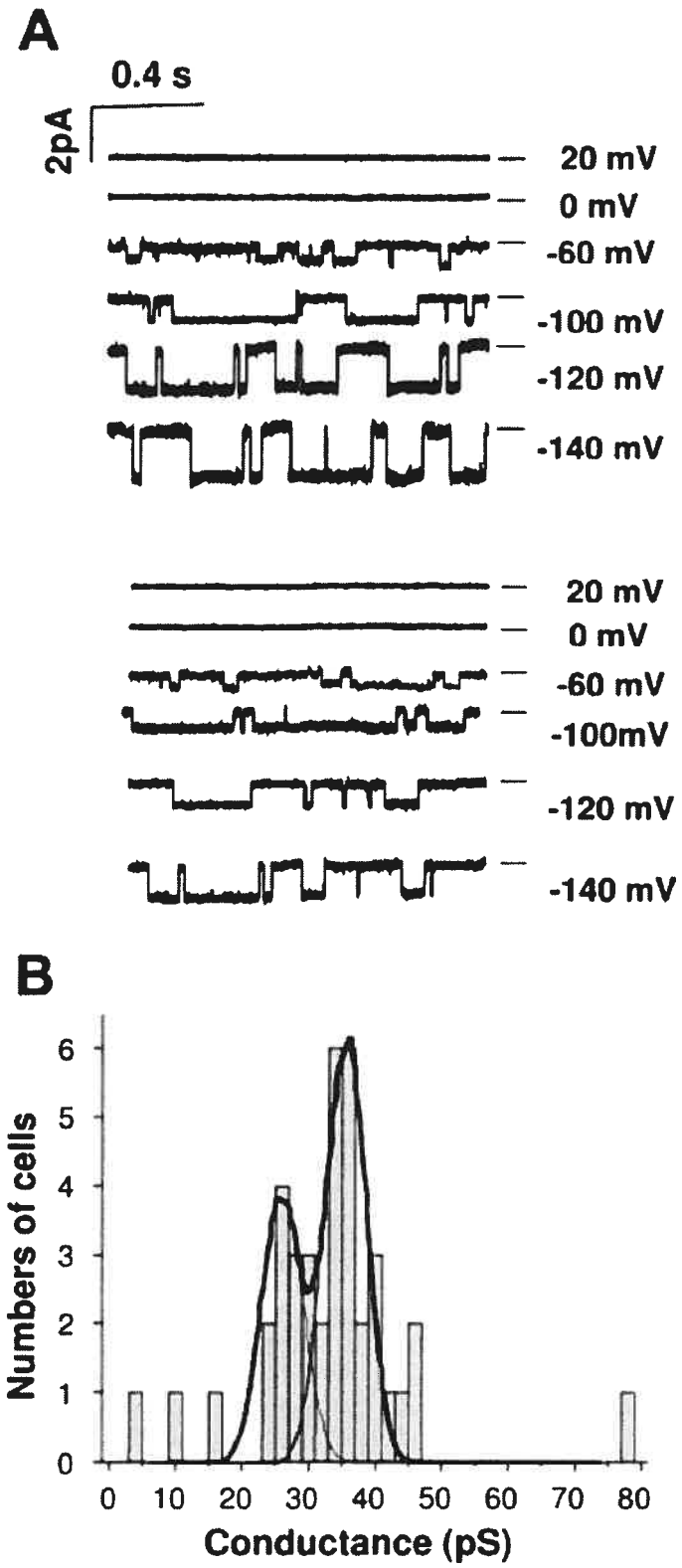
A
0.4 s
2pA
20 mV
0 mV
-60 mV
-100 mV
-120 mV
-140 mV
20 mV
0 mV
-60 mV
-100mV
-120 mV
-140 mV
B
Numbers of cells
0
1
2
3
4
5
6
0 10 20 30 40 50 60 70 80
Conductance (pS)

Figure 46: Distribution of single-channel conductances of endogenous Kir channels in HAECs.

***A*:** typical single-channel currents at different membrane potentials recorded from HAECs in the cell-attached configuration. Bath and pipette solution contained 156 mM [K^+]. The closed level of the channel is indicated by a bar to the *right* of each trace. The two examples show the most prevalent unitary conductances observed in these experiments.

***B*:** conductance histograms of single-channel recording. The single-channel slope conductance was calculated by performing linear regression analysis from cell-attached recordings at membrane potentials in the range of –60 to –140 mV. The histogram was generated in 2-pS bin steps. The bimodal histograms were fitted with two Gaussians of the same width (thin lines). The sum of the two Gaussians is indicated by a heavy black line.

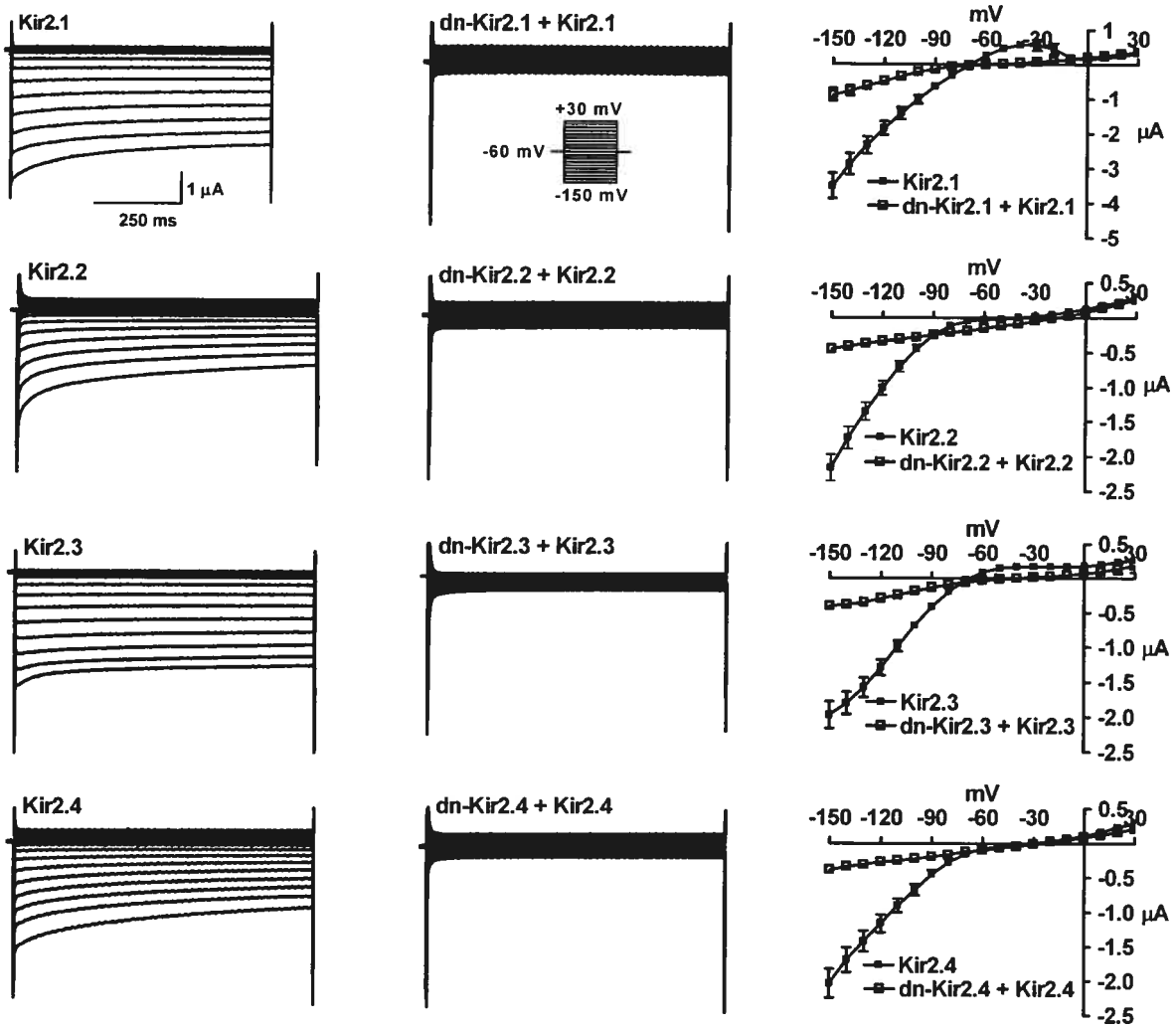

Figure 47: Suppression of Kir2.x current by dominant-negative (dn-) Kir2.x constructs.

Left*:** representative recordings of Kir2.x wild-type recordings in *Xenopus* oocytes. Representative recordings of coexpression of Kir2.x channels with the respective dn-Kir2.x construct are shown in ***middle images. Kir2 currents were elicited by voltage steps from a holding potential of –60 mV to step potentials between –150 mV and +30 mV in 10-mV increments as shown by the voltage protocol in the *inset*. ***Right*:** mean current-voltage (*I-V*) relationships of Kir2.1 (n = 7), Kir2.1 + dn-Kir2.1 (n = 9), Kir2.2 (n = 9), Kir2.2 + dn-Kir2.2 (n = 9), Kir2.3 (n = 9), Kir2.3 + dn-Kir2.3 (n = 5), Kir2.4 (n = 9), and Kir2.4 + dn-Kir2.4 (n = 9) as indicated.

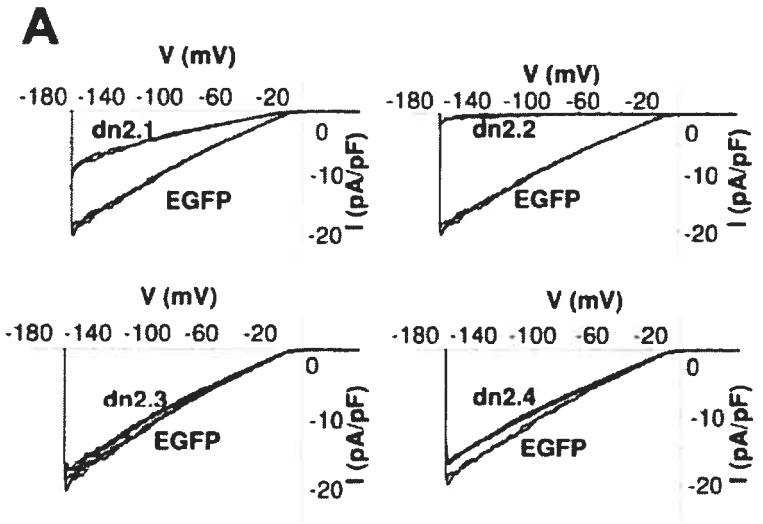
A
V (mV)
-180 -140 -100 -60 -20
dn2.1
EGFP
0
-10
-20
I (pA/pF)
V (mV)
-180 -140 -100 -60 -20
dn2.2
EGFP
0
-10
-20
I (pA/pF)
V (mV)
-180 -140 -100 -60 -20
dn2.3
EGFP
0
-10
-20
I (pA/pF)
V (mV)
-180 -140 -100 -60 -20
dn2.4
EGFP
0
-10
-20
I (pA/pF)

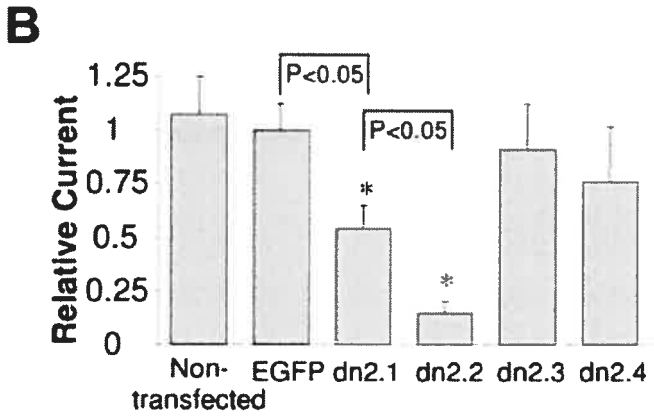
B
Relative Current
1.25
1
0.75
0.5
0.25
0
P<0.05
P<0.05
*
*
Non-transfected
EGFP
dn2.1
dn2.2
dn2.3
dn2.4

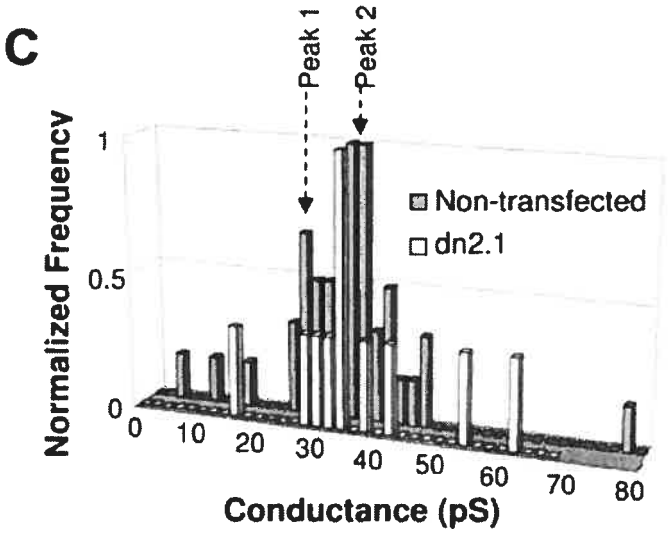
C
Peak 1
Peak 2
Normalized Frequency
1
0.5
0
Non-transfected
dn2.1
0
10
20
30
40
50
60
70
80
Conductance (pS)

Figure 48: Inhibition of the endogenous I_K in HAECs by dnKir2.x constructs.

***A*:** currents recorded in HAECs transfected with pIRES2-EGFP, pIRES2-EGFP-dnKir2.1, pIRES2-EGFP-dnKir2.2, pIRES2-EGFP-dnKir2.3, or pIRES2-EGFP-dnKir2.4.

***B*:** average current densities in native HAECs (n = 10) and in HAECs transfected with dnKir2.1 (n = 15), dnKir2.2 (n = 13), dnKir2.3 (n = 14), or dnKir2.4 (n = 19) normalized to the average current density in control cells (transfected with pIRES2-EGFP; n = 26). Each point is the mean ± S.E.M. The external solution contained 156 mM [K^+].

***C*:** conductance histograms of single-channel recording in cells expressing dnKir2.1 (light bars), compared with the histogram obtained from control cells (dark bars).

PART III: GENERAL DISCUSSION AND CONCLUSION

CHAPTER XI: DISCUSSION OF RESULTS.

XI-1 Major Novel Contributions and Significance in Context of Literature

In this thesis, we present data that has considerably contributed to the understanding of the molecular composition of native inward rectifier currents carried by Kir2 channels in different biological systems. Major novelties presented in this thesis are:

1. Kir2.1 and Kir2.4 subunits co-assemble. Resulting Kir2.1-Kir2.4 channels are functional and have unique biophysical properties distinct from Kir2.1, Kir2.4 or the algebraic sum of both. Our study is one of the first two publications (Preisig-Muller *et al.* (2002) and Schram *et al.* (2002a)) demonstrating heteromeric Kir2 channel assembly. Presentation of preliminary results at international scientific conferences represented the first demonstration of heterotetramer formation amongst Kir2 subfamily members (Schram *et al.*, 2000a; Schram *et al.*, 2000b).

2. Heteromeric assembly of Kir2 subunits might underlie human cardiac I_{K1}. Our data presents the first analysis of Kir2 subunit function in human heart and strongly supports the notion that a substantial proportion of human cardiac I_{K1} may result from heteromultimeric formation among Kir2 subunits (Schram *et al.*, 2003).

3. Kir2.2 current might represent the major K^+-conductance in human aortic endothelial cells. Our data is the first demonstration that human aortic endothelial cells express all four Kir2 subfamily members and not only Kir2.1, as previously believed (Forsyth *et al.*, 1997; Kamouchi *et al.*, 1997; Eschke *et al.*, 2002). Our study shows that both Kir2.1 and Kir2.2 are functionally important in HAECs and that the major conductance in these cells might be carried by Kir2.2 currents (Fang *et al.*, 2005).

The following pages will discuss our results in context of the current literature.

XI-1.1 Kir2.1 and Kir2.4 form Heteromeric Channels with Distinct Properties

XI-1.1.1 Primary Novelty and Results Reported in this Study

In this study, we showed that Kir2.4 and Kir2.1 subunits co-associate and that resulting heteromeric channels are functional and have distinct biophysical properties.

When mRNA of Kir2.1 and a dominant negative (dn-) Kir2.4 mutant were co-injected in *Xenopus* oocytes, Kir2.1 currents were completely suppressed. Similarly, co-expression of Kir2.4 with dn-Kir2.1 mRNA resulted in complete suppression of Kir2.1 currents indicating subunit co-assembly. Kir2.4 co-precipitated with Kir2.1 from Cos-7 cells transfected with both Kir2.1 and Kir2.4 cDNA affirming that both subunits co-assemble with a tight physical association. To determine whether co-assembled channels are functional and if so, to evaluate their properties, we constructed a chimeric construct, in which Kir2.1 and Kir2.4 cDNA were covalently linked. Translation of this DNA resulted in a protein with Kir2.1 and Kir2.4 physically attached, and any channels formed would have had to be composed of co-assembled Kir2.1 and Kir2.4. Kir2.1/Kir2.4 chimeras conducted robust current demonstrating that heteromeric channels were functional. Ba^{2+}-block of Kir2.1/Kir2.4 chimeras was different from Kir2.1 or Kir2.4 homomers alone or from what would have been expected from the simple sum of properties of homomeric channels indicating that channels resulting from Kir2.1/Kir2.4 co-assembly have distinct biophysical properties. Ba^{2+} blocking properties of co-expressed Kir2.1 and Kir2.4 subunits were identical to those of Kir2.1/Kir2.4 chimeras indicating that formation of Kir2.1/Kir2.4 heteromers occurs spontaneously and is preferred over formation of Kir2.1 and Kir2.4 homotetramers (Schram *et al.*, 2002a).

XI-1.1.2 Discussion of Results in Context of the Literature

First evidence for potential formation of Kir2 heteromers was controversial (Fink *et al*, 1996a; Tinker *et al*, 1996). However, while our manuscript was in submission another study was published, which provided strong evidence for heterotetramer formation between Kir2.1, Kir2.2 and Kir2.3 subunits (Preisig-Muller *et al.*, 2002). Many of the techniques used in this study were identical to methods we

had previously published (Schram *et al.*, 2000a; Schram *et al.*, 2000b). Preisig-Müller et al. showed that Kir2.1-3 channel subunits co-assemble via interactions of their C- and N-termini. While not clarifying the exact mechanism for Kir2 channel assembly, these results resolved the apparent controversy between the results of Fink and Tinker who had found the N-terminus (Fink *et al*, 1996a) or part of the M2 segment and the C-terminus (Tinker *et al*, 1996) were essential for assembly of Kir2 subfamily channels. Similar to our results, Preisig-Müller and co-workers showed that chimeric construct of Kir2.x/Kir2.y subunits were functional and had Ba^{2+} blocking properties that differed substantially from the value expected for independent expression of homomeric channels. Co-expression of dn-Kir2.x constructs with wild-type Kir2.x channels generated both homomeric and heteromeric dominant-negative effects. Kir2.1 and Kir2.3 co-immunoprecipitated in membrane extracts from isolated guinea pig cardiomyocytes. In addition, the authors reported that Kir2.1 mutants related to Andersen's syndrome suppressed Kir2 current in homo- and heteromeric Kir2 channels thus emphasizing the pathophysiological relevance of Kir2 channel heteromerization (Preisig-Muller *et al.*, 2002).

Our results are different from data published by Tinker et al. (1996) in that our data suggests spontaneous co-assembly of Kir2.1 and Kir2.4 subunits whereas Tinker et al. reported that formation of homomultimers is by far the preferred reaction when Kir2.1 is co-expressed with either Kir2.2 or Kir2.3 (Tinker *et al.*, 1996). While it could be argued that co-assembly between Kir2.1 and Kir2.4 is due to distinct properties of the Kir2.4 subunit which are not present in Kir2.2 or Kir2.3, the data of Fink et al (1996) who reported formation of Kir2.1/Kir2.3 heteromultimers (Fink *et al.*, 1996a) and Preisig-Müller et al. (2002) who provided convincing evidence for the formation of Kir2 heteromeric channels consisting of Kir2.1, Kir2.2 and Kir2.3 subunits in both a heterologous expression system and in vivo strongly supports our data. Our findings are similar to those of Preisig-Müller et al. in that we show that Kir2.1 and Kir2.4 can co-assemble, that covalently linked Kir2.1/Kir2.4 channels conduct robust current, and that Ba^{2+}-blocking properties of Kir2.1/Kir2.4 currents are different from their homomeric constituents. Like Preisig-Müller et al., we found that dn-Kir2 constructs suppress currents of other Kir2 subfamily members when co-

expressed in a heterologous expression system. While Preisig-Müller et al. co-precipitated Kir2.1 and Kir2.3 from ventricular myocytes of guinea pigs, we co-precipitated Kir2.1 and Kir2.4 from Cos-7 cells co-transfected with Kir2.1-His6 and Kir2.4-Flag constructs. Whereas we found that Ba^{2+} sensitivity of chimeric Kir2.1/Kir2.4 and co-expressed Kir2.1/Kir2.4 channels was higher than that of either Kir2.4 or Kir2.1, Preisig-Müller reported that co-assembled Kir2.x/Kir2.y currents had Ba^{2+} sensitivities in the range of those of the more sensitive homomeric constituent subunit (Preisig-Muller *et al.*, 2002). However, absolute values reported by Preisig-Müller for heteromeric Kir2.x/Kir2.y channels is in good agreement with our data (Preisig-Muller *et al.*, 2002; Schram *et al.*, 2002a).

Taken together, our data in context of the literature strongly suggests that formation of functionally distinct heteromeric Kir2 channels in vivo may represent a commonly occurring mechanism to achieve diversity of Kir2 channel function.

XI-1.1.3 Potential Scientific Significance of Results Reported

Heteromerization is an important contributor to functional diversity of K^+ channels (Coetzee *et al.*, 1999). Kir2.4 is expressed in the central (Topert *et al.*, 1998; Hughes *et al.*, 2000) and peripheral nervous system (Liu *et al.*, 2001). It was previously assumed that Kir2.4 expression in the CNS is limited to various cranial nerve motor neuron nuclei in the midbrain, pons, and medulla. Kir2.4 mRNA expression as evaluated by Northern blot analysis was also seen in rat heart but to a lesser extent than in the brain (Topert *et al.*, 1998). Recent data, however, points to a much more important physiological role of Kir2.4 than previously assumed. Using polyclonal monospecific affinity-purified antibodies against the less conserved carboxy-terminal sequences of Kir2 subunits Pruss et al. (2005) demonstrated a far more widespread distribution of Kir2.4 in rat brain than previously reported. Strong co-localization of Kir2.4 and Kir2.1 is found in Layers II – VI in the neocortex. In the hippocampus, Kir2.4 and Kir2.1 co-localize in the granule cell layer of the dentate gyrus, CA1-CA3 regions, the basal nucleus of Meynert and the basal ganglia. Particularly strong co-localization of all four Kir2 subunits is found in the neocortex and the granule cell layer of the dentate gyrus. In the oculomotor nucleus and

hypothalamic supraoptic nucleus, Kir2.4 co-localizes with Kir2.2. Co-localization of Kir2.4 with Kir2.3 and Kir2.1 is found in the deep nuclei of the cerebellum (Pruss *et al.*, 2005). In rat striatum, Kir2.4 channels are localized to striatal patch compartment and giant cholinergic interneurons, important structures in basal ganglia circuitry and thus in movement disorders such as Parkinson's disease (Pruss *et al.*, 2003). Thus, heteromeric Kir2.1/Kir2.4 channels (and other Kir2.4 subunit-containing heteromeric channels) might represent ion channels specifically tailored to modulation of neuronal excitability in specific tissues through fine tuning of cellular excitability (Karschin *et al.*, 1996; Liu *et al.*, 2001).

XI-1.2 Comparison of Barium Block of Cardiac I_{K1} with Homo- and Heteromeric Kir2 Channel Complexes

XI-1.2.1 Primary Novelty and Results Reported in this Study

In this thesis, we present the first study to compare properties of heteromeric Kir2 channels with those of native cardiac I_{K1}. High-potency block by Ba^{2+} is a hallmark property of I_{K1} and channels of the Kir2 family. We defined Ba^{2+} blocking properties of different Kir2 channels and showed that Ba^{2+} block is a valuable pharmacological tool to distinguish between Kir2 subunits (Schram *et al.*, 1999a; Schram *et al.*, 1999b; Schram *et al.*, 2000a). This approach has been generally accepted in the scientific community and was adopted in several publications (Liu *et al.*, 2001; Preisig-Muller *et al.*, 2002; Zobel *et al.*, 2003; Fang *et al.*, 2005).

To analyze Ba^{2+} blocking properties of Kir2.1-3 subunits and compare them to human cardiac I_{K1}, we expressed homomeric Kir2.1-3 channels in *Xenopus* oocytes. Cardiac I_{K1} was recorded from single ventricular myocytes isolated from myocardial biopsies of normal human hearts. Five different Ba^{2+} concentrations were applied and responses to Ba^{2+} measured and analyzed. Our results showed that Ba^{2+} block of homomeric Kir2.1-3 currents was concentration and voltage-dependent, similar to cardiac I_{K1}. However, Ba^{2+} sensitivity of I_{K1} in human ventricular myocytes was greater and kinetics showed slower time-dependent onset of block than Ba^{2+} block of currents carried by homomeric Kir2 channels. Using the same strategy, we then proceeded to evaluate the potential significance of heteromeric channels formed by

Kir2 subunits known be expressed in the human heart (Wang *et al.*, 1998). To compare Ba^{2+} blocking properties of heteromeric Kir2.x/Kir2.y channels, we co-injected various combinations of two distinct Kir2 subunits in a 1:1 stoichiometry in *Xenopus* oocytes and studied their responses to different concentrations of Ba^{2+}. Channels resulting from Kir2.1/Kir2.2, Kir2.1/Kir2.4 and Kir2.2/Kir2.3 heteromultimer formation were more sensitive to Ba^{2+} than either of their homomeric constituents, and had Ba^{2+} sensitivities similar to cardiac I_{K1}. No difference in Ba^{2+} sensitivity was noted between Kir2.2 and heteromeric Kir2 channels. Time-dependent onset of Ba^{2+} block was significantly slower in Kir2.1/Kir2.2 and Kir2.1/Kir2.3 channels when compared to homomeric Kir2 channels, but matching Ba^{2+} blocking kinetics of cardiac I_{K1}. Onset of block was somewhat faster in Kir2.2/Kir2.3 channels.

XI-1.2.2 Potential Significance of Results in Context of the Literature

Besides ours, five other studies have been published that examined the potential molecular composition of cardiac I_{K1} in different tissues. Nakamura et al. (1998) found that application of Kir2.1 antisense oligonucleotides significantly but incompletely suppressed I_{K1} in rat ventricular myocytes. The authors concluded that Kir2.1 is the major contributor to rat ventricular I_{K1} and that other subunits must play a role (Nakamura *et al.*, 1998). Zaritsky et al (2001) constructed mice in which the genes coding for Kir2.1 or Kir2.2 had been deleted. Consistent with results obtained from Nakamura et al, Kir2.1 knockout mice showed a significant reduction in I_{K1} current but displayed measurable remaining inward rectifier current. Deletion of the Kir2.2 gene resulted in a 50% suppression of I_{K1}. These results indicate that in mouse ventricular myocyte Kir2.1 is the main determinant of I_{K1} and that Kir2.2 must be present in about 50% of native channel complexes (Zaritsky *et al.*, 2001). Liu et al. (2001) cloned Kir2.1-3 from guinea pig cardiomyocytes. Using immunocytochemistry they demonstrated that Kir2.4 expression in guinea pig heart is restricted to neuronal tissue. Based on Ba^{2+} sensitivity and the single channel conductance of native I_{K1} in guinea pig cardiomyocytes, the authors concluded that Kir2.2 homomeric channels underlie the major Kir conductance in guinea pig heart. No quantification of Kir2 mRNA or protein was published (Liu *et al.*, 2001). Preisig-

Müller et al. (2002) showed that Kir2.x/Kir2.y chimeric constructs have similar single channel conductances between 28-30 pS, that Kir2.1 and Kir2.2 spontaneously co-assemble and that Ba^{2+} blocking properties of co-assembled channels are identical to that of chimeric Kir2.x/Kir2.y chimeric constructs. Physical association in native tissue was demonstrated by co-immunoprecipitation of Kir2.1 and Kir2.3 from single cardiomyocytes. Yeast two-hybrid experiments showed interaction of C- and N-termini of different Kir2 subunits (Preisig-Muller *et al.*, 2002). However, no comparison between heteromeric Kir2.x/Kir2.y channels and cardiac I_{K1} was performed. Zobel et al. (2003) transfected rabbit cardiomyocytes with dn-Kir2.1 and / or dn-Kir2.2 subunits. Both transfection with dn-Kir2.1 or dn-Kir2.2 decreased I_{K1} density by about 70%, as did co-transfection with both dn-Kir2.1 and dn-Kir2.2. Increasing amounts of transfected dn-Kir2 cDNA did not cause any further decrease in cardiac I_{K1}. Functional properties such as Ba^{2+} sensitivity of the remaining current were unaffected. Kir2.3 protein was not detected in these cells and transfection with a dn-Kir2.3 subunit had no effect on native I_{K1} current (Zobel *et al.*, 2003). The authors concluded that native I_{K1} in rabbit cardiomyocytes must at least consist of Kir2.1 and Kir2.2 subunits. Residual Kir current after dn-Kir2 transfection could be caused by insufficient current suppression by the dominant negative Kir2.x subunit(s), a channel turn-over rate resulting in rapid regeneration of functional Kir2 channels or the presence of an unknown Kir2 subunit.

The major novelty of our data in the context of these studies is that our study is the first and only study to date to compare properties of heteromeric Kir2 channels to human cardiac I_{K1}. Our data is in good agreement with the above mentioned studies in that it strongly supports the notion that a substantial proportion of cardiac I_{K1} may result from Kir2 heteromultimer formation. Similar to Preisig-Müller et al. and in agreement with our data on Kir2.1/Kir2.4 heteromer formation, our data shows that Ba^{2+}-block of co-expressed Kir2 subunit current is not simply the algebraic sum of individual subunit responses. In addition we show that the response of native human I_{K1} to Ba^{2+} is more similar to that of co-injected subunits than of each subunit expressed alone, supporting the notion that Kir2 heteromer formation plays a role in human cardiac I_{K1}.

It is important to mention at this point, that currents carried by Kir2.2 co-injected with either Kir2.1 or Kir2.3 had Ba^{2+} sensitivity indistinguishable from homomeric Kir2.2 channels. A similar observation was made by Preisig-Müller et al. This observation is important for the interpretation of data published by Liu et al. (2001). Based upon Ba^{2+} sensitivity and single channel conductance the authors concluded that Kir2.2 is the major conductance in guinea pig cardiomyocytes (Liu *et al.*, 2001). Biochemical and functional data obtained in various species however points to a predominant role of Kir2.1 in native I_{K1} in different species (Nakamura *et al.*, 1999b; Wang *et al.*, 1998; Melnyk *et al.*, 2002; Zaritsky *et al.*, 2001). Liu and colleagues neither measured Kir2 mRNA nor protein expression in guinea pig cardiomyocytes. As discussed above, Ba^{2+} blocking properties of heteromeric channels are indistinguishable from those of Kir2.2 (Schram *et al.*, 2002a; Schram *et al.*, 2003; Preisig-Muller *et al.*, 2002). Therefore, the guinea pig findings are in good agreement with a prominent role of Kir2 heteromeric channels in guinea pig I_{K1}.

XI-1.3 Kir2 Channels in HAECs

XI-1.3.1 Primary Novelty and Results Reported in this Study

In this study we have shown that Kir2.1-4 are expressed in human aortic endothelial cells and that only Kir2.1 and Kir2.2 appear to be of functional relevance. Our results point to Kir2.2 as the primary determinant of inward rectifier current in HAECs.

Inward rectifier currents were found in 85% of HAECs under resting conditions, consistent with a resting membrane potential of -79.0 ± 2.0 mV. ECs are known to change their ion channel expression pattern during culture (Nilius & Droogmans, 2001) and it is important to note that culturing of HAECs had no effect on current density and rectification properties. Messenger RNA of all four Kir2 subfamily members was detected in HAECs by RT-PCR. Real-time PCR showed that Kir2.2 mRNA expression was strongest, followed by intermediate Kir2.4 mRNA expression. Kir2.1 mRNA expression levels were lower than Kir2.2 or Kir2.4. Kir2.3 mRNA expression was weak and Kir2.3 protein was not detected. Protein expression of Kir2.1, Kir2.2 was in agreement with transcript levels. No Kir2.3 protein was

detected. A Kir2.4 antibody was not available. Transfection with dn-Kir2.1 and dn-Kir2.2 subunits significantly decreased endogenous HAEC currents with dn-Kir2.2 causing stronger current suppression than dn-Kir2.1. Transfection with dn-Kir2.3 or dn-Kir2.4 did not affect native HAEC currents. Ba^{2+} blocked native HAEC currents with strong potency. Single channel analysis revealed two peaks of single channel conductances similar to those measured from heterologously expressed Kir2.1 and Kir2.2. Transfection with a dn-Kir2.1 subunit eliminated one of the two peaks.

Taken together, our results indicate that Kir2.1 and Kir2.2 contribute to native inward rectifier currents in HAECs and that Kir2.2 appears to be the predominant channel subunit.

XI-1.3.2 Potential Significance of Results in Context of the Literature

Very little data is available on the molecular composition of endogenous inward rectifier currents in ECs. The evaluation of ionic currents in ECs is made difficult by the ability of cultured ECs to condition their media and change their ion channel expression pattern in conditioned media (Nilius & Droogmans, 2001). In our system, current densities were similar in freshly isolated and low passage HAECs, supporting the relevance of the system. Previous studies have found only Kir2.1 to be expressed in ECs (Kamouchi *et al.*, 1997; Eschke *et al.*, 2002; Hoger *et al.*, 2002; Yang *et al.*, 2003a) and no inward rectifier currents have been detected in mouse or rabbit aortic endothelial cells (Rusko *et al.*, 1992).

Here we show that all four members of the Kir2 family, including Kir2.4, are expressed in HAECs. We found Kir2.2 and Kir2.1 to be the expressed on both the mRNA and protein level. Kir2.2 expression was prominent when assessed with biochemical or functional methods. Kir2.3 mRNA expression was low and no Kir2.3 protein was detected. Kir2.4 mRNA was abundant but Kir2.4 protein was not measured. Lack of pH dependence and high Ba^{2+} sensitivity of native HAEC current as well as lack of current suppression by a dn-Kir2.4 construct suggest that Kir2.4 homomeric channels do not play an important role in HAECs. However, the contribution of Kir2.4 subunits to heteromeric Kir2.2/Kir2.4 and Kir2.1/Kir2.4 channels can not be excluded.

In summary, our study is the first to demonstrate that all four Kir2 family members are expressed in HAECs and that native EC Kir current might be dominated by Kir2.2 channels.

XI-2 Potential Limitations

We have not included the evaluation of Kir2.1/Kir2.4 heteromultimers as potential contributors to cardiac I_{K1} in our publication. Kir2.4 mRNA expression has been shown in the heart by Northern blot analysis (Topert *et al.*, 1998). RT-PCR has revealed the presence of Kir2.4 in both human atrial and ventricular tissue and Ba^{2+} blocking properties of Kir2.1/Kir2.4 provided striking resemblance of human ventricular I_{K1} (Schram *et al.*, 2000a). In guinea pigs, Kir2.4 has been found in whole tissue but not in isolated myocytes and capillary fragments. Immunohistochemistry has revealed that in guinea pig cardiac tissue, Kir2.4 expression is limited to perikarya of local parsympathetic ganglia and axons (Liu *et al.*, 2001). Our results demonstrating Kir2.4 mRNA expression in human heart were obtained with non intron-spanning primers from whole tissue. Therefore it can not be excluded that we amplified Kir2.4 from cardiac neuronal tissue or genomic DNA. Species specific differences in subunit composition of cardiac I_{K1} are well recognized (Nakamura *et al.*, 1998; Wang *et al.*, 1998; Zaritsky *et al.*, 2001; Zobel *et al.*, 2003; Dhamoon *et al.*, 2004). Lack of Kir2.4 expression in guinea pig cardiomyocytes therefore does not exclude potential Kir2.4 expression in cardiomyocytes of other species. Zobel et al. reported incomplete I_{K1} current suppression in rabbit ventricular myocytes transfected with dn-Kir2.1 or dn-Kir2.2 subunits. Kir2.3 was not detected in these cells (Zobel *et al.*, 2003). Residual current could therefore be due to Kir2.4 conductance. However, Ba^{2+} sensitivity of residual currents was not compatible with Kir2.4 homomultimers. One might also expect that in the case of heteromeric Kir2 subunit assembly, Kir2.4 current would be suppressed by dn-Kir2.1 subunits (Schram *et al.*, 2002a). On the other hand, dn-Kir2.3 and dn-Kir2.4 subunits had no effect on endogenous HAEC currents (Fang *et al.*, 2005) while dn-Kir2.4 subunits resulted in suppression of Kir2.1 current when co-expressed in *Xenopus* oocytes (Schram *et al.*, 2002a). It therefore cannot be excluded that dominant negative subunits might have different effects on

currents in a native system than when they are co-expressed with functional Kir2 subunits in a heterologous expression system.

In summary, Kir2.4 expression in cardiomyocytes might explain certain experimental findings and future experiments on localization and quantity of Kir2.4 protein expression might delineate a role for Kir2.4 in cardiac tissue in different species. However, current data does not support a functional role of Kir2.4 in cardiomyocytes and we therefore did not include the possibility of Kir2.1/Kir2.4 heteromer formation in our analyses of human cardiac I_{K1}.

We have not recorded single channel conductances in both the Kir2.1/Kir2.4 co-expression study and the Kir2.1-3 heterotetramer study. Single-channel conductances are often measured and various Kir2.1-3 heteromultimeric channels were found to have single-channel conductances distinct from their homomeric constituents but similar to each other. Picones et al. have studied single channel conductances of Kir2.1 and reported multiple values ranging from 2-33 pS (Picones *et al.*, 2001). We therefore believe that single-channel analyses may not provide clear insight into the molecular composition of native inward rectifier channels and have thus not performed single channel analyses.

In the analyses of the molecular composition of inward rectifier K^+-conductance in endothelial cells, we have concluded that Kir2.4 is present on the transcriptional level but not functionally important. This conclusion was based on the lack of pH modulation, Ba^{2+} blocking properties, and lack of current suppression by transfection of native cells with a dn-Kir2.4 subunit. Our conclusion bears two major weaknesses: First, Kir2.4 protein was not measured. In order to prove that Kir2.4 is not translated into protein, the absence of such protein would have to be proven by western blot experiments. Second, our data evaluated only potential homomeric channel assembly and did not investigate the potential role of heteromeric Kir2 subunit channels in endothelial cells. The assumption that Kir2.2 is the major contributor to endothelial inward rectifier current is based on strong Kir2.2 mRNA and protein expression, most potent native current reduction by transfection with a dn-Kir2.2 subunit and a single channel conductance that is compatible with Kir2.2

and not affected by transfection with a dn-Kir2.1 subunit. The major single channel conductance and Ba^{2+} sensitivity of native cells we report in this study are compatible with values reported for Kir2.1-3 heteromultimers (Preisig-Muller *et al.*, 2002;Schram *et al.*, 2003). We can not exclude that heteromultimer formation of Kir2 subunits contributes to native Kir current in HAECs but the fact that dn-Kir2.3 and dn-Kir2.4 subunits did not suppress native current suggests that these subunits might not be functionally important. Potential formation of Kir2.1/Kir2.2 heteromultimers can not be assessed by methods used in this study.

XI-3 Future Directions

It is currently generally accepted, that only Kir2.1, Kir2.2 and Kir2.3 subunits are expressed in cardiac tissue. However, this assumption is based on one study only, who found restriction of Kir2.4 to neuronal tissue in guinea pig heart (Liu *et al.*, 2001). Inter-species variations in cardiac Kir subunit are well known (Dhamoon *et al.*, 2004) and reflected in functional studies (Nakamura *et al.*, 1998; Zaritsky *et al.*, 2001; Zobel *et al.*, 2003). In addition, members of the same group who reported the absence of Kir2.4 in cardiomyocytes now found far more widespread distribution of Kir2.4 in rat brain with newly designed antibodies targeted to the less well conserved Kir2 C-terminal and reported lack of sensitivity of their Kir2.4 antibody for previously reported low Kir2.4 protein expression in the brain (Pruss *et al.*, 2003; Pruss *et al.*, 2005). Growing evidence of an important physiological role of Kir2.4 in the brain (Pruss *et al.*, 2003; Pruss *et al.*, 2005) and the demonstration of Kir2.4 expression in non-neuronal tissues (Fang *et al.*, 2005) justifies a re-evaluation of the role of Kir2.4 in the heart in different species. Kir2.4 might be expressed in human cardiomyocytes as shown by RT-PCR and Ba^{2+} blocking properties of Kir2.1/Kir2.4 (Schram *et al.*, 2000a). In rabbit cardiomyocytes, sustained inward rectifier current after suppression of Kir2.1 and Kir2.2 might be attributable to Kir2.4 channels. Suggested experiments include screening for Kir2.4 mRNA with intron-spanning primers and western blot experiments in isolated single myocytes. Immunocytochemistry could demonstrate subcellular localization of Kir2.4 subunits and possible co-localization with other Kir2 subfamily members.

Substantial co-localization of Kir2.4 with other Kir2 family subunits is found in the brain (Pruss *et al.*, 2005). A particularly important subunit appears to be Kir2.2 (Pruss *et al.*, 2003; Pruss *et al.*, 2005). No data exists on functional Kir2.4 and Kir2.2 assembly. In the context of its potential physiological importance in the brain, co-assembly between Kir2.2 and Kir2.4 should be structurally and functionally investigated. Experiments to be performed include already established methods such as yeast two hybrid systems, functional evaluation of heterologously expressed chimeric Kir2.2/Kir2.4 constructs and channels resulting from co-expression of Kir2.2 and Kir2.4, co-expression of Kir2.4 with dn-Kir2.2 and vice versa, and co-precipitation of Kir2.2 and Kir2.4 from brain tissue. A Kir2.4 knockout model might provide insight into the physiological importance of Kir2.4 by showing functional consequences of its absence. However, extensive co-localization of Kir2 subunits in the brain might provide a "back-up" mechanism by which one Kir2 subunit might substitute the loss of another Kir2 subunit in the brain (Pruss *et al.*, 2003) thus diminishing the usefulness of a Kir2.4 knockout model.

Nothing is known about the structural changes occurring during Kir channel co-assembly. Regardless of their subunit composition, heteromeric Kir2 channels have higher Ba^{2+} sensitivity (with the exception of Kir2.2) and different time-dependence of block than their homomeric constituents (Preisig-Muller *et al.*, 2002; Schram *et al.*, 2002a; Schram *et al.*, 2003). Modeling studies could try to simulate the dynamics of channel co-assembly and provide insight into structural changes occurring during channel assembly and their functional consequences. A very interesting observation is that Ba^{2+} block of homomeric Kir2.4 channels is virtually voltage-independent. Mutation of S142 to a threonine, the corresponding amino acid in Kir2.1, Kir2.2 and Kir2.3, confers strong voltage-dependence of block as seen in the other Kir2 subfamily members (Herrera et al., 2006). S142 is located at the C-terminal end of the pore-helix. In general, K^+ channels have a highly conserved threonine at this position (Doyle *et al.*, 1998; Jiang *et al.*, 2002b; Jiang *et al.*, 2003a; Long *et al.*, 2005a) which is essential for stabilization of the K^+-ion in the central water filled cavity (Morais-Cabral *et al.*, 2001). A functional tetrameric channel would therefore have the carboxy terminals of four threonines pointing at the center

of the central cavity, coordinating the permeant ion. Heteromeric Kir2.1/Kir2.4 channels show strong voltage-dependence of block despite the fact that only two threonines are available to coordinate the permeating ion in the center of the water filled cavity. Obtaining a crystal structure of a heteromeric channel assembly would be of great interest because it would allow us to see structural changes underlying heterotetramer specific channel properties. Due to its unique biophysical properties, Kir2.4 would be an interesting candidate in such a heteromeric channel.

Kir2.4 western blots should be performed in HAECs to confirm the absence of Kir2.4 protein. The absence of native current suppression in HAECs by dn-Kir2.4 is surprising since dn-Kir2.4 suppresses Kir2.1 current when heterologously expressed in *Xenopus* oocytes (Schram *et al.*, 2002a). A possible explanation could be that heteromerization of Kir2 channels somehow "rescues" or "protects" the channel protein from defective ion channel subunits. A similar concept has been suggested by Pruss et al. in brain tissue, where extensive differential co-localization of Kir2 subunits might account for formation of heteromeric Kir2 channels "rescuing" native inward rectifier current in Andersen's syndrome, where mutations of Kir2.1 suppress native Kir current in a dominant negative fashion (Preisig-Muller *et al.*, 2002; Pruss *et al.*, 2003). This hypothesis would be difficult to prove but heterologous co-expression of a Kir2.1/Kir2.4 chimeric construct with Kir2.1 and dn-Kir2.4 may represent an experimental approach. Further necessary experiments to investigate the role of heterotetramers in HAECs include co-precipitation of Kir2 subunits from HAECs. Immunocytochemistry would be helpful to determine the subcellular localization of Kir2 subunits. Another approach to evaluate the functional role of distinct Kir2 subunits is the application of si-RNA. Kir2.1 and Kir2.2 knockout models exists (Zaritsky *et al.*, 2000; Zaritsky *et al.*, 2001), however, might not represent a good model for investigation of Kir2 subunits in MAEC due to the lack of inward rectifier currents in freshly isolated cells from mice indicating inter-species differences in Kir expression (Rusko J., *et al.* 1992).

XI-4 Conclusions

We have investigated the molecular basis of inward rectifier current in different biological systems and examined the potential role of Kir2 heterotetramers. Kir2.1 associates with Kir2.4 subunits to form functional heteromeric channels with Ba^{2+}-blocking properties different from those of homomeric channels. Heteromeric assembly of Kir2.1/Kir2.4 channels might be functionally important in the brain where significant co-localization of Kir2 subunits occurs. Heteromeric Kir2 channels consisting of Kir2.1-3 subunits have Ba^{2+} blocking properties resembling human cardiac I_{K1}, supporting the notion that native I_{K1} may at least partly result from heteromultimer formation among Kir2 subunits. All four Kir2 family members are expressed in human aortic endothelial cells but only Kir2.1 and Kir2.2 seem to be functionally important. Based upon biophysical properties, Kir2.2 appears to be the dominant conductance in these cells.

Taken together, our results suggest that formation of heteromeric Kir2 channels may represent a common physiological mechanism to achieve diversity of functionally distinct inward rectifier channels, specifically tailored to adjust Kir2 channel function to distinct physiological requirements in distinct tissues. The relative importance of different Kir2 subunits might differ between tissues.

CHAPTER XII: REFERENCES.

Abbott, G. W., Butler, M. H., Bendahhou, S., Dalakas, M. C., Ptacek, L. J., & Goldstein, S. A. (2001). MiRP2 forms potassium channels in skeletal muscle with Kv3.4 and is associated with periodic paralysis. *Cell* **104**, 217-231.

Abbott, G. W., Sesti, F., Splawski, I., Buck, M. E., Lehmann, M. H., Timothy, K. W., Keating, M. T., & Goldstein, S. A. (1999). MiRP1 forms I_{Kr} potassium channels with HERG and is associated with cardiac arrhythmia. *Cell* **97**, 175-187.

Abraham, M. R., Jahangir, A., Alekseev, A. E., & Terzic, A. (1999). Channelopathies of inwardly rectifying potassium channels. *FASEB J.* **13**, 1901-1910.

Adams, D. J. & Hill, M. A. (2004). Potassium channels and membrane potential in the modulation of intracellular calcium in vascular endothelial cells. *J. Cardiovasc. Electrophysiol.* **15**, 598-610.

Adelbrecht, C., Murer, M. G., Lauritzen, I., Lesage, F., Ladzunski, M., Agid, Y., & Raisman-Vozari, R. (1997). An immunocytochemical study of a G-protein-gated inward rectifier K^+ channel (GIRK2) in the weaver mouse mesencephalon. *Neuroreport* **8**, 969-974.

Aggarwal, S. K. & MacKinnon, R. (1996). Contribution of the S4 segment to gating charge in the Shaker K^+ channel. *Neuron* **16**, 1169-1177.

Aguilar-Bryan, L., Nichols, C. G., Wechsler, S. W., Clement, J. P., Boyd, A. E., III, Gonzalez, G., Herrera-Sosa, H., Nguy, K., Bryan, J., & Nelson, D. A. (1995). Cloning of the beta cell high-affinity sulfonylurea receptor: a regulator of insulin secretion. *Science* **268**, 423-426.

Akao, M., Otani, H., Horie, M., Takano, M., Kuniyasu, A., Nakayama, H., Kouchi, I., Murakami, T., & Sasayama, S. (1997). Myocardial ischemia induces differential regulation of KATP channel gene expression in rat hearts. *J. Clin. Invest* **100**, 3053-3059.

Akselrod, S., Gordon, D., Ubel, F. A., Shannon, D. C., Berger, A. C., & Cohen, R. J. (1981). Power spectrum analysis of heart rate fluctuation: a quantitative probe of beat-to-beat cardiovascular control. *Science* **213**, 220-222.

Alagem, N., Dvir, M., & Reuveny, E. (2001). Mechanism of Ba^{2+} block of a mouse inwardly rectifying K^+ channel: differential contribution by two discrete residues. *J. Physiol.* **534**, 381-393.

Allard, B., Lazdunski, M., & Rougier, O. (1995). Activation of ATP-dependent K^+ channels by metabolic poisoning in adult mouse skeletal muscle: role of intracellular Mg^{2+} and pH. *J. Physiol.* **485**, 283-296.

Allen, T. W., Andersen, O. S., & Roux, B. (2004). On the importance of atomic fluctuations, protein flexibility, and solvent in ion permeation. *J. Gen. Physiol.* **124**, 679-690.

Allen, T. W., Bliznyuk, A., Rendell, A. P., Kyuucak, S., & Chung, S. H. (2000). The potassium channel: Structure, selectivity and diffusion. *J. Chem. Phys.* **112**, 8191-8204.

Allen, T. W. & Chung, S. H. (2001). Brownian dynamics study of an open-state KcsA potassium channel. *Biochim. Biophys. Acta* **1515**, 83-91.

An, W. F., Bowlby, M. R., Betty, M., Cao, J., Ling, H. P., Mendoza, G., Hinson, J. W., Mattsson, K. I., Strassle, B. W., Trimmer, J. S., & Rhodes, K. J. (2000). Modulation of A-type potassium channels by a family of calcium sensors. *Nature* **403**, 553-556.

Anantharam, A. & Abbott, G. W. (2005). Does hERG coassemble with a beta subunit? Evidence for roles of MinK and MiRP1. *Novartis Found. Symp.* **266**, 100-112.

Angus, J. A. (1996). Role of the endothelium in the genesis of cardiovascular disease. *Clin. Exp. Pharmacol.Physiol.* **23**, S16-22.

Antcliff, J. F., Haider, S., Proks, P., Sansom, M. S., & Ashcroft, F. M. (2005). Functional analysis of a structural model of the ATP-binding site of the K_{ATP} channel Kir6.2 subunit. *EMBO J.* **24**, 229-239.

Antzelevitch, C. & Sicouri, S. (1994). Clinical relevance of cardiac arrhythmias generated by afterdepolarizations. Role of M cells in the generation of U waves, triggered activity and torsade de pointes. *J. Am. Coll. Cardiol.* **23**, 259-277.

Antzelevitch, C., Sicouri, S., Litovsky, S. H., Lukas, A., Krishnan, S. C., Di Diego, J. M., Gintant, G. A., & Liu, D. W. (1991). Heterogeneity within the ventricular wall. Electrophysiology and pharmacology of epicardial, endocardial, and M cells. *Circ. Res.* **69**, 1427-1449.

Apkon, M. & Nerbonne, J. M. (1991). Characterization of two distinct depolarization-activated K^+ currents in isolated adult rat ventricular myocytes. *J. Gen. Physiol.* **97**, 973-1011.

Aqvist, J. & Luzhkov, V. (2000). Ion permeation mechanism of the potassium channel. *Nature* **404**, 881-884.

Armstrong, C. M. (1969). Inactivation of the potassium conductance and related phenomena caused by quaternary ammonium ion injection in squid axons. *J. Gen. Physiol.* **54**, 553-575.

Armstrong, C. M. (1971). Interaction of tetraethylammonium ion derivatives with the potassium channels of giant axons. *J. Gen. Physiol.* **58**, 413-437.

Armstrong, C. M. & Bezanilla, F. (1974). Charge movement associated with the opening and closing of the activation gates of the Na channels. *J. Gen. Physiol.* **63**, 533-552.

Armstrong, C. M., and S. R. Taylor. (1980). Interaction of barium ions with potassium channels in squid giant axons. *Biophys. J.* **30**, 473-488.

Asano, Y., Davidenko, J. M., Baxter, W. T., Gray, R. A., & Jalife, J. (1997). Optical mapping of drug-induced polymorphic arrhythmias and torsade de pointes in the isolated rabbit heart. *J. Am. Coll. Cardiol.* **29**, 831-842.

Ashcroft, F. M. (1988). Adenosine 5'-triphosphate-sensitive potassium channels. *Annu. Rev. Neurosci.* **11**, 97-118.

Ashcroft, F. M. & Gribble, F. M. (2000a). New windows on the mechanism of action of K_{ATP} channel openers. *Trends Pharmacol. Sci.* **21**, 439-445.

Ashcroft, F. M. & Gribble, F. M. (2000b). Tissue-specific effects of sulfonylureas: lessons from studies of cloned K_{ATP} channels. *J. Diabetes Complications* **14**, 192-196.

Ashcroft, F. M. & Rorsman, P. (1989). Electrophysiology of the pancreatic beta-cell. *Prog. Biophys. Mol. Biol.* **54**, 87-143.

Ashcroft, S. J. & Ashcroft, F. M. (1990). Properties and functions of ATP-sensitive K^+ channels. *Cell Signal.* **2**, 197-214.

Ashfield, R., Gribble, F. M., Ashcroft, S. J., & Ashcroft, F. M. (1999). Identification of the high-affinity tolbutamide site on the SUR1 subunit of the K_{ATP} channel. *Diabetes* **48**, 1341-1347.

Ashford, M. L., Boden, P. R., & Treherne, J. M. (1990). Glucose-induced excitation of hypothalamic neurones is mediated by ATP-sensitive K^+ channels. *Pflugers Arch.* **415**, 479-483.

Babenko, A. P., Aguilar-Bryan, L., & Bryan, J. (1998). A view of sur/KIR6.X, K_{ATP} channels. *Annu. Rev. Physiol.* **60**, 667-687.

Babenko, A. P., Gonzalez, G., & Bryan, J. (1999a). The tolbutamide site of SUR1 and a mechanism for its functional coupling to K_{ATP} channel closure. *FEBS Lett.* **459**, 367-376.

Babenko, A. P., Gonzalez, G., & Bryan, J. (1999b). Two regions of sulfonylurea receptor specify the spontaneous bursting and ATP inhibition of K_{ATP} channel isoforms. *J. Biol. Chem.* **274**, 11587-11592.

Badou, A., Basavappa, S., Desai, R., Peng, Y. Q., Matza, D., Mehal, W. Z., Kaczmarek, L. K., Boulpaep, E. L., & Flavell, R. A. (2005). Requirement of voltage-gated calcium channel beta4 subunit for T lymphocyte functions. *Science* **307**, 117-121.

Bahring, R., Dannenberg, J., Peters, H. C., Leicher, T., Pongs, O., & Isbrandt, D. (2001). Conserved Kv4 N-terminal domain critical for effects of Kv channel-interacting protein 2.2 on channel expression and gating. *J. Biol. Chem.* **276**, 23888-23894.

Baker, O. S., Larsson, H. P., Mannuzzu, L. M., & Isacoff, E. Y. (1998). Three transmembrane conformations and sequence-dependent displacement of the S4 domain in shaker K^+ channel gating. *Neuron* **20**, 1283-1294.

Baranauskas, G., Tkatch, T., Nagata, K., Yeh, J. Z., & Surmeier, D. J. (2003). Kv3.4 subunits enhance the repolarizing efficiency of Kv3.1 channels in fast-spiking neurons. *Nat. Neurosci.* **6**, 258-266.

Barhanin, J., Lesage, F., Guillemare, E., Fink, M., Lazdunski, M., & Romey, G. (1996). KvLQT1 and lsK (minK) proteins associate to form the I_{Ks} cardiac potassium current. *Nature* **384**, 78-80.

Barry, D. M. & Nerbonne, J. M. (1996). Myocardial potassium channels: electrophysiological and molecular diversity. *Annu. Rev. Physiol.* **58**, 363-394.

Barry, D. M., Trimmer, J. S., Merlie, J. P., & Nerbonne, J. M. (1995). Differential expression of voltage-gated K^+ channel subunits in adult rat heart. Relation to functional K^+ channels? *Circ. Res.* **77**, 361-369.

Barry, D. M., Xu, H., Schuessler, R. B., & Nerbonne, J. M. (1998). Functional knockout of the transient outward current, long-QT syndrome, and cardiac remodeling in mice expressing a dominant-negative Kv4 alpha subunit. *Circ. Res.* **83**, 560-567.

Bass, R. B., Strop, P., Barclay, M., & Rees, D. C. (2002). Crystal structure of Escherichia coli MscS, a voltage-modulated and mechanosensitive channel. *Science* **298**, 1582-1587.

Baukrowitz, T., Schulte, U., Oliver, D., Herlitze, S., Krauter, T., Tucker, S. J., Ruppersberg, J. P., & Fakler, B. (1998). PIP_2 and PIP as determinants for ATP inhibition of K_{ATP} channels. *Science* **282**, 1141-1144.

Bausch, S. B., Patterson, T. A., Ehrengruber, M. U., Lester, H. A., Davidson, N., & Chavkin, C. (1995). Colocalization of mu opioid receptors with GIRK1 potassium channels in the rat brain: an immunocytochemical study. *Receptors Channels* **3**, 221-241.

Beech, D. J., Zhang, H., Nakao, K., & Bolton, T. B. (1993). K^+ channel activation by nucleotide diphosphates and its inhibition by glibenclamide in vascular smooth muscle cells. *Br. J. Pharmacol.* **110**, 573-582.

Beeler, G. W., Jr. & Reuter, H. (1970). Voltage clamp experiments on ventricular myocarial fibres. *J. Physiol.* **207**, 165-190.

Bekkers, J. M. (2000). Distribution and activation of voltage-gated potassium channels in cell-attached and outside-out patches from large layer 5 cortical pyramidal neurons of the rat. *J. Physiol.* **525 Pt 3**, 611-620.

Bender, K., Wellner-Kienitz, M. C., Inanobe, A., Meyer, T., Kurachi, Y., & Pott, L. (2001). Overexpression of monomeric and multimeric GIRK4 subunits in rat atrial myocytes removes fast desensitization and reduces inward rectification of muscarinic K^+ current (I_{KACh}). Evidence for functional homomeric GIRK4 channels. *J. Biol. Chem.* **276**, 28873-28880.

Benians, A., Leaney, J. L., Milligan, G., & Tinker, A. (2003). The dynamics of formation and action of the ternary complex revealed in living cells using a G-protein-gated K^+ channel as a biosensor. *J. Biol. Chem.* **278**, 10851-10858.

Berneche, S. & Roux, B. (2000). Molecular dynamics of the KcsA K^+ channel in a bilayer membrane. *Biophys. J.* **78**, 2900-2917.

Berneche, S. & Roux, B. (2001). Energetics of ion conduction through the K^+ channel. *Nature* **414**, 73-77.

Berneche, S. & Roux, B. (2003). A microscopic view of ion conduction through the K^+ channel. *Proc. Natl. Acad. Sci. U.S.A.* **100**, 8644-8648.

Berneche, S. & Roux, B. (2005). A gate in the selectivity filter of potassium channels. *Structure. (Camb.)* **13**, 591-600.

Bernstein, J. (1902). Untersuchungen zur Thermodynamik der elektrischen Stroeme. Erster Theil. *Pflugers Arch.* **92**, 521-562.

Bernstein, J. (1912). *Elektrobiologie* Vieweg, Braunschweig.

Bettahi, I., Marker, C. L., Roman, M. I., & Wickman, K. (2002). Contribution of the Kir3.1 subunit to the muscarinic-gated atrial potassium channel I_{KACh}. *J. Biol. Chem.* **277**, 48282-48288.

Beuckelmann, D. J., Nabauer, M., & Erdmann, E. (1993). Alterations of K^+ currents in isolated human ventricular myocytes from patients with terminal heart failure. *Circ. Res.* **73**, 379-385.

Bezanilla, F. (2000). The voltage sensor in voltage-dependent ion channels. *Physiol. Rev.* **80**, 555-592.

Bezanilla, F. (2002). Voltage sensor movements. *J. Gen. Physiol.* **120**, 465-473.

Bichet, D., Haass, F. A., & Jan, L. Y. (2003). Merging functional studies with structures of inward-rectifier K^+ channels. *Nat. Rev. Neurosci.* **4**, 957-967.

Biermans, G., Vereecke, J. & Carmeliet, E. (1987). The mechanism of the inactivation of the inward-rectifying K^+ current during hyperpolarizing steps in guinea-pig ventricular myocytes. *Pflugers Arch.* **410**, 604–613.

Biggin, P. C., Smith, G. R., Shrivastava, I., Choe, S., & Sansom, M. S. (2001). Potassium and sodium ions in a potassium channel studied by molecular dynamics simulations. *Biochim. Biophys. Acta.* **1510**, 1-9.

Billette, J. (1987). Atrioventricular nodal activation during periodic premature stimulation of the atrium. *Am. J. Physiol.* **252**, H163-177.

Birch, K. A., Pober, J. S., Zavoico, G. B., Means, A. R., & Ewenstein, B. M. (1992). Calcium/calmodulin transduces thrombin-stimulated secretion: studies in intact and minimally permeabilized human umbilical vein endothelial cells. *J. Cell Biol.* **118**, 1501-1510.

Bischofberger, J., Geiger, J. R., & Jonas, P. (2002). Timing and efficacy of Ca^{2+} channel activation in hippocampal mossy fiber boutons. *J. Neurosci.* **22**, 10593-10602.

Bkaily, G., d'Orleans-Juste, P., Naik, R., Perodin, J., Stankova, J., Abdulnour, E., & Rola-Pleszczynski, M. (1993). PAF activation of a voltage-gated R-type Ca^{2+} channel in human and canine aortic endothelial cells. *Br. J. Pharmacol.* **110**, 519-520.

Blaine, J. T. & Ribera, A. B. (1998). Heteromultimeric potassium channels formed by members of the Kv2 subfamily. *J. Neurosci.* **18**, 9585-9593.

Bleeker, W. K., Mackaay, A. J., Masson-Pevet, M., Bouman, L. N., & Becker, A. E. (1980). Functional and morphological organization of the rabbit sinus node. *Circ. Res.* **46**, 11-22.

Blondeau, N., Plamondon, H., Richelme, C., Heurteaux, C., & Lazdunski, M. (2000). K_{ATP} channel openers, adenosine agonists and epileptic preconditioning are stress signals inducing hippocampal neuroprotection. *Neuroscience* **100**, 465-474.

Boim, M. A., Ho, K., Shuck, M. E., Bienkowski, M. J., Block, J. H., Slightom, J. L., Yang, Y., Brenner, B. M., & Hebert, S. C. (1995). ROMK inwardly rectifying ATP-sensitive K^+ channel. II. Cloning and distribution of alternative forms. *Am. J. Physiol.* **268**, F1132-1140.

Bond, C. T., Pessia, M., Xia, X. M., Lagrutta, A., Kavanaugh, M. P., & Adelman, J. P. (1994). Cloning and expression of a family of inward rectifier potassium channels. *Receptors.Channels* **2**, 183-191.

Born, G., Rabelink, T., & Smith, T. (1998). *Endothelium and Cardiovascular Disease* Science Press, London.

Born, G. V. R. & Schwartz, C. J. (1997). *Vascular endothelium: Physiology, pathology and therapeutics.* Schatthauer Verlag, Stuttgart, Germany.

Bosch, R. F., Gaspo, R., Busch, A. E., Lang, H. J., Li, G. R., & Nattel, S. (1998). Effects of the chromanol 293B, a selective blocker of the slow, component of the delayed rectifier K^+ current, on repolarization in human and guinea pig ventricular myocytes. *Cardiovasc. Res.* **38**, 441-450.

Bossu, J. L., Elhamdani, A., & Feltz, A. (1992a). Voltage-dependent calcium entry in confluent bovine capillary endothelial cells. *FEBS Lett.* **299**, 239-242.

Bossu, J. L., Elhamdani, A., Feltz, A., Tanzi, F., Aunis, D., & Thierse, D. (1992b). Voltage-gated Ca entry in isolated bovine capillary endothelial cells: evidence of a new type of BAY K 8644-sensitive channel. *Pflugers Arch.* **420**, 200-207.

Bossu, J. L., Feltz, A., Rodeau, J. L., & Tanzi, F. (1989). Voltage-dependent transient calcium currents in freshly dissociated capillary endothelial cells. *FEBS Lett.* **255**, 377-380.

Bou-Abboud, E., Li, H., & Nerbonne, J. M. (2000). Molecular diversity of the repolarizing voltage-gated K^+ currents in mouse atrial cells. *J. Physiol.* **529**, 345-358.

Bou-Abboud, E. & Nerbonne, J. M. (1999). Molecular correlates of the calcium-independent, depolarization-activated K^+ currents in rat atrial myocytes. *J.Physiol.* **517**, 407-420.

Boyett, M. R., Kirby, M. S., Orchard, C. H., & Roberts, A. (1988). The negative inotropic effect of acetylcholine on ferret ventricular myocardium. *J. Physiol.* **404**, 613-635.

Boyle, W. A. & Nerbonne, J. M. (1991). A novel type of depolarization-activated K^+ current in isolated adult rat atrial myocytes. *Am. J. Physiol.* **260**, H1236-1247.

Brahmajothi, M. V., Campbell, D. L., Rasmusson, R. L., Morales, M. J., Trimmer, J. S., Nerbonne, J. M., & Strauss, H. C. (1999). Distinct transient outward potassium current (I_{to}) phenotypes and distribution of fast-inactivating potassium channel alpha subunits in ferret left ventricular myocytes. *J. Gen. Physiol.* **113**, 581-600.

Brahmajothi, M. V., Morales, M. J., Liu, S. G., Rasmusson, R. L., Campbell, D. L., & Strauss, H. C. (1996). In situ hybridization reveals extensive diversity of K^+ channel mRNA in isolated ferret cardiac myocytes. *Circ. Res.* **78**, 1083-1089.

Brahmajothi, M. V., Morales, M. J., Rasmusson, R. L., Campbell, D. L., & Strauss, H. C. (1997a). Heterogeneity in K^+ channel transcript expression detected in isolated ferret cardiac myocytes. *Pacing Clin. Electrophysiol.* **20**, 388-396.

Brahmajothi, M. V., Morales, M. J., Reimer, K. A., & Strauss, H. C. (1997b). Regional localization of ERG, the channel protein responsible for the rapid component of the delayed rectifier K^+ current in the ferret heart. *Circ. Res.* **81**, 128-135.

Bredt, D. S., Wang, T. L., Cohen, N. A., Guggino, W. B., & Snyder, S. H. (1995). Cloning and expression of two brain-specific inwardly rectifying potassium channels. *Proc. Natl. Acad. Sci.U.S.A.* **92**, 6753-6757.

Breitwieser, G. E. & Szabo, G. (1985). Uncoupling of cardiac muscarinic and beta-adrenergic receptors from ion channels by a guanine nucleotide analogue. *Nature* **317**, 538-540.

Breitwieser, G. E. & Szabo, G. (1988). Mechanism of muscarinic receptor-induced K^+ channel activation as revealed by hydrolysis-resistant GTP analogues. *J. Gen. Physiol.* **91**, 469-493.

Brismar, T. & Collins, V. P. (1989). Inward rectifying potassium channels in human malignant glioma cells. *Brain Res.* **480**, 249-258.

Broadhead, M. W., Kharbanda, R. K., Peters, M. J., & MacAllister, R. J. (2004). K_{ATP} channel activation induces ischemic preconditioning of the endothelium in humans in vivo. *Circulation* **110**, 2077-2082.

Brown, D. A., Gahwiler, B. H., Griffith, W. H., & Halliwell, J. V. (1990). Membrane currents in hippocampal neurons. *Prog. Brain Res.* **83**, 141-160.

Browne, D. L., Gancher, S. T., Nutt, J. G., Brunt, E. R., Smith, E. A., Kramer, P., & Litt, M. (1994). Episodic ataxia/myokymia syndrome is associated with point mutations in the human potassium channel gene, KCNA1. *Nat. Genet.* **8**, 136-140.

Bruggemann, A., Pardo, L. A., Stuhmer, W., & Pongs, O. (1993). Ether-a-go-go encodes a voltage-gated channel permeable to K^+ and Ca^{2+} and modulated by cAMP. *Nature* **365**, 445-448.

Bryant, S. M., Wan, X., Shipsey, S. J., & Hart, G. (1998). Regional differences in the delayed rectifier current (I_{Kr} and I_{Ks}) contribute to the differences in action potential duration in basal left ventricular myocytes in guinea-pig. *Cardiovasc. Res.* **40**, 322-331.

Burgen, A. S. & Terroux, K. G. (1953). On the negative inotropic effect in the cat's auricle. *J. Physiol.* **120**, 449-464.

Busch, A. E., Eigenberger, B., Jurkiewicz, N. K., Salata, J. J., Pica, A., Suessbrich, H., & Lang, F. (1998). Blockade of HERG channels by the class III antiarrhythmic azimilide: mode of action. *Br. J. Pharmacol.* **123**, 23-30.

Busch, A. E., Suessbrich, H., Waldegger, S., Sailer, E., Greger, R., Lang, H., Lang, F., Gibson, K. J., & Maylie, J. G. (1996). Inhibition of I_{Ks} in guinea pig cardiac myocytes and guinea pig IsK channels by the chromanol 293B. *Pflugers Arch.* **432**, 1094-1096.

Butler, A., Wei, A. G., Baker, K., & Salkoff, L. (1989). A family of putative potassium channel genes in Drosophila. *Science* **243**, 943-947.

Bywater, R. A., Campbell, G. D., Edwards, F. R., & Hirst, G. D. (1990). Effects of vagal stimulation and applied acetylcholine on the arrested sinus venosus of the toad. *J. Physiol.* **425**, 1-27.

Caballero, R., Pourrier, M., Schram, G., Delpon, E., Tamargo, J., & Nattel, S. (2003). Effects of flecainide and quinidine on Kv4.2 currents: voltage dependence and role of S6 valines. *Br. J. Pharmacol.* **138**, 1475-1484.

Callewaert, G., Carmeliet, E., & Vereecke, J. (1984). Single cardiac Purkinje cells: general electrophysiology and voltage- clamp analysis of the pace-maker current. *J. Physiol.* **349**, 643-661.

Cannon, R. O., III (1998). Role of nitric oxide in cardiovascular disease: focus on the endothelium. *Clin. Chem.* **44**, 1809-1819.

Capener, C. E., Proks, P., Ashcroft, F. M., & Sansom, M. S. (2003). Filter flexibility in a mammalian K^+ channel: models and simulations of Kir6.2 mutants. *Biophys. J.* **84**, 2345-2356.

Carmeliet, E. (1977). Repolarisation and frequency in cardiac cells. *J. Physiol. (Paris)* **73**, 903-923.

Carmeliet, E. (1992). Voltage- and time-dependent block of the delayed K^+ current in cardiac myocytes by dofetilide. *J. Pharmacol. Exp. Ther.* **262**, 809-817.

Carmeliet, E. (1993). K^+ channels and control of ventricular repolarization in the heart. *Fundam. Clin. Pharmacol.* **7**, 19-28.

Carmeliet, E. & Mubagwa, K. (1986). Characterization of the acetylcholine-induced potassium current in rabbit cardiac Purkinje fibres. *J. Physiol.* **371**, 219-237.

Cha, A., Snyder, G. E., Selvin, P. R., & Bezanilla, F. (1999). Atomic scale movement of the voltage-sensing region in a potassium channel measured via spectroscopy. *Nature* **402**, 809-813.

Chanchevalap, S., Yang, Z., Cui, N., Qu, Z., Zhu, G., Liu, C., Giwa, L. R., Abdulkadir, L., & Jiang, C. (2000). Involvement of histidine residues in proton sensing of ROMK1 channel. *J. Biol. Chem.* **275**, 7811-7817.

Chandy, K. G. (1991). Simplified gene nomenclature. *Nature* **352**, 26.

Chandy, K. G. & Gutman, G. A. (1993). Nomenclature for mammalian potassium channel genes. *Trends Pharmacol. Sci.* **14**, 434.

Chang, G., Spencer, R. H., Lee, A. T., Barclay, M. T., & Rees, D. C. (1998). Structure of the MscL homolog from Mycobacterium tuberculosis: a gated mechanosensitive ion channel. *Science* **282**, 2220-2226.

Chatterjee, S., Al Mehdi, A. B., Levitan, I., Stevens, T., & Fisher, A. B. (2003). Shear stress increases expression of a K_{ATP} channel in rat and bovine pulmonary vascular endothelial cells. *Am. J. Physiol. Cell Physiol.* **285**, C959-967.

Chen, F., Wetzel, G. T., Friedman, W. F., & Klitzner, T. S. (1991). Single-channel recording of inwardly rectifying potassium currents in developing myocardium. *J. Mol. Cell. Cardiol.* **23**, 259-267.

Chen, S. C., Ehrhard, P., Goldowitz, D., & Smeyne, R. J. (1997). Developmental expression of the GIRK family of inward rectifying potassium channels: implications for abnormalities in the weaver mutant mouse. *Brain Res.* **778**, 251-264.

Cheng, J., Kamiya, K., Liu, W., Tsuji, Y., Toyama, J., & Kodama, I. (1999). Heterogeneous distribution of the two components of delayed rectifier K^+ current: a potential mechanism of the proarrhythmic effects of methanesulfonanilideclass III agents. *Cardiovasc. Res.* **43**, 135-147.

Chittajallu, R., Chen, Y., Wang, H., Yuan, X., Ghiani, C. A., Heckman, T., McBain, C. J., & Gallo, V. (2002). Regulation of Kv1 subunit expression in oligodendrocyte progenitor cells and their role in G1/S phase progression of the cell cycle. *Proc. Natl. Acad. Sci. U.S.A.* **99**, 2350-2355.

Choi, B. R., Liu, T., & Salama, G. (2001). The distribution of refractory periods influences the dynamics of ventricular fibrillation. *Circ. Res.* **88**, E49-E58.

Chutkow, W. A., Makielski, J. C., Nelson, D. J., Burant, C. F., & Fan, Z. (1999). Alternative splicing of sur2 Exon 17 regulates nucleotide sensitivity of the ATP-sensitive potassium channel. *J. Biol. Chem.* **274**, 13656-13665.

Chutkow, W. A., Pu, J., Wheeler, M. T., Wada, T., Makielski, J. C., Burant, C. F., & McNally, E. M. (2002). Episodic coronary artery vasospasm and hypertension develop in the absence of Sur2 K_{ATP} channels. *J.Clin.Invest.* **110**, 203-208.

Chutkow, W. A., Simon, M. C., Le Beau, M. M., & Burant, C. F. (1996). Cloning, tissue expression, and chromosomal localization of SUR2, the putative drug-binding subunit of cardiac, skeletal muscle, and vascular K_{ATP} channels. *Diabetes* **45**, 1439-1445.

Clancy, S. M., Fowler, C. E., Finley, M., Suen, K. F., Arrabit, C., Berton, F., Kosaza, T., Casey, P. J., & Slesinger, P. A. (2005). Pertussis-toxin-sensitive Galpha subunits selectively bind to C-terminal domain of neuronal GIRK channels: evidence for a heterotrimeric G-protein-channel complex. *Mol. Cell Neurosci.* **28**, 375-389.

Clapham, D. E. (1994). Direct G protein activation of ion channels? *Annu. Rev. Neurosci.* **17**, 441-464.

Clapham, D. E. & Neer, E. J. (1997). G protein beta gamma subunits. *Annu. Rev. Pharmacol. Toxicol.* **37**, 167-203.

Clark, J. D., Schievella, A. R., Nalefski, E. A., & Lin, L. L. (1995). Cytosolic phospholipase A2. *J. Lipid Mediat. Cell Signal.* **12**, 83-117.

Clark, R. B., Giles, W. R., & Imaizumi, Y. (1988). Properties of the transient outward current in rabbit atrial cells. *J. Physiol.* **405**, 147-168.

Clement, J. P., Kunjilwar, K., Gonzalez, G., Schwanstecher, M., Panten, U., Aguilar-Bryan, L., & Bryan, J. (1997). Association and stoichiometry of K_{ATP} channel subunits. *Neuron* **18**, 827-838.

Clemo, H. F. & Belardinelli, L. (1986). Effect of adenosine on atrioventricular conduction. I: Site and characterization of adenosine action in the guinea pig atrioventricular node. *Circ. Res.* **59**, 427-436.

Codina, J., Yatani, A., Grenet, D., Brown, A. M., & Birnbaumer, L. (1987). The alpha subunit of the GTP binding protein Gk opens atrial potassium channels. *Science* **236**, 442-445.

Coetzee, W. A., Amarillo, Y., Chiu, J., Chow, A., Lau, D., McCormack, T., Moreno, H., Nadal, M. S., Ozaita, A., Pountney, D., Saganich, M., Vega-Saenz, d. M., & Rudy, B. (1999). Molecular diversity of K^+ channels. *Ann. N. Y. Acad. Sci.* **868**, 233-285.

Cohen, N. A., Brenman, J. E., Snyder, S. H., & Bredt, D. S. (1996). Binding of the inward rectifier K^+ channel Kir 2.3 to PSD-95 is regulated by protein kinase A phosphorylation. *Neuron* **17**, 759-767.

Conti, L. R., Radeke, C. M., Shyng, S. L., & Vandenberg, C. A. (2001). Transmembrane topology of the sulfonylurea receptor SUR1. *J. Biol. Chem.* **276**, 41270-41278.

Cooper, E. C., Milroy, A., Jan, Y. N., Jan, L. Y., & Lowenstein, D. H. (1998). Presynaptic localization of Kv1.4-containing A-type potassium channels near excitatory synapses in the hippocampus. *J. Neurosci.* **18**, 965-974.

Coppen, S. R., Kodama, I., Boyett, M. R., Dobrzynski, H., Takagishi, Y., Honjo, H., Yeh, H. I., & Severs, N. J. (1999). Connexin45, a major connexin of the rabbit sinoatrial node, is co-expressed with connexin43 in a restricted zone at the nodal-crista terminalis border. *J. Histochem. Cytochem.* **47**, 907-918.

Coraboeuf, E. & Carmeliet, E. (1982). Existence of two transient outward currents in sheep cardiac Purkinje fibers. *Pflugers Arch.* **392**, 352-359.

Cordeiro, J. M., Spitzer, K. W., & Giles, W. R. (1998). Repolarizing K^+ currents in rabbit heart Purkinje cells. *J. Physiol.* **508**, 811-823.

Corey, S. & Clapham, D. E. (1998). Identification of native atrial G-protein-regulated inwardly rectifying K^+ (GIRK4) channel homomultimers. *J. Biol. Chem.* **273**, 27499-27504.

Cortes, D. M., Cuello, L. G., & Perozo, E. (2001). Molecular architecture of full-length KcsA: role of cytoplasmic domains in ion permeation and activation gating. *J. Gen. Physiol.* **117**, 165-180.

Courtemanche, M., Ramirez, R. J., & Nattel, S. (1998). Ionic mechanisms underlying human atrial action potential properties: insights from a mathematical model. *Am. J. Physiol.* **275**, H301-321.

Crawford, R. M., Jovanovic, S., Budas, G. R., Davies, A. M., Lad, H., Wenger, R. H., Robertson, K. A., Roy, D. J., Ranki, H. J., & Jovanovic, A. (2003). Chronic mild hypoxia protects heart-derived H9c2 cells against acute hypoxia/reoxygenation by regulating expression of the SUR2A subunit of the ATP-sensitive K^+ channel. *J. Biol. Chem.* **278**, 31444-31455.

Cuello, L. G., Cortes, D. M., & Perozo, E. (2004). Molecular architecture of the KvAP voltage-dependent K^+ channel in a lipid bilayer. *Science* **306**, 491-495.

Curran, M. E., Splawski, I., Timothy, K. W., Vincent, G. M., Green, E. D., & Keating, M. T. (1995). A molecular basis for cardiac arrhythmia: HERG mutations cause long QT syndrome. *Cell* **80**, 795-803.

Dart, C. & Standen, N. B. (1995). Activation of ATP-dependent K^+ channels by hypoxia in smooth muscle cells isolated from the pig coronary artery. *J. Physiol.* **483**, 29-39.

Dart, C., Leyland, M. L., Spencer, P. J., Stanfield, P. R. & Sutcliffe, M. J. (1998). The selectivity filter of a potassium channel, murine Kir2.1, investigated using scanning cysteine mutagenesis. *J. Physiol.* **511**, 25–32.

Dascal, N. (1997). Signalling via the G protein-activated K^+ channels. *Cell Signal.* **9**, 551-573.

Daut, J., Maier-Rudolph, W., von Beckerath, N., Mehrke, G., Gunther, K., & Goedel-Meinen, L. (1990). Hypoxic dilation of coronary arteries is mediated by ATP-sensitive potassium channels. *Science* **247**, 1341-1344.

Daut, J., Standen, N. B., & Nelson, M. T. (1994). The role of the membrane potential of endothelial and smooth muscle cells in the regulation of coronary blood flow. *J. Cardiovasc. Electrophysiol.* **5**, 154-181.

Davis, L. D. & Temte, J. V. (1969). Electrophysiological actions of lidocaine on canine ventricular muscle and Purkinje fibers. *Circ. Res.* **24**, 639-655.

Decher, N., Uyguner, O., Scherer, C. R., Karaman, B., Yuksel-Apak, M., Busch, A. E., Steinmeyer, K., & Wollnik, B. (2001). hKChIP2 is a functional modifier of hKv4.3 potassium channels: cloning and expression of a short hKChIP2 splice variant. *Cardiovasc. Res.* **52**, 255-264.

Deck, K. A. & Trautwein, W. (1964). Ionic currents in cardiac excitation. *Pflugers Arch. Gesamte Physiol. Menschen.Tiere.* **280**, 63-80.

Deedwania, P. C. (2000). Endothelium: a new target for cardiovascular therapeutics. *J. Am. Coll. Cardiol.* **35**, 67-70.

del Camino, D., Holmgren, M., Liu, Y., & Yellen, G. (2000). Blocker protection in the pore of a voltage-gated K^+ channel and its structural implications. *Nature* **403**, 321-325.

del Camino, D. & Yellen, G. (2001). Tight steric closure at the intracellular activation gate of a voltage-gated K^+ channel. *Neuron* **32**, 649-656.

Del Castillo, J. & Katz, B. (1955). Production of membrane potential changes in the frog's heart by inhibitory nerve impulses. *Nature* **175**, 1035.

Del Castillo, J. & Moore, J. W. (1959). On increasing the velocity of a nerve impulse. *J. Physiol.* **148**, 665-670.

DePaoli, A. M., Bell, G. I., & Stoffel, M. (1994). G protein-activated inwardly rectifying potassium channel (GIRK1/KGA) mRNA in adult rat heart and brain by in situ hybridization histochemistry. *Mol. Cell. Neurosci.* **5**, 515-522.

Derst, C., Hirsch, J. R., Preisig-Muller, R., Wischmeyer, E., Karschin, A., Doring, F., Thomzig, A., Veh, R. W., Schlatter, E., Kummer, W., & Daut, J. (2001a). Cellular localization of the potassium channel Kir7.1 in guinea pig and human kidney. *Kidney Int.* **59**, 2197-2205.

Derst, C., Karschin, C., Wischmeyer, E., Hirsch, J. R., Preisig-Muller, R., Rajan, S., Engel, H., Grzeschik, K., Daut, J., & Karschin, A. (2001b). Genetic and functional linkage of Kir5.1 and Kir2.1 channel subunits. *FEBS Lett.* **491**, 305-311.

Derst, C., Konrad, M., Kockerling, A., Karolyi, L., Deschenes, G., Daut, J., Karschin, A., & Seyberth, H. W. (1997). Mutations in the ROMK gene in antenatal Bartter

syndrome are associated with impaired K^+ channel function. *Biochem. Biophys. Res. Commun.* **230**, 641-645.

Deschenes, I., DiSilvestre, D., Juang, G. J., Wu, R. C., An, W. F., & Tomaselli, G. F. (2002). Regulation of Kv4.3 current by KChIP2 splice variants: a component of native cardiac I_{to}? *Circulation* **106**, 423-429.

Deschenes, I. & Tomaselli, G. F. (2002). Modulation of Kv4.3 current by accessory subunits. *FEBS Lett.* **528**, 183-188.

Dhamoon, A. S., Pandit, S. V., Sarmast, F., Parisian, K. R., Guha, P., Li, Y., Bagwe, S., Taffet, S. M., & Anumonwo, J. M. (2004). Unique Kir2.x properties determine regional and species differences in the cardiac inward rectifier K^+ current. *Circ. Res.* **94**, 1332-1339.

Di Diego, J. M., Sun, Z. Q., & Antzelevitch, C. (1996). I_{to} and action potential notch are smaller in left vs. right canine ventricular epicardium. *Am. J. Physiol.* **271**, H548-561.

DiFrancesco, D. (1993). Pacemaker mechanisms in cardiac tissue. *Annu. Rev. Physiol.* **55**, 455-472.

DiFrancesco, D., Ducouret, P., & Robinson, R. B. (1989). Muscarinic modulation of cardiac rate at low acetylcholine concentrations. *Science* **243**, 669-671.

DiFrancesco, D. & Tromba, C. (1988). Inhibition of the hyperpolarization-activated current (I_f) induced by acetylcholine in rabbit sino-atrial node myocytes. *J. Physiol.* **405**, 477-491.

DiMarco, J. P., Sellers, T. D., Berne, R. M., West, G. A., & Belardinelli, L. (1983). Adenosine: electrophysiologic effects and therapeutic use for terminating paroxysmal supraventricular tachycardia. *Circulation* **68**, 1254-1263.

Diochot, S., Drici, M. D., Moinier, D., Fink, M., & Lazdunski, M. (1999). Effects of phrixotoxins on the Kv4 family of potassium channels and implications for the role of I_{to1} in cardiac electrogenesis. *Br. J. Pharmacol.* **126**, 251-263.

Dissmann, E., Wischmeyer, E., Spauschus, A., Pfeil, D. V., Karschin, C., & Karschin, A. (1996). Functional expression and cellular mRNA localization of a G protein-activated K^+ inward rectifier isolated from rat brain. *Biochem. Biophys. Res. Commun.* **223**, 474-479.

Dittrich, M. & Daut, J. (1999). Voltage-dependent K^+ current in capillary endothelial cells isolated from guinea pig heart. *Am. J. Physiol.* **277**, H119-127.

Dixon, J. E. & McKinnon, D. (1994). Quantitative analysis of potassium channel mRNA expression in atrial and ventricular muscle of rats. *Circ. Res.* **75**, 252-260.

Dixon, J. E., Shi, W., Wang, H. S., McDonald, C., Yu, H., Wymore, R. S., Cohen, I. S., & McKinnon, D. (1996). Role of the Kv4.3 K^+ channel in ventricular muscle. A molecular correlate for the transient outward current. *Circ. Res.* **79**, 659-668.

Dobrev, D., Graf, E., Wettwer, E., Himmel, H. M., Hala, O., Doerfel, C., Christ, T., Schuler, S., & Ravens, U. (2001). Molecular basis of downregulation of G-protein-coupled inward rectifying K^+ current (I_{KACh}) in chronic human atrial fibrillation: decrease in GIRK4 mRNA correlates with reduced I_{KACh} and muscarinic receptor-mediated shortening of action potentials. *Circulation* **104**, 2551-2557.

Dobrzynski, H., Marples, D. D., Musa, H., Yamanushi, T. T., Henderson, Z., Takagishi, Y., Honjo, H., Kodama, I., & Boyett, M. R. (2001). Distribution of the muscarinic K^+ channel proteins Kir3.1 and Kir3.4 in the ventricle, atrium, and sinoatrial node of heart. *J. Histochem. Cytochem.* **49**, 1221-1234.

Domene, C., Doyle, D. A., & Venien-Bryan, C. (2005). Modeling of an ion channel in its open conformation. *Biophys. J.* **89**, L01-03.

Domene, C., Grottesi, A., & Sansom, M. S. (2004). Filter flexibility and distortion in a bacterial inward rectifier K^+ channel: simulation studies of KirBac1.1. *Biophys. J.* **87**, 256-267.

Domene, C. & Sansom, M. S. (2003). Potassium channel, ions, and water: simulation studies based on the high resolution X-ray structure of KcsA. *Biophys. J.* **85**, 2787-2800.

Domotor, E., Abbott, N. J., & Adam-Vizi, V. (1999). Na^+-Ca^{2+} exchange and its implications for calcium homeostasis in primary cultured rat brain microvascular endothelial cells. *J. Physiol.* **515**, 147-155.

Doring, F., Derst, C., Wischmeyer, E., Karschin, C., Schneggenburger, R., Daut, J., & Karschin, A. (1998). The epithelial inward rectifier channel Kir7.1 displays unusual K^+ permeation properties. *J. Neurosci.* **18**, 8625-8636.

Doupnik, C. A., Davidson, N., & Lester, H. A. (1995). The inward rectifier potassium channel family. *Curr. Opin. Neurobiol.* **5**, 268-277.

Doupnik, C. A., Davidson, N., Lester, H. A., & Kofuji, P. (1997). RGS proteins reconstitute the rapid gating kinetics of gbetagamma-activated inwardly rectifying K^+ channels. *Proc. Natl. Acad. Sci. U.S.A.* **94**, 10461-10466.

Doyle, D. A. (2004). Structural changes during ion channel gating. *Trends Neurosci.* **27**, 298-302.

Doyle, D. A., Morais, C. J., Pfuetzner, R. A., Kuo, A., Gulbis, J. M., Cohen, S. L., Chait, B. T., & MacKinnon, R. (1998). The structure of the potassium channel: molecular basis of K^+ conduction and selectivity. *Science* **280**, 69-77.

Drake, C. T., Bausch, S. B., Milner, T. A., & Chavkin, C. (1997). GIRK1 immunoreactivity is present predominantly in dendrites, dendritic spines, and somata in the CA1 region of the hippocampus. *Proc. Natl. Acad. Sci.U.S.A.* **94**, 1007-1012.

Drici, M. D., Diochot, S., Terrenoire, C., Romey, G., & Lazdunski, M. (2000). The bee venom peptide tertiapin underlines the role of I_{KACh} in acetylcholine-induced atrioventricular blocks. *Br. J. Pharmacol.* **131**, 569-577.

Drouin, E., Charpentier, F., Gauthier, C., Laurent, K., & Le Marec, H. (1995). Electrophysiologic characteristics of cells spanning the left ventricular wall of human heart: evidence for presence of M cells. *J. Am. Coll. Cardiol.* **26**, 185-192.

Drysdale, R., Warmke, J., Kreber, R., & Ganetzky, B. (1991). Molecular characterization of eag: a gene affecting potassium channels in Drosophila melanogaster. *Genetics* **127**, 497-505.

Du, J., Tao-Cheng, J. H., Zerfas, P., & McBain, C. J. (1998). The K^+ channel, Kv2.1, is apposed to astrocytic processes and is associated with inhibitory postsynaptic membranes in hippocampal and cortical principal neurons and inhibitory interneurons. *Neuroscience* **84**, 37-48.

Duan, D. Y., Fermini, B., & Nattel, S. (1992). Sustained outward current observed after I_{to1} inactivation in rabbit atrial myocytes is a novel Cl^- current. *Am. J. Physiol.* **263**, H1967-1971.

Dunne, M. J., Illot, M. C., & Peterson, O. H. (1987). Interaction of diazoxide, tolbutamide and and ATP on nucleotide-dependent K^+ channels in an insulin-secreting cell line. *J. Membr. Biol.* **99**, 215-224.

Duprat, F., Girard, C., Jarretou, G., & Lazdunski, M. (2005). Pancreatic two P domain K^+ channels TALK-1 and TALK-2 are activated by nitric oxide and reactive oxygen species. *J. Physiol.* **562**, 235-244.

Duprat, F., Lesage, F., Fink, M., Reyes, R., Heurteaux, C., & Lazdunski, M. (1997). TASK, a human background K^+ channel to sense external pH variations near physiological pH. *EMBO J.* **16**, 5464-5471.

Eaton,D.C., Brodwick,M.S. (1980). Effects of barium on the potassium conductance of squid axon. *J.Gen.Physiol.* **75**, 727-750.

Edwards, G., Dora, K. A., Gardener, M. J., Garland, C. J., & Weston, A. H. (1998). K^+ is an endothelium-derived hyperpolarizing factor in rat arteries. *Nature* **396**, 269-272.

Edwards, G. & Weston, A. H. (1993). The pharmacology of ATP-sensitive potassium channels. *Annu. Rev. Pharmacol. Toxicol.* **33**, 597-637.

Ehrlich, J. R., Cha, T. J., Zhang, L., Chartier, D., Villeneuve, L., Hebert, T. E., & Nattel, S. (2004). Characterization of a hyperpolarization-activated time-dependent potassium current in canine cardiomyocytes from pulmonary vein myocardial sleeves and left atrium. *J. Physiol.* **557**, 583-597.

El Sherif, N., Caref, E. B., Yin, H., & Restivo, M. (1996). The electrophysiological mechanism of ventricular arrhythmias in the long QT syndrome. Tridimensional mapping of activation and recovery patterns. *Circ. Res.* **79**, 474-492.

Elinder, F., Arhem, P., & Larsson, H. P. (2001). Localization of the extracellular end of the voltage sensor S4 in a potassium channel. *Biophys. J.* **80**, 1802-1809.

Emeis, J. J., Eijnden-Schrauwen, Y., van den Hoogen, C. M., de Priester, W., Westmuckett, A., & Lupu, F. (1997). An endothelial storage granule for tissue-type plasminogen activator. *J. Cell Biol.* **139**, 245-256.

England, S. K., Uebele, V. N., Shear, H., Kodali, J., Bennett, P. B., & Tamkun, M. M. (1995). Characterization of a voltage-gated K^+ channel beta subunit expressed in human heart. *Proc.Natl.Acad.Sci.U.S.A.* **92**, 6309-6313.

Escande, D., Coulombe, A., Faivre, J. F., Deroubaix, E., & Coraboeuf, E. (1987). Two types of transient outward currents in adult human atrial cells. *Am. J. Physiol.* **252**, H142-148.

Eschke, D., Richter, M., Brylla, E., Lewerenz, A., Spanel-Borowski, K., & Nieber, K. (2002). Identification of inwardly rectifying potassium channels in bovine retinal and choroidal endothelial cells. *Ophthalmic Res.* **34**, 343-348.

Escoubas, P., Diochot, S., Celerier, M. L., Nakajima, T., & Lazdunski, M. (2002). Novel tarantula toxins for subtypes of voltage-dependent potassium channels in the Kv2 and Kv4 subfamilies. *Mol. Pharmacol.* **62**, 48-57.

Fakler, B., Bond, C. T., Adelman, J. P., & Ruppersberg, J. P. (1996). Heterooligomeric assembly of inward-rectifier K^+ channels from subunits of different subfamilies: Kir2.1 (IRK1) and Kir4.1 (BIR10). *Pflugers Arch.* **433**, 77-83.

Fakler, B., Brandle, U., Bond, C., Glowatzki, E., Konig, C., Adelman, J. P., Zenner, H. P., & Ruppersberg, J. P. (1994). A structural determinant of differential sensitivity of cloned inward rectifier K^+ channels to intracellular spermine. *FEBS Lett.* **356**, 199-203.

Fakler, B., Brandle, U., Glowatzki, E., Weidemann, S., Zenner, H. P., & Ruppersberg, J. P. (1995). Strong voltage-dependent inward rectification of inward rectifier K^+ channels is caused by intracellular spermine. *Cell* **80**, 149-154.

Falk, T., Meyerhof, W., Corrette, B. J., Schafer, J., Bauer, C. K., Schwarz, J. R., & Richter, D. (1995). Cloning, functional expression and mRNA distribution of an inwardly rectifying potassium channel protein. *FEBS Lett.* **367**, 127-131.

Fan, Z. & Makielski, J. C. (1997). Anionic phospholipids activate ATP-sensitive potassium channels. *J. Biol. Chem.* **272**, 5388-5395.

Fang, Y., Schram, G., Romanenko, V., Shi, C., Conti, L., Vandenberg, C. A., Davies, P. F., Nattel, S., & Levitan, I. (2005). Functional expression of Kir2.x in human aortic endothelial cells: the dominant role of Kir2.2. *Am. J. Physiol. Cell Physiol.* **289**, C1134-1144

Faraldo-Gomez, J. D., Forrest, L. R., Baaden, M., Bond, P. J., Domene, C., Patargias, G., Cuthbertson, J., & Sansom, M. S. (2004). Conformational sampling and dynamics of membrane proteins from 10-nanosecond computer simulations. *Proteins* **57**, 783-791.

Fareh, S., Villemaire, C., & Nattel, S. (1998). Importance of refractoriness heterogeneity in the enhanced vulnerability to atrial fibrillation induction caused by tachycardia-induced atrial electrical remodeling. *Circulation* **98**, 2202-2209.

Fedida, D. & Giles, W. R. (1991). Regional variations in action potentials and transient outward current in myocytes isolated from rabbit left ventricle. *J. Physiol.* **442**, 191-209.

Felix, J. P., Bugianesi, R. M., Schmalhofer, W. A., Borris, R., Goetz, M. A., Hensens, O. D., Bao, J. M., Kayser, F., Parsons, W. H., Rupprecht, K., Garcia, M. L., Kaczorowski, G. J., & Slaughter, R. S. (1999). Identification and biochemical characterization of a novel nortriterpene inhibitor of the human lymphocyte voltage-gated potassium channel, Kv1.3. *Biochemistry* **38**, 4922-4930.

Feng, J., Wible, B., Li, G. R., Wang, Z., & Nattel, S. (1997). Antisense oligodeoxynucleotides directed against Kv1.5 mRNA specifically inhibit ultrarapid delayed rectifier K^+ current in cultured adult human atrial myocytes. *Circ. Res.* **80**, 572-579.

Feng, J., Yue, L., Wang, Z., & Nattel, S. (1998). Ionic mechanisms of regional action potential heterogeneity in the canine right atrium. *Circ. Res.* **83**, 541-551.

Fermini, B., Wang, Z., Duan, D., & Nattel, S. (1992). Differences in rate dependence of transient outward current in rabbit and human atrium. *Am. J. Physiol.* **263**, H1747-H1754.

Ficker, E., Taglialatela, M., Wible, B. A., Henley, C. M., & Brown, A. M. (1994). Spermine and spermidine as gating molecules for inward rectifier K^+ channels. *Science* **266**, 1068-1072.

Findlay, I. (1994). The ATP sensitive potassium channel of cardiac muscle and action potential shortening during metabolic stress. *Cardiovasc. Res.* **28**, 760-761.

Fink, M., Duprat, F., Heurteaux, C., Lesage, F., Romey, G., Barhanin, J., & Lazdunski, M. (1996a). Dominant negative chimeras provide evidence for homo and heteromultimeric assembly of inward rectifier K^+ channel proteins via their N-terminal end. *FEBS Lett.* **378**, 64-68.

Fink, M., Duprat, F., Lesage, F., Heurteaux, C., Romey, G., Barhanin, J., & Lazdunski, M. (1996b). A new K^+ channel beta subunit to specifically enhance Kv2.2 (CDRK) expression. *J. Biol. Chem.* **271**, 26341-26348.

Fink, M., Duprat, F., Lesage, F., Reyes, R., Romey, G., Heurteaux, C., & Lazdunski, M. (1996c). Cloning, functional expression and brain localization of a novel unconventional outward rectifier K^+ channel. *EMBO J.* **15**, 6854-6862.

Finn, J. T., Grunwald, M. E., & Yau, K. W. (1996). Cyclic nucleotide-gated ion channels: an extended family with diverse functions. *Annu. Rev. Physiol.* **58**, 395-426.

Fiset, C., Clark, R. B., Shimoni, Y., & Giles, W. R. (1997). Shal-type channels contribute to the Ca^{2+}-independent transient outward K^+ current in rat ventricle. *J. Physiol.* **500**, 51-64.

Forsyth, S. E., Hoger, A., & Hoger, J. H. (1997). Molecular cloning and expression of a bovine endothelial inward rectifier potassium channel. *FEBS Lett.* **409**, 277-282.

Frearson, J. A., Harrison, P., Scrutton, M. C., & Pearson, J. D. (1995). Differential regulation of von Willebrand factor exocytosis and prostacyclin synthesis in electropermeabilized endothelial cell monolayers. *Biochem. J.* **309**, 473-479.

Freichel, M., Vennekens, R., Olausson, J., Stolz, S., Philipp, S. E., Weissgerber, P., & Flockerzi, V. (2005). Functional role of TRPC proteins in native systems: implications from knockout and knock-down studies. *J. Physiol.* **567**, 59-66.

Fujita, A. & Kurachi, Y. (2000). Molecular aspects of ATP-sensitive K^+ channels in the cardiovascular system and K^+ channel openers. *Pharmacol. Ther.* **85**, 39-53.

Fujita, S., Inanobe, A., Chachin, M., Aizawa, Y., & Kurachi, Y. (2000). A regulator of G protein signalling (RGS) protein confers agonist-dependent relaxation gating to a G protein-gated K^+ channel. *J. Physiol.* **526**, 341-347.

Fujiwara, N., Higashi, H., Shimoji, K., & Yoshimura, M. (1987). Effects of hypoxia on rat hippocampal neurones in vitro. *J. Physiol.* **384**, 131-151.

Furchgott, R. F. & Zawadzki, J. V. (1980). The obligatory role of endothelial cells in the relaxation of arterial smooth muscle by acetylcholine. *Nature* **288**, 373-376.

Furukawa, T., Kimura, S., Furukawa, N., Bassett, A. L., & Myerburg, R. J. (1992). Potassium rectifier currents differ in myocytes of endocardial and epicardial origin. *Circ. Res.* **70**, 91-103.

Furukawa, T., Myerburg, R. J., Furukawa, N., Bassett, A. L., & Kimura, S. (1990). Differences in transient outward currents of feline endocardial and epicardial myocytes. *Circ. Res.* **67**, 1287-1291.

Gahwiler, B. H. & Brown, D. A. (1985). GABAB-receptor-activated K^+ current in voltage-clamped CA3 pyramidal cells in hippocampal cultures. *Proc. Natl. Acad. Sci. U.S.A.* **82**, 1558-1562.

Gandhi, C. S. & Isacoff, E. Y. (2002). Molecular models of voltage sensing. *J. Gen. Physiol.* **120**, 455-463.

Ganetzky, B., Robertson, G. A., Wilson, G. F., Trudeau, M. C., & Titus, S. A. (1999). The eag family of K^+ channels in Drosophila and mammals. *Ann. N. Y. Acad. Sci.* **868**, 356-369.

Ganetzky, B. & Wu, C. F. (1983). Neurogenetic analysis of potassium currents in Drosophila: synergistic effects on neuromuscular transmission in double mutants. *J. Neurogenet.* **1**, 17-28.

Garcia-Palmieri, M. R. (1997). The endothelium in health and in cardiovascular disease. *P. R. Health Sci .J.* **16**, 136-141.

Garlid, K. D., Paucek, P., Yarov-Yarovoy, V., Murray, H. N., Darbenzio, R. B., D'Alonzo, A. J., Lodge, N. J., Smith, M. A., & Grover, G. J. (1997). Cardioprotective effect of diazoxide and its interaction with mitochondrial ATP-sensitive K^+ channels. Possible mechanism of cardioprotection. *Circ. Res.* **81**, 1072-1082.

Garnier, D., Nargeot, J., Ojeda, C., & Rougier, O. (1978). The action of acetylcholine on background conductance in frog atrial trabeculae. *J. Physiol.* **274**, 381-396.

Gauldie, J., Hanson, J. M., Rumjanek, F. D., Shipolini, R. A., & Vernon, C. A. (1976). The peptide components of bee venom. *Eur. J. Biochem.* **61**, 369-376.

Geiger, J. R. & Jonas, P. (2000). Dynamic control of presynaptic Ca^{2+} inflow by fast-inactivating K^+ channels in hippocampal mossy fiber boutons. *Neuron* **28**, 927-939.

Gendron, M. E., Thorin, E., & Perrault, L. P. (2004). Loss of endothelial K_{ATP} channel-dependent, NO-mediated dilation of endocardial resistance coronary arteries in pigs with left ventricular hypertrophy. *Br. J. Pharmacol.* **143**, 285-291.

Giles, W. & Noble, S. J. (1976). Changes in membrane currents in bullfrog atrium produced by acetylcholine. *J. Physiol.* **261**, 103-123.

Giles, W. R. & Imaizumi, Y. (1988). Comparison of potassium currents in rabbit atrial and ventricular cells. *J. Physiol.* **405**, 123-145.

Giles, W. R. & van Ginneken, A. C. (1985). A transient outward current in isolated cells from the crista terminalis of rabbit heart. *J. Physiol.* **368**, 243-264.

Gilman, A. G. (1987). G proteins: transducers of receptor-generated signals. *Annu. Rev. Biochem.* **56**, 615-649.

Gilman, A. G. (1995). Nobel Lecture. G proteins and regulation of adenylyl cyclase. *Biosci. Rep.* **15**, 65-97.

Gintant, G. A. (1995). Regional differences in I_K density in canine left ventricle: role of I_{Ks} in electrical heterogeneity. *Am. J. Physiol.* **268**, H604-613.

Gintant, G. A. (1996). Two components of delayed rectifier current in canine atrium and ventricle. Does I_{Ks} play a role in the reverse rate dependence of class III agents? *Circ. Res.* **78**, 26-37.

Gintant, G. A. (2000). Characterization and functional consequences of delayed rectifier current transient in ventricular repolarization. *Am. J. Physiol. Heart Circ. Physiol.* **278**, H806-817.

Glowatzki, E., Fakler, G., Brandle, U., Rexhausen, U., Zenner, H. P., Ruppersberg, J. P., & Fakler, B. (1995). Subunit-dependent assembly of inward-rectifier K^+ channels. *Proc. R. Soc. Lond. B. Biol. Sci.* **261**, 251-261.

Goldman-Wohl, D. S., Chan, E., Baird, D., & Heintz, N. (1994). Kv3.3b: a novel Shaw type potassium channel expressed in terminally differentiated cerebellar Purkinje cells and deep cerebellar nuclei. *J. Neurosci.* **14**, 511-522.

Goldstein, S. A. & Miller, C. (1993). Mechanism of charybdotoxin block of a voltage-gated K^+ channel. *Biophys. J.* **65**, 1613-1619.

Gomez, A. M., Benitah, J. P., Henzel, D., Vinet, A., Lorente, P., & Delgado, C. (1997). Modulation of electrical heterogeneity by compensated hypertrophy in rat left ventricle. *Am. J. Physiol.* **272**, H1078-1086.

Graier, W. F., Groschner, K., Schmidt, K., & Kukovetz, W. R. (1992). SK&F 96365 inhibits histamine-induced formation of endothelium-derived relaxing factor in human endothelial cells. *Biochem. Biophys. Res. Commun.* **186**, 1539-1545.

Graier, W. F., Paltauf-Doburzynska, J., Hill, B. J., Fleischhacker, E., Hoebel, B. G., Kostner, G. M., & Sturek, M. (1998). Submaximal stimulation of porcine endothelial cells causes focal Ca^{2+} elevation beneath the cell membrane. *J. Physiol.* **506**, 109-125.

Greenstein, J. L., Wu, R., Po, S., Tomaselli, G. F., & Winslow, R. L. (2000). Role of the calcium-independent transient outward current I_{to1} in shaping action potential morphology and duration. *Circ. Res.* **87**, 1026-1033.

Gribble, F. M., Proks, P., Corkey, B. E., & Ashcroft, F. M. (1998a). Mechanism of cloned ATP-sensitive potassium channel activation by oleoyl-CoA. *J. Biol. Chem.* **273**, 26383-26387.

Gribble, F. M. & Reimann, F. (2003). Sulphonylurea action revisited: the post-cloning era. *Diabetologia* **46**, 875-891.

Gribble, F. M., Tucker, S. J., & Ashcroft, F. M. (1997). The essential role of the Walker A motifs of SUR1 in K_{ATP} channel activation by Mg-ADP and diazoxide. *EMBO J.* **16**, 1145-1152.

Gribble, F. M., Tucker, S. J., Seino, S., & Ashcroft, F. M. (1998b). Tissue specificity of sulfonylureas: studies on cloned cardiac and beta-cell K_{ATP} channels. *Diabetes* **47**, 1412-1418.

Grigg, J. J., Kozasa, T., Nakajima, Y., & Nakajima, S. (1996). Single-channel properties of a G-protein-coupled inward rectifier potassium channel in brain neurons. *J. Neurophysiol.* **75**, 318-328.

Gross, E. R., Peart, J. N., Hsu, A. K., Grover, G. J., & Gross, G. J. (2003). K_{ATP} opener-induced delayed cardioprotection: involvement of sarcolemmal and mitochondrial K_{ATP} channels, free radicals and MEK1/2. *J. Mol. Cell Cardiol.* **35**, 985-992.

Gross, G. J. & Auchampach, J. A. (1992). Blockade of ATP-sensitive potassium channels prevents myocardial preconditioning in dogs. *Circ. Res.* **70**, 223-233.

Gross, G. J. & Peart, J. N. (2003). K_{ATP} channels and myocardial preconditioning: an update. *Am. J. Physiol. Heart Circ. Physiol.* **285**, H921-930.

Grottesi, A., Domene, C., Haider, S., & Sansom, M. S. P. (2005). Investigating open pore structure: Essential dynamics sampling of motions performed by the inner S6 helix bundle in KirBac. *Biophys. J.* **88**, 105A.

Grover, G. J., Sleph, P. G., & Dzwonczyk, S. (1992). Role of myocardial ATP-sensitive potassium channels in mediating preconditioning in the dog heart and their possible interaction with adenosine A1-receptors. *Circulation* **86**, 1310-1316.

Guidoni, L., Torre, V., & Carloni, P. (1999). Potassium and sodium binding to the outer mouth of the K^+ channel. *Biochemistry* **38**, 8599-8604.

Gulbis, J. M., Mann, S., & MacKinnon, R. (1999). Structure of a voltage-dependent K^+ channel beta subunit. *Cell* **97**, 943-952.

Gulbis, J. M., Zhou, M., Mann, S., & MacKinnon, R. (2000). Structure of the cytoplasmic beta subunit-T1 assembly of voltage-dependent K^+ channels. *Science* **289**, 123-127.

Guo, D. & Lu, Z. (2000). Mechanism of IRK1 channel block by intracellular polyamines. *J. Gen. Physiol.* **115**, 799-814.

Guo, J., Mitsuiye, T., & Noma, A. (1997). The sustained inward current in sino-atrial node cells of guinea-pig heart. *Pflugers Arch.* **433**, 390-396.

Guo, J., Ono, K., & Noma, A. (1995). A sustained inward current activated at the diastolic potential range in rabbit sino-atrial node cells. *J. Physiol.* **483**, 1-13.

Guo, W., Li, H., Aimond, F., Johns, D. C., Rhodes, K. J., Trimmer, J. S., & Nerbonne, J. M. (2002). Role of heteromultimers in the generation of myocardial transient outward K^+ currents. *Circ. Res.* **90**, 586-593.

Guo, W., Li, H., London, B., & Nerbonne, J. M. (2000). Functional consequences of elimination of $I_{to,f}$ and $I_{to,s}$: Early afterdepolarizations, atrioventricular block, and ventricular arrhythmias in mice lacking Kv1.4 and expressing a dominant-negative Kv4 alpha subunit. *Circ. Res.* **87**, 73-79.

Guo, W., Xu, H., London, B., & Nerbonne, J. M. (1999). Molecular basis of transient outward K^+ current diversity in mouse ventricular myocytes. *J. Physiol.* **521**, 587-599.

Gutman, G. A., Chandy, K. G., Adelman, J. P., Aiyar, J., Bayliss, D. A., Clapham, D. E., Covarriubias, M., Desir, G. V., Furuichi, K., Ganetzky, B., Garcia, M. L., Grissmer, S., Jan, L. Y., Karschin, A., Kim, D., Kuperschmidt, S., Kurachi, Y., Lazdunski, M., Lesage, F., Lester, H. A., McKinnon, D., Nichols, C. G., O'Kelly, I., Robbins, J., Robertson, G. A., Rudy, B., Sanguinetti, M., Seino, S., Stuehmer, W., Tamkun, M. M., Vandenberg, C. A., Wei, A., Wulff, H., & Wymore, R. S. (2003). International Union of Pharmacology. XLI. Compendium of voltage-gated ion channels: potassium channels. *Pharmacol. Rev.* **55**, 583-586.

Hackos, D. H., Chang, T. H., & Swartz, K. J. (2002). Scanning the intracellular s6 activation gate in the shaker K^+ channel. *J. Gen. Physiol.* **119**, 521-532.

Hagiwara, N., Irisawa, H., & Kameyama, M. (1988). Contribution of two types of calcium currents to the pacemaker potentials of rabbit sino-atrial node cells. *J. Physiol.* **395**, 233-253.

Hagiwara, S., Kusano, K., & Saito, N. (1961). Membrane changes of Onchidium nerve cell in potassium-rich media. *J. Physiol.* **155**, 470-489.

Hagiwara S., Miyazaki S., & Rosenthal N. P. (1976). Potassium current and the effect of cesium on this current during anomalous rectification of the egg cell membrane of a starfish. *J. Gen. Physiol.* **67**, 621-638.

Haider, S., Antcliff, J. F., Proks, P., Sansom, M. S., & Ashcroft, F. M. (2005). Focus on Kir6.2: a key component of the ATP-sensitive potassium channel. *J. Mol. Cell Cardiol.* **38**, 927-936.

Hall, A. E., Hutter, O. F., & Noble, D. (1963). Current-voltage relations of Purkinje fibres in sodium-deficient solutions. *J. Physiol.* **166**, 225-240.

Hamada, E., Takikawa, R., Ito, H., Iguchi, M., Terano, A., Sugimoto, T., & Kurachi, Y. (1990). Glibenclamide specifically blocks ATP-sensitive K^+ channel current in atrial myocytes of guinea pig heart. *Jpn. J. Pharmacol.* **54**, 473-477.

Hambrock, A., Preisig-Muller, R., Russ, U., Piehl, A., Hanley, P. J., Ray, J., Daut, J., Quast, U., & Derst, C. (2002). Four novel splice variants of sulfonylurea receptor 1. *Am. J. Physiol. Cell Physiol.* **283**, C587-598.

Han, W., Wang, Z., & Nattel, S. (2000). A comparison of transient outward currents in canine cardiac Purkinje cells and ventricular myocytes. *Am. J. Physiol. Heart Circ. Physiol.* **279**, H466-474.

Han, W., Wang, Z. G., & Nattel, S. (2001a). Expression profile of ion channel mRNA in canine cardiac Purkinje fibers - A basis for electrophysiological specificity? *Circulation* **104**, 133.

Han, W., Zhang, L., & Nattel, S. (2001b). Properties of potassium currents in human cardiac purkinje fibers. Circulation 104 [suppl II], II-26.

Han, W., Zhang, L., Schram, G., & Nattel, S. (2002). Properties of potassium currents in Purkinje cells of failing human hearts. *Am. J. Physiol. Heart Circ. Physiol.* **283**, H2495-2503.

Hancox, J. C. & Mitcheson, J. S. (1997). Ion channel and exchange currents in single myocytes isolated from the rabbit atrioventricular node. *Can. J. Cardiol.* **13**, 1175-1182.

Harris, R. E., Larsson, H. P. & Isacoff, E. Y. (1998). A permanent ion binding site located between two gates of the Shaker K^+ channel. *Biophys. J.* **74**, 1808–1820.

Hartzell, H. C. (1979). Adenosine receptors in frog sinus venosus: slow inhibitory potentials produced by adenine compounds and acetylcholine. *J. Physiol.* **293**, 23-49.

Hartzell, H. C., Mery, P. F., Fischmeister, R., & Szabo, G. (1991). Sympathetic regulation of cardiac calcium current is due exclusively to cAMP-dependent phosphorylation. *Nature* **351**, 573-576.

Hartzell, H. C. & Simmons, M. A. (1987). Comparison of effects of acetylcholine on calcium and potassium currents in frog atrium and ventricle. *J. Physiol.* **389**, 411-422.

Harvey, R. D. & Ten Eick, R. E. (1989). Voltage-dependent block of cardiac inward-rectifying potassium current by monovalent cations. *J. Gen. Physiol.* **94**, 349–361.

Hearse, D. J. (1998). Myocardial protection during ischemia and reperfusion. *Mol. Cell. Biochem.* **186**, 177-184.

Hedin, K. E., Lim, N. F., & Clapham, D. E. (1996). Cloning of a *Xenopus* laevis inwardly rectifying K^+ channel subunit that permits GIRK1 expression of I_{KACh} currents in oocytes. *Neuron* **16**, 423-429.

Heginbotham, L., Lu, Z., Abramson, T., & MacKinnon, R. (1994). Mutations in the K^+ channel signature sequence. *Biophys. J.* **66**, 1061-1067.

Heinemann, S. H., Rettig, J., Graack, H. R., & Pongs, O. (1996). Functional characterization of Kv channel beta-subunits from rat brain. *J. Physiol.* **493**, 625-633.

Hepler, J. R. (1999). Emerging roles for RGS proteins in cell signalling. *Trends Pharmacol. Sci.* **20**, 376-382.

Hernandez-Sanchez, C., Basile, A. S., Fedorova, I., Arima, H., Stannard, B., Fernandez, A. M., Ito, Y., & LeRoith, D. (2001). Mice transgenically overexpressing sulfonylurea receptor 1 in forebrain resist seizure induction and excitotoxic neuron death. *Proc. Natl. Acad .Sci. U.S.A.* **98**, 3549-3554.

Herrera, D., Schram, G, Mamarbachi, M., Wang, Z., Parent, L., & Nattel, S. (2005). Differences in barium block of KIR2.1 versus KIR2.4: Structural determinants of voltage-dependent block. *Can. J. Cardiol.* **21**, 180C

Herrera, D., Schram, G., Mamarbachi, A., Wang, Z., Parent, L., & Nattel, S. (2006). Molecular Determinants of Barium Block on Kir2.1 vs. Kir2.4: Two Residues Confer Voltage- but Not Concentration-Dependence of Barium Block. *Biophys. J.***176a,** 835-Plat

Hestrin, S. (1987). The properties and function of inward rectification in rod photoreceptors of the tiger salamander. *J. Physiol.* **390**, 319-333.

Heurteaux, C., Bertaina, V., Widmann, C., & Lazdunski, M. (1993). K^+ channel openers prevent global ischemia-induced expression of c-fos, c-jun, heat shock protein, and amyloid beta-protein precursor genes and neuronal death in rat hippocampus. *Proc. Natl. Acad. Sci. U.S.A.* **90**, 9431-9435.

Heurteaux, C., Lauritzen, I., Widmann, C., & Lazdunski, M. (1995). Essential role of adenosine, adenosine A1 receptors, and ATP-sensitive K^+ channels in cerebral ischemic preconditioning. *Proc. Natl. Acad. Sci. U.S.A.* **92**, 4666-4670.

Hibino, H., Fujita, A., Iwai, K., Yamada, M., & Kurachi, Y. (2004). Differential assembly of inwardly rectifying K^+ channel subunits, Kir4.1 and Kir5.1, in brain astrocytes. *J. Biol. Chem.* **279**, 44065-44073.

Hicks, G. A., Hudson, A. L., & Henderson, G. (1994). Localization of high affinity [3H]glibenclamide binding sites within the substantia nigra zona reticulata of the rat brain. *Neuroscience* **61**, 285-292.

Higgins, C. F. (1992). ABC transporters: from microorganisms to man. *Annu. Rev. Cell Biol.* **8**, 67-113.

Hille, B. (2001). *Ion Channels of Excitable Membranes*, 3 ed. Sinauer Associates, Inc., Sunderland, Massachusetts, U.S.A.

Hille, B., Armstrong, C. M., & MacKinnon, R. (1999). Ion channels: from idea to reality. *Nat. Med.* **5**, 1105-1109.

Himmel, H. M., Rauen, U., & Ravens, U. (2001). Microvascular endothelial cells from human omentum lack an inward rectifier K^+ current. *Physiol. Res.* **50**, 547-555.

Himmel, H. M., Wettwer, E., Li, Q., & Ravens, U. (1999). Four different components contribute to outward current in rat ventricular myocytes. *Am. J. Physiol.* **277**, H107-118.

Himmel, H. M., Whorton, A. R., & Strauss, H. C. (1993). Intracellular calcium, currents, and stimulus-response coupling in endothelial cells. *Hypertension* **21**, 112-127.

Hiraoka, M. & Kawano, S. (1989). Calcium-sensitive and insensitive transient outward current in rabbit ventricular myocytes. *J. Physiol.* **410**, 187-212.

Hirst, G. D., Bramich, N. J., Edwards, F. R., & Klemm, M. (1992). Transmission at autonomic neuroeffector junctions. *Trends Neurosci.* **15**, 40-46.

Ho, K., Nichols, C. G., Lederer, W. J., Lytton, J., Vassilev, P. M., Kanazirska, M. V., & Hebert, S. C. (1993). Cloning and expression of an inwardly rectifying ATP-regulated potassium channel. *Nature* **362**, 31-38.

Hodgkin, A. L. (1958). Ionic movements and electrical activity in giant nerve fibres. *Proc. R. Soc. Lond. B. Biol. Sci.* **148**, 1-37.

Hodgkin, A. L. & Huxley, A. F. (1952). A quantitative description of membrane current and its application to conduction and excitation in nerve. *J. Physiol.* **117**, 500-544.

Hodgkin, A. L. & Keynes, R. D. (1955). The potassium permeability of a giant nerve fibre. *J. Physiol.* **128**, 61-88.

Hoffman, B. F., Paes de Carvalho, A., & De Mello, W. C. (1959). Electrical activity of single fibers of the atrioventricular node. *Circ. Res.* **7**, 11-18.

Hoffman, D. A., Magee, J. C., Colbert, C. M., & Johnston, D. (1997). K^+ channel regulation of signal propagation in dendrites of hippocampal pyramidal neurons. *Nature* **387**, 869-875.

Hogan, P. M. & Davis, L. D. (1968). Evidence for specialized fibers in the canine right atrium. *Circ. Res.* **23**, 387-396.

Hoger, J. H., Ilyin, V. I., Forsyth, S., & Hoger, A. (2002). Shear stress regulates the endothelial Kir2.1 ion channel. *Proc. Natl. Acad. Sci. U.S.A.* **99**, 7780-7785.

Hogg, D. S., Albarwani, S., Davies, A. R., & Kozlowski, R. Z. (1999). Endothelial cells freshly isolated from resistance-sized pulmonary arteries possess a unique K^+ current profile. *Biochem. Biophys. Res. Commun.* **263**, 405-409.

Hoglund, M., Siden, T., & Rohme, D. (1992). The isolation of evolutionarily conserved Eag I end-clones from mouse chromosome 17 using cloned DNA. *DNA Cell Biol.* **11**, 613-619.

Holmgren, M., Jurman, M. E., & Yellen, G. (1996). N-type inactivation and the S4-S5 region of the Shaker K^+ channel. *J. Gen. Physiol.* **108**, 195-206.

Holyoake, J., Domene, C., Bright, J. N., & Sansom, M. S. (2004). KcsA closed and open: modelling and simulation studies. *Eur. Biophys. J.* **33**, 238-246.

Hondeghem, L. M. & Snyders, D. J. (1990). Class III antiarrhythmic agents have a lot of potential but a long way to go. Reduced effectiveness and dangers of reverse use dependence. *Circulation* **81**, 686-690.

Horie, M., Irisawa, H., & Noma, A. (1987). Voltage-dependent magnesium block of adenosine-triphosphate-sensitive potassium channel in guinea-pig ventricular cells. *J. Physiol.* **387**, 251-272.

Horio, Y., Morishige, K., Takahashi, N., & Kurachi, Y. (1996). Differential distribution of classical inwardly rectifying potassium channel mRNAs in the brain: comparison of IRK2 with IRK1 and IRK3. *FEBS Lett.* **379**, 239-243.

Horn, R. (2002). Coupled movements in voltage-gated ion channels. *J. Gen. Physiol.* **120**, 449-453.

Hoshi, T., Zagotta, W. N., & Aldrich, R. W. (1990). Biophysical and molecular mechanisms of Shaker potassium channel inactivation. *Science* **250**, 533-538.

Howarth, F. C., Levi, A. J., & Hancox, J. C. (1996). Characteristics of the delayed rectifier K current compared in myocytes isolated from the atrioventricular node and ventricle of the rabbit heart. *Pflugers Arch.* **431**, 713-722.

Huang, C. L., Feng, S., & Hilgemann, D. W. (1998). Direct activation of inward rectifier potassium channels by PIP_2 and its stabilization by Gbetagamma. *Nature* **391**, 803-806.

Hughes, B. A., Kumar, G., Yuan, Y., Swaminathan, A., Yan, D., Sharma, A., Plumley, L., Yang-Feng, T. L., & Swaroop, A. (2000). Cloning and functional expression of human retinal kir2.4, a pH-sensitive inwardly rectifying K^+ channel. *Am. J. Physiol. Cell Physiol.* **279**, C771-C784.

Hugnot, J. P., Salinas, M., Lesage, F., Guillemare, E., de Weille, J., Heurteaux, C., Mattei, M. G., & Lazdunski, M. (1996). Kv8.1, a new neuronal potassium channel subunit with specific inhibitory properties towards Shab and Shaw channels. *EMBO J.* **15**, 3322-3331.

Hume, J. R. & Uehara, A. (1985). Ionic basis of the different action potential configurations of single guinea-pig atrial and ventricular myocytes. *J. Physiol.* **368**, 525-544.

Hutter, O. F. & Trautwein, W. (1955). Vagal and sympathetic effects on the pacemaker fibers in the sinus venosus of the heart. *J. Gen. Physiol.* **39**, 715-733.

Hwang, P. M., Cunningham, A. M., Peng, Y. W., & Snyder, S. H. (1993a). CDRK and DRK1 K^+ channels have contrasting localizations in sensory systems. *Neuroscience* **55**, 613-620.

Hwang, P. M., Fotuhi, M., Bredt, D. S., Cunningham, A. M., & Snyder, S. H. (1993b). Contrasting immunohistochemical localizations in rat brain of two novel K^+ channels of the Shab subfamily. *J. Neurosci.* **13**, 1569-1576.

Ibarra, J., Morley, G. E., & Delmar, M. (1991). Dynamics of the inward rectifier K^+ current during the action potential of guinea pig ventricular myocytes. *Biophys. J.* **60**, 1534-1539.

Imoto, Y., Ehara, T., & Matsuura, H. (1987). Voltage- and time-dependent block of I_{K1} underlying Ba^{2+}-induced ventricular automaticity. *Am. J. Physiol.* **252**, H325-333.

Inagaki, N., Gonoi, T., Clement, J. P., Namba, N., Inazawa, J., Gonzalez, G., Aguilar-Bryan, L., Seino, S., & Bryan, J. (1995a). Reconstitution of I_{KATP}: an inward rectifier subunit plus the sulfonylurea receptor. *Science* **270**, 1166-1170.

Inagaki, N., Gonoi, T., Clement, J. P., Wang, C. Z., Aguilar-Bryan, L., Bryan, J., & Seino, S. (1996). A family of sulfonylurea receptors determines the pharmacological properties of ATP-sensitive K^+ channels. *Neuron* **16**, 1011-1017.

Inagaki, N., Gonoi, T., & Seino, S. (1997). Subunit stoichiometry of the pancreatic beta-cell ATP-sensitive K^+ channel. *FEBS Lett.* **409**, 232-236.

Inagaki, N., Tsuura, Y., Namba, N., Masuda, K., Gonoi, T., Horie, M., Seino, Y., Mizuta, M., & Seino, S. (1995b). Cloning and functional characterization of a novel ATP-sensitive potassium channel ubiquitously expressed in rat tissues, including pancreatic islets, pituitary, skeletal muscle, and heart. *J. Biol. Chem.* **270**, 5691-5694.

Inanobe, A., Fujita, S., Makino, Y., Matsushita, K., Ishii, M., Chachin, M., & Kurachi, Y. (2001). Interaction between the RGS domain of RGS4 with G protein alpha subunits mediates the voltage-dependent relaxation of the G protein-gated potassium channel. *J. Physiol.* **535**, 133-143.

Inanobe, A., Morishige, K. I., Takahashi, N., Ito, H., Yamada, M., Takumi, T., Nishina, H., Takahashi, K., Kanaho, Y., Katada, T., & . (1995). G beta gamma directly binds to the carboxyl terminus of the G protein-gated muscarinic K^+ channel, GIRK1. *Biochem. Biophys. Res. Commun.* **212**, 1022-1028.

Inomata, N., Ishihara, T., & Akaike, N. (1991). Mechanisms of the anticholinergic effect of SUN 1165 in comparison with flecainide, disopyramide and quinidine in single atrial myocytes isolated from guinea-pig. *Br. J. Pharmacol.* **104**, 1007-1011.

Inoue, I., Nagase, H., Kishi, K., & Higuti, T. (1991). ATP-sensitive K^+ channel in the mitochondrial inner membrane. *Nature* **352**, 244-247.

Inoue, M., Nakajima, S., & Nakajima, Y. (1988). Somatostatin induces an inward rectification in rat locus coeruleus neurones through a pertussis toxin-sensitive mechanism. *J. Physiol.* **407**, 177-198.

Iouzalen, L., Lantoine, F., Pernollet, M. G., Millanvoye-Van Brussel, E., Devynck, M. A., & David-Dufilho, M. (1996). SK&F 96365 inhibits intracellular Ca^{2+} pumps and raises cytosolic Ca^{2+} concentration without production of nitric oxide and von Willebrand factor. *Cell Calcium* **20**, 501-508.

Irisawa, H., Brown, H. F., & Giles, W. (1993). Cardiac pacemaking in the sinoatrial node. *Physiol. Rev.* **73**, 197-227.

Isacoff, E. Y., Jan, Y. N., & Jan, L. Y. (1990). Evidence for the formation of heteromultimeric potassium channels in *Xenopus* oocytes. *Nature* **345**, 530-534.

Ishii, K., Yamagishi, T., & Taira, N. (1994). Cloning and functional expression of a cardiac inward rectifier K^+ channel. *FEBS Lett.* **338**, 107-111.

Ishii, M. & Kurachi, Y. (2003). Physiological actions of regulators of G-protein signaling (RGS) proteins. *Life Sci 74*, 163-171

Isomoto, S., Kondo, C., & Kurachi, Y. (1997). Inwardly rectifying potassium channels: their molecular heterogeneity and function. *Jpn. J. Physiol.* **47**, 11-39.

Isomoto, S., Kondo, C., Takahashi, N., Matsumoto, S., Yamada, M., Takumi, T., Horio, Y., & Kurachi, Y. (1996a). A novel ubiquitously distributed isoform of GIRK2 (GIRK2B) enhances GIRK1 expression of the G-protein-gated K^+ current in *Xenopus* oocytes. *Biochem. Biophys. Res. Commun.* **218**, 286-291.

Isomoto, S., Kondo, C., Yamada, M., Matsumoto, S., Higashiguchi, O., Horio, Y., Matsuzawa, Y., & Kurachi, Y. (1996b). A novel sulfonylurea receptor forms with BIR (Kir6.2) a smooth muscle type ATP-sensitive K^+ channel. *J. Biol. Chem.* **271**, 24321-24324.

Ito, H., Hosoya, Y., Inanobe, A., Tomoike, H., & Endoh, M. (1995). Acetylcholine and adenosine activate the G protein-gated muscarinic K^+ channel in ferret ventricular myocytes. *Naunyn Schmiedebergs Arch. Pharmacol.* **351**, 610-617.

Ito, H., Takikawa, R., Kurachi, Y., & Sugimoto, T. (1989). Anti-cholinergic effect of verapamil on the muscarinic acetylcholine receptor-gated K^+ channel in isolated guinea-pig atrial myocytes. *Naunyn Schmiedebergs Arch. Pharmacol.* **339**, 244-246.

Ivanina, T., Varon, D., Peleg, S., Rishal, I., Porozov, Y., Dessauer, C. W., Keren-Raifman, T., & Dascal, N. (2004). Galphai1 and Galphai3 differentially interact with, and regulate, the G protein-activated K^+ channel. *J. Biol. Chem.* **279**, 17260-17268.

Jan, L. Y. (1999). Studies of voltage-dependent and inwardly rectifying potassium channels. In *Potassium ion channels: Molecular structure, function , and disease*, eds. Kurachi, Y., Jan, L. Y., & Lazdunski, M., pp. 1-5. Academic Press, San Diego.

Jan, L. Y. & Jan, Y. N. (1997). Cloned potassium channels from eukaryotes and prokaryotes. *Annu. Rev. Neurosci.* **20**, 91-123.

Janigro, D., Nguyen, T. S., Gordon, E. L., & Winn, H. R. (1996). Physiological properties of ATP-activated cation channels in rat brain microvascular endothelial cells. *Am. J. Physiol* **270**, H1423-H1434.

Janigro, D., West, G. A., Gordon, E. L., & Winn, H. R. (1993). ATP-sensitive K^+ channels in rat aorta and brain microvascular endothelial cells. *Am. J. Physiol.* **265**, C812-821.

Jelacic, T. M., Kennedy, M. E., Wickman, K., & Clapham, D. E. (2000). Functional and biochemical evidence for G-protein-gated inwardly rectifying K^+ (GIRK) channels composed of GIRK2 and GIRK3. *J. Biol. Chem.* **275**, 36211-36216.

Jentsch, T. J. (2000). Neuronal KCNQ potassium channels: physiology and role in disease. *Nat. Rev. Neurosci.* **1**, 21-30.

Jeong, S. W. & Ikeda, S. R. (2001). Differential regulation of G protein-gated inwardly rectifying K^+ channel kinetics by distinct domains of RGS8. *J. Physiol.* **535**, 335-347.

Jiang, C., Qu, Z., & Xu, H. (2002a). Gating of inward rectifier K^+ channels by proton-mediated interactions of intracellular protein domains. *Trends Cardiovasc. Med.* **12**, 5-13.

Jiang, Y., Lee, A., Chen, J., Cadene, M., Chait, B. T., & MacKinnon, R. (2002b). Crystal structure and mechanism of a calcium-gated potassium channel. *Nature* **417**, 515-522.

Jiang, Y., Lee, A., Chen, J., Cadene, M., Chait, B. T., & MacKinnon, R. (2002c). The open pore conformation of potassium channels. *Nature* **417**, 523-526.

Jiang, Y., Lee, A., Chen, J., Ruta, V., Cadene, M., Chait, B. T., & MacKinnon, R. (2003a). X-ray structure of a voltage-dependent K^+ channel. *Nature* **423**, 33-41.

Jiang, Y., Pico, A., Cadene, M., Chait, B. T., & MacKinnon, R. (2001). Structure of the RCK domain from the E. coli K^+ channel and demonstration of its presence in the human BK channel. *Neuron* **29**, 593-601.

Jiang, Y., Ruta, V., Chen, J., Lee, A., & MacKinnon, R. (2003b). The principle of gating charge movement in a voltage-dependent K^+ channel. *Nature* **423**, 42-48.

Jiang, Y. & MacKinnon, R. (2000). The barium site in a potassium channel by x-ray crystallography. *J. Gen. Physiol.* **115**, 269–272.

Jin, T., Peng, L., Mirshahi, T., Rohacs, T., Chan, K. W., Sanchez, R., & Logothetis, D. E. (2002). The βγ-subunits of G proteins gate a K^+ channel by pivoted bending of a transmembrane segment. *Mol. Cell* **10**, 469-481.

Jin, W. & Lu, Z. (1998). A novel high-affinity inhibitor for inward-rectifier K^+ channels. *Biochemistry* **37**, 13291-13299.

Jin, W. & Lu, Z. (1999). Synthesis of a stable form of tertiapin: a high-affinity inhibitor for inward-rectifier K^+ channels. *Biochemistry* **38**, 14286-14293.

Johnston, D., Hoffman, D. A., Magee, J. C., Poolos, N. P., Watanabe, S., Colbert, C. M., & Migliore, M. (2000). Dendritic potassium channels in hippocampal pyramidal neurons. *J. Physiol.* **525**, 75-81.

Josephson, I. R. & Brown, A. M. (1986). Inwardly rectifying single-channel and whole cell K^+ currents in rat ventricular myocytes. *J. Membr. Biol.* **94**, 19-35.

Josephson, I. R., Sanchez-Chapula, J., & Brown, A. M. (1984). Early outward current in rat single ventricular cells. *Circ. Res.* **54**, 157-162.

Josephson, I. R. & Sperelakis, N. (1990). Developmental increases in the inwardly-rectifying K^+ current of embryonic chick ventricular myocytes. *Biochim. Biophys. Acta* **1052**, 123-127.

Jow, F., Sullivan, K., Sokol, P., & Numann, R. (1999). Induction of Ca^{2+}-activated K^+ current and transient outward currents in human capillary endothelial cells. *J. Membr. Biol.* **167**, 53-64.

Jurkiewicz, N. K. & Sanguinetti, M. C. (1993). Rate-dependent prolongation of cardiac action potentials by a methanesulfonanilide class III antiarrhythmic agent. Specific block of rapidly activating delayed rectifier K^+ current by dofetilide. *Circ. Res.* **72**, 75-83.

Kaab, S., Dixon, J., Duc, J., Ashen, D., Nabauer, M., Beuckelmann, D. J., Steinbeck, G., McKinnon, D., & Tomaselli, G. F. (1998). Molecular basis of transient outward potassium current downregulation in human heart failure: a decrease in Kv4.3 mRNA correlates with a reduction in current density. *Circulation* **98**, 1383-1393.

Kaibara, M., Nakajima, T., Irisawa, H., & Giles, W. (1991). Regulation of spontaneous opening of muscarinic K^+ channels in rabbit atrium. *J. Physiol.* **433**, 589-613.

Kajimura, M. & Curry, F. E. (1999). Endothelial cell shrinkage increases permeability through a Ca^{2+}-dependent pathway in single frog mesenteric microvessels. *J. Physiol.* **518**, 227-238.

Kalsi, A. S., Greenwood, K., Wilkin, G., & Butt, A. M. (2004). Kir4.1 expression by astrocytes and oligodendrocytes in CNS white matter: a developmental study in the rat optic nerve. *J. Anat.* **204**, 475-485.

Kamb, A., Iverson, L. E., & Tanouye, M. A. (1987). Molecular characterization of Shaker, a Drosophila gene that encodes a potassium channel. *Cell* **50**, 405-413.

Kamouchi, M., Van Den, B. K., Eggermont, J., Droogmans, G., & Nilius, B. (1997). Modulation of inwardly rectifying potassium channels in cultured bovine pulmonary artery endothelial cells. *J. Physiol.* **504**, 545-556.

Karschin, A., Wischmeyer, E., Davidson, N., & Lester, H. A. (1994a). Fast inhibition of inwardly rectifying K^+ channels by multiple neurotransmitter receptors in oligodendroglia. *Eur. J. Neurosci.* **6**, 1756-1764.

Karschin, C., Dissmann, E., Stuhmer, W., & Karschin, A. (1996). IRK(1-3) and GIRK(1-4) inwardly rectifying K^+ channel mRNAs are differentially expressed in the adult rat brain. *J. Neurosci.* **16**, 3559-3570.

Karschin, C. & Karschin, A. (1997). Ontogeny of gene expression of Kir channel subunits in the rat. *Mol. Cell Neurosci.* **10**, 131-148.

Karschin, C. & Karschin, A. (1999). Distribution of inwardly rectifying potassium channels in the brain. In *Potassium ion channels: Molecular structure, function, and diseases*, eds. Kurachi, Y., Jan, L. Y., & Lazdunski, M., pp. 273-289. Academic Press, San Diego.

Karschin, C., Schreibmayer, W., Dascal, N., Lester, H., Davidson, N., & Karschin, A. (1994b). Distribution and localization of a G protein-coupled inwardly rectifying K^+ channel in the rat. *FEBS Lett.* **348**, 139-144.

Katayama, J., Yakushiji, T., & Akaike, N. (1997). Characterization of the K^+ current mediated by 5-HT1A receptor in the acutely dissociated rat dorsal raphe neurons. *Brain Res.* **745**, 283-292.

Katnik, C. & Adams, D. J. (1995). An ATP-sensitive potassium conductance in rabbit arterial endothelial cells. *J. Physiol.* **485**, 595-606.

Katnik, C. & Adams, D. J. (1997). Characterization of ATP-sensitive potassium channels in freshly dissociated rabbit aortic endothelial cells. *Am. J. Physiol.* **272**, H2507-2511.

Katsura, K., Minamisawa, H., Ekholm, A., Folbergrova, J., & Siesjo, B. K. (1992). Changes of labile metabolites during anoxia in moderately hypo- and hyperthermic rats: correlation to membrane fluxes of K^+. *Brain Res.* **590**, 6-12.

Katz, B. (1949). Les constantes électrique de la membrane du muscle. *Arch. Sci. Physiol.* **3**, 285-299.

Kenna, S., Roper, J., Ho, K., Hebert, S., Ashcroft, S. J., & Ashcroft, F. M. (1994). Differential expression of the inwardly-rectifying K^+ channel ROMK1 in rat brain. *Brain Res. Mol. Brain Res.* **24**, 353-356.

Kenyon, J. L. & Gibbons, W. R. (1979). 4-Aminopyridine and the early outward current of sheep cardiac Purkinje fibers. *J. Gen. Physiol.* **73**, 139-157.

Khanna, R., Roy, L., Zhu, X., & Schlichter, L. C. (2001). K^+ channels and the microglial respiratory burst. *Am. J. Physiol. Cell Physiol.* **280**, C796-806.

Kirchhof, C. J., Bonke, F. I., & Allessie, M. A. (1988). Evidence for the presence of electrotonic depression of pacemakers in the rabbit atrioventricular node. The effects of uncoupling from the surrounding myocardium. *Basic Res. Cardiol.* **83**, 190-201.

Kiss, L., LoTurco, J., & Korn, S. J. (1999). Contribution of the selectivity filter to inactivation in potassium channels. *Biophys. J.* **76**, 253-263.

Kitamura, H., Yokoyama, M., Akita, H., Matsushita, K., Kurachi, Y., & Yamada, M. (2000). Tertiapin potently and selectively blocks muscarinic K^+ channels in rabbit cardiac myocytes. *J. Pharmacol. Exp. Ther.* **293**, 196-205.

Klishin, A., Sedova, M., & Blatter, L. A. (1998). Time-dependent modulation of capacitative Ca^{2+} entry signals by plasma membrane Ca^{2+} pump in endothelium. *Am. J. Physiol.* **274**, C1117-1128.

Kobayashi, T., Ikeda, K., Ichikawa, T., Abe, S., Togashi, S., & Kumanishi, T. (1995). Molecular cloning of a mouse G-protein-activated K^+ channel (mGIRK1) and distinct distributions of three GIRK (GIRK1, 2 and 3) mRNAs in mouse brain. *Biochem. Biophys. Res. Commun.* **208**, 1166-1173.

Kobertz, W. R. & Miller, C. (1999). K^+ channels lacking the 'tetramerization' domain: implications for pore structure. *Nat. Struct. Biol.* **6**, 1122-1125.

Kofuji, P., Hofer, M., Millen, K. J., Millonig, J. H., Davidson, N., Lester, H. A., & Hatten, M. E. (1996). Functional analysis of the weaver mutant GIRK2 K^+ channel and rescue of weaver granule cells. *Neuron* **16**, 941-952.

Korngreen, A. & Sakmann, B. (2000). Voltage-gated K^+ channels in layer 5 neocortical pyramidal neurones from young rats: subtypes and gradients. *J. Physiol.* **525**, 621-639.

Korth, R. M., Hirafuji, M., Benveniste, J., & Russo-Marie, F. (1995). Human umbilical vein endothelial cells: specific binding of platelet-activating factor and cytosolic calcium flux. *Biochem. Pharmacol.* **49**, 1793-1799.

Koumi, S., Sato, R., Nagasawa, K., & Hayakawa, H. (1997). Activation of inwardly rectifying potassium channels by muscarinic receptor-linked G protein in isolated human ventricular myocytes. *J. Membr. Biol.* **157**, 71-81.

Kovoor, P., Wickman, K., Maguire, C. T., Pu, W., Gehrmann, J., Berul, C. I., & Clapham, D. E. (2001). Evaluation of the role of I_{KACh} in atrial fibrillation using a mouse knockout model. *J. Am. Coll. Cardiol.* **37**, 2136-2143.

Kozasa T, Kaziro Y, Ohtsuka T, Grigg JJ, Nakajima S & Nakajima Y (1996). G protein specificity of the muscarine-induced increase in an inward rectifier current in AtT-20 cells. *Neurosci Res* 26:289–297.

Koyama, H., Morishige, K., Takahashi, N., Zanelli, J. S., Fass, D. N., & Kurachi, Y. (1994). Molecular cloning, functional expression and localization of a novel inward rectifier potassium channel in the rat brain. *FEBS Lett.* **341**, 303-307.

Kramer, J. W., Post, M. A., Brown, A. M., & Kirsch, G. E. (1998). Modulation of potassium channel gating by coexpression of Kv2.1 with regulatory Kv5.1 or Kv6.1 alpha-subunits. *Am. J. Physiol.* **274**, C1501-1510.

Krapivinsky, G., Gordon, E. A., Wickman, K., Velimirovic, B., Krapivinsky, L., & Clapham, D. E. (1995a). The G-protein-gated atrial K^+ channel I_{KACh} is a heteromultimer of two inwardly rectifying K^+-channel proteins. *Nature* **374**, 135-141.

Krapivinsky, G., Krapivinsky, L., Wickman, K., & Clapham, D. E. (1995b). G beta gamma binds directly to the G protein-gated K^+ channel, I_{KACh}. *J. Biol. Chem.* **270**, 29059-29062.

Kreusch, A., Pfaffinger, P. J., Stevens, C. F., & Choe, S. (1998). Crystal structure of the tetramerization domain of the Shaker potassium channel. *Nature* **392**, 945-948.

Kubo, Y., Baldwin, T. J., Jan, Y. N., & Jan, L. Y. (1993a). Primary structure and functional expression of a mouse inward rectifier potassium channel. *Nature* **362**, 127-133.

Kubo, Y. & Murata, Y. (2001). Control of rectification and permeation by two distinct sites after the second transmembrane region in Kir2.1 K^+ channel. *J. Physiol.* **531**, 645-660.

Kubo, Y., Reuveny, E., Slesinger, P. A., Jan, Y. N., & Jan, L. Y. (1993b). Primary structure and functional expression of a rat G-protein-coupled muscarinic potassium channel. *Nature* **364**, 802-806.

Kullmann, D. M. (2002). The neuronal channelopathies. *Brain* **125**, 1177-1195.

Kuo, A., Gulbis, J. M., Antcliff, J. F., Rahman, T., Lowe, E. D., Zimmer, J., Cuthbertson, J., Ashcroft, F. M., Ezaki, T., & Doyle, D. A. (2003). Crystal structure of the potassium channel KirBac1.1 in the closed state. *Science* **300**, 1922-1926.

Kuo, H. C., Cheng, C. F., Clark, R. B., Lin, J. J., Lin, J. L., Hoshijima, M., Nguyen-Tran, V. T., Gu, Y., Ikeda, Y., Chu, P. H., Ross, J., Giles, W. R., & Chien, K. R. (2001). A defect in the Kv channel-interacting protein 2 (KChIP2) gene leads to a complete loss of I_{to} and confers susceptibility to ventricular tachycardia. *Cell* **107**, 801-813.

Kuo, L. & Chancellor, J. D. (1995). Adenosine potentiates flow-induced dilation of coronary arterioles by activating K_{ATP} channels in endothelium. *Am. J. Physiol.* **269**, H541-549.

Kurachi, Y. & Ishii, M. (2004). Cell signal control of the G protein-gated potassium channel and its subcellular localization. *J. Physiol.* **554**, 285-294.

Kurachi, Y., Ito, H., Sugimoto, T., Katada, T., & Ui, M. (1989). Activation of atrial muscarinic K^+ channels by low concentrations of beta gamma subunits of rat brain G protein. *Pflugers Arch.* **413**, 325-327.

Kurachi, Y., Nakajima, T., & Sugimoto, T. (1986a). Acetylcholine activation of K^+ channels in cell-free membrane of atrial cells. *Am. J. Physiol.* **251**, H681-684.

Kurachi, Y., Nakajima, T., & Sugimoto, T. (1986b). On the mechanism of activation of muscarinic K^+ channels by adenosine in isolated atrial cells: involvement of GTP-binding proteins. *Pflugers Arch.* **407**, 264-274.

Kurachi, Y., Nakajima, T., & Sugimoto, T. (1987). Quinidine inhibition of the muscarine receptor-activated K^+ channel current in atrial cells of guinea pig. *Naunyn Schmiedebergs Arch. Pharmacol.* **335**, 216-218.

Kurachi, Y., Tung, R. T., Ito, H., & Nakajima, T. (1992). G protein activation of cardiac muscarinic K^+ channels. *Prog. Neurobiol.* **39**, 229-246.

Kurokawa, J., Abriel, H., & Kass, R. S. (2001). Molecular basis of the delayed rectifier current I_{Ks}in heart. *J. Mol. Cell Cardiol.* **33**, 873-882.

Kurose, H., Katada, T., Haga, T., Haga, K., Ichiyama, A., & Ui, M. (1986). Functional interaction of purified muscarinic receptors with purified inhibitory guanine nucleotide regulatory proteins reconstituted in phospholipid vesicles. *J. Biol. Chem.* **261**, 6423-6428.

Kuryshev, Y. A., Gudz, T. I., Brown, A. M., & Wible, B. A. (2000). KChAP as a chaperone for specific K^+ channels. *Am. J. Physiol. Cell Physiol.* **278**, C931-941.

Kuryshev, Y. A., Wible, B. A., Gudz, T. I., Ramirez, A. N., & Brown, A. M. (2001). KChAP/Kvbeta1.2 interactions and their effects on cardiac Kv channel expression. *Am. J. Physiol. Cell Physiol.* **281**, C290-299.

Kus, T. & Sasyniuk, B. I. (1975). Electrophysiological actions of disopyramide phosphate on canine ventricular muscle and purkinje fibers. *Circ. Res.* **37**, 844-854.

Kusaka, S., Horio, Y., Fujita, A., Matsushita, K., Inanobe, A., Gotow, T., Uchiyama, Y., Tano, Y., & Kurachi, Y. (1999). Expression and polarized distribution of an inwardly rectifying K^+ channel, Kir4.1, in rat retinal pigment epithelium. *J. Physiol.* **520**, 373-381.

Kusaka, S., Inanobe, A., Fujita, A., Makino, Y., Tanemoto, M., Matsushita, K., Tano, Y., & Kurachi, Y. (2001). Functional Kir7.1 channels localized at the root of apical processes in rat retinal pigment epithelium. *J. Physiol.* **531**, 27-36.

Kwan, H. Y., Leung, P. C., Huang, Y., & Yao, X. (2003). Depletion of intracellular Ca^{2+} stores sensitizes the flow-induced Ca^{2+} influx in rat endothelial cells. *Circ. Res.* **92**, 286-292.

Lacey, M. G., Mercuri, N. B., & North, R. A. (1987). Dopamine acts on D2 receptors to increase potassium conductance in neurones of the rat substantia nigra zona compacta. *J. Physiol.* **392**, 397-416.

Lacey, M. G., Mercuri, N. B., & North, R. A. (1988). On the potassium conductance increase activated by GABAB and dopamine D2 receptors in rat substantia nigra neurones. *J. Physiol.* **401**, 437-453.

Lane, P. W. (1964). *Mouse News Letter* 30-32.

Lanier, S. M. (2004). AGS proteins, GPR motifs and the signals processed by heterotrimeric G proteins. *Biol. Cell* **96**, 369-372.

Lantoine, F., Iouzalen, L., Devynck, M. A., Millanvoye-Van Brussel, E., & David-Dufilho, M. (1998). Nitric oxide production in human endothelial cells stimulated by histamine requires Ca^{2+} influx. *Biochem. J.* **330**, 695-699.

Larsson, H. P., Baker, O. S., Dhillon, D. S., & Isacoff, E. Y. (1996a). Transmembrane movement of the shaker K^+ channel S4. *Neuron* **16**, 387-397.

Larsson, O., Deeney, J. T., Branstrom, R., Berggren, P. O., & Corkey, B. E. (1996b). Activation of the ATP-sensitive K^+ channel by long chain acyl-CoA - A role in modulation of pancreatic beta-cell glucose sensitivity. *J. Biol. Chem.* **271**, 10623-10626.

Laube, G., Roper, J., Pitt, J. C., Sewing, S., Kistner, U., Garner, C. C., Pongs, O., & Veh, R. W. (1996). Ultrastructural localization of Shaker-related potassium channel subunits and synapse-associated protein 90 to septate-like junctions in rat cerebellar Pinceaux. *Brain Res. Mol. Brain Res.* **42**, 51-61.

Lauritzen, I., de Weille, J., Adelbrecht, C., Lesage, F., Murer, G., Raisman-Vozari, R., & Lazdunski, M. (1997). Comparative expression of the inward rectifier K^+ channel GIRK2 in the cerebellum of normal and weaver mutant mice. *Brain Res.* **753**, 8-17.

Lee, J. K., John, S. A., & Weiss, J. N. (1999). Novel gating mechanism of polyamine block in the strong inward rectifier K^+ channel Kir2.1. *J. Gen. Physiol.* **113**, 555-564.

Lees-Miller, J. P., Kondo, C., Wang, L., & Duff, H. J. (1997). Electrophysiological characterization of an alternatively processed ERG K^+ channel in mouse and human hearts. *Circ. Res.* **81**, 719-726.

Lei, M., Honjo, H., Kodama, I., & Boyett, M. R. (2001). Heterogeneous expression of the delayed-rectifier K^+ currents I_{Kr} and I_{Ks} in rabbit sinoatrial node cells. *J. Physiol.* **535**, 703-714.

Lesage, F., Guillemare, E., Fink, M., Duprat, F., Heurteaux, C., Fosset, M., Romey, G., Barhanin, J., & Lazdunski, M. (1995). Molecular properties of neuronal G-protein-activated inwardly rectifying K^+ channels. *J. Biol. Chem.* **270**, 28660-28667.

Lesage, F., Guillemare, E., Fink, M., Duprat, F., Lazdunski, M., Romey, G., & Barhanin, J. (1996a). TWIK-1, a ubiquitous human weakly inward rectifying K^+ channel with a novel structure. *EMBO J.* **15**, 1004-1011.

Lesage, F., Lauritzen, I., Duprat, F., Reyes, R., Fink, M., Heurteaux, C., & Lazdunski, M. (1997). The structure, function and distribution of the mouse TWIK-1 K^+ channel. *FEBS Lett.* **402**, 28-32.

Lesage, F. & Lazdunski, M. (2000). Molecular and functional properties of two-pore-domain potassium channels. *Am. J. Physiol. Renal Physiol.* **279**, F793-F801.

Lesage, F., Reyes, R., Fink, M., Duprat, F., Guillemare, E., & Lazdunski, M. (1996b). Dimerization of TWIK-1 K^+ channel subunits via a disulfide bridge. *EMBO J.* **15**, 6400-6407.

Li, D., Zhang, L., Kneller, J., & Nattel, S. (2001). Potential ionic mechanism for repolarization differences between canine right and left atrium. *Circ. Res.* **88**, 1168-1175.

Li, G. R., Feng, J., Yue, L., Carrier, M., & Nattel, S. (1996). Evidence for two components of delayed rectifier K^+ current in human ventricular myocytes. *Circ. Res.* **78**, 689-696.

Li, M., Jan, Y. N., & Jan, L. Y. (1992). Specification of subunit assembly by the hydrophilic amino-terminal domain of the Shaker potassium channel. *Science* **257**, 1225-1230.

Li-Smerin, Y., Hackos, D. H., & Swartz, K. J. (2000). A localized interaction surface for voltage-sensing domains on the pore domain of a K^+ channel. *Neuron* **25**, 411-423.

Liao, Y. J., Jan, Y. N., & Jan, L. Y. (1996). Heteromultimerization of G-protein-gated inwardly rectifying K^+ channel proteins GIRK1 and GIRK2 and their altered expression in weaver brain. *J. Neurosci.* **16**, 7137-7150.

Lieu, D. K., Pappone, P. A., & Barakat, A. I. (2004). Differential membrane potential and ion current responses to different types of shear stress in vascular endothelial cells. *Am. J. Physiol. Cell Physiol.* **286**, C1367-1375.

Lim, S. T., Antonucci, D. E., Scannevin, R. H., & Trimmer, J. S. (2000). A novel targeting signal for proximal clustering of the Kv2.1 K^+ channel in hippocampal neurons. *Neuron* **25**, 385-397.

Lipton, P. (1999). Ischemic cell death in brain neurons. *Physiol Rev.* **79**, 1431-1568.

Litovsky, S. H. & Antzelevitch, C. (1988). Transient outward current prominent in canine ventricular epicardium but not endocardium. *Circ. Res.* **62**, 116-126.

Litovsky, S. H. & Antzelevitch, C. (1989). Rate dependence of action potential duration and refractoriness in canine ventricular endocardium differs from that of epicardium: role of the transient outward current. *J. Am. Coll. Cardiol.* **14**, 1053-1066.

Liu, D. W. & Antzelevitch, C. (1995). Characteristics of the delayed rectifier current (I_{Kr} and I_{Ks}) in canine ventricular epicardial, midmyocardial, and endocardial myocytes. A weaker I_{Ks} contributes to the longer action potential of the M cell. *Circ. Res.* **76**, 351-365.

Liu, D. W., Gintant, G. A., & Antzelevitch, C. (1993). Ionic bases for electrophysiological distinctions among epicardial, midmyocardial, and endocardial myocytes from the free wall of the canine left ventricle. *Circ. Res.* **72**, 671-687.

Liu, G. X., Derst, C., Schlichthorl, G., Heinen, S., Seebohm, G., Bruggemann, A., Kummer, W., Veh, R. W., Daut, J., & Preisig-Muller, R. (2001). Comparison of cloned Kir2 channels with native inward rectifier K^+ channels from guinea-pig cardiomyocytes. *J. Physiol.* **532**, 115-126.

Liu, Q. & Flavahan, N. A. (1997). Hypoxic dilatation of porcine small coronary arteries: role of endothelium and K_{ATP}-channels. *Br. J. Pharmacol.* **120**, 728-734.

Liu, X. K., Yamada, S., Kane, G. C., Alekseev, A. E., Hodgson, D. M., O'Cochlain, F., Jahangir, A., Miki, T., Seino, S., & Terzic, A. (2004). Genetic disruption of Kir6.2, the pore-forming subunit of ATP-sensitive K^+ channel, predisposes to catecholamine-induced ventricular dysrhythmia. *Diabetes* **53**, S165-168.

Liu, Y., Holmgren, M., Jurman, M. E., & Yellen, G. (1997). Gated access to the pore of a voltage-dependent K^+ channel. *Neuron* **19**, 175-184.

Liu, Y., Jurman, M. E., & Yellen, G. (1996). Dynamic rearrangement of the outer mouth of a K^+ channel during gating. *Neuron* **16**, 859-867.

Liu, Y., Sato, T., O'Rourke, B., & Marban, E. (1998). Mitochondrial ATP-dependent potassium channels: novel effectors of cardioprotection? *Circulation* **97**, 2463-2469.

Loboda, A., Melishchuk, A., & Armstrong, C. (2001). Dilated and defunct K^+ channels in the absence of K^+. *Biophys. J.* **80**, 2704-2714.

Loewi, O. (1921). Über humorale Übertragbarkeit der Herznervenwirkung. *Pflugers Arch.* **189**, 239-242.

Loewi, O. & Navaratil, E. (1926). Übertragbarkeit der Herznervenwirkung, X. Mitteilung. Über das Schicksal des Vagusstoffs. *Pflugers Arch.* **214**, 678-688.

Logothetis, D. E., Kurachi, Y., Galper, J., Neer, E. J., & Clapham, D. E. (1987). The beta gamma subunits of GTP-binding proteins activate the muscarinic K^+ channel in heart. *Nature* **325**, 321-326.

London, B., Trudeau, M. C., Newton, K. P., Beyer, A. K., Copeland, N. G., Gilbert, D. J., Jenkins, N. A., Satler, C. A., & Robertson, G. A. (1997). Two isoforms of the mouse ether-a-go-go-related gene coassemble to form channels with properties similar to the rapidly activating component of the cardiac delayed rectifier K^+ current. *Circ. Res.* **81**, 870-878.

Long, S. B., Campbell, E. B., & MacKinnon, R. (2005a). Crystal structure of a mammalian voltage-dependent shaker family K^+ channel. *Science* **309**, 897-903.

Long, S. B., Campbell, E. B., & MacKinnon, R. (2005b). Voltage sensor of Kv1.2: Structural basis of electromechanical coupling. *Science* **309**, 903-908.

Lopatin, A. N., Makhina, E. N., & Nichols, C. G. (1994). Potassium channel block by cytoplasmic polyamines as the mechanism of intrinsic rectification. *Nature* **372**, 366-369.

Lopatin, A. N., Makhina, E. N., & Nichols, C. G. (1995). The mechanism of inward rectification of potassium channels: "long-pore plugging" by cytoplasmic polyamines. *J. Gen. Physiol.* **106**, 923-955.

Lopatin, A. N. & Nichols, C. G. (2001). Inward rectifiers in the heart: an update on I_{K1}. *J. Mol. Cell Cardiol.* **33**, 625-638.

Lopes, C. M., Zhang, H., Rohacs, T., Jin, T., Yang, J., & Logothetis, D. E. (2002). Alterations in conserved Kir channel-PIP_2 interactions underlie channelopathies. *Neuron* **34**, 933-944.

Lopez, G. A., Jan, Y. N., & Jan, L. Y. (1994). Evidence that the S6 segment of the Shaker voltage-gated K^+ channel comprises part of the pore. *Nature* **367**, 179-182.

Lourdel, S., Paulais, M., Cluzeaud, F., Bens, M., Tanemoto, M., Kurachi, Y., Vandewalle, A., & Teulon, J. (2002). An inward rectifier K^+ channel at the basolateral membrane of the mouse distal convoluted tubule: similarities with Kir4-Kir5.1 heteromeric channels. *J. Physiol.* **538**, 391-404.

Lu, T., Wu, L., Xiao, J., & Yang, J. (2001a). Permeant ion-dependent changes in gating of Kir2.1 inward rectifier potassium channels. *J. Gen. Physiol.* **118**, 509-522.

Lu, T., Zhu, Y. G., & Yang, J. (1999). Cytoplasmic amino and carboxyl domains form a wide intracellular vestibule in an inwardly rectifying potassium channel. *Proc. Natl. Acad. Sci. U.S.A.* **96**, 9926-9931.

Lu, Z., Klem, A. M., & Ramu, Y. (2001b). Ion conduction pore is conserved among potassium channels. *Nature* **413**, 809-813.

Lu, Z., Klem, A. M., & Ramu, Y. (2002). Coupling between voltage sensors and activation gate in voltage-gated K^+ channels. *J. Gen. Physiol.* **120**, 663-676.

Lu, Z. & MacKinnon, R. (1994). Electrostatic tuning of Mg^{2+} affinity in an inward-rectifier K^+ channel. *Nature* **371**, 243-246.

Luckhoff, A. & Busse, R. (1990). Calcium influx into endothelial cells and formation of endothelium-derived relaxing factor is controlled by the membrane potential. *Pflugers Arch.* **416**, 305-311.

Luckhoff, A. & Clapham, D. E. (1992). Inositol 1,3,4,5-tetrakisphosphate activates an endothelial Ca^{2+}-permeable channel. *Nature* **355**, 356-358.

Ludwig, J., Terlau, H., Wunder, F., Bruggemann, A., Pardo, L. A., Marquardt, A., Stuhmer, W., & Pongs, O. (1994). Functional expression of a rat homologue of the voltage gated either a go-go potassium channel reveals differences in selectivity and activation kinetics between the Drosophila channel and its mammalian counterpart. *EMBO J.* **13**, 4451-4458.

Luscher, C., Jan, L. Y., Stoffel, M., Malenka, R. C., & Nicoll, R. A. (1997). G protein-coupled inwardly rectifying K^+ channels (GIRKs) mediate postsynaptic but not presynaptic transmitter actions in hippocampal neurons. *Neuron* **19**, 687-695.

Luscher, T. F. (1994). The endothelium and cardiovascular disease - a complex relation. *NEJM* **330**, 1081-1083.

Luzhkov, V. B. & Aqvist, J. (2001). K^+/Na^+ selectivity of the KcsA potassium channel from microscopic free energy perturbation calculations. *Biochim. Biophys. Acta* **1548**, 194-202.

MacKinnon, R. (1991). Determination of the subunit stoichiometry of a voltage-activated potassium channel. *Nature* **350**, 232-235.

MacKinnon, R. (2003). Potassium channels. *FEBS Lett.* **555**, 62-65.

MacKinnon, R. (2004). Nobel Lecture. Potassium channels and the atomic basis of selective ion conduction. *Biosci. Rep.* **24**, 75-100.

MacKinnon, R. & Miller, C. (1988). Mechanism of charybdotoxin block of the high-conductance, Ca^{2+}-activated K^+ channel. *J. Gen. Physiol.* **91**, 335-349.

Main, M. C., Bryant, S. M., & Hart, G. (1998). Regional differences in action potential characteristics and membrane currents of guinea-pig left ventricular myocytes. *Exp. Physiol.* **83**, 747-761.

Majumder, K., De Biasi, M., Wang, Z., & Wible, B. A. (1995). Molecular cloning and functional expression of a novel potassium channel beta-subunit from human atrium. *FEBS Lett.* **361**, 13-16.

Makhina, E. N., Kelly, A. J., Lopatin, A. N., Mercer, R. W., & Nichols, C. G. (1994). Cloning and expression of a novel human brain inward rectifier potassium channel. *J. Biol. Chem.* **269**, 20468-20474.

Maletic-Savatic, M., Lenn, N. J., & Trimmer, J. S. (1995). Differential spatiotemporal expression of K^+ channel polypeptides in rat hippocampal neurons developing in situ and in vitro. *J. Neurosci.* **15**, 3840-3851.

Mao, J., Wu, J., Chen, F., Wang, X., & Jiang, C. (2003). Inhibition of G-protein-coupled inward rectifying K^+ channels by intracellular acidosis. *J. Biol. Chem.* **278**, 7091-7098.

Marban, E. (2002). Cardiac channelopathies. *Nature* **415**, 213-218.

Marchenko, S. M. & Sage, S. O. (1994). Mechanism of acetylcholine action on membrane potential of endothelium of intact rat aorta. *Am. J. Physiol.* **266**, H2388-2395.

Markworth, E., Schwanstecher, C., & Schwanstecher, M. (2000). ATP mediates closure of pancreatic beta-cell ATP-sensitive potassium channels by interaction with 1 of 4 identical sites. *Diabetes* **49**, 1413-1418.

Martin, R. L., Koumi, S., & Ten Eick, R. E. (1995). Comparison of the effects of internal Mg^{2+} on I_{K1} in cat and guinea-pig cardiac ventricular myocytes. *J. Mol. Cell Cardiol.* **27**, 673-691.

Martina, M., Yao, G. L., & Bean, B. P. (2003). Properties and functional role of voltage-dependent potassium channels in dendrites of rat cerebellar Purkinje neurons. *J. Neurosci.* **23**, 5698-5707.

Mascher, D. & Peper, K. (1969). Two components of inward current in myocardial muscle fibers. *Pflugers Arch.* **307**, 190-203.

Matsuda, H., Saigusa, A., & Irisawa, H. (1987). Ohmic conductance through the inwardly rectifying K^+ channel and blocking by internal Mg^{2+}. *Nature* **325**, 156-159.

Matsuo, M., Kioka, N., Amachi, T., & Ueda, K. (1999a). ATP binding properties of the nucleotide-binding folds of SUR1. *J. Biol. Chem.* **274**, 37479-37482.

Matsuo, M., Tucker, S. J., Ashcroft, F. M., Amachi, T., & Ueda, K. (1999b). NEM modification prevents high-affinity ATP binding to the first nucleotide binding fold of the sulphonylurea receptor, SUR1. *FEBS Lett.* **458**, 292-294.

Mazhari, R., Greenstein, J. L., Winslow, R. L., Marban, E., & Nuss, H. B. (2001). Molecular interactions between two long-QT syndrome gene products, HERG and KCNE2, rationalized by in vitro and in silico analysis. *Circ. Res.* **89**, 33-38.

McDonald, T. V., Yu, Z., Ming, Z., Palma, E., Meyers, M. B., Wang, K. W., Goldstein, S. A., & Fishman, G. I. (1997). A minK-HERG complex regulates the cardiac potassium current I_{Kr}. *Nature* **388**, 289-292.

McMorn, S. O., Harrison, S. M., Zang, W. J., Yu, X. J., & Boyett, M. R. (1993). A direct negative inotropic effect of acetylcholine on rat ventricular myocytes. *Am. J. Physiol.* **265**, H1393-1400.

McNamara, N. M., Averill, S., Wilkin, G. P., Dolly, J. O., & Priestley, J. V. (1996). Ultrastructural localization of a voltage-gated K^+ channel alpha subunit Kv1.2 in the rat cerebellum. *Eur. J. Neurosci.* **8**, 688-699.

McNamara, N. M., Muniz, Z. M., Wilkin, G. P., & Dolly, J. O. (1993). Prominent location of a K^+ channel containing the alpha subunit Kv1.2 in the basket cell nerve terminals of rat cerebellum. *Neuroscience* **57**, 1039-1045.

McNicholas, C. M., Wang, W., Ho, K., Hebert, S. C., & Giebisch, G. (1994). Regulation of ROMK1 K^+ channel activity involves phosphorylation processes. *Proc. Natl. Acad. Sci. U.S.A.* **91**, 8077-8081.

Melnyk, P., Zhang, L., Shrier, A., & Nattel, S. (2002). Differential distribution of Kir2.1 and Kir2.3 subunits in canine atrium and ventricle. *Am. J. Physiol. Heart Circ. Physiol.* **283**, H1123-1133.

Mendelowitz, D., Bacal, K., & Kunze, D. L. (1992). Bradykinin-activated calcium influx pathway in bovine aortic endothelial cells. *Am. J. Physiol.* **262**, H942-948.

Merideth, J., Mendez, C., Mueller, W. J., & Moe, G. K. (1968). Electrical excitability of atrioventricular nodal cells. *Circ. Res.* **23**, 69-85.

Miake, J., Marban, E., & Nuss, H. B. (2002). Biological pacemaker created by gene transfer. *Nature* **419**, 132-133.

Miake, J., Marban, E., & Nuss, H. B. (2003). Functional role of inward rectifier current in heart probed by Kir2.1 overexpression and dominant-negative suppression. *J. Clin. Invest.* **111**, 1529-1536.

Miki, T., Liss, B., Minami, K., Shiuchi, T., Saraya, A., Kashima, Y., Horiuchi, M., Ashcroft, F., Minokoshi, Y., Roeper, J., & Seino, S. (2001). ATP-sensitive K^+ channels in the hypothalamus are essential for the maintenance of glucose homeostasis. *Nat. Neurosci.* **4**, 507-512.

Miki, T., Suzuki, M., Shibasaki, T., Uemura, H., Sato, T., Yamaguchi, K., Koseki, H., Iwanaga, T., Nakaya, H., & Seino, S. (2002). Mouse model of Prinzmetal angina by disruption of the inward rectifier Kir6.1. *Nat. Med.* **8**, 466-472.

Mirshahi, T., Mittal, V., Zhang, H., Linder, M. E., & Logothetis, D. E. (2002). Distinct sites on G protein beta gamma subunits regulate different effector functions. *J. Biol. Chem.* **277**, 36345-36350.

Mitcheson, J. S., Chen, J., Lin, M., Culberson, C., & Sanguinetti, M. C. (2000). A structural basis for drug-induced long QT syndrome. *Proc. Natl. Acad. Sci. U.S.A.* **97**, 12329-12333.

Miyake, M., Christie, M. J., & North, R. A. (1989). Single potassium channels opened by opioids in rat locus ceruleus neurons. *Proc. Natl. Acad. Sci. U.S.A.* **86**, 3419-3422.

Miyashita, T. & Kubo, Y. (1997). Localization and developmental changes of the expression of two inward rectifying K^+-channel proteins in the rat brain. *Brain Res.* **750**, 251-263.

Mohammad, S., Zhou, Z., Gong, Q., & January, C. T. (1997). Blockage of the HERG human cardiac K^+ channel by the gastrointestinal prokinetic agent cisapride. *Am. J. Physiol.* **273**, H2534-2538.

Moore, T. M., Brough, G. H., Babal, P., Kelly, J. J., Li, M., & Stevens, T. (1998a). Store-operated calcium entry promotes shape change in pulmonary endothelial cells expressing Trp1. *Am. J. Physiol.* **275**, L574-582.

Moore, T. M., Chetham, P. M., Kelly, J. J., & Stevens, T. (1998b). Signal transduction and regulation of lung endothelial cell permeability. Interaction between calcium and cAMP. *Am. J. Physiol.* **275**, L203-222.

Morais-Cabral, J. H., Zhou, Y., & MacKinnon, R. (2001). Energetic optimization of ion conduction rate by the K^+ selectivity filter. *Nature* **414**, 37-42.

Moreau, C., Jacquet, H., Prost, A. L., D'hahan, N., & Vivaudou, M. (2000). The molecular basis of the specificity of action of K_{ATP} channel openers. *EMBO J.* **19**, 6644-6651.

Moreau, C., Prost, A. L., Derand, R., & Vivaudou, M. (2005). SUR, ABC proteins targeted by K_{ATP} channel openers. *J. Mol. Cell Cardiol.* **38**, 951-963.

Morishige, K., Takahashi, N., Jahangir, A., Yamada, M., Koyama, H., Zanelli, J. S., & Kurachi, Y. (1994). Molecular cloning and functional expression of a novel brain-specific inward rectifier potassium channel. *FEBS Lett.* **346**, 251-256.

Moritz, W., Leech, C. A., Ferrer, J., & Habener, J. F. (2001). Regulated expression of adenosine triphosphate-sensitive potassium channel subunits in pancreatic beta-cells. *Endocrinology* **142**, 129-138.

Mourre, C., Ben Ari, Y., Bernardi, H., Fosset, M., & Lazdunski, M. (1989). Antidiabetic sulfonylureas: localization of binding sites in the brain and effects on the hyperpolarization induced by anoxia in hippocampal slices. *Brain Res.* **486**, 159-164.

Munk, A. A., Adjemian, R. A., Zhao, J., Ogbaghebriel, A., & Shrier, A. (1996). Electrophysiological properties of morphologically distinct cells isolated from the rabbit atrioventricular node. *J. Physiol.* **493**, 801-818.

Murai, T., Kakizuka, A., Takumi, T., Ohkubo, H., & Nakanishi, S. (1989). Molecular cloning and sequence analysis of human genomic DNA encoding a novel membrane protein which exhibits a slowly activating potassium channel activity. *Biochem. Biophys. Res. Commun.* **161**, 176-181.

Murakoshi, H. & Trimmer, J. S. (1999). Identification of the Kv2.1 K^+ channel as a major component of the delayed rectifier K^+ current in rat hippocampal neurons. *J. Neurosci.* **19**, 1728-1735.

Murata, Y., Fujiwara, Y., & Kubo, Y. (2002). Identification of a site involved in the block by extracellular Mg^{2+} and Ba^{2+} as well as permeation of K^+ in the Kir2.1 K^+ channel. *J. Physiol.* **544**, 665-677.

Murer, G., Adelbrecht, C., Lauritzen, I., Lesage, F., Lazdunski, M., Agid, Y., & Raisman-Vozari, R. (1997). An immunocytochemical study on the distribution of two G-protein-gated inward rectifier potassium channels (GIRK2 and GIRK4) in the adult rat brain. *Neuroscience* **80**, 345-357.

Murrell-Lagnado, R. D. & Aldrich, R. W. (1993a). Energetics of Shaker K^+ channels block by inactivation peptides. *J. Gen. Physiol.* **102**, 977-1003.

Murrell-Lagnado, R. D. & Aldrich, R. W. (1993b). Interactions of amino terminal domains of Shaker K^+ channels with a pore blocking site studied with synthetic peptides. *J. Gen. Physiol.* **102**, 949-975.

Murry, C. E., Jennings, R. B., & Reimer, K. A. (1986). Preconditioning with ischemia: a delay of lethal cell injury in ischemic myocardium. *Circulation* **74**, 1124-1136.

Nabauer, M., Beuckelmann, D. J., Uberfuhr, P., & Steinbeck, G. (1996). Regional differences in current density and rate-dependent properties of the transient outward current in subepicardial and subendocardial myocytes of human left ventricle. *Circulation* **93**, 168-177.

Nadal, M. S., Ozaita, A., Amarillo, Y., Vega-Saenz, d. M., Ma, Y., Mo, W., Goldberg, E. M., Misumi, Y., Ikehara, Y., Neubert, T. A., & Rudy, B. (2003). The CD26-related dipeptidyl aminopeptidase-like protein DPPX is a critical component of neuronal A-type K^+ channels. *Neuron* **37**, 449-461.

Nakahira, K., Shi, G., Rhodes, K. J., & Trimmer, J. S. (1996). Selective interaction of voltage-gated K^+ channel beta-subunits with alpha-subunits. *J. Biol. Chem.* **271**, 7084-7089.

Nakajima, T., Kurachi, Y., Ito, H., Takikawa, R., & Sugimoto, T. (1989). Anti-cholinergic effects of quinidine, disopyramide, and procainamide in isolated atrial myocytes: mediation by different molecular mechanisms. *Circ. Res.* **64**, 297-303.

Nakajima, Y., Nakajima, S., & Inoue, M. (1988). Pertussis toxin-insensitive G protein mediates substance P-induced inhibition of potassium channels in brain neurons. *Proc. Natl. Acad. Sci. U.S.A.* **85**, 3643-3647.

Nakamura, N., Suzuki, Y., Sakuta, H., Ookata, K., Kawahara, K., & Hirose, S. (1999a). Inwardly rectifying K^+ channel Kir7.1 is highly expressed in thyroid follicular cells, intestinal epithelial cells and choroid plexus epithelial cells: implication for a functional coupling with Na^+/K^+-ATPase. *Biochem. J.* **342**, 329-336.

Nakamura, T. Y., Artman, M., Rudy, B., & Coetzee, W. A. (1998). Inhibition of rat ventricular I_{K1} with antisense oligonucleotides targeted to Kir2.1 mRNA. *Am. J. Physiol.* **274**, H892-900.

Nakamura, T. Y., Lee, K., Artman, M., Rudy, B., & Coetzee, W. A. (1999b). The role of Kir2.1 in the genesis of native cardiac inward-rectifier K^+ currents during pre- and postnatal development. *Ann. N. Y. Acad. Sci.* **868**, 434-437.

Nakaya, H., Takeda, Y., Tohse, N., & Kanno, M. (1991). Effects of ATP-sensitive K^+ channel blockers on the action potential shortening in hypoxic and ischaemic myocardium. *Br. J. Pharmacol.* **103**, 1019-1026.

Nakayama, T. & Irisawa, H. (1985). Transient outward current carried by potassium and sodium in quiescent atrioventricular node cells of rabbits. *Circ. Res.* **57**, 65-73.

Nattel, S., Khairy, P., & Schram, G. (2001). Arrhythmogenic ionic remodeling: adaptive responses with maladaptive consequences. *Trends Cardiovasc. Med.* **11**, 295-301.

Nattel, S. & Quantz, M. A. (1988). Pharmacological response of quinidine induced early afterdepolarisations in canine cardiac Purkinje fibres: insights into underlying ionic mechanisms. *Cardiovasc. Res.* **22**, 808-817.

Navaratnam, D. S., Escobar, L., Covarrubias, M. & Oberholtzer, J. C. (1995). Permeation properties and differential expression across the auditory receptor epithelium of an inward rectifier K^+ channel cloned from the chick inner ear. *J. Biol. Chem.* **270**, 19238–19245.

Navarro, B., Corey, S., Kennedy, M., & Clapham, D. (1999). G-protein-gated potassium channels: Implication for the weaver mouse. In *Potassium ion channels: Molecular structure, function, and diseases*, eds. Kurachi, Y., Jan, L. Y., & Lazdunski, M., pp. 295-320. Academic Press, San Diego.

Neer, E. J. (1995). Heterotrimeric G proteins: organizers of transmembrane signals. *Cell* **80**, 249-257.

Neer, E. J. & Clapham, D. E. (1988). Roles of G protein subunits in transmembrane signalling. *Nature* **333**, 129-134.

Nelson, M. T. & Quayle, J. M. (1995). Physiological roles and properties of potassium channels in arterial smooth muscle. *Am. J. Physiol.* **268**, C799-822.

Nerbonne, J. M. (2000). Molecular basis of functional voltage-gated K^+ channel diversity in the mammalian myocardium. *J. Physiol.* **525**, 285-298.

Neusch, C., Rozengurt, N., Jacobs, R. E., Lester, H. A., & Kofuji, P. (2001). Kir4.1 potassium channel subunit is crucial for oligodendrocyte development and in vivo myelination. *J. Neurosci.* **21**, 5429-5438.

Newman, E. A. (1993). Inward-rectifying potassium channels in retinal glial (Muller) cells. *J. Neurosci.* **13**, 3333-3345.

Neyton, J. & Miller, C. (1988a). Potassium blocks barium permeation through a calcium-activated potassium channel. *J. Gen. Physiol.* **92**, 549–567.

Neyton, J. & Miller, C. (1988b). Discrete Ba^{2+} block as a probe of ion occupancy and pore structure in the high-conductance Ca^{2+} -activated K^+ channel. *J. Gen. Physiol.* **92**, 569-586.

Nichols, C. G. & Lederer, W. J. (1991). Adenosine triphosphate-sensitive potassium channels in the cardiovascular system. *Am. J. Physiol.* **261**, H1675-1686.

Nichols, C. G. & Lopatin, A. N. (1997). Inward rectifier potassium channels. *Annu. Rev. Physiol* **59**, 171-191.

Nichols, C. G. & Lopatin, A. N. (1999). Inwardly rectifying potassium channels: Mechanisms of rectification. In *Potassium ion channels. Molecular structure, function, and diseases*, eds. Kurachi, Y., Jan, L. Y., & Lazdunski, M., pp. 159-176. Academic Press, San Diego.

Nichols, C. G., Shyng, S. L., Nestorowicz, A., Glaser, B., Clement, J. P., Gonzalez, G., Aguilar-Bryan, L., Permutt, M. A., & Bryan, J. (1996). Adenosine diphosphate as an intracellular regulator of insulin secretion. *Science* **272**, 1785-1787.

Nilius, B. & Droogmans, G. (2001). Ion channels and their functional role in vascular endothelium. *Physiol. Rev.* **81**, 1415-1459.

Nilius, B., Viana, F., & Droogmans, G. (1997). Ion channels in vascular endothelium. *Annu. Rev. Physiol.* **59**, 145-170.

Nimigean, C. M. & Miller, C. (2002). Na^+ block and permeation in a K^+ channel of known structure. *J. Gen. Physiol.* **120**, 323-335.

Nishida, M. & MacKinnon, R. (2002). Structural basis of inward rectification: cytoplasmic pore of the G protein-gated inward rectifier GIRK1 at 1.8 A resolution. *Cell* **111**, 957-965.

Noble, D. (1965). Electrical properties of cardiac muscle attributable to inward going (anomalous) rectification. *J. Cell. Comp. Physiol.* **66**, 127-136.

Noble, D. & Tsien, R. W. (1969). Outward membrane currents activated in the plateau range of potentials in cardiac Purkinje fibres. *J. Physiol.* **200**, 205-231.

Noma, A. (1983). ATP-regulated K^+ channels in cardiac muscle. *Nature* **305**, 147-148.

Noma, A., Morad, M., & Irisawa, H. (1983). Does the "pacemaker current" generate the diastolic depolarization in the rabbit SA node cells? *Pflugers Arch.* **397**, 190-194.

Noma, A. & Trautwein, W. (1978). Relaxation of the ACh-induced potassium current in the rabbit sinoatrial node cell. *Pflugers Arch.* **377**, 193-200.

North, R. A. (1989). Twelfth Gaddum memorial lecture. Drug receptors and the inhibition of nerve cells. *Br. J. Pharmacol.* **98**, 13-28.

Noskov, S. Y., Berneche, S., & Roux, B. (2004). Control of ion selectivity in potassium channels by electrostatic and dynamic properties of carbonyl ligands. *Nature* **431**, 830-834.

Numaguchi, H., Mullins, F. M., Johnson, J. P., Jr., Johns, D. C., Po, S. S., Yang, I. C., Tomaselli, G. F., & Balser, J. R. (2000). Probing the interaction between inactivation gating and Dd-sotalol block of HERG. *Circ. Res.* **87**, 1012-1018.

Ohmori, H. (1978). Inactivation kinetics and steady-state current noise in the anomalous rectifier of tunicate egg cell membranes. *J. Physiol.* **281**, 77–99.

Ohno-Shosaku, T. & Yamamoto, C. (1992). Identification of an ATP-sensitive K^+ channel in rat cultured cortical neurons. *Pflugers Arch.* **422**, 260-266.

Ohya, S., Morohashi, Y., Muraki, K., Tomita, T., Watanabe, M., Iwatsubo, T., & Imaizumi, Y. (2001). Molecular cloning and expression of the novel splice variants of K^+ channel-interacting protein 2. *Biochem. Biophys. Res. Commun.* **282**, 96-102.

Oike, M., Droogmans, G., Casteels, R., & Nilius, B. (1993). Electrogenic Na^+/K^+-transport in human endothelial cells. *Pflugers Arch.* **424**, 301-307.

Okuyama, Y., Yamada, M., Kondo, C., Satoh, E., Isomoto, S., Shindo, T., Horio, Y., Kitakaze, M., Hori, M., & Kurachi, Y. (1998). The effects of nucleotides and

potassium channel openers on the SUR2A/Kir6.2 complex K^+ channel expressed in a mammalian cell line, HEK293T cells. *Pflugers Arch.* **435**, 595-603.

Olesen, S. P., Clapham, D. E., & Davies, P. F. (1988). Haemodynamic shear stress activates a K^+ current in vascular endothelial cells. *Nature* **331**, 168-170.

Oliva, C., Cohen, I. S., & Pennefather, P. (1990). The mechanism of rectification of I_{K1} in canine Purkinje myocytes. *J. Gen. Physiol.* **96**, 299-318.

Osterrieder, W., Yang, Q. F., & Trautwein, W. (1981). The time course of the muscarinic response to ionophoretic acetylcholine application to the S-A node of the rabbit heart. *Pflugers Arch.* **389**, 283-291.

Oudit, G. Y., Kassiri, Z., Sah, R., Ramirez, R. J., Zobel, C., & Backx, P. H. (2001). The molecular physiology of the cardiac transient outward potassium current I_{to} in normal and diseased myocardium. *J. Mol. Cell Cardiol.* **33**, 851-872.

Oudit, G. Y., Ramirez, R. J., & Backx, P. H. (2004). Voltage-regulated potassium channels. In *Cardiac electrophysiology - from cell to bedside*, eds. Zipes, D. P. & Jalife, J., pp. 19-32. Saunders, Philadelphia.

Ozaita, A., Martone, M. E., Ellisman, M. H., & Rudy, B. (2002). Differential subcellular localization of the two alternatively spliced isoforms of the Kv3.1 potassium channel subunit in brain. *J. Neurophysiol.* **88**, 394-408.

Pain, T., Yang, X. M., Critz, S. D., Yue, Y., Nakano, A., Liu, G. S., Heusch, G., Cohen, M. V., & Downey, J. M. (2000). Opening of mitochondrial K_{ATP} channels triggers the preconditioned state by generating free radicals. *Circ. Res.* **87**, 460-466.

Paltauf-Doburzynska, J., Posch, K., Paltauf, G., & Graier, W. F. (1998). Stealth ryanodine-sensitive Ca^{2+} release contributes to activity of capacitative Ca^{2+} entry and nitric oxide synthase in bovine endothelial cells. *J. Physiol.* **513**, 369-379.

Papazian, D. M. (1999). Potassium channels: some assembly required. *Neuron* **23**, 7-10.

Papazian, D. M., Silverman, W. R., Lin, M. C., Tiwari-Woodruff, S. K., & Tang, C. Y. (2002). Structural organization of the voltage sensor in voltage-dependent potassium channels. *Novartis. Found. Symp.* **245**, 178-190.

Parekh, A. B. & Penner, R. (1997). Store depletion and calcium influx. *Physiol. Rev.* **77**, 901-930.

Parsegian, A. (1969). Energy of an ion crossing a low dielectric membrane: solutions to four relevant electrostatic problems. *Nature* **221**, 844-846.

Pascual, J. M., Shieh, C. C., Kirsch, G. E., & Brown, A. M. (1995). Multiple residues specify external tetraethylammonium blockade in voltage-gated potassium channels. *Biophys. J.* **69**, 428-434.

Patel, A. J. & Lazdunski, M. (2004). The 2P-domain K^+ channels: role in apoptosis and tumorigenesis. *Pflugers Arch.* **448**, 261-273.

Patel, A. J., Lazdunski, M., & Honore, E. (2001). Lipid and mechano-gated 2P domain K^+ channels. *Curr. Opin. Cell Biol.* **13**, 422-428.

Patel, V., Brown, C., Goodwin, A., Wilkie, N., & Boarder, M. R. (1996). Phosphorylation and activation of p42 and p44 mitogen-activated protein kinase are required for the P2 purinoceptor stimulation of endothelial prostacyclin production. *Biochem. J.* **320**, 221-226.

Patil, N., Cox, D. R., Bhat, D., Faham, M., Myers, R. M., & Peterson, A. S. (1995). A potassium channel mutation in weaver mice implicates membrane excitability in granule cell differentiation. *Nat. Genet.* **11**, 126-129.

Pearson, W. L., Dourado, M., Schreiber, M., Salkoff, L., & Nichols, C. G. (1999). Expression of a functional Kir4 family inward rectifier K^+ channel from a gene cloned from mouse liver. *J. Physiol.* **514**, 639-653.

Pearson, W. L. & Nichols, C. G. (1998). Block of the Kir2.1 channel pore by alkylamine analogues of endogenous polyamines. *J. Gen. Physiol.* **112**, 351-363.

Pegan, S., Arrabit, C., Zhou, W., Kwiatkowski, W., Collins, A., Slesinger, P. A., & Choe, S. (2005). Cytoplasmic domain structures of Kir2.1 and Kir3.1 show sites for modulating gating and rectification. *Nat. Neurosci.* **8**, 279-287.

Peleg, S., Varon, D., Ivanina, T., Dessauer, C. W., & Dascal, N. (2002). $G_{\alpha i}$ controls the gating of the G protein-activated K^+ channel, GIRK. *Neuron* **33**, 87-99.

Pereon, Y., Demolombe, S., Baro, I., Drouin, E., Charpentier, F., & Escande, D. (2000). Differential expression of KvLQT1 isoforms across the human ventricular wall. *Am. J. Physiol. Heart Circ. Physiol.* **278**, H1908-1915.

Perier, F., Radeke, C. M., & Vandenberg, C. A. (1994). Primary structure and characterization of a small-conductance inwardly rectifying potassium channel from human hippocampus. *Proc. Natl. Acad. Sci. U.S.A.* **91**, 6240-6244.

Perney, T. M., Marshall, J., Martin, K. A., Hockfield, S., & Kaczmarek, L. K. (1992). Expression of the mRNAs for the Kv3.1 potassium channel gene in the adult and developing rat brain. *J. Neurophysiol.* **68**, 756-766.

Pessia, M., Imbrici, P., D'Adamo, M. C., Salvatore, L., & Tucker, S. J. (2001). Differential pH sensitivity of Kir4.1 and Kir4.2 potassium channels and their modulation by heteropolymerisation with Kir5.1. *J. Physiol.* **532**, 359-367.

Pessia, M., Tucker, S. J., Lee, K., Bond, C. T., & Adelman, J. P. (1996). Subunit positional effects revealed by novel heteromeric inwardly rectifying K^+ channels. *EMBO J.* **15**, 2980-2987.

Pfaffinger, P. J., Martin, J. M., Hunter, D. D., Nathanson, N. M., & Hille, B. (1985). GTP-binding proteins couple cardiac muscarinic receptors to a K^+ channel. *Nature* **317**, 536-538.

Picones, A., Keung, E., & Timpe, L. C. (2001). Unitary conductance variation in Kir2.1 and in cardiac inward rectifier potassium channels. *Biophys. J.* **81**, 2035-2049.

Plaster, N. M., Tawil, R., Tristani-Firouzi, M., Canun, S., Bendahhou, S., Tsunoda, A., Donaldson, M. R., Iannaccone, S. T., Brunt, E., Barohn, R., Clark, J., Deymeer, F., George, A. L., Jr., Fish, F. A., Hahn, A., Nitu, A., Ozdemir, C., Serdaroglu, P., Subramony, S. H., Wolfe, G., Fu, Y. H., & Ptacek, L. J. (2001). Mutations in Kir2.1 cause the developmental and episodic electrical phenotypes of Andersen's syndrome. *Cell* **105**, 511-519.

Pogwizd, S. M., Schlotthauer, K., Li, L., Yuan, W., & Bers, D. M. (2001). Arrhythmogenesis and contractile dysfunction in heart failure: Roles of sodium-calcium exchange, inward rectifier potassium current, and residual beta-adrenergic responsiveness. *Circ. Res.* **88**, 1159-1167.

Ponce, A., Bueno, E., Kentros, C., Vega-Saenz, d. M., Chow, A., Hillman, D., Chen, S., Zhu, L., Wu, M. B., Wu, X., Rudy, B., & Thornhill, W. B. (1996). G-protein-gated inward rectifier K^+ channel proteins (GIRK1) are present in the soma and dendrites as well as in nerve terminals of specific neurons in the brain. *J. Neurosci.* **16**, 1990-2001.

Ponce, A., Vega-Saenz, d. M., Kentros, C., Moreno, H., Thornhill, B., & Rudy, B. (1997). K^+ channel subunit isoforms with divergent carboxy-terminal sequences carry distinct membrane targeting signals. *J. Membr. Biol.* **159**, 149-159.

Pond, A. L., Scheve, B. K., Benedict, A. T., Petrecca, K., Van Wagoner, D. R., Shrier, A., & Nerbonne, J. M. (2000). Expression of distinct ERG proteins in rat, mouse, and human heart. Relation to functional I_{Kr} channels. *J. Biol. Chem.* **275**, 5997-6006.

Pongs, O., Kecskemethy, N., Muller, R., Krah-Jentgens, I., Baumann, A., Kiltz, H. H., Canal, I., Llamazares, S., & Ferrus, A. (1988). Shaker encodes a family of putative potassium channel proteins in the nervous system of Drosophila. *EMBO J.* **7**, 1087-1096.

Pourrier, M., Herrera, D., Caballero, R., Schram, G., Wang, Z., & Nattel, S. (2004). The Kv4.2 N-terminal restores fast inactivation and confers KChIP2 modulatory effects on N-terminal-deleted Kv1.4 channels. *Pflugers Arch.* **449**, 235-247.

Pourrier, M., Schram, G., & Nattel, S. (2003a). Properties, expression and potential roles of cardiac K^+ channel accessory subunits: MinK, MiRPs, KChIP, and KChAP. *J. Membr. Biol.* **194**, 141-152.

Pourrier, M., Zicha, S., Ehrlich, J., Han, W., & Nattel, S. (2003b). Canine ventricular KCNE2 expression resides predominantly in Purkinje fibers. *Circ. Res.* **93**, 189-191.

Preisig-Muller, R., Schlichthorl, G., Goerge, T., Heinen, S., Bruggemann, A., Rajan, S., Derst, C., Veh, R. W., & Daut, J. (2002). Heteromerization of Kir2.x potassium channels contributes to the phenotype of Andersen's syndrome. *Proc. Natl. Acad. Sci. U.S.A.* **99**, 7774-7779.

Proks, P., Capener, C. E., Jones, P., & Ashcroft, F. M. (2001). Mutations within the P-loop of Kir6.2 modulate the intraburst kinetics of the ATP-sensitive potassium channel. *J. Gen. Physiol.* **118**, 341-353.

Pruss, H., Derst, C., Lommel, R., & Veh, R. W. (2005). Differential distribution of individual subunits of strongly inwardly rectifying potassium channels (Kir2 family) in rat brain. *Brain Res. Mol. Brain Res.* **139**, 63-79.

Pruss, H., Wenzel, M., Eulitz, D., Thomzig, A., Karschin, A., & Veh, R. W. (2003). Kir2 potassium channels in rat striatum are strategically localized to control basal ganglia function. *Brain Res. Mol. Brain Res.* **110**, 203-219.

Qu, Z., Yang, Z., Cui, N., Zhu, G., Liu, C., Xu, H., Chanchevalap, S., Shen, W., Wu, J., Li, Y., & Jiang, C. (2000). Gating of inward rectifier K^+ channels by proton-mediated interactions of N- and C-terminal domains. *J. Biol. Chem.* **275**, 31573-31580.

Quayle, J. M., Bonev, A. D., Brayden, J. E., & Nelson, M. T. (1995). Pharmacology of ATP-sensitive K^+ currents in smooth muscle cells from rabbit mesenteric artery. *Am. J. Physiol.* **269**, C1112-1118.

Quayle, J. M., Nelson, M. T., & Standen, N. B. (1997). ATP-sensitive and inwardly rectifying potassium channels in smooth muscle. *Physiol. Rev.* **77**, 1165-1232.

Quesada, I., Rovira, J. M., Martin, F., Roche, E., Nadal, A., & Soria, B. (2002). Nuclear K_{ATP} channels trigger nuclear Ca^{2+} transients that modulate nuclear function. *Proc. Natl. Acad. Sci. U.S.A.* **99**, 9544-9549.

Raab-Graham, K. F., Radeke, C. M., & Vandenberg, C. A. (1994). Molecular cloning and expression of a human heart inward rectifier potassium channel. *Neuroreport* **5**, 2501-2505.

Reimann, F. & Ashcroft, F. M. (1999). Inwardly rectifying potassium channels. *Curr. Opin. Cell Biol.* **11**, 503-508.

Reis, A. F. & Velho, G. (2002). Sulfonylurea receptor -1 (SUR1): genetic and metabolic evidences for a role in the susceptibility to type 2 diabetes mellitus. *Diabetes Metab.* **28**, 14-19.

Rettig, J., Heinemann, S. H., Wunder, F., Lorra, C., Parcej, D. N., Dolly, J. O., & Pongs, O. (1994). Inactivation properties of voltage-gated K^+ channels altered by presence of beta-subunit. *Nature* **369**, 289-294.

Rettig, J., Wunder, F., Stocker, M., Lichtinghagen, R., Mastiaux, F., Beckh, S., Kues, W., Pedarzani, P., Schroter, K. H., Ruppersberg, J. P., & . (1992). Characterization of a Shaw-related potassium channel family in rat brain. *EMBO J.* **11**, 2473-2486.

Reuveny, E., Jan, Y. N. & Jan, L. Y. (1996). Contributions of a negatively charged residue in the hydrophobic domain of the Kir2.1 inwardly rectifying K^+ channel to K^+-selective permeation. *Biophys. J.* **70**, 754–761.

Rhodes, K. J., Carroll, K. I., Sung, M. A., Doliveira, L. C., Monaghan, M. M., Burke, S. L., Strassle, B. W., Buchwalder, L., Menegola, M., Cao, J., An, W. F., & Trimmer, J. S. (2004). KChIPs and Kv4 alpha subunits as integral components of A-type potassium channels in mammalian brain. *J. Neurosci.* **24**, 7903-7915.

Rhodes, K. J., Strassle, B. W., Monaghan, M. M., Bekele-Arcuri, Z., Matos, M. F., & Trimmer, J. S. (1997). Association and colocalization of the Kvbeta1 and Kvbeta2 beta-subunits with Kv1 alpha-subunits in mammalian brain K^+ channel complexes. *J. Neurosci.* **17**, 8246-8258.

Romanenko, V. G., Rothblat, G. H., & Levitan, I. (2002). Modulation of endothelial inward-rectifier K^+ current by optical isomers of cholesterol. *Biophys. J.* **83**, 3211-3222.

Roper, J. & Ashcroft, F. M. (1995). Metabolic inhibition and low internal ATP activate K_{ATP} channels in rat dopaminergic substantia nigra neurones. *Pflugers Arch.* **430**, 44-54.

Rosati, B., Pan, Z., Lypen, S., Wang, H. S., Cohen, I., Dixon, J. E., & McKinnon, D. (2001). Regulation of KChIP2 potassium channel beta subunit gene expression underlies the gradient of transient outward current in canine and human ventricle. *J. Physiol.* **533**, 119-125.

Ross, E. M. & Wilkie, T. M. (2000). GTPase-activating proteins for heterotrimeric G proteins: regulators of G protein signaling (RGS) and RGS-like proteins. *Annu. Rev. Biochem.* **69**, 795-827.

Rougier, O., Vassort, G., & Stampfli, R. (1968). Voltage clamp experiments on frog atrial heart muscle fibres with the sucrose gap technique. *Pflugers Arch. Gesamte Physiol. Menschen.Tiere.* **301**, 91-108.

Roux, B. (2005). Ion conduction and selectivity in K^+ channels. *Annu. Rev. Biophys. Biomol. Struct.* **34**, 153-171.

Roux, B. & MacKinnon, R. (1999). The cavity and pore helices in the KcsA K^+ channel: electrostatic stabilization of monovalent cations. *Science* **285**, 100-102.

Rusko, J., Tanzi, F., van Breemen, C., & Adams, D. J. (1992). Calcium-activated potassium channels in native endothelial cells from rabbit aorta: conductance, Ca^{2+} sensitivity and block. *J. Physiol.* **455**, 601-621.

Ruta, V. & MacKinnon, R. (2004). Localization of the voltage-sensor toxin receptor on KvAP. *Biochemistry* **43**, 10071-10079.

Sabirov, R. Z., Okada, Y. & Oiki, S. (1997a). Two-sided action of protons on an inward rectifier K^+ channel (Kir2.1). *Pflugers Arch.* **433**, 428–434.

Sabirov, R. Z., Tominaga, T., Miwa, A., Okada, Y., & Oiki, S. (1997b). A conserved arginine residue in the pore region of an inward rectifier K^+ channel (IRK1) as an external barrier for cationic blockers. *J. Gen. Physiol.* **110**, 665-677.

Sadja, R., Alagem, N., & Reuveny, E. (2003). Gating of GIRK channels: details of an intricate, membrane-delimited signaling complex. *Neuron* **39**, 9-12.

Saitoh, O., Kubo, Y., Miyatani, Y., Asano, T., & Nakata, H. (1997). RGS8 accelerates G-protein-mediated modulation of K^+ currents. *Nature* **390**, 525-529.

Sakmann, B., Noma, A., & Trautwein, W. (1983). Acetylcholine activation of single muscarinic K^+ channels in isolated pacemaker cells of the mammalian heart. *Nature* **303**, 250-253.

Sakmann, B. & Trube, G. (1984a). Conductance properties of single inwardly rectifying potassium channels in ventricular cells from guinea-pig heart. *J. Physiol.* **347**, 641-657.

Sakmann, B. & Trube, G. (1984b). Voltage-dependent inactivation of inward-rectifying single-channel currents in the guinea-pig heart cell membrane. *J.Physiol.* **347**, 659-683.

Sakura, H., Trapp, S., Liss, B., & Ashcroft, F. M. (1999). Altered functional properties of K_{ATP} channel conferred by a novel splice variant of SUR1. *J. Physiol.* **521**, 337-350.

Salkoff, L. (1983). Drosophila mutants reveal two components of fast outward current. *Nature* **302**, 249-251.

Samie, F. H., Berenfeld, O., Anumonwo, J., Mironov, S. F., Udassi, S., Beaumont, J., Taffet, S., Pertsov, A. M., & Jalife, J. (2001). Rectification of the background potassium current: a determinant of rotor dynamics in ventricular fibrillation. *Circ. Res.* **89**, 1216-1223.

Sanada, S., Kitakaze, M., Asanuma, H., Harada, K., Ogita, H., Node, K., Takashima, S., Sakata, Y., Asakura, M., Shinozaki, Y., Mori, H., Kuzuya, T., & Hori, M. (2001). Role of mitochondrial and sarcolemmal K_{ATP} channels in ischemic preconditioning of the canine heart. *Am. J. Physiol. Heart Circ. Physiol.* **280**, H256-263.

Sands, Z., Grottesi, A., & Sansom, M. S. (2005). Voltage-gated ion channels. *Curr. Biol.* **15**, R44-R47.

Sanguinetti, M. C., Curran, M. E., Zou, A., Shen, J., Spector, P. S., Atkinson, D. L., & Keating, M. T. (1996). Coassembly of KvLQT1 and minK (IsK) proteins to form cardiac I_{Ks} potassium channel. *Nature* **384**, 80-83.

Sanguinetti, M. C., Johnson, J. H., Hammerland, L. G., Kelbaugh, P. R., Volkmann, R. A., Saccomano, N. A., & Mueller, A. L. (1997). Heteropodatoxins: peptides isolated from spider venom that block Kv4.2 potassium channels. *Mol. Pharmacol.* **51**, 491-498.

Sanguinetti, M. C. & Jurkiewicz, N. K. (1991). Delayed rectifier outward K^+ current is composed of two currents in guinea pig atrial cells. *Am. J. Physiol.* **260**, H393-399.

Sano, Y., Mochizuki, S., Miyake, A., Kitada, C., Inamura, K., Yokoi, H., Nozawa, K., Matsushime, H., & Furuichi, K. (2002). Molecular cloning and characterization of Kv6.3, a novel modulatory subunit for voltage-gated K^+ channel Kv2.1. *FEBS Lett.* **512**, 230-234.

Sansom, M. S., Shrivastava, I. H., Bright, J. N., Tate, J., Capener, C. E., & Biggin, P. C. (2002). Potassium channels: structures, models, simulations. *Biochim. Biophys. Acta* **1565**, 294-307.

Sarmast, F., Kolli, A., Zaitsev, A., Parisian, K., Dhamoon, A. S., Guha, P. K., Warren, M., Anumonwo, J. M., Taffet, S. M., Berenfeld, O., & Jalife, J. (2003). Cholinergic atrial fibrillation: I_{KACh} gradients determine unequal left/right atrial frequencies and rotor dynamics. *Cardiovasc. Res.* **59**, 863-873.

Sato, N., Tanaka, H., Habuchi, Y., & Giles, W. R. (2000). Electrophysiological effects of ibutilide on the delayed rectifier K^+ current in rabbit sinoatrial and atrioventricular node cells. *Eur. J. Pharmacol.* **404**, 281-288.

Scannevin, R. H., Murakoshi, H., Rhodes, K. J., & Trimmer, J. S. (1996). Identification of a cytoplasmic domain important in the polarized expression and clustering of the Kv2.1 K^+ channel. *J. Cell Biol.* **135**, 1619-1632.

Schoppa, N. E., McCormack, K., Tanouye, M. A., & Sigworth, F. J. (1992). The size of gating charge in wild-type and mutant Shaker potassium channels. *Science* **255**, 1712-1715.

Schoppa, N. E. & Sigworth, F. J. (1998). Activation of Shaker potassium channels. II. Kinetics of the V2 mutant channel. *J. Gen. Physiol.* **111**, 295-311.

Schram, G., Herrera, D., Mamarbachi, M., Wang, Z. G., Parent, L., & Nattel, S. (2005). Differences in barium block of Kir2.1 vs Kir2.4 : H5 segment confers voltage-but not concentration-dependence of block. *Biophys. J.* **88**, 107A.

Schram, G., Melnyk, P., Pourrier, M., Wang, Z., & Nattel, S. (2002a). Kir2.4 and Kir2.1 K^+ channel subunits co-assemble: a potential new contributor to inward rectifier current heterogeneity. *J. Physiol.* **544**, 337-349.

Schram, G., Melnyk, P., Pourrier, M., Wang, Z. G., & Nattel, S. (2000a). Kir2.4: A novel contributor to human cardiac I_{K1} heterogeneity. *Circulation* **102**, 285.

Schram, G., Pourrier, M., Melnyk, P., & Nattel, S. (2002b). Differential distribution of cardiac ion channel expression as a basis for regional specialization in electrical function. *Circ.Res.* **90**, 939-950.

Schram, G., Pourrier, M., Melnyk, P., Wang, Z. G., & Nattel, S. (2000b). Kir2.1 coassembles with Kir2.4 to form heterotetrameric inward rectifier channels. *Biophys. J.* **78**, 466A.

Schram, G., Pourrier, M., Wang, Z., White, M., & Nattel, S. (2003). Barium block of Kir2 and human cardiac inward rectifier currents: evidence for subunit-heteromeric contribution to native currents. *Cardiovasc. Res.* **59**, 328-338.

Schram, G., Wang, Z., & Nattel, S. (1999a). Differences in barium block among various inward rectifier subunit clones. *Biophys. J.* **76**, A72.

Schram, G., Wang, Z., & Nattel, S. (1999b). Molecular composition of human cardiac I_{K1} evaluated by barium blocking profile. *Circulation* **100**, 633.

Schram, G., Zhang, L., Derakhchan, K., Ehrlich, J. R., Belardinelli, L., & Nattel, S. (2004). Ranolazine: ion-channel-blocking actions and in vivo electrophysiological effects. *Br .J. Pharmacol.* **142**, 1300-1308.

Schreieck, J., Wang, Y., Gjini, V., Korth, M., Zrenner, B., Schomig, A., & Schmitt, C. (1997). Differential effect of beta-adrenergic stimulation on the frequency-dependent electrophysiologic actions of the new class III antiarrhythmics dofetilide, ambasilide, and chromanol 293B. *J. Cardiovasc. Electrophysiol.* **8**, 1420-1430.

Schulteis, C. T., Nagaya, N., & Papazian, D. M. (1998). Subunit folding and assembly steps are interspersed during Shaker potassium channel biogenesis. *J. Biol. Chem.* **273**, 26210-26217.

Seino, S. & Miki, T. (2003). Physiological and pathophysiological roles of ATP-sensitive K^+ channels. *Prog. Biophys. Mol. Biol.* **81**, 133-176.

Seiss-Geuder, M., Mehrke, G., & Daut, J. (1992). Sustained hyperpolarization of cultured guinea pig coronary endothelial cells induced by adenosine. *J. Cardiovasc. Pharmacol.* **20**, S97-100.

Seoh, S. A., Sigg, D., Papazian, D. M., & Bezanilla, F. (1996). Voltage-sensing residues in the S2 and S4 segments of the Shaker K^+ channel. *Neuron* **16**, 1159-1167.

Sesti, F. & Goldstein, S. A. (1998). Single-channel characteristics of wild-type I_{Ks} channels and channels formed with two minK mutants that cause long QT syndrome. *J. Gen. Physiol.* **112**, 651-663.

Sharma, N., Crane, A., Clement, J. P., Gonzalez, G., Babenko, A. P., Bryan, J., & Aguilar-Bryan, L. (1999). The C terminus of SUR1 is required for trafficking of K_{ATP} channels. *J. Biol. Chem.* **274**, 20628-20632.

Shen, N. V., Chen, X., Boyer, M. M., & Pfaffinger, P. J. (1993). Deletion analysis of K^+ channel assembly. *Neuron* **11**, 67-76.

Shen, N. V. & Pfaffinger, P. J. (1995). Molecular recognition and assembly sequences involved in the subfamily- specific assembly of voltage-gated K^+ channel subunit proteins. *Neuron* **14**, 625-633.

Sheng, M., Tsaur, M. L., Jan, Y. N., & Jan, L. Y. (1992). Subcellular segregation of two A-type K^+ channel proteins in rat central neurons. *Neuron* **9**, 271-284.

Shi, G., Nakahira, K., Hammond, S., Rhodes, K. J., Schechter, L. E., & Trimmer, J. S. (1996). Beta subunits promote K^+ channel surface expression through effects early in biosynthesis. *Neuron* **16**, 843-852.

Shieh, C. C., Coghlan, M., Sullivan, J. P., & Gopalakrishnan, M. (2000). Potassium channels: molecular defects, diseases, and therapeutic opportunities. *Pharmacol. Rev.* **52**, 557-594.

Shieh, R. C., Chang, J. C. & Arreola, J. (1998). Interaction of Ba^{2+} with the pores of the cloned inward rectifier K^+ channel Kir2.1 expressed in *Xenopus* oocytes. *Biophys. J.* **75**, 2313–2322.

Shieh, C. C. & Kirsch, G. E. (1994). Mutational analysis of ion conduction and drug binding sites in the inner mouth of voltage-gated K^+ channels. *Biophys. J.* **67**, 2316-2325.

Shimokawa, H. & Takeshita, A. (1995). Endothelium-dependent regulation of the cardiovascular system. *Intern. Med.* **34**, 939-946.

Shimoni, Y., Clark, R. B., & Giles, W. R. (1992). Role of an inwardly rectifying potassium current in rabbit ventricular action potential. *J. Physiol.* **448**, 709-727.

Shimura, M., Yuan, Y., Chang, J. T., Zhang, S., Campochiaro, P. A., Zack, D. J., & Hughes, B. A. (2001). Expression and permeation properties of the K^+ channel Kir7.1 in the retinal pigment epithelium. *J. Physiol.* **531**, 329-346.

Shinagawa, K., Shiroshita-Takeshita, A., Schram, G., & Nattel, S. (2003). Effects of antiarrhythmic drugs on fibrillation in the remodeled atrium: insights into the mechanism of the superior efficacy of amiodarone. *Circulation* **107**, 1440-1446.

Shioya, T., Matsuda, H., & Noma, A. (1993). Fast and slow blockades of the inward-rectifier K^+ channel by external divalent cations in guinea-pig cardiac myocytes. *Pflugers Arch.* **422**, 427-435.

Shiroshita-Takeshita, A., Schram, G., Lavoie, J., & Nattel, S. (2004). Effect of simvastatin and antioxidant vitamins on atrial fibrillation promotion by atrial-tachycardia remodeling in dogs. *Circulation* **110**, 2313-2319.

Shrivastava, I. H. & Sansom, M. S. (2000). Simulations of ion permeation through a potassium channel: molecular dynamics of KcsA in a phospholipid bilayer. *Biophys. J.* **78**, 557-570.

Shrivastava, I. H., Tieleman, D. P., Biggin, P. C., & Sansom, M. S. (2002). K^+ versus Na^+ ions in a K^+ channel selectivity filter: a simulation study. *Biophys. J.* **83**, 633-645.

Shyng, S., Ferrigni, T., & Nichols, C. G. (1997). Regulation of K_{ATP} channel activity by diazoxide and MgADP. Distinct functions of the two nucleotide binding folds of the sulfonylurea receptor. *J. Gen. Physiol.* **110**, 643-654.

Shyng, S. & Nichols, C. G. (1997). Octameric stoichiometry of the K_{ATP} channel complex. *J. Gen. Physiol.* **110**, 655-664.

Shyng, S. L., Barbieri, A., Gumusboga, A., Cukras, C., Pike, L., Davis, J. N., Stahl, P. D., & Nichols, C. G. (2000a). Modulation of nucleotide sensitivity of ATP-sensitive potassium channels by phosphatidylinositol-4-phosphate 5-kinase. *Proc. Natl. Acad. Sci. U.S.A.* **97**, 937-941.

Shyng, S. L., Cukras, C. A., Harwood, J., & Nichols, C. G. (2000b). Structural determinants of PIP_2 regulation of inward rectifier K_{ATP} channels. *J. Gen. Physiol.* **116**, 599-608.

Shyng, S. L. & Nichols, C. G. (1998). Membrane phospholipid control of nucleotide sensitivity of K_{ATP} channels. *Science* **282**, 1138-1141.

Sicouri, S. & Antzelevitch, C. (1991). A subpopulation of cells with unique electrophysiological properties in the deep subepicardium of the canine ventricle. The M cell. *Circ. Res.* **68**, 1729-1741.

Sicouri, S. & Antzelevitch, C. (1993). Drug-induced afterdepolarizations and triggered activity occur in a discrete subpopulation of ventricular muscle cells (M cells) in the canine heart: quinidine and digitalis. *J. Cardiovasc. Electrophysiol.* **4**, 48-58.

Signorini, S., Liao, Y. J., Duncan, S. A., Jan, L. Y., & Stoffel, M. (1997). Normal cerebellar development but susceptibility to seizures in mice lacking G protein-coupled, inwardly rectifying K^+ channel GIRK2. *Proc. Natl. Acad. Sci. U.S.A.* **94**, 923-927.

Silver, M. R. & DeCoursey, T. E. (1990). Intrinsic gating of inward rectifier in bovine pulmonary artery endothelial cells in the presence or absence of internal Mg^{2+}. *J. Gen. Physiol.* **96**, 109-133.

Silverman, S. K., Kofuji, P., Dougherty, D. A., Davidson, N., & Lester, H. A. (1996a). A regenerative link in the ionic fluxes through the weaver potassium channel underlies the pathophysiology of the mutation. *Proc. Natl. Acad. Sci. U.S.A.* **93**, 15429-15434.

Silverman, S. K., Lester, H. A., & Dougherty, D. A. (1996b). Subunit stoichiometry of a heteromultimeric G protein-coupled inward- rectifier K^+ channel. *J. Biol. Chem.* **271**, 30524-30528.

Silverman, S. K., Lester, H. A., & Dougherty, D. A. (1998). Asymmetrical contributions of subunit pore regions to ion selectivity in an inward rectifier K^+ channel. *Biophys. J.* **75**, 1330-1339.

Simon, M. I., Strathmann, M. P., & Gautam, N. (1991). Diversity of G proteins in signal transduction. *Science* **252**, 802-808.

Singh, B. N. & Vaughan Williams, E. M. (1970). A third class of anti-arrhythmic action. Effects on atrial and ventricular intracellular potentials, and other pharmacological actions on cardiac muscle, of MJ 1999 and AH 3474. *Br. J. Pharmacol.* **39**, 675-687.

Slesinger, P. A., Patil, N., Liao, Y. J., Jan, Y. N., Jan, L. Y., & Cox, D. R. (1996). Functional effects of the mouse weaver mutation on G protein-gated inwardly rectifying K^+ channels. *Neuron* **16**, 321-331.

Sodickson, D. L. & Bean, B. P. (1996). GABAB receptor-activated inwardly rectifying potassium current in dissociated hippocampal CA3 neurons. *J. Neurosci.* **16**, 6374-6385.

Soom, M., Schonherr, R., Kubo, Y., Kirsch, C., Klinger, R., & Heinemann, S. H. (2001). Multiple PIP_2 binding sites in Kir2.1 inwardly rectifying potassium channels. *FEBS Lett.* **490**, 49-53.

Southan, A. P. & Robertson, B. (1998). Patch-clamp recordings from cerebellar basket cell bodies and their presynaptic terminals reveal an asymmetric distribution of voltage-gated potassium channels. *J. Neurosci.* **18**, 948-955.

Southan, A. P. & Robertson, B. (2000). Electrophysiological characterization of voltage-gated K^+ currents in cerebellar basket and purkinje cells: Kv1 and Kv3 channel subfamilies are present in basket cell nerve terminals. *J. Neurosci.* **20**, 114-122.

Spach, M. S. (1995). Microscopic Basis of anisotropic propagation in the heart: The nature of current flow at a cellular level. In *Cardiac Electrophysiology: From cell to bedside*, eds. Zipes, D. P. & Jalife, J., pp. 204-216. WB Saunders Co, Philadelphia,Pa.

Spach, M. S., Dolber, P. C., & Anderson, P. A. (1989). Multiple regional differences in cellular properties that regulate repolarization and contraction in the right atrium of adult and newborn dogs. *Circ. Res.* **65**, 1594-1611.

Spector, P. S., Curran, M. E., Keating, M. T., & Sanguinetti, M. C. (1996). Class III antiarrhythmic drugs block HERG, a human cardiac delayed rectifier K^+ channel. Open-channel block by methanesulfonanilides. *Circ. Res.* **78**, 499-503.

Splawski, I., Shen, J., Timothy, K. W., Lehmann, M. H., Priori, S., Robinson, J. L., Moss, A. J., Schwartz, P. J., Towbin, J. A., Vincent, G. M., & Keating, M. T. (2000). Spectrum of mutations in long-QT syndrome genes. KVLQT1, HERG, SCN5A, KCNE1, and KCNE2. *Circulation* **102**, 1178-1185.

Standen, N. B. & Stanfield, P. R. (1978). A potential- and timedependent blockade of inward rectification in frog skeletal musclefibres by barium and strontium ions. *J. Physiol.* **280**,169–191.

Standen, N. B. & Stanfield, P. R. (1980). Rubidium block and rubidium permeability of the inward rectifier of frog skeletal muscle fibres. *J. Physiol.* **304**, 415–435.

Stanfield, P. R., Davies, N. W., Shelton, P. A., Sutcliffe, M. J., Khan, I. A., Brammar, W. J., & Conley, E. C. (1994). A single aspartate residue is involved in both intrinsic gating and blockage by Mg^{2+} of the inward rectifier, IRK1. *J. Physiol.* **478**, 1-6.

Stanfield, P. R., Nakajima, S., & Nakajima, Y. (2002). Constitutively active and G-protein coupled inward rectifier K^+ channels: Kir2.0 and Kir3.0. *Rev. Physiol. Biochem. Pharmacol.* **145**, 47-179.

Starace, D. M. & Bezanilla, F. (2004). A proton pore in a potassium channel voltage sensor reveals a focused electric field. *Nature* **427**, 548-553.

Starkus, J. G., Heinemann, S. H., & Rayner, M. D. (2000). Voltage dependence of slow inactivation in Shaker potassium channels results from changes in relative K^+ and Na^+ permeabilities. *J. Gen. Physiol.* **115**, 107-122.

Starkus, J. G., Kuschel, L., Rayner, M. D., & Heinemann, S. H. (1997). Ion conduction through C-type inactivated Shaker channels. *J. Gen. Physiol.* **110**, 539-550.

Stern, D., Brett, J., Harris, K., & Nawroth, P. (1986). Participation of endothelial cells in the protein C-protein S anticoagulant pathway: the synthesis and release of protein S. *J. Cell Biol.* **102**, 1971-1978.

Stocker, M., Hellwig, M., & Kerschensteiner, D. (1999). Subunit assembly and domain analysis of electrically silent K^+ channel alpha-subunits of the rat Kv9 subfamily. *J. Neurochem.* **72**, 1725-1734.

Stonehouse, A. H., Pringle, J. H., Norman, R. I., Stanfield, P. R., Conley, E. C., & Brammar, W. J. (1999). Characterisation of Kir2.0 proteins in the rat cerebellum and hippocampus by polyclonal antibodies. *Histochem. Cell Biol.* **112**, 457-465.

Storm, J. F. (2000). K^+ channels and their distribution in large cortical pyramidal neurones. *J. Physiol.* **525**, 565-566.

Strauss, H. C., Bigger, J. T., Jr., & Hoffman, B. F. (1970). Electrophysiologial and beta-receptor blocking effects of MJ 1999 on dog and rabbit cardiac tissue. *Circ. Res.* **26**, 661-678.

Sturgess, N. C., Ashford, M. L., Cook, D. L., & Hales, C. N. (1985). The sulphonylurea receptor may be an ATP-sensitive potassium channel. *Lancet* **2**, 474-475.

Suessbrich, H., Schonherr, R., Heinemann, S. H., Attali, B., Lang, F., & Busch, A. E. (1997). The inhibitory effect of the antipsychotic drug haloperidol on HERG potassium channels expressed in *Xenopus* oocytes. *Br. J. Pharmacol.* **120**, 968-974.

Suessbrich, H., Waldegger, S., Lang, F., & Busch, A. E. (1996). Blockade of HERG channels expressed in *Xenopus* oocytes by the histamine receptor antagonists terfenadine and astemizole. *FEBS Lett.* **385**, 77-80.

Sui, J. L., Petit-Jacques, J., & Logothetis, D. E. (1998). Activation of the atrial KACh channel by the betagamma subunits of G proteins or intracellular Na^+ ions depends on the presence of phosphatidylinositol phosphates. *Proc. Natl. Acad. Sci.U.S.A.* **95**, 1307-1312.

Sukhareva, M., Hackos, D. H., & Swartz, K. J. (2003). Constitutive activation of the Shaker Kv channel. *J. Gen. Physiol.* **122**, 541-556.

Suzuki, M., Li, R. A., Miki, T., Uemura, H., Sakamoto, N., Ohmoto-Sekine, Y., Tamagawa, M., Ogura, T., Seino, S., Marban, E., & Nakaya, H. (2001). Functional roles of cardiac and vascular ATP-sensitive potassium channels clarified by Kir6.2-knockout mice. *Circ. Res.* **88**, 570-577.

Suzuki, Y., Yasuoka, Y., Shimohama, T., Nishikitani, M., Nakamura, N., Hirose, S., & Kawahara, K. (2003). Expression of the K^+ channel Kir7.1 in the developing rat kidney: role in K^+ excretion. *Kidney Int.* **63**, 969-975.

Swartz, K. J. & MacKinnon, R. (1997). Hanatoxin modifies the gating of a voltage-dependent K^+ channel through multiple binding sites. *Neuron* **18**, 665-673.

Tabor, C. W. & Tabor, H. (1984). Polyamines. *Annu. Rev. Biochem.* **53**, 749-790.

Taborsky, G. J., Jr., Ahren, B., & Havel, P. J. (1998). Autonomic mediation of glucagon secretion during hypoglycemia: implications for impaired alpha-cell responses in type 1 diabetes. *Diabetes* **47**, 995-1005.

Taglialatela, M., Ficker, E., Wible, B. A., & Brown, A. M. (1995). C-terminus determinants for Mg^{2+} and polyamine block of the inward rectifier K^+ channel IRK1. *EMBO J.* **14**, 5532-5541.

Taglialatela, M., Wible, B. A., Caporaso, R., & Brown, A. M. (1994). Specification of pore properties by the carboxyl terminus of inwardly rectifying K^+ channels. *Science* **264**, 844-847.

Taglialatela, M, Drewe J. A.& Brown, A. M. (1993). Barium blockade of a clonal potassium channel and its regulation by a critical pore residue. *Mol. Pharmacol.* **44**, 180-190

Takeda, K., Schini, V., & Stoeckel, H. (1987). Voltage-activated potassium, but not calcium currents in cultured bovine aortic endothelial cells. *Pflugers Arch.* **410**, 385-393.

Takumi, T., Ohkubo, H., & Nakanishi, S. (1988). Cloning of a membrane protein that induces a slow voltage-gated potassium current. *Science* **242**, 1042-1045.

Tan, K. T., Watson, S. P., & Lip, G. Y. (2004). The endothelium and platelets in cardiovascular disease: potential targets for therapeutic intervention. *Curr. Med. Chem. Cardiovasc. Hematol. Agents* **2**, 169-178.

Tanemoto, M., Fujita, A., Higashi, K., & Kurachi, Y. (2002). PSD-95 mediates formation of a functional homomeric Kir5.1 channel in the brain. *Neuron* **34**, 387-397.

Tanemoto, M., Kittaka, N., Inanobe, A., & Kurachi, Y. (2000). In vivo formation of a proton-sensitive K^+ channel by heteromeric subunit assembly of Kir5.1 with Kir4.1. *J. Physiol.* **525**, 587-592.

Tang, W., Qin, C. L., & Yang, X. C. (1995). Cloning, localization, and functional expression of a human brain inward rectifier potassium channel (hIRK1). *Receptors. Channels* **3**, 175-183.

Tang, W. & Yang, X. C. (1994). Cloning a novel human brain inward rectifier potassium channel and its functional expression in *Xenopus* oocytes. *FEBS Lett.* **348**, 239-243.

Tempel, B. L., Papazian, D. M., Schwarz, T. L., Jan, Y. N., & Jan, L. Y. (1987). Sequence of a probable potassium channel component encoded at Shaker locus of Drosophila. *Science* **237**, 770-775.

Terzic, A., Jahangir, A., & Kurachi, Y. (1995). Cardiac ATP-sensitive K^+ channels: regulation by intracellular nucleotides and K^+ channel-opening drugs. *Am. J. Physiol.* **269**, C525-545.

Thomas, D., Gut, B., Wendt-Nordahl, G., & Kiehn, J. (2002). The antidepressant drug fluoxetine is an inhibitor of human ether-a-go- go-related gene (HERG) potassium channels. *J. Pharmacol. Exp. Ther.* **300**, 543-548.

Thomas, P. M., Cote, G. J., Wohllk, N., Haddad, B., Mathew, P. M., Rabl, W., Aguilar-Bryan, L., Gagel, R. F., & Bryan, J. (1995). Mutations in the sulfonylurea receptor gene in familial persistent hyperinsulinemic hypoglycemia of infancy. *Science* **268**, 426-429.

Thomzig, A., Wenzel, M., Karschin, C., Eaton, M. J., Skatchkov, S. N., Karschin, A., & Veh, R. W. (2001). Kir6.1 is the principal pore-forming subunit of astrocyte but not neuronal plasma membrane K_{ATP} channels. *Mol. Cell Neurosci.* **18**, 671-690.

Timpe, L. C., Schwarz, T. L., Tempel, B. L., Papazian, D. M., Jan, Y. N., & Jan, L. Y. (1988). Expression of functional potassium channels from Shaker cDNA in *Xenopus* oocytes. *Nature* **331**, 143-145.

Tinker, A., Jan, Y. N., & Jan, L. Y. (1996). Regions responsible for the assembly of inwardly rectifying potassium channels. *Cell* **87**, 857-868.

Titus, S. A., Warmke, J. W., & Ganetzky, B. (1997). The Drosophila erg K^+ channel polypeptide is encoded by the seizure locus. *J. Neurosci.* **17**, 875-881.

Tiwari-Woodruff, S. K., Lin, M. A., Schulteis, C. T., & Papazian, D. M. (2000). Voltage-dependent structural interactions in the Shaker K^+ channel. *J. Gen. Physiol.* **115**, 123-138.

Topert, C., Doring, F., Derst, C., Daut, J., Grzeschik, K. H., & Karschin, A. (2000). Cloning, structure and assignment to chromosome 19q13 of the human Kir2.4 inwardly rectifying potassium channel gene (KCNJ14). *Mamm. Genome* **11**, 247-249.

Topert, C., Doring, F., Wischmeyer, E., Karschin, C., Brockhaus, J., Ballanyi, K., Derst, C., & Karschin, A. (1998). Kir2.4: a novel K^+ inward rectifier channel associated with motoneurons of cranial nerve nuclei. *J. Neurosci.* **18**, 4096-4105.

Torrecilla, M., Marker, C. L., Cintora, S. C., Stoffel, M., Williams, J. T., & Wickman, K. (2002). G-protein-gated potassium channels containing Kir3.2 and Kir3.3 subunits mediate the acute inhibitory effects of opioids on locus ceruleus neurons. *J. Neurosci.* **22**, 4328-4334.

Tracey, W. R. & Peach, M. J. (1992). Differential muscarinic receptor mRNA expression by freshly isolated and cultured bovine aortic endothelial cells. *Circ. Res.* **70**, 234-240.

Trapp, S., Haider, S., Jones, P., Sansom, M. S., & Ashcroft, F. M. (2003). Identification of residues contributing to the ATP binding site of Kir6.2. *EMBO J.* **22**, 2903-2912.

Trautwein, W. & Dudel, J. (1958). Zum Mechanismus der Membranwirkung des Acetylcholines an der Herzmuskelfaser. *Pflugers Arch.* **266**, 324-334.

Trimmer, J. S. (1991). Immunological identification and characterization of a delayed rectifier K^+ channel polypeptide in rat brain. *Proc. Natl. Acad. Sci. U.S.A.* **88**, 10764-10768.

Trimmer, J. S. (1998). Regulation of ion channel expression by cytoplasmic subunits. *Curr. Opin. Neurobiol.* **8**, 370-374.

Trimmer, J. S. & Rhodes, K. J. (2004). Localization of voltage-gated ion channels in mammalian brain. *Annu. Rev. Physiol.* **66**, 477-519.

Trube, G., Rorsman, P., & Ohno-Shosaku, T. (1986). Opposite effects of tolbutamide and diazoxide on the ATP-dependent K^+ channel in mouse pancreatic beta-cells. *Pflugers Arch.* **407**, 493-499.

Tse, F. W., Fraser, D. D., Duffy, S., & MacVicar, B. A. (1992). Voltage-activated K^+ currents in acutely isolated hippocampal astrocytes. *J. Neurosci.* **12**, 1781-1788.

Tseng, G. N. (2001). I_{Kr}: the hERG channel. *J. Mol. Cell Cardiol.* **33**, 835-849.

Tseng, G. N. & Hoffman, B. F. (1989). Two components of transient outward current in canine ventricular myocytes. *Circ. Res.* **64**, 633-647.

Tu, L., Santarelli, V., Sheng, Z., Skach, W., Pain, D., & Deutsch, C. (1996). Voltage-gated K^+ channels contain multiple intersubunit association sites. *J. Biol. Chem.* **271**, 18904-18911.

Tucker, S. J., Bond, C. T., Herson, P., Pessia, M., & Adelman, J. P. (1996). Inhibitory interactions between two inward rectifier K^+ channel subunits mediated by the transmembrane domains. *J. Biol. Chem.* **271**, 5866-5870.

Tucker, S. J., Gribble, F. M., Zhao, C., Trapp, S., & Ashcroft, F. M. (1997). Truncation of Kir6.2 produces ATP-sensitive K^+ channels in the absence of the sulphonylurea receptor. *Nature* **387**, 179-183.

Ueda, K., Inagaki, N., & Seino, S. (1997). MgADP antagonism to Mg^{2+}-independent ATP binding of the sulfonylurea receptor SUR1. *J. Biol. Chem.* **272**, 22983-22986.

Ueda, K., Komine, J., Matsuo, M., Seino, S., & Amachi, T. (1999a). Cooperative binding of ATP and MgADP in the sulfonylurea receptor is modulated by glibenclamide. *Proc. Natl. Acad. Sci. U.S.A.* **96**, 1268-1272.

Ueda, K., Matsuo, M., Tanabe, K., Morita, K., Kioka, N., & Amachi, T. (1999b). Comparative aspects of the function and mechanism of SUR1 and MDR1 proteins. *Biochim. Biophys. Acta* **1461**, 305-313.

Unwin, N. (1993). Nicotinic acetylcholine receptor at 9 Å resolution. *J. Mol. Biol.* **229**, 1101-1124.

Unwin, N. (1995). Acetylcholine receptor channel imaged in the open state. *Nature* **373**, 37-43.

Vaca, L. & Kunze, D. L. (1995). IP_3-activated Ca^{2+} channels in the plasma membrane of cultured vascular endothelial cells. *Am. J. Physiol.* **269**, C733-738.

Valentin, S. & Schousboe, I. (1996). Factor Xa enhances the binding of tissue factor pathway inhibitor to acidic phospholipids. *Thromb. Haemost.* **75**, 796-800.

Vandenberg, C. A. (1987). Inward rectification of a potassium channel in cardiac ventricular cells depends on internal magnesium ions. *Proc. Natl. Acad. Sci. U.S.A.* **84**, 2560-2564.

Vandenberg, C. A. (1994). Cardiac inward rectifier potassium channels. In *Ion channels in the cardiovascular system*, eds. Spooner, P. M. & Brown, A. M., Futura Publishing, New York.

Vanoli, E., Priori, S. G., Nakagawa, H., Hirao, K., Napolitano, C., Diehl, L., Lazzara, R., & Schwartz, P. J. (1995). Sympathetic activation, ventricular repolarization and I_{Kr} blockade: implications for the antifibrillatory efficacy of potassium channel blocking agents. *J. Am. Coll. Cardiol.* **25**, 1609-1614.

Vargas, F. F., Caviedes, P. F., & Grant, D. S. (1994). Electrophysiological characteristics of cultured human umbilical vein endothelial cells. *Microvasc. Res.* **47**, 153-165.

Varro, A., Nanasi, P. P., Lathrop, D. A.. (1993). Potassium currents in isolated human atrial and ventricular cardiocytes. *Acta Physiol Scand.* **149**, 133-142.

Varro, A., Balati, B., Iost, N., Takacs, J., Virag, L., Lathrop, D. A., Csaba, L., Talosi, L., & Papp, J. G. (2000). The role of the delayed rectifier component I_{Ks} in dog ventricular muscle and Purkinje fibre repolarization. *J. Physiol.* **523**, 67-81.

Vergara, C. & Latorre, R. (1983). Kinetics of Ca^{2+}-activated K^+ channels from rabbit muscle incorporated into planar bilayers. Evidence for a Ca^{2+} and Ba^{2+} blockade. *J. Gen. Physiol.* **82**, 543-568.

Vergara, C., Alvarez, O., & Latorre, R. (1999). Localization of the K^+ lock-in and the Ba^{2+} binding sites in a voltage-gated calcium-modulated channel. Implications for survival of K^+ permeability. *J. Gen. Physiol.* **114**, 365–376.

Verkerk, A. O., Veldkamp, M. W., Abbate, F., Antoons, G., Bouman, L. N., Ravesloot, J. H., & van Ginneken, A. C. (1999). Two types of action potential configuration in single cardiac Purkinje cells of sheep. *Am. J. Physiol.* **277**, H1299-1310.

Vinet, R. & Vargas, F. F. (1999). L- and T-type voltage-gated Ca^{2+} currents in adrenal medulla endothelial cells. *Am. J. Physiol.* **276**, H1313-1322.

Voets, T., Droogmans, G., & Nilius, B. (1996). Membrane currents and the resting membrane potential in cultured bovine pulmonary artery endothelial cells. *J. Physiol.* **497**, 95-107.

Volders, P. G., Sipido, K. R., Carmeliet, E., Spatjens, R. L., Wellens, H. J., & Vos, M. A. (1999). Repolarizing K^+ currents I_{to1} and I_{Ks} are larger in right than left canine ventricular midmyocardium. *Circulation* **99**, 206-210.

Volk, T., Nguyen, T. H., Schultz, J. H., & Ehmke, H. (1999). Relationship between transient outward K^+ current and Ca^{2+} influx in rat cardiac myocytes of endo- and epicardial origin. *J. Physiol.* **519**, 841-850.

Wahler, G. M. (1992). Developmental increases in the inwardly rectifying potassium current of rat ventricular myocytes. *Am. J. Physiol.* **262**, C1266-1272.

Walker, B. D., Singleton, C. B., Tie, H., Bursill, J. A., Wyse, K. R., Valenzuela, S. M., Breit, S. N., & Campbell, T. J. (2000). Comparative effects of azimilide and ambasilide on the human ether-a-go-go-related gene (HERG) potassium channel. *Cardiovasc. Res.* **48**, 44-58.

Walker, J. E., Saraste, M., Runswick, M. J., & Gay, N. J. (1982). Distantly related sequences in the alpha- and beta-subunits of ATP synthase, myosin, kinases and other ATP-requiring enzymes and a common nucleotide binding fold. *EMBO J.* **1**, 945-951.

Wang, H., Han, H., Zhang, L., Shi, H., Schram, G., Nattel, S., & Wang, Z. (2001). Expression of multiple subtypes of muscarinic receptors and cellular distribution in the human heart. *Mol. Pharmacol.* **59**, 1029-1036.

Wang, H., Kunkel, D. D., Martin, T. M., Schwartzkroin, P. A., & Tempel, B. L. (1993a). Heteromultimeric K^+ channels in terminal and juxtaparanodal regions of neurons. *Nature* **365**, 75-79.

Wang, H., Kunkel, D. D., Schwartzkroin, P. A., & Tempel, B. L. (1994a). Localization of Kv1.1 and Kv1.2, two K^+ channel proteins, to synaptic terminals, somata, and dendrites in the mouse brain. *J. Neurosci.* **14**, 4588-4599.

Wang, X. J., Reynolds, E. R., Deak, P., & Hall, L. M. (1997). The seizure locus encodes the Drosophila homolog of the HERG potassium channel. *J. Neurosci.* **17**, 882-890.

Wang, Z., Feng, J., Shi, H., Pond, A., Nerbonne, J. M., & Nattel, S. (1999). Potential molecular basis of different physiological properties of the transient outward K^+ current in rabbit and human atrial myocytes. *Circ. Res.* **84**, 551-561.

Wang, Z., Fermini, B., & Nattel, S. (1993b). Delayed rectifier outward current and repolarization in human atrial myocytes. *Circ. Res.* **73**, 276-285.

Wang, Z., Fermini, B., & Nattel, S. (1993c). Sustained depolarization-induced outward current in human atrial myocytes. Evidence for a novel delayed rectifier K^+ current similar to Kv1.5 cloned channel currents. *Circ. Res.* **73**, 1061-1076.

Wang, Z., Fermini, B., & Nattel, S. (1994b). Rapid and slow components of delayed rectifier current in human atrial myocytes. *Cardiovasc. Res.* **28**, 1540-1546.

Wang, Z., Fermini, B., & Nattel, S. (1995). Effects of flecainide, quinidine, and 4-aminopyridine on transient outward and ultrarapid delayed rectifier currents in human atrial myocytes. *J. Pharmacol. Exp. Ther.* **272**, 184-196.

Wang, Z., Yue, L., White, M., Pelletier, G., & Nattel, S. (1998). Differential distribution of inward rectifier potassium channel transcripts in human atrium versus ventricle. *Circulation* **98**, 2422-2428.

Warmke, J., Drysdale, R., & Ganetzky, B. (1991). A distinct potassium channel polypeptide encoded by the Drosophila eag locus. *Science* **252**, 1560-1562.

Warmke, J. W. & Ganetzky, B. (1994). A family of potassium channel genes related to eag in Drosophila and mammals. *Proc. Natl. Acad. Sci.U.S.A.* **91**, 3438-3442.

Warren, M., Guha, P. K., Berenfeld, O., Zaitsev, A., Anumonwo, J. M., Dhamoon, A. S., Bagwe, S., Taffet, S. M., & Jalife, J. (2003). Blockade of the inward rectifying potassium current terminates ventricular fibrillation in the guinea pig heart. *J. Cardiovasc. Electrophysiol.* **14**, 621-631.

Watanabe, Y. & Dreifus, L. S. (1968). Sites of impulse formation within the atio-ventricular junction of the rabbit. *Circ. Res.* **333**, 717-727.

Watsky, M. A., Cooper, K., & Rae, J. L. (1992). Transient outwardly rectifying potassium channel in the rabbit corneal endothelium. *J. Membr. Biol.* **128**, 123-132.

Weerapura, M., Nattel, S., Chartier, D., Caballero, R., & Hebert, T. E. (2002). A comparison of currents carried by HERG, with and without coexpression of MiRP1, and the native rapid delayed rectifier current. Is MiRP1 the missing link? *J. Physiol.* **540**, 15-27.

Weidmann, S. (1955). Rectifier properties of Purkinje fibers. *Am. J. Physiol.* **183**, 671.

Weik, R. & Neumcke, B. (1989). ATP-sensitive potassium channels in adult mouse skeletal muscle: characterization of the ATP-binding site. *J. Membr. Biol.* **110**, 217-226.

Weiser, M., Bueno, E., Sekirnjak, C., Martone, M. E., Baker, H., Hillman, D., Chen, S., Thornhill, W., Ellisman, M., & Rudy, B. (1995). The potassium channel subunit KV3.1b is localized to somatic and axonal membranes of specific populations of CNS neurons. *J. Neurosci.* **15**, 4298-4314.

Wellman, G. C. & Bevan, J. A. (1995). Barium inhibits the endothelium-dependent component of flow but not acetylcholine-induced relaxation in isolated rabbit cerebral arteries. *J. Pharmacol. Exp. Ther.* **274**, 47-53.

Wettwer, E., Amos, G. J., Posival, H., & Ravens, U. (1994). Transient outward current in human ventricular myocytes of subepicardial and subendocardial origin. *Circ. Res.* **75**, 473-482.

White, J. A., McAlpine, P. J., Antonarakis, S., Cann, H., Eppig, J. T., Frazer, K., Frezal, J., Lancet, D., Nahmias, J., Pearson, P., Peters, J., Scott, A., Scott, H., Spurr, N., Talbot, C., Jr., & Povey, S. (1997). Guidelines for human gene nomenclature (1997). HUGO Nomenclature Committee. *Genomics* **45**, 468-471.

Wible, B. A., De Biasi, M., Majumder, K., Taglialatela, M., & Brown, A. M. (1995). Cloning and functional expression of an inwardly rectifying K^+ channel from human atrium. *Circ. Res.* **76**, 343-350.

Wible, B. A., Yang, Q., Kuryshev, Y. A., Accili, E. A., & Brown, A. M. (1998). Cloning and expression of a novel K^+ channel regulatory protein, KChAP. *J. Biol. Chem.* **273**, 11745-11751.

Wickenden, A. D., Jegla, T. J., Kaprielian, R., & Backx, P. H. (1999). Regional contributions of Kv1.4, Kv4.2, and Kv4.3 to transient outward K^+ current in rat ventricle. *Am. J. Physiol.* **276**, H1599-1607.

Wickman, K., Karschin, C., Karschin, A., Picciotto, M. R., & Clapham, D. E. (2000). Brain localization and behavioral impact of the G-protein-gated K^+ channel subunit GIRK4. *J. Neurosci.* **20**, 5608-5615.

Wickman, K., Nemec, J., Gendler, S. J., & Clapham, D. E. (1998). Abnormal heart rate regulation in GIRK4 knockout mice. *Neuron* **20**, 103-114.

Wickman, K. D., Iniguez-Lluhl, J. A., Davenport, P. A., Taussig, R., Krapivinsky, G. B., Linder, M. E., Gilman, A. G., & Clapham, D. E. (1994). Recombinant G-protein beta gamma-subunits activate the muscarinic-gated atrial potassium channel. *Nature* **368**, 255-257.

Wimpey, T. L. & Chavkin, C. (1991). Opioids activate both an inward rectifier and a novel voltage-gated potassium conductance in the hippocampal formation. *Neuron* **6**, 281-289.

Wu, C. F., Ganetzky, B., Haugland, F. N., & Liu, A. X. (1983). Potassium currents in Drosophila: different components affected by mutations of two genes. *Science* **220**, 1076-1078.

Wu, S. N., Nakajima, T., Yamashita, T., Hamada, E., Hazama, H., Iwasawa, K., Omata, M., & Kurachi, Y. (1994). Molecular mechanism of cibenzoline-induced anticholinergic action in single atrial myocytes: comparison with effect of disopyramide. *J. Cardiovasc. Pharmacol.* **23**, 618-623.

Wymore, R. S., Gintant, G. A., Wymore, R. T., Dixon, J. E., McKinnon, D., & Cohen, I. S. (1997). Tissue and species distribution of mRNA for the I_{Kr}-like K^+ channel, erg. *Circ. Res.* **80**, 261-268.

Xie, L. H., Horie, M., & Takano, M. (1999). Phospholipase C-linked receptors regulate the ATP-sensitive potassium channel by means of phosphatidylinositol 4,5-bisphosphate metabolism. *Proc. Natl. Acad. Sci. U.S.A.* **96**, 15292-15297.

Xie, L. H., John, S. A., & Weiss, J. N. (2002). Spermine block of the strong inward rectifier potassium channel Kir2.1: dual roles of surface charge screening and pore block. *J. Gen. Physiol.* **120**, 53-66.

Xu, H., Guo, W., & Nerbonne, J. M. (1999a). Four kinetically distinct depolarization-activated K^+ currents in adult mouse ventricular myocytes. *J. Gen. Physiol.* **113**, 661-678.

Xu, H., Li, H., & Nerbonne, J. M. (1999b). Elimination of the transient outward current and action potential prolongation in mouse atrial myocytes expressing a dominant negative Kv4 alpha subunit. *J.Physiol.* **519**, 11-21.

Xu, Z. C., Yang, Y., & Hebert, S. C. (1996). Phosphorylation of the ATP-sensitive, inwardly rectifying K^+ channel, ROMK, by cyclic AMP-dependent protein kinase. *J. Biol. Chem.* **271**, 9313-9319.

Yamada, K. & Inagaki, N. (2005). Neuroprotection by K_{ATP} channels. *J. Mol. Cell. Cardiol.* **38**, 945-949.

Yamada, M., Inanobe, A., & Kurachi, Y. (1998). G protein regulation of potassium ion channels. *Pharmacol. Rev.* **50**, 723-760.

Yamada, M., Isomoto, S., Matsumoto, S., Kondo, C., Shindo, T., Horio, Y., & Kurachi, Y. (1997). Sulphonylurea receptor 2B and Kir6.1 form a sulphonylurea-sensitive but ATP-insensitive K^+ channel. *J. Physiol.* **499**, 715-720.

Yamada, M. & Kurachi, Y. (1995). Spermine gates inward-rectifying muscarinic but not ATP-sensitive K^+ channels in rabbit atrial myocytes. Intracellular substance-mediated mechanism of inward rectification. *J. Biol. Chem.* **270**, 9289-9294.

Yamaguchi, K., Nakajima, Y., Nakajima, S., & Stanfield, P. R. (1990). Modulation of inwardly rectifying channels by substance P in cholinergic neurones from rat brain in culture. *J. Physiol.* **426**, 499-520.

Yamamoto, Y., Chen, G., Miwa, K., & Suzuki, H. (1992). Permeability and Mg^{2+} blockade of histamine-operated cation channel in endothelial cells of rat intrapulmonary artery. *J Physiol,* **450**, 395-408.

Yang, D., MacCallum, D. K., Ernst, S. A., & Hughes, B. A. (2003a). Expression of the inwardly rectifying K^+ channel Kir2.1 in native bovine corneal endothelial cells. *Invest. Ophthalmol. Vis. Sci.* **44**, 3511-3519.

Yang, D., Pan, A., Swaminathan, A., Kumar, G., & Hughes, B. A. (2003b). Expression and localization of the inwardly rectifying potassium channel Kir7.1 in native bovine retinal pigment epithelium. *Invest. Ophthalmol. Vis. Sci.* **44**, 3178-3185.

Yang, E. K., Alvira, M. R., Levitan, E. S., & Takimoto, K. (2001). Kvbeta subunits increase expression of Kv4.3 channels by interacting with their C termini. *J. Biol. Chem.* **276**, 4839-4844.

Yang, J., Jan, Y. N., & Jan, L. Y. (1995). Control of rectification and permeation by residues in two distinct domains in an inward rectifier K^+ channel. *Neuron* **14**, 1047-1054.

Yang, Z., Xu, H., Cui, N., Qu, Z., Chanchevalap, S., Shen, W., & Jiang, C. (2000). Biophysical and molecular mechanisms underlying the modulation of heteromeric Kir4.1-Kir5.1 channels by CO_2 and pH. *J. Gen. Physiol.* **116**, 33-45.

Yao, Z., Cavero, I., & Gross, G. J. (1993). Activation of cardiac K_{ATP} channels: an endogenous protective mechanism during repetitive ischemia. *Am. J. Physiol.* **264**, H495-504.

Yatani, A., Codina, J., Brown, A. M., & Birnbaumer, L. (1987). Direct activation of mammalian atrial muscarinic potassium channels by GTP regulatory protein G_k. *Science* **235**, 207-211.

Yatani, A., Mattera, R., Codina, J., Graf, R., Okabe, K., Padrell, E., Iyengar, R., Brown, A. M., & Birnbaumer, L. (1988). The G protein-gated atrial K^+ channel is stimulated by three distinct Gi alpha-subunits. *Nature* **336**, 680-682.

Yellen, G., Jurman, M. E., Abramson, T., & MacKinnon, R. (1991). Mutations affecting internal TEA blockade identify the probable pore-forming region of a K^+ channel. *Science* **251**, 939-942.

Yellen, G., Sodickson, D., Chen, T. Y., & Jurman, M. E. (1994). An engineered cysteine in the external mouth of a K^+ channel allows inactivation to be modulated by metal binding. *Biophys J* **66**, 1068-1075.

Yellon, D. M. & Downey, J. M. (2003). Preconditioning the myocardium: from cellular physiology to clinical cardiology. *Physiol. Rev.* **83**, 1113-1151.

Yeola, S. W. & Snyders, D. J. (1997). Electrophysiological and pharmacological correspondence between Kv4.2 current and rat cardiac transient outward current. *Cardiovasc. Res.* **33**, 540-547.

Yifrach, O. & MacKinnon, R. (2002). Energetics of pore opening in a voltage-gated K^+ channel. *Cell* **111**, 231-239.

Yue, L., Feng, J., Gaspo, R., Li, G. R., Wang, Z., & Nattel, S. (1997). Ionic remodeling underlying action potential changes in a canine model of atrial fibrillation. *Circ. Res.* **81**, 512-525.

Yue, L., Feng, J., Li, G. R., & Nattel, S. (1996a). Characterization of an ultrarapid delayed rectifier potassium channel involved in canine atrial repolarization. *J.Physiol.* **496**, 647-662.

Yue, L., Feng, J., Li, G. R., & Nattel, S. (1996b). Transient outward and delayed rectifier currents in canine atrium: properties and role of isolation methods. *Am. J. Physiol.* **270**, H2157-2168.

Yue, L., Wang, Z., Rindt, H., & Nattel, S. (2000). Molecular evidence for a role of Shaw (Kv3) potassium channel subunits in potassium currents of dog atrium. *J. Physiol.* **527**, 467-478.

Yue, L. X., Melnyk, P., Gaspo, R., Wang, Z. G., & Nattel, S. (1999). Molecular mechanisms underlying ionic remodeling in a dog model of atrial fibrillation. *Circ. Res.* **84**, 776-784.

Yusaf, S. P., Wray, D., & Sivaprasadarao, A. (1996). Measurement of the movement of the S4 segment during the activation of a voltage-gated potassium channel. *Pflugers Arch.* **433**, 91-97.

Zaccai, G. (2000). How soft is a protein? A protein dynamics force constant measured by neutron scattering. *Science* **288**, 1604-1607.

Zagotta, W. N., Hoshi, T., & Aldrich, R. W. (1990). Restoration of inactivation in mutants of Shaker potassium channels by a peptide derived from ShB. *Science* **250**, 568-571.

Zaritsky, J. J., Eckman, D. M., Wellman, G. C., Nelson, M. T., & Schwarz, T. L. (2000). Targeted disruption of Kir2.1 and Kir2.2 genes reveals the essential role of the inwardly rectifying K^+ current in K^+-mediated vasodilation. *Circ. Res.* **87**, 160-166.

Zaritsky, J. J., Redell, J. B., Tempel, B. L., & Schwarz, T. L. (2001). The consequences of disrupting cardiac inwardly rectifying K^+ current (I_{K1}) as revealed by the targeted deletion of the murine Kir2.1 and Kir2.2 genes. *J. Physiol.* **533**, 697-710.

Zawar, C., Plant, T. D., Schirra, C., Konnerth, A., & Neumcke, B. (1999). Cell-type specific expression of ATP-sensitive potassium channels in the rat hippocampus. *J. Physiol.* **514**, 327-341.

Zerangue, N., Schwappach, B., Jan, Y. N., & Jan, L. Y. (1999). A new ER trafficking signal regulates the subunit stoichiometry of plasma membrane K_{ATP} channels. *Neuron* **22**, 537-548.

Zhang, H. & Bolton, T. B. (1995). Activation by intracellular GDP, metabolic inhibition and pinacidil of a glibenclamide-sensitive K^+ channel in smooth muscle cells of rat mesenteric artery. *Br. J. Pharmacol.* **114**, 662-672.

Zhang, H., Holden, A. V., Kodama, I., Honjo, H., Lei, M., Varghese, T., & Boyett, M. R. (2000). Mathematical models of action potentials in the periphery and center of the rabbit sinoatrial node. *Am. J. Physiol. Heart Circ. Physiol.* **279**, H397-421.

Zhang, M., Jiang, M., & Tseng, G. N. (2001). minK-related peptide 1 associates with Kv4.2 and modulates its gating function: potential role as beta subunit of cardiac transient outward channel? *Circ. Res.* **88**, 1012-1019.

Zhang, Q., Pacheco, M. A., & Doupnik, C. A. (2002). Gating properties of GIRK channels activated by $G_{\alpha o}$- and $G_{\alpha i}$-coupled muscarinic m2 receptors in *Xenopus* oocytes: the role of receptor precoupling in RGS modulation. *J. Physiol.* **545**, 355-373.

Zhang, S., Zhou, Z., Gong, Q., Makielski, J. C., & January, C. T. (1999). Mechanism of block and identification of the verapamil binding domain to HERG potassium channels. *Circ. Res.* **84**, 989-998.

Zhou, L., Zhang, C. L., Messing, A., & Chiu, S. Y. (1998). Temperature-sensitive neuromuscular transmission in Kv1.1 null mice: role of potassium channels under the myelin sheath in young nerves. *J. Neurosci.* **18**, 7200-7215.

Zhou, M., Morais-Cabral, J. H., Mann, S., & MacKinnon, R. (2001a). Potassium channel receptor site for the inactivation gate and quaternary amine inhibitors. *Nature* **411**, 657-661.

Zhou, W., Qian, Y., Kunjilwar, K., Pfaffinger, P. J., & Choe, S. (2004). Structural insights into the functional interaction of KChIP1 with Shal-type K^+ channels. *Neuron* **41**, 573-586.

Zhou, Y. & MacKinnon, R. (2003). The occupancy of ions in the K^+ selectivity filter: charge balance and coupling of ion binding to a protein conformational change underlie high conduction rates. *J. Mol. Biol.* **333**, 965-975.

Zhou, Y. & MacKinnon, R. (2004). Ion binding affinity in the cavity of the KcsA potassium channel. *Biochemistry* **43**, 4978-4982.

Zhou, Y., Morais-Cabral, J. H., Kaufman, A., & MacKinnon, R. (2001b). Chemistry of ion coordination and hydration revealed by a K^+ channel- Fab complex at 2.0 Å resolution. *Nature* **414**, 43-48.

Zhou, Z., Vorperian, V. R., Gong, Q., Zhang, S., & January, C. T. (1999). Block of HERG potassium channels by the antihistamine astemizole and its metabolites desmethylastemizole and norastemizole. *J. Cardiovasc. Electrophysiol.* **10**, 836-843.

Zhu, X. R., Netzer, R., Bohlke, K., Liu, Q., & Pongs, O. (1999a). Structural and functional characterization of Kv6.2 a new gamma-subunit of voltage-gated potassium channel. *Receptors. Channels* **6**, 337-350.

Zhu, X. R., Wulf, A., Schwarz, M., Isbrandt, D., & Pongs, O. (1999b). Characterization of human Kv4.2 mediating a rapidly-inactivating transient voltage-sensitive K^+ current. *Receptors. Channels* **6**, 387-400.